THE DEVELOPMENT OF SEISMIC DETAILING AND DESIGN FOR MORE RESILIENT BRIDGE PIERS

Brandon McHaffie

Be(Hons) – Structural Engineering

Supervisors:

Prof. Alessandro Palermo – Professor in Structural Engineering, University of Canterbury,

Dr John Wood – John wood Consulting

Submitted in [partial] fulfilment of the requirements for the degree of Doctor of Philosophy

Civil and Natural Resources Engineering

University of Canterbury

[2020]

Abstract

In the last century, the seismic design of structures has been continuously evolving. Particularly, when compared to other design requirements such as gravity, traffic and wind loads. In the past 50 years, there has been notable advancements in the way structures are detailed and the design philosophy used for designed. Much of this advancement takes place due to learnings from past earthquakes. The first part of this thesis investigates the 2016, 7.8 (M_w) Kaikōura Earthquake, which caused severe plastic hinge damage to six bridge structures. Each of these structures is investigated to determine whether current provisions of detailing for ductility are sufficient, what future improvements are necessary, and whether current displacement-based design procedures would accurately capture this damage given the recorded ground motion data obtained. It was concluded that current codes do not adequately prevent buckling of longitudinal reinforcement and that simplified displacement-based design procedures can predict peak displacements with adequate accuracy. This investigation was taken a step further to try and estimate the residual capacity of a plastic hinge. The residual capacity of a plastic hinge that formed on the River Road Bridge was estimated using material testing techniques (Vickers Hardness) and NLTH. This analysis indicates that the structure has sufficient capacity to prevent collapse in future earthquakes.

Dissipative Controlled Rocking (DCR) is an alternative detail that can be used in place of a traditional plastic hinge. DCR has many advantages over plastic hinges, including repairable damage and no residual deformation. However, to date, this detailing has only been implemented once. The main reason for this is the additional cost associated with this detail. The second part of this thesis focuses on the development of displacement-based design methods for DCR connections to try and gain efficiencies and account for the benefits of DCR. In particular, an alternative design philosophy is presented where the Collapse Avoidance Limit State (CALS) is the crucial design level and the DCLS level can be altered based on the acceptable risk of replacing dissipaters – a higher risk of dissipater replacement means the dissipaters can be designed to a lower DCLS strain limit. This strategy is further adapted for dissipaters that are not damaged, such as the lead extrusion damper, to fully exclude

the DCLS. The alternative design philosophy was found to reduce the base shear demands by between 20-40% reducing foundation and pier cap sizes.

Due to the proposal of the alternative design philosophy, there were several gaps in the design framework, such as CALS performance limits. Therefore, dissipater, Post-Tensioning (PT) and P-Delta limits were proposed for the CALS. A parametric analysis was carried out to allow the estimation of key preliminary design inputs such as the yield rotation and neutral axis location. This research was also used to propose geometric ratios that ensure DCR connections can achieve the desired performance limits. Design tables were also developed that allow the quick and easy preliminary design of DCR connections.

In addition to the alternative design philosophy, experimental testing of alternative devices was also carried to try and gain further cost efficiency and detailing simplicity. The double tube and optimised double tube axial dissipater were investigated. These dissipaters were found to have a lower cost (~30% cheaper) than the currently preferred four groove axial dissipater but have less low-cycle fatigue capacity. An alternative device, the lead extrusion damper was also tested, which was found to have good performance after a number of tests. No damage was recorded to the device and therefore, this device could offer a no-damage (no replacement, no DCLS design level) alternative to axial dissipaters. Application of these devices to the Wigram Magdala Bridge was investigated, and in addition to the simplified detailing that can be used, the cost of a 300kN lead extrusion damper is around $800 while the cost of a 190kN axial dissipater is around 800$. Therefore, overall it would cost less to improve performance, and simplify detailing.

Table of Contents

List of Figures

List of Tables

List of Abbreviations

ABC - Accelerated Bridge Construction

Af – Fuse Area

At – Treaded Area

ADRS - Acceleration Displacement Response Spectrum

CSM – Capacity Spectrum Method

BRF - Buckling Restrained Fuse

BM – Bridge Manual

CALS - Collapse Avoidance Limit State, formerly termed MCE

CHS - Circular Hollow Section

COM - Centre of Mass

CR - Controlled Rocking

DAD - Damage Avoidance Design

DCLS - Damage Control Limit State, formerly termed ULS

DCR – Dissipative Controlled Rocking

DBD – Displacement Based Design

DDBD - Direct Displacement Based Design

Dxx - Deformed Grade 300 rebar of xx diameter

EPP - Elastic Perfectly Plastic

FEM - Finite Element Modelling

HDxx - High Strength Deformed Grade 500 rebar of xx diameter

HRxx - High Strength Plain Grade 500 rebar of xx diameter

ID - Inside Diameter

MBA - Monolithic Beam Analogy

MCE - Maximum Credible Earthquake

Mxx - Metric coarse thread of xx diameter

NA - Neutral Axis

NLTA - Nonlinear Time History Analysis

NLTH – Non-linear Time History

NZS - New Zealand Standard

NZTA - New Zealand Transport Agency

OD - Outside Diameter

PRESSS - Precast Seismic Structural System

ptMBA - Post-tensioned only Monolithic Beam Analogy

PT – Post-tensioning

P −Δ - Second order effects arising from global deformation

P – δ - Second order effects arising from member deformation

rMBA - Revisited Monolithic Beam Analogy

RC - Reinforced Concrete

SLS – Serviceability Limit State

SDOF - Single Degree of Freedom

Statement of Original Authorship

The work contained in this thesis has not been previously submitted to meet requirements for an award at this or any other higher education institution. To the best of my knowledge and belief, the thesis contains no material previously published or written by another person except where due reference is made.

Signature: Brandon McHaffie

Date: 01/03/2020

Acknowledgements

There are many people who have supported me along this difficult and enlightening journey. I would like to thank my supervisor, Prof. Alessandro Palermo, for his guidance and support that he provided during my time as a PhD student. I would like to thank my co-supervisor John Wood for his assistance and expertise throughout the course of my research. I would like to thank Quake Centre and WSP for assisting with financial support. I would also like to thank Gavin Geats, Mosese Fifita, Peter Coursey and Russel McConchie who assisted with laboratory testing. I would like to thank friends and colleagues who have provided me with invaluable support, advice and technical knowledge throughout. Lastly, I would like to thank my family and Partner for their unconditional understanding, love and support even in the most difficult of times.

Chapter 1: Introduction and Scope

Bridges are a key part of infrastructure, both in New Zealand and throughout the world. They provide critical links between towns and cities, often facilitating shorter routes between critical locations. Therefore, when bridges are damaged it can either isolate a community altogether, or at the very least, significantly increase travel times, which impacts the ability of communities to obtain critical goods. Therefore, to minimise impacts on society it is important to design and build the most resilient infrastructure possible.

Currently, seismic resilience relies on capacity design. Developed in the 1970's, capacity design is still the preferred design philosophy used to ensure structures can withstand earthquakes (Priestley et al., 1996). In capacity design, well detailed elements, typically called plastic hinges, are designed to be damaged. This allows the structure to dissipate energy and displace further than it could elastically, reducing the overall moment and shear demands on the structure. All other elements of the structure are designed to have enough capacity to ensure they remain undamaged. Displacement ductility is used to describe or quantify the acceptable level of damage allowed to occur in the plastic hinges. While this method of design has, for the most part, prevented collapse of structures in recent earthquakes (Kawashima & Buckle, 2013; Palermo et al., 2017a; Roberts, 2001), significant damage (Figure 1-1) has still occurred, which was costly and time consuming to repair. Given the importance of detailing on the ductility capacity of the structure, it is important to learn from the damage that has occurred in past earthquakes. This is especially important as reinforced concrete, detailed for ductility, is still more common than any other seismic design strategy.

Figure 1-1: Damage to the Lower Mason River Bridge (Left) and residual drift at the Waima River Bridge (Right).

Alternatives to plastic hinging, and the idea of ductility, which reduce the demand by elongating the period or displacements have previously been developed. Probably the most widely adopted is the use of seismic isolation such as lead rubber bearings (Skinner et al., 1991). Typically, for bridges, these devices would be placed between the beams (superstructure) and the pier (substructure). They allow the beams to move independently of the pier, providing displacement capacity to the structure, shifting the period, ultimately reducing displacement and force demands on the pier.

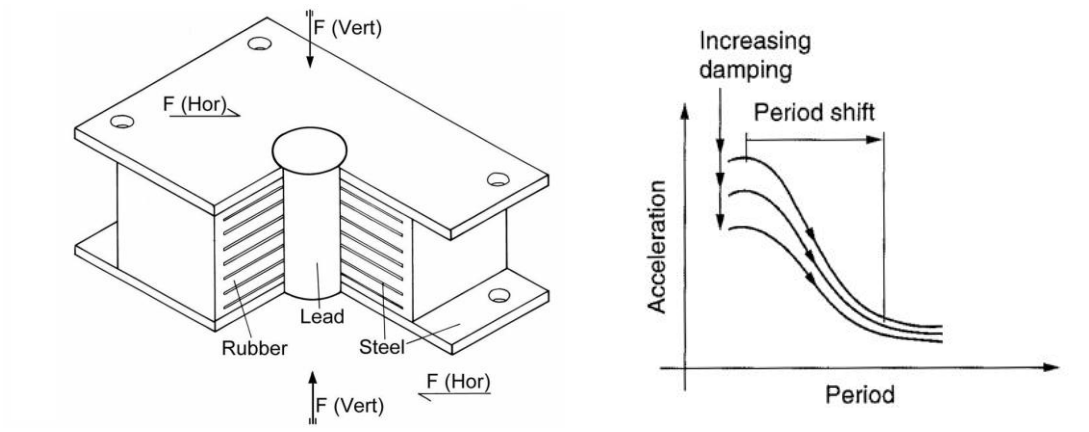

Figure 1-2: Left - lead rubber bearing retrieved from (Skinner et al., 1991) Right – Illustration of the period shift (Kelly, Skinner, & Robinson, 2010).

Though these devices effectively reduce base shear demand there are some issues:

- The vertical flexibility can cause unseating of the beams which induces large torsional stresses in the deck and adjacent beams.
- The bearings have limited self-centering ability and hence residual displacements of the superstructure are likely to cause alignment issues.

- They add significant cost to construction.

An alternative approach could be low damage repairable plastic hinges. Development of low damage connections can eliminate the issues discussed above for both plastic hinges and seismic isolation. Low damage connections are not significantly different to plastic hinges – there are still elements that are capacity protected and elements that are designed to yield. However, there are two key differences; the first is that the damaged elements (typically dissipaters) are designed to be readily replaced, the second is that PT is used to provide recentering capacity to the connection. The first application of the Precast Seismic Structural System (PRESSS) to bridges (Palermo et al., 2005) was in the form of Dissipative Controlled Rocking (DCR). However, similar systems were experimentally tested prior to this by Mander & Cheng, (1997).

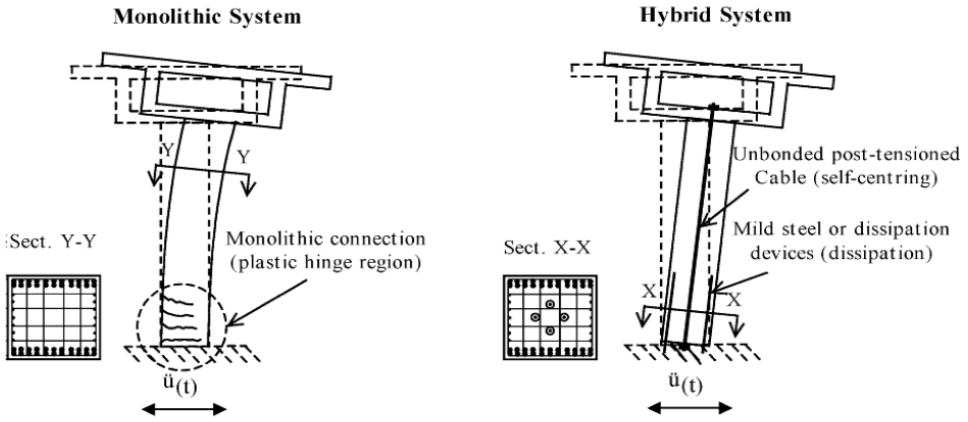

Figure 1-3: Monolithic and DCR systems in their application to bridge piers retrieved from (Palermo et al., 2005).

The DCR system is basically designed to be a replaceable plastic hinge – it dissipates energy and responds in a similar manner to the plastic hinge but has been cleverly detailed to ensure it can be repaired. The DCR connection utilises a rocking interface which is clamped together using PT and dissipaters allowing the combined benefits of rocking and energy dissipation to be utilised. Essentially, rather than the plastic hinge accommodating the inelastic rotation, the rocking interface and yielding dissipaters accommodate it. Residual drifts, typical of plastic hinges, are eliminated through the implementation of PT which acts to recenter the structure. Since the dissipaters can be readily replaced, the DCR connection can be repaired quickly and easily, restoring the connection back to its as-built capacity. However, there is

additional cost associated with the implementation of these connections (Routledge et al., 2016). This is particularly evident when trying to conform to current codes largely intended for reinforced plastic hinge design such as the NZTA Bridge Manual, (2018) and AASHTO, (2017). Therefore, there is a need to develop design procedures and standards which accommodate DCR and other low damage connections.

The research presented within this thesis has two independent sections. The first section investigates structures damaged in the Kaikōura Earthquake, particularly those with plastic hinges. Investigating these structures will help develop learnings from the damage and determine whether improvements can be made to the detailing. In addition, a procedure for estimating the residual capacity of a plastic hinge is presented. This is particularly important given plastic hinges are still the most widely adopted method of resisting seismic demands in bridges. The second section investigates DCR connections and presents an alternative design philosophy, including the parameters required to design using such a philosophy. Key design inputs such as yield rotation, CALS strain limits and neutral axis location are presented, which can be easily implemented during the preliminary design stage. In addition, alternative dissipative devices are examined to try and improve the efficiency of DCR connections.

1.1 PLASITC HINGE PERFORMANCE

1.1.1 Problem Statement

The main purpose of this research is to learn from the 2016 Kaikōura Earthquake (Palermo et al., 2017). In particular, understanding whether the design procedures and detailing requirements that are currently defined by code are proficient at ensuring plastic hinges and ductility demands can be achieved. Furthermore, given plastic hinges have been the preferred design strategy for the last 50 years, to understand whether the residual capacity of plastic hinges can be assessed given recent developments in material testing.

1.1.2 Scope and Objectives

The scope of this research is limited to bridges most severely damaged in the 2016 Kaikōura Earthquake. Of particular interest is the damage to the plastic hinge zones. The key objectives of this research are as follows:

1. Determine, through modelling in conjunction with observed damage after the Kaikōura Earthquake, whether current codes are adequate to ensure plastic hinges can reliably meet performance (ductility) requirements.
2. Assess through modelling and material testing, the residual capacity of a plastic hinge which developed as a result of the Kaikōura Earthquake.

1.2 DISSIPATIVE CONTROLLED ROCKING

1.2.1 Problem Statement

DCR connections have been well developed along with appropriate modelling and analysis procedures. Their performance, and the performance of modelling techniques, has been extensively confirmed through experimental testing and modelling. However, to date, only one structure (Wigram Magdala Bridge) has been constructed which implements this technology. The main reasons for this being the additional cost associated with DCR connections when compared to traditional plastic hinges and the additional perceived design complexity. Therefore, it is important to ensure these connections are designed in a manner that accounts for their attributes, such as having repairable damage and predictable performance. Taking these benefits into account will allow more efficient design of DCR connections.

1.2.2 Scope and Objectives

This section is aimed optimising DCR connections. This is achieved both through design and the development of dissipative devices. This is split into the following objectives:

1. Develop and present an alternative design philosophy for low damage connections (specifically DCR connections).

2. Determine suitable strain limits for components used in DCR connections to allow them to be designed using the alternative design philosophy.
3. Optimise DCR connections through the development of dissipative devices.
4. Determine key DBD parameters for preliminary design of DCR connections including yield rotation, NA location, suitable geometric ratios and design tables.

1.3 THESIS OUTLINE

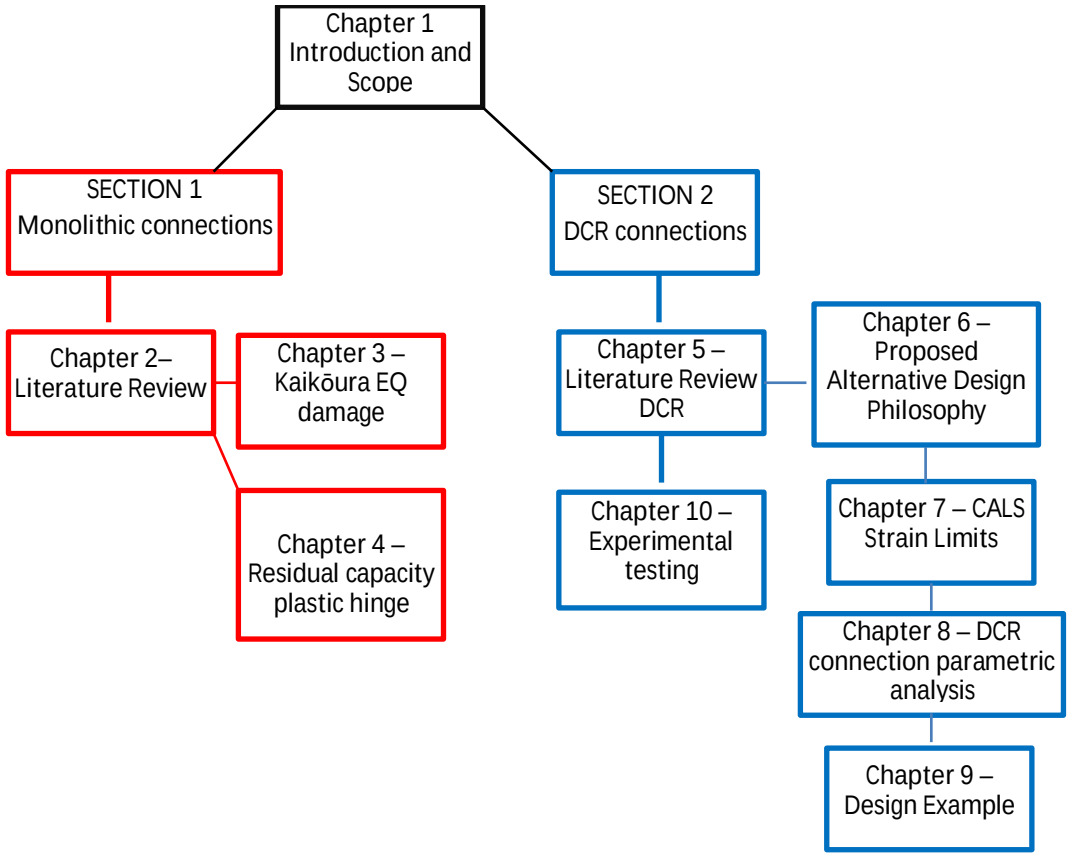

Figure 1-4: General overview of the Thesis

Chapter 2: Presents the most recent and relevant research on plastic hinges and aspects relating to their residual capacity. This chapter will also present the novelty of the research in Chapters 3 and 4.

Chapter 3: Reviews the most severe plastic hinge damage that resulted during the 2016 Kaikōura Earthquake. Simplified modelling and NLTH analysis are used to estimate how the level of shaking compared to both the design standards at the time and modern standards. The damage is then correlated to expected damage. The detailing is examined to determine if changes are likely to improve future performance.

Chapter 4: Investigates the River Road Bridge which was damaged during the Kaikōura Earthquake and was very difficult to retrofit and repair due to detailing of the pier-pile cap connection. The investigation is aimed at estimating the residual capacity of the hinge.

Chapter 5: Reviews the most recent and relevant research on DCR connections, associated devices and design methods. This chapter presents the novelty of the research in subsequent Chapters (6-10)

Chapter 6: Proposes an alternative design philosophy for DCR connections, and other low damage connections, and the reason why such a shift in design thinking is required/warranted. The overall intent of this philosophy is to increase the cost-competitiveness of DCR connections compared to traditional plastic hinges.

Chapter 7: Proposes strain limits for the CALS (to be used for the alternative design philosophy). These were found using NLTH and appropriate fatigue models.

Chapter 8: Presents a parametric analysis of DCR connections and includes relationships that allow the estimation of the yield rotation, NA location and optimum geometric ratios which ensure desired performance limits and displacement can be achieved.

Chapter 9: Presents the design of a prototype pier using the alternative design philosophy and traditional DBD. Comparisons are then made between the different design methods.

Chapter 10: Presents experimental testing on alternative dissipative devices including cheaper axial dissipaters and lead extrusion dampers.

SECTION ONE – THE PLASTIC HINGE

Chapter 2: Literature Review

This chapter provides an overview of the most recent literature related to plastic hinges. In particular, designing the longitudinal reinforcement of plastic hinges against buckling, which is required to ensure plastic hinges can meet the ductility requirements outlined in current codes such as NZS 3101:2006 and the New Zealand Transport Agency Bridge Manual (2018). Additionally, recent literature on assessing the residual capacity of plastic hinges is reviewed.

2.1 PREVENTING BUCKLING OF LONGITUDINAL REINFORCEMENT

The Kaikōura Earthquake caused damage to a number of plastic hinges (Palermo et al., 2017; Wood & McHaffie, 2020). The plastic hinge damage typically included, high strain in reinforcement, crushing and spalling of concrete, flexural cracking, buckling of reinforcement (that ultimately led to fracture of reinforcement in one case) and residual drifts. Most of this damage is repairable provided plastic strains in the steel are low enough that they can survive future seismic events (Cuevas & Pampanin, 2017). However, buckling is critical as it engenders low cycle fatigue and leads to premature fracture of reinforcement (Priestley et al., 2007).

The current requirements for anti-buckling are stipulated in the concrete standard (NZS 3101, 2006). This standard both limits the maximum spacing of lateral ties and ensures that there are enough ties to overcome the buckling tendency of the main bars at the tie location. However, these recommendations where developed based on experience and intuition without any strong quantitative research. International guidelines note the importance of transverse reinforcement, though typically these are not considered individually. For example, American Standards (AASHTO, 2017) provide explicit criteria for the confinement and assume this is sufficient to prevent buckling. The buckling of longitudinal reinforcement has been studied in the past Dhakal (2005) proposed that the max spacing of the lateral ties be determined using equation 2.1.

$$S_{\max} \leq \lambda_{bmax} \frac{d_b}{\sqrt{\frac{fy}{100}}} \qquad 2\text{-}1$$

Where λ_b is a buckling parameter defined as:

$$\lambda_b = \frac{L}{d_b}\sqrt{\frac{f_y}{100}} \qquad 2\text{-}2$$

λ_{bmax} is based on the maximum allowable drop in compression stress from an element. At the time, derivation was made for a maximum drop in stress of 10%. This was further developed by Dhakal & Su (2018) for full and limited ductility and a drop in compressive strength of 15%. Where the maximum spacings are shown in equation 2-3 and 2-4.

For full ductility: $$S_{\max} \leq 14 \frac{d_b}{\sqrt{\frac{fy}{100}}} \qquad 2\text{-}3$$

For limited ductility; $$S_{\max} \leq 18 \frac{d_b}{\sqrt{\frac{fy}{100}}} \qquad 2\text{-}4$$

For Grade 300E reinforcement this results in a spacing of $8d_b$. This is larger than the current spacing of $6d_b$ outlined in NZS3101:2006. Several other attempts have been made (Bresler & Gilbert, 1961; Dhakal, 2005; Dutta & Mander, 1998; Pantazopoulou, 1998; Scribner, 1986) to allow the design of longitudinal reinforcement against buckling. However, these studies make various assumption with varying results and recommendations. Dhakal & Su (2018) have proposed a design strategy to prevent against buckling. This strategy is based on theoretical derivation and experimental verification (over 100 tests) with good agreement. In addition, it has been developed specifically for application to the New Zealand Concrete Standards (NZS 3101, 2006). Therefore, this procedure will be examined to determine whether this may have resulted in improved plastic hinge performance. The proposed design procedure is outlined below:

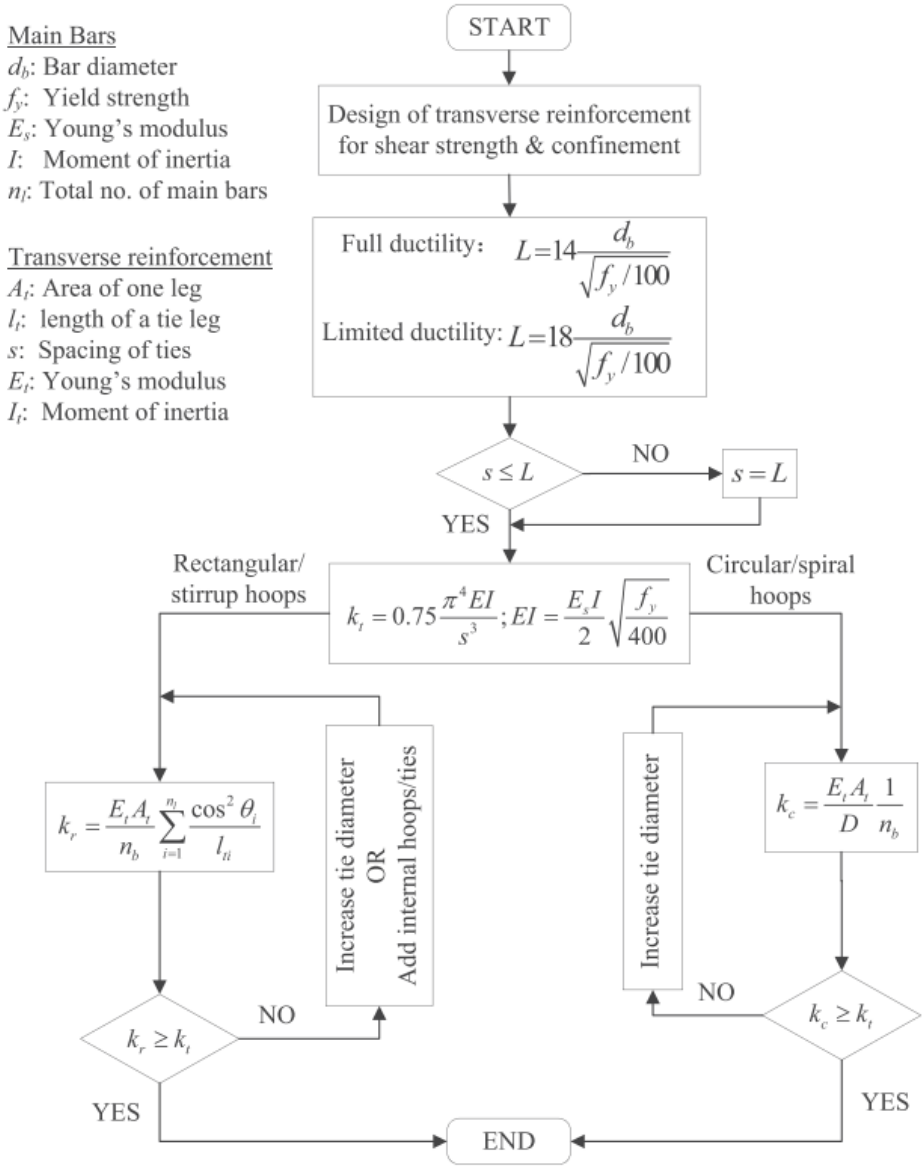

Figure 2-1: Design procedure for preventing anti-buckling, retrieved from (Rajesh Prasad Dhakal & Su, 2018).

This design procedure was verified by significant experimental and numerical research. While the research within this thesis does not intend to develop these equations, it does aim to investigate whether this procedure would have resulted in more conservative anti-buckling requirements and whether these would have improved the performance of the plastic hinges damaged in the Kaikōura Earthquake.

2.2 RESIDUAL CAPACITY – PLASTIC HINGE

To date there is very little (likely none) codified assistance or guidance relating to the estimation of the residual capacity of a plastic hinge, particularly pertaining to the fatigue life. However, (Cuevas & Pampanin, 2014) recently proposed a method for

estimating the residual capacity of a plastic hinge, which includes the following key steps:

1. Use displacement-based design to estimate the design displacements.
2. Estimate the equivalent number of cycles the structure experienced using equivalent design code cycles (Mander & Rodgers, 2013).
3. Determine number of cycles until failure.
4. Estimate remaining fatigue life based on number of cycles experienced and total cycles until failure.

This process was developed for incorporation into the displacement-based design framework and is intended for simplified analysis. As such simplifications in the process such as the use of equivalent code cycles limit the accuracy of the method. The residual cyclic capacity doesn't account for the specific response in question and the peak strains rely on the accuracy of the design methods. In addition, it cannot directly account for strain ageing affects.

Strain ageing is a phenomenon many carbon steels exhibit after being subjected to plastic strains. The effects are time and temperature dependent and result in significant changes to the strain dependant change in mechanical properties. Strain ageing encompasses three different process: strain hardening, strain ageing and strain embrittlement (Erasmus & Pussegoda, 1977). Consider the case where steel with a strain-ageing tendency is strained in tension beyond its yield up to stress A (Figure 2-2). When the steel is then unloaded and reloaded immediately, the steel will exhibit plastic behaviour back to stress A, and then strain hardening will occur as if the test had not stopped. However, if the specimen was unloaded, aged and reloaded, the yield point appears at a higher stress (point B); this is strain ageing. In addition, the ultimate tensile strength is higher, and ductility is reduced. Strain ageing also causes an increase in transition temperature – strain-ageing embrittlement (Erasmus & Pussegoda, 1977). Therefore, this effect must be considered when trying to assess the residual capacity of a plastic hinge as the ultimate strain capacity and hence displacement capacity reduces.

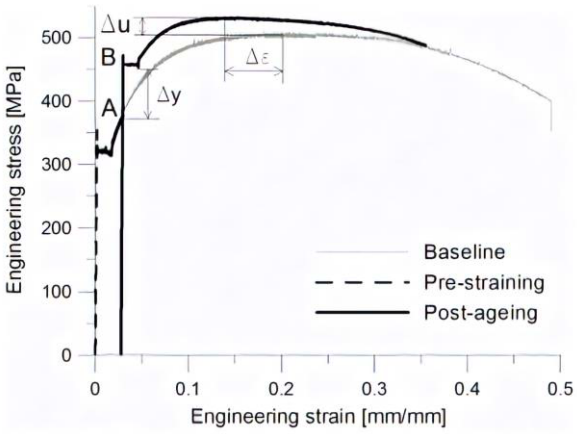

Figure 2-2: Shows the strain ageing affect on G300E reinforcement retrieved from (Loporcaro, 2017)

Strain ageing effects, though well understood, have previously been difficult to predict accurately. However, the development of material testing techniques and artificial ageing techniques have been significant in the past decade. One benefit of this testing is the ability to predict the effect of strain ageing and plastic strain in reinforcement thus aiding the determination of remaining capacity.

The main two testing methods test the hardness by physically indenting the metallic material of interest. Leeb hardness testing (Kompatscher, 2004) is a non-destructive test method which uses the increased hardness of the steel to estimate plastic strain. This test method has been used for the assessment of eccentrically braced frames (Nashid, Ferguson and Clifton et al., 2014) and for the assessment of reinforcement in earthquake damaged buildings (Allington, 2011). One key advantage of the Leeb hardness test is that it is non-destructive, and testing can be carried out in-situ. However, the method has some drawbacks; there are no published relationships between hardness, plastic strain and remaining ductility with adequate accuracy for reliable damage assessment. In addition, strain ageing is not accounted for in these methods and the boundary restraint of reinforcement can affect the results of the hardness testing (Loporcaro, Pampanin and Kral, 2018). Vickers hardness testing is an alternative hardness test which is more intrusive, requiring the removal of damaged bars. This allows the error associated with fixity of the bars to be minimised. In addition, the relationships between hardness, plastic strain, strain ageing and residual strain capacity are well defined with acceptable levels of error (Loporcaro et al., 2018).

Given the material testing techniques can help determine properties of the bar and residual plastic strain, the only remaining variable is the low cycle fatigue life.

Fracture of longitudinal reinforcement due to low-cycle fatigue is one of the most common failure modes that can occur in flexural members during an earthquake, especially for structures located in regions with high seismicity. Therefore, the ability to characterise this behaviour is critical for understanding how a plastic hinge will behave and how much fatigue capacity remains in the reinforcement.

Low cycle fatigue is most prominent when between 1 and 5 fully reversed cycles of large strains up to or larger than 6% may be expected (Mander, Panthaki and Kasalanati, 1994). Mander utilised the Coffin-Manson (Coffin, 1954; Manson, 1953) fatigue life relationship and concluded that a single equation based on plastic strain (εp), and number of cycles (Nf), could be developed and applied to all reinforcing steels:

$$\varepsilon p = 0.08(Nf)^{-0.5}$$

Kunnath, El-Bahy and Stone (1997) found that the model proposed by Mander and Cheng (1994) under-predicted the final damage state of all their column specimens. In particular, they found that the model was capable of predicting low-cycle fatigue of longitudinal reinforcement only, however confinement failure prior to low cycle fatigue could not be captured. They proposed a more conservative equation:

$$\varepsilon p = 0.065(Nf)^{-0.436}$$

These experimental studies indicated that the fatigue life might be influenced by bar diameter. Kunnath, Kanvinde and Xiao et al (2009) carried out further low cycle fatigue testing on #11 and #14 bars which correspond to a 36 and 43mm diameter rebar respectively. The resulting fatigue equation was proposed:

$$\varepsilon p = 0.071(Nf)^{-0.493}$$

This was further refined for smaller diameter bars by (Kunnath, Kanvinde and Xiao et al, 2009) and is likely to be slightly conservative for G300 reinforcement typically used with New Zealand.

$$\varepsilon p = 0.068(Nf)^{-0.5}$$

The Palmgren-Miner rule was developed to allow the estimation of fatigue due to many cycles (Miner, 1945). The rule allows the calculation of cumulative damage, when the damage index exceeds 1 fracture is likely.

$$D = \Sigma \frac{N_i}{N_{fi}}$$

Where D is the cumulative damage, $N_i$is the number of strain cycles at a given strain, and N_{fi} is the number of cycles until failure at the given strain.

2.3 PLASTIC HINGE REPAIR

Capacity design, as it currently stands, allows the formation of a plastic hinge, which allows a reduction in design forces. However, it is well understood that when plastic hinges form the residual capacity is limited and repair is necessary to ensure adequate performance in future seismic events. Repair strategies for severely damaged bridge columns have been experimentally tested in the past. These strategies include, repairing the plastic hinge regions by adding new longitudinal reinforcement, jacketing of the damaged region to force plastic hinging to form elsewhere and jacketing of the region to enable re-development of a plastic hinge. Experimental testing of these strategies by Lawrance and Jacks (1990), Lehman, Gookin and Nacamuli et al (2001), Rutledge, Kowalsky and Seracino et al (2014), have shown that these repairs are effective and restore the hinges to the original design levels. Cuevas & Pampanin (2014) investigated the use of a commercial epoxy to repair plastic hinges damaged in the 2011 Christchurch earthquakes. The cracks were up to 1mm wide. The repair strategy allowed some distribution of damage outside the repaired area, had similar energy dissipation to the original joint and resulted in a reduced secant stiffness that wasn't significant at ULS levels.

2.4 CAPACITY SPECTRUM METHOD

The Capacity Spectrum Method (CSM) was developed as a rapid evaluation method for a pilot seismic risk project of the Puget Sound Naval Shipyard for the U.S. Navy (Freeman et al., 1975). It was later used as a procedure to correlate earthquake ground motions with the observed building performance. The CSM takes a graphical representation of the global force-displacement capacity curve of the structure and compares it to the response spectrum representation of the earthquake demands. The global force-displacement or capacity curve is achieved through a static pushover, and the demand curve is represented by the earthquake response spectra. If the capacity curve intercepts the envelope of the demand curve, the building survives the earthquake. The intersection of the capacity curve and appropriately damped demand

curve represents the inelastic displacement of the structure (Freeman, 2004). The alternative to this method is DDBD (Priestley et al., 2007), which is essentially a reverse process of the CSM. Target displacements and ductility ratios are selected to determine the required period, damping and hence required capacity. However, the CSM provides a graphical representation, which allows engineers to easily understand the relationship between the demand and the capacity, allowing the optimisation of any given design.

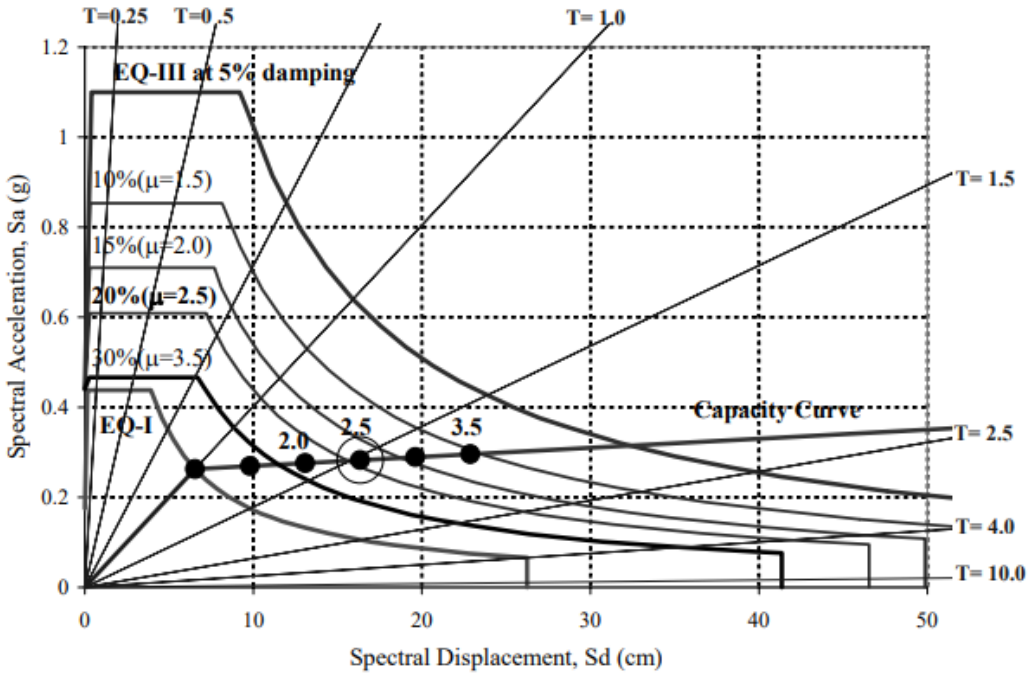

Figure 2-3: Capacity Spectrum Method (Freeman, 2004)

Chapter 3: Performance of Bridge Structures Damaged in the Kaikōura Earthquake

3.1 INTRODUCTION

The magnitude 7.8 Kaikōura earthquake that occurred on the 14th November 2016 had an epicentre 17km north–east of Culverden and 62km south-west of Kaikōura. The earthquake lasted for almost two minutes and occurred along multiple fault lines causing widespread damage (Figure 3-1). The main fault ruptures and strong levels of shaking were located on the north-east coast of the South Island causing major damage to critical road and rail transportation networks (Stringer et al., 2017)

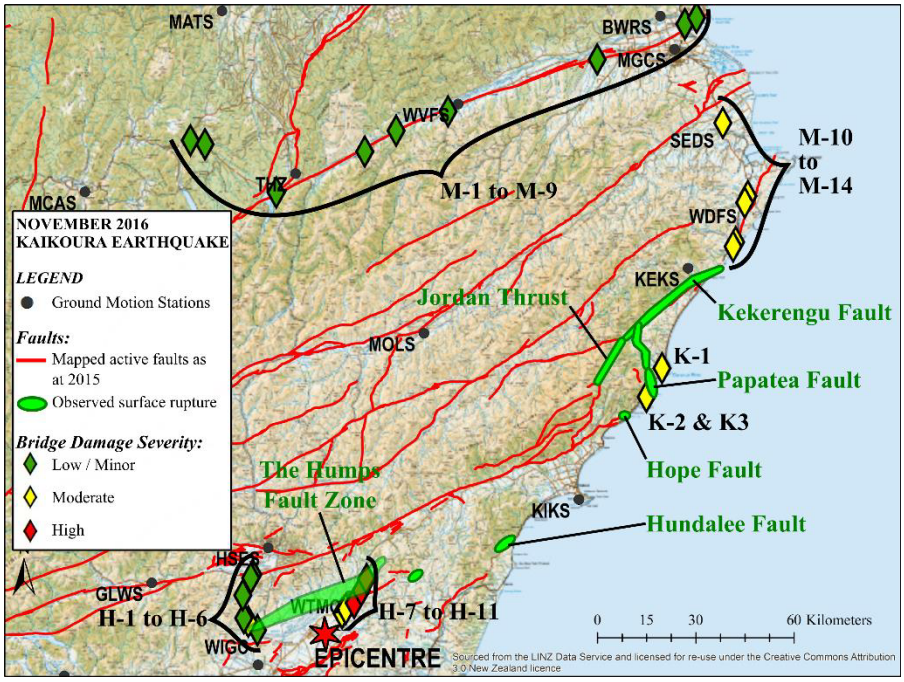

Figure 3-1: Map of inspected bridges with surface fault rupture observations (Palermo et al., 2017)

Over 300 bridge structures were inspected following the earthquake. Of these, 21 suffered significant damage, 11 suffered moderate damage and three suffered major damage including two structures that were near collapse (Figure 3-2 and Figure 3-3).

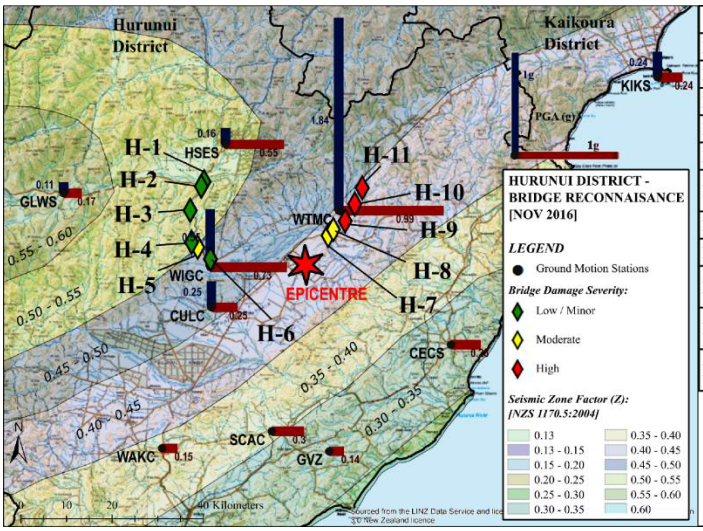

ID	Bridge Name	Route
H1	Hanmer River Bridge	SH7A
H2	Waiau Ferry Bridge	SH7A
H3	Glenallan Stream Bridge	SH7
H4	Brown Stream Bridge	SH7
H5	Stinking Stream Bridge	SH7
H6	Leslie Road Bridge	Leslie Hills Road
H7	Waiau River Bridge	SH70
H8	River Road Bridge	River Road
H9	Lower Mason Bridge	Inland Road
H10	Lottery River Bridge	Inland Road
H11	Wandle River Bridge	Inland Road

Figure 3-2: Location of damaged bridge structures in the Hurunui District and maximum recorded PGA (Palermo et al., 2017).

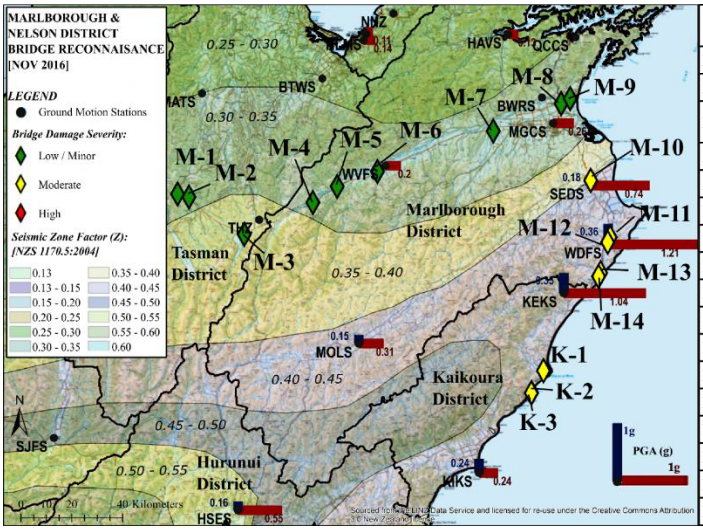

ID	Bridge Name	Route
M1	Hope River Bridge	SH63
M2	Buller River Bridge	SH63
M3	Black Valley Stream Bridge	SH63
M4	Wairau River Bridge	SH63
M5	Branch River Bridge	SH63
M6	Wye River Bridge	SH63
M7	Waihopai River Bridge	SH63
M8	Ferry Road Bridge	Ferry Road
M9	Neal Road Bridge	Neal Road
M10	Awatere River Bridge	SH1
M11	Flaxbourne River Bridge	SH1
M12	Needles Creek Bridge	SH1
M13	Waima River Bridge	SH1
M14	Waima Overbridge	SH1
K1	Clarence River Bridge	SH1
K2	Mororimu Overbridge	SH1
K3	Mororimu Stream Bridge	SH1

Figure 3-3: Location of damaged bridge structures in the Marlborough District and maximum recorded PGA (Palermo et al., 2017).

Of particular interest in the context of this research, are the six bridges that had significant plastic hinge damage. These were River Road Bridge, Lower Mason Bridge, Lottery River Bridge, Wandle River Bridge, Waima River Bridge and the Awatere River Bridge. The structures near the epicentre were all located near strong motion accelerometers, which recorded the ground motions. This presents a unique opportunity as there is little published information on the back analysis of bridges damaged in earthquakes. With the accelerometers providing an input ground motion, observed damage can be compared to predicted damage based on design guidelines. Therefore, these structures can provide insights into the probable reasons for damage and indicate improvements that can be made in design to prevent future damage. In

the following sections of this chapter, the damaged structures previously listed will be investigated and analysed to identify the accuracy of current codes along with the shortfalls of current detailing. Suggestions will then be presented on possible improvements.

3.2 TYPICAL MODELLING APPROACH USED FOR PLASTIC HINGE ASSESSMENT.

The intent of the following case studies is to try and determine the peak displacements of the piers and the expected number of cycles (strain) in the reinforcement. This section discusses the modelling approach used for pushover and NLTH analysis.

3.2.1 Pushover Response

The pushover response of the pier itself was determined using the software Cumbia (Montejo & Kowalsky, 2007). This Matlab script allows the determination of the Moment-Curvature response given the plastic hinge layout. Furthermore, a Force-Displacement response can be obtained based on an assumed plastic hinge length. It uses the confined concrete model proposed by Mander, et al., (1988) and a reinforcing steel model proposed by King & Priestley, (1986). The combination of these models allows the estimation of a plastic hinge's capacity beyond yield (providing buckling does not occur). Buckling onset is predicted by the Moyer & Kowalsky, (2003) and Berry & Eberhard, (2005) models. These models are calibrated to experimental results. The key material inputs for each bridge are tabulated in the subsequent sections. However, the key definitions for the input of the stress strain curves are shown in Table 3-1. Material strength used in the subsequent sections are based on drawings, and have not been calibrated or altered based on material testing.

Table 3-1: Material relation inputs for Cumbia.

End of yield plateau	**Ultimate Strain**	**Ultimate strain**	**Max unconfined conc strain**	**Unconfined concrete strain**	**Elastic Modulus Conc**
esh	esu	esm	espall	eco	Ec
0.008	0.10/0.12	0.10	0.0064	0.002	5000sqrt(f'c)

Figure 3-4 show a typical pushover response obtained from Cumbia for an arbitrary bridge pier. This shows how the Modified Takeda Hysteresis inputs (Figure 3-5) was obtained. K_0 is the initial stiffness and K_1 is the post yielding stiffness. The bilinear factor r is obtained by dividing the post-yielding stiffness K_1, by the initial stiffness K_0.

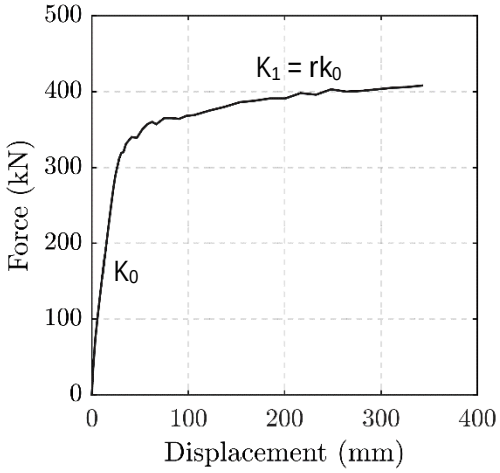

Figure 3-4: Illustration of the k0 and k1 stiffness's.

3.2.2 Non-Linear Time History Analysis

Using the Cumbia outputs (Force - Displacement), Non-linear time history analysis could be carried out, in Ruaumoko (Carr, 2004). A typical layout is shown in Figure 3-5 for a pier with bearings and soil flexibility included. The Moment-Curvature or Force – Displacement response from Cumbia was used to define the Modified Takeda hysteresis rule used to model the plastic hinges. A frame member was used to model the pier, which requires only elastic section properties.

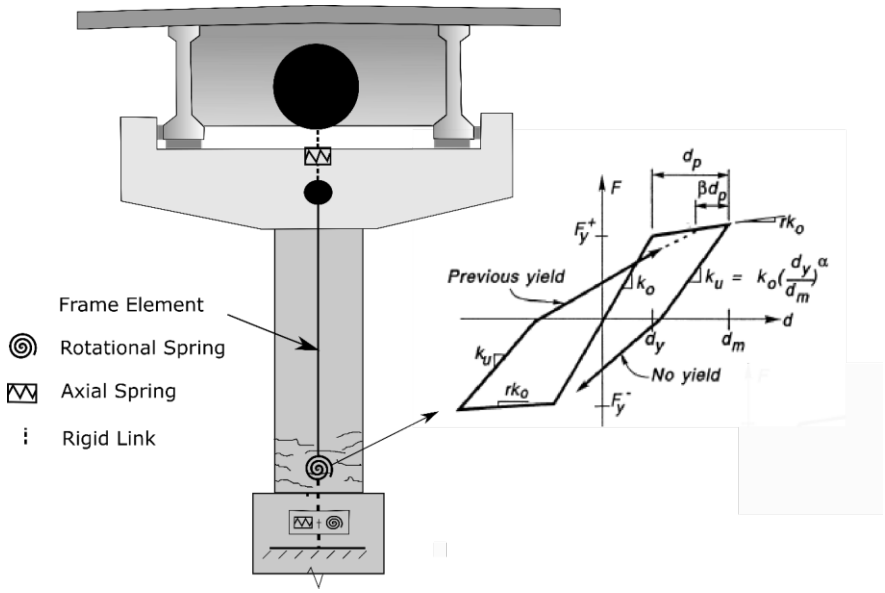

Figure 3-5: Typical SDOF system layout for pier with bearings and soil stiffness included.

Table 3-2: Key parameter inputs for the Modified Takeda Hysteresis Rule.

Ko	β	α	NF
Initial stiffness from pushover curve	k_0/k_1	0.3	1

Penders method (Pender, 1996) was used to estimate the rotational and transverse stiffness at the top of the piles, which were modelled using Multi Linear Elastic Hysteresis rules based on the outputs from analysis. This rule allows the definition of the gradients of each portion of the rule and loads and unloads elastically with no hysteretic behaviour. Bearings were modelled in the same way but used an infinite stiffness at the point the beams contact shear keys transferring the full lateral force into the piers.

3.3 LOWER MASON AND LOTTERY RIVER BRIDGE

The Lower Mason River Bridge and Lottery River Bridge have almost identical designs apart from different pier heights and number of spans. Both structures suffered significant damage including, damage to frangible deck joint details (knock-of details), bearing unseating and plastic hinge damage (Figure 3-6). Of the two structures, it was

the Lower Mason River Bridge which suffered the more severe damage. Therefore, it will be investigated in this section. Given the similar details of the structures, it is not necessary to investigate the Lottery River Bridge separately.

The Lower Mason River Bridge was constructed in 1986. It consists of eight 20.5m spans which combine to give a total bridge length of 164m. The spans are simply supported and consist of two 1.5m deep precast I beams that support a 200mm cast in-situ reinforced concrete deck. The superstructure is supported by 1m wide octagonal piers founded on 1.5m diameter steel encased reinforced concrete piles.

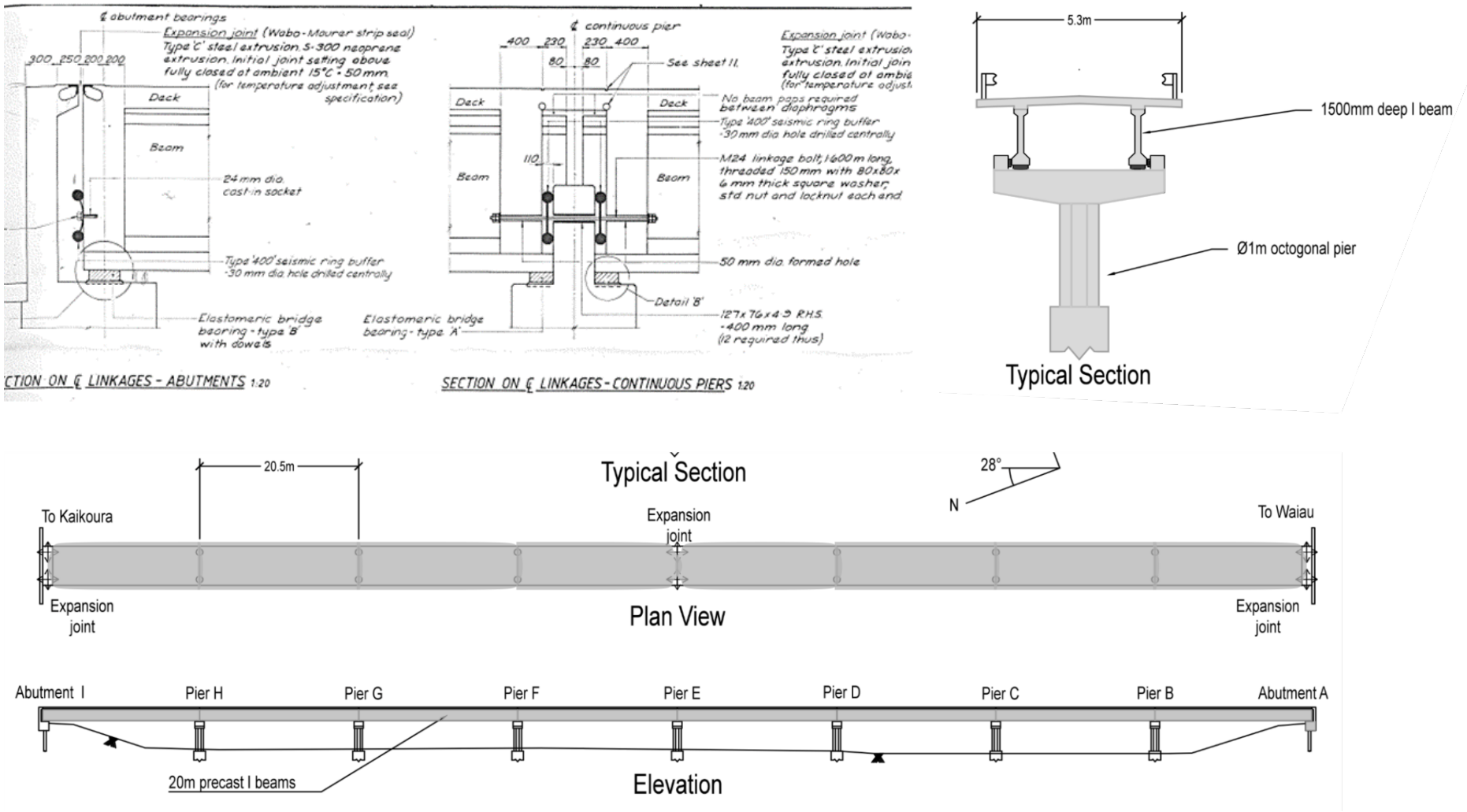

Figure 3-6: Key layout and detail information for the Lower Mason River Bridge.

Figure 3-7: General view of the Lower Mason River Bridge.

3.3.1 Plastic Hinge Performance

Plastic hinges formed at the base of all piers. The level of damage to piers typically increased towards the centre of the bridge. Flexural cracking and spalling was observed on all piers. In addition, longitudinal reinforcement buckled on all piers apart from the central pier (Pier E) which only exhibited severe spalling. Pier E is located at the centre of the bridge below a longitudinal movement joint in the deck. Also, Pier E does not have transverse shear keys restraining the superstructure (Figure 3-7). Therefore, it is likely that the force transferred into this pier was limited to that which the bearing could transfer, reducing force and displacement demands in the transverse direction. The other piers had transverse shear keys which transferred greater lateral loads into the piers at large displacements. This resulted in significant demands and thus damage to the piers. Figure 3-8 shows the damage observed at each pier. As discussed, six of the seven piers had buckled reinforcement and five had fractured reinforcement, evidence of this is illustrated in Figure 3-9. The most severe damage occurred to Pier D which had 9 fractured bars, 7 buckled bars and no undamaged bars. In addition, the core concrete had crushed. Based on typical design strain limits and an assumed ductility of 6 this level of damage was greater than expected.

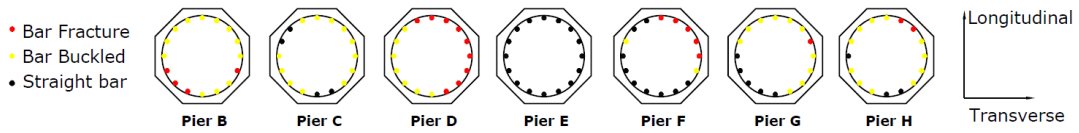

Figure 3-8: Damage to individual reinforcement bars and indicates which piers exhibited the worst damage.

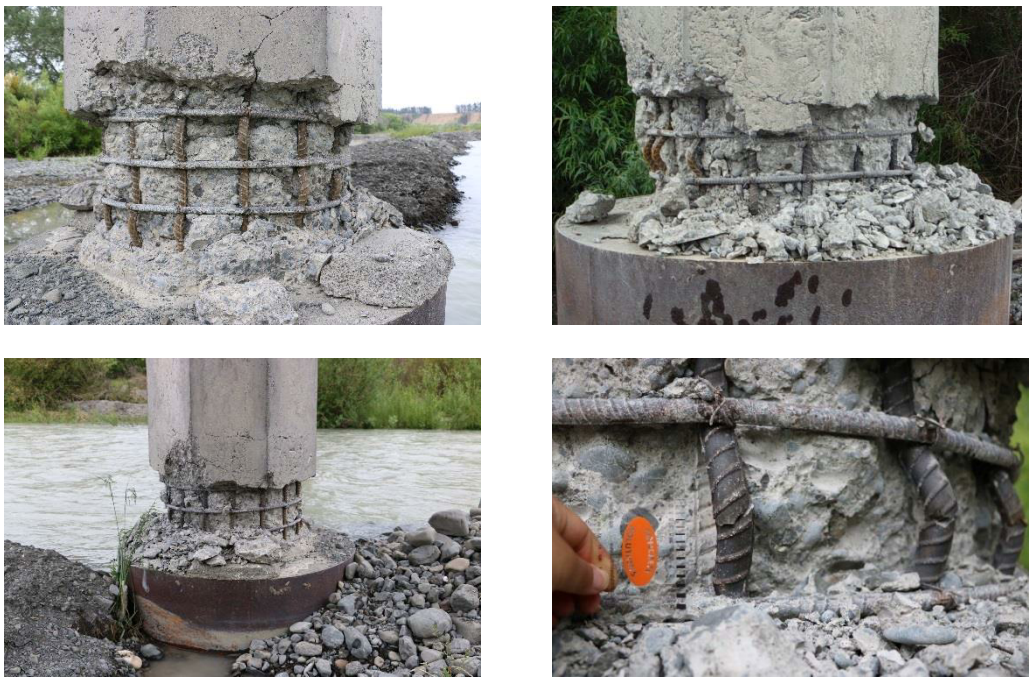

Figure 3-9: Evidence of severe plastic hinge damage including spalling, bar buckling and fracture.

3.3.2 Bridge Analysis

In order to better understand the performance of the bridge and design standards, an analysis to determine the expected displacements as a result of the Kaikōura Earthquake was undertaken. The most severe plastic hinge damage observed was in the transverse direction. The abutments moved inwards, towards the centre of the bridge causing the central movement joint to close, essentially locking up the structure. This would likely result in significant load being transferred to the abutments, reducing the load on the piers in the longitudinal direction. Therefore, analysis was only carried out in the transverse direction and is expected to represent the largest demand on the piers.

As shown in Figure 3-2 the Lower Mason River Bridge was within 2km of the Te Mara Farm (WTMC) strong motion recording station. Though the bridge location and recording station location likely have slightly different soil characteristics, it is

expected that the WTMC recording station will provide a good estimate of the level of shaking experienced by the Lower Mason River Bridge.

The acceleration records from this station were resolved into the longitudinal and transverse components (Figure 3-10). The resolved components were then compared to the spectrum given in NZS1170.5 for a 1/1000 (Z = 0.45, Site Soil D) year annual probability of exceedance event which represents a current bridge design earthquake. Given this was previously a State Highway bridge (Importance Level 2) it is likely this would correspond to a ULS or DCLS event. The comparison shows that the transverse demand is higher than the longitudinal demand which is consistent with the damage patterns observed. Because of the large number of simply supported spans and the lack of transverse restraint at the abutments a SDOF model based on a single pier and tributary mass is expected to give a good indication of the transverse performance.

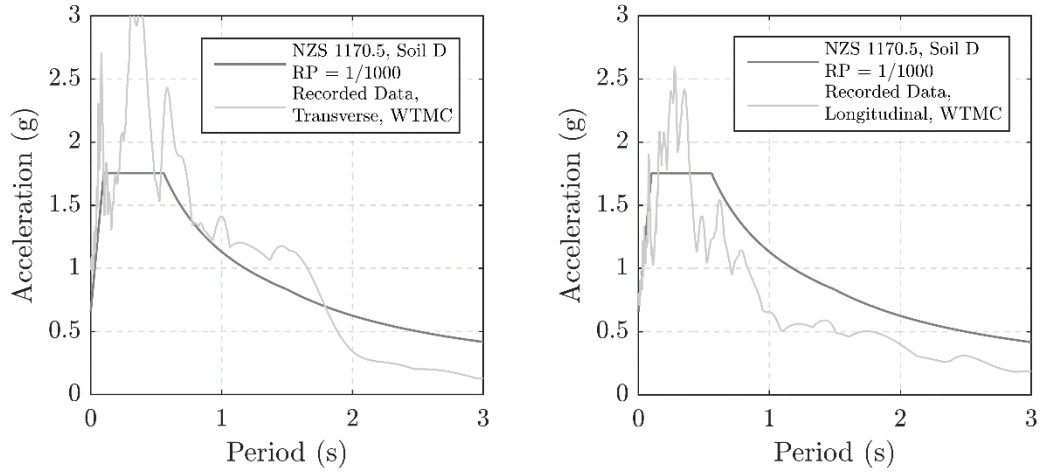

Figure 3-10: 5% Damped acceleration spectra for the transverse and longitudinal directions at the Lower Mason Bridge.

To assess the expected performance of the pier, a moment curvature analysis was carried out using the as built detailing of the plastic hinge. The software Cumbia (Montejo & Kowalsky, 2007) was used to estimate the strains in the reinforcement and concrete and develop a pushover curve for the pier. The Cumbia inputs are shown in Table 3-3. Probable material strengths were used in accordance with the NZ Bridge Manual (NZTA, 2018). The Cumbia software uses concrete stress-strain properties for confined concrete as defined by (Mander, Priestley, & Park, 1988) and steel stress-strain properties defined by (King & Priestley, 1986). Foundation flexibility was estimated using the elastic continuum theory (Pender, 1996).

Table 3-3: Key pier properties and probable strengths used to determine plastic hinge performance.

Lower Mason Column Details	
Diameter	1000 mm
Cover to longitudinal bars	66 mm
Number of longitudinal bars	16
Diameter of longitudinal bars	24 mm
Diameter of transverse steel	16 mm
Spacing of transverse steel	125 mm
Type of Transverse reinforcement	hoops
Axial load (at base of column)	1288 kN
Concrete compressive strength	32.5 MPa
Long steel yielding stress	310 MPa
Long steel max. stress	469 MPa
Transverse steel yielding stress	310 MPa
Member Length	5182 mm

The CSM was used to assess the demands on the structure (Figure 3-11). The capacity curves represent the most severely damaged pier (closest to the central pier). The recorded demand spectrum is obtained from the resolved transverse ground motion recording, multiplied by the damping reduction factor (NZTA, 2016) associated with 15% damping. The pushover curve intercepts the demand curve at approximately 275mm which indicates this was the peak transverse displacement for the pier. However, the pushover curve does not intercept the NZS 1170.5 1/1000 annual probability of exceedance ADRS curve. This is an indication that the pier may have been designed for a lesser earthquake than the 1/1000 annual probability of exceedance previously assumed. This is not surprising given the design spectrum was likely derived using NZS4203:1992, which used risk factors that are typically much lower (ordinary bridge annual probability of exceedance is 1/650 years).

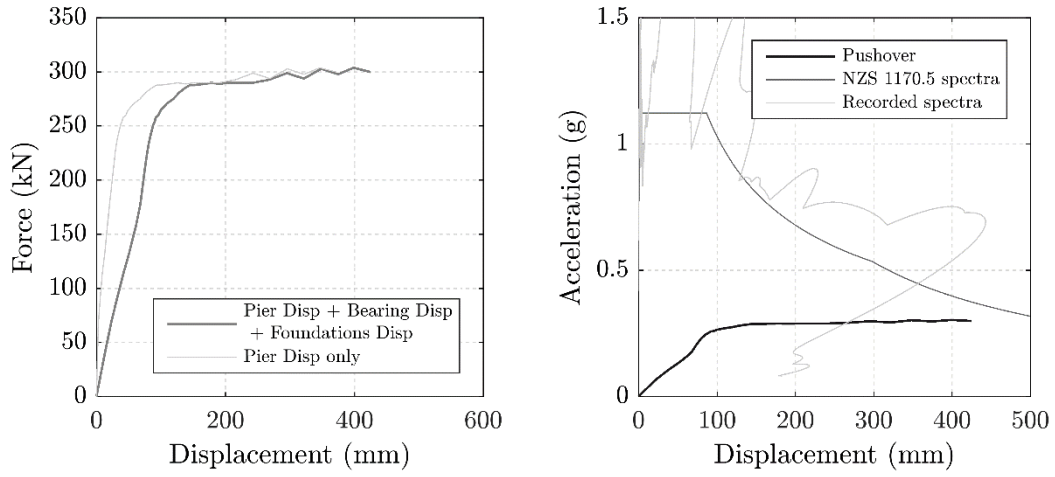

Figure 3-11: Left-Pushover curves, Right- Intercept found using the CSM.

The current strain limit for steel would govern the DCLS displacement if designed to modern standards (NZTA, 2018). With the detailing used in the Lower Mason River Bridge, the maximum allowable displacement at the DCLS would be 190mm (based on the hoop spacing given in the NZTA Bridge Manual, Equation 3-4) which is significantly less than the displacement reached during the Kaikōura Earthquake. A Force Based Design approach would result in an allowable displacement (based on a yield of 45mm and a ductility factor of 4, with no allowance for foundation flexibility or bearings) of approximately 180mm. One area of concern arises with the use of FBD – ductility is not specifically related to the detailing. It is well known that the deformation capacity of a plastic hinge is related to the detailing i.e. having close stirrup spacings etc. NZS3101:2006 and the NZTA Bridge manual are the governing design standards which specify the minimum stirrup spacing to ensure adequate confinement and anti-buckling. Given the plastic hinge detailing meets these minimum requirements, it would appear that these alone are insufficient to ensure the plastic hinge performs in the desired manner. This will be further discussed in Section 3-7.

Based on the Moyer-Kowalsky buckling criteria (Moyer & Kowalsky, 2003), which are criteria defined within Cumbia, buckling would be estimated to occur at a displacement of 215mm. Therefore, although NZS3101:2006 and the current NZTA Bridge Manual allow the stirrup spacing used, buckling would be expected in the ground motions recorded during the Kaikōura Earthquake. This indicates that if using force-based design and modern design codes, plastic hinges could be expected to perform poorly if designed to minimum standards. Displacements at critical performance limits are summarised in Table 3-2.

Table 3-4: Key damage predictors

Performance Limit	Displacement
Yield Displacement (includes bearing and foundation components)	84 mm
Displacement Ductility	4
DCLS Steel Strain Limit Reached	190 mm
Buckling M-K Criterion	215 mm
Buckling B-E Criterion	322 mm

NLTH was carried out using a SDOF lumped plasticity model and a tributary mass approach (Figure 3-5) to check that the damping among other variables were obtained with sufficient accuracy. The NLTH analysis discussed throughout this chapter was all carried out using Ruaumoko (Carr, 2004). The reinforced concrete was modelled using a modified Takeda hysteresis rule and bearings and soil displacements were accommodated using multi linear elastic rules (Carr, 2004) with rotational and axial springs as previously discussed. The shear keys were modelled by giving the axial spring infinite stiffness once they contacted the bearings on the shear keys. P-Delta effects were include in the analysis.

This analysis was only carried out in the transverse direction for reasons discussed previously in this section. The analysis shows that the pushover has predicted the peak displacement relatively well. Again, the displacements reached are well beyond the DCLS and the prediction of buckling onset.

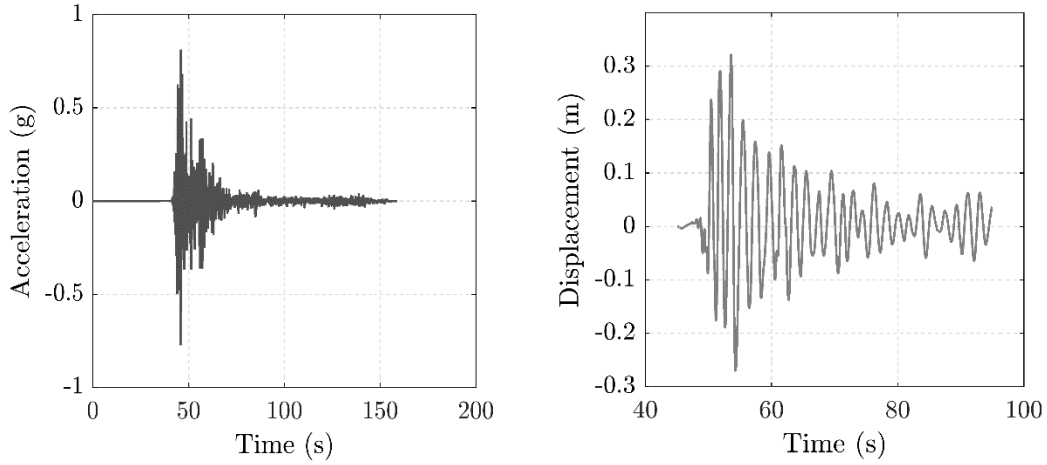

Figure 3-12: Left-Input ground motion for NLTH, Right-Displacement response of SDOF.

The peak displacement computed by the NLTH analysis is 310mm. This correlates to a bar strain of around 7% giving further evidence that the level of shaking was beyond the design level. At this level of strain (assuming only a single monotonic load) bar fracture would not be expected. Though it is likely that fracture would occur after only a few cycles at the high level of strain, the severe nature of the buckling likely contributed to the fractures (very high strains in the curvature resulting from buckling). The buckling was so severe that it is likely that very few strain cycles (low cycle fatigue) contributed to the fracture of bars, which ultimately put the structure in a near collapse scenario (Figure 3-9). In general, there was good agreement between NLTH, the CSM and the observed damage, excluding the buckled/fractured reinforcement. However, the reinforcement damage was the result of a hoop spacing that was too wide rather than inaccurate demands.

3.4 WANDLE RIVER BRIDGE

The Wandle River Bridge was constructed in 1986 and is part of a curved alignment. It consists of two end spans 16.7m in length, a central span 17.6m in length and a total bridge length of 51m (Figure 3-14). The spans are simply supported and consist of five 576mm deep precast double core beams. The superstructure is supported by 1m wide octagonal piers founded on 1.5m diameter steel encased reinforced concrete piles.

Figure 3-13: General view of the Wandle River Bridge

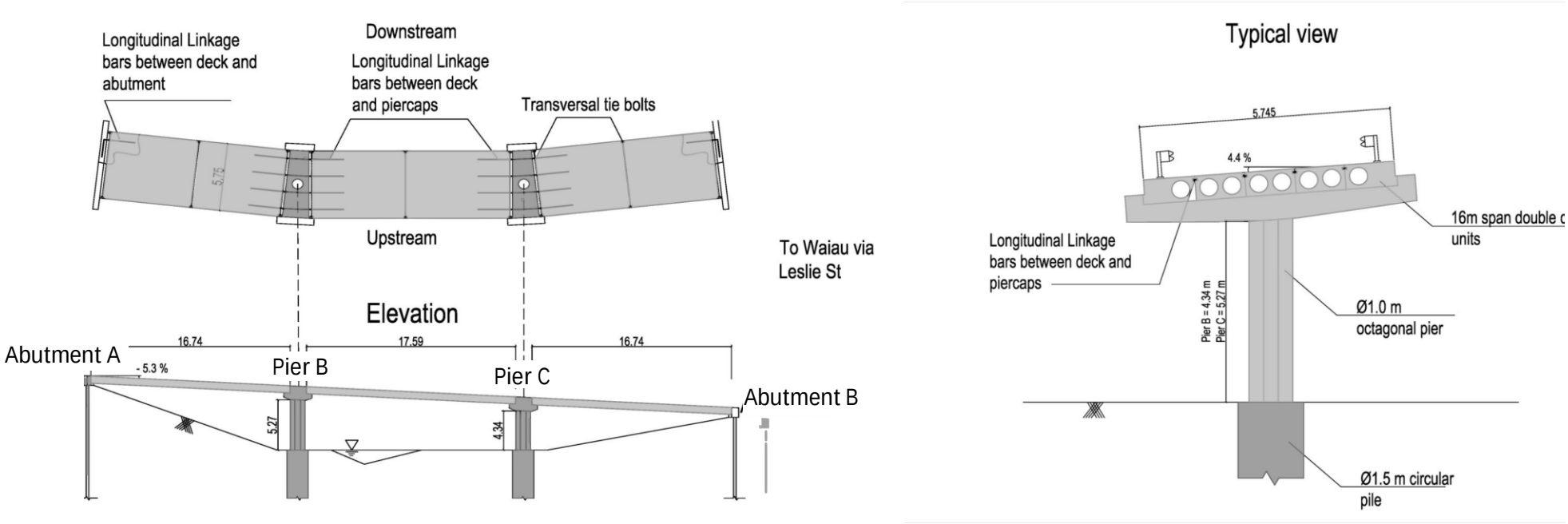

Figure 3-14: Layout of the Wandle River bridge

3.4.1 Plastic Hinge Performance

Plastic hinges formed at the base of both piers. Pier C, the shorter of the two piers, exhibited flexural cracking, spalling, degradation of core concrete and buckling in eight of the 20 longitudinal bars (Figure 3-15). Major flexural cracking and spalling was observed at Pier B (Figure 3-16). For both piers, the riverbed level partially covered the plastic hinge zones and prevented observation of potentially, more severe damage.

Figure 3-15: Bar buckling, and plastic hinge damage observed at Pier B.

Figure 3-16: Flexural cracks and spalling observed at Pier C.

The plastic hinge damage observed, was not as severe as that seen in the Lower Mason River Bridge which had fractured reinforcement. However, the bridge was closed following the earthquake and has since been demolished. The reason for this was the significant residual drifts observed in both piers. Pier B had a residual drift of around 6 and Pier C had a residual drift of around 7%. The residual displacements at the pier tops were around 370mm (Figure 3-17). At the deck level the displacements were in the order of 500mm. Initially, some of this permanent deformation was thought to have occurred as a result of the reasonably shallow piles rotating. However, during demolition of the structure, the piles were vertical indicating that the rotation was fully accommodated by the plastic hinges. Both positive and negative points can be made about this damage. The positive, plastic hinges underwent CALS drift levels (7%) without collapse. The negative, large residual drifts led to loss of functionality.

Figure 3-17: Left – Residual deformation in Pier C, Right – Residual deformation Pier B.

3.4.2 Bridge Analysis

The Wandle River Bridge lies approximately 5km from the WTMC recording station. Although there is likely to be some variability between the shaking at the WTMC recording station and the bridge site, the WTMC records should provide a good indication of the level of shaking at the Wandle River Bridge. The records from the WTMC recording station were resolved into the longitudinal and transverse directions for the structure (Figure 3-18). The spectral acceleration aligns well with a NZ1170.5 1/1000 (Z = 0.45, Site Soil C) annual probability of exceedance event in the transverse direction. The soil class was assumed to be soil class C given the large residual displacement, though it is noted that the soil at the site could potentially be soil class B. Since the structure is simply supported and the demands are lower in the longitudinal direction a simple analysis in only the transverse direction was undertaken.

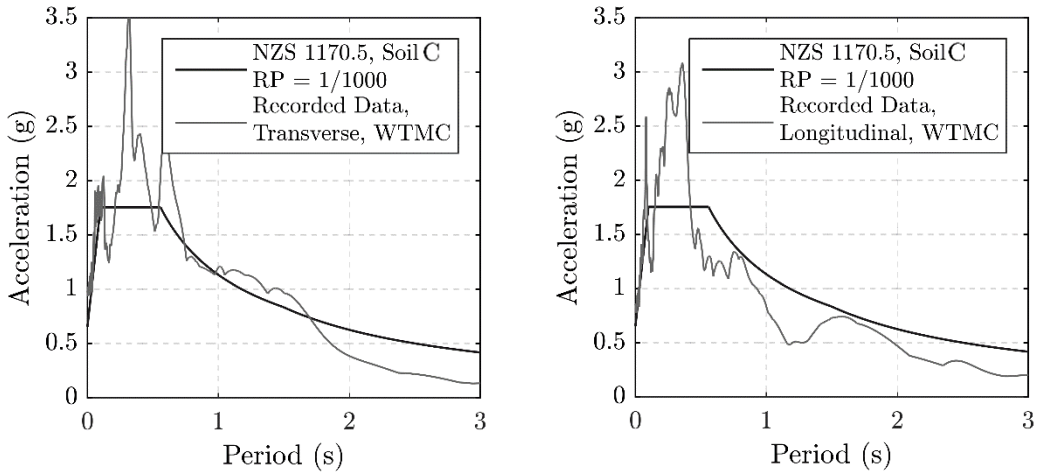

Figure 3-18: 5% Damped acceleration spectra for the transverse and longitudinal directions at the Wandle River Bridge.

The expected performance (pushover curve) for the plastic hinges in piers B and C was estimated using the inputs shown in Table 3-5 which were obtained from design drawings. Foundation flexibility was estimated using Pender (1996).

Table 3-5: Key pier properties and probable strengths used to determine plastic hinge performance

Wandle Column Details	**Pier B**	**Pier C**
Octagonal width	1000 mm	1000mm
Number of longitudinal bars	20	20
Diameter of longitudinal bars	28 mm	28mm
Diameter of transverse steel	16 mm	16 mm
Spacing of transverse steel	120 mm	120 mm
Type of Transverse reinforcement	hoops	hoops
Axial load (at base of column)	1090 kN	1070kN
Concrete compressive strength	32.5 MPa	32.5 MPa
Long steel yielding stress	310 MPa	310 MPa
Transverse steel yielding stress	310 MPa	310 MPa
Member Length – height of CoG of superstructure above top of pile.	6170 mm	5230 mm

The pushover curves that were obtained from the moment curvature analysis and modified to include foundation flexibility are shown in Figure 3-19. The direction of the recorded ground motions was corrected to calculate a spectrum aligned with the transverse direction of the bridge and multiplied by the damping reduction factor (NZTA, 2016) associated with 16% damping. The pushover curve intercepts the damped spectra at 305mm for the most severely damaged pier (Pier C). This is less than the residual displacement of 370mm indicating this analysis does not very accurately capture the demands on the pier.

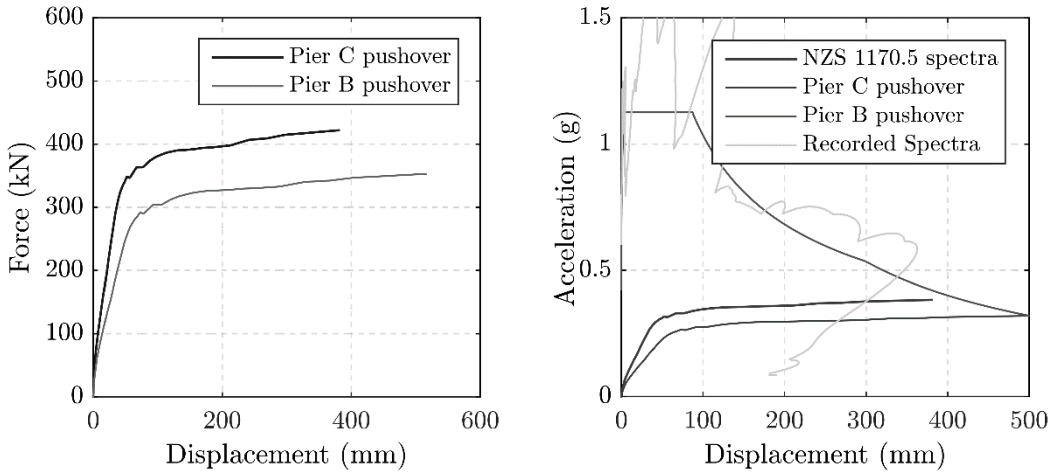

Figure 3-19: Left – Pushover curves for both piers, Right – Demands found using CSM (Soil Class C).

Based on the estimated displacement obtained from the ADRS-pushover analysis the plastic hinge damage expected would be spalling of cover concrete and strains in longitudinal reinforcement of up to 7%. This strain was estimated from Cumbia at the calculated displacement. Buckling of longitudinal reinforcement would not be expected until the CoG displacement reached around 370-400mm. The reason that the reinforcement did buckle is that the actual displacement reached by pier was around 370mm (500mm at the deck level), which is much larger than estimated. At this level of displacement, which the piers must have undergone (at least), buckling would be expected in both piers based the M-K and B-E buckling models (Table 3-6). The CSM has underpredicted demands for this structure.

Table 3-6: Key damage predicters

Performance Limit	**Displacement Reached**	
	Pier B	***Pier C***
Yield displacement	58 mm	45mm
Displacement Ductility (Pier only)	5.3	6.1
DCLS Steel Strain Limit (Bridge Manual)	232mm	181mm
Cover Strain Limit (Bridge Manual)	252mm	212mm
Buckling M-K Criterion	378mm	281mm
Buckling B-E Criterion	405mm	308mm
Calculated EQ Demand Displacement	275mm	305mm
Measured Residual Displacement (at effective height)	375mm	364mm

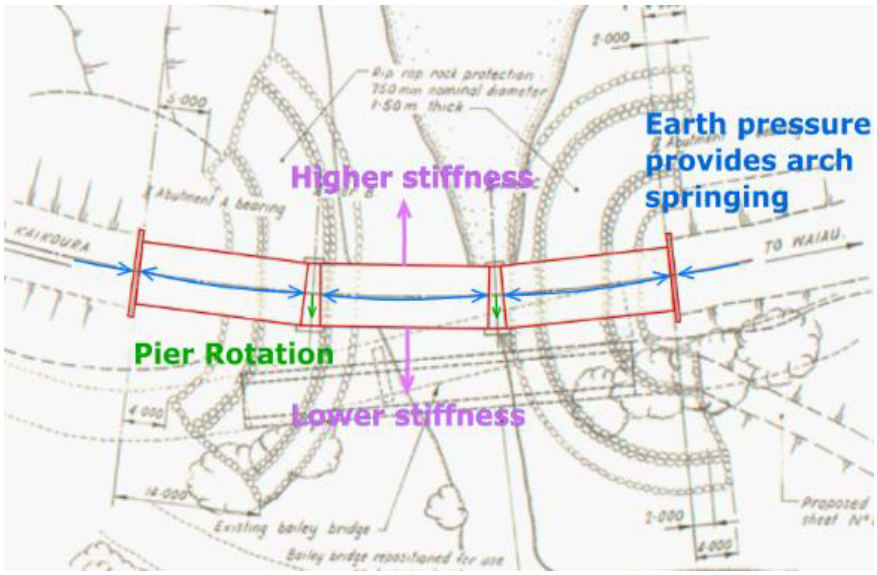

Figure 3-20: Curved horizontal alignment of the Wandle River Bridge.

The inconsistency between the estimated response and measured residual drift could due to:

- The simplified assumption that a SDOF system is sufficient to capture the real response.
- The recorded ground motions being significantly different to those experienced at the given site.

A SDOF model inherently assumes a symmetrical superstructure when in fact the curvature of the deck can contribute to accumulation of displacement in one direction. The interaction of the superstructure with abutments could reduce the level of displacement in one direction and in turn cause larger displacements in the opposite direction (Figure 3-20). Another possibility is that a large initial displacement caused P-Delta effects, significant enough to cause a ratcheting effect. However, this would be observed in a SDOF NLTH analysis. Finally, the difference in the recorded ground motion and input ground motion where significantly different. In order to try and rule out the simplicity of the modelling regime, more complex modelling was undertaken.

Initially, a SDOF model was developed for Pier B (6.17m tall). The same procedure described in Section 3.2 was implemented. The peak displacement recorded was 254mm, very similar to that obtained using the capacity spectrum method. The residual displacement (Figure 3-21) was 91mm, significantly less than that observed at the site. From

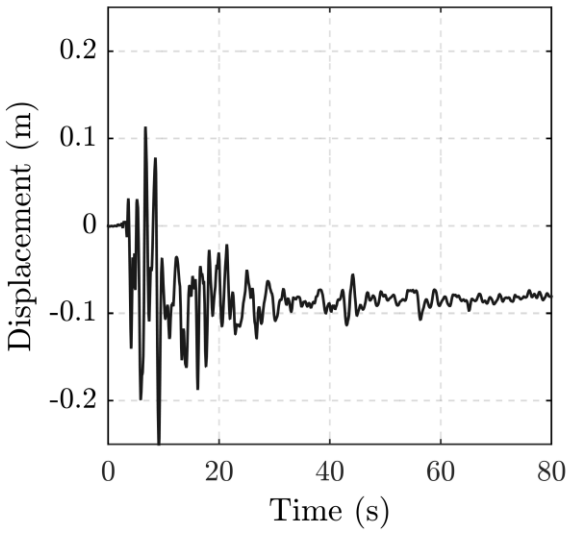

Figure 3-21: Displacement history for Pier B (6.17m tall).

Given the results are still significantly different to those expected a more complex Multi-Degree of Freedom (MDOF) Model was carried out. The horizontal curvature and change in height were included the model. The following assumptions were made:

1. Abutments were assumed to be fixed (though connection to abutment was not).
2. The deck was assumed to act rigidly (all beams have infinite shear strength between them).
3. Input motions at piers and abutments occurred in phase simultaneously.

Assumption one was made on the basis that a fully fixed abutment would lead to a worse ratcheting of displacement in one direction, resulting in larger peak displacements in the negative transverse direction and reduced peak displacement in the positive transverse direction. This is because, due to the geometry of the structure, diagonal compression struts would lock up the structure in the positive transverse direction. Including soil structure interaction would reduce the available forces and thus allow larger displacements in the positive transverse direction and less severe ratcheting. The deck was assumed rigid for the same reason, displacement in the higher stiffness direction (Figure 3-20) will lock up the structure and develop a worse ratcheting toward the lower stiffness direction. The model layout is shown in (Figure 3-23 and Figure 3-23). For each span the five beams are modelled using frame elements. The beams are connected to the pier using contact elements and elastic

springs. The contact elements have infinite compression capacity and have the option to insert a gap, which was set to 3mm for this structure. These elements were used to model the contact of the beams with pier and were critical to ensuring the curvature of the structure resulted in a high stiffness in the positive transverse direction. The bilinear elastic springs, used to represent the bearings, were given stiffness and yield capacities as outlined in the GRANOR Elastomeric Bearing catalogue (GRANOR, 2018) for the tributary width of the bearing. Beams are connected to adjacent beams over piers, and to abutments, using an elastic, tension only spring element with a gap. These springs are not shown in Figure 3-22 below but are located at the midpoint between beam centres (in line with black beam edge lines). There are four linkages at each of the piers. The gap element used, allows the user to define a displacement or gap before the element engages. The stiffness of the spring was defined as the axial stiffness of each linkage bar. Seismic mass was lumped at quarter points along the span (in each beam) with the seismic mass of the pier and headstock lumped at piers.

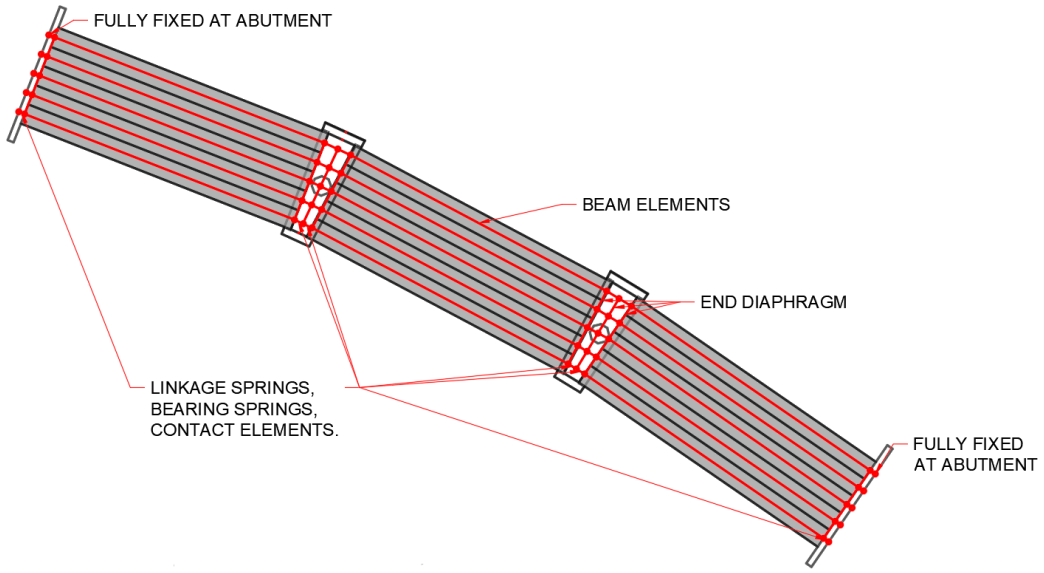

Figure 3-22: Generalise model showing the key elements used for NLTH implementation in Ruaumoko (Carr, 2004)

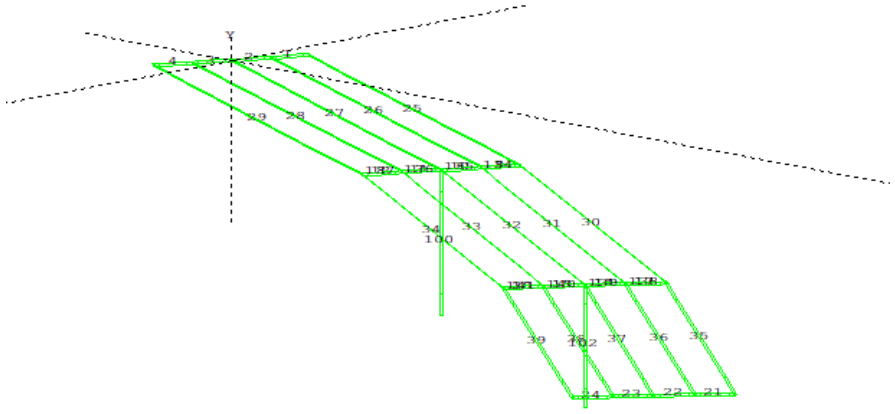

Figure 3-23: MDOF model in Ruaumoko 3D (Carr, 2004)

Both horizontal components of the ground motions were used in the NLTH. Pier B underwent the largest displacement in both the positive and negative transverse direction. In the positive direction (the stiffer direction – inside of the curve) the pier reached a displacement of 111mm while in the negative direction the pier reached a peak displacement of -165mm, significantly less than the 254mm observed from the simplified SDOF. In addition, the residual displacement has halved as a result of including the interaction of the deck.

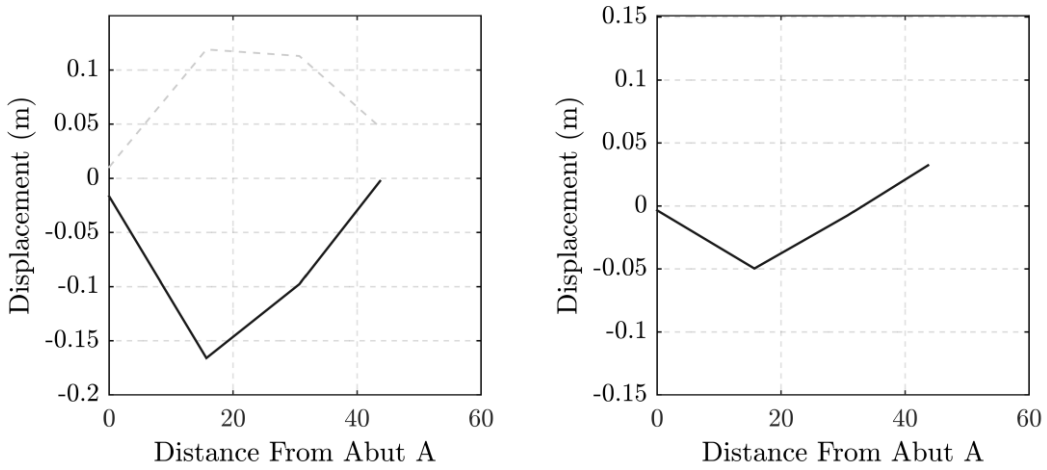

Figure 3-24: Left - Displacement profile/envelope of peak displacements, Right – Residual displacement profile.

Though the displacement history of Pier B has a similar form to that of the model which did not include the interaction of the beams and abutments, its peak displacement, residual drift and fundamental period is significantly reduced. This is not surprising for this short structure since the deck limits displacements and transfers additional load back to the abutments.

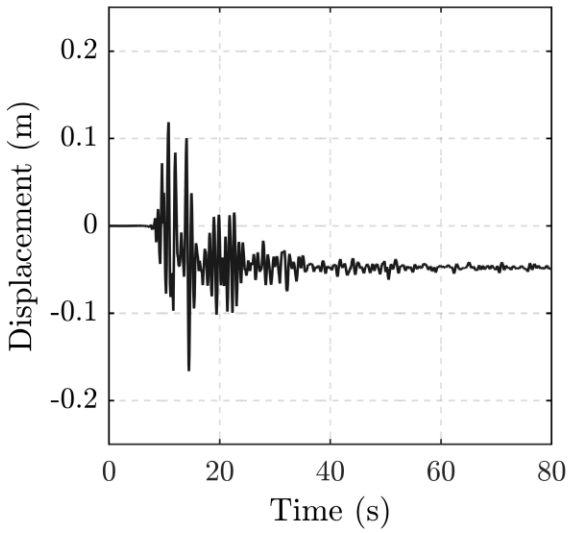

Figure 3-25: Displacement history of Pier B, from MDOF model.

Therefore, this structure, and likely any structure with few spans, can be conservatively modelled as SDOF structures on the basis that considerable demands are transferred to abutments through linkages and compression of deck elements. However, if the outcomes of a SDOF model are unfavourable and result in demolition or costly repairs, a MDOF model should be undertaken to more accurately understand the behaviour of the structure.

3.5 RIVER ROAD BRIDGE

The River Road Bridge is 197m in length with 10 internal spans of 16.2m and two end spans of 16.4m. The structure is 4.6m wide and carries a single lane of traffic. The superstructure consists of five 576mm deep precast pre-stressed concrete double hollow core units. The substructure is made up of 900mm diameter circular single-column hammerhead piers founded on pilecaps supported by six raked UC steel H piles (Figure 3-27). The structure is extensively investigated in the following chapter and therefore only a summary of the damage and analysis is presented here.

Figure 3-26: General view of the River Road Bridge

3.5.1 Plastic Hinge Performance

Plastic hinges formed at the base of all piers, except the pier nearest to the west abutment, with varying levels of damage. All piers had flexural cracks over the bottom half of their height. Ten of the eleven piers had spalling in the transverse direction. The damage generally increased towards the centre of the structure, with piers nearer the abutments having the least damage. This is due to the abutments providing a stiffer support at either end resulting in the typical parabolic type displacement profile. Piers with exposed piles also suffered less damage than piers which had soil surrounding the pile cap (Figure 3-28). This is likely due to the increased flexibility of the pier/piles, which reduces inelastic demands on the plastic hinge.

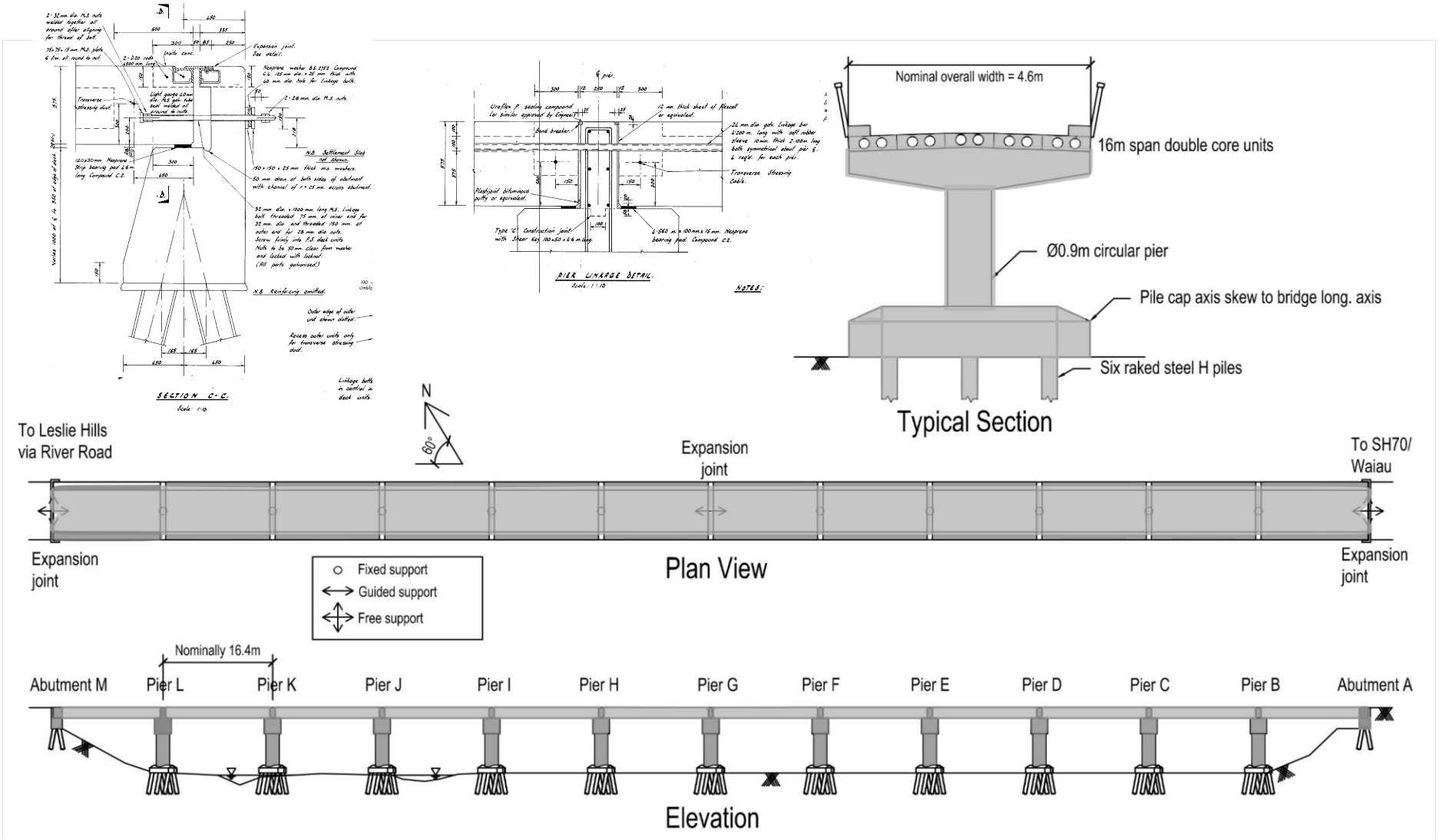

Figure 3-27: Layout of the River Road Bridge

In general, the plastic hinges performed relatively well at the River Road Bridge with damage mostly limited to flexural cracking (yielding of longitudinal reinforcement) and spalling of cover concrete. However, two piers had slightly buckled longitudinal reinforcement. At the locations buckling was observed, the stirrup spacing was larger than specified (due to construction error). More specifically, the measured spiral pitch was up to 120 mm rather than the 75mm specified in design (Figure 3-29).

Figure 3-28: Left – Plastic hinge damage of pier with exposed piles, Right – Plastic hinge damage of pier with soil surrounding pier cap.

Figure 3-29: Left – Typical plastic hinge damage, Right – Onset of buckling at location with 120mm stirrup spacing.

3.5.2 Bridge Analysis

In the longitudinal direction the Kaikōura Earthquake generated demands in excess of a 1/1000 annual probability of exceedance event while in the transverse direction the level of shaking was much less than this and probably in the order of a 1/500 annual probability of exceedance event. The spalling damage was more severe in the transverse direction than the longitudinal. This is likely to be a result of the

longitudinal interaction with abutments that provide additional damping and stiffness, reducing the demand on the piers.

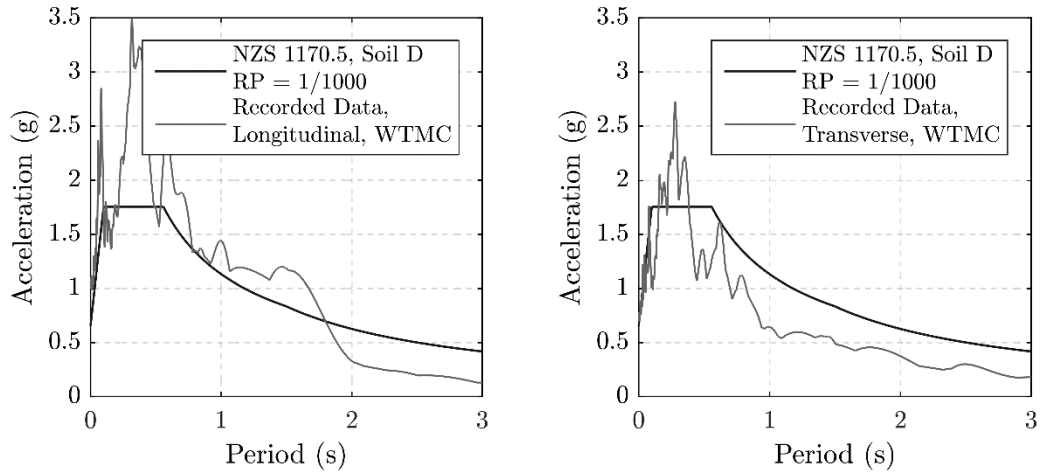

Figure 3-30: 5% Damped acceleration spectra for the transverse and longitudinal directions at the River Road Bridge.

To determine the expected performance (strain in reinforcement and concrete), the moment-curvature software Cumbia was used. The inputs used to generate the pushover or capacity curve are tabulated below. The as-designed stirrup spacing of 75mm was initially used for the analysis as this was representative of most piers.

Table 3-7: Column properties and probable strengths used to determine plastic hinge performance

River Road Column Details	
Diameter	900 mm
Cover to longitudinal bars	66 mm
Number of longitudinal bars	14
Diameter of longitudinal bars	28 mm
Diameter of transverse steel	16 mm
Spacing of transverse steel	75 mm
Type of Transverse reinforcement	hoops
Axial load	908 kN
Concrete compressive strength	32.5 MPa
Long steel yielding stress	310 MPa
Long steel max. stress	469 MPa
Transverse steel yielding stress	310 MPa
Member Length (Height of CoG)	3623 mm

Displacement based design methods (Priestley et al., 2007) were used to determine the demands on the piers. This analysis, shown in Chapter 4, indicated that

the peak displacement at the CoG was 110mm. At this displacement, yielding of longitudinal bars and spalling of cover concrete would be expected. This is very similar to the damage that was observed, though buckling of longitudinal reinforcement was not expected. As previously discussed the spiral pitch was 120mm where the isolated buckling was observed. However, even accounting for this increased spacing buckling is not expected until much larger displacements of around 160mm (Chapter 4). Therefore, a similar outcome to the Lower Mason River Bridge presents itself – current design standards do not prevent the buckling of longitudinal reinforcement (spiral pitch specified in in the NZTA Bridge Manual and NZS3101:2006 is approximately 6 x the longitudinal bar diameter = 168 mm). The CSM was found to accurately predict the demand and damage observed.

Given the type of structure (particularly the pile cap shape), repair of this structure was expected to be difficult and expensive. Therefore, material testing and analysis was used to determine the residual capacity of the plastic hinge (refer to Chapter 4 for more detail).

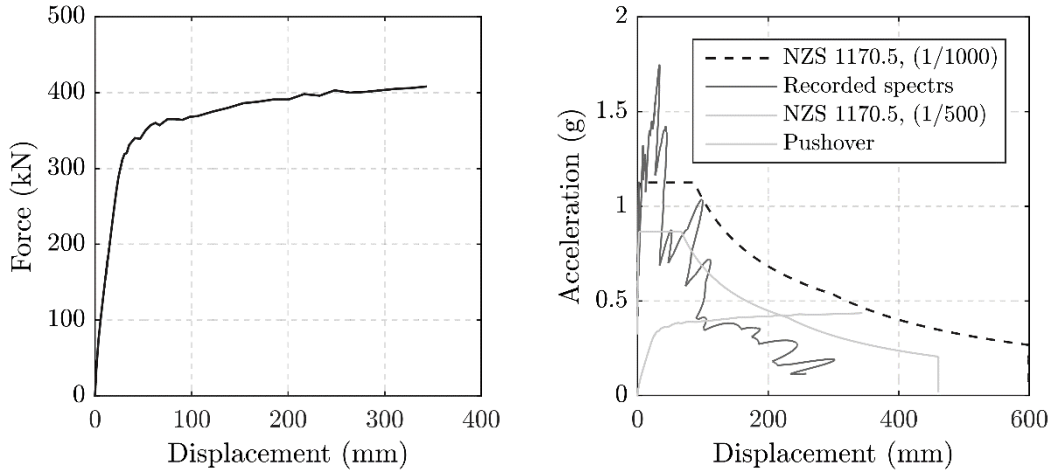

Figure 3-31: Left - Pushover curves, Right - Pushover curve overlaid with damped recorded spectrum.

3.6 AWATERE RIVER BRIDGE

The Awatere River Bridge was designed in 2004 and opened in 2007. It replaced a historic structure that combined both road and rail via a one-way through truss. The historic structure remains as a rail bridge with only the road deck removed. The bridge is made up of eight 27.4m internal spans and two end spans of 27.2m, for a total length of approximately 274m (Figure 3-32). The carriageway width is 10m, consisting of two 3.5m lanes with 1.5m wide shoulders. The superstructure consists of precast pre-

stressed concrete U beams and deck slab units (Figure 3-32). Cast in-situ diaphragms and slab topping provide continuity of the superstructure over the piers. The nine piers are reinforced concrete twin-column portal frames. The 1m diameter reinforced concrete columns are founded on 1.2m drilled piles. The clear distance between the pile and bottom of the cap beam is 5.5m. At the abutments, the superstructure U-beams are seated on elastomeric bearing pads which allow rotation and longitudinal movement. Transverse movement is restricted by concrete shear keys cast integral with the abutment seating beams.

Figure 3-32: General View of the Awatere River Bridge

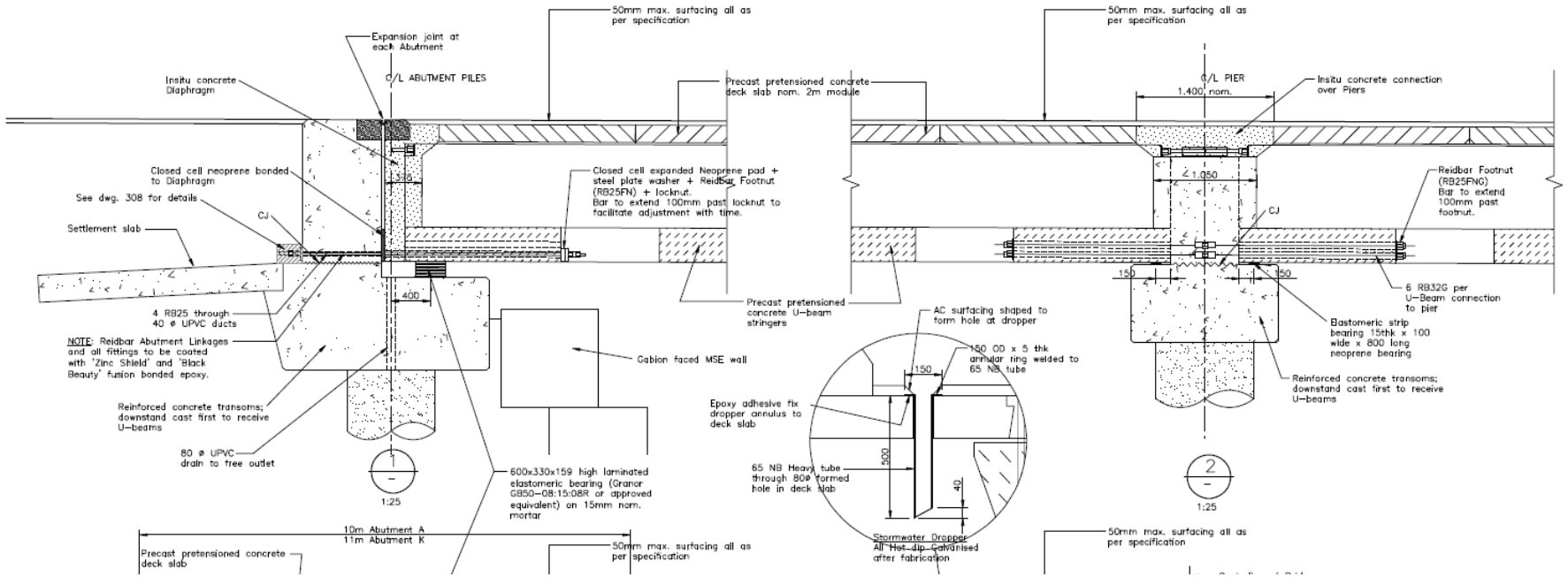

Figure 3-33: Abutment-beam and beam-beam/pier connections.

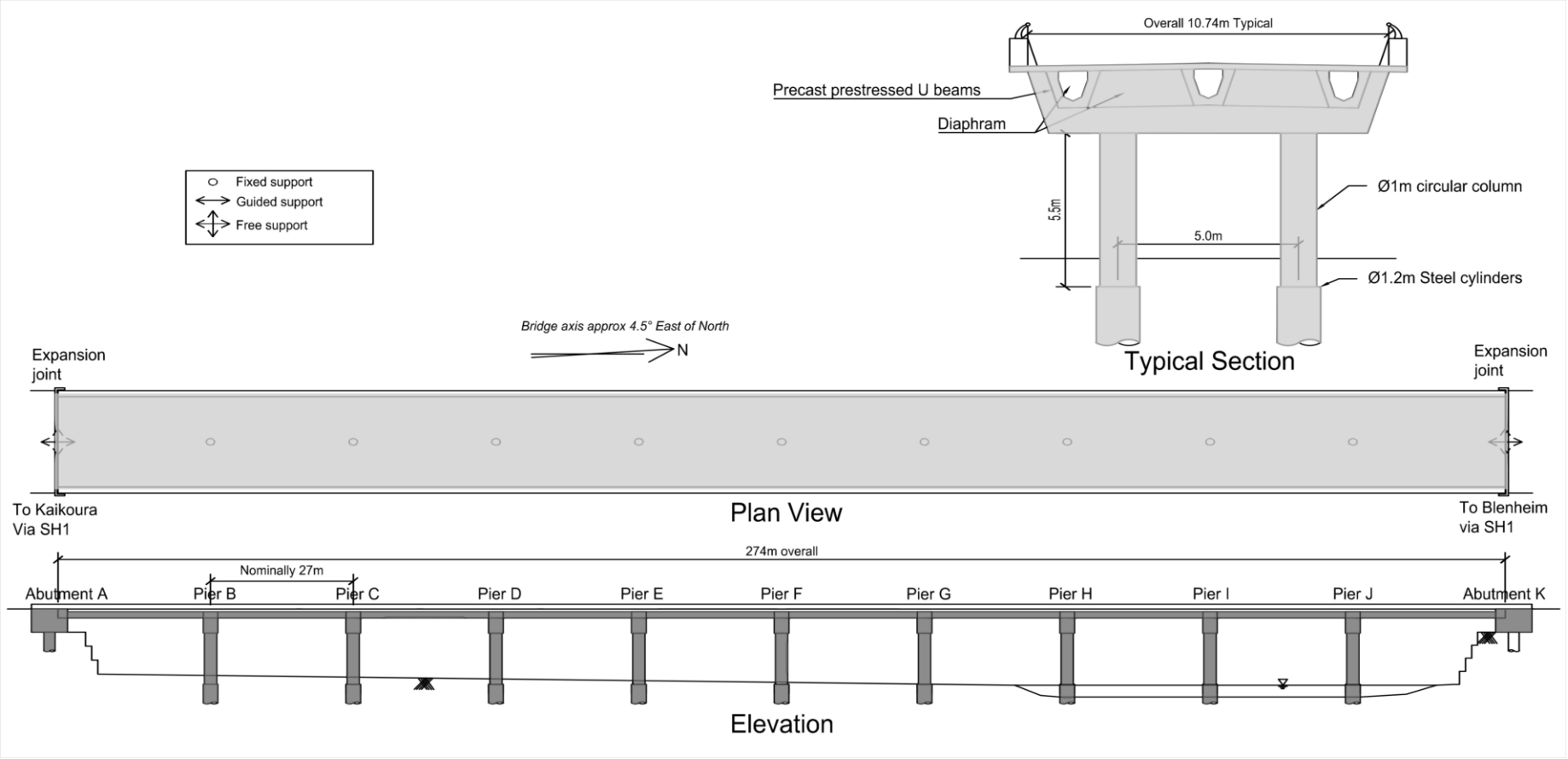

Figure 3-34: Layout of the Awatere River Bridge

3.6.1 Plastic Hinge Performance

The Awatere River Bridge sustained flexural cracking and spalling at the piers. However, the bridge was also subjected to strong ground shaking in the 2013 Seddon earthquake which resulted in column hinging and linkage bar damage (Divers, 2013). Therefore, some of the spalling was attributed to spall repairs undertaken following 2013 Earthquake.

Flexural cracking in the cover concrete, within 1.5m of the top of the pier columns, was observed. Most of the pier columns also had cracking and spalling at their base, just above the top of the pile. Again, it is not clear whether the damage occurred in the 2013 Seddon earthquake or the 2016 Kaikōura Earthquake. However, given the level of shaking and the fact that spalled concrete was laying at the base of the pier appeared to be new, it is likely that the damage developed during the Kaikōura Earthquake.

Figure 3-35: Plastic hinge damage observed at Awatere River Bridge.

3.6.2 Bridge Analysis

The bridge is located 114 km from the epicenter of the Kaikōura Earthquake. The peak horizontal ground acceleration (PGA) recorded in Seddon, at the SEDS strong motion station, 1.5 km south of the bridge, was 0.76g. The SEDS recording station is the closest to the Awatere River Bridge and has been used to estimate the level of damage at the site. As shown in Figure 3-36 below, the Kaikōura earthquake generated shaking intensity similar to a 1/500 annual probability of exceedance event for the structure which has an elastic period in the transverse direction of 0.9 seconds.

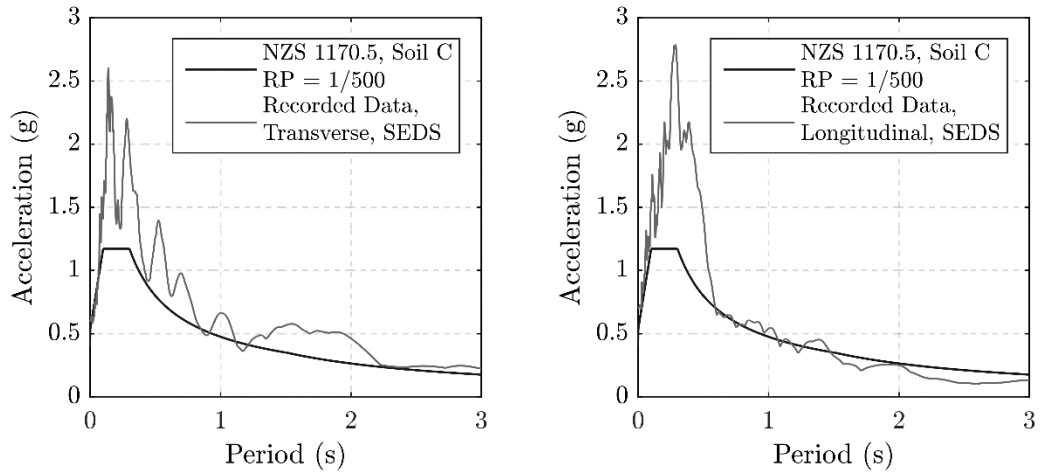

Figure 3-36: 5% Damped acceleration spectra for the transverse and longitudinal directions at the Awatere River Bridge.

To investigate the column damage, a static pushover analysis in the transverse direction of the piers was performed using Cumbia. The tributary mass assumption was used to estimate the transverse response of the central piers. The dynamic weight of 4,100kN was used for the analysis. This included the U beams, topping, pier cap, diaphragm and one third of the column weight. Table 3-6 summarises the inputs used for the analysis of the column and Figure 3-11 shows the pushover response of the top and bottom sections of the pier.

Table 3-8: Properties and probable strengths used to determine the performance of the plastic hinge.

Awatere Column Details	
Diameter	1000 mm
Cover to longitudinal bars	94 mm
Number of longitudinal bars	24 in top, 16 at base
Diameter of longitudinal bars	25 mm
Diameter of transverse steel	20 mm
Spacing of transverse steel	150 mm
Type of Transverse reinforcement	hoops
Axial load at base of column	2050 kN
Concrete compressive strength	52 MPa
Long steel yielding stress	550 MPa
Long steel max. stress	660 MPa
Transverse steel yielding stress	550 MPa
Member Length from top of pile to underside of pier cap	5500 mm

Approximate displacement demands on the piers as a result of the Kaikōura earthquake were obtained using the CSM. Specifically, the recorded spectra were used instead of the design spectra. Recorded accelerations from the Seddon strong motion recording station (SEDS) were used to derive the displacement spectra. This can now be done using accelerometers installed on the bridge; however, at the time of the Kaikōura earthquake these accelerometers were not installed. The ground accelerations recorded by (SEDS) were geometrically rotated to represent the transverse acceleration input at the Awatere River Bridge.

The damped displacement response spectrum is estimated below (Figure 3-37) with 8% damping (calculated in accordance with the Bridge Manual). An estimation of the pushover curve was carried out by assuming no soil structure interaction and ignoring the axial load contribution induced by the portal frame. The height of the structure (for determination of pier properties) was taken as the mid height of the pier. The pushover curve intercepts the demand curve at approximately 90mm. This corresponds to a ductility demand of 2.5 for the top hinge

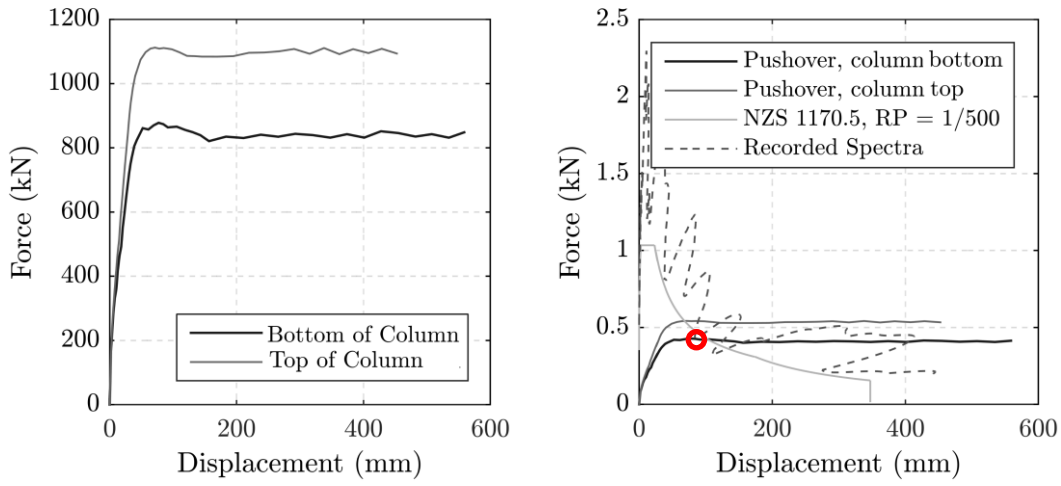

Figure 3-37: Left - Pushover curves, Right - Pushover curve overlaid with damped recorded spectrum.

At 90mm the Cumbia pushover analysis estimates that the pier will have yielded, and some minor spalling is likely. Therefore, the damage observed matches very well with that estimated using simplified analysis. Table 3-9 shows that the plastic hinges are well away from meeting DCLS performance limits.

Table 3-9: Key damage predictors.

Performance Limit	Displacement Reached (mm)
Yield Reached	64
DCLS Steel Strain Limit Reached	284
Buckling M-K Criterion	161
Buckling B-E Criterion	419

To further investigate the performance of the plastic hinges, NLTH analysis was performed. A lumped plasticity model was adopted. The plastic hinge was modelled with a rotational spring using a modified Takeda hysteresis rule with a backbone curve to match that from the Cumbia pushover. The pier cap was given its elastic section properties. Though this is not a perfect way to model the portal frame it is expected to provide a good estimation of the expected response.

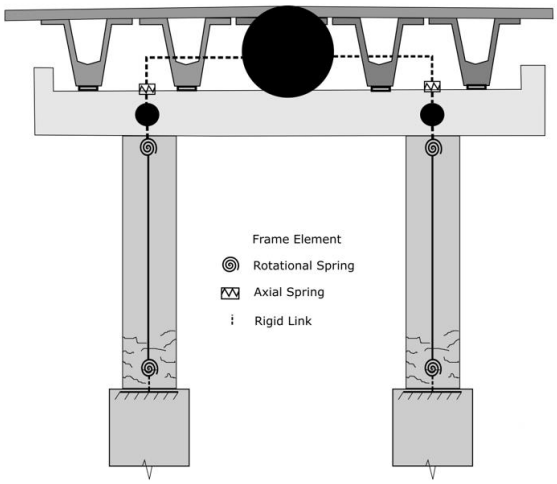

Figure 3-38: Modelling layout used for the Awatere River Bridge

Due to the accelerometers that were added to the structure after the Kaikōura Earthquake, which allow model calibration including the damping ratio, a unique opportunity presented itself. Estimating damping ratios for real structures subject to moderate ground shaking is very difficult and hence there is relatively sparse information on this important topic. Typically, recommended damping ratios are based largely on the few detailed case histories as well as expert judgment. The analysis presented here is somewhat unique in that the structure is monitored by accelerometers

along the span. In addition, the ground motion input is recorded by an accelerometer on the ground at the site (Wood, 2017).

Given the input ground motion and the response of the structure, the model can be calibrated by altering the damping ratio to represent the recorded response of the structure. To date, the recorded ground motions have been relatively small, so information about the performance in strong shaking is currently unavailable. However, the present records verify that the modelling assumptions correctly capture the response of the structure. As shown in Figure 3-39 the model represents the recorded acceleration very well for a damping ratio of 3%. This is in agreement with current practice, where the damping ratio in bridges is typically assumed to be between 3 and 5%. The aftershock motion recorded was particularly small and well below yield of the structure. The input ground motion used was captured by an accelerometer located at the north end of the structure and acceleration comparison was made with an accelerometer located at the middle of the bridge on the super structure.

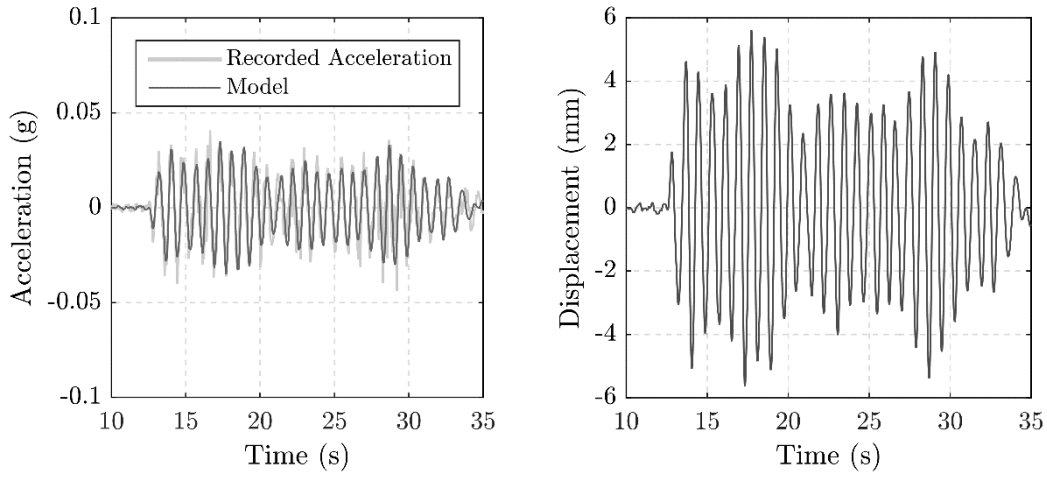

Figure 3-39: left – Comparison between recorded response at centre of bridge and modelled response of central pier. Right – Displacement history of modelled response.

Figure 3-39 shows very good agreement between the calculated and recorded response. The recorded peak acceleration was 0.044g and the models peak acceleration was 0.037g. This indicates that the input motion from the south end of the bridge was representative of the motion at the base of the pier where the superstructure recorder was located. This would indicate that travelling wave effects were probably not very significant. A complete model could be set up and analysed to investigate travelling wave effects. Moreover, it may be possible to estimate the apparent wave speed from the two sets of records measured by the ground instruments. However, the data

recording frequency of 50Hz was too low to allow this; hence, it has been increased to 200Hz and the time lag effect can be investigated in future aftershocks (Wood, 2017).

Knowing the damping ratios for the structure, the SDOF model was subjected to the Kaikōura ground motion recorded by the SEDS accelerometer located in Seddon.

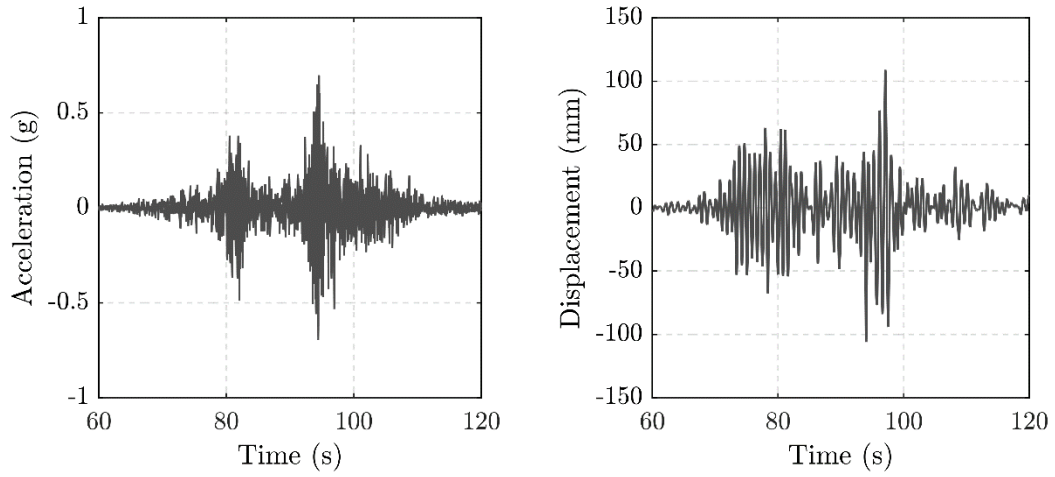

Figure 3-40: Left - Input acceleration history recorded by SEDS accelerometer, Right – Displacement history output from modelled response.

NLTH analysis indicates that the pier has displaced approximately 102mm at the peak response. This corresponds well to the CSM and indicates that simplified procedures accurately predict the demands.

The Awatere River Bridge provides an example of how modern plastic hinges are expected to perform. One of the reasons for this is that the structure is designed in 2006 to modern design standards (NZS 3101, 2006) and with modern construction techniques (though the same minimum hoop spacing requirements of the other bridges apply, so the use of "modern" design standards does not necessarily account for the good performance). Using the current Bridge Manual formula for minimum hoop spacing (Equation 3-5) gives a spacing of 105mm, which is significantly less than the 150mm used in the design (NZS3101:2006 gives a spacing of 150 mm). If the displacement demands had been greater in the earthquake, the bars in the plastic hinge zone would probably have buckled. Therefore, though the performance appears to be better than other piers examined, it is a result of the lower demand rather than the modern detailing (which hasn't changed).

The maximum displacement of the pier was 102mm, which corresponds to a steel strain of 0.02 or 2% (estimated using Cumbia). The steel strain level reached in

the plastic hinges is relatively low given the ultimate strain capacity is usually assumed to be 10% for G500 seismic reinforcement used in the columns. However, this is not the first seismic event the structure has been subjected to and the same repaired cracks appear to be opening, indicating that the strains could be concentrated at these locations rather than spreading uniformly along the length of the plastic hinge.

The DCLS strain for steel is 6%, this is the maximum allowable in accordance with the Bridge Manual based on best case detailing. If the Awatere River Bridge was designed to this standard it would be expected that the bars could reach this strain in a design level event. Knowing that the cyclic strain capacity of the bar is likely to be at least 10%, and possibly more, it is accepted that even with some residual strain this structure would safely survive another design level earthquake. The uncertainty that remains is how the structure will perform in a CALS event now that some fatigue capacity has been utilised.

This results in significant uncertainty associated with the residual displacement capacity of the pier (peak displacement and cyclic life). This uncertainty is further increased due to effects such as low cycle fatigue and strain ageing (for G300 reinforcing, for G500 there are no strain ageing effects). The result is that, either, additional unknown risk must be accepted or intrusive testing of the reinforcement in the plastic hinges must be carried out to determine the level of risk being accepted. If these show the damage to the steel is unacceptable the bridge must be strengthened.

3.7 WAIMA RIVER BRIDGE

The Waima River Bridge was constructed in 1975, it carries two lanes of traffic across the Waima River and is located on State Highway 1, a critical South Island road network. The overall length of the structure is 150m, with eight 18.7m spans. The simply supported spans are made up of four prestressed concrete I beams that are 1220mm deep. The beams support a 180mm deep reinforced concrete deck. The spans are supported by headstocks that are integral with 1.52m diameter reinforced concrete piers. The piers are founded on 1.52m diameter steel encased concrete piles. A seismic retrofit of the structure tied the superstructure in with the piers and abutments. The general arrangement of the structure is shown in Figure 3-41.

Figure 3-41: General View of the Waima River Bridge

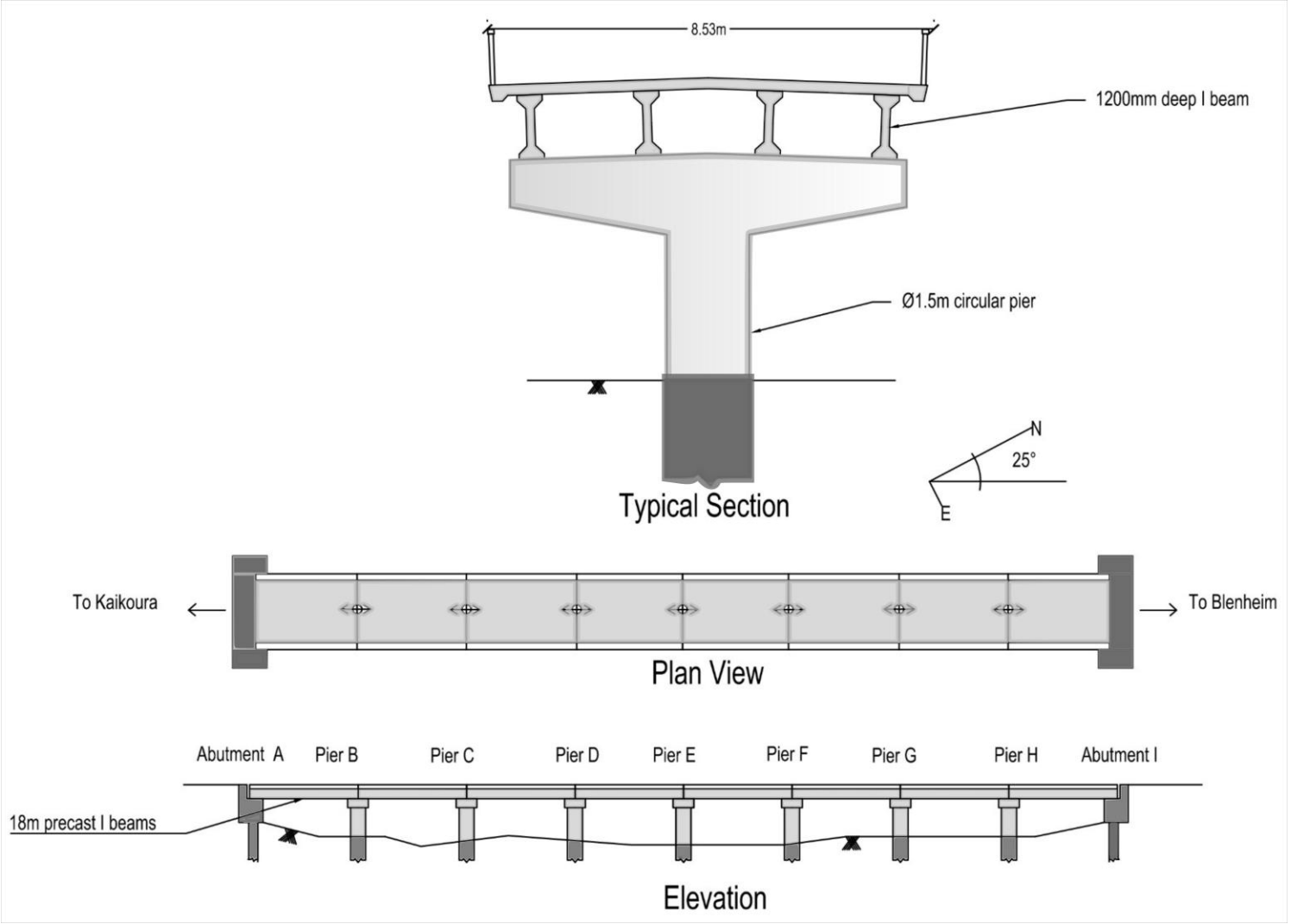

Figure 3-42: Layout of the Waima River Bridge

3.7.1 Plastic Hinge Performance

When the bridge was initially inspected, gravels covered around 1m of the base of the pier, completely hiding the plastic hinges. Given the significant residual drifts it was obvious plastic hinges had formed (or some other deep-seated failure had occurred). Consequently, excavation down to the top of the piles was carried out on the 5 central piers (which had largest residual displacement). Given the large residual drifts, the damage to the plastic hinges appeared minimal. The extent of damage was limited to vertical and horizontal cracking. This crack pattern and lack of spalling/buckling is attributed to the highly confined plastic hinge regions. The columns had 19mm diameter stirrups spaced at 75mm centres over their full height. Misalignment of columns at the pile-column interface shown in Figure 3-43 is thought to be a construction imperfection.

Figure 3-43: Plastic hinge damage after excavation (occurred below ground level).

Perhaps more significant than the damage observed at the plastic hinge were the residual drifts. Though it did not manifest as visual damage (spalling and buckling) in the plastic hinge, it is a direct result of plastic hinge deformation. As shown in Figure 3-44, the displacement profile has the expected parabolic shape along the length of the bridge, with the piers near the centre of the bridge having the largest displacement (at the abutments the spans were restrained transversely by shear keys and abutment piles). The measured drifts and estimated displacements at deck level are shown in Table 3-10.

Figure 3-44: Evidence of post-earthquake residual drifts of piers.

Table 3-10: Residual drifts at the Waima River Bridge.

	Pier B	**Pier C**	**Pier D**	**Pier E**	**Pier F**	**Pier G**	**Pier H**
Drift %	0	2	2	3.5	4.4	3.2	2.4
Displacement at deck level (mm)	0	140	140	240	300	220	160

3.7.2 Bridge Analysis

The central pier of the Waima River Bridge was modelled using a SDOF lumped plasticity model carrying the tributary mass. Given the structure is simply supported, this is expected to accurately predict the response of a pier near the centre (Pier F). This will represent the maximum displacement of all piers as seen by the displacement profile of the superstructure and the fact that the load carried back to the abutments is likely small.

Two recording stations the KEKS and WDFS were relatively close to the site at 7km and 14km away respectively. In this case the KEKS recording station was used as the shaking intensity was much larger in the transverse direction. However, the KEKS accelerometer is in Soil Class B soils and the Waima River Bridge is on site C soil so it is likely that the shaking at the Waima is larger than that assumed in the analysis. However, the KEKS data is used here as the best estimate for computing the maximum displacement of the central pier. Given this assumption, the level of shaking exceeded a 1/1000 annual probability of exceedance event.

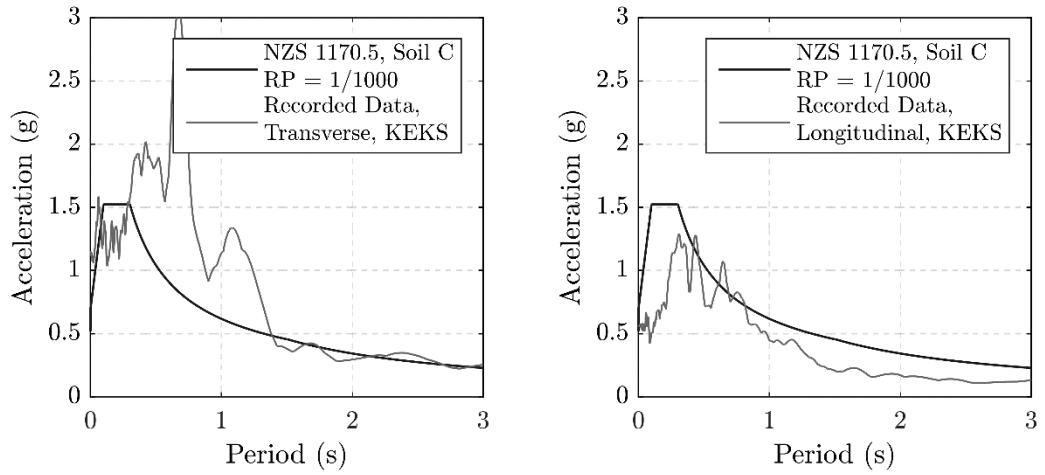

Figure 3-45: 5% Damped acceleration spectra for the transverse and longitudinal directions at the Waima River Bridge.

The level of damage can be further understood through pushover analysis in the transverse direction using Cumbia and a SDOF model with the tributary mass of the superstructure. The parameters shown in Table 3-11 were used as inputs for the pushover analysis.

Table 3-11: Properties and probable strengths used to determine the performance of the plastic hinge.

Waima Column Details	
Diameter	1524 mm
Cover to longitudinal bars	94 mm
Number of longitudinal bars	33
Diameter of longitudinal bars	32 mm
Diameter of transverse steel	19 mm
Spacing of transverse steel	75 mm
Type of Transverse reinforcement	hoops
Axial load	2187 kN
Concrete compressive strength	32.5 MPa
Long steel yielding stress	305 MPa
Long steel max. stress	458 MPa
Transverse steel yielding stress	305 MPa
Height of dynamic mass above top of pile	6105 mm

The recorded demand curve is obtained from the ground motion recorded at the KEKS station corrected to match the transverse direction of the Waima River Bridge. The recorded spectra were damped by 18% using the damping reduction factor outlined in the NZTA Bridge Manual. The capacity or pushover curve intercepts the

demand or ADRS curve at approximately 215mm (Figure 3-46). This represents the peak displacement the structure would be expected to undergo. The current maximum residual maximum displacement is 300mm (at Pier F) indicating that the KEKS input motion underestimates the demands at the site.

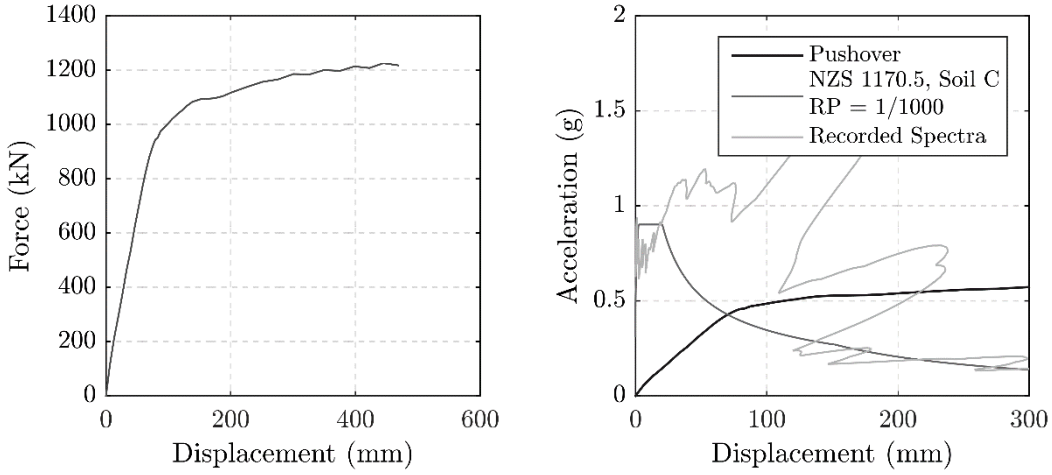

Figure 3-46: Left – Pushover curve for piers, Right – Demands found using the CSM.

As shown in Table 3-12 buckling would not be expected to occur at the predicted displacements or the residual displacement. This matches the observed damage.

Table 3-12: Key damage predictors.

Performance Limit	Displacement Reached (mm)
Yield Displacement (Including foundation component)	71
DCLS Steel Strain Limit Reached. Based on BM limits	300
Buckling M-K Criterion	320
Buckling B-E Criterion	-

NLTH was carried out using a SDOF lumped plasticity model and a tributary mass approach to ensure the damping, among other variables, were obtained with sufficient accuracy. The reinforced concrete was modelled using a modified Takeda hysteresis rule and bearings and soil displacements were modelled using linear elastic rules. A 5% damping ratio was adopted. The analysis gave a peak displacement of 230mm which was in reasonable agreement with the pushover analysis peak displacement of 215mm. It does however verify that the input ground motion was probably not an accurate representation of the shaking observed at the site as the measured residual displacement was 300m.

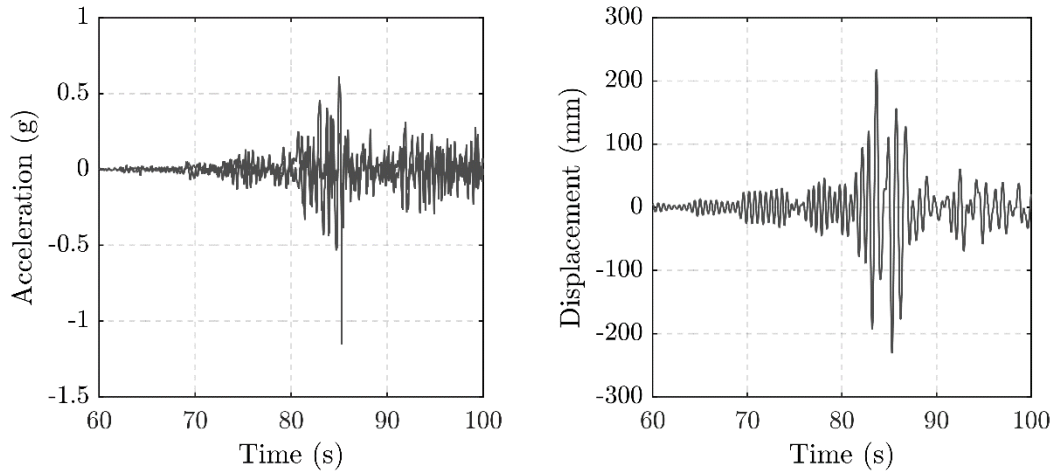

Figure 3-47: Left - Acceleration history of the KEKS recording, Right – Displacement history of the Waima River Bridge.

3.8 SHORTFALLS OF PLASTIC HINGES AND CURRENT STANDARDS

While there were no structures that collapsed after the intense shaking caused by the Kaikōura earthquake, and most plastic hinges performed as expected, the analysis carried out highlights two particular types of damage that led to the poor performance of plastic hinges. The first is residual drift, which affected two of the structures investigated and led to the deconstruction of one. The second is buckling of longitudinal reinforcement, which almost resulted in the collapse of the Lower Mason River Bridge. The first issue, residual drift, is ultimately a property of a plastic hinge. It can be minimised by reducing maximum drifts and axial loads but can't be prevented altogether (unless designing for very low displacements). The second, buckling of longitudinal reinforcement, is an issue that can be avoided with good detailing.

Evidence of this can be found by comparing the Waima River Bridge to the Lower Mason River Bridge. Both had similar anti-buckling requirements (Table 3-12) and both were subjected to large drifts. However, the Lower Mason had severe buckling with fractured bars while the Waima performed well with only flexural cracks. The key difference between the two plastic hinges was the level of confinement and anti-buckling reinforcement provided. The Waima had 19mm diameter bars at 75mm centres while the Lower Mason had 16mm diameter bars at 125mm centres. Consequently, the Waima River Bridge had significantly less concrete degradation and no evidence of buckling (Figure 3-48) compared to the Lower Mason which had buckled and fractured reinforcement. The buckling criteria (M-K and B-E) used in the assessments appeared to be conservative compared to the stirrup spacing used.

However, given these are largely experimental based empirical relationships a more refined method of determining the required amount of anti-buckling reinforcement is sought.

Figure 3-48: Left – Plastic hinge at the Lower Mason River Bridge, Right – Plastic hinge at the Waima River Bridge

All the structures which had buckled longitudinal reinforcement were designed to the provisions outlined in NZS3101:2006. This standard specifies that the anti-buckling centre-to-centre spacing for spirals or circular hoops be the smaller of one quarter of the diameter of the cross section of the member or six times the diameter of the longitudinal bar to be restrained. The volumetric ratio required for the restraint of longitudinal bars against buckling is calculated in accordance with equation 3-1 where A_{st} is the area of a longitudinal bar, d_b is the diameter of the longitudinal bar, d_c is the diameter of the concrete core. The equation is derived to ensure that the amount of transverse reinforcement is enough to overcome the buckling tendency of the longitudinal reinforcement. It was developed based on experience and intuition with very little quantitative evidence (R. Dhakal, 2005). It is noted that in some cases the confinement required may exceed that required in Eq 3-2 below (typically when axial load ratios are low). The maximum anti-buckling stirrup spacing can be determined using Eq 3-4.

$$\rho_s = \frac{A_{st} f_y}{110 d_c f_{yt} d_b} \qquad 3\text{-}1$$

Where,

$$\rho_s = \frac{V_s}{V_c} = \frac{A_h \pi d_c}{A_c s} \qquad 3\text{-}2$$

Rearranged,

$$s = \frac{A_h \pi d_c}{A_c \rho_s} \qquad 3\text{-}3$$

Combining 3-1 and 3-2 and rearranging,

$$s = \frac{440 A_h f_{yt} d_b}{f_y A_{st}} \qquad 3\text{-}4$$

When using displacement-based design methods, to enable the full development of longitudinal reinforcement tensile strain without buckling, the spacing must meet the upper limit set out in equation 3-5 (Priestley et al., 2007). Typically, equation 3-5 is more conservative than NZS3101:2006. The NZTA Bridge Manual gives values of f_u/f_y of 1.4 and 1.2 for Grade 300 and 500 reinforcement respectively.

$$s = (3 + 6\left(\frac{f_u}{f_y} - 1\right))d_{bl} \qquad 3\text{-}5$$

Table 3.11 shows the observed damage, observed spacings and design spacings for the structures damaged in the Kaikoura Earthquake. Ticks indicate that the hinge had the specified damage and blanks indicate that the hinge did not show signs of the damage. All of the hinges had stirrup spacings which comply with both equations 3-3 and 3-5. In fact, the specified spacing was often significantly less than required. Therefore, these provisions do not effectively prevent buckling of longitudinal reinforcement in bridge piers.

Table 3.11: Summary of the severe damaged observed at the bridge sites and observed stirrup spacing parameters compared to design spacings.

Structure	Intensity	Buckling	Bar Fracture	Residual Drift	Specified Stirrup Spacing	Stirrup Spacing[1]	Design Spacing[2]
Lower Mason	1/1000	✓	✓		125mm	140mm	130mm
River Road	1/500	✓			75mm	120mm	151mm
Wandle	1/1000	✓		✓	120mm	120mm	151mm
Waima	>1/1000			✓	75mm	75mm	150mm

[1] Maximum stirrup spacing observed (typically at location of buckled reinforcement)

[2] Design Spacing taken as the most conservative of equations 3-3 and 3-4 and $6d_b$ from NZS3101:2006.

The current version of the Bridge Manual uses equation 3-6 to determine the DCLS strain limit for steel in tension. This is based on the volumetric ratio of transverse steel to core concrete (ρ_s). Presumably, in most scenarios, it is desirable for

the tensile strain in steel to be close to the upper limit of $0.5\varepsilon_{sul}$ as this will allow the largest pier displacement and hence smallest design moment. ε_{sul} is the ultimate strain capacity of a bar which is taken at the maximum stress. To achieve this the volumetric ratio has to be a minimum 0.0108 (For Grade 300 steel). It is noted that using the maximum steel strain limit might give smaller diameter columns, higher displacements and undesirable P-Delta effects that will possibly lead to residual displacement following an earthquake. Therefore, it may not always be desirable to use this upper limit.

$$\varepsilon_{sd} = 0.015 + 6(\rho_s - 0.005) \leq 0.5\varepsilon_{sul} \qquad 3\text{-}6$$

As shown in Table 3.12 the stirrup spacing required to mobilise the full tensile capacity of the reinforcement is much smaller than current design guidelines allow. Given the plastic hinge damage and spacings observed in the Kaikōura Earthquake, it would appear this stirrup spacing is much more conservative and would provide adequate protection against buckling. However, designing to these maximum strain limits could cause issues such as significant residual drifts, more substantial P-Delta effects and more severe low cycle fatigue behaviour.

Table 3.12: Required stirrup spacing to achieve full tensile strain capacity of longitudinal reinforcement.

Structure	**Stirrup Spacing**	**Stirrup Spacing[1]**	**Design Spacing[2]**	**Spacing to reach full tensile strain capacity**
Lower Mason	125mm	140mm	130mm	80mm
River Road	75mm	120mm	151mm	95mm
Wandle	120mm	120mm	151mm	85mm
Waima	75mm	75mm	150mm	75mm

[1] Maximum stirrup spacing observed (typically at location of buckled reinforcement).

[2] Design Spacing taken as the most conservative of equations 3-4 and 3-5 and $6d_b$ from NZS3101:2006.

(Dhakal & Su, 2018) also proposed a strategy for preventing anti-buckling that has been well verified through experimental and numerical studies. The design process for this is outlined in Chapter 2 (Literature Review). It assumes shear and confinement have been designed for. Following that, it sets out a maximum spacing which is higher than currently stipulated in NZS3101:2006 and other codes (Priestley et al., 2007).

However, it does impose additional requirements relating to the stiffness of the transverse reinforcement. Table 3.13 shows the key design parameters used to determine the lateral stiffness requirements of the tie. It was assumed the as built spacings of the connection were appropriate to resist shear and meet confinement requirements. According to the design strategy proposed by (Dhakal & Su, 2018), in all cases, it was found that the lateral ties had insufficient stiffness to prevent buckling.

Table 3.13: Shows the current stiffness (k_c) and design requirements (k_t) for the four of the bridges damaged in the Kaikōura Earthquake.

	d_b (mm)	f_y (MPa)	s (mm)	Hoop Dia. (mm)	n_t	**β**	n_b	d_t (mm)	k_t (Gpa.mm)	k_c (Gpa.mm)
Lower Mason	24	310	125	868	16	0.85	1	16	54	46
River Road	28	310	75	768	14	0.86	1	16	460	52
Wandle	28	310	120	868	20	1.15	3	16	112	15
Waima	32	305	75	1336	33	1.63	3	19	778	14

Where d_b is the diameter of the longitudinal bar, s is the spacing of the stirrups or spiral, n_t is the total number of longitudinal bars, β is number of bar layers that touch each other on the projected line, n_b is the number of buckling-prone main bars, k_t lateral stiffness required to restrict buckling bar, k_c lateral stiffness of transverse reinforcement.

However, use of this formulation in the bridges examined results in transverse reinforcement (as spaced currently) to be larger than 25mm. This is significantly higher than current standards would require and seems impractical. This procedure is certainly more conservative than other standards that currently exist for the bridges investigated. The research and proposed design strategy have been validated through experimental testing (Dhakal & Su, 2018). However, the largest specimen investigated appears to be around 600mm in diameter which is around half the size of the piers investigated here. The lateral stiffness required is used to ensure the bar can only buckle between consecutive ties. That is to say, as the spacing reduces, the stiffness required to ensure bar buckling occurs between consecutive ties increases. Adding additional transverse reinforcement, with lower stiffness would result in higher mode buckling, but potentially improved seismic performance.

Although preventing buckling by adding more, or stiffer transverse reinforcement has been the focus, it is near impossibly to prevent buckling under high levels of strain. Therefore, a more efficient method to ensure the reliable performance of a plastic hinge is to reduce the displacements and strains at the design level.

However, this is going to result in less efficient connections and hence designers are unlikely to want adopt this strategy.

3.9 RECOMMENDATIONS

It has been proven that current provisions for detailing of the plastic hinge are not sufficient to prevent buckling of longitudinal reinforcement. Though requirements in the NZTA Bridge Manual are certainly stricter, a high design level strain needs to be used to increase the number of stirrups to what appears to be a desirable level. Of course, using a high steel strain has its own limits in that this means larger drifts can be designed for, which leads to increased risk of P-Delta effects and residual drifts. These issues can be easily solved by applying limits to the peak drifts (in the same way FBD currently limits maximum allowable ductility) and the minimum design strain used to calculate the required transverse reinforcement.

Dhakal et al., (2018) have proposed what appears to be the most conservative design strategy. It has been validated by significant experimental and numerical research. Therefore, is likely to be the most reliable strategy moving forward. The strategy indicates that the buckling observed in the plastic hinges investigated is likely related to the stiffness of the ties as well as the spacing i.e the buckling length of the longitudinal reinforcement was longer than the spacing between ties. However, this design method results in overly large stirrups, which are thought to be impractical. Therefore, until more research on the method proposed by Dhaka et al., (2018) is presented, it is proposed that the anti-buckling reinforcement be designed in accordance with the NZTA Bridge Manual (Eq 3-7) assuming a peak tensile strain is desired (even if it is not used).

$$\rho_s = \frac{0.5\varepsilon_{sul} - 0.015}{6} + 0.005 \qquad 3\text{-}7$$

Where ε_{sul} is taken as 0.1 for G500 and 0.12 for G300 steel reinforcement.

3.10 CONCLUSIONS

A number of bridge structures that were damaged as a result of the 14 November 2016 Kaikōura earthquake were examined. Of particular interest were those that had severe plastic hinge damage. Each structure was analysed, using NLTH, CSM, and ground motion inputs from the nearest strong motion recording station. The NLTH analysis was carried out on all investigated structures with the exception of the Wandle River Bridge, where geometric complexities led to a response that could not be replicated by simple analysis. In general, it was found that structures (designed using FBD) typically had damage that was worse than that which would be expected given the level of shaking at the sites. However, the CSM and displacement-based design (since displacement-based design is essentially the reverse process of the CSM) accurately predicted displacements and damage levels for structures that had accelerometers near the site, located on soil with similar properties. It was the detailing of the plastic hinge zone that led to the poorer than expected performance. Residual drifts and buckling of longitudinal reinforcement were noted as the main area of concern.

An investigation indicated that current standards such as the New Zealand concrete standard and other international displacement based guidelines (NZS 3101, 1995; NZTA, 2018; Priestley et al., 2007) provide anti-buckling requirements that are insufficient to ensure buckling does not occur. This is based on the observed damage and the fact that the plastic hinges investigated met the latest provisions for anti-buckling. The recently released Bridge Manual (NZTA, 2018) limits the ultimate tensile strain based on the volumetric ratio of transverse reinforcement to core concrete. This formula is much more conservative than the others examined and would appear, at least in the cases examined in this chapter to provide a more conservative approach to protect against anti-buckling (provided the maximum tensile strain is used). A more evidence based approach, the method proposed by Dhakal et al., 2018, resulted in overly larger transverse stirrup requirements (>25mm). Therefore, at this stage designing to the following is recommended:

$$\rho_s = \frac{0.5\varepsilon_{sul} - 0.015}{6} + 0.005 \qquad 3\text{-}7$$

Further experimental research to verify the applicability of the approach proposed by Dhakal et al., (2018) to larger scale bridge piers where a number of

longitudinal bars (typically three) require restraint should be carried out to determine the applicability of the theory to larger connections and ensure the theory results in practically achievable solutions.

Chapter 4: Assessing the Residual Capacity of Moderately Damaged Plastic Hinges

4.1 INTRODUCTION

The transportation network of the entire north-east portion of the South Island was severely affected by the magnitude 7.8 Kaikōura Earthquake (Palermo, Liu and Rias et al., 2017). While several structures showed signs of distress, including approach and pier settlement, unseating of spans from bearings, flexural cracking and damage to frangible joint (knock-off) elements and shear keys among other items, severe plastic hinge damage was only observed in structures close to the fault ruptures (Wood and McHaffie, 2017). Most of these structures could be readily repaired or did not need repair. However, due to the structural form of the River Road Bridge repairs were likely to be complex and expensive.

Capacity design, as it currently stands, allows the formation of a plastic hinge as a means of reducing design forces. However, it is well understood that when plastic hinges form, the residual capacity is limited, and repair is necessary to ensure adequate performance in future seismic events. As discussed in Chapter 2, there are strategies that allow the repair of plastic hinges depending on the severity of the damage and structural form. However, for moderately damaged plastic hinges it is possible that these costly repair strategies are unnecessary.

Estimating the residual capacity of plastic hinges is difficult due to various phenomena that occur to longitudinal reinforcement as a result of loading history. These phenomena include strain hardening, strain ageing, low cycle fatigue, and buckling; all of which are complicated and difficult to predict. The cost benefits of being able to estimate the residual capacity of a plastic hinge are significant, especially when several structures are damaged each of which, may have several plastic hinges. However, in the past, the residual capacity has been virtually impossible to estimate due to a lack of information on the loading history, strain ageing, plastic strain levels

and low cycle fatigue behaviour. In the case of the River Road Bridge, information on the loading history was recorded (via the WTMC strong motion recorder), and material testing techniques that can estimate the loss in strain capacity due to strain ageing and the plastic strain in the bar have been developed. This chapter illustrates, through a case study, how the residual capacity of a plastic hinge, which formed during the Kaikōura earthquake, can be estimated using material testing and NLTH analysis.

4.2 EARTHQUAKE INTENSITY AND DAMAGE

The Mason River Bridge, located about 5km from the Kaikōura Earthquake epicentre, was one of the structures that exhibited plastic hinge damage at the base of the piers. The structure, designed in 1979, supports one lane of traffic on pretensioned double hollow core beams. The overall length of the structure is 197m, which is made up of 12 simply supported 16m long spans. The piers are reinforced concrete with a 900mm diameter single column supported on longitudinally raked steel H piles. The piles are founded on 5m of medium dense gravels that are on top of clay bound and cemented gravels, correlating to Soil Class D in the New Zealand loadings code (NZS 1170.5, 2004). The plan view and elevation of this structure are shown in Figure 3-26 (Chapter 3).

Figure 4-1: Mason River Bridge

The Mason River Bridge was situated within 5km of the WTMC (Te Mara Farm Waiau) strong motion recording station. The peak horizontal ground acceleration at

the WTMC site was 0.99g. When the WTMC records were resolved into the transverse direction of the bridge, the acceleration and displacement spectra were less than a 1/500 annual probability of exceedance event for a Class D soil with a seismic hazard factor of 0.45 (Figure 4-2). Given the proximity of this recording station to the Mason River Bridge the recorded ground motion is assumed to represent the demands at the site. The fundamental period of vibration of the bridge piers was around 0.6 seconds. If the structure is assumed to be Importance Level 2 the Mason River Bridge experienced a level of shaking below a design level (DCLS) 1/1000 annual exceedance probability event.

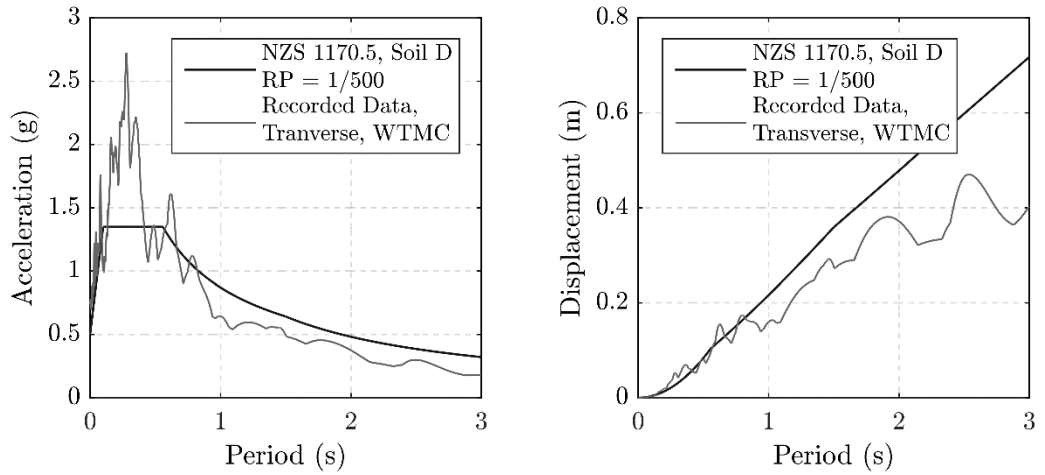

Figure 4-2: Shows a comparison between the recorded spectra (at WTMC station) and the design spectrum for the site (NZS1170.5, 2004).

The shaking caused significant damage to the structure. As expected, the superstructure was in reasonable condition with minor residual displacements of 5-15mm at both abutments indicating movement of the superstructure longitudinally. Further evidence of superstructure movement was also seen at the central expansion joint. Linkage rods and shear keys prevented excess movements of the superstructure in relation to the piers. The damage to the sub-structure was limited to plastic hinges which formed at the base of all except one of the piers but with varying levels of damage. However, the most significant damage was located at the piers near the centre of the bridge. The plastic hinge damage was moderate and included flexural cracks, spalling, yielding of longitudinal reinforcement and isolated buckling of longitudinal reinforcement (Figure 4-3). The buckling was only observed in two piers that were near the centre of the bridge and a total of 4 bars were found with minor buckling in the space between the confining spiral. While the damage sustained by the bridge is

considerable, the bridge was deemed to have enough capacity to remain trafficable to legal highway vehicles.

Figure 4-3: Plastic hinge damage observed at the Mason River Bridge.

4.3 ANALYSIS

To investigate the column damage, a single bridge pier was analysed in the transverse direction through a static pushover using Cumbia (Montejo and Kowalsky, 2007). A seismic mass of 938kN was used for analysis which included the double hollow core beams, pier cap, and one third of the column weight.

Table 4-1: Pier properties used for analysis

COLUMN PROPERTIES	
Diameter	900mm
Diameter of Long. Bars	28mm
Diameter of confinement spiral	16mm
Pitch of confinement spiral	75mm
Axial load at base of column	938kN
Concrete comp. strength	35MPa
Long. steel yield stress	275MPa

The CSM was used to determine the demands on the piers. Given that the event closely matched a 1/500 annual probability of exceedance event an ADRS curve was developed from the design spectra in NZS 1170.5 (also used in the Bridge Manual) for this annual exceedance probability. As shown in Figure 4.4 the normalised pushover

curve intercepted the 1/500 annual exceedance probability demand spectrum. Both the recorded and derived spectrum were corrected for the transverse bridge direction and 16% damping. The intersection indicates that the maximum expected displacement in the earthquake is 120mm (Figure 4.4). From the pushover analysis, at this displacement, yielding of longitudinal bars and spalling of cover concrete would be expected. However, bars would not be expected to buckle, which was observed at a location where a construction error had increased the design spiral pitch of 75mm to approximately 120mm. To prevent bar buckling the Bridge Manual and Priestley et al, (2007) recommend the stirrup spacing on circular columns should not exceed:

$$s = (3 + 6(\frac{f_u}{f_y} - 1))d_{bl} \qquad 4\text{-}1$$

Where f_u is the ultimate stress, f_y is the yield stress and d_{bl} is the diameter of the longitudinal bar being restrained against buckling. For a longitudinal bar diameter of 28mm and Grade 300 steel this relationship would give a maximum spacing of 151mm. The New Zealand concrete standard (NZS3101:2006) would allow a maximum stirrup spacing of 168mm (6 x d_{bl}). However, these limits have been found to be ineffective at preventing buckling. Even with the maximum observed pitch of 120mm the NZTA Bridge Manual and other design guidelines indicate that the Mason River columns should be protected against buckling for design level strains.

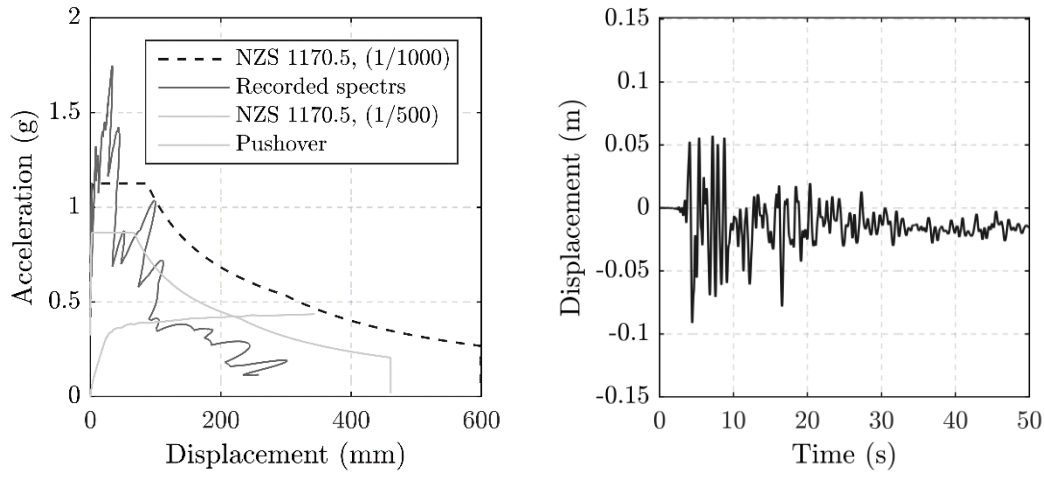

Figure 4-4: Left – CSM, Right – Displacement history from NLTH analysis.

To further investigate the performance of the plastic hinge, NLTH analysis was carried out using Ruaumoko. The ground motion recorded at the WTMC sites was resolved to match the transverse direction of River Road Bridge. Analysis was only

undertaken in the transverse direction due to complexities in the longitudinal direction related to soil-structure interaction at the abutments. In addition, although flexural cracking was observed in the longitudinal direction, the most severe spalling damage was observed in the transverse direction. This indicates that a significant portion of seismic load in the longitudinal direction was transferred to abutments and that the transverse direction was most critical for the piers (Figure 4-5).

Figure 4-5: Illustrates the damage patterns being most severe in the transverse direction.

To ensure that a SDOF model accurately captured the response of the structure a MDOF model was used to compare the peak response of the central pier. The general layout of this model is shown in Figure 4-6. This shows the end two spans, however, all 12 spans were modelled using Ruaumoko3D (Carr, 2004). In addition, the four linkages used in the model (at beam edges) are not shown. There were four linkages in total. A similar approach was taken as discussed in Section 3.4, for the Wandle River Bridge. Linkages at the abutments and piers were modelled using elastic springs with initial stiffness equivalent to the axial stiffness. No properties in the direction perpendicular to the spring were defined. The rubber strip bearings were modelled with elastic springs, properties for these elastic bearing were obtained from the GRANOR bearing catalogue (GRANOR, 2018). Details of the bearings and linkages are shown in Section 3.5.1. Gaps were used for the compression only springs (contact elements) and tension only springs (linkages).

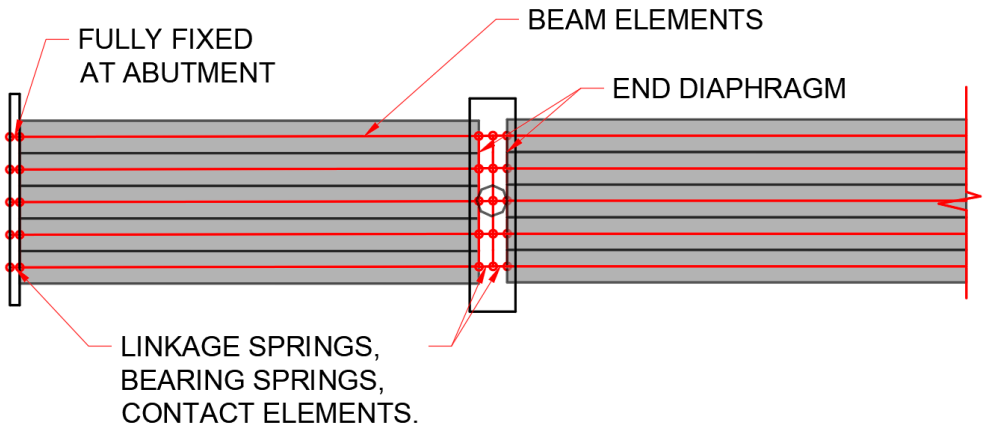

Figure 4-6: Generalised MDOF model layout for Abutment A and Pier B.

The displacement profile or envelope at the maximum displacement and the residual displacement following the earthquake are shown in Figure 4-7. In this case, due to the length, width, peak displacement and boundary conditions (gaps between spans and abutments), there was minimal interaction from the deck. In fact, for all spans apart from the end two, there was no contribution from the linkage bars or the compression only elements. This resulted in a relatively flat profile for the central piers. Essentially, each pier acts independently from the other. Therefore, provided the piers are the same size, height and are carrying the same seismic mass as the adjacent pier, little difference in response between the SDOF and the MDOF system is expected. This is shown in Figure 4-8, where the response between the SDOF and MDOF are almost identical. There is a slight difference due to the strip bearing properties implemented in the MDOF system. However, this resulted in a 0.1s period elongation and a 2mm increase in peak displacement. Therefore, a SDOF model is sufficient for estimating the bar strains, number of cycles, and fatigue life.

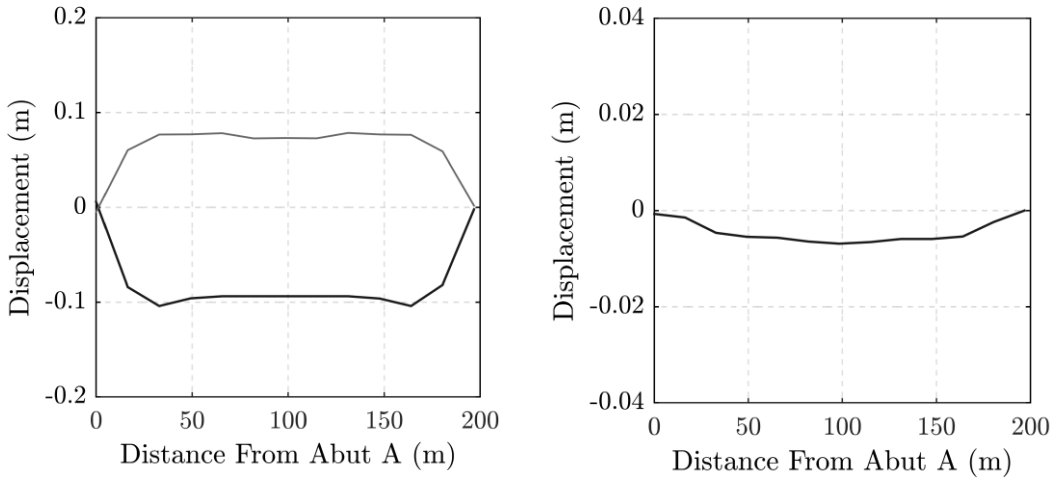

Figure 4-7: Left- Displacement profile/envelope from SDOF model, Right – Residual displacement profile.

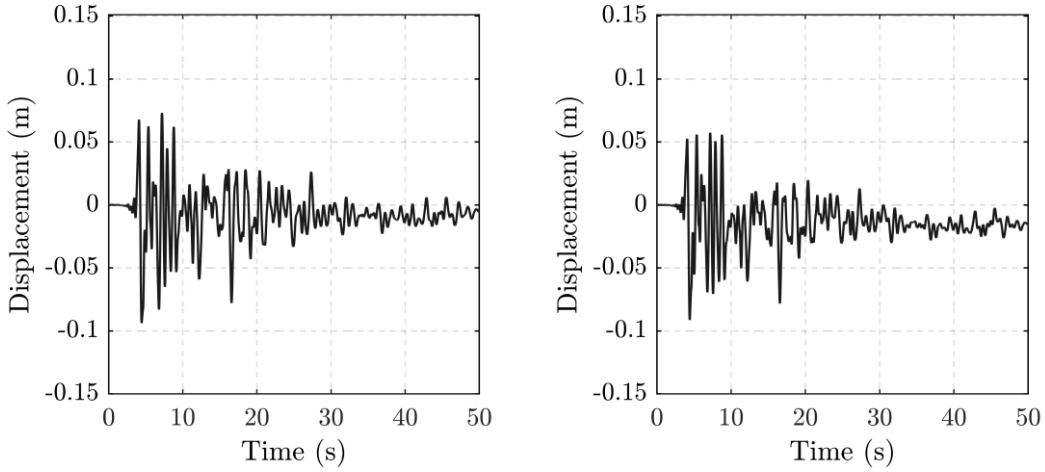

Figure 4-8: Left: Response of central pier within MDOF, Right: Response of central pier modelled as SDOF.

A lumped plasticity model was adopted for the simplified SDOF. The plastic hinge was modelled with a rotational spring using a modified Takeda hysteresis rule with properties to match the moment-curvature relationship obtained through section analysis. A user specified damping ratio of 5% was used. All other elements were modelled in accordance with the procedure outlined in Chapter 3. Given the backbone curve is based on the pushover from Cumbia, it is expected that displacements from NLTH will agree with the CSM method. However, the NLTH analysis will give information on the number of cycles, strain levels and confirm damping relations currently outlined (NZTA, 2018).

The results from this analysis predicted a maximum displacement response of 110mm validating the CSM method. The displacement response from the two analysis procedures corresponds to a tensile strain in the longitudinal reinforcing of about 0.032-0.035mm/mm or 3.2-3.5% (from the Cumbia pushover). This indicates that the longitudinal reinforcement has been plastically strained and therefore the monotonic and cyclic strain capacity will be reduced. Furthermore, strain ageing of the reinforcement, which had a specified yield stress of 275 MPa, will result in further reduction of the ultimate tensile strain (UTS) that can be developed by the damaged reinforcement (Loporcaro, Pampanin and Kral, 2018). The cyclic capacity will also be compromised as a result of low cycle fatigue. Therefore, many areas of uncertainty remain, making the assessment of the residual capacity difficult. However, recent material testing methods developed at the University of Canterbury (UoC) provide insight into the remaining strain capacity in the reinforcement.

4.4 MATERIAL TESTING

As discussed in the Literature review the development of material testing techniques has been significant in the past decade. Because of this advancement, the properties of the reinforcement bars after being subjected to plastic strains can be estimated (Loporcaro, Pampanin and Kral, 2018). Vickers hardness testing, which is more intrusive than the alternative Leeb hardness test was selected for this structure. This was chosen to minimise the error associated with fixity of the bars in on-site Leeb testing. In addition, the relationships between hardness, plastic strain, strain ageing and residual strain capacity are well defined with acceptable levels of error (Loporcaro, Pampanin and Kral, 2018). Tensile testing was also used to determine the residual monotonic strain capacity after strain ageing and plastic straining.

Initially, three damaged samples of rebar were removed from the three most severely damaged piers (Figure 4-9). The damaged specimens were removed from the bars loaded in the transverse direction and were assumed to be at the location of maximum strain, which was determined based on the damage (crack) patterns. Undamaged bars were removed from the top of the pier, where the strain in the bar was likely to be elastic. The bars were then tested by the Mechanical Department at the UoC. Loporcaro (2018) describes the testing method. The damaged bars were intended to represent the most severely damaged bars and the undamaged bars were

used to get an undamaged baseline along with a calibration curve for hardness versus pre-strain.

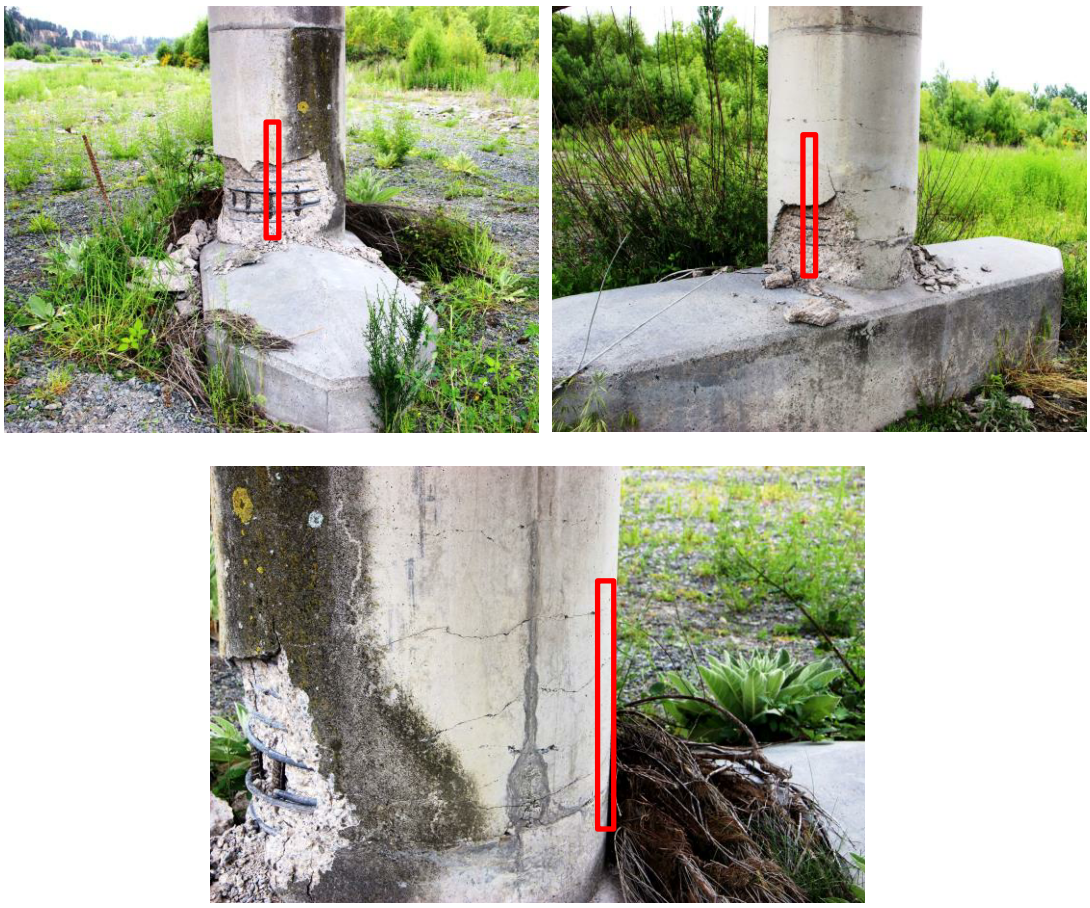

Figure 4-9: Location of bars removed for testing.

4.5 HARDNESS CALIBRATION AND FURTHER TESTING

The Vickers hardness (HV) of the undamaged specimens was constant over the length of the bar as expected. The results from these hardness tests were used as a baseline. Loporcaro (2018) related the Vickers hardness to pre-strain as shown in Figure 4-10.

The most damaged specimen had an increase in hardness, when compared to the undamaged specimen, of 30.1 HV which corresponds to a pre-strain of 0.042mm/mm or 4.2%. This correlation was found using the universal calibration curve shown in Figure 4-4 which is for strain aged G300 reinforcement. This indicates that the strain in the bar is slightly higher than predicted by the pushover and NLTH analyses (4.2% compared to 3.5%).

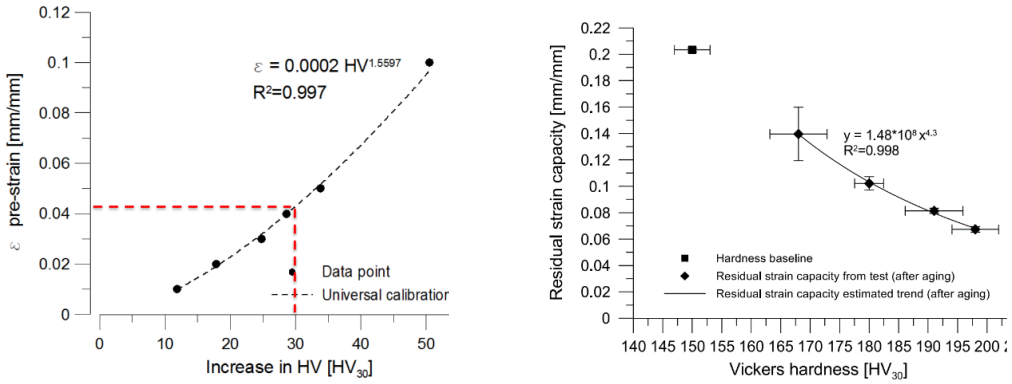

Figure 4-10: Calibration curves used to determine the pre-strain and residual strain capacity (Report Upper Mason Rebar Damage, UoC Mechanical Dept).

In addition to the pre-strain, calibration curves have also been developed to determine the residual monotonic strain capacity (Figure 4-10). This could be used to eliminate the need for tensile testing. However, given the bars from the Mason River Bridge are almost 40 years old (with a specified yield stress less than for G300 steel) it is likely the metal composition is somewhat different, so in this situation tensile testing was used to determine the residual monotonic strain capacity rather than relying on the previously developed calibration curves.

4.6 TENSILE TESTING

Tensile testing of the undamaged bars indicated the yield stress of the bars waa 273MPa, with an ultimate tensile strain of 0.21mm/mm. Ultimate tensile strain was defined as the strain at which maximum tensile stress was achieved, with the fracture strain being significantly greater than this. The yield stress specified on the design drawings was 275MPa which is consistent with the test results. Tensile testing of the damaged reinforcement indicated that the yield stress was between 300-313MPa, indicating strain hardening and strain ageing had occurred as expected. The ultimate strength was between 450-475MPa, with ultimate tensile strains between 0.139mm/mm and 0.162mm/mm. This testing was done over a year after the seismic event so this reduction in strain capacity is due to strain ageing combined with residual plastic strains. The most severely damaged bar lost 33% of the ultimate tensile strain capacity (Figure 4-11).

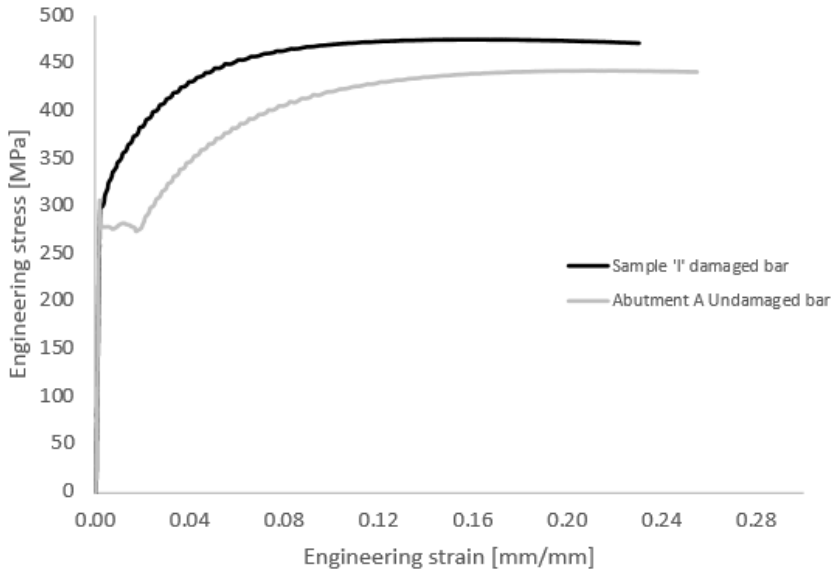

Figure 4-11: Stress strain properties of reinforcement tested at the UoC.

In the current NZTA Bridge Manual, the ultimate tensile strain is assumed to be 0.10mm/mm for G500 bars and 0.12mm/mm for G300 bars. This is consistent with the strain limits specified in international displacement based guidelines (Priestley, Calvi, & Kowalsky, 2007). A further reduction is taken to determine the appropriate DCLS strain. This reduction is to account for the following:

a) Under cyclic loading the effective ultimate tensile strain is reduced by the peak compressive strain (Priestley, Calvi and Kowalsky, 2007).

b) Once high tensile strains have been developed, longitudinal reinforcement becomes susceptible to buckling and fracture (low-cycle fatigue).

DBD guidelines propose that in order to account for these phenomena, the steel strain limit at the DCLS should be 0.6 of the ultimate tensile strain, ε_{su} provided concrete compression strains in the plastic hinge section do not govern. Therefore, the tensile tests indicate that even with the previous loading and strain ageing the residual ultimate tensile strain capacity of reinforcement is still above the design limit. Therefore, using the design DCLS strain levels would still be conservative in a monotonic scenario. However, this design strain limit assumes no previous cycles and the low cycle fatigue capacity needs to be assessed to ensure the damaged reinforcement can undergo several cycles of 4-5% strain in a future seismic event.

4.7 FATIGUE PREDICTION

Fracture of longitudinal reinforcement due to low-cycle fatigue is one of the most common failure modes that can occur in flexural members, especially for structures located in regions with high seismicity. Low cycle fatigue is most prominent when between 1 and 5 fully reversed cycles of large strains up to or larger than 6% may be expected (Mander, Panthaki and Kasalanati, 1994). Mander utilised the Coffin-Manson (Coffin, 1954; Manson, 1953) fatigue life relationship and concluded that a single equation based on plastic strain (εp), and number of cycles (Nf), could be developed and applied to all reinforcing steels:

$$\varepsilon p = 0.08(Nf)^{-0.5} \qquad 4\text{-}2$$

The rebar used to derive equation 4-2 had an UTS of 18% which is similar to the UTS of undamaged specimens from Mason River Bridge. The properties of the bars tested do not exactly match that of G300 or the G275 bar used in the bridge; however, the strain results of the testing done by Kunnath et al (2009) are likely to be slightly conservative for this structure. Therefore, the following relationship will provide a conservative estimate of the cyclic capacity of the bars at Mason River Bridge.

$$\varepsilon p = 0.068(Nf)^{-0.5} \qquad 4\text{-}3$$

To evaluate the damage to the steel resulting from repeated cyclic loads the Palmgren-Miner rule was used (Miner, 1945). The following rule allows the calculation of cumulative damage from different strain amplitude peaks. When the damage index exceeds 1 or 100% fracture is likely. This relationship is shown in Eq 4-4.

$$D = \Sigma \frac{N_i}{N_{fi}} \qquad 4\text{-}4$$

Where D is the cumulative damage, $N_i$is the number of full strain cycles at a given strain, and N_{fi} is the number of cycles until failure at the given strain. The present analysis will conservatively focus on the outer most bar which underwent the largest strain cycles. Based on NLTH analysis a strain history was developed as shown in Figure 4-12.

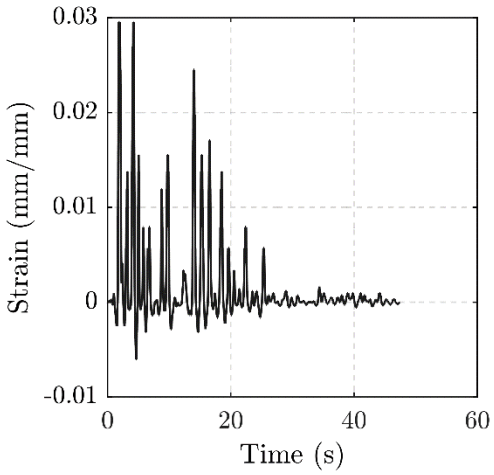

Figure 4-12: Strain history of the reinforcements

By using Miners rule in conjunction with the fatigue model developed by Kunnath et al, (2009) the cumulative damage was obtained using the strain history shown in Figure 4-12. This was done using the results from NLTH combined with the Cumbia pushover analysis (displacements correlated back to strains in reinforcement).

The total damage (fatigue life used) in the outermost bar is estimated to be 21% (a value of 100% damage indicates failure of the bar or that the full fatigue capacity of the bar has been utilised). To account for the fact that hardness testing showed a maximum plastic strain of 4%, the strain history was scaled up so that the peak strain in the steel was 4%. This resulted in the damage increasing slightly to 23%. At these levels of strain, the number of cycles to failure is around 20. Therefore, the slight increase in strain has a small effect on the cumulative fatigue damage. In fact, for strains of 6% or below the damage from a full-cycle is less than 10%. Therefore, it can be concluded that for low cycle fatigue, large cycles above 6% have a significant effect, and moderate strains below 6% have a minor effect on fatigue life in the context of seismic performance. Given the damage to the extreme reinforcement is around 20%, the low cycle fatigue capacity is sufficient to withstand at least three future events of similar magnitude and duration.

Table 4-2: Low cycle fatigue damage for scaled strain histories. S1 is the scale factor used to increase the peak strain to 4% (1.35). S2 is used to scale to CALS (1.5).

Event Size	Cumulative Damage
Kaikōura EQ	21%
S1xKaikōura EQ (DCLS)	23%
S1xS2xKaikōura EQ (CALS)	52%

Since the Kaikōura Earthquake does not represent the worst possible ground motion, the strain history that included the 1.35 scale factor was further scaled (Table 4-2) up by 1.5 to represent a CALS event (total scale factor to get to the CALS is 1.35x1.5=2). This is expected to provide a good estimate of the type of strain history that could be expected in a CALS earthquake. At this level of shaking it would be conceivable that reinforcement is at or near its low cycle fatigue capacity. However, the maximum strain reached by the outermost bar is 6%. The total damage as a result of the scaled strain history is 52%. Given the current estimated damage of 23%, the total damage after a future CALS event would be 75%. This shows that from a low cycle fatigue perspective, assuming buckling is prevented, the bars have enough strain capacity to survive a future CALS event. It is noted that a more correct approach for determining the remaining fatigue capacity would be to use ground motion scaling for the DCLS and CALS events to determine the likely future fatigue demands. However, given the proximity of the earthquake to the structure, the scaling adopted is thought to be a good representation of the shaking that could be experienced in future events.

4.8 REPAIR STRATEGY

Material testing and analysis has confirmed that the reinforcement likely has sufficient capacity to provide the required ductility in future seismic events. This conclusion is dependent upon the longitudinal bars being sufficiently restrained against buckling. Therefore, it is important to close up the spiral spacing. As discussed earlier, plastic hinge damage to other structures has indicated that the transverse reinforcement provisions in the Bridge Manual and DBD guidelines do not necessarily ensure adequate anti-buckling restraint. Therefore, a more conservative stirrup spacing of 90mm stirrup was used. There were locations in the plastic hinge regions where the maximum pitch of the spiral exceeded the 90mm limit. In these locations, additional

stirrup reinforcement was installed to protect the main reinforcement from buckling in the future.

The four longitudinal bars that buckled in the Kaikōura Earthquake and the bars removed for testing were replaced by cutting out the sections of bar and welding in new sections of reinforcement. This repair strategy, although not ideal, is permitted by NZS 3101, 2006 for the grade of reinforcement used in the bridge.The remaining damage on all piers was repaired through crack injection and concrete patch repairs. This was justified as the strains in the most severely damaged piers were found to be ok, and therefore strains in the less damage piers would be lower with more additional cyclic strain capacity than is stated within this Chapter.

4.9 CONCLUSIONS

The Mason River Bridge sustained plastic hinge damage as a result of the Kaikōura Earthquake. Simplified analysis indicated that the outermost bar underwent a maximum strain of 3.2%. Hardness testing confirmed that the strain experienced by the steel was around 4% and was used to verify the level of strain hardening, strain ageing and the residual strain capacity of the yielded bars. Monotonic tensile testing of the bars indicated the residual strain capacity was larger than 14%. This is larger than the strain capacity assumed in design (12% for G300). Therefore, the monotonic strain capacity was assumed to be sufficient to survive future design level events even when strain ageing is accounted for. However, the monotonic strain capacity of the bar is of less concern than the cyclic capacity. The cyclic capacity was estimated using a fatigue model proposed by Kunnath, Kanvinde and Xiao et al (2009) and was found to be sufficient to sustain a future CALS event.

The analysis assumes that bars are adequately restrained against buckling so the spiral spacings where checked with additional stirrups installed to ensure a maximum spacing of 90mm. Replacement of buckled reinforcement and concrete have restored the capacity of the hinge so that it can service a future CALS event. The testing and analysis costs were around 5-10% of the original estimated repair costs and provided considerable cost savings compared with the alternative of extensive column repairs and strengthening.

Though this chapter provided a logic-based strategy for estimating the residual capacity of a hinge, it could be further developed and verified through experimental

testing i.e pseudo-dynamic testing, which would provide a realistic strain history. After being damaged the residual capacity could be assessed, failure predicted, and further testing carried out to determine how failure correlates to that predicted using the method presented in this chapter. In addition, cyclic testing of the damaged specimen could provided further evidence of the residual fatigue capacity of the bar.

SECTION TWO – DCR

Chapter 5: Literature Review

5.1 DISSIPATIVE CONTROLLED ROCKING

Research on the seismic design of reinforced concrete bridges, has focused on improving performance to reduce the physical damage and residual drift associated with plastic hinging. Previously developed, damage-resistant technologies intend to minimise post-earthquake damage in the bridge structure, providing continued functionality for the transportation network. DCR (Figure 5-1) combines mild steel which provides energy dissipation, PT which provides an additional contribution to moment capacity and recentering, and steel armoring which prevents severe concrete damage at the rocking interface. Due to the steel armoring, damage is confined to the external or internal dissipative devices. These devices could be bonded or partially unbonded reinforcement, axial dissipative devices, lead dampers, friction dampers or viscous dampers. Both internal and external dissipative devices have advantages over one and other. External dissipative devices provide easier access for inspection and repair. However, they are susceptible to the elements (durability), are visually unappealing and susceptible to vandalism. Internal dissipative devices can't be inspected or repaired however they are not exposed to the elements.

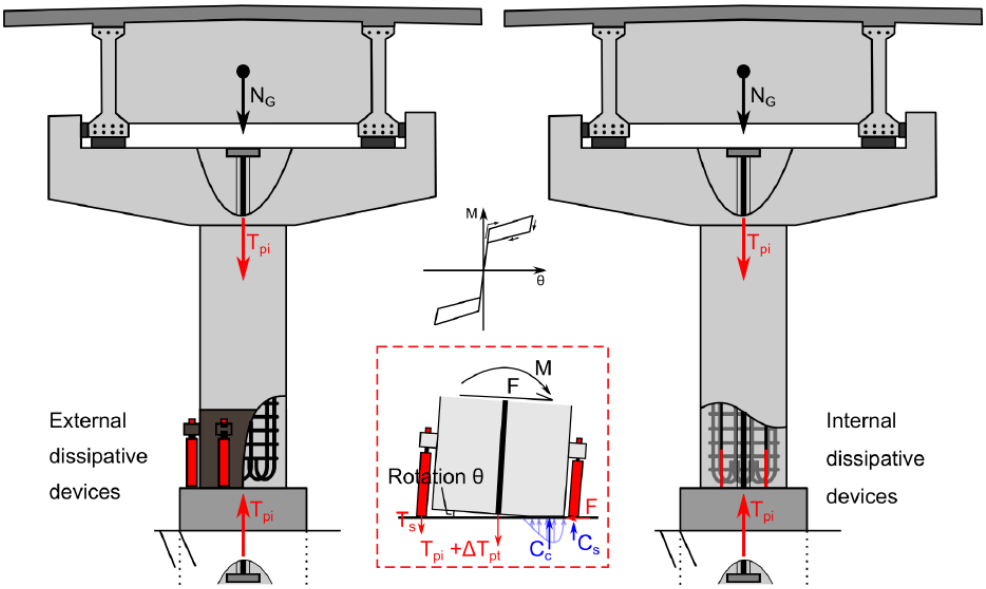

Figure 5-1: Components and free body diagram of DCR connections for bridge piers that are detailed with external (left) and internal (right) dissipative devices (Liu, 2018).

The main advantages of DCR connections, if detailed appropriately, are the elimination of residual drifts and the minimisation of structural damage, which are desirable features for resilient structures and networks. Low damage technologies on bridges facilitate repair and inspection by incorporating external replaceable dissipaters that can be unbolted and reinserted without any need for temporary supports or restraints. Since the extent of damage is significantly limited, no significant cracking away from the main rocking interfaces is expected, even after a collapse avoidance limit state event, and no significant spalling is expected at or near the rocking interfaces. Additionally, unlike plastic hinge design, low damage systems prevent residual drifts on the bridge due to their self-centering nature. Finally, control over damage leads to minimised traffic disruption after an earthquake, reducing indirect costs due to downtime on the transportation network.

Dissipative Controlled Rocking (DCR) is based on the Hybrid connection first developed by (Stone et al., 1995), which looked at using the combination of mild steel and PT as a means of connecting precast elements. This was taken further with the development of the so-called Hybrid PRESSS system which was intended as an alternative to the traditional plastic hinge (Priestley, 1996). Though relying on similar structural features to the connections designed as part of the PRESSS program, the mechanics are slightly different for bridge piers. This is due to the axial load, which in

addition to PT, provides the connection with recentering. That is to say, that a pier not integrally connected to the foundation (a gap can open) without mechanical devices such as PT and dissipative devices would **rock** in the event of an earthquake. Adding PT allows the designer to **control** the re-centering capability of the connections and mild steel **dissipates** energy and reduces the number of displacement cycles before the structure stops vibrating. As a result the term **DCR** was coined by (Liu & Palermo, 2016b), which accurately describes the behavior of the connection. From this point on, within this document, the so called Hybrid and Hybrid PRESSS system will be referred to as DCR. Any connection which combines opening of a single large crack (preferably armoured), PT and dissipative devices will be classed as a DCR connection.

The first record of testing on DCR connections in buildings was carried out at the at the University of Washington (Stone et al., 1995). Significant further testing and refinement was then carried out at the University of California, San Diego as part of the PREcast Seismic Structural System (PRESSS) program (Priestley, 1996). The first adaptation of this technology to bridge piers was carried out by Palermo (2004) which showed promising improvement in performance compared to traditional monolithic plastic hinges (Palermo et al., 2005).

Since this first proposed application in bridge piers there have been numerous studies on the applications of DCR. At the University of Canterbury most of these studies have been aimed at the detailing and performance of a single connection.

Experimental validation of the performance of bridge piers implementing DCR, including comparison to a traditional plastic hinge (benchmark), was carried out by (Marriott, Boys, Pampanin, & Palermo, 2006). This study showed a stable hysteretic behavior, minimal residual drifts and very little stiffness degradation.

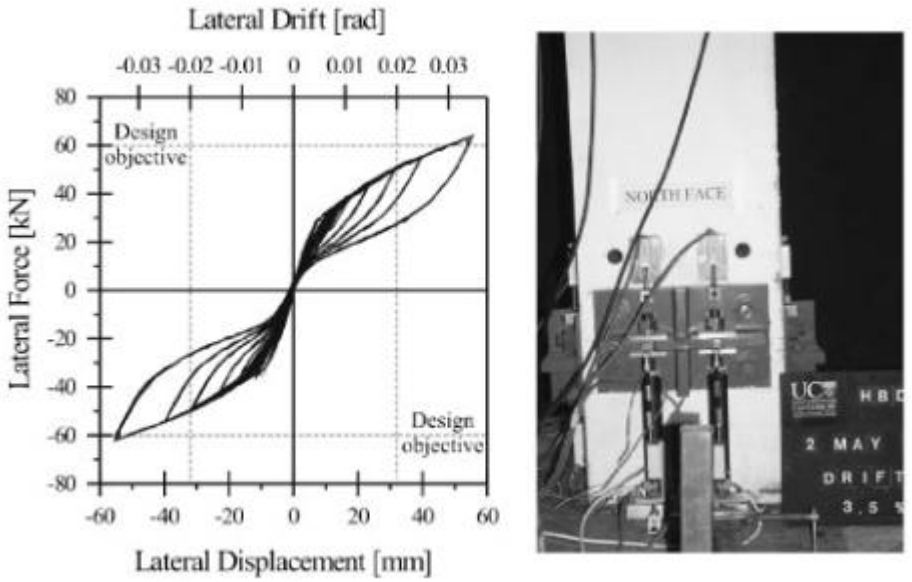

Figure 5-2: Specimen tested by (Marriott et al., 2009) and the resulting hysteretic behaviour.

Research on the performance of DCR connections with replaceable (external) dissipative devices was carried out by (Marriott et al., 2009). The experimental investigation included quasi-static and pseudo-dynamic testing (Figure 5-2). This was found to perform well with the most notable performance increase being the lack of softening in the hysteretic behavior compared to the traditional plastic hinge benchmark.

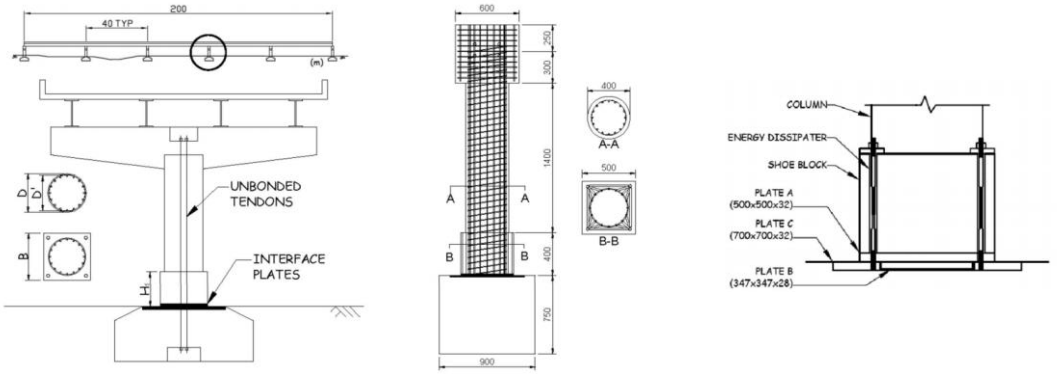

Figure 5-3: Details of the DAD pier and details used retrieved from (Solberg et al., 2009).

Testing on a cantilever pier, including quasi-static and pseudo-dynamic, was carried out by (Solberg et al., 2009). The pier was designed in accordance with the Damage Avoidance Design (DAD) philosophy initiated by (Mander & Cheng, 1997). This design philosophy essentially uses special detailing to avoid damage. The

specimen showed signs of only minor damage which included concrete crushing and fine flexural cracking.

Further development, through the application of velocity dependant dissipaters combined with displacement dependant dissipaters, was carried out by (Kam et al., 2010). The numerical study showed having both hysteretic and viscous dampers was found to improve the performance of DCR connections for both near and far field earthquakes.

An Advanced Flag Shape system consisting of velocity dependent and displacement dependent dissipaters placed in parallel, in addition to the recentering provided by the unbonded tendons/bars was also tested under shake table tests (Marriott et al., 2008).

(White, 2014) investigated a number of controlled damage connections. These were essentially designed to perform in a similar manner to plastic hinges (cracking, spalling and yielding) but with confined damage so that the plastic hinge could be readily repaired. PT was incorporated in these connections to limit residual drifts after an earthquake. Options for repairing the damage incudes the use of couplers or additional retrofitted brackets that would allow the addition of external dissipative devices (Figure 5-4).

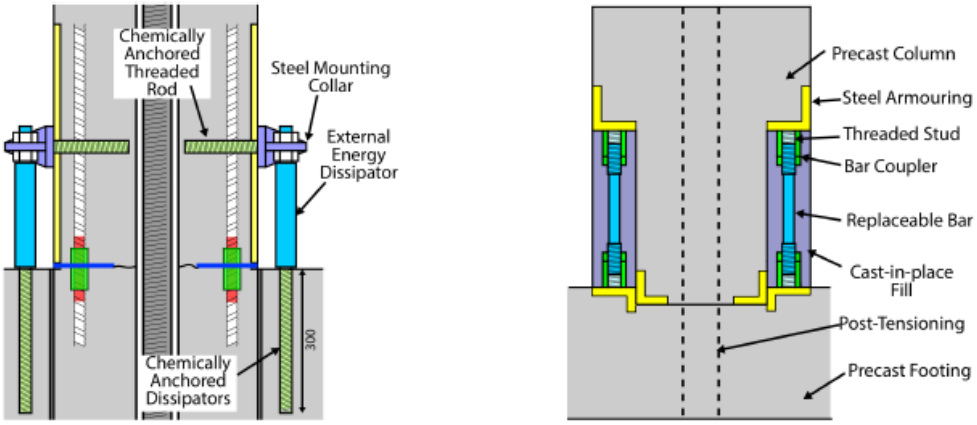

Figure 5-4: Left – Shows the externally fitted brackets and dissipaters, Right – Shows the replaceable dissipaters through the use of couplers (retrieved from White, 2014).

(Mashal & Palermo, 2014) investigated the application of DCR in the Accelerated Bridge Construction (ABC) framework. Essentially, ABC uses prefabricated elements to reduce the construction time. Given DCR requires a rocking interface it lends itself well to ABC as the pier and pile cap or pier cap elements can

be precast (cast separately rather than integral). Testing on a half scale bent with DCR and high damage connections (plastic hinge equivalent) showed satisfactory performance of the DCR connection with reduced residual drifts and damage.

(Chegini, 2018) investigated, both experimentally and numerically, seismic resistance of a structure which allowed the deck to rock - the connections which dissipate energy are located within the superstructure (between spans). The PT that runs the length of the superstructure acts to re-center the structure. Though the performance of the system was suitable, there is significant further research related to type of superstructure, geometry, bearing and abutment seating's, link slabs, and displacement profile required before application is possible.

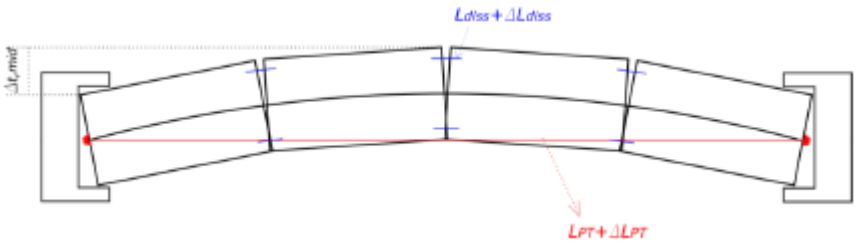

Figure 5-5: DCR through the superstructure (red is PT and blue are dissipative devices) retrieved from (Chegini, 2018).

(Liu, 2018) investigated methods of adding additional robustness to DCR connections. This investigation was carried out through quasi-static testing. In the first experiment, two sets of dissipaters were used across a single joint. One set was activated at very small drifts, while the second set did not activate until larger levels of drift. This means that the strains and fatigue levels are much lower safeguarding these sets of dissipaters against fracture. Liu also investigated hierarchical activation of dissipaters across multiple rocking joints. In addition, testing was carried out where DCR and pile cap rocking were combined. In all cases the desired performance was achieved with stable hysteretic behavior.

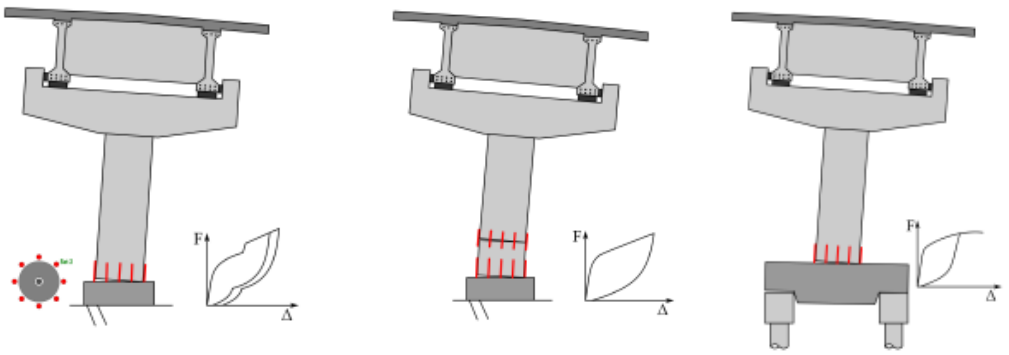

Figure 5-6: Left – Hierarchical activation across a single interface, Middle – Hierarchical activation across multiple interfaces, Right – Pile cap rocking combined with DCR (Retrieved from Liu, 2018)

Overseas the research is more aimed at how a DCR connection can be applied as part of ABC, particularly in the US. Dual shell columns with PT and energy dissipation (internal and external) were experimentally (static and dynamic) and numerically investigated by (Guerrini et al., 2015; Guerrini et al., 2012; Moustafa & Elgawady, 2016). Moustafa et al., 2016 used an inner and outer steel shell, used an inner steel shell combined with an outer FRP shell. The shells are intended to act as form-work, provide confinement and replace reinforcement (outer shell).

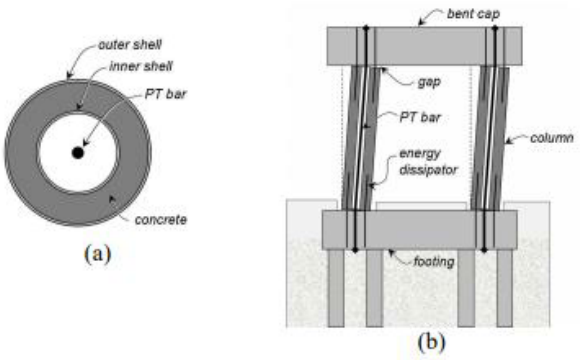

Figure 5-7: Self centering precast dual-shell steel rocking column retrieved from (Guerrini et al., 2015).

The application of DCR for tall segmental concrete bridge piers, which are commonly used in ABC due to their size and therefore the ease by which they can be moved, was investigated by (Sideris, Aref, & Filiatrault, 2014, Wang, et al., 2008). This was further developed through experimental testing with the addition of sliding-rocking joints with an aim of increasing energy dissipation and reducing the seismic demand (Sideris et al., 2014). Wang et al, (2018) extended these studies by using high performance materials in the columns to reduce damage to the concrete (crushing).

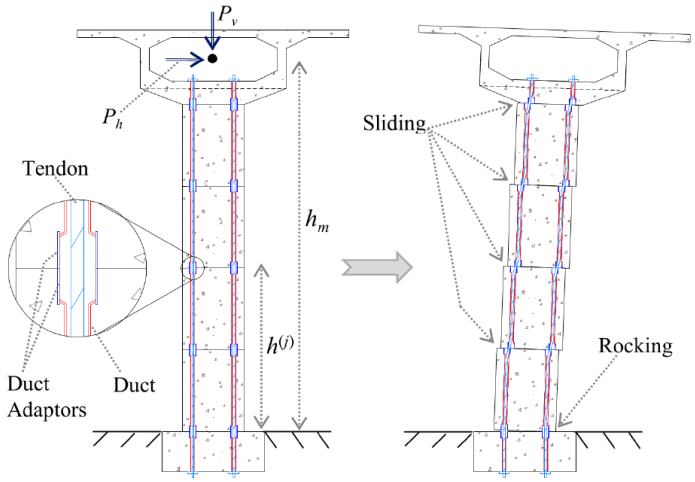

Figure 5-8: Segmental pier which can dissipater energy through combined rocking and sliding at multiple interfaces (Retrieved from (Sideris et al., 2014)).

A new bridge bent system was developed by (Thonstad et al., 2016) highlighted the potential application of DCR in accelerated bridge construction in seismic regions. The system had internal unbonded steel reinforcement for energy dissipation. Shake table testing of a quarter scale two span bridge underwent minimal damage and reliable behavior.

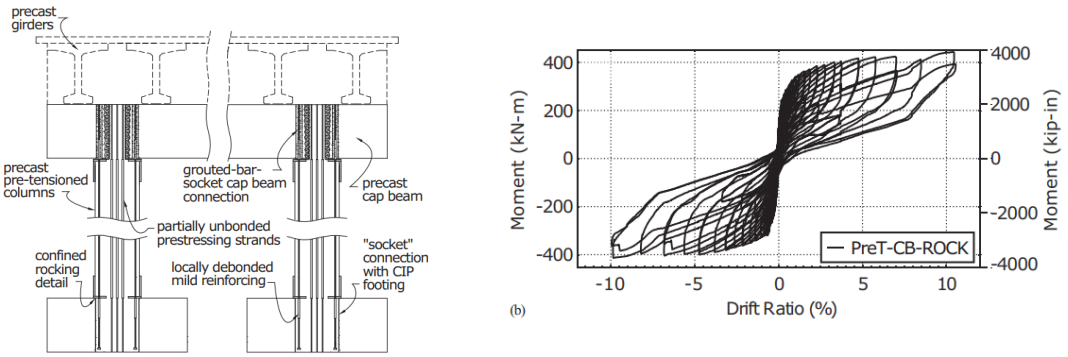

Figure 5-9: Detailing used in the experimental test setup and reliable performance hysteretic behaviour at large drifts.

Ou, (2007) experimentally tested a number of precast segmental bridge columns that used unbonded post-tensioning. The study used longitudinal reinforcement to dissipate energy. In addition, models were presented for modelling of both the monotonic and cyclic behavior of the piers (Ou et al.,2007).

Studies at the University of Nevada have investigated the use of non-traditional materials, such as ultrahigh-performance concrete, engineered cementitious composite

and nickel-titanium shape memory alloy (Mehrsoroush & Saiidi, 2016). The materials were used to improve the performance of ABC connections. The damage was found to be less than traditional plastic hinges, with the ability to survive extreme drifts and reduced residual displacements.

These studies on bridge piers incorporating DCR have shown improved performance than the alternative monolithic connections. In addition, they provide solutions to a number of challenging design problems. The main drawback of low damage technologies is that due to additional components and current lack of implementation there is an increased construction cost. In reality, this is likely offset by the minimised traffic disruption and safer repair methods as well as the other advantages associated with using ABC and precast elements. However, those benefits are not easily measurable nor are they easily understood at a design level by owners and decision makers. Therefore, to ensure this technology can be utilised in cost competitive environments their efficiency must be improved. This research aims to improve their efficiency in two ways. The first is to investigate dissipative devices, which account for much of the difficulty, risk and cost, to develop more efficient dissipaters. The second is to look at the way these connections are designed and develop alternative design methods for connections with replaceable dissipative devices and reliable performance at the CALS.

5.2 PASSIVE ENERGY DISSIPATIVE DEVICES

As previously discussed, one of the key components of DCR is the dissipative devices. In fact, since all other components are designed to remain elastic, these devices determine the overall performance of the connection; a poorly designed dissipative device could lead to poor energy dissipation, premature loss of capacity and excess displacements. In addition, much of the increased cost associated with implementing DCR connections is related to fabricating the devices. The following section investigates previously developed, and currently available dissipative devices.

5.2.1 Metallic Damper

There are currently a wide range of dissipation devices that rely on the stable hysteretic behaviour of mild steel to dissipate energy. Initially, these devices were developed to be used in seismic isolation applications (Kelly, Skinner, & Heine, 1972; Skinner et al., 1980). The devices developed for this application include the torsional

beam damper, the U-shaped flexural plate damper, the cantilever plate damper and the lead extrusion damper. To date, only the U-shaped flexural plate and lead extrusion damper have been tested as part of a DCR connection.

The development of the PRESSS system and DCR has led to the invention of many dissipation devices, designed specifically for the application. Perhaps the most common has been advancement of the buckling restrained fuse type dissipater. This is an axial dissipation device which yields in tension and compression. The popularity of this device for application in DCR is probably due to the simplicity and cost-effectiveness of the devices. In addition, using these devices makes the connection design most similar to plastic hinge design. Christopoulos et al., (2002) were the first to experimentally test energy dissipating bars. Further development of the devices was carried out at the university of Canterbury where several variations were conceived (Marriott, 2009; White, 2014) for application in connections with external and internal dissipative devices. The dry dissipaters, which do not require the injection of grout or other materials on-site, have become the most popular.

White, (2014) developed and experimentally tested three dry type buckling restrained fuses that have an application to DCR connections (which incorporate the external dissipative devices). These included the split tube, the supported bar and the grooved dissipater (Figure 5-10). All three variations of axial dissipaters had stable hysteretic behaviour along with a monotonic strain capacity similar to rebar. One concern raised by White (2014) was the low cyclic fatigue capacity of the grooved type dissipater. However, investigations carried out by Liu (2018) have verified the low cycle fatigue performance of the grooved dissipater and characterised the fatigue life relationship for the four-groove type dissipater.

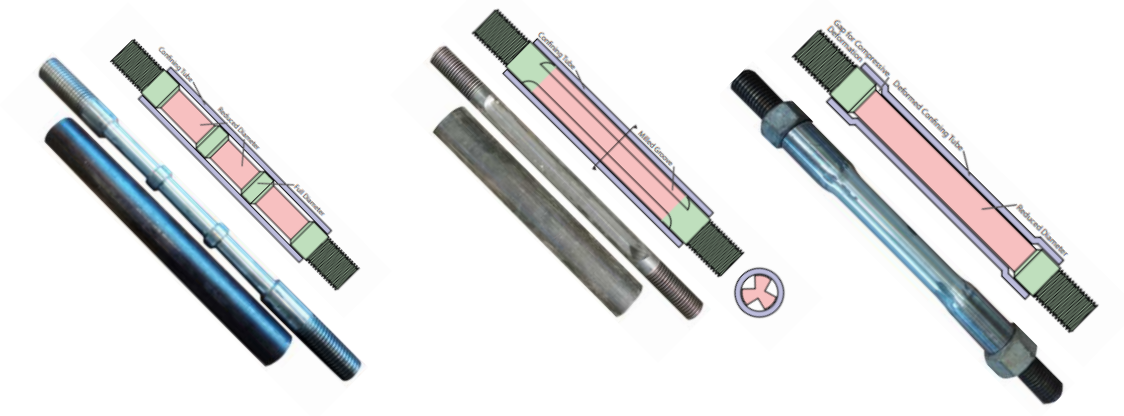

Figure 5-10: Dry type dissipaters developed by (White, 2014)

The lead extrusion damper was first conceived by (Robinson & Greenbank, 1976) for application in seismic isolation. Two types of lead extrusion dampers exist, the bulged shaft type and the constricted tube type. The devices provide a resisting force and dissipation capacity by forcing the lead material through a hole or an orifice, altering its shape (Rodgers, et al., 2009). Application of the lead extrusion damper was limited initially due to the size of the devices. (Rodgers, 2009) developed the high force to volume damper which could create resisting forces between 120kN and 400kN and was sized appropriately for application into precast connections (Mander et al., 2009) and steel frame connections (Rodgers, 2009). The devices have a large advantage over the buckling restrained and fuse type dissipaters as energy can be dissipated without damage, and hence need to replace the device after a seismic event. This is done by utilising the rheological properties and crystallisation temperature of lead (Rodgers, 2009).

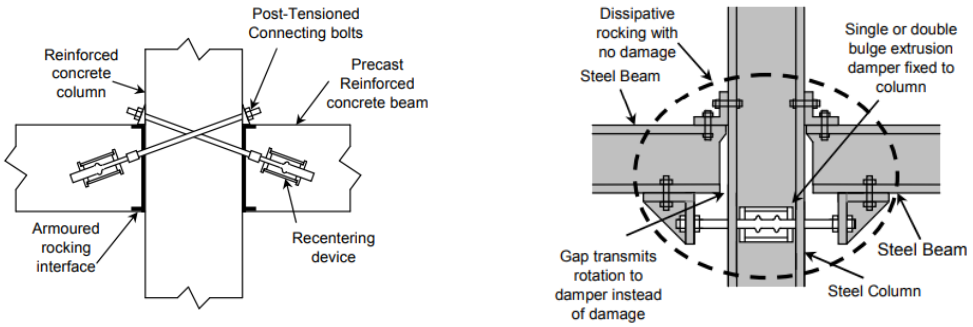

Figure 5-11: Left – Schematic of implementation in precast concrete connection, Right – Schematic of application to steel beam column joint.

5.2.2 Friction Damper

The application of friction devices to rocking connections has been limited. This is likely due to potential durability and corrosion issues particularly at the friction interface. (Constantinou, Reinhorn, et al., 1991) developed a displacement control device which had energy dissipation characteristics in strong earthquakes and also has re-centering characteristics. A rotational friction device was developed by (Morgen & Kurama, 2004) for application in a beam-column rocking joint.

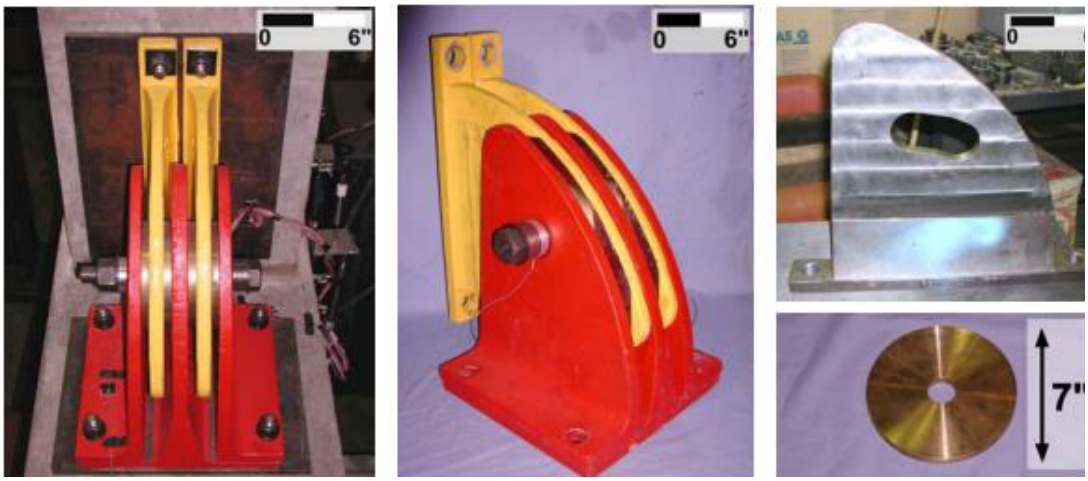

Figure 5-12: Rotational friction damper retrieved from (Morgen & Kurama, 2004)

5.2.3 Fluid Viscous Damper

Fluid viscous dampers have been used across a range of applications in structures. However, their application in bridges has been a little scarcer. The first proposed application of viscous dampers as dissipation devices in bridge piers was by Palermo et al., (2005). This was further developed and tested by Marriott, (2009). As previously mentioned Kam et al., (2010) used a combination of viscous dampers and hysteretic dampers to improve performance to near and far field earthquakes (since the viscous dampers are velocity dependant). Fluid viscous dampers have improved performance when compared to hysteretic dampers as there are no fatigue issues – they will not be damaged or require replacement after large seismic events. However, the reason they are not a preferred option for application in DCR connections is likely related to their high cost.

5.3 DISPLACEMENT BASED DESIGN OF DCR CONNECTIONS

In the last century seismic design of structures has been constantly evolving. Particularly, when compared to other design requirements such as gravity, traffic and wind loads. Seismic design began with the perception that the earthquake force could simply be quantified by assuming a force proportional to the mass of the structure i.e the lateral design force was taken as say 10% of the mass of the structure. This was further adapted in the 1940's where the influence of the structural period in modifying the intensity of forces was incorporated. Though structural demands were still based on an elastic structural response. In the 1960's and 1970's experimental and empirical results showed that well detailed structures could survive earthquakes much larger than the elastic capacity would allow. Thus, the idea of ductility was coined as a means of using elastic analysis and accounting for the non-linear behaviour (Calvi et al., 2008). The ductility factors, specifically adapted for reinforced concrete, where markedly different in different countries. Eventually, the realisation that strength was important for reducing displacements and strains but not necessarily for predicting or preventing collapse (Priestley et al., 2007) led to the idea that displacements, deformations and strains are more important than strength.

In the following decades a number of design philosophies based on deformation capacity rather than strength were developed, often termed performance-based design philosophies. Some of these even attempted to incorporate financial data and a client-based approach to quantify acceptable risk. Direct Displacement Based Design (DDBD) was first introduced by (Priestley, 1995). Fundamentally, this philosophy proposes that a structure should be designed to achieve a specified performance level, which can be defined by a displacement or strain limit (higher strains relate to more damage). The process was developed over the next decade which eventuated in a displacement based design guideline (Priestley et al., 2007).

AASHTO Specifications are an example of the use of capacity design principles. These principles are then supplemented using a force-based design strategy outlined in AASHTO LRFD Bridge Design Specification (AASHTO, 2017). Similar to New Zealand codes, they have an operational classification which effectively alters the accepted risk of collapse. Essential bridges are designed for a 1/1000 year annual exceedance probability. The response modification factor (R) is then used as a means to reduce the design demand to account for ductility. This factor is intended to ensure

the seismic performance of a bridge based on the following principles (U.S. Department of Transportation Federal Highway Administration, 2014):

1. Small-moderate earthquakes are resisted elastically with little damage.
2. Realistic seismic ground motion intensities are used to determine the elastic demand forces that are subsequently reduced by the fact R to use for design.
3. Shaking from large earthquakes should not cause collapse, if possible, damage should be detectable and accessible for inspection and repair as necessary.

The allowable ductility level is then reduced or increased based on the operational classification of the structure. This is a logical step as the damage is related to ductility. Therefore, more critical bridges are expected to have less damage than less critical structures. New Zealand codes outline a similar strategy, however rather than reducing the acceptable damage in a given design earthquake, the design earthquake is increased. Though there are some small differences, in essence, the overarching aim is to ensure a low risk of collapse in a design level event. In AASHTO, collapse must be prevented but significant damage and disruption is accepted in a 1/1000-year annual exceedance probability. Earthquakes beyond this are not explicitly considered.

Displacement-based design methods are also codified in the AASHTO Guide Specifications for LRFD Seismic Bridge Design (AASHTO, 2011). In this guide the displacements are specifically checked but the upper limit on the response modification factor still applies. This seismic bridge design guide also outlines requirements for different earthquake resisting systems. However, though mention of other systems such as seismic isolation and fuses are mentioned, DCR connections would still be required to be designed in the same manner as a plastic hinge. Appendix A1 (AASHTO, 2011), allows for the use of rocking foundation with an upper ductility limit of 8 provided the P-Delta moment demand is less than 25% of the capacity of the section. It can be concluded that for traditional plastic hinges, and therefore DCR connections, design is ultimately based on a low risk of collapse. However, collapse is not explicitly considered (apart from in the detailing and displacement limits).

For single piers at the design level, the response modification factor is between 1.5 and 3 depending on the operational classification (importance level of the

structure). For comparison to New Zealand codes, this response modification factor can be altered by dividing the allowable ductility by the return period factor, which is used to alter the risk based on the importance of the structure. For a single column pier this response modification factor would range between 1.8 and 4. Therefore, the AASHTO guidelines outline similar damage levels to those outlined for the DCLS within New Zealand. The critical difference being that the NZTA Bridge Manual outlines provisions for design at the CALS should it require consideration. The CALS is taken as 1.5 time the DCLS demands. It is implied that designing to the DCLS ensures life safety at the CALS and this does not require explicit consideration.

The ductility demands outlined in AASHTO are similar to that defined in the NZTA Bridge Manual for a DCLS level. The annual exceedance probability of an ordinary bridge designed for the no collapse level using the AASHTO guidelines is 1/1000 years. Similarly, the annual exceedance probability for an Importance Level 3 (standard highway bridge) within New Zealand is 1/1000 years. New Zealand has an additional design level beyond this – the CALS which is the no collapse level and has an annual exceedance probability less than 1/2500 years though this is not always explicitly considered during design. Therefore, it could be argued that the no collapse level and corresponding ductility limits defined in AASHTO are similar to the DCLS level and ductility limits defined in the NZTA Bridge Manual. Neither code outline special design procedures to allow repairable structures to be designed to lesser earthquakes in either manual.

Eurocode 8 (EN, 1998) is similar to the NZTA and AASHTO standards. Capacity design principles and ductility factors are used to resist seismic forces. The allowable ductility factor (q) outlined in Eurocode 8 is up to 3.5. To ensure this level of ductility/damage can sustained by the structure, detailing requirements are set out, similar to both AASHTO and the NZTA Bridge Manual.

All three of the standards investigated allow damage to occur as a means of dissipating energy. The allowable level of damage is based on probability of failure, ease for access and repair and allowable reductions in strength. The ductility factors used are tailored to damage within plastic hinge zones.

As current codes stand, there is no benefit in having a structural system that dissipates energy but remains elastic (viscous damper) or dissipates energy with replaceable elements (axial dissipaters). Currently, both codes ensure life safety by

ensuring ductility demands at a given design level are sufficiently low, though often the CALS is not explicitly considered. In the NZTA Bridge Manual the CALS is defined as 1.5 times the DCLS for structures where design at this level is necessary. This research proposes that DCR connections be designed for the CALS. Given the large demands (and low annual exceedance probabilities) this is not practical or economic for monolithic connections (in part due to the unreliable performance, concrete degradation, buckling etc that is required to survive CALS demands). Chapters 6 – 9 investigate the effects of employing such a philosophy (designing to the CALS) with a particular emphasis on DCR connections. It is noted that this philosophy could easily be adopted for any system that has recentering, repairable elements (or elastic) and predictable performance at the CALS level.

Chapter 6: Proposed Alternative Design Philosophy

6.1 INTRODUCTION

DCR connections are inherently more robust and resilient than plastic hinges because they have an extra element, PT, which provides a significant portion of the section's moment capacity. In addition, if designed appropriately, it is easy to ensure that all elements, apart from the dissipation devices, remain elastic. The downside is that these connections currently cost slightly more to construct than traditional monolithic piers. This chapter introduces an alternative design philosophy for DCR connections that better captures the improved performance of the connections without compromising on life safety. It also highlights some current gaps in design frameworks that need to be investigated further for this design philosophy to be implemented in design.

Seismic resilience in bridge design within New Zealand, and throughout the world (El Sebai, 2009) is currently rather crudely considered based on the Importance Level (IL) determined for a particular bridge structure. The importance level is based on the potential loss of human life and the economic, social and environmental consequences of bridge failure. The IL is then used to define the return period for Serviceability Limit State (SLS), Ultimate Limit State (ULS) and the Maximum Credible Earthquake (MCE). In New Zealand, these limit states have recently been more appropriately renamed for seismic design in the latest version of the Bridge Manual (NZTA, 2018) and other international displacement-based seismic design provisions (Priestley et al., 2007), as Serviceability Limit State (SLS), Damage Control Limit State (DCLS) and Collapse Avoidance Limit State (CALS) respectively. These new terms help clarify that what used to be termed Ultimate Limit State is not in fact about life safety but rather about controlling damage, and it is the CALS that is about ensuring life safety. Ironically, the majority of structures designed to these limit states use plastic hinges, which have little ability to limit and control damage since the

damage is difficult to model and predict. In addition, accurately predicting the performance at the CALS is problematic due to the cyclic degradation of the hinge.

After several recent significant earthquakes in New Zealand (NZTA, 2012; Palermo et al., 2017), there has been a shift in the seismic design strategy towards minimising earthquake damage and facilitating repair (controlling damage). Consequently, several innovative strategies have been implemented that can achieve these objectives. This is particularly evident in multi-story building structures where the use of bracing systems, base isolation and DCR among others are common. In the bridging sector, these low damage systems are less common. In New Zealand and many other countries around the world, bridges are typically publicly owned. Given the large combined value of these assets, damage to a few isolated structures as a result of a seismic event is of little financial consequence. Particularly, when consideration is given to the discounted cost of this damage. As a result, bridge structures are often designed to achieve a pre-defined level of service at a minimum construction cost (in the majority of cases). However, as demonstrated by the Christchurch and Kaikōura earthquake (Wood & McHaffie, 2017; Palermo et al, 2011) this does not necessarily result in resilient infrastructure.

Given the change in design strategy, towards controlling damage as outlined by the invention of the "Damage Control Limit State", technologies such as DCR become advantageous due to the repairability, controlled damage and performance predictability. Although these traits specifically relate to the critical objectives of design guidelines and the use of this technology can lead to better infrastructure resilience, there is no direct economic advantage in using DCR or other low damage connections. Therefore, an alternative design philosophy for low damage connections that have seismic detailing which is predictable and repairable is proposed. The intent of this proposal is to allow designers to design DCR or any other low damage connections more efficiently. This philosophy enables the designer to better utilise the strain/deformation capacity of the connections. Fully utilising member strain capacities can reduce force/moment demands on the connections and their components, foundations and pier caps.

This chapter is specifically focused on introducing an alternative design philosophy for DCR connections, although the philosophy could be extended and

adapted to any connection type which has easily repairable damage and predictable performance up until the CALS level.

6.2 BACKGROUND

The alternative design philosophy was developed due to some complexities associated with the design of the Wigram Magdala Link Bridge (Routledge et al., 2016). Completed in 2016, the Wigram Magdala Link Bridge (WML) in southwest Christchurch crosses State Highway 73 (SH73) to link several suburbs to the city centre and comprises three spans of 32m, 35m and 32m in length. The superstructure comprises simply supported 1.5m deep prestressed concrete Super Tee beams with a 200mm thick in-situ deck. The two piers each comprise a headstock beam supported by two 1.5m-diameter columns which in turn are supported on large piled footings.

Figure 6-1: Wigram Magdala Link Bridge after construction completed.

The need for a structure to provide this link was identified in a scheme assessment for the Christchurch City Council (CCC) in 2009. As a separate project, the New Zealand Transport Agency (NZTA) constructed the Christchurch Southern Motorway in 2011, which also crosses SH73 and runs parallel with the then-proposed WML Bridge. As part of this motorway project, the pier foundations for the WML Bridge were also constructed, in advance, to minimise traffic disruption on SH73 during the future bridge construction. This allowed CCC to design and construct the remainder of the bridge later to suit the council's funding programme. It also created

an unusual situation where one consultant designed the foundations for an assumed bridge that was later to be designed by another consultant.

Opus (now operating as WSP) was commissioned by CCC to design the remainder of the bridge using the completed foundations. However, in the period between foundation construction and design of the bridge, the NZTA Bridge Manual was revised, changing the design criteria for the new bridge. The changes recognised the increased seismic hazard in the aftermath of the Christchurch Earthquakes and SH73 was reclassified as a Primary Lifeline Route with a higher importance level. The increased seismic demands due to the Bridge Manual changes, coupled with the fact that the foundation designers had already relied upon a high degree of ductility, meant that the design seismic base shear to be accommodated was 40% higher than the foundations had been designed for.

In New Zealand, Primary Lifeline Routes are categorised based on volume of traffic carried, strategic route importance and redundancy of the regional road network. The reason structures on Primary Lifeline Routes are designed for larger earthquakes is to reduce the risk of significant disruption to these critical roads. Conversely, the consequence of designing the structure for a smaller earthquake is a higher likelihood of damage and potentially collapse in a smaller event.

To capacity-protect the weaker foundation a lower strength pier column connection was provided using DCR. A smaller DCLS earthquake was considered to enable this. Whilst this could have also been achieved with conventional plastic hinges in the columns, the low-damage details ensured that damage expected in the design earthquake would be highly controlled and minor, having minimal effect on the post-earthquake serviceability. The low-damage details are also easily repaired requiring minimal disruption. Therefore, the higher likelihood of damage due to the smaller design earthquake was offset by the minor consequences of the expected damage. To demonstrate that the design had not compromised on the level of protection against collapse, no reduction was considered for the Collapse Avoidance Limit State Earthquake (CALS). This innovative solution to enable the use of a reduced design level earthquake was accepted by NZTA in this circumstance.

In summary, the Wigram Magdala Bridge was designed as an Importance Level 3 structure for the CALS and Importance Level 2 structure for the DCLS. This design

strategy allowed the structure to be designed for a lower base shear with an uncompromised collapse capacity.

6.3 PROPOSED DESIGN PHILOSOPHY

Given the logic previously discussed a new design philosophy is proposed for bridges with low-damage details (repairable connections with reliable CALS performance), where the DCLS demands can be relaxed and the CALS and SLS events are considered the critical design level events. This is further justified by considering the performance objectives outlined in the appropriate design guidelines. In the NZTA Bridge Manual and other international displacement/performance-based design guidelines, a specific set of performance objectives is set out for each design level. These performance objectives relate to levels of damage and the impacts on downtime and cost of repair. For the DCLS, the critical performance requirement is that the level of damage is such that repairs are feasible, repairs can be undertaken within a moderate time span and the repaired damage does not reduce live load capacity. For the CALS, the main performance requirement is to ensure life safety by avoiding the collapse of the structure.

As shown in Figure 6-2 (left) for a conventional reinforced concrete plastic hinge, as the demand level increases from SLS to DCLS there is an increasing level of damage and thus increasing repair costs. After yielding of longitudinal reinforcement, the concrete begins to form significant cracks (which would require repair) and then begins to spall. Beyond the DCLS, the plastic hinge degrades in a manner that is difficult to predict accurately. Figure 6-2 (right) illustrates the idea (based on authors opinion and experience) of the cost increasing drastically as the damage increases. The Figure does not include bar buckling or failure as this is highly dependent on the detailing used. Beyond the DCLS the damage continues to increase and estimating the level of damage and remaining capacity becomes difficult. This results in complex repairs or possibly even unrepairable plastic hinge zones. For this reason, the annual probability of exceedance of the DCLS for a plastic hinge, cannot be reduced as to do so would also increase the level of damage and cost of repair.

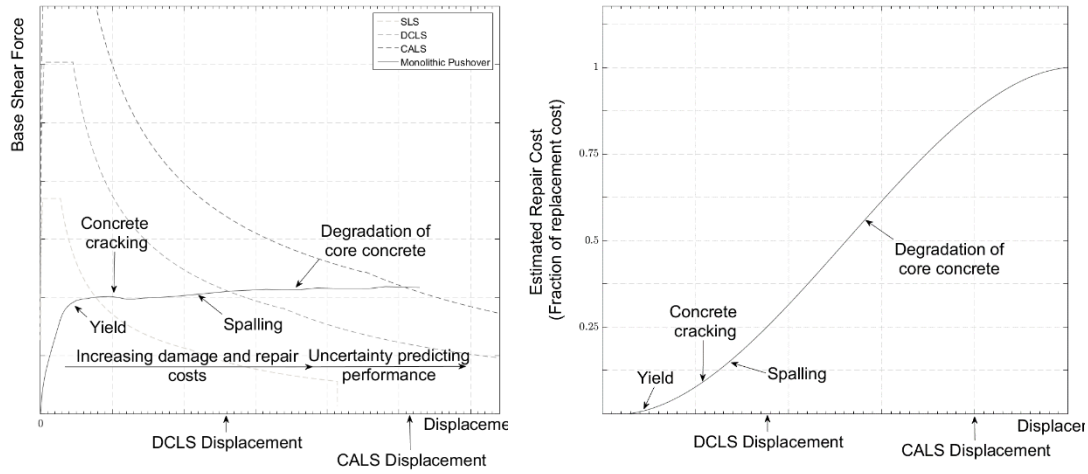

Figure 6-2: Left - Pushover response of a monolithic connection overlaid on ADRS demand curves (CSM), Right - Approximate relationship between increasing displacement/damage and cost of repair.

For a DCR connection, damage is confined to the dissipative devices. Steel armouring prevents the concrete from degrading (and limits cracking), and the PT is designed to yield beyond the CALS (Figure 6-3). As shown in Figure 6-3 (right), which illustrates the assumed cost of repair based on research carried out for RC frames (Ramirez et al., 2012), once the replacement of dissipaters is required the only increased cost associated with larger demands is the increased number of dissipaters that need replacement. This shows that, assuming the superstructure is not damaged, for any level of shaking up to the CALS displacement, the DCLS performance objective is met because the replacement of dissipaters is the only required repair. This implies that designing to a specific DCLS level is unnecessary. Therefore, the CALS becomes the key design level for low-damage connections, or specifically in this case DCR connections. Therefore, it is logical that the CALS level can be designed for, and the requirements at the DCLS level can be relaxed or neglected altogether.

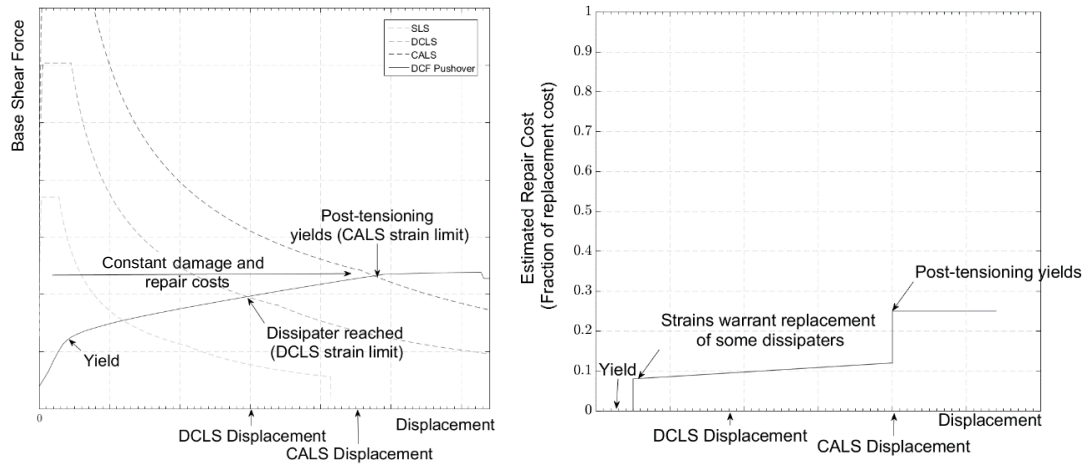

Figure 6-3: Left - Pushover response of a DCR connection overlaid on ADRS demand curves (CSM), Right - Estimated relationship (based on cost of dissipaters and author experience, it is for illustration only not expected to be accurate) between increasing displacement/damage and cost of repair.

To better understand the implications of this design philosophy, consider an Importance Level 3 structure. The DCLS annual probability of exceedance is 1/1500 (R = 1.5), the near-fault factor is taken as 1, hazard factor (Z) is 0.4 and soil class C is assumed. A displacement-based design procedure was used to design two connections with the pier assumed fixed at the base. The strain limits shown in Table 6-1 were used to define the maximum achievable drift at a given design level. Instability due to P-Delta effects was also considered when designing at the CALS. It is noted that at this stage there is little information about the CALS strain limits (other than the conservative 7.5% limit) for axial dissipative devices, so the values used here are simply shown to illustrate the alternative design philosophy (for any device).

Table 6-1: Strain limits used when designing DCR connections

	DCLS Strain Limits	CALS Strain Limits
Dissipaters	5%	10% (Dependant on dissipative devices used)
PT	~60-70% yield	Yield Strain (Dependant on material used)

As is currently common practice, the first connection was designed to achieve the DCLS strain limits. This means the DCLS strain level in the dissipaters is reached at the DCLS displacement. The second connection was designed for the CALS. At this level, the strain in the dissipaters should not exceed 10% (or the appropriate CALS strain level for the dissipative device), this is below the monotonic strain capacity but allows for a reduction in capacity due to low cycle fatigue. However, there is little

research that defines the appropriate dissipater strain level, as such this is investigated in Chapter 7. The PT was designed not to yield until after the CALS displacement. With the geometry used in this scenario, it was yielding of the PT which was the most critical and consequently governed design. By designing the pier in this way, the CALS displacement can be reached by fully utilizing the material capacity of the dissipaters.

Figure 6-4 shows the pushover curve for the two connections overlaid on the ADRS curves (CSM), derived in accordance with the NZTA Bridge Manual and NZS1170.5:2004. Both connections intercept the CALS demand curve before the PT yields. Given that the PT and axial load provide about 60% of the moment capacity for the pier, even if a number of dissipaters were to fracture, collapse would not be expected. Therefore, the structure is protected against collapse and life safety is ensured for both designs. However, the connection explicitly designed for the CALS is more efficient; less materials are used, the base shear demand is smaller and overstrength demands on capacity protected elements are reduced. The only drawbacks being that larger displacements occur in each seismic event and, at the DCLS displacement, the strains in the outer dissipaters exceed 5% (replacement required in smaller seismic events). However, as previously discussed, increased displacements and strains at the DCLS do not mean a sacrifice in performance as the connection can be readily repaired by replacing dissipaters. Moreover, in Chapter 7 it is shown that for mild steel dissipaters if the peak dissipater strain, reached during a seismic event, is less than 6%, only 10-15% of the dissipater fatigue life is utilised. Therefore, the dissipater will be able to survive future DCLS events and thus not require immediate replacement.

For DCR connections designed to the CALS, it would require a 1/1000 annual probability of exceedance earthquake to constitute consideration for dissipater replacement. For the traditionally designed DCR connection it would require a 1/1500 annual probability of exceedance event before replacement of dissipaters is considered. Therefore, the downfall is more frequent replacement of dissipaters. It should be noted that this repair cost is still likely to be considerably smaller than a monolithic connection designed for a 1/1500 APE event that is subjected to a 1/1000 APE event, as concrete cracking/spalling would require repair and there may be uncertainty in the future performance. In addition, considerable assessment would

likely be required to confirm adequate future performance. Consideration is also required for the displacement capacity of the superstructure. Allowing increased pier displacements mean the superstructure needs to be able to facilitate the larger displacements. Therefore, there are limitations on the peak displacement the pier can be designed for.

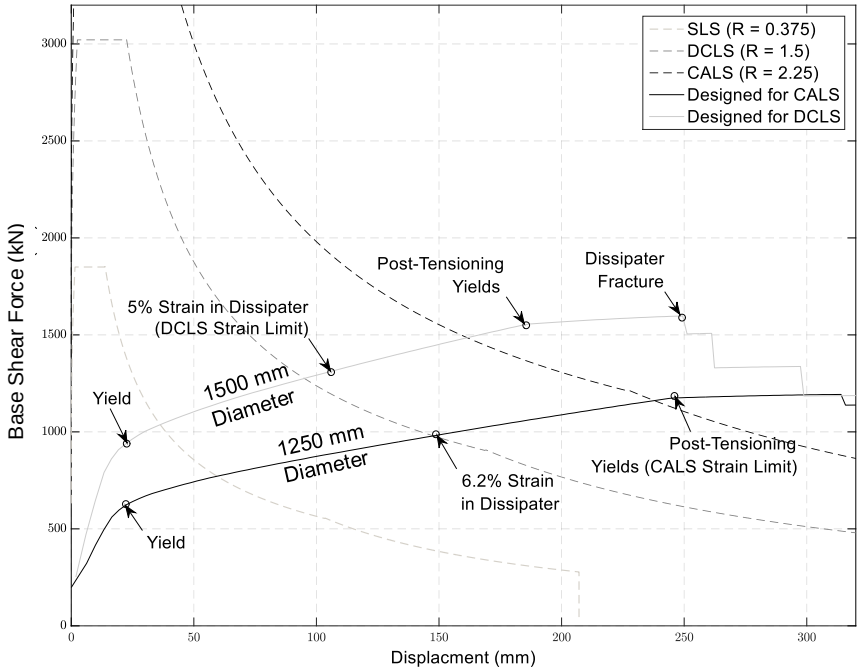

Figure 6-4: Pushover curves for DCR connection designed to satisfy DCLS; and using the alternative design philosophy (i.e. to satisfy CALS but not DCLS) (Pushover curves developed in accordance with the proves discussed in Chapter 8).

Table 6-2 tabulates the connection components used to achieve designs at the respective design levels. It shows that although larger displacements need to be accommodated, base shear demands and the dissipater connection materials can be reduced by about 25%. Moreover, this reduction is satisfied with only a small decrease in performance at the DCLS compared to a DCR connection designed using the current displacement-based design framework. There is no decrease in performance when compared to a monolithic connection. In fact, for all ground motions which exceed the DCLS, the DCR connection designed to the CALS will have better performance with lower repair costs than the monolithic connection. In addition to the material savings tabulated, because of the reduced base shear demand, further material savings will result from requiring smaller piles and pile-caps.

Table 6-2: Comparison between DCR connections designed to satisfy DCLS; and using the alternative design philosophy (i.e. to satisfy CALS but not DCLS

Property	Design - CALS	Design - DCLS	% Difference
Seismic Weight (kN)	3000	3000	0
Pier Diameter (mm)	1250	1500	-15%
Pier Height (mm)	5000	5000	0
DCLS Displacement (mm)	146	105	+28%
CALS Displacement (mm)	250	172	+31%
Number of mild steel dissipators	8	10	-20%
PT Diameter (mm^2)	50	75	-50%
Yield Capacity (kNm)	605kN	920kN	-35%
Base Shear Demand at CALS (kN)	1153	1490	-23%
Initial Stiffness (kNm)	35200	26200	-25%

6.4 CONCLUSIONS

This chapter introduced the benefits of DCR connections, including improved resilience and repairability. It was shown that these connections are not yet widely implemented due to the additional cost associated with these connections (extra construction complexity adds to cost). Therefore, an alternative design philosophy which can increase the cost-competitiveness of DCR connections (or any easily repairable connections with reliable CALS performance) was presented. The change in philosophy, of designing to the CALS and neglecting the DCLS, is a simple one that can promote the efficient design of DCR connections as was demonstrated through a simple example. Although the alternative design philosophy results in higher displacements, it was shown that the connection is still likely to have better performance than the monolithic connection. A simple case study comparing the two philosophies resulted in a reduction in base shear of 23% which results in reductions in moment demand of the foundations.

Chapters 7-9 build upon the alternative design philosophy presented in this Chapter. Chapter 7 outlines strain and performance limits for the DCR connections at the CALS. Chapter 8 provides further inputs into the DBD framework including detailed design tables. Chapter 9 is a case study which illustrates the design process. The performance of the connection, designed using the alternative design philosophy, is compared against traditional DBD through NLTH.

Chapter 7: Appropriate CALS Limits for DCR connections

In the previous chapter an alternative design philosophy, where the CALS is the critical design level, was proposed. Given strain limits for the CALS are not currently well defined for this design level, this chapter presents strain limits for DCR connections that implement grooved mild steel dissipaters and PT. Other mild steel dissipaters are likely to have a similar fatigue life provided they are well detailed. These strain limits are derived using results from NLTH analysis and the low cycle fatigue characteristics proposed by Liu, 2018. In particular, SDOF multi-spring models, designed with various strain limits are subjected to ground motions scaled to the DCLS and CALS. Initially, this Chapter intends to define what levels of damage and strain might be acceptable for DCR connections implemented in bridge piers. This Chapter will propose strain limits for axial dissipaters, PT and propose P-Delta limits.

7.1 INTRODUCTION

Table 7-1 (NZTA, 2018) shows the performance objectives for bridges designed to resist earthquake loading. Previous Chapters (Chapters 5&6) showed that for DCR connections with an armoured interface, the damage is constrained to the dissipative devices and therefore, in a CALS event, these connections provide immediate functionality and post-earthquake repair is easily achievable through replacement of some or all of the dissipaters. The main performance objective at the CALS is to prevent collapse. Theoretically, for a DCR connection, this would allow significant damage to the PT, rupture of some dissipaters and damage to the rocking interface. However, given the improved performance and resilience of DCR connections, it is possible to define strain limits that exceed the performance objectives shown in Table 7-1

Table 7-1: Performance objectives for bridges in NZ (NZTA, 2018).

	Minor Earthquake (SLS)	Design Level Earthquake (DCLS)	Major Earthquake (CALS)
Immediate Functionality	Minimal disruption to traffic. Full functionality is maintained.	Usable by emergency traffic within three days	Usable by emergency traffic after temporary repair.
Functionality post-earthquakee repair	Minimal reinstatement is necessary to cater for all design level actions. All damage to be repairable within one month	Feasible to economically reinstate to cater for all design-level actions, including repeat design level earthquake, and serviceability for traffic.	Capable of permanent repair, but possibly with reduced load capacity.
Acceptable Damage	No Damage to primary structural members. Damage to secondary members and non-structural elements shall not be such as to impede the operational functionality of the structure. Deck joint seals may be dislodged but should be readily reinstatable. Knock of elements should not be damaged or dislodged	Damage may be significant; temporary repair may be required.	Damage may be extensive; collapse prevented.

Table 7-2 shows the authors interpretation of how the performance objectives, shown in Table 7-1, relate to the level of damage in a DCR connection. Achieving these levels of damage would ensure that the connection and hence structure (provided capacity design principles are followed) is repairable after being subjected to a CALS level earthquake. The significant advantage over plastic hinges is that for seismic events between the DCLS and CALS, the connection can be repaired to 100% of the

original capacity by replacing external dissipaters. This implies a constant level of damage between the DCLS and CALS events.

Table 7-2: Performance Objectives for DCR connections.

Minor Earthquake (SLS)	Design Level Earthquake (DCLS)	Major Earthquake (CALS)
No damage to the connection. Gap openings and displacements minimal	Mild steel in dissipaters yields and reaches strains which match DCLS limits. No damage to concrete/steel interface which affects the capacity. Elastic cracking to pier above steel armouring. Potential yielding of PT if it can be easily replaced (not desirable in most circumstances).	PT close to yielding (if unreplaceable). Mild steel in dissipaters reaches CALS strain limits.

To meet the damage levels shown in Table 7-2, PT should be designed to yield at, or just after, the CALS displacement is reached. Conversely, dissipative devices can be severely damaged with rupture to a small number. Rupture is only acceptable because PT and axial load provide around 60% of the moment capacity of the connection (additional elements result in improved resilience). However, in general this should be avoided. Damage to the connection interface should be minimal such as minor cracking (to ensure concrete repairs are minimal or not required at all). P-Delta demands should be limited to ensure collapse is prevented.

7.2 STRAIN LIMITS FOR POST-TENSIONING

Given it is acceptable for the PT to reach yield at the CALS, the corresponding strain limit is simply dependant on the type of PT used. Grade 1030 Macalloy bar was used which has a strain of 0.037 at 70% of the ultimate stress (Macalloy Bar Systems, 2009).

7.3 STRAIN LIMITS FOR DISSIPATERS

Determining the CALS strain limit for dissipative devices is more complex. This is because there is no pre-defined strain limit such as yield. Instead the ultimate capacity of steel dissipative devices is based on their low-cycle fatigue characteristics, which alter depending on the typed of dissipater used (Liu, 2018). A strain limit of 5% has been defined for the DCLS and 8.5% for CALS in the PRESSS handbook (Pampanin et al., 2010). However, these limits were estimated using quasi-static

experimental results that do not necessarily reflect the strain histories which dissipaters are subjected to during a seismic event. In addition, recent work carried out by (Liu, 2018) has quantified the low cycle fatigue behaviour of grooved type dissipaters. This allows the estimation of damage and rupture resulting from low-cycle fatigue to be predicted through NLTH analysis.

Additional complexity is added due to the assumption that it is possible that dissipaters are damaged in seismic events lower than the CALS. Practically, it is assumed that for levels of shaking below the DCLS, dissipaters would not be replaced. In addition, it has been argued that the DCLS design level is somewhat arbitrary and can be altered based on the economic effects of doing so. This allows the DCLS dissipater strain to be altered so long as the combined damage resulting from a DCLS earthquake and from a CALS earthquake is less than 100% (fracture does not occur). It is still important to define a DCLS level and corresponding strain limit as this gives information on dissipater replacement. Obviously, should the asset owner choose to accept a high frequency of dissipater replacement the strain limit at the DCLS could be low and consequently the CALS strain limit would be much higher. This is discussed in more detail in the following sections.

To further understand the implications, and show the concepts discussed above a parametric study was carried out on five connections, each designed to the CALS, using peak strains ranging between 6% and 14%. This allowed the cumulative damage to the extreme fibre dissipater to be determined using NLTH analyses.

7.3.1 Design Inputs

In order to estimate the appropriate strain limit for buckling restrained fuse type mild steel dissipaters, NLTH analysis was carried out on prototype connections. The connections were designed using the alternative design philosophy and displacement-based design. The prototype structure consists of eight super T-beams supported by a single hammerhead pier which carries an axial load of 2520kN. Seismic inputs for the design are shown in Table 7-3. The hazard factor used has been selected to represent areas of relatively high seismicity as this is the most likely application for low damage (DCR) connections. Higher seismic demands could be selected but conditions significantly worse are expected to be rare. Soil interaction has been neglected.

Table 7-3: Earthquake characteristics for design of pier.

Parameter	SLS	DCLS	CALS
Importance Level	3+	3+	3+
Hazard factor, Z	0.3	0.3	0.3
Soil Class	C	C	C
Annual Probability of Exceedance	1/100 years	1/1500years	~1/6500 years
Return period factor, R	0.5 (0.25)	1.5	2.25
Near fault factor	1	1	1
Structural performance factor, Sp	1	1	1

*Importance level 3+ is an importance level specific to the NZTA Bridge Manual (NZTA, 2018) and is defined as a bridge structure situated on a national highway which carries a high number of vehicles per day.

All five of the connections have been designed so that the PT yields beyond the CALS. The fuse lengths (Table 7-5) were altered so that the dissipater strain at the CALS varies between 6% and 14%. For DCR connections, this can be easily done by simply altering the length of the dissipater. However, there are limitations on this, as the length increases relative to the diameter (dissipater becomes slenderer) the dissipater becomes more prone to global instability (dissipater buckling) and hence premature failure (Sarti, 2015). This analysis assumes the dissipaters are designed with thick anti-buckling tubes such that global instability is prevented.

The DCR connection capacity selected represents the weakest possible connection that satisfies the CALS level. This is done by using the smallest PT bar diameter that is able to ensure recentering along with the minimum mild steel area. In addition, base shear demands were based on the maximum displacement the structure could reach without yielding the PT. This is essentially the basis of the alternative design philosophy. Therefore, the weakest possible connection was designed using the alternative design philosophy.

The resulting pushover curve crosses the ADRS curve at a higher displacement and lower force than would typically be allowable using traditional design strategies. The initial PT force is set to be less than 10% of the yield force. The reason for this configuration is to ensure the displacement demand on the pier, and consequently strain demand on the dissipaters, is equivalent to the maximum feasible demands on this type of connection. Higher initial prestress would lead to less remaining strain capacity in the PT and lower displacement capacity of the pier resulting in lower strain demands in the dissipaters. The final pier dimensions are shown in Table 7-4. The

fused length of the dissipaters was then altered to achieve the range of strain levels shown in Table 7-5.

Table 7-4: Details of connection used to examine dissipater strain levels.

Prototype pier Details	
Effective height	7000mm
Column Diameter	1200mm
Dissipater Length	Table 7-5
Length of PT	10000mm
Diameter of PT	100mm
Axial Load	2520 kN
Number of Dissipaters	12
Dissipater Area	6100mm^2

Table 7-5: Fuse lengths examined and strain level in DCLS and CALS earthquake events.

Fuse Length (mm)	**400**	**500**	**550**	**600**	**650**	**700**	**900**
DCLS Strain (%)	10	8	7	6.5	6	5.5	4.5
CALS Strain (%)	14	11	10	9	8.5	8	6

The initial strain levels in the dissipaters were determined by using the damped acceleration displacement response spectrum curves overlaid with pier pushover curves. The intercept of the two represents the peak displacement that would be expected in a DCLS or CALS event. An example of the connection pushover and acceleration displacement response spectrum curves is shown in Figure 7-1 for a connection with a fuse length of 500mm. At the CALS the strain in the outermost dissipater is expected to reach 11%.

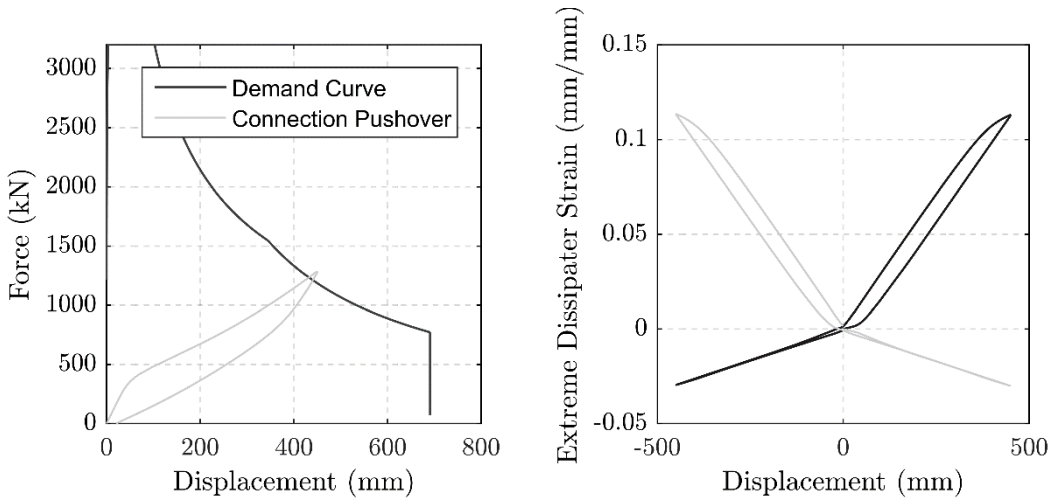

Figure 7-1: Left – CSM for the CALS, Right – Strain demand for extreme fibre dissipater (500mm fuse length)

Determination of the allowable level of strain in a design limit event is determined by the likely strain history and low cycle fatigue damage that is imposed on the dissipater. Not only that, but some consideration must be given to the fact that multiple seismic events could be expected over the lifetime of the structure. Consideration must be given to not only the level at which they will fracture, but also the level of strain or strain history the dissipater has previously been subjected to. In order to estimate the strain history that a given dissipater will be subjected to in a DCLS and CALS event, NLTH analysis has been carried out using ground motions scaled to the DCLS and CALS events (Figure 7-2).

7.3.2 Ground Motion Scaling

Ground motion scaling was carried out in accordance with NZS1170.5:2004 to obtain strain histories for the DCLS and CALS level earthquakes. The elastic fundamental period (T) was calculated to be 0.9s. The ground motion was scaled between 0.4T and 1.3T as set out in NZS1170.5:2004. Initially all ground motions that complied with the k1 (between 0.33 and 3) and D1 (less than log (1.5)) factors where considered irrespective of soil type. K1 is the scale factor which results in minimised error between the target spectrum and ground motion over the period range of interest. For the DCLS there were 104 compatible ground motions and for the CALS there where 57 compatible ground motions. NLTH analysis was then completed and ground motions that excited the model to the largest displacements were selected. Soil types that varied significantly from that assumed in design were filtered out and the

remaining ground motions were checked to ensure they met the family scaling factor (k2). The final ground motions used are shown in Figure 7-2. Ground motions and their scaling factors are listed in Table 7-6 and Table 7-7. There were 11 compatible ground motions at the DCLS and 8 compatible ground motions for the CALS.

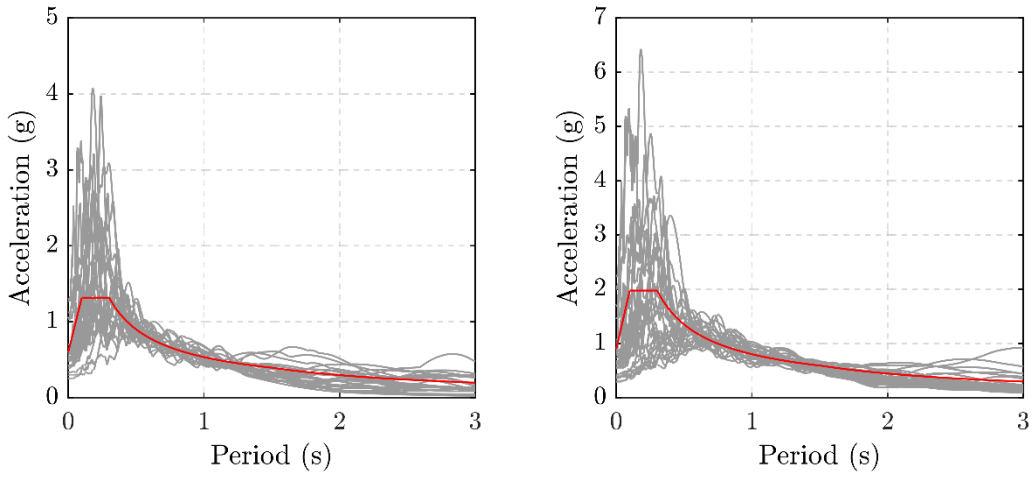

Figure 7-2: Left - Ground motions scaled to DCLS design spectrum (red(, Right – Ground motions scaled to the CALS spectrum (red).

Table 7-6: Ground Motions used for the DCLS analysis.

Record Sequence Number	EQID	Earthquake Name	Year	Magnitude	EpiD (km)	HypD (km)	Soil Class	PGA (g)	PGV (cm/sec)	Scale Factor (k1)
159	0050	Imperial Valley-06	1979	6.5	3	10	D	0.29	33.9	1.71
183	0050	Imperial Valley-06	1979	6.5	28	30	D	0.54	56.8	1.24
292	0068	Irpinia, Italy-01	1980	6.9	30	32	C	0.29	46.9	1.72
571	0109	Taiwan SMART1(45)	1986	7.3	73	75	D	0.17	24.9	1.85
729	0116	Superstition Hills-02	1987	6.5	29	31	D	0.19	32.3	2.90
806	0118	Loma Prieta	1989	6.9	42	46	D	0.21	35.3	2.12
1048	0127	Northridge-01	1994	6.7	3	18	D	0.41	48.0	1.45
1077	0127	Northridge-01	1994	6.7	22	28	D	0.59	31.2	1.50
1120	0129	Kobe, Japan	1995	6.9	13	22	E	0.65	117.1	0.7
1209	0137	Chi-Chi, Taiwan	1999	7.6	55	56	D	0.18	23.3	2.18
1324	0137	Chi-Chi, Taiwan	1999	7.6	136	136	D	0.11	20.9	2.9

Table 7-7: Ground Motions used for the CALS analysis

Record Sequence Number	EQID	Earthquake Name	YEAR	Magnitude	EpiD (km)	HypD (km)	Soil Class	PGA (g)	PGV (cm/sec)	Scale Factor (k1)
159	50	Imperial Valley-06	1979	6.5	3	10	D	0.29	33.9	2.38
183	0050	Imperial Valley-06	1979	6.5	28	30	D	0.54	56.8	1.9
292	0068	Irpinia, Italy-01	1980	6.9	30	32	C	0.29	46.9	2.61
571	0109	Taiwan SMART1(45)	1986	7.3	73	75	D	0.17	24.9	2.77
1077	0127	Northridge-01	1994	6.7	22	28	D	0.59	31.2	2.28
1500	0137	Chi-Chi, Taiwan	1999	7.62	42	43	D	0.1	34.7	3
1528	0137	Chi-Chi, Taiwan	1999	7.62	45	46	D	0.2	61.5	2.66
1535	0137	Chi-Chi, Taiwan	1999	7.62	126	127	D	0.0	8.0	2.57

7.3.3 Time History Model

OpenSEES was used to undertake the NLTH analysis. An axial spring model was selected over the alternative rotational spring model due to the additional details (strain in axial dissipaters) that can be captured using this modelling technique. It also provides additional benefits such as being able to track the neutral axis. Although this typically requires more computational effort than the rotational spring model, due to the simplicity of the model this was insignificant.

The method for modelling this type of connection in OpenSEES was based on the method proposed by (Sarti, 2015). First conceived by Spieth et al., (2004), this method was further adapted and compared by (Palermo, 2004; Pampanin et al., 2010). Further adaption so that the specific geometry can be used, eliminating the need for calibration based on moment-rotation analysis was carried out by (Liu, 2018). However, it still requires that the axial springs and locations be correctly defined. Previously, (Sarti, 2015) found that the Lobatto quadrature rule provided sufficient accuracy to estimate the location and weighting of the axial springs for rectangular sections. However, (Liu, 2018) found that using the Lobatto quadrature integration rule provided insufficient accuracy to replicate the experimental results for a circular connection and instead proposed the use of a multi-dimensional numerical integration (cubature) rules. This method inherently accounts for the geometry of the section when defining weightings of integration points (location of springs) and was found to accurately represent the experimental behaviour. Therefore, this methodology was adopted for the analysis undertaken in the following sections. The spring locations used and their weighting are shown in Table 7-8. The weighting represents the portion of the total connection stiffness to be applied to the axial spring (Section 7.3.6).

Table 7-8: Weighting and spring locations for a 1D circular sections (compressed from a 2D integration rule).

Spring Location	Weighting
±0.4596D	*w1 = 0.0376*
±0.3718D	*w2 = 0.0753*
±0.2979D	*w3 = 0.0512*
±0.2410D	*w4 = 0.1025*
±0.1420D	*w5 = 0.0753*
±0.0921D	*w6 = 0.1025*
0	*w7 = 0.1111*

The overall modelling scheme is illustrated in Figure 7-3. As shown the super-structure mass, which includes the deck, beams and 1/3rd of the column is assumed to act at the centre of mass, 7m above the point of fixity. The PT bar is 10m long, which accounts for the embedment length in the foundation and pier cap. The compression only springs and dissipaters are pinned at the ground level (along the black line). Though the pier cap is shown, this was not included in the model. The individual elements are discussed in the following section.

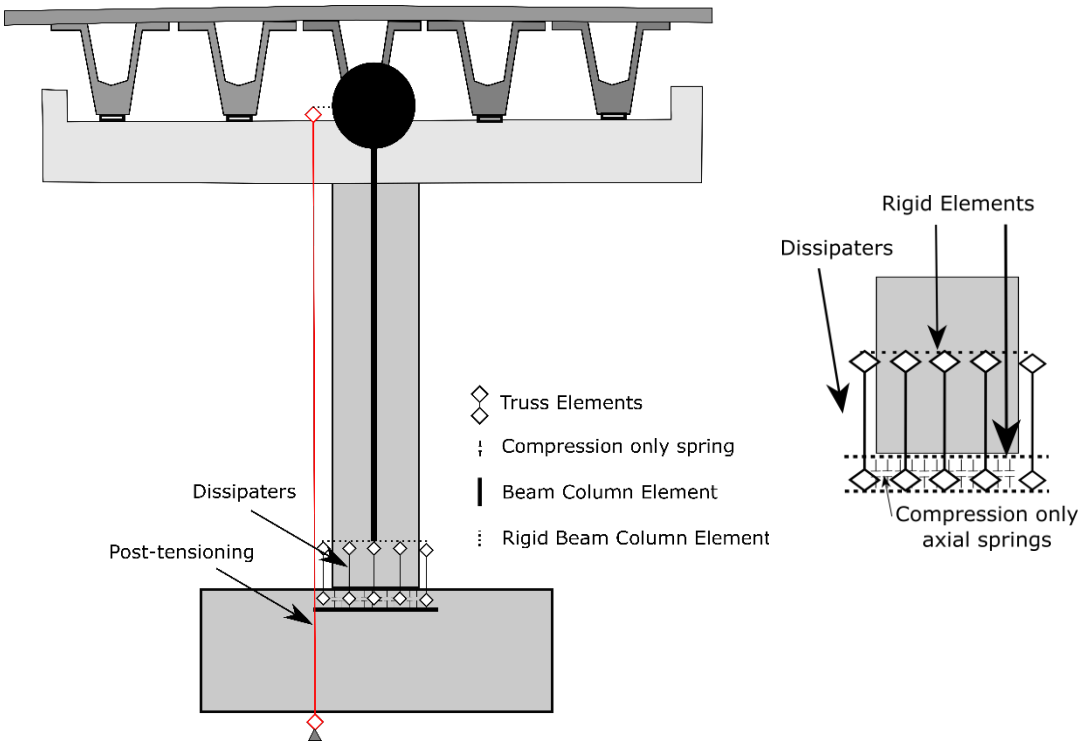

Figure 7-3: Structural scheme of OpenSEES model.

7.3.4 Mild Steel Dissipaters

The mild steel dissipaters were modelled using a Giuffré-Menegotto-Pinto model (Steel02). The inputs used are based on test data for the four groove type dissipaters discussed in Chapter 10. The data for this type of dissipater (Table 7-9) is calibrated based on experimental testing and was retrieved from (Liu, 2018). The variable definition can be found in the OpenSEES user guides.

Table 7-9: Material values used for input into OpenSEES model (Steel02).

E_0 (GPa)	σ_y (MPa)	b	R0	cR1	cR2	a1	a2	a3	a4	sigInit
200	300	0.008	20	0.925	0.15	0.04	1	0	1	0

To capture the low cycle fatigue behaviour of the dissipaters, a fatigue material was used with the inputs outlined in Table 7-10 (obtained from (Liu & Palermo, 2020)). This element uses the log-log relation based on the Coffin-Manson relationship discussed in Chapter 2&4. In addition, the model uses Miners rule (Miner, 1945) to record the accumulated damage. Damage of 1.0 or 100% represents failure of the

element. The fatigue characteristics (Table 7-10) have been based on the calibration of the fatigue curve for the four groove dissipaters carried out by (Liu & Palermo, 2020).

Table 7-10: Material values used to model the fatigue in OpenSEES.

E0	***m***	***Max***
0.1887	0.43	0.2

E0 is the monotonic strain capacity and ***m*** is the slop of the Coffin-Manson curve in log-log space and ***Max*** is the ultimate tensile strain of the steel.

7.3.5 Post-Tensioning

The material model used for the PT, which consisted of a Macalloy bar (Macalloy Bar Systems, 2009), was a Ramberg-Osgood function. The parameters were calibrated based on the material behaviour specified in the Macalloy Bar Design Manual.

Table 7-11: Material values used for input into OpenSEES model.

E_0 (GPa)	σ_{pty} (MPa)	a	n	ε_{su}
170	880	0.001	25.1	6%

7.3.6 Concrete

The concrete interface is modelled using compression only springs, assigned with linear elastic properties in compression (based on experimental results and steel armouring preventing high strains and crushing etc). The total stiffness of the rocking interface can be calculated using Eq 7-1 below. For an end joint the effective length $Leff$ can be taken as the diameter of the section D (Liu, 2018). Thus, the interface stiffness can be calculated using Eq 7-2.

$$k_{interface} = \frac{EA}{Leff} \qquad 7\text{-}1$$

$$k_{interface} = \frac{EA}{D} \qquad 7\text{-}2$$

Each compression only spring can then be assigned a stiffness based on the interface stiffness and weightings from Eq 7-3.

$$k_{i,spring} = k_{interface} \times w_i \qquad 7\text{-}3$$

(Liu, 2018) showed that modelling in this way resulted in the modelled system being less stiff than the experimental system. In Liu's analysis, the interface stiffness was increased, by increasing the area of the interface. However, this has not been carried out in the present study as a lower spring stiffness will result in larger displacement and strain demands which is conservative when determining the fatigue life of dissipaters.

7.3.7 Verification of Model

Although many of the model components and strategies have been previously developed and validified against experimental test results, further verification is given below for the experimental testing carried out by Liu, 2018. The quasistatic testing parameters are shown in Table 7-12. The key parameters are summarised in Table 7-12. The modelling approach and variables used are discussed in the previous sections.

Table 7-12: Summary of geometrics used in experiments and numerical model.

Parameter	**Value**
Axial Load, N	1028 kN
Effective height, H_e	4000mm
Pier Diameter, D	1000mm
Dissipater Area, A	490mm^2
Number of Dissipaters	8 total
Area PT	1963mm^2

Figure 7-4 shows that the numerical model captures the behaviour of the experimentally tested pier relatively well. There is some disagreement at displacements below 50mm, which is when the neutral axis changes most rapidly,

increasing the capacity of the connection at the lower drifts (increased lever arm). However, in the experimental test the neutral axis shifted much more gradually than is typical. This is thought to be related to a construction imperfection at the interface. Specifically, that the interface was not completely flat and was perhaps slightly curved.

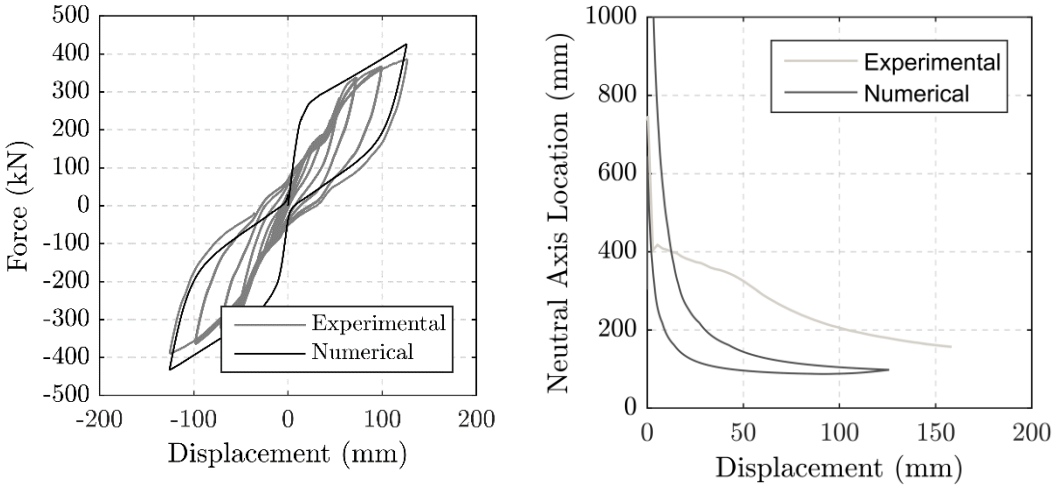

Figure 7-4: Left – Comparison between experimental test and numerical pushover (up to 3% drift), Right – comparison between predicted neutral axis and measured neutral axis.

The strain in the dissipaters is overpredicted by the numerical model by around 1% strain at the peak strain (Figure 7-5). This will result in conservative damage estimates for the model. This is thought to be an acceptable margin of error and give some conservatism when estimating the fatigue capacity of the dissipaters. This verification indicated that the modelling method could satisfactorily be extended to consider the prototype structure.

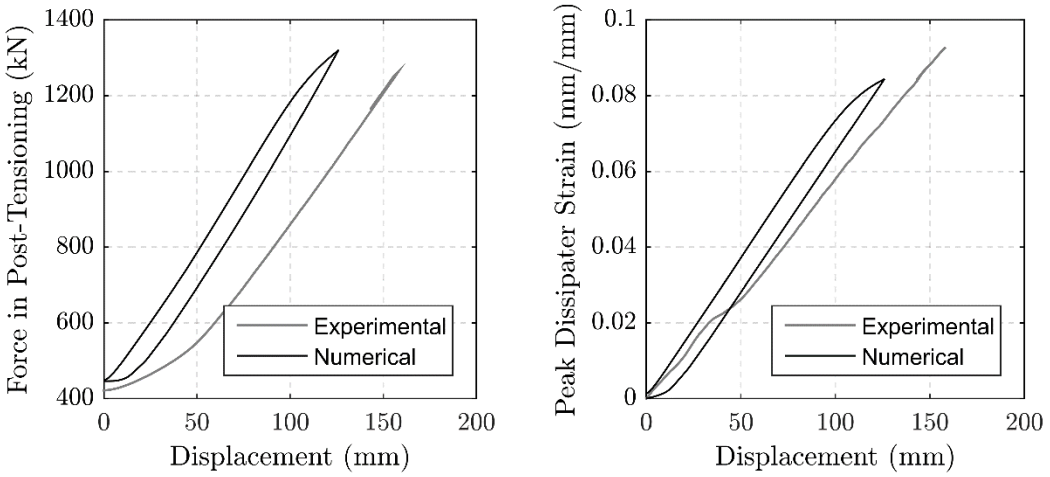

Figure 7-5: Left – Comparison between the predicted force (numerical) and measured force (experimental), Right – Comparison between peak dissipater strain.

Further verification of this model was undertaken through comparison with another experimental test carried out at UC by Liu, 2018. Good agreement was found between the model and experimental response further verifying the applicability of the model.

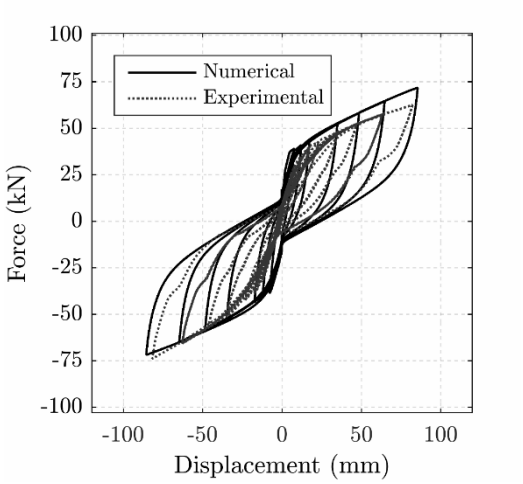

Figure 7-6: Comparison between multi-spring model and experimental results (Liu, 2018)

7.3.8 Damage at the DCLS

The host of models given in Tables 7-4 and 7-5 were then subjected to the scaled ground motions. The cumulative damage in the extreme fibre dissipater on each side of the connection was recorded (OpenSEES using Miners rule) for each ground motion. The results for each of the ground motions is shown in Figure 7-7 to Figure 7-12. 100% damage indicates low cycle fatigue failure of the dissipater has occurred. The results from the analysis are summarised in Table 7-13. In this scenario for the earthquakes selected all significant cycles were complete after 40s.

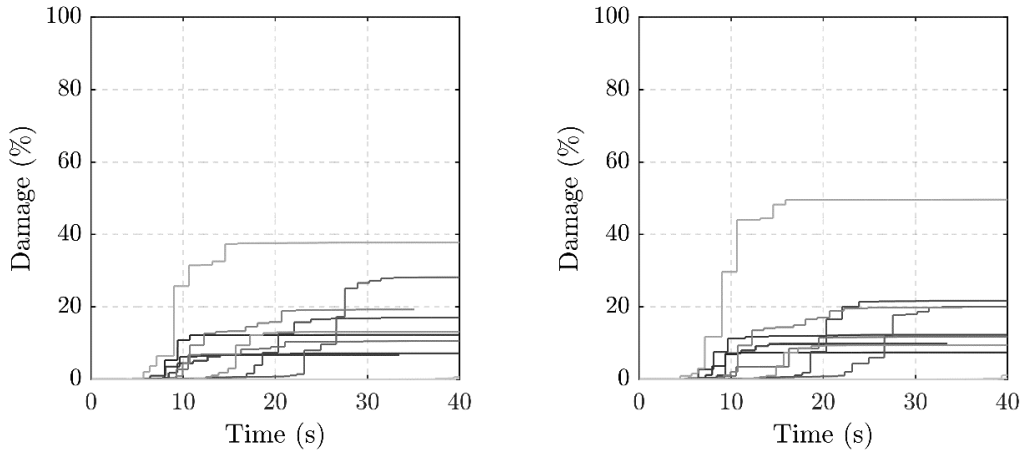

Figure 7-7: Dissipater damage for connections with 400mm unbonded dissipater length. Left represents the LHS and right represents the RHS dissipater.

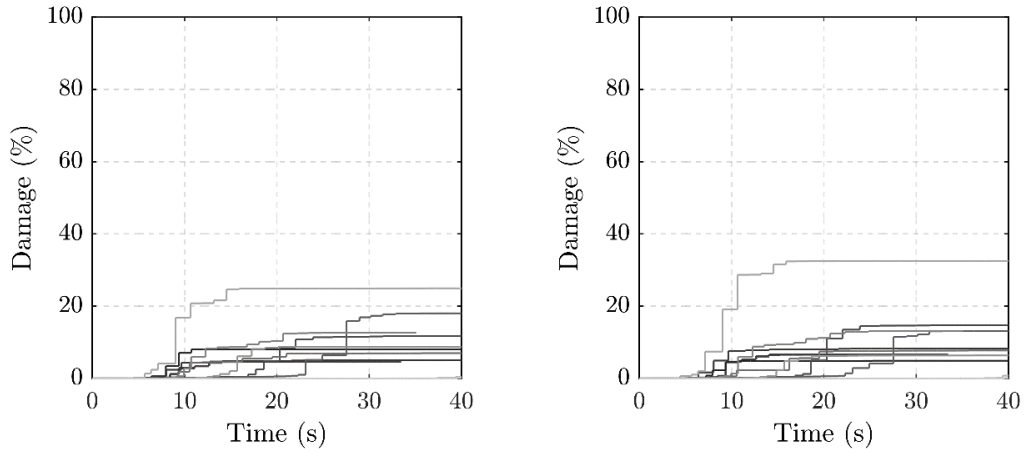

Figure 7-8: Dissipater damage for connections with 500mm unbonded dissipater length. Left represents the LHS and right represents the RHS dissipater.

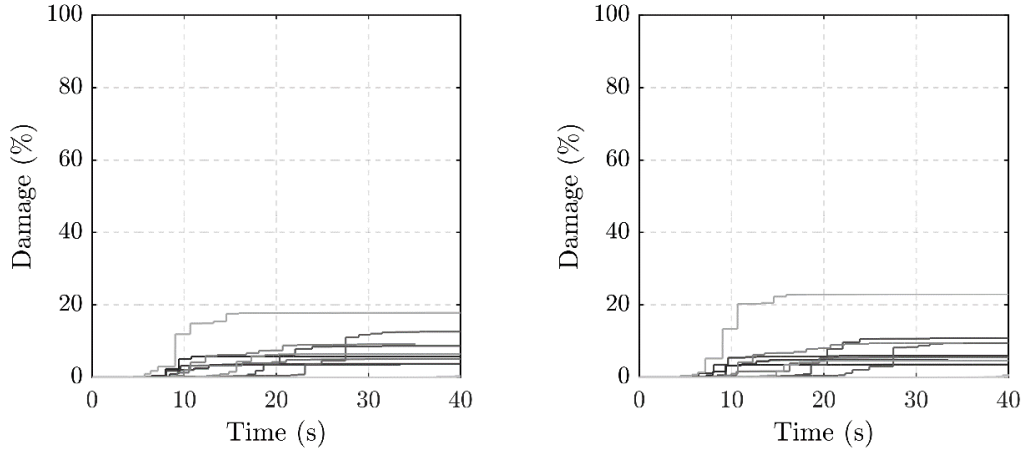

Figure 7-9: Dissipater damage for connections with 600mm unbonded dissipater length. Left represents the LHS and right represents the RHS dissipater.

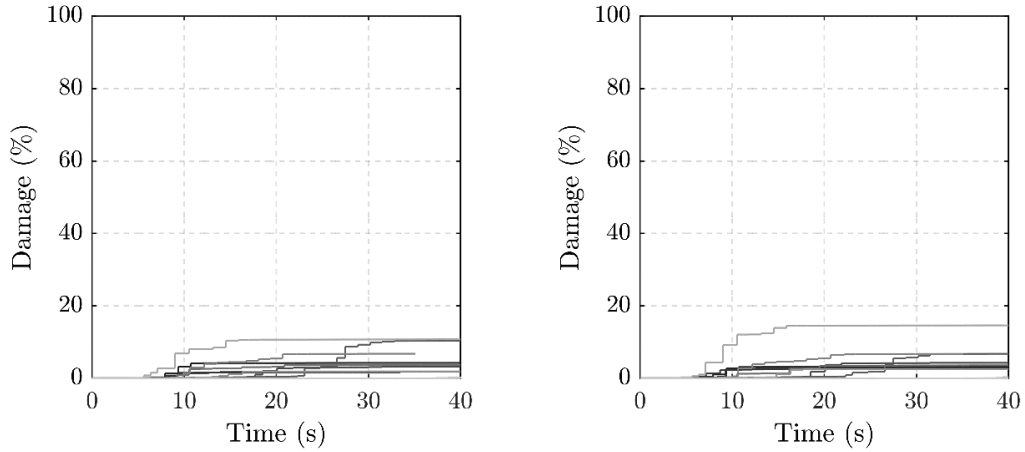

Figure 7-10: Dissipater damage for connections with 650mm unbonded dissipater length. Left represents the LHS and right represents the RHS dissipater.

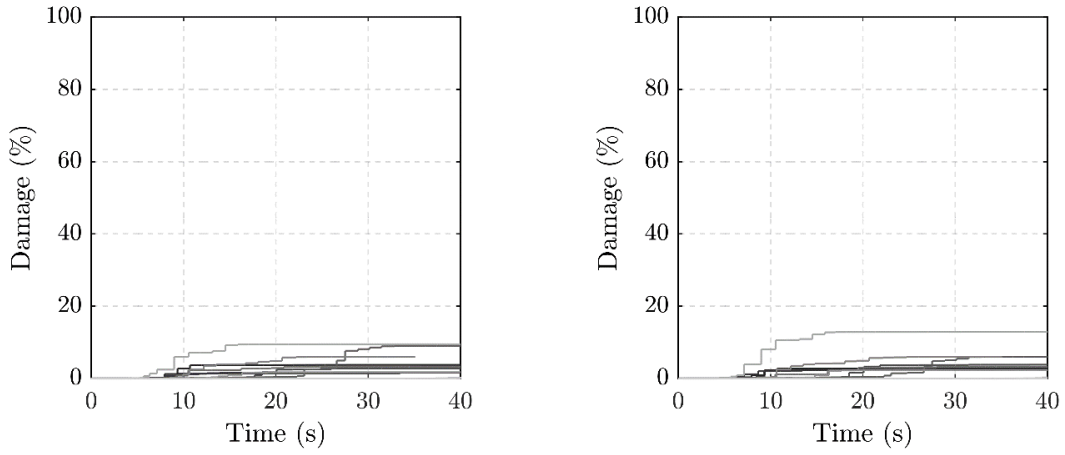

Figure 7-11: Dissipater damage for connections with 700mm unbonded dissipater length. Left represents the LHS and right represents the RHS dissipater.

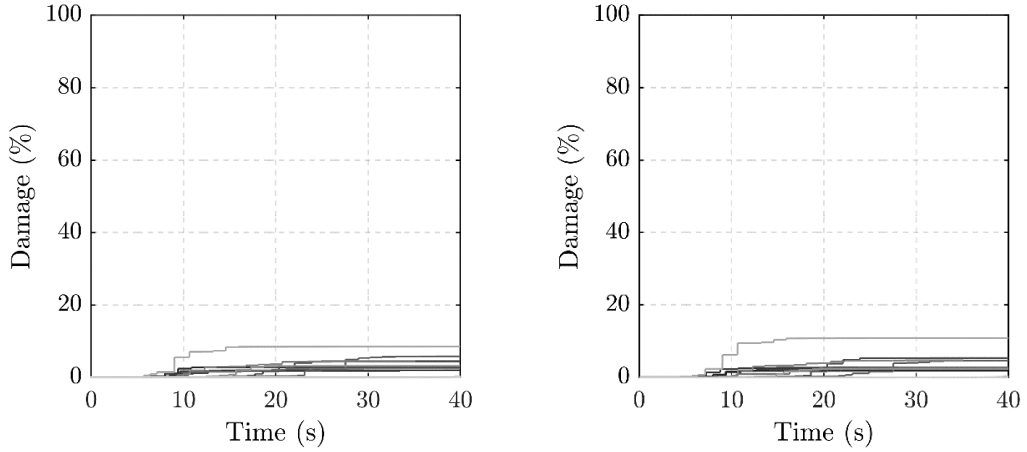

Figure 7-12: Dissipater damage for connections with 900mm unbonded dissipater length. Left represents the LHS and right represents the RHS dissipater.

The peak displacement recorded in all cases was within 10% of the estimated peak displacement of 325mm which was derived from the CSM. This allows a good estimation of the number of cycles and the consequent expected fatigue life demand on the four-grooved dissipater. The results show that the shorter unbonded lengths lead to higher peak strains and therefore more of the fatigue life is utilised. For peak strains of around 10%, almost half of the fatigue life was used and for peak strains of 5% only a tenth of the fatigue life was used. Current guidelines, specifically the PRESSS handbook (Pampanin et al., 2010) recommend a damage control limit state strain of 5%, which would result in the utilisation of a 10^{th} of the fatigue life. Table 7-14 shows

the fatigue life used if the structure is subjected to two DCLS events. However, this will be discussed further in the next section as the CALS is the critical design level.

Table 7-13: Summary of total dissipater damage for extreme fibre dissipater after a single DCLS earthquake.

	Unbonded Length of Dissipater (mm)					
	400	**500**	**600**	**650**	**700**	**900**
Peak Displacement (mm)	346	348	349	342	343	349
Peak Dissipater Strain (%)	10.3	8.4	7.3	6.4	6	5.1
Cumulative Damage (%)	49.6	32.4	23	14.5	12.8	10.8

Table 7-14: Summary of total dissipater damage for extreme fibre dissipater after two DCLS earthquakes.

	Unbonded Length of Dissipater (mm)					
	400	**500**	**600**	**650**	**700**	**900**
Peak Displacement (mm)	346	348	349	342	343	349
Peak Dissipater Strain (%)	10.3	8.4	7.3	6.4	6	5.1
Cumulative Damage (%)	99.2	64.8	46	29	25.6	21.6

7.3.9 Damage at the CALS

The connection described in Table 7-4 was also subjected to earthquakes scaled to the CALS level. The results for all ground motions and each unbonded length of dissipater are shown in Figure 7-13 to Figure 7-18. It becomes immediately obvious that the fatigue damage is much more severe for the CALS. This is due to the nature of low-cycle fatigue, where a small number of high strain cycles cause more fatigue damage than a high number of lower strain cycles (See Chapter 2 and 4 for further details on low cycle fatigue characteristics). The results are summarised in Table 7-15.

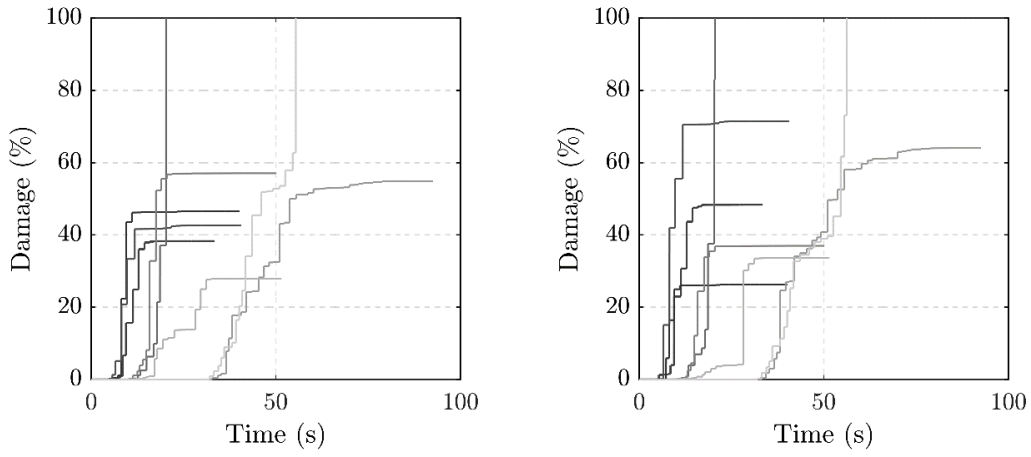

Figure 7-13: Dissipater damage for connections with 400mm unbonded dissipater length. Left represents the LHS and right represents the RHS dissipater.

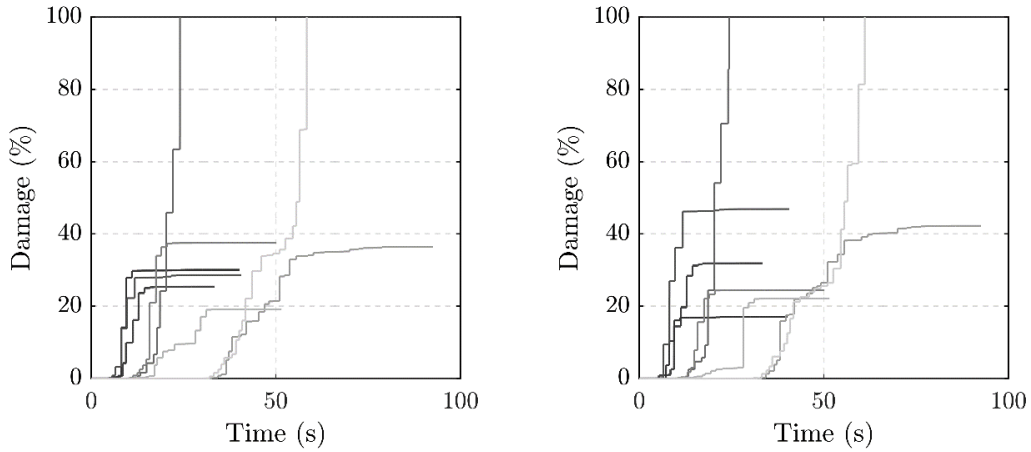

Figure 7-14: Dissipater damage for connections with 500mm unbonded dissipater length. Left represents the LHS and right represents the RHS dissipater.

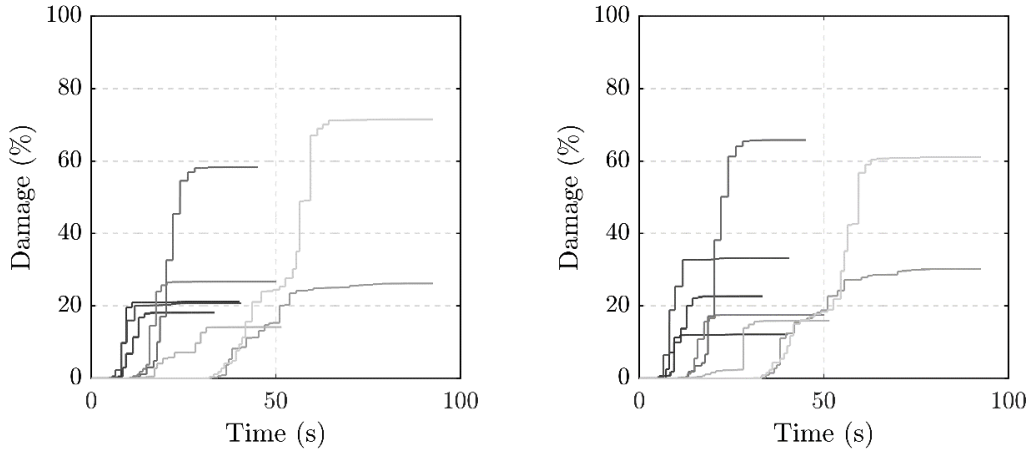

Figure 7-15: Dissipater damage for connections with 600mm unbonded dissipater length. Left represents the LHS and right represents the RHS dissipater.

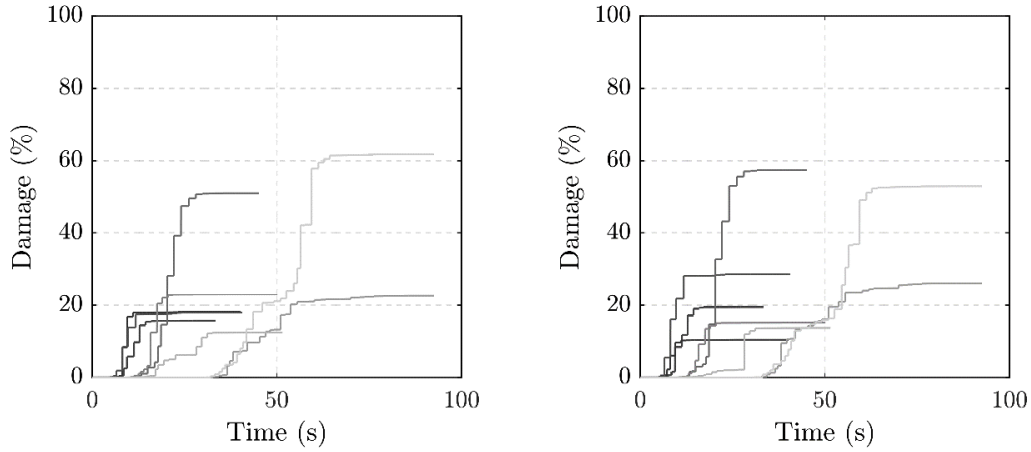

Figure 7-16: Dissipater damage for connections with 650mm unbonded dissipater length. Left represents the LHS and right represents the RHS dissipater.

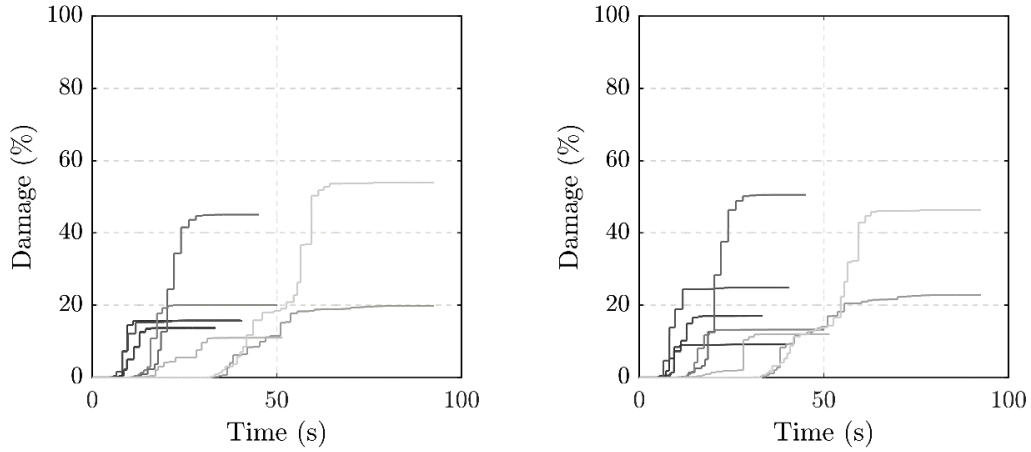

Figure 7-17: Dissipater damage for connections with 700mm unbonded dissipater length. Left represents the LHS and right represents the RHS dissipater.

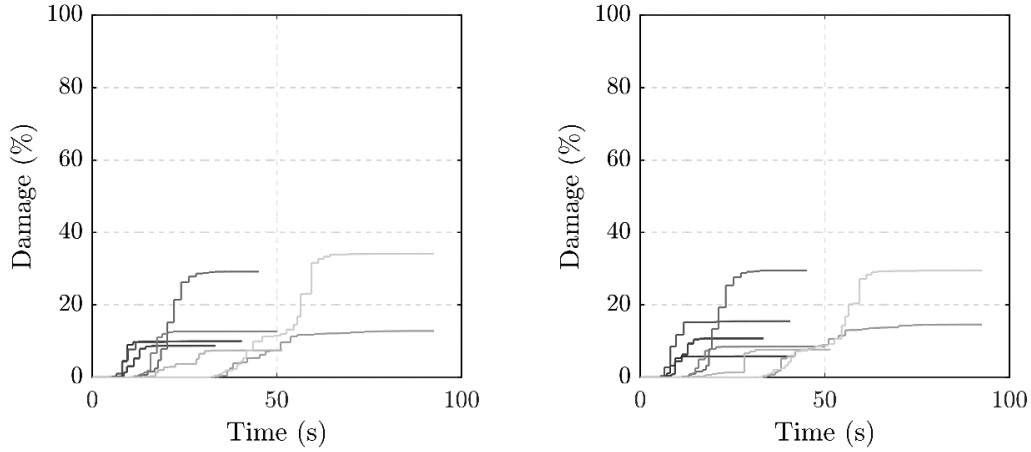

Figure 7-18: Dissipater damage for connections with 900mm unbonded dissipater length. Left represents the LHS and right represents the RHS dissipater (100 seconds included all the significant acceleration cycles).

The peak displacement recorded in all cases was within 10% of the estimated peak displacement. This resulted from selection of the ground motions to provide a good representation of the strain history and expected fatigue demand on the four-grooved dissipater during a design level event. The results show that the shorter unbonded lengths led to higher peak strains and therefore, more of the fatigue life is used. For peak strains above 12% the dissipaters would be expected to fracture and for peak strains of 6% only a 3rd (35%) of the fatigue life was used. Current guidelines, specifically the PRESSS handbook (Pampanin et al., 2010) recommend a collapse avoidance limit state strain of 7.5%, which would result in the utilisation of between 44% and 51% of the fatigue life. Therefore, if the dissipaters are to be replaced in every seismic event, a strain limit (for the CALS) could be as high as 11%. Although this is possible, for the repairable DCR connections it is not altogether that practical. Therefore, the two following options are most practical.

1. Set a DCLS strain level that must be adhered to and set the CALS so that the dissipaters can go through a DCLS and CALS event (fixed values for all connections).
2. Set the DCLS strain limit based on economics and cost of repair and set the CALS limit to ensure a CALS event can be sustained (a higher DCLS limit will reduce the CALS limit).

Table 7-15: Summary of total dissipater damage for extreme fibre dissipater after a CALS earthquake

	Unbonded Length of Dissipater (mm)					
	400	**500**	**600**	**650**	**700**	**900**
Peak Displacement (mm)	460	460	459	459	459	459
Peak Dissipater Strain (%)	14.7	11.9	10.5	9.1	8.5	6.1
Cumulative Damage (%)	100	100	72	61	53	35

It is recommended that both DCLS and CALS strain limits be specified (Option 1). The reason for this is that they can be adopted without use of the alternative design philosophy and it also keeps the design process simple. Table 7-16 and Table 7-17 have been provided should Option 1 be preferred. These tables show the amount of low cycle fatigue damage estimated for a DCLS event followed by a CALS event. If a DCLS strain level of 6% and a CALS strain of 9% is selected the fatigue life used after

sequential DCLS and CALS events is less than 74%. Alternatively, if the client wished to reduce the risk of repair, a higher DCLS strain limit could be selected and lower CALS strain limit could be selected. Further reduction in risk could be achieved by designing the dissipaters for two DCLS events and a CALS (Table 7-17). The risk can most easily be quantified in displacement-based design by setting the design displacement to that which correlates to the strain level of interest and altering the risk factor (R) until the force demand is below the capacity provided. The risk factor correlates to the annual exceedance probability which indicates the risk.

he values tabulated are highly sensitive to the ground motion type, and scaling method used. Moreover, ground motions are highly variable and the host of compatible ground motions is relatively small. In addition, the ground motions are selected to specifically match the design spectrum displacement. Therefore, it would be prudent to err on the conservative side when selecting the appropriate strain levels. However, these strain levels represent the peak strains in the outermost dissipater and therefore even pushing the connections further than the design level would result in the fracture of only the outermost dissipater which provides a small percentage of the capacity (4% for 10 dissipaters in a connection where the mild steel dissipaters only provide 40% of the sections capacity). Given these points, the fact that the CALS is approximately 1.5 times the DCLS and the high variability in near and far field motions a DCLS strain level of 6% and a CALS strain of 9% is recommended. This results in less than 74% of the fatigue life of the dissipater being used. The DCLS strain limit aligns well with that used for the steel reinforcing in traditional plastic hinges and provides ample displacement capacity (probably in excess of that which can be accommodated by the superstructure).

Table 7-16 and Table 7-17 show the combined damage for DCLS and CALS events. For example, if the strain level selected at the DCLS is 6% and the damage selected for the CALS is 10.5% the total expected low cycle fatigue damage caused by a DCLS event followed by a CALS event is expected to be 84.8%.

Table 7-16: Summary of combined damage levels (%) for DCLS and CALS earthquakes.

		DCLS Strain Levels					
		10.3	**8.4**	**7.3**	**6.4**	**6**	**5**
CALS Strain Levels	**14.7**	149.6	132.4	123	114.5	112.8	110.8
	11.9	149.6	132.4	123	114.5	112.8	110.8
	10.5	121.6	104.4	95	86.5	84.8	82.8
	9.1	110.6	93.4	84	75.5	73.8	71.8
	8.5	102.6	85.4	76	67.5	65.8	63
	6.1	84.6	67.4	58	49.5	47.8	45

An alternative option is to select the a lower DCLS strain level of say 5% and set the CALS strain level to 10.5%. If using the alternative design philosophy this results in the connection being able to reach larger displacements. The DCLS strain limit of 5% implies that after an earthquake that induces strains larger than 5%, dissipaters require replacement. Therefore, larger displacements can be accepted on the basis of more frequent (or higher risk) of repair. This aligns with the idea that the CALS can be altered based on the risk and cost of repair.

Alternatively, if the client wished to reduce the risk of repair, a higher DCLS strain limit could be selected and lower CALS strain limit could be selected. Further reduction in risk could be achieved by designing the dissipaters for two DCLS events and a CALS (Table 7-17). The risk can most easily be quantified in displacement-based design by setting the design displacement to that which correlates to the strain level of interest and altering the risk factor (R) until the force demand is below the capacity provided. The risk factor correlates to the annual exceedance probability which indicates the risk.

Table 7-17: Summary of combined damage levels (%) for two DCLS earthquake and a single CALS earthquake.

		DCLS Strain Levels				
		10.3	**8.4**	**7.3**	**6.4**	**6**
CALS Strain Levels	**14.7**	199.2	164.8	146	129	125.6
	11.9	199.2	164.8	146	129	125.6
	10.5	171.2	136.8	118	101	97.6
	9.1	160.2	125.8	107	90	86.6
	8.5	152.2	117.8	99	82	78.6
	6.1	134.2	99.8	81	64	60.6

7.4 P-DELTA EFFECTS

Being able to ensure that the PT and dissipative devices can undergo significant drifts before yielding is somewhat redundant if another failure mechanism governs design. P-Delta effects have always been an important consideration for bridges. Typically, for building structures, it would be uncommon to see design drifts exceeding 2.5% due to the damage to non-structural elements. However, for bridges, which are typically taller and slenderer, design drifts are more commonly determined based on material strain limits which allow drifts of more than 4% to be reached. With DCR connections which can achieve higher drifts again due to the control over the unbonded length of dissipaters and PT is even more critical to examine how P-Delta effects could affect or govern the design of these connections. Particularly when designing using the proposed alternative design philosophy.

In the current version of the NZTA Bridge Manual the P-Delta moment is limited to 10% of the pier-base moment capacity at the DCLS. If it exceeds this the design moment is to be increased by 50% of the P-Delta moment. In addition, for reinforced concrete piers, the P-Delta moment is limited to 25% of the pier base moment capacity to prevent ratcheting (Priestley et al., 1996). Ratcheting is where the displacement of a pier increases in one direction rather than the pier being displaced about a zero displacement (pier does not reach zero displacement before being reloaded). This often results in significant residual displacement after a seismic event. These guidelines propose practical limits to ensure that the moment capacity of the connection is

sufficient to prevent significant residual displacements. However, they do not account for differences in mechanics associated with DCR connections to be discussed herein. The mechanics of P-Delta effects and how they relate to dissipative-controlled rocking connections are examined and P-Delta limits are recommended.

As previously discussed current design approaches utilise some form of stability index which compares the magnitude of the P-Delta force at the design level to the design base moment (Eq 7.4).

$$Stability\ Index = \frac{P\Delta_{max}}{M_{DCLS}} \qquad 7\text{-}4$$

In the NZTA bridge manual if this stability index is less than 0.1. P-Delta effects can be ignored. This is consistent with work done by (Park & Paulay, 1975) which indicated that for reinforced concrete buildings a suitable stability index is 0.085. For a stability index larger than the given limit the moment capacity is increased by 50% of the of the calculated P-Delta effect to prevent excess displacements because of the additional moment demand. Another way of countering P-Delta effects is to increase the expected design displacement. This was proposed by Priestley in DDBD (Priestley, Calvi, & Kowalsky, 2007) and is shown Eq 7-5.

$$\Delta^*_{max} = \frac{\Delta_{max}}{1-\theta_\Delta} = \frac{\mu_\Delta \Delta_y}{1-\theta_\Delta} \qquad 7\text{-}5$$

Where,
$$\theta_\Delta = \frac{P\Delta_{max}}{M} \qquad 7\text{-}6$$

Δ_{max} is the max displacement, Δ_y is the yield displacement, μ_Δ the displacement ductility, P is the axial load and M is the moment capacity of the section. The implementation of these methods is only necessary for connections where P-Delta effects are significant. Previous research on these matters indicate that the significance of P-Delta is dependent upon the shape of the hysteretic response. This is explained in depth by Priestley, et al., 2007. Essentially, the findings indicate that the material used and resulting hysteretic behaviour determines whether the connection is likely to be affected by P-Delta effects as shown in Figure 7-19. For the elastoplastic hysteresis after the structure is initially loaded beyond yield, to point A, the structure unloads to B. As a result of further shaking the structure then reloads along the same line at the

same stiffness. Given that B is closer to A than C, it is more likely that further displacement will occur in the positive direction as less excitation is required to reach the backbone curve. Therefore, in a long ground motion, it is likely that D and E would be reached potentially leading to failure, but certainly larger displacements than would be expected if P-Delta effects are excluded from analysis.

The stiffness degrading Takeda hysteresis, which is the preferred hysteretic rule for reinforced concrete, responds quite differently. Because of the reduced unloading stiffness, there is a much smaller residual displacement at B. Additionally elastic cycles cause the residual displacement to reduce along the lines C-D-E as a result of the stiffness degradation. Therefore, the tendency for displacement to accumulate in one direction which would occur with elasto-plastic response is much less likely. Research on this (Priestley et al., 1996) has concluded that provided the second slope stiffness Ks is positive the structural response is stable and the increase in displacement is minor. This was shown to be guaranteed provided P-Delta effects do not exceed 30% of the total moment.

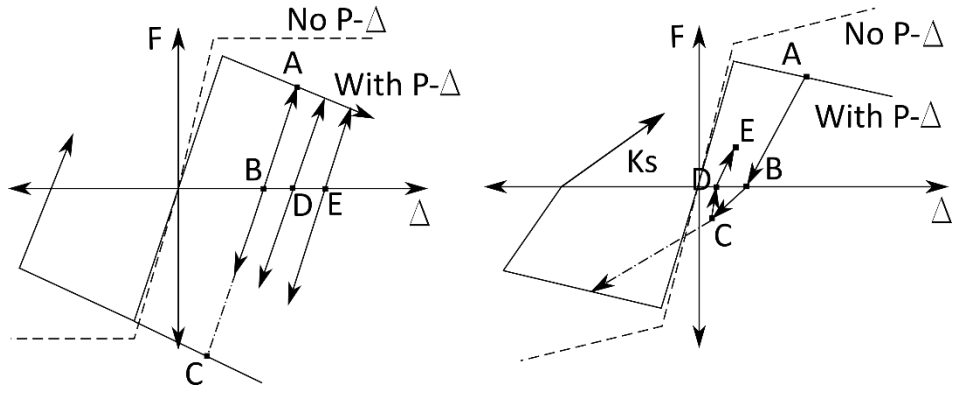

Figure 7-19: Effect of hysteresis rule on p-delta response. Left) Elaso-plastic hysteresis, Right) Degrading Takeda hysteresis.

For DCR connections this logic is even more simple to understand, as after any loading history the connection unloads towards a zero-residual displacement as a result of the recentering capability of the PT. In addition, the PT typically generates a very large post-yielding stiffness as discussed previously. As a result, even with P-Delta effects included, the post yielding stiffness is still typically positive. In addition, the hysteretic behaviour is similar to that of the Takeda hysteresis rule in that it has a tendency to re-center rather than accumulate displacements in one direction. This

means that DCR connections could conservatively be designed under the same guidelines as traditional plastic hinges. However, given the proposed alternative design philosophy which is going to give the potential for DCR connections to reach larger displacements (probably much larger than researched previously), this must be confirmed.

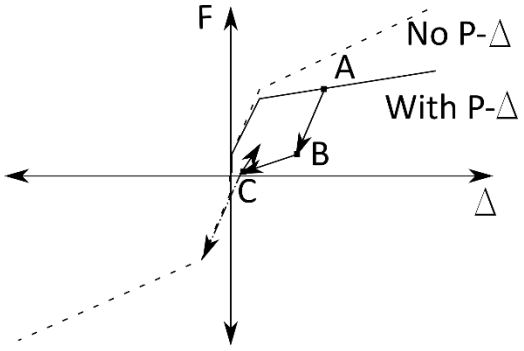

Figure 7-20: Hysteresis response of a DCR connection.

To examine the P-Delta effects on DCR connections a parametric analysis was carried out with the OpenSEES model used to develop suitable dissipater strain limits (Table 7-4). The model was subjected to ground motions scaled to the CALS (Table 7-7).

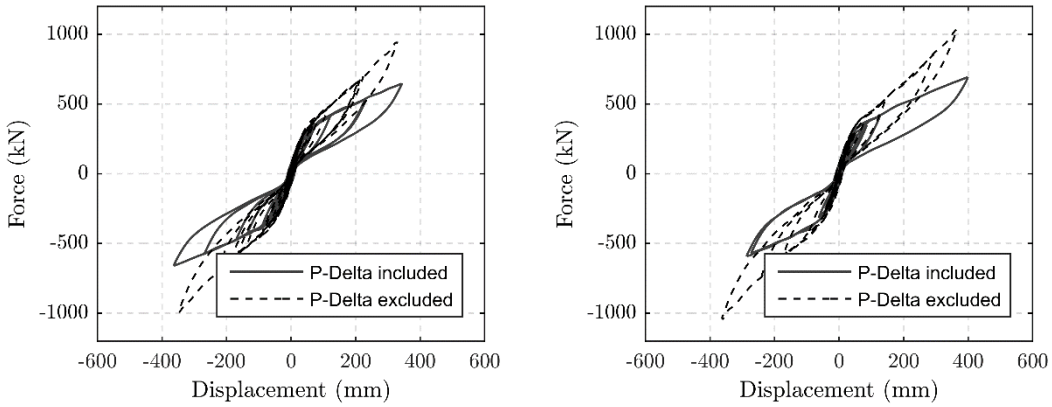

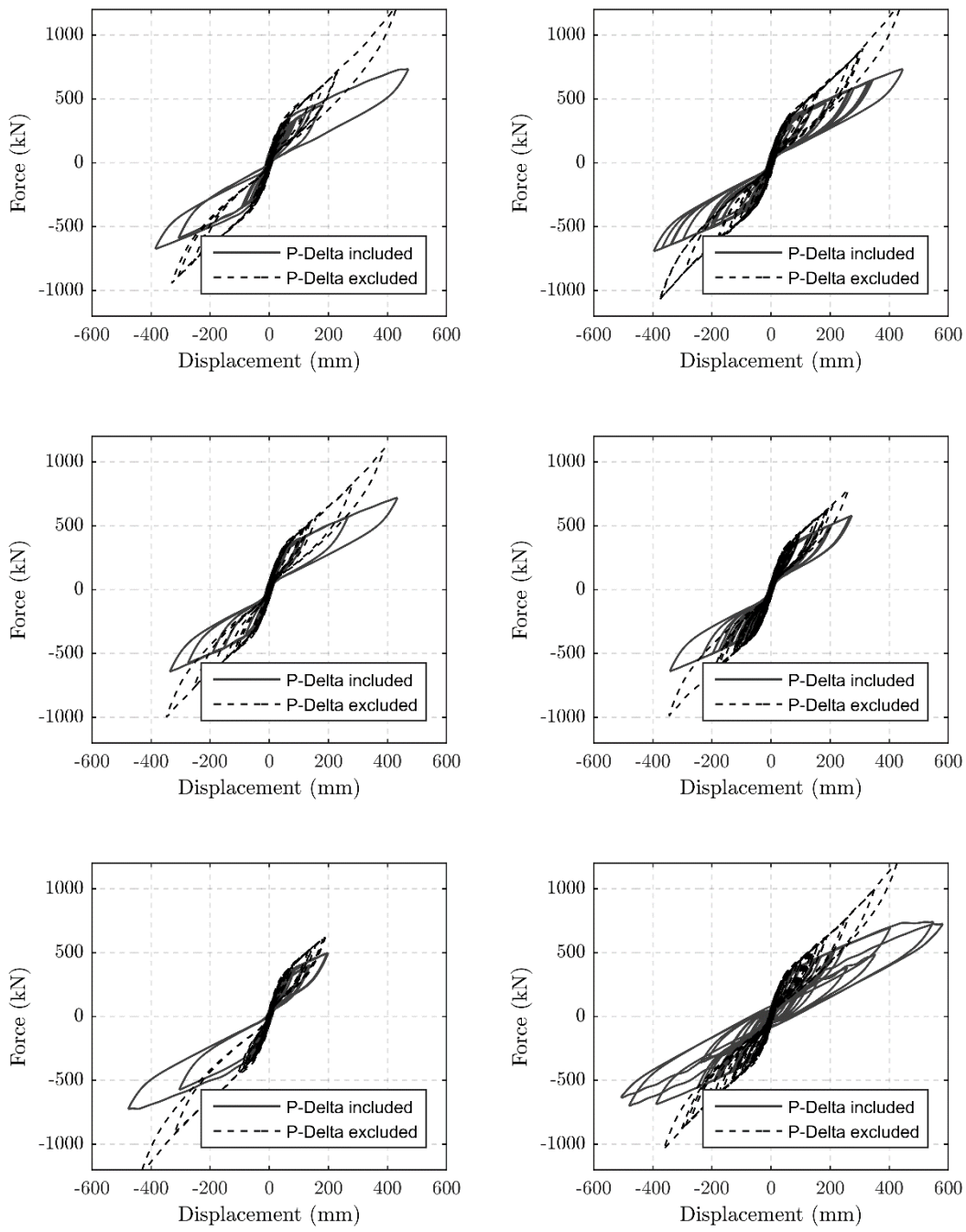

Figure 7-21: The effects of including P-Delta effects.

For this connection, which was designed using the alternative design philosophy, P-Delta effects reduced the moment capacity by up to 40% which resulted in increased displacements of up to 20% (Figure 7-22). In all cases, the P-Delta moment was less than 30% of the moment capacity of the connection. Despite this the displacements still increased by up to 20% which is significant. However, none of the connections became unstable, even though in one instance the additional displacement lead to fracture of a dissipater and yielding of the PT. Another notable point is that increasing

P-Delta demands did not lead to increased displacements, in fact the increase in displacement is relatively constant for all levels of P-Delta moments. This is somewhat controlled by the reduced effective period and the slope of the spectrum at large displacements.

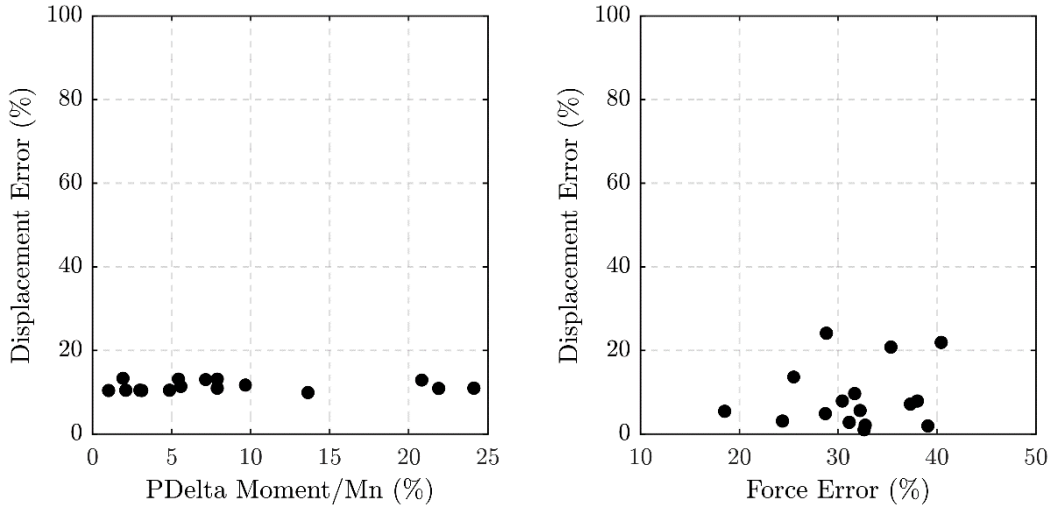

Figure 7-22: Additional displacement and moment demands on the structure due to P-Delta effects (error resulting from ignoring P-Delta effects).

Mn is the nominal moment capacity and the P-Delta moment is found by multiplying the gravity load at the effective height by the peak displacement. The force and displacement error represent the change in displacement or force when compared to the connection with P-Delta effects excluded.

Given there is additional displacement response that results from including the additional moment demand and reduced capacity due to P-Delta it is recommended that P-Delta effects be considered in the design. This can be simply achieved by calculating the capacity with the axial load located at the approximate displaced location and ensuring the capacity is greater than the demands including P-Delta.

For single column piers a logical upper limit on the maximum displacement is when the centre of mass of the pier approaches the critical section neutral axis location. The reason for setting this limit is that the gravity load will contribute to overturning beyond this. In addition, the axial load will no longer act to provide recentering. This is illustrated in Figure 7-23, since the neutral axis location becomes constant at larger drifts, as the pier rocks over the gravity load contribution to moment capacity reduces (due to a reducing lever arm), at the neutral axis location its contribution is zero and beyond the neutral axis location it contributes to overturning. In this scenario, the only

way for the pier to recenter is if the contribution from PT is large enough to overcome both the moment contribution from the dissipaters and the overturning capacity from gravity load which is unlikely.

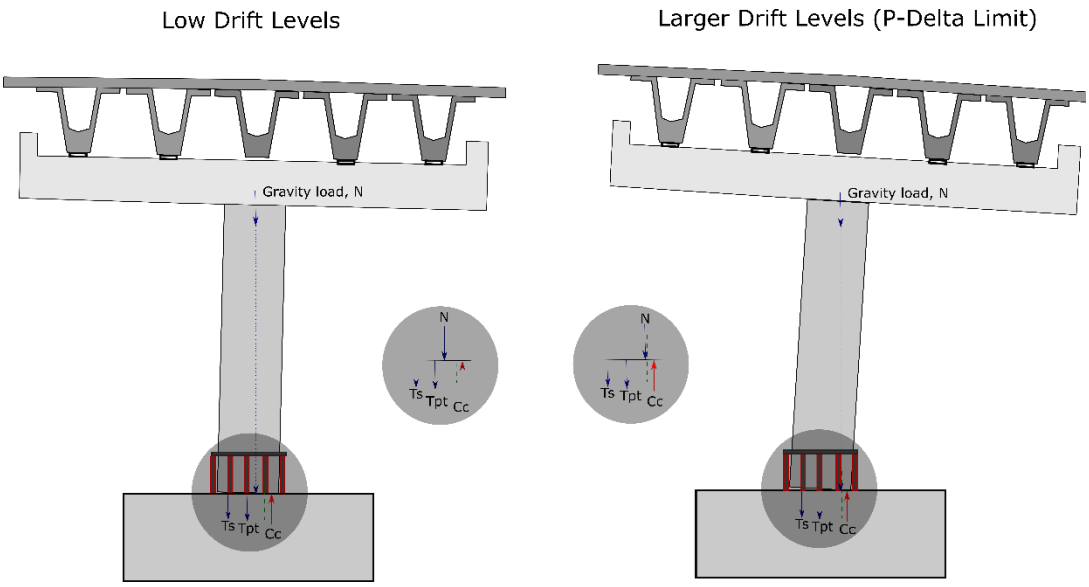

Figure 7-23: Shows how the displacement at the top of the pier influence the section capacity.

For a single column pier with PT at the centre this would yield the following limit for the displacement including P-Delta effects:

$$\Delta_{pdelta} = 0.5D - NA$$

Assuming a diameter of 1000 mm this formulation would result in drift limits of 7% and 3.5% for 5m tall and 10m tall piers respectively. This is probably a conservative upper-bound limit. As shown in Figure 7-24 (left) the deck has some torsional rigidity (dependant on the superstructure) which would provide additional re-centering, altering the location of the axial load application and reducing moment demands. However, this effect is likely to be small for longer, multiple span bridges. A pier bent is less likely to be susceptible to P-Delta demands due to the stiffness of the pier cap which would alter the location of the application of the gravity load as shown in Figure 7-24 (right). Therefore, the pier would have to displace by more than 0.7D before the gravity load contributed to overturning (assuming the gravity load acts at the neutral axis location at the top of the columns).

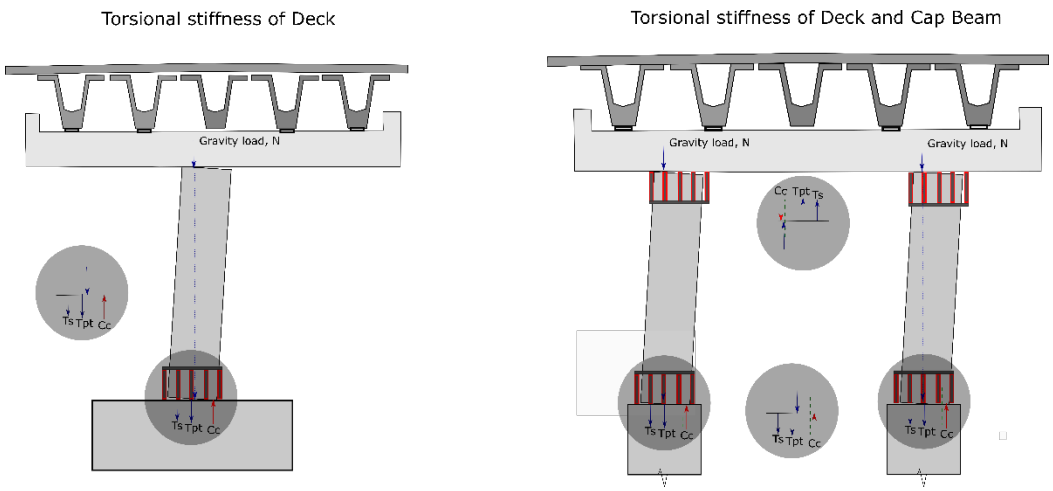

Figure 7-24: Potential effects of deck interaction on piers

7.5 CONCLUSIONS

In this chapter extensive NLTH analysis was undertaken on a prototype bridge pier to determine P-Delta displacements and dissipater strain limits that are applicable to DCR connections. The assumptions made to model this were:

- Base of pier was fixed (pile cap rigid) no soil-structure interaction is assumed.
- The fatigue model proposed by (Liu & Palermo, 2020) accurately predicts rupture of a given grooved axial device.
- Selected ground motions accurately capture the number of cycles (at high strain) that will be experienced by the connections.

These assumptions and the subsequent modelling resulted in the following outcomes:

- PT was defined as being able to reach yield at the CALS.
- Dissipater strain levels were recommended at 9% for the CALS and 6% for the DCLS.
- P-Delta was investigated and found to be significant, thus it's recommended that reductions in capacity and increases in demands be accounted for during design.
- Upper limits on the P-Delta displacements, proportional to the diameter, were proposed for single column piers based on geometric considerations.

To further this research, similar fatigue relationships for G500 dissipaters can be developed. These relations can then be used to derive DCLS and CALS strain limits for these higher-grade dissipaters. Moreover, further development on the type of GM and the expected number of cycles experienced in an earthquake can be completed. Further increases in the strain limits, for G300 dissipaters, could be used if strain ageing affects could be accounted for.

Chapter 8: Parametric Analysis of DCR Connections

8.1 INTRODUCTION

DCR connections are more challenging to design efficiently than traditional plastic hinges. This is because of the additional parameters that can be altered; these include, the unbonded length of PT and dissipaters, the diameter of the PT and the initial prestressing force in the PT. The additional elements can lead to many different connection designs for the same design demand, not all of which achieve the desired efficiency. This chapter provides information for simplifying the design of DCR connections. The key outcomes of this chapter are as follows:

- Development of simplified equations that allow the estimation of yield rotation.
- Development of relationships for determining the neutral axis location (allowing the section analysis).
- Define key design parameters for DCR connections that limit the post-yielding stiffness to allow their application in FBD (same design strategy as monolithic connections – apply overstrength to yield capacity).
- Define geometric ratio ranges that ensure DCR connections can reach their CALS drift.
- Develop design tables that speed up preliminary design.

To undertake these objectives parametric analysis will be undertaken. Specifically, all elements that contribute to each parameter will be defined. From this relationsips will be developed to allow the estimation of the parameters such as the yield rotation and neutral axis location. Similarly, this parametric analysis will allow the determination of geometric ratios, such as the ratio of the unbonded length of PT and connection diameter, that are suitable for the CALS. Finally, the parametric analysis will allow the development of design tables which will further speed up the

design process and allow designers to quickly determine the appropriateness of the DCR connection.

8.2 SECTION BEHAVIOUR OF DCR CONNECTIONS

DCR connections behave differently to plastic hinges. The key differences are that a single crack opens rather than the formation of several flexural cracks as is typically seen in plastic hinges and that unbonded reinforcement and PT violate the strain compatibility conditions. The monolithic beam analogy (MBA) allows member compatibility to be derived by imposing equal member deflections between a system implementing DCR and an equivalent plastic hinge (Pampanin et al., 2001, 2010). This compatibility allows the estimation of the compression strain for a given rotation, ϑ, at the extreme fibre of the DCR connection as shown in 8-1.

$$\varepsilon_c = \left[\frac{\vartheta L_{cant}}{\left(L_{cant} - \frac{L_p}{2}\right) L_p} + \emptyset_y\right] . c \qquad 8\text{-}1$$

.

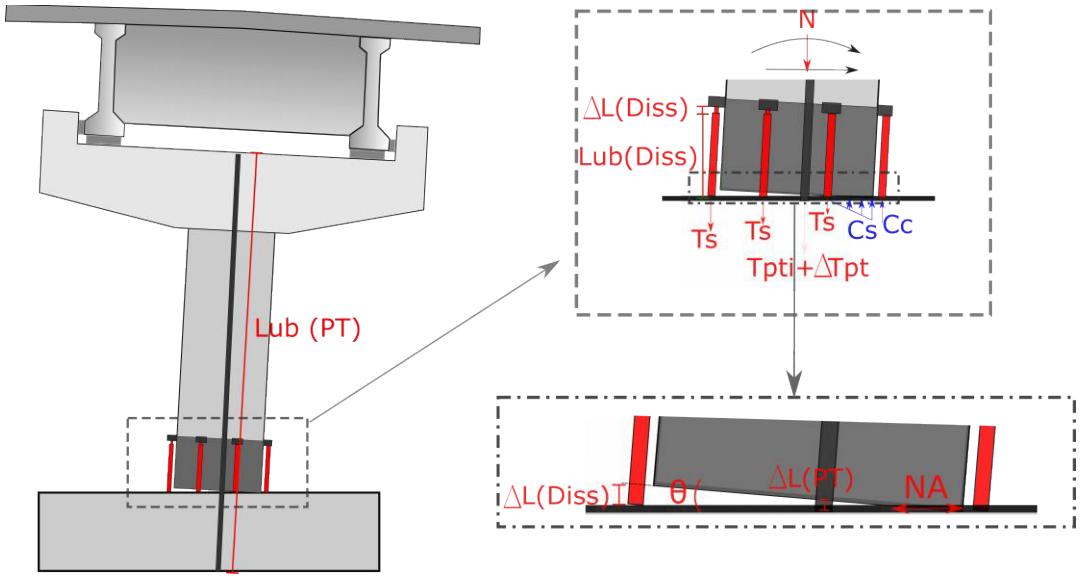

Figure 8-1: Shows the section response for a given rotation θ.

With the compression strain at the extreme fibre known, an assumed linear distribution (for a steel armoured connection) of concrete strains allows the calculation of the resultant compression force in the concrete based on an assumed neutral axis location. As shown in Figure 8-1, once an assumed neutral axis location is determined, the strain in the external dissipaters and post-tensioning can also be calculated through

simple geometry. Forces in each element are calculated using desired material models and the neutral axis is altered such that the sum of the force is 0, as depicted in Figure 8-4. Though this method is termed section analysis it incorporates the unbonded length of PT and dissipaters which is critical.

8.3 MODELLING

Several non-linear modelling techniques have previously been developed and investigated for modelling the behaviour of DCR connections (Palermo et al., 2005, 2007; Pampanin et al., 2001; Sritharan et al., 1999). Previously in this thesis, rotational spring and multi-spring models have been used depending on the purpose of the model, and the detail required. These modelling techniques have various levels of complexity with consequent advantages and disadvantages. Both are well suited to NLTH analysis and require significant user input to alter each model. Therefore, a more simple model was developed and used for this Chapter given that the aim is to develop pushover curves rather than capture variables like the number of cycles experienced in an earthquake.

Matlab was used to develop a simplified axial spring model. Initially, this model was developed to use in NLTH analysis but was computationally inefficient. However, it was sufficient for monotonic loading, and in particular, it lends itself to parametric analysis. This method of modelling allows the investigation of many parameters.

8.3.1 Simplified Axial Spring Model - Matlab

The simplified axial spring model is a hybrid of the axial spring model and section analysis. Section analysis can be easily carried out for DCR connections. Typically, analysis is carried out at key points such as decompression, yield and the design drift. Values between these key points can be interpolated. This method relies on accurately estimating the yield rotation, design drift and any other key points. It is not very accurate for points between the yield and design drift, as this is typically linearly interpolated. In addition, it requires the designer to know when materials will yield (as this will cause a change in stiffness). This method uses the Monolithic Beam Analogy (MBA) (Pampanin et al., 2010), or variations of this such as the revised Monolithic Beam Analogy (rMBA) (Palermo et al., 2017) or ptMBA (Marriot, 2009).

The simplified axial spring model used in this chapter utilises the ptMBA, for sections with external dissipative devices. The ptMBA allows the estimation of the peak concrete strains, which can be used with an assumed distribution, to find the concrete contribution at a given displacement. The model uses material properties and an iterative process to determine the stress-strain behaviour and hence axial stiffness of elements such as the dissipaters, PT and concrete. Each element is represented by an axial spring, with the concrete split into many elements or springs. Then, in a similar manner to plastic hinges, the neutral axis can be calculated by iterating until the sum of axial forces action on the section is zero.

The behaviour of concrete is assumed to be linear. This is acceptable given the concrete has steel armouring to prevent large peak stresses and strains in the extreme fibre of the concrete. Previous experimental testing has validated this assumption.

The PT is modelled using the back-bone curve of the Ramberg-Osgood function (Equation 8-2). The properties used (Table 8-1) are calibrated from technical data for Macalloy bars (Macalloy Bar Systems, 2009).

$$\sigma_{pt}(\varepsilon_{pt}) = E_{pt}\epsilon_{pt}\left(a + \frac{b}{(1 + (c\epsilon_{pt})^n)^p}\right) \qquad 8\text{-}2$$

Table 8-1: Parameters used for the Ramberg-Osgood function.

σ_{pty}	σ_{ptu}	ε_{ptu}	E_{pt}	a	b	c	n	p
830Mpa	1030Mpa	0.06	180GPa	0.01	1.15	215	4.97	0.2

Where the inputs a,b,c,n and P are recommended by (Collins & Mitchell, 1997). The material model for the concrete is assumed to be linear (remains elastic). This assumption is reasonable as long as compression strains in the concrete are below the crushing strain limit, typically assumed to be 0.002. Finally, for the mild steel dissipaters, the path dependant Menegotto-Pinto (Dhakal & Maekawa, 2002) is used. It is noted, that the path dependent Menegotto-Pinto relationship is not fully utilised as only the pushover is required. However, the code implemented was initially developed for NLTH.

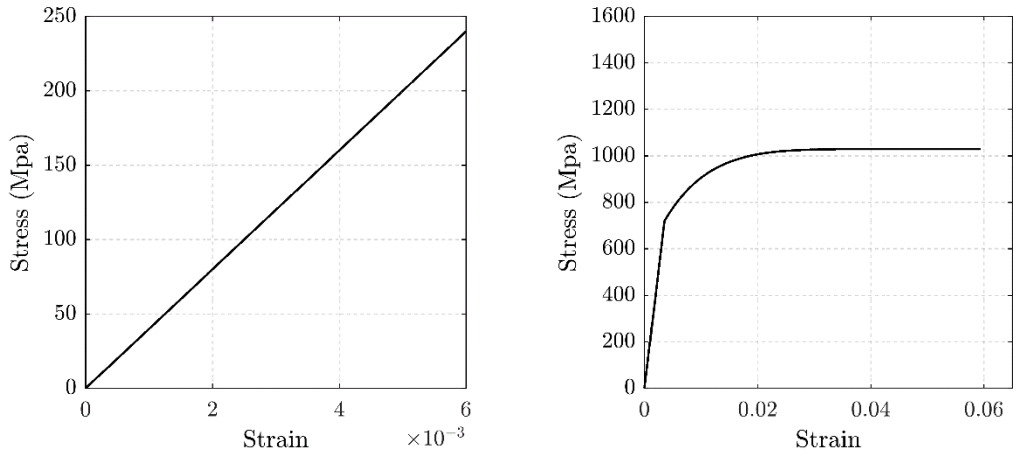

Figure 8-2: Left – Linear stress strain behaviour used for steel armoured concrete ($E = 4700 \times \sqrt{fc28}$), Right – Stress strain behaviour used for PT behaviour.

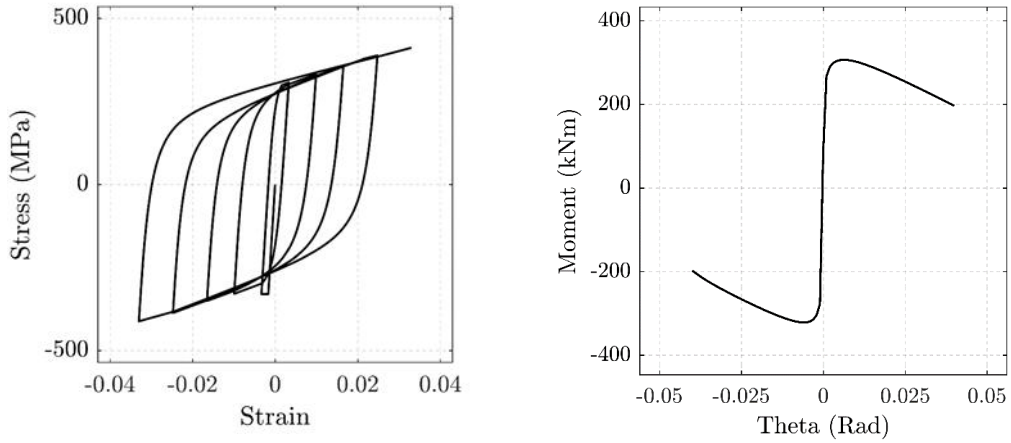

Figure 8-3: Left - Menegotto-Pinto material model used for steel dissipaters, Right – Moment contribution of axial load.

At each timestep, or displacement for a pushover, an iterative procedure is implemented in Matlab to find the strains and stresses in each element such that force equilibrium is reached. The iterative procedure, as shown in Figure 8-4, is used to solve for equilibrium by altering the neutral axis location until the sum of contributing forces is less than a tolerance (1kN).

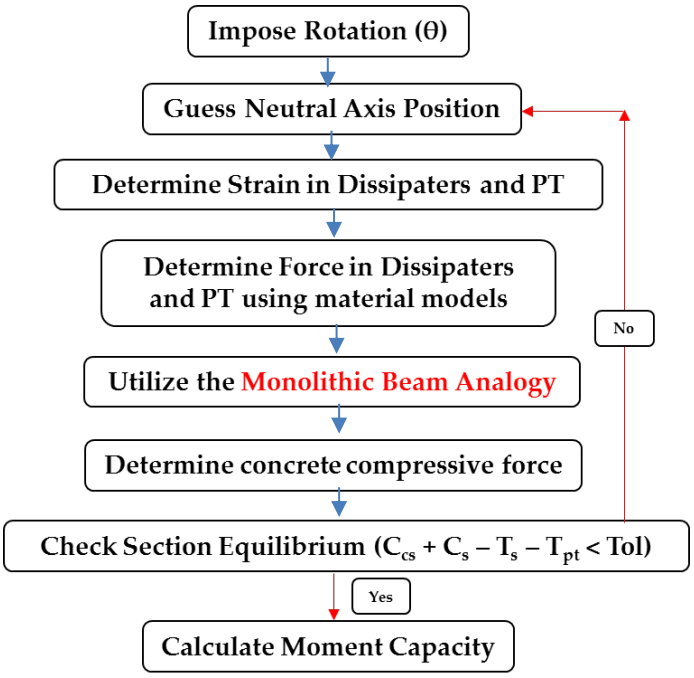

Figure 8-4: Iterative procedure used to obtain section capacity.

Where C_{cs} is steel encased concrete compression force, C_s is the compression force of the dissipaters, T_s is the tension force in the steel dissipaters and T_{pt} is the tension force in the PT.

8.3.2 Model Validation

The model was validated against experimental testing carried out at UoC by Liu et al, (2016) and further verified against testing carried out in Chapter 10. Figure 8-5 and Figure 8-6 show that the numerical model captures the behaviour of the experimentally tested pier relatively well. There is some disagreement at displacements below 50mm which is when the neutral axis changes rapidly, increasing the capacity of the connection at the lower drifts (increased lever arm). However, in the experimental test the neutral axis shifted much more gradually than is typical. This is thought to be related to a construction imperfection at the interface. Specifically, that the interface was not completely flat and was perhaps slightly curved. Similar to the multi-spring model used in OpenSEES, the model over-predicted the dissipater strain. However, at displacements exceeding 150mm (once the neutral axis location converged), good agreement was found.

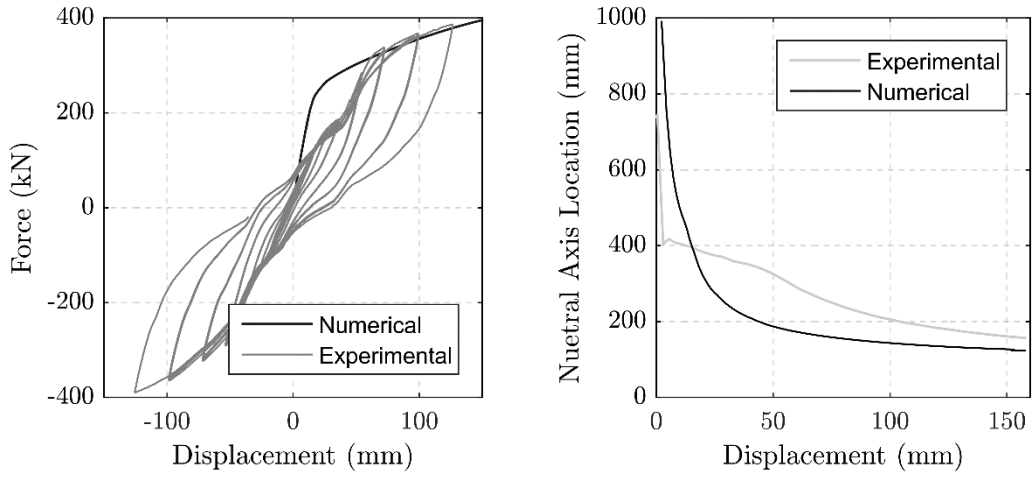

Figure 8-5: Left – Force-Displacement response, Right – Location of the neutral axis.

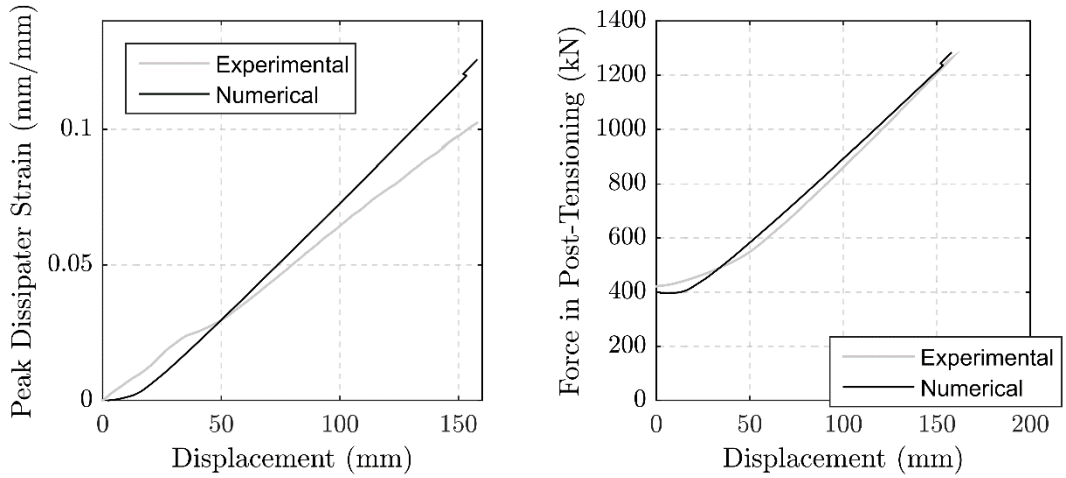

Figure 8-6: Left – Strain in extreme fibre dissipater, Right – Total PT force.

The model was also subjected to the same loading history that was carried out during the experimental testing and compared. The first experiment test was carried out by Liu et al, (2016) . The model, without calibration, accurately predicted the response under these conditions even during unloading. The error between the model and experimental results can be, to some extent, contributed to the experimental imperfections. In this instance significant dissipater slippage due to threads not being fully engaged was noted. The second comparison was made to experimental testing carried out by Liu, 2019. Again, the peak displacements and forces matched the experimental results very well. However, there was some error on the backbone curve, again this is related to experimental imperfections, in this case due to not having a perfectly flat interface. It is concluded that this modelling technique can accurately model the pushover and cyclic behaviour of DCR connections.

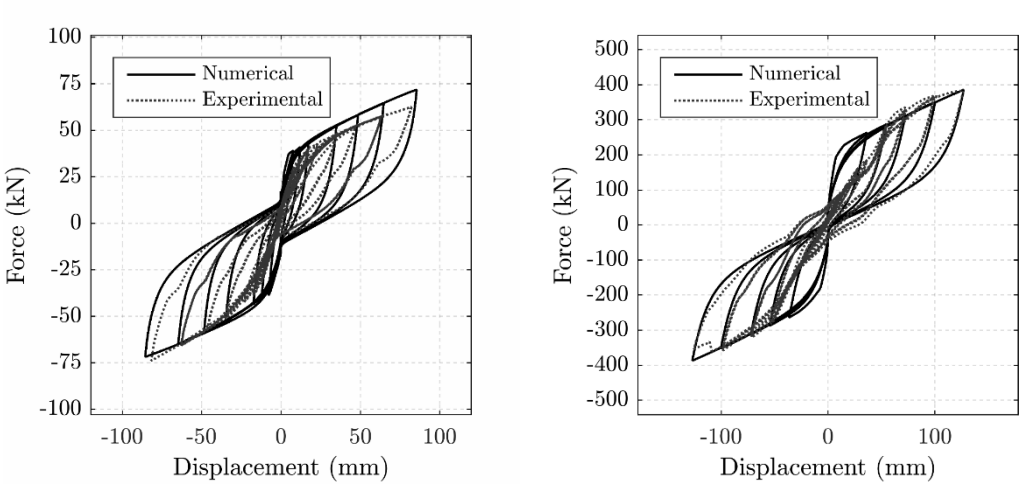

Figure 8-7: Comparison to experimental data obtained from testing, Left – comparison against Liu et al, (2016), Right – Comparison against testing carried out in Chapter 10.

8.4 YIELD ROTATION

As discussed in Chapter 2, the yield rotation is critical for determining the hysteretic damping and hence base shear demands on the pier. For DCR connections, a "yielding" type behaviour is evident for connections that do not include dissipaters, and for those which do (Figure 8-8). It is clear from these figures that this so called "yielding", for connections without dissipaters, is due to the reduction in moment contribution from axial load. This effect is due to the position of the neutral axis and the assumption that the axial load of the superstructure acts at the centre of the pier. The neutral axis quickly reaches a level where it becomes stable and changes only very slightly. Conversely, the top of the pier constantly increases in displacement. Therefore, the lever arm between the neutral axis and centre of the pier top is always decreasing (once the neutral axis becomes stable). Although this does look like yielding, it is a geometrical non-linearity and therefore not included within the determination of the yield rotation.

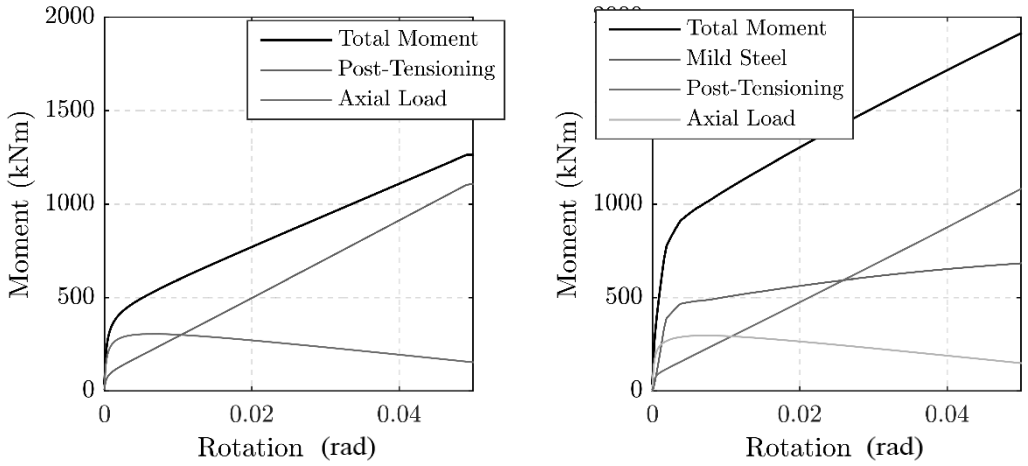

Figure 8-8: Left – Moment-rotation contributions of a connection with no dissipative devices (controlled rocking), Right – Moment-rotation contributions of a connection with dissipative devices (DCR).

It is important to define the yield rotation carefully because it is used to determine ductility and hence hysteretic damping. Eq 8-3 shows the dependence of the equivalent viscous damping on the system displacement ductility, μ, and type of structural system, R_ξ (NZTA, 2018):

$$\xi_{eq} = 0.05 + R_\xi\left(\frac{\mu - 1}{\mu\pi}\right) \qquad 8\text{-}3$$

The hysteretic damping is a means of capturing the damping associated with non-linear response. In displacement-based design the hysteretic damping is dependent upon the ductility, and hence the yield rotation. Therefore, it is not logical to define a yield rotation for DCR connections without dissipaters as they do not exhibit non-elastic behaviour. For DCR connections without dissipaters, the yield rotation need not be known as the hysteretic damping should be taken as the 5% that is often assumed for an elastic system. The dissipation due to impact is minimal and can be neglected.

As previously discussed, DCR connections are complex due to the number of contributing variables that can affect the moment rotation response of the connection. These include the connection diameter, PT diameter, initial PT stress, unbonded length of the PT, axial load, yield strain and unbonded length of the dissipative devices. The recentering ratio is also a variable that needs to be considered as shown in Figure 8-9.

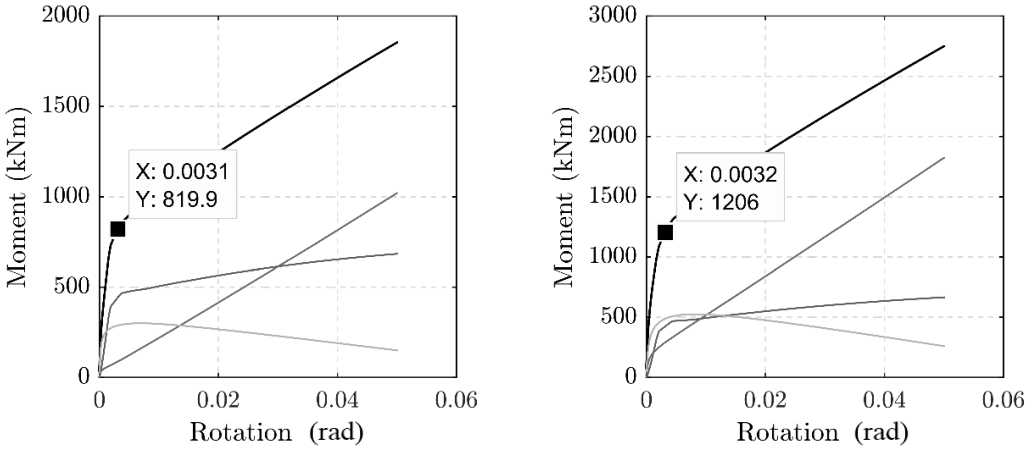

Figure 8-9: Left-Moment-rotation response of connections with low re-centering ratio λ = 1.15, Right – Moment-rotation response of a connection with a high re-centering ratio λ = 2.

The recentering ratio referred to above is defined as:

$$\lambda = \frac{M_{pt} + M_n}{M_s} > 1.15 \qquad 8\text{-}4$$

Where M_{pt}, M_s, and M_n are the moment contributions from PT, dissipaters and axial load respectively. Many of these variables can be eliminated as the they have little influence on the yield rotation. Figure 8-9 shows that altering the force contribution from axial load and PT has little effect on the yield rotation. This is intuitive since the PT force increases linearly and the axial load level is constant. The reduction in moment contribution is a result of the variation in neutral axis location which is highly sensitive to the rotation but is mostly unaffected by any other parameters (particularly for λ ratios used in design). Thus, the yield rotation is dependent upon, the yield strain of the dissipative device, the unbonded length of the dissipative device and the diameter of the connection. Notably, all of these parameters affect the level of strain in the dissipater or the yield strain of the dissipater. The height of the pier only affects the yield displacement and so can also be excluded from the parametric analysis.

Figure 8-10 shows that there is a clear relationship between the diameter and yield rotation. This relationship strengthens when examining Grade 300 and Grade 500 dissipaters separately. This is particularly evident for connections which have a large diameter and short unbonded prestressing length.

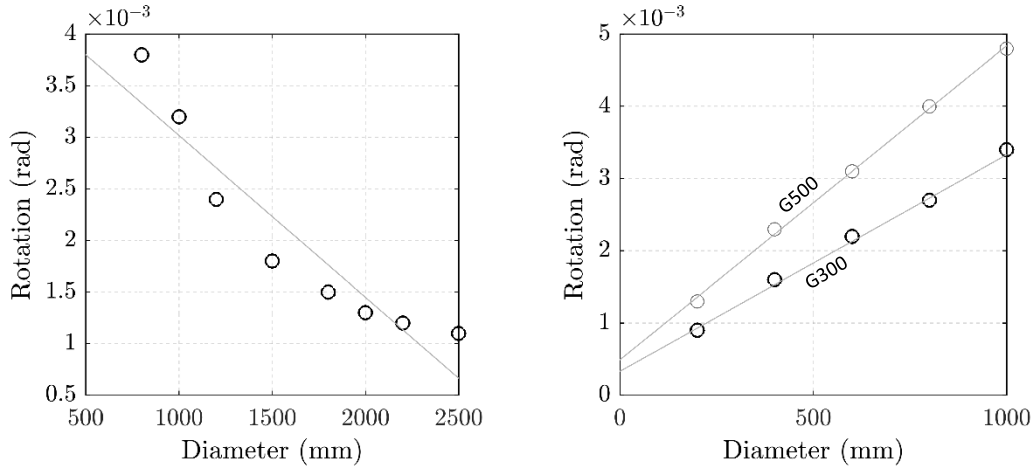

Figure 8-10: Left-Relationship between yield rotation and connection diameter, Right-Shows the difference between G300 and G500 dissipaters.

The strengthening influence of the dissipater grade at larger diameters is due to the geometry. Connections with a small dissipater length relative to the connection diameter (Lub/D<0.5) have their yield rotation dominated by the axial load contribution. For larger unbonded lengths (Lub/D>0.5) the yield rotation is dominated by dissipaters and hence the yield strain of the devices.

Two linear relationships and hence simple equations exist for G300 and G500 bars. While it would be simpler to have one equation, the error would be significant. Further simplification can be made by noting that if the connection diameter increases , the yield rotation reduces. However, increasing the unbonded length of the dissipative device would act to offset this by increasing the yield rotation. Therefore, the yield rotation relationship can be simplified by investigating the parameter Lub/D for each steel grade.

Initially, equations were developed using the parameters, typical of design, shown in Table 8-2 below. A total of 260 connections were examined for each grade of steel (G300 and G500 only). The Lub/D ratio ranges from 0 to 1, going outside this range is physically impractical (unlikely that dissipater length is larger than connection diameter). It was found that altering the PT, initial prestress and axial load only resulted in small errors (~10%). Therefore, the formulae relating the yield rotation to Lub/D can accurately represent all practical geometric and force contribution effects.

Table 8-2: Range of variables used to define the yield rotation of circular sections.

Parameter	Variable Range
Connection Diameter/width (mm)	1000,1500,2000,2500
PT Diameter (mm)	30,75,100,150
Unbonded Length Dissipater (mm)	250,500,7500,1000
Axial Load	$0\text{-}0.05A_g f'_c$
Initial Prestress	$0.1f_{pty}, 0.2f_{pty}, 0.4f_{pty}$
Re-centering Ratio (λ)	0.8 – 2.5

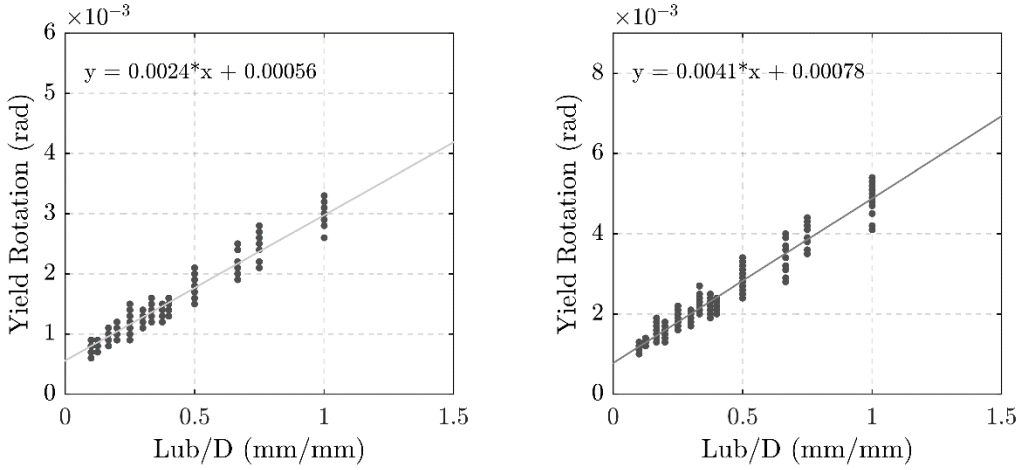

Figure 8-11: Left – Yield rotation relationship for G300 dissipaters, Right – Yield rotation behaviour for G500 dissipaters.

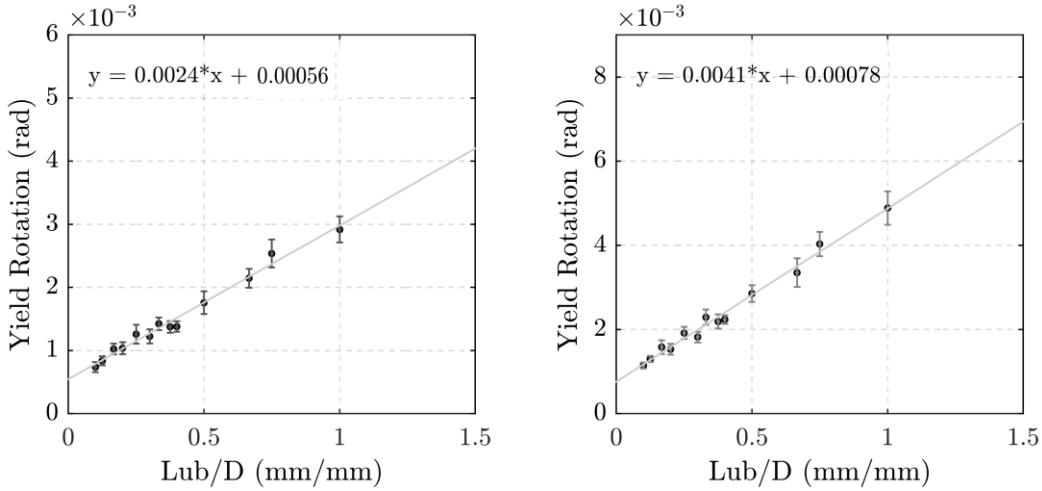

Figure 8-12: Shows one standard deviation for the connections examined.

Figure 8-11 and Figure 8-12 show the proposed relationships (lines of best fit), and standard deviation. The simple linear relationships allow the estimation of the yield rotation. The maximum error between the predicted yield rotation and the actual

yield rotation was 15% which is acceptable for design. The proposed linear relationships are shown in the table below.

Table 8-3: Proposed relationships used to determine the yield rotation of DCR connections with steel armouring at the interface and mild steel dissipaters.

Grade 300	Grade 500
$\vartheta_{yield} = 0.0024\frac{L_{ub}}{D} + 0.00056$	$\vartheta_{yield} = 0.0041\frac{L_{ub}}{D} + 0.00078$

This relationship can be further simplified by noting that the multipliers (0.0024 and 0.0041) are both multiples of the yield strain ε_y. Therefore, the yield rotation of a DCR connection can be estimated using the following:

$$\vartheta_{yield} = 1.62\frac{\varepsilon_y L_{ub}}{D} + 0.00056 \quad 8\text{-}5$$

8.4.1 Yield Displacement

For short piers which have insignificant elastic contributions the yield displacement can be estimated by simply multiplying the yield rotation by the height of the pier. For tall piers (and more correctly for short piers), which have significant elastic contributions in the pier above the connection, estimating the yield displacement is more difficult as the yield force is required. The force at the yield rotations are tabulated in Appendix B. Estimating the yield displacement can then be carried out using the following equations:

$$\Delta_{el} = \frac{F L_{cant}^3}{3(0.3EI)} \quad 8\text{-}6$$

$$\Delta_{gap} = \vartheta_y L_{cant} \quad 8\text{-}7$$

$$\Delta_{tot} = \Delta_{el} + \Delta_{gap} \quad 8\text{-}8$$

Where F is the base shear force, L_{cant} is the effective height, E is the elastic modulus, I the moment of inertia, Δ_{gap} is the deflection at the top of the pier due to interface rotation, ϑ_y is the yield rotation and Δ_{el} is the elastic displacement of the pier.

The ptMBA can also be used to calculate the elastic displacement. The force used must correspond to the force capacity at the given rotation.

8.5 NEUTRAL AXIS LOCATION

The neutral axis location is found using the ptMBA and a modified section analysis, as previously described, that includes unbonded length of dissipaters and PT. However, this process is timely, and during preliminary design, it is often helpful to be able to estimate the neutral axis location quickly. This allows designers to easily evaluate strains in dissipaters and PT at various design levels, which results in significant design efficiency. Therefore, a parametric analysis was undertaken to determine which parameters have a significant effect on the neutral axis location. Simple relations that give a simple estimation of the neutral axis location are then presented.

8.5.1 Key Parameters

Using the section analysis procedure described previously each parameter affecting the connection was investigated. The first variable investigated is the diameter. The values of the other variables (which are constant) are tabulated in Table 8-4.

Table 8-4: Connection parameters used to determine the influence of Diameter.

Axial Load (kN)	PT Dia (mm)	Fuse length dissipater (mm)	Prestress (Tpti/Tpty)	Connection Diameter (mm)	Lcant (mm)	Recentering ratio (λ)
2000	50	1000	0.1	1000	6000	1.24
2000	50	1000	0.1	1200	6000	1.41
2000	50	1000	0.1	1500	6000	1.59
2000	50	1000	0.1	1800	6000	1.72
2000	50	1000	0.1	2000	6000	1.79

Results from the section analysis are shown in Figure 8-13. These results show that the diameter has an insignificant effect on the location of the neutral axis with a maximum error of 21mm at 2% drift. The diameter does not significantly affect the neutral axis location because the neutral axis determined based on section equilibrium (compression = tension). At low drift levels the variation is higher due to the differing

diameters. However, this variation rapidly reduces as the neutral axis location reaches its asymptote.

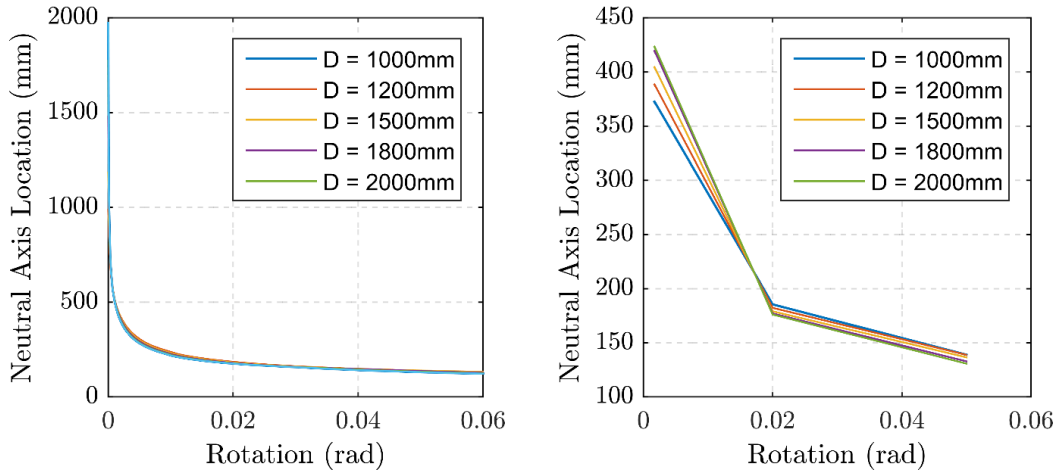

Figure 8-13: Left – Neutral axis location variance, Right Neutral axis location at Yield, Design (2%) and CALS (5%) drifts.

Table 8-5: Connection parameters used to determine the influence of Lcant.

Axial Load (kN)	PT Dia (mm)	Fuse length dissipater (mm)	Prestress (Tpti/Tpty)	Connection Diameter (mm)	Lcant (mm)	Recentering ratio (λ)
2000	50	1000	0.1	1500	5000	1.67
2000	50	1000	0.1	1500	6000	1.59
2000	50	1000	0.1	1500	8000	1.45
2000	50	1000	0.1	1500	10000	1.32
2000	50	1000	0.1	1500	12000	1.20

The cantilever lengths examined are shown in Table 8-5. The results show that varying the cantilever length results in some variation in the location of the neutral axis. Mainly because a taller pier has a longer unbonded length of PT. Therefore, at the design drift, the force contribution from PT is less for taller piers than it is for shorter piers meaning the total axial load is reduced. Therefore the compression forces in the concrete are lower.

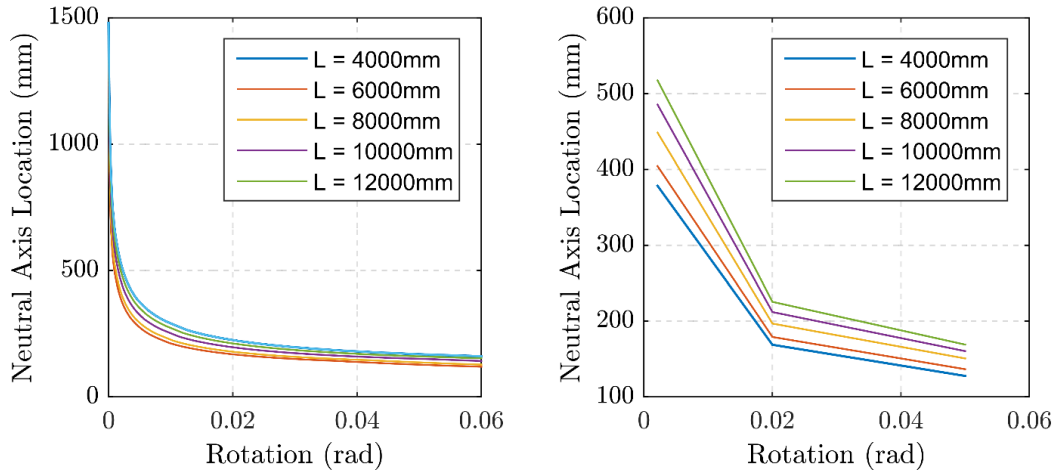

Figure 8-14: Left – Neutral axis location variance, Right Neutral axis location at Yield, Design (2%) and CALS (5%) drifts.

Table 8-6: Connection parameters used to determine the influence of PT diameter.

Axial Load (kN)	PT Dia (mm)	Fuse length dissipater (mm)	Prestress (Tpti/Tpty)	Connection Diameter (mm)	Lcant (mm)	Recentering ratio (λ)
2000	25	1000	0.1	1500	6000	1.44
2000	50	1000	0.1	1500	6000	1.59
2000	75	1000	0.1	1500	6000	1.75
2000	100	1000	0.1	1500	6000	1.86
2000	125	1000	0.1	1500	6000	1.92

The PT diameters examined are shown in Table 8-6. The results (Figure 8-15) show that varying the PT diameter results in a small variation in the location of the neutral axis. Similar to the cantilever length, this variation is due to the additional force in the PT. A larger diameter results in a more substantial force contribution and therefore a larger neutral axis location.

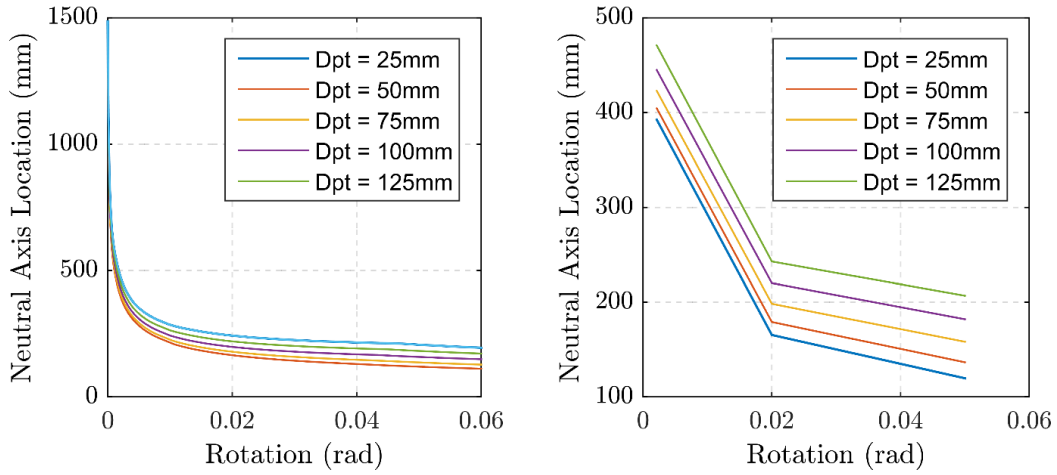

Figure 8-15: Left – Neutral axis location variance, Right Neutral axis location at Yield, Design (2%) and CALS (5%) drifts.

The variation of initial prestress examined were between 10% and 50% of the yield stress. The recentering ratio for these connections was 1.55. This variation in the initial prestress has little effect on the neutral axis location, as shown in Figure 8-16.

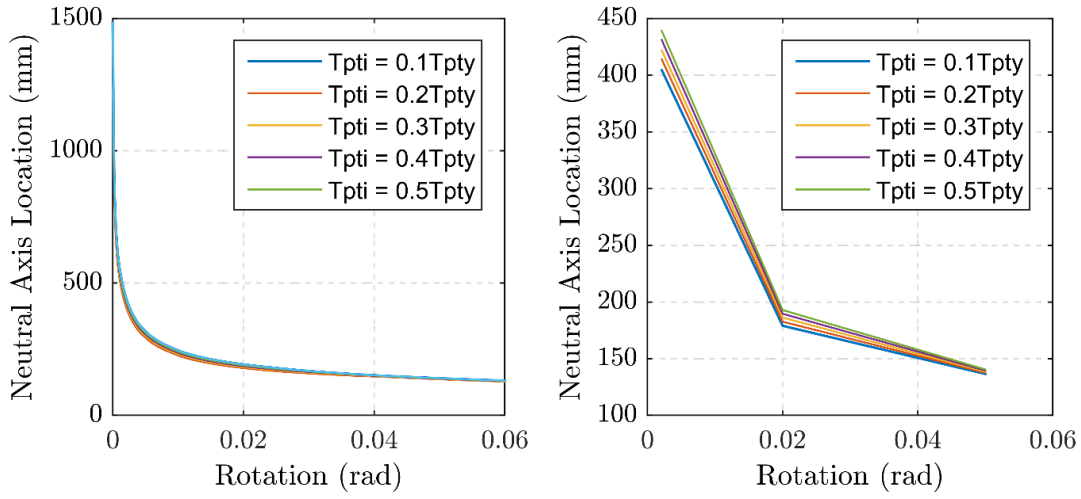

Figure 8-16: Left – Neutral axis location variance, Right Neutral axis location at Yield, Design (2%) and CALS (5%) drifts.

The axial loads examined were 2000kN, 4000kN and 6000kN. The results show that varying the axial load results in a small variation in the location of the neutral axis. This makes sense given a larger axial load will result in a larger area of concrete required to balance the section forces.

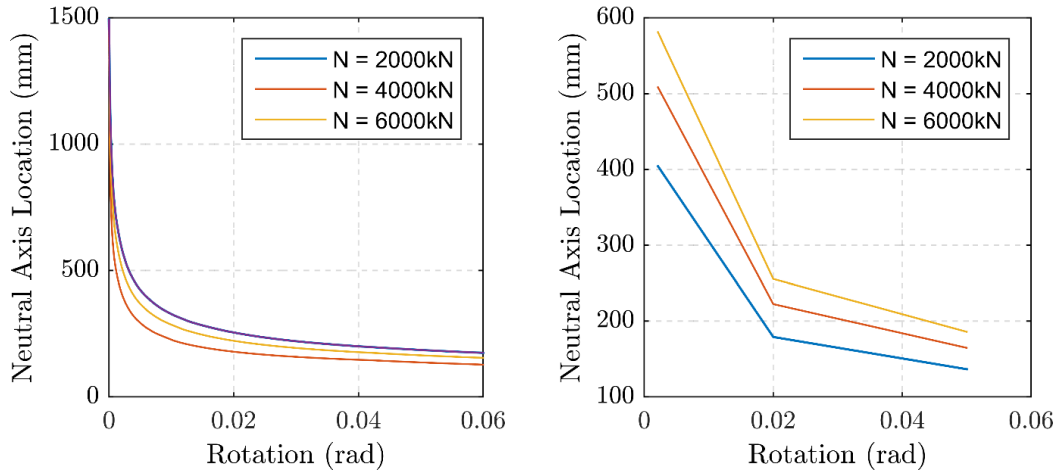

Figure 8-17: Left – Neutral axis location variance, Right Neutral axis location at Yield, Design (2%) and CALS (5%) drifts.

Figure 8-14, Figure 8-15 and Figure 8-17 show that the axial load, cantilever length and diameter of PT have the most influence on the neutral axis location. This is because they all increase the section force for a given drift, increasing this means a larger compression area is required to achieve section equilibrium. These effects are captured with one variable, total force on the section, which includes the forces from the dissipaters, PT and axial load. Further influence from the cantilever length is due to the ptMBA, used to estimate the peak strain (Marriott, 2009), which includes the variable, Lcant.

Table 8-7: Range of Connections Examined (1125 connections total)

Axial Load (kN)	PT Dia (mm)	Fuse length dissipater (mm)	Prestress (Tpti/Tpty)	Connection Diameter (mm)	Lcant (mm)
2000 - 6000	25 -125	1000	0.1-0.5	1000-2000	4000-12000

Initially, the NA location was determined as a function of the axial force acting on the section. Table 8-7 shows the range of connections examined, of which there are 1125. The results are shown in Figure 8-18.

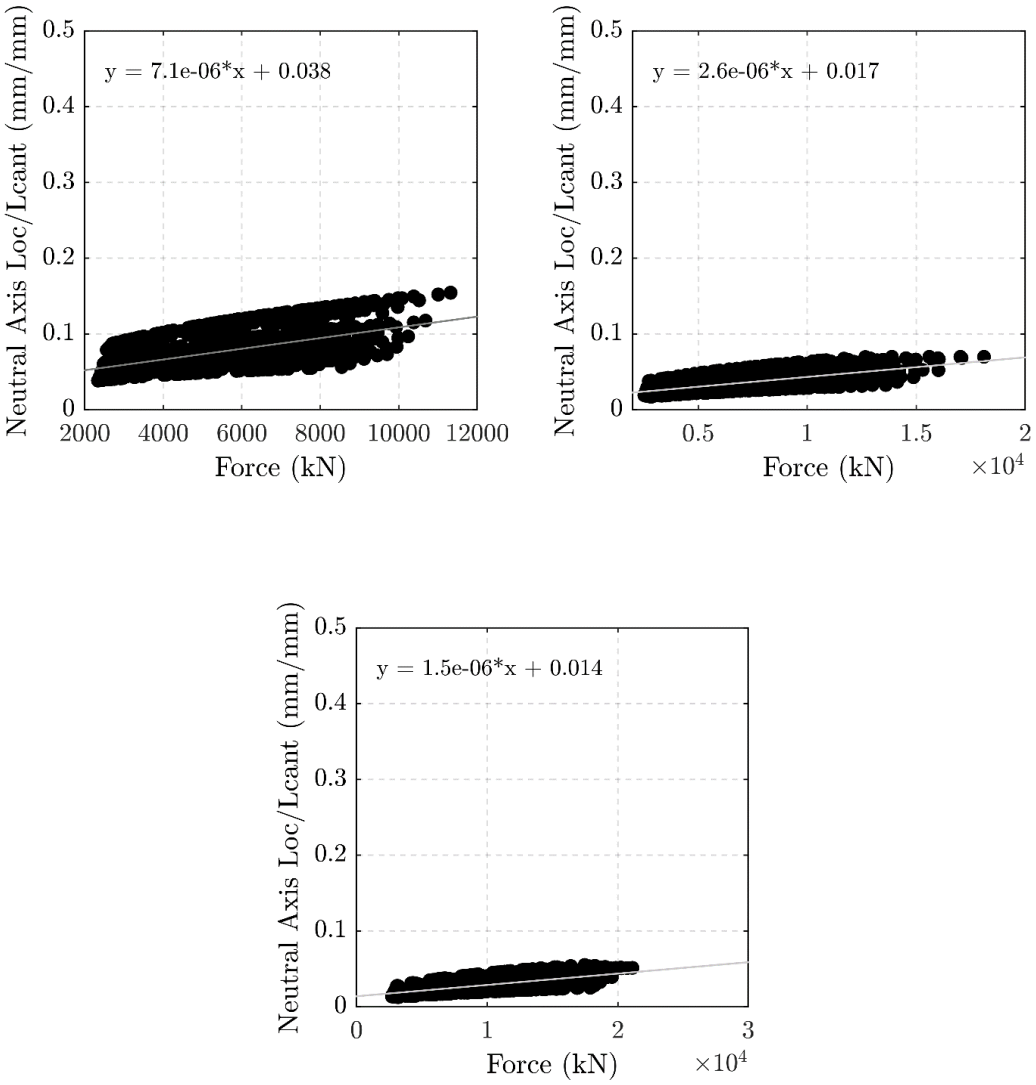

Figure 8-18: Shows the variance of the NA/Lcant with Force. Top Left – Yield, Top Right – DCLS, Bottom – CALS.

Based on the results, lines of best fit were added to enable the estimation of the neutral axis location. The proposed relationships are shown in Table 8-8. The relationships, based on the total axial force acting on the connection, and the neutral axis location normalised by Lcant provide a reasonable estimation of the neutral axis location.

Table 8-8: Equations used to estimate the NA location.

	Equation
Yield	$NA_{yield} = (7.1e^{-6}F + 0.038)Lcant$
DCLS	$NA_{DCLS} = (2.6e^{-6}F + 0.017)Lcant$
CALS	$NA_{CALS} = (1.5e^{-6}F + 0.014)Lcant$

Where F is the sum of the axial load, PT force and total dissipater force and $Lcant$ is the effective height of the pier. To use these values the unbonded length of the PT should be within 30% of the cantilever length ($Lcant$). Given the stress in the PT is a function of the NA location, this formulation still requires iteration, though less than a full section analysis. A less accurate formulation, but likely sufficient for preliminary design, can be found by using more straightforward relationships, which exclude the force variation.

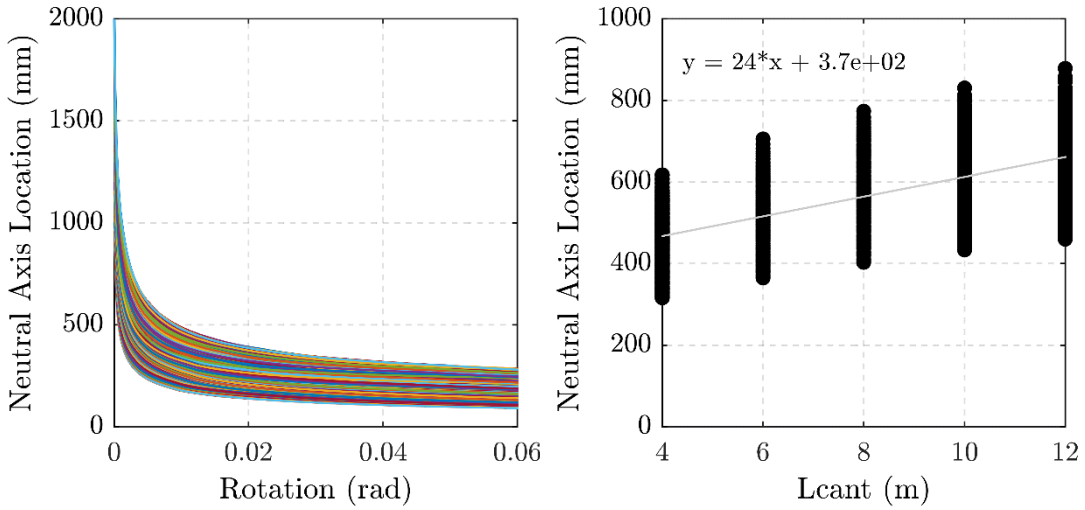

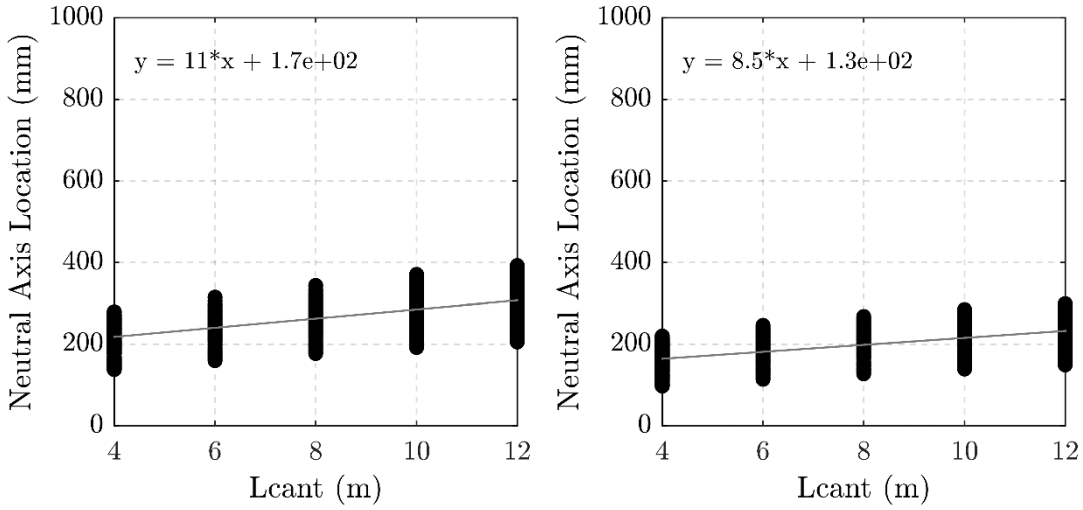

Figure 8-19: Top Left – Tracking of neutral axis for all connections examined, Top Right, Influence of Lcant on the neutral axis location at yield, Bottom Left – Influence of Lcant on the neutral axis location at DCLS, Bottom Right – Influence of Lcant on the neutral axis location at CALS.

The results of the parametric analysis accounting for only a variation in Lcant only are shown in Figure 8-19. At the DCLS and CALS drifts the error is up to 85mm. The error at yield is 217mm. This significant error is due to the rapid changes in the neutral axis location at low drifts. The results for DCLS and CALS are sufficiently accurate for preliminary design. The proposed relationships are tabulated below (Table 8-9).

Table 8-9: Shows equations suitable for estimating the neutral axis location and maximum possible error.

	Equation	**Error**
Yield	NA_{yield} = 24$Lcant$ + 370	+-217mm (33%)
DCLS	NA_{DCLS} = 11$Lcant$ + 170	+-85mm (28%)
CALS	NA_{CALS} = 8.5$Lcant$ + 130	+-65mm (28%)

8.6 DESIGNING FOR OVERSTRENGTH

In traditional capacity design, the capacity protected elements such as the piles and pile caps are designed to have a capacity larger than the over-strength capacity of the ductile element. This strength hierarchy is established to ensure that a ductile failure mechanism occurs, which helps prevent unexpected brittle collapse. For bridges, a column sway behaviour that allows the formation of ductile plastic hinging

in the piers is used. To ensure this formation does not damage other elements, the overstrength factor to be applied to the plastic hinge must account for the following:

- The probability that the actual yield strength of steel is greater than the lower characteristic value.
- Increase in the strength of steel beyond the yield strength due to strain hardening.
- Confinement of concrete.
- Any additional reinforcement placed during construction that is unaccounted for in calculations.

Currently, the concrete code (NZS3101:2006) defines the overstrength factor of reinforced concrete with G300 and G500 steel as 1.25 and 1.35 respectively. In addition, the concrete compressive strength is increased by 15MPa.

In New Zealand, seismic design strategies currently uses both Grade 300E and 500E reinforcement. (Previously, Grade 275 and 380 were the standard steel grades.) These over-strength factors have proven to be a sufficient means of ensuring capacity protected elements remain undamaged in design level events. However, additional consideration must be given to the external dissipaters. This is due to the axial dissipaters potentially having an increased axial capacity in compression (Liu, 2018) . The increased axial capacity can come about due to interaction of the internal dissipater with the external confining tube.

The purpose of the external confining tube is to prevent buckling and ensure the dissipater provides stable hysteretic behaviour. It is important to leave a gap between the confining tube and internal dissipater to minimise the loads induced in the confining tube under compression and buckling. Therefore, the gap between the dissipater and its confining tube must be sufficient to accommodate expansion of the core under compression (Poisson's effect) and small enough to limit buckling of the dissipater. This can achieve by filling the space with an elastic material or allowing the confining tube to expand elastically. However, this gap must be well controlled as poor design can lead to engagement of the external tube, increased curvature demands (buckling) and reduced fatigue capacity.

Designing the gap to allow for Poisson expansion will not fully prevent engagement of the confining tube, as buckling will induce friction on the internal walls of the confining tube. As this is unavoidable, the overstrength factor should incorporate a compression overstrength factor, β, which accounts for the force that is transferred to the confining tube through friction. The overstrength factors for the dissipater in compression should include material overstrength factors in addition to the specific overstrength factor for the dissipaters in compression. The adjusted compression strength in compression would be:

$$\beta \emptyset_{steel} f_y \qquad 8\text{-}9$$

Where f_y is the yield stress, $\emptyset_{steel}$ is the overstrength of steel and β is a buckling factor relating to engagement of the confining tube (not known for four groove axial dissipaters). The overstrength factor for the dissipaters in tension would not need to be altered. For Buckling Restrained Braces (BRB), the US Standard AISC 341 (AISC, 2011) stipulates that the compression adjustment factor shall be calculated as the ratio of maximum compression force to the maximum tension force of the test specimen at strains corresponding to the expected deformations. In no case shall β be less than 1 and β factors larger than 1.5 would indicate the dissipater has been poorly designed. For BRB type braces there is a requirement that at least one experimental test is done to get a proper understanding of the behaviour of the dissipater.

There are several key points to note here. The first is that when we consider a DCR connection which is designed to re-centre with a $\lambda > 1.15$ the dissipater (mild steel) contribution to the total moment capacity is less than 40%. In addition, this effect is only applied to the small number of dissipaters in compression. Since the neutral axis typically converges to less than 0.15D, only 20% of the dissipaters are likely to be affected. This results in only 8% of the total moment capacity being affected. Therefore, even if the dissipaters capacity in compression is increased by 50%, which is unlikely, the overall increase in moment capacity would be less than 5%. Therefore, the overstrength factor could either be conservatively taken as 1.5, or simply neglected altogether, without significantly impacting the design of the connections. If it were to be considered, this would be applied in Eq 8-9 to only the dissipaters in compression and only to determine the overstrength capacity. Given the increase is less than 5% these effects are ignored throughout this chapter.

With DCR connections PT is an additional component which influences the increase in moment capacity beyond yielding. The PT typically results in significant post-yielding stiffness of the overall connection. This is particularly evident for squat piers, pier bents (more than one gap opening) or connections with a large PT area because displacements cause a larger increase in stress or force in the PT. Given this additional contribution, it is not acceptable to simply apply an overstrength factor to the yield capacity of the connection as this would, in many cases, severely underestimate the actual capacity of the connection at the CALS.

The proposed design philosophy for DCR connections discussed in Chapter 7, which is to design for the CALS, has an added benefit in that applying the overstrength factor to the CALS capacity means that the effects of PT can be easily captured through section analysis. Since yielding of the PT is not intended, no overstrength factor is needed to account for better than expected yield strength or strain hardening as these effects would occur beyond CALS and are minimal for PT (the PT would load and unload along the elastic portion of the stress-strain curve where only small errors exist). Therefore, for DCR connections designed using the alternative design philosophy, or complying with geometric constraints in the following sections, the upper bound material overstrength factors proposed by (Priestley et al., 2007) are recommended in lieu of more detailed information on the dissipaters:

$$\emptyset_{steel} = 1.3 f_y \qquad 8\text{-}10$$

$$\emptyset_{concrete} = 1.7 f'_c \qquad 8\text{-}11$$

Where these overstrength factors are applied to the material capacities, and the moment capacity is calculated using section analysis.

8.6.1 Post Yielding Stiffness

The post-yielding stiffness is an important parameter that can have a significant effect on capacity design principles. As discussed in the previous section, for monolithic connections the post-yielding stiffness is typically small, which makes designing for overstrength relatively straight forward as an overstrength factor is applied directly to the yield capacity. Given current design strategies are still preferred

by designers, this section recommends geometric constraints that would allow traditional design strategies to be applied to DCR connections. In particular, these ratios intend to limit the post-yielding stiffness to ensure capacity design principles can be applied to DCR connections (so as to prevent excessively large overstrength capacity requirements on piles etc).

To determine and verify the key variables that affect the post yielding stiffness a preliminary analysis was undertaken. This analysis was carried out using the modelling method presented earlier in this chapter. As shown in Figure 8-20, regardless of the re-centering ratio (combination of contributions from axial load, PT and dissipaters), the post yielding stiffness is dominated by the PT. In general, the increase in moment capacity due to strain hardening in the dissipaters is offset by the reduction in capacity resulting from the reducing moment contribution from axial load. The post-yielding stiffness (k_{py}) is the rotational stiffness, taken as the slope from the moment-rotation relationship for the connection (Figure 8-19).

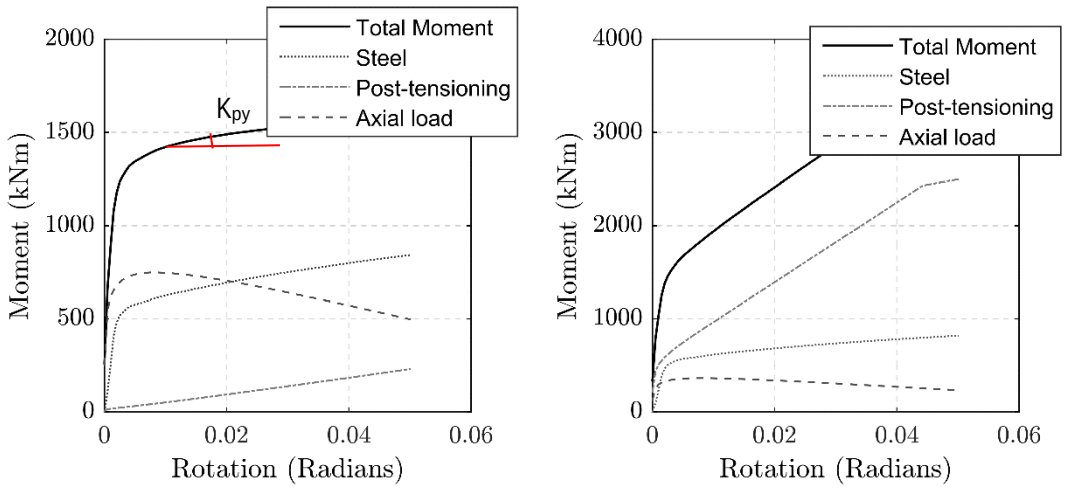

Figure 8-20: Left – Post yielding stiffness of a connection with low Mpt/Mn ratio of 0.15, Right – Post yielding stiffness of a connection with a high Mpt/Mn ratio of 2.2.

The reduction in axial load moment is a consequence of the axial load, acting at the centre of the column, approaching the neutral axis as the column rocks over.

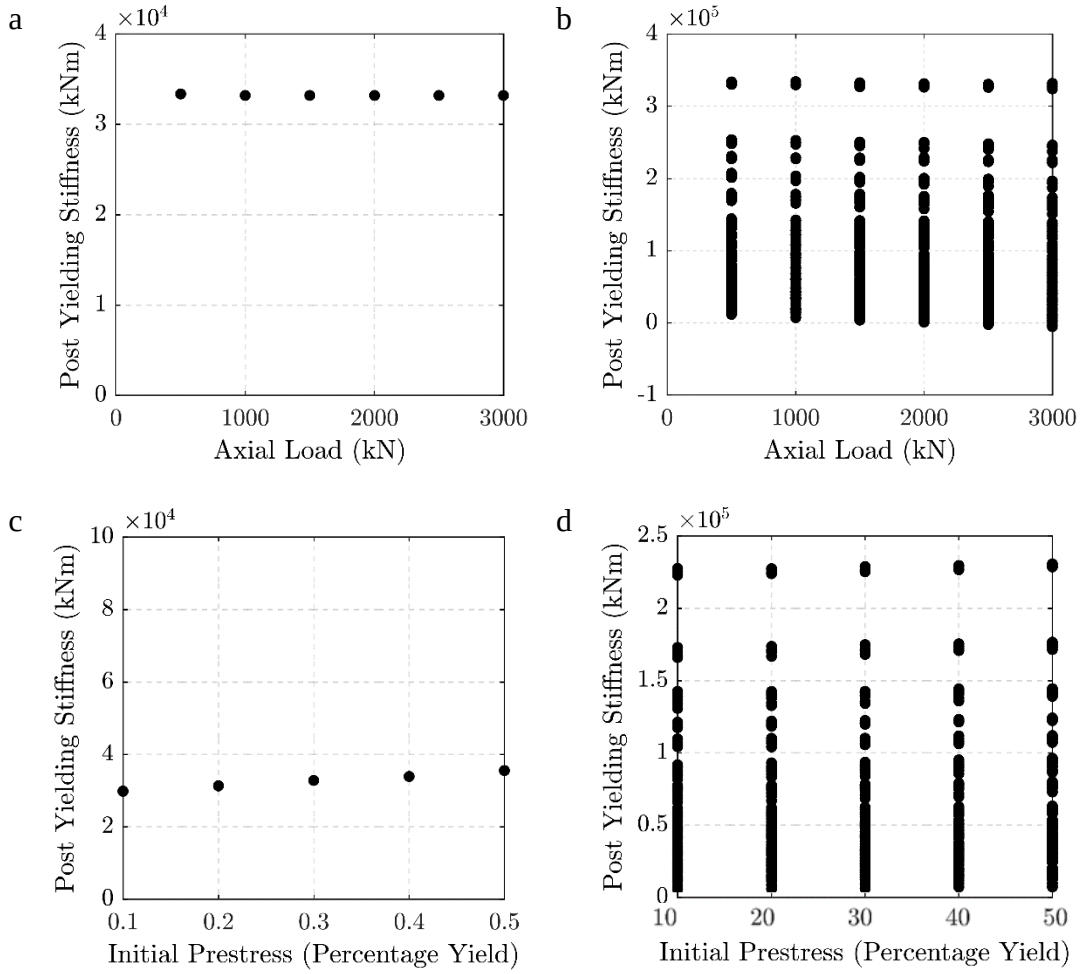

Figure 8-21: a/b – Shows how the axial load influences the post-yielding stiffness, b/c – Shows how the initial prestress influences the post-yielding stiffness (slope of the Moment-rotation plot)

Figure 8-21 and Figure 8-22 show the results from the preliminary analysis. The figures on the left show the variation of the single variable while all other variables are fixed. The figures on the right show the variation of the single variable in conjunction with the variation of all other variables. As shown in Figure 8-22 , the axial load and initial prestress have no significant effect on the post yielding stiffness, provided the PT does not yield. Conversely, the diameter of the connection, PT diameter and the pier height all have a significant effect on the post-yielding stiffness. As previously discussed, the post-yielding stiffness of the connection is dominated by the contribution from PT. Therefore, it is not surprising that PT diameter, pier diameter and the unbonded length of PT (assumed to be equal to the pier height) affect the force in the PT as they all influence the stress or strain in the PT.

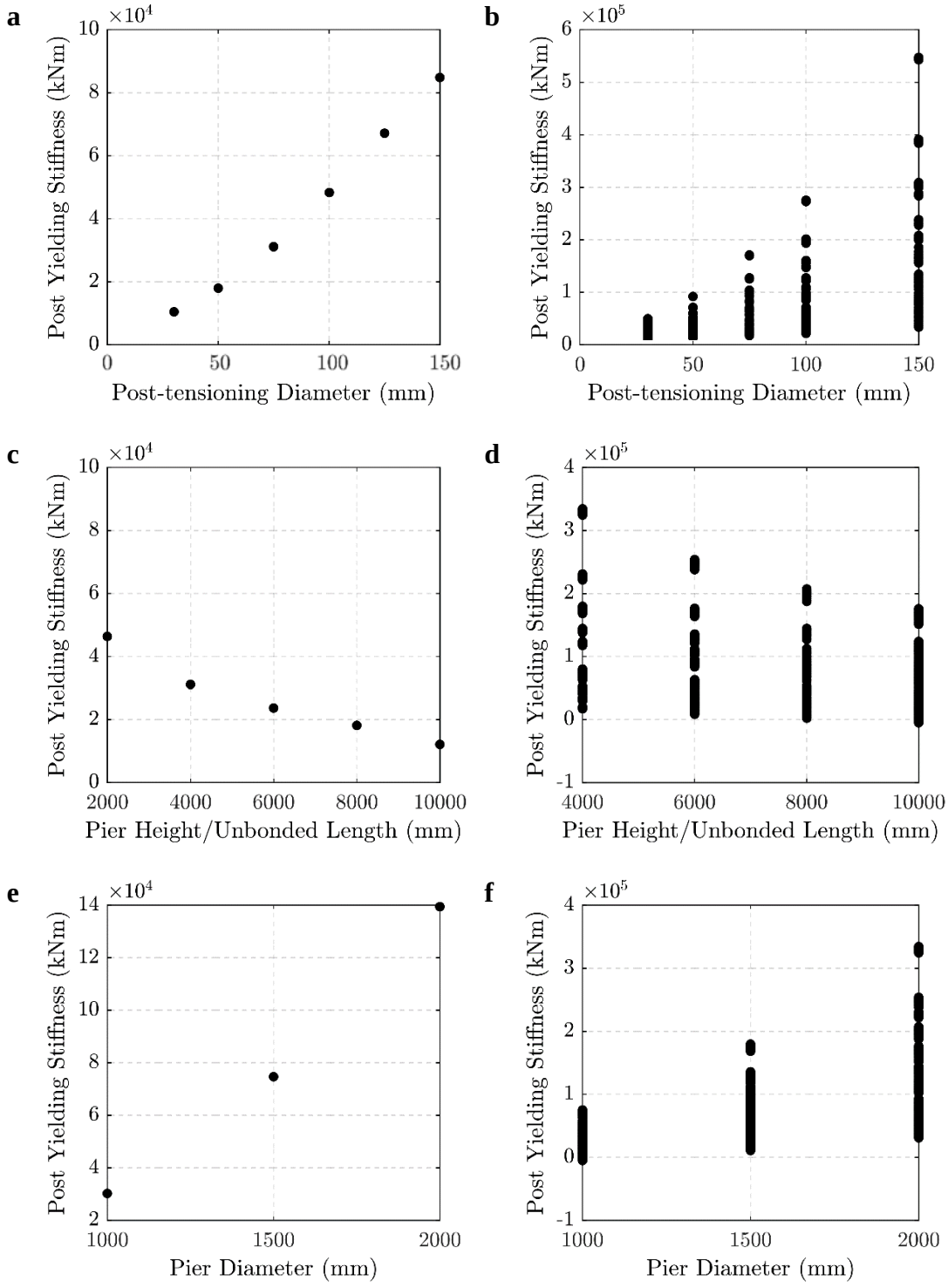

Figure 8-22 a/b – Shows how the PT diameter affects the post-yielding stiffness, c/d – Shows how the unbonded length affects the post-yielding stiffness, c/d – Shows how the pier diameter affects the post-yielding stiffness.

The effect of each of these parameters is shown in Figure 8-24 and Figure 8-25 below. The axial load includes only the gravity load as this shows how the gravity load influences the post-yielding stiffness given its contribution is typically negative (Figure 8-20). It was found that there is a relatively flat gradient for axial load ratios

less than 0.1*Agf'c*, which are typical in seismically designed bridges. This illustrates that the axial load plays an insig

nificant role on the post yielding stiffness. The exception being for axial load ratios in excess of *0.1Agf'c*, which are not examined here as they are unlikely to ever be reached in regions with high seismicity. This is because the diameter required to generate sufficient moment capacity is typically much larger than the diameter needed to provide adequate axial load capacity.

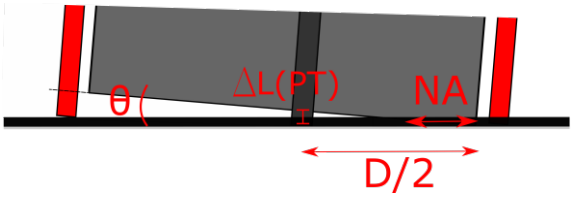

$$\Delta F_{pt} = \frac{E_{pt} A_{pt} \vartheta (\frac{D}{2} - NA)}{L_{ub,pt}}$$

Figure 8-23: Shows how the force in the PT is calculated.

The initial prestress also generates a negligible increase in post-yielding stiffness. This is because the prestressing force only increases the stress in the PT bar and has no effect on the stress-strain relationship as shown in Figure 8-23. The variables that alter the post-yielding stiffness significantly are the diameter of PT, unbonded length of PT (in this analysis, Lcant) and the diameter of the connection.

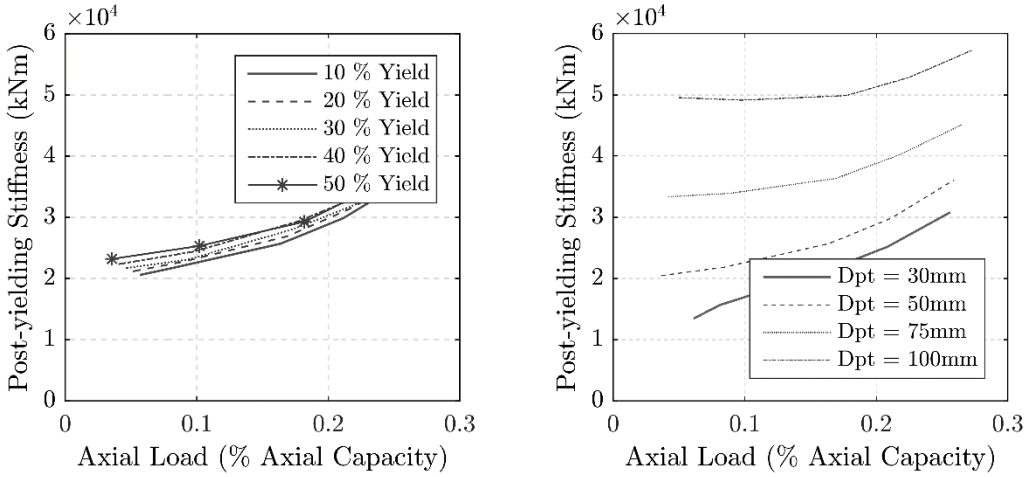

Figure 8-24: Influence of axial load on the post-yielding stiffness, Left – Varying initial prestress, Right – Varying PT diameter.

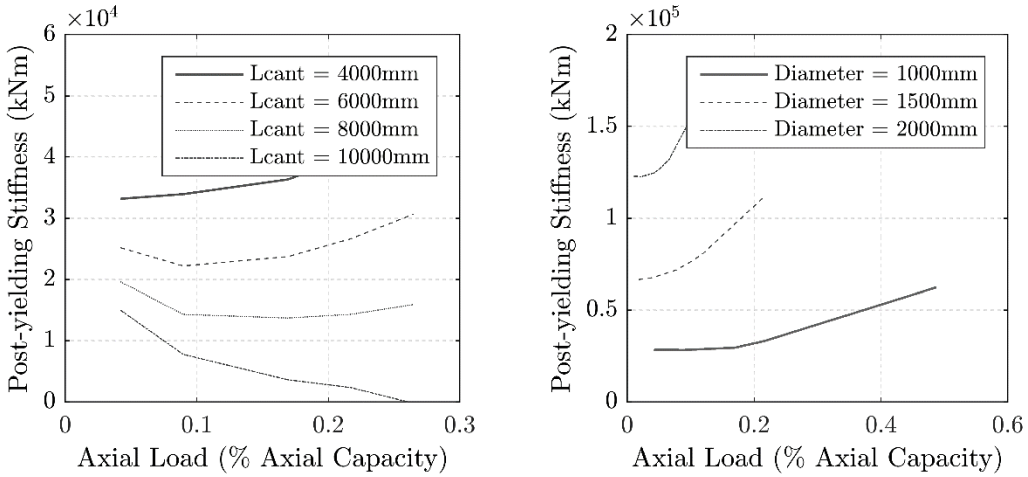

Figure 8-25: Influence of axial load on the post-yielding stiffness, Left – Varying unbonded length, Right – Pier diameter.

The post yielding stiffness is highly influenced by the diameter of the PT because the strain in the PT is constant for a given rotation, pier diameter and unbonded length. Therefore, the increasing moment capacity simply comes as a result of the increased force contribution which results from the larger area. The unbonded length and diameter cause different strain levels in the PT, the diameter by increasing the lever arm and the unbonded length by directly influencing the strain. A smaller unbonded length and larger diameter result in increased strain. Conversely, a larger unbonded length and reduced diameter result in decreased strain.

In order to define suitable geometric ranges that give a post-yielding stiffness suitable for traditional design, the ranges of post-yielding stiffness that are acceptable must be defined. Figure 8-26 illustrates a range of post-yielding stiffnesses. All of the connections shown include over strength effects such as strain hardening of mild steel. Therefore, some increase in the predicted moment capacity is acceptable.

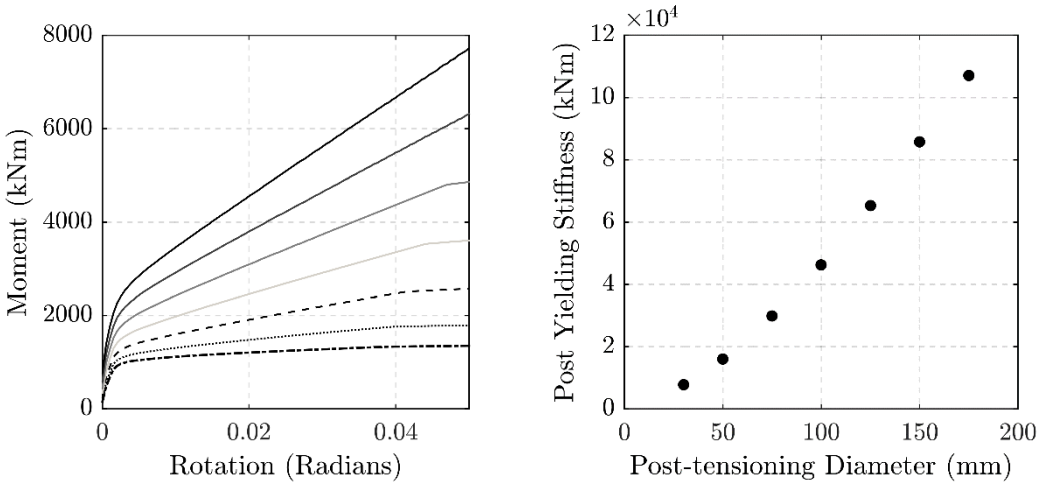

Figure 8-26: Shows the various levels of post-yielding stiffness.

Table 8-10 shows the tabulated values of the post-yielding stiffness and the equivalent over-strength factors. In this analysis yield strengths and upper bound material strengths were used, so material overstrength factors are included. The overstrength factors used in this analysis are shown in equations 8-10 and 8-11. The remaining increase is a result of the contribution from PT.

Table 8-10: Tabulated values of the post-yield stiffness and equivalent overstrength factor defined as ($M_{Collapse}/M_{Design}$).

	M_{Design} (2% Drift)	$M_{Collapse}$ (4.5% Drift)	Post-yielding Stiffness (kNm)	Overstrength Factor
Connection 1	1208	1341	5480	1.11
Connection 2	1480	1776	12000	1.20
Connection 3	1907	2537	25200	1.33
Connection 4	2495	3544	42560	1.42
Connection 5	3101	4683	63640	1.51
Connection 6	3811	5908	84320	1.55
Connection 7	4555	7197	105560	1.58

When the range of connections with various levels of post-yielding stiffness are investigated, all of them have an increase in strength beyond the design level. To conform to current design strategies (FBD), the post-yielding stiffness for DCR connections is assumed to be around 9000kNm which results in less than a 25% increase in capacity beyond the yield. This is similar to typical increases in the strength

of plastic hinges, which increase by a similar amount when assessed using upper bound material strengths.

This post-yielding stiffness includes overstrength factors (strain hardening and upper bound strengths). Although this might be quite limiting for DCR connections designed using current design philosophies, the post-yielding stiffness could be an advantage as discussed in depth in Chapter 6. Using the alternative design philosophy means that the connection is assessed at the CALS and the over strength capacity is therefore only related to maximum possible material strengths. Therefore, a theoretical limit on the post-yielding stiffness is not required.

Figure 8-27 shows how the unbonded length, pier diameter and PT influence the post-yielding stiffness. The horizontal red line shows the assumed acceptable post-yielding stiffness for traditional design strategies (9000kNm).

Unbonded Length PT – 3000mm

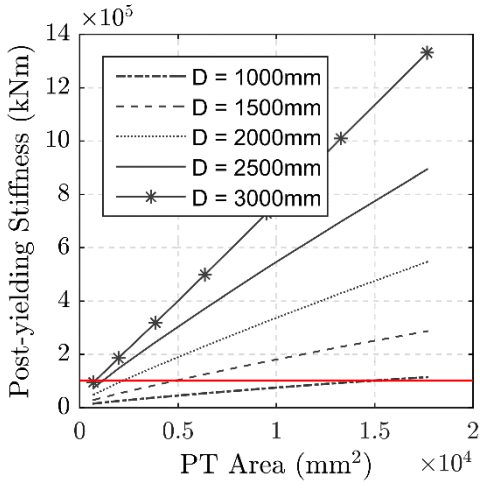

Unbonded Length PT – 4000mm

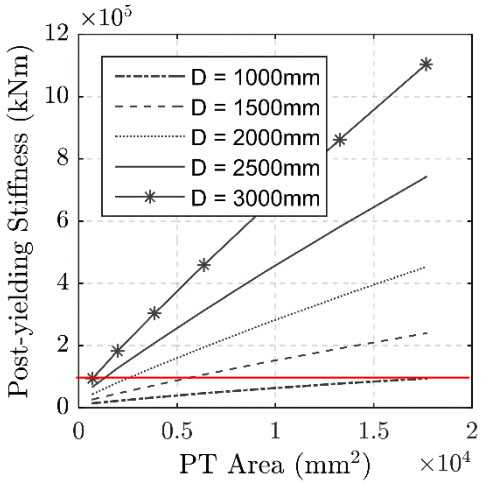

Unbonded Length PT – 5000mm

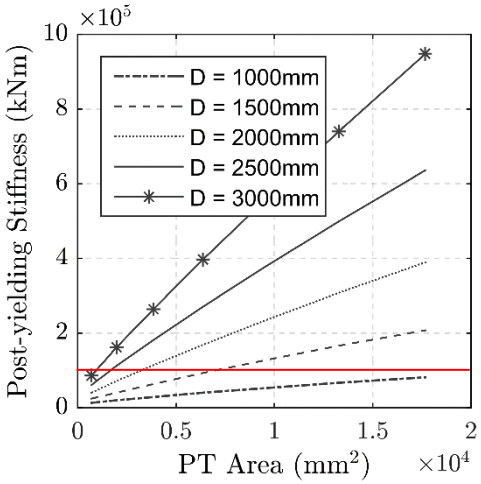

Unbonded Length PT – 6000mm

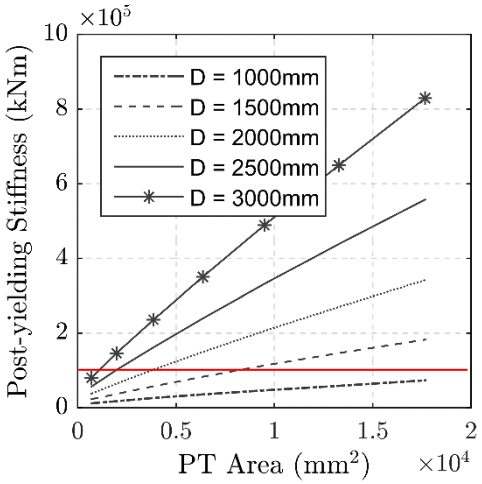

Unbonded Length PT – 7000mm

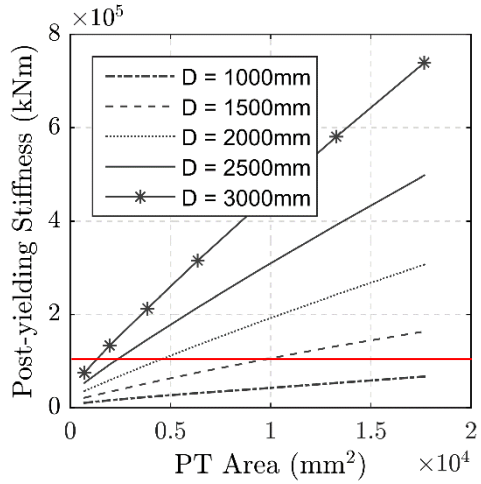

Unbonded Length PT – 8000mm

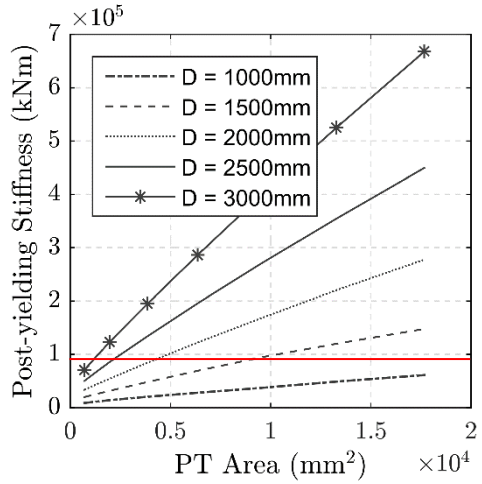

Unbonded Length PT – 9000mm

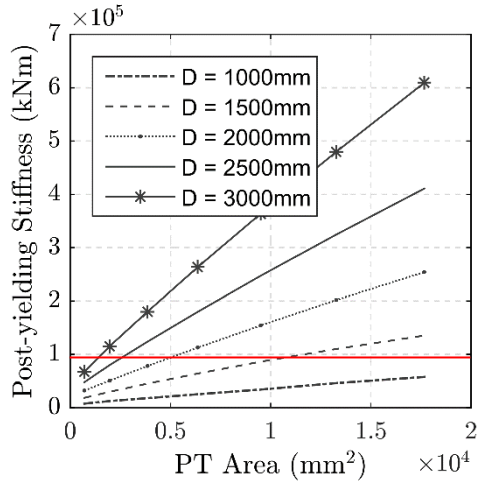

Unbonded Length PT – 10000mm

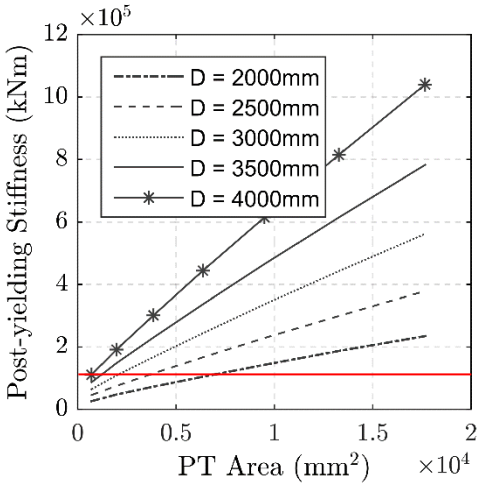

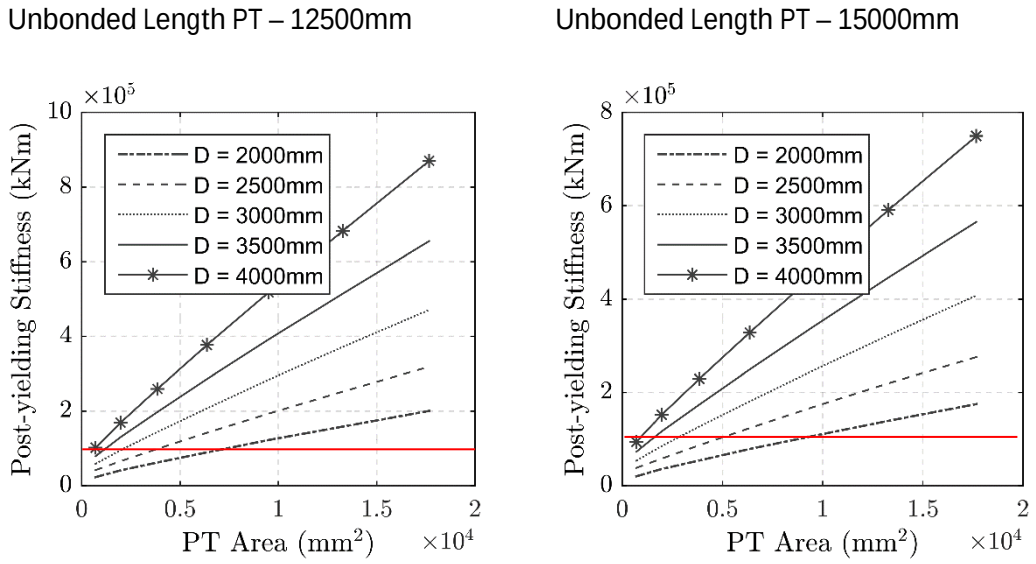

Figure 8-27: Shows the effect of each parameter on the post yielding stiffness.

Table 8-11 and Table 8-12 provide upper limits on the diameter of PT for a given pier diameter and unbonded length of PT. Conforming to the values in this table will ensure that the post yielding stiffness gives a CALS section capacity that is below 1.25 times the yield capacity.

Table 8-11: Maximum diameter of PT for given pier diameter and unbonded length of PT.

Cantilever Length (mm)	**Pier Diameter (mm)**						
	1000	**1500**	**2000**	**2500**	**3000**	**3500**	**4000**
3000	135	80	50	30	-	-	-
4000	150	90	60	35	-	-	-
5000	160	95	65	40	30	-	-
6000	170	100	70	45	35	-	-
7000	-	105	75	50	40	-	-
8000	-	110	80	55	45	-	-
9000	-	115	85	60	50	-	-
10000	-	-	90	65	55	45	30
12500	-	-	95	70	60	50	35
15000	-	-	100	75	65	55	40

Table 8-12: Dimensionless ratio A_{pt}/A_c

Cantilever Length (mm)	Pier Diameter (mm)						
	1000	**1500**	**2000**	**2500**	**3000**	**3500**	**4000**
3000	1.82	0.28	0.06	0.01	-	-	-
4000	2.25	0.36	0.09	0.02	-	-	-
5000	2.56	0.40	0.11	0.03	0.01	-	-
6000	2.89	0.44	0.12	0.03	0.01	-	-
7000	-	0.49	0.14	0.04	0.02	-	-
8000	-	0.54	0.16	0.05	0.02	-	-
9000	-	0.59	0.18	0.06	0.03	-	-
10000	-	-	0.20	0.07	0.03	0.02	0.01
12500	-	-	0.23	0.08	0.04	0.02	0.01
15000	-	-	0.25	0.09	0.05	0.02	0.01

8.7 ACHIEVING CALS DRIFT LIMITS

8.7.1 Post-Tensioning

A key design objective for any type of connection is the ability of the connection to avoid a collapse scenario in high levels of shaking. One of the key design objectives for DCR connections is ensuring the PT does not yield. A preliminary analysis was undertaken to determine the key variables associated with the onset of yielding in the PT.

Figure 8-28 shows that there are three parameters which have a significant influence on the rotation at which the PT yields. Specifically, initial PT stress, cantilever length and connection diameter.

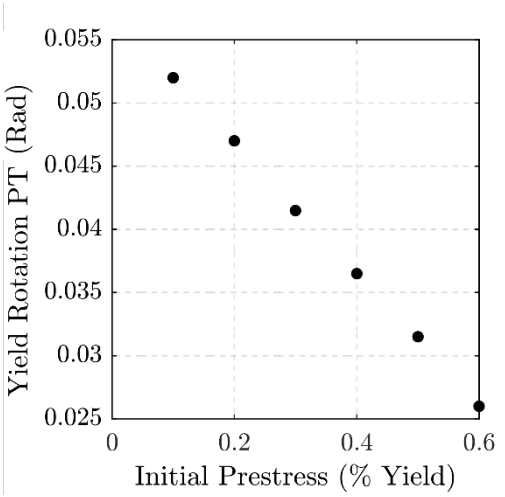
Yield Rotation PT (Rad)
0.055
0.05
0.045
0.04
0.035
0.03
0.025
0
0.2
0.4
0.6
Initial Prestress (% Yield)

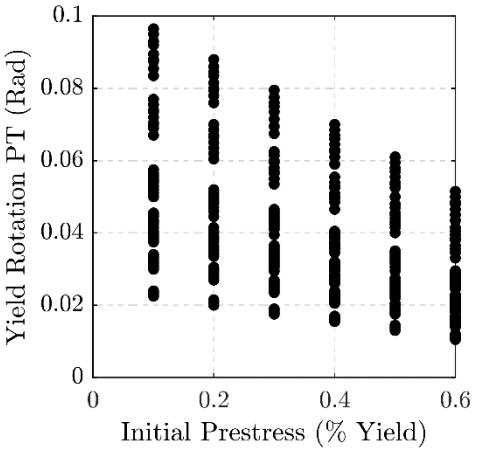
Yield Rotation PT (Rad)
0.1
0.08
0.06
0.04
0.02
0
0
0.2
0.4
0.6
Initial Prestress (% Yield)

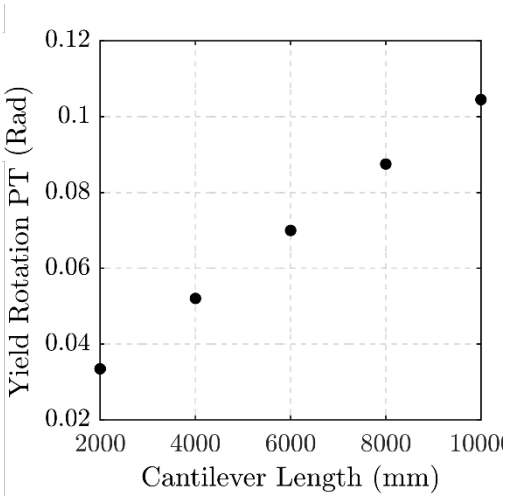
Yield Rotation PT (Rad)
0.12
0.1
0.08
0.06
0.04
0.02
2000
4000
6000
8000
Cantilever Length (mm)

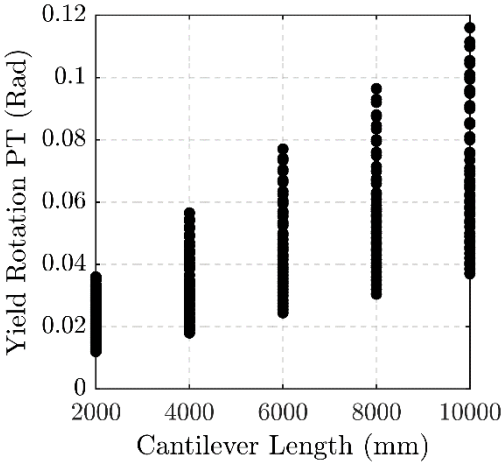
Yield Rotation PT (Rad)
0.12
0.1
0.08
0.06
0.04
0.02
0
2000
4000
6000
8000
10000
Cantilever Length (mm)

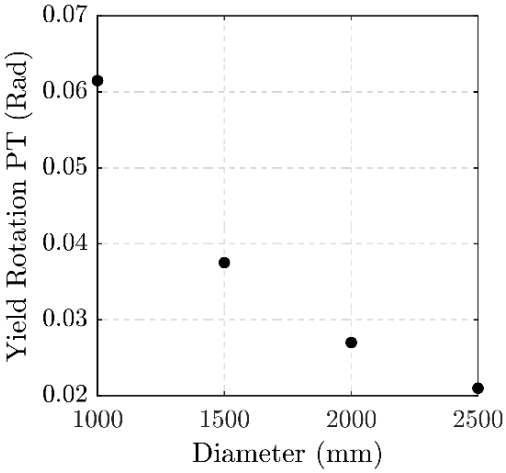
Yield Rotation PT (Rad)
0.07
0.06
0.05
0.04
0.03
0.02
1000
1500
2000
2500
Diameter (mm)

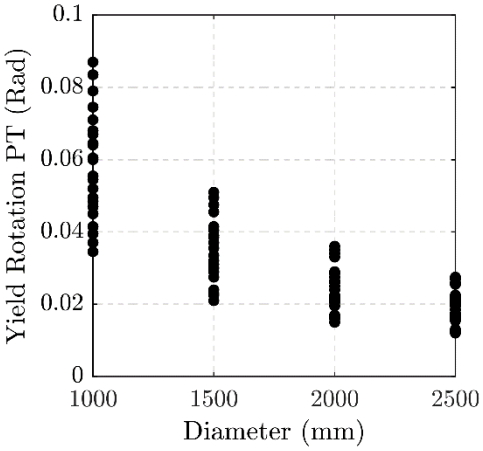
Yield Rotation PT (Rad)
0.1
0.08
0.06
0.04
0.02
0
1000
1500
2000
2500
Diameter (mm)

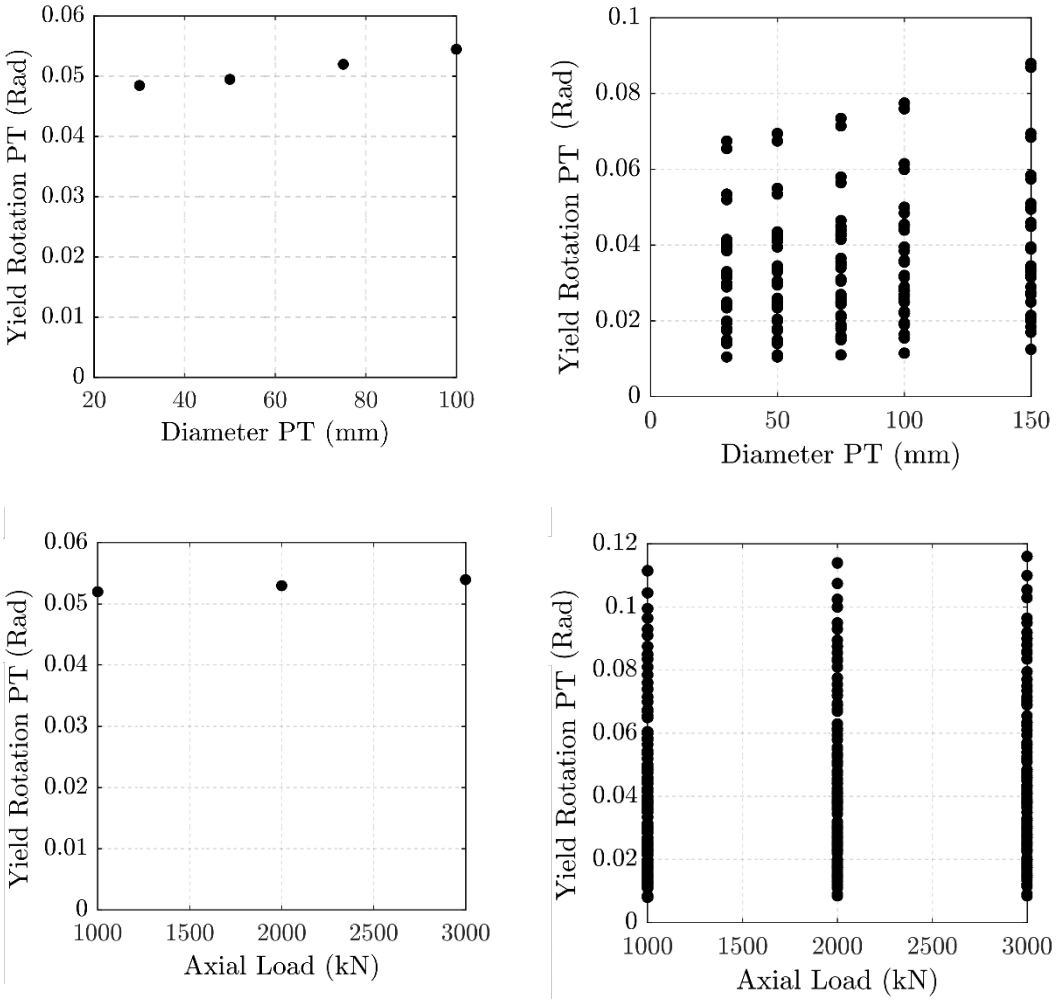

Figure 8-28: Influence of parameters on the rotation that PT yields at.

The CALS displacement for any given DCR connection is dependent on external variables such as the type of superstructure and specific design requirements like importance level and seismic hazard. However, typical DCLS drifts are of the order of 3% with CALS drift being of the order of 4.5%. This is the CALS drift used to determine which combination of the relevant variables are suitable for design.

The figures below show how the key parameters, including the unbonded length, diameter of PT and initial prestress, influence the yield rotation of the PT. The yield rotation of the PT is important since it is a key performance objective that the PT does not yield at the CALS. Geometries that ensure the PT yields beyond 4.5% drift are shown in Table 8-11. The yield stress assumed in this analysis is 70% of the ultimate stress (720Mpa).

L = 3000mm, Dpt = 30mm

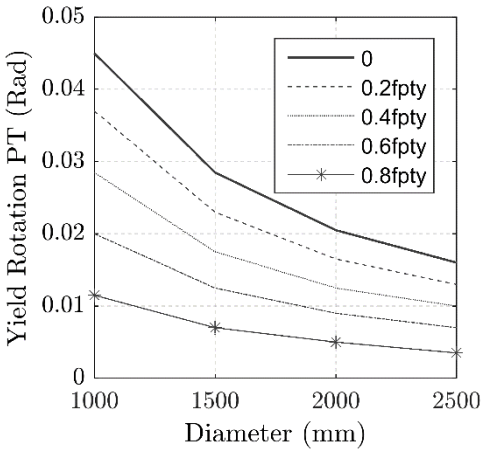

L = 3000mm, Dpt = 100mm

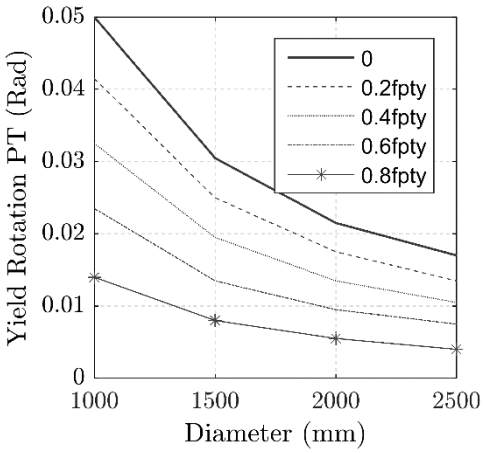

L = 4000mm, Dpt = 30mm

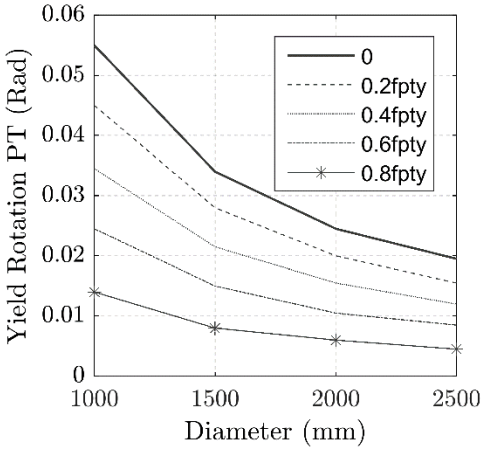

L = 4000mm, Dpt = 100mm

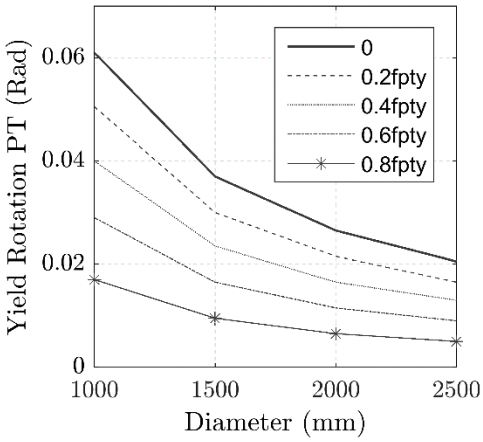

L = 5000mm, Dpt = 30mm

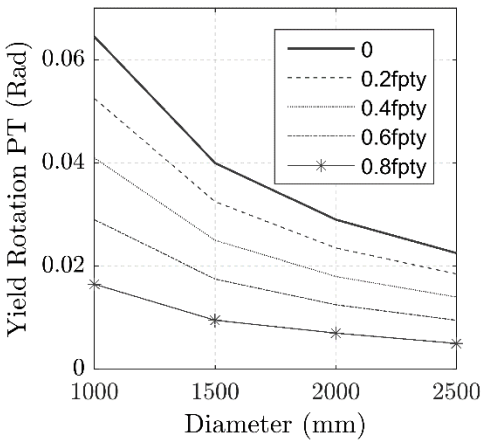

L = 5000mm, Dpt = 100mm

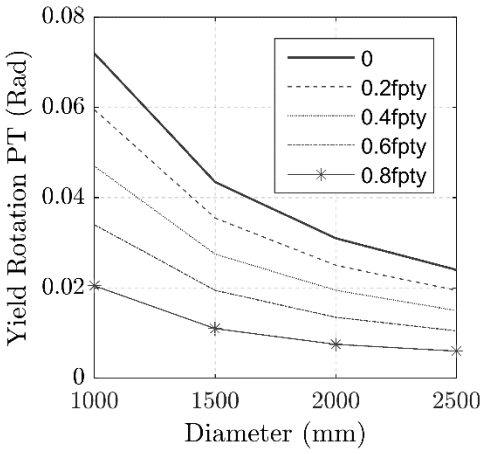

L = 6000mm, Dpt = 30mm

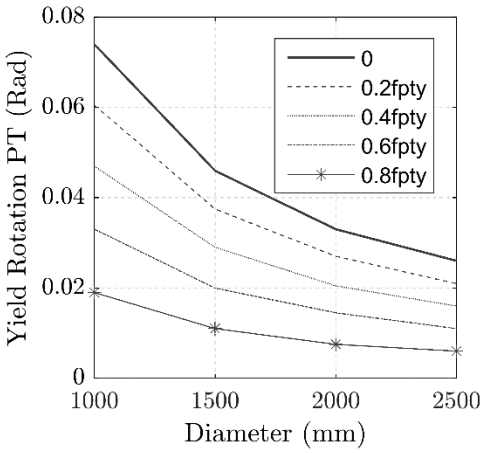

L = 6000mm, Dpt = 100mm

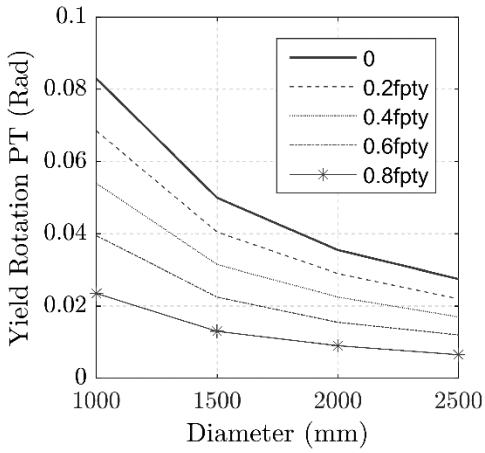

L = 7000mm, Dpt = 30mm

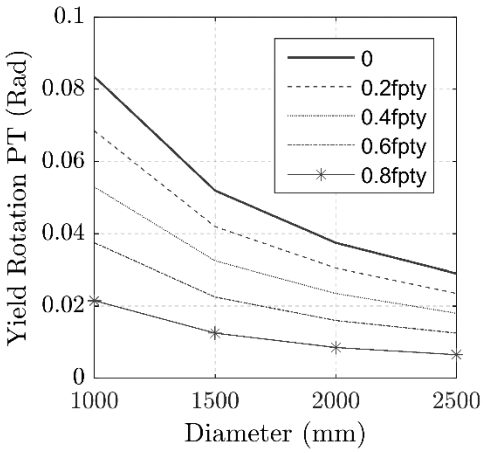

L = 7000mm, Dpt = 100mm

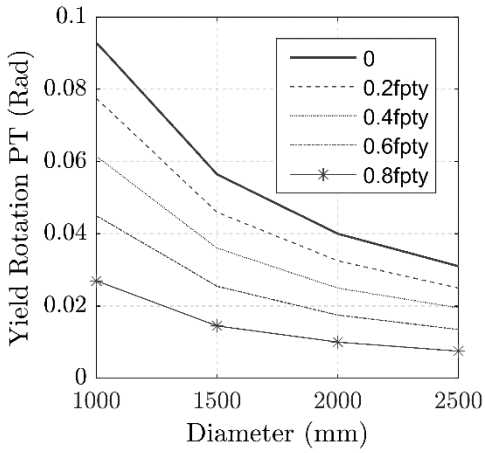

L = 8000mm, Dpt = 30mm

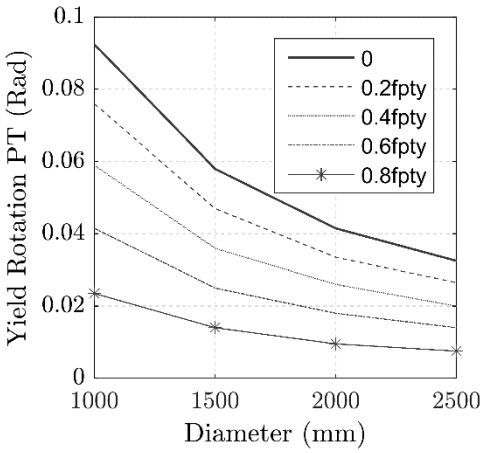

L = 8000mm, Dpt = 100mm

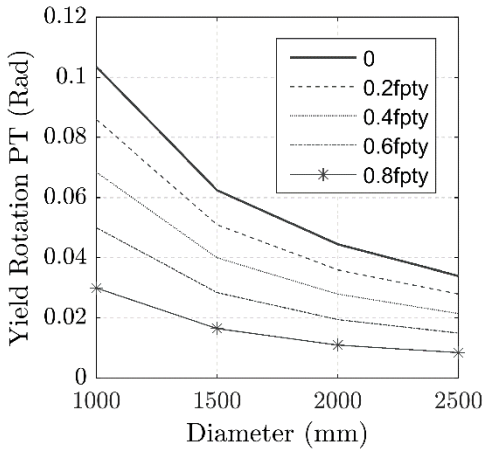

L = 9000mm, Dpt = 30mm

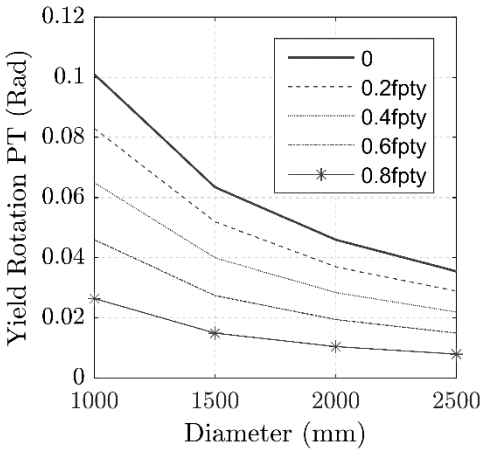

L = 9000mm, Dpt = 100mm

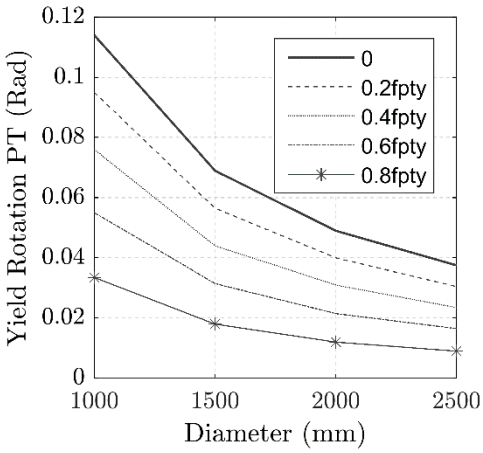

L = 10000mm, Dpt = 30mm

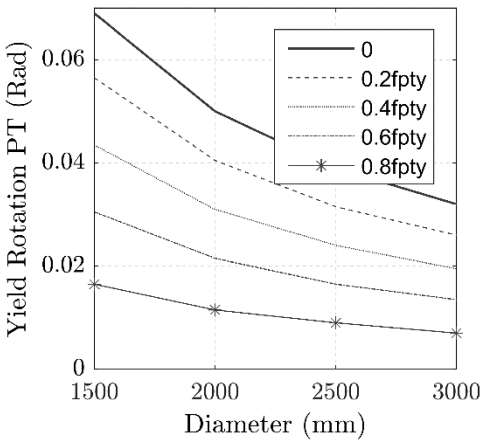

L = 10000mm, Dpt = 100mm

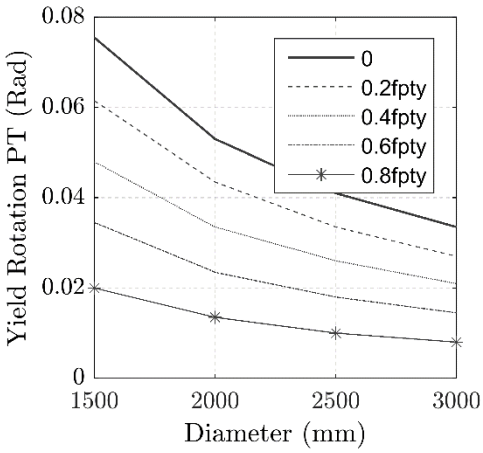

L = 12500mm, Dpt = 30mm

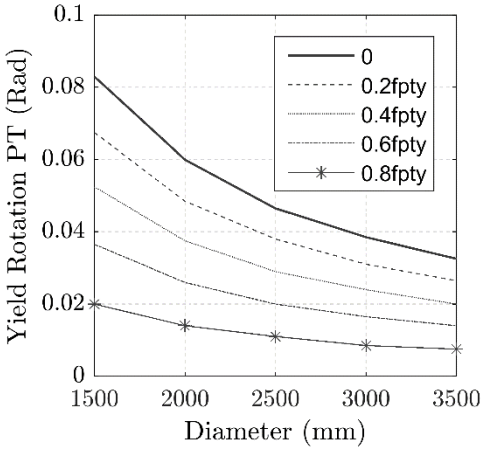

L = 12500mm, Dpt = 150mm

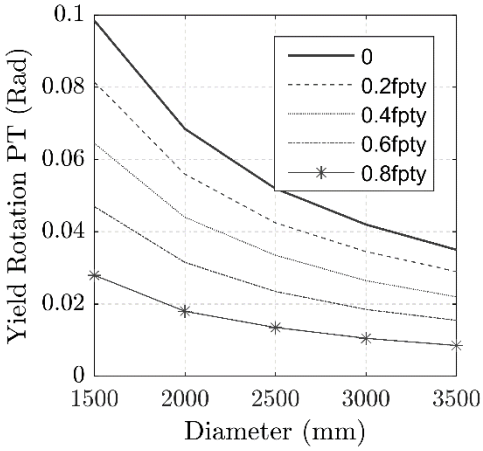

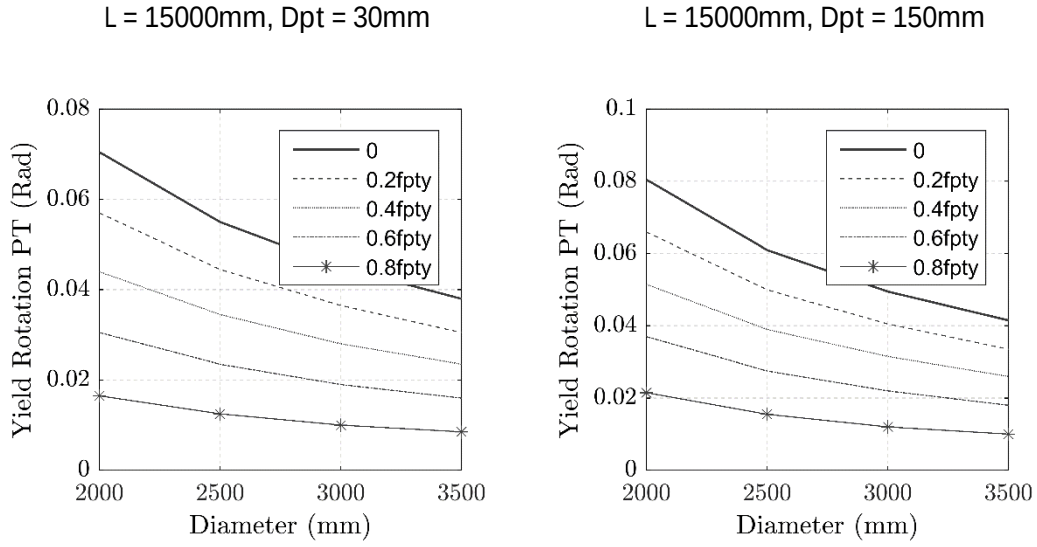

Figure 8-29: Shows the influence of initial prestress, pier diameter and unbonded length on the rotation or drift at which the PT yields.

The results from Figure 8-27 are shown in the tables below. For a given diameter and unbonded length (cantilever length) the allowable initial prestress is reported. Grey portions of the table illustrate either geometric ratios that are improbable, inefficient or not achievable. An upper and lower bound of PT diameters were found to have minimal influence, with a maximum increase in allowable prestress of 20%. The tables allow the quick and simple estimation of the maximum initial prestress of PT with a given unbonded length (cantilever length) and diameter. Following the values in these table will ensure the pier can achieve a CALS of 4.5% without yielding the PT.

Table 8-13: Lower bound, PT diameter is 30mm

Cantilever Length (mm)	Diameter (mm)								
	1000	1250	1500	1750	2000	2250	2500	2750	3000
3000	0	-	-	-	-	-	-	-	-
4000	20%	0	-	-	-	-	-	-	-
5000	20%	20%	-	-	-	-	-	-	-
6000	40%	20%	0	-	-	-	-	-	-
7000	40%	40%	0	-	-	-	-	-	-
8000	40%	40%	20%	0	-	-	-	-	-
9000	60%	40%	20%	20%	0	-	-	-	-
10000	60%	60%	40%	20%	0	0	-	-	-
12500	60%	60%	40%	40%	20%	0	0	-	-
15000	60%	60%	60%	40%	40%	20%	20%	0	0

Table 8-14: Upper bound, PT diameter is 100mm for unbonded lengths below 10m and 150mm for unbonded lengths above 10m.

Cantilever Length (mm)	Diameter (mm)								
	1000	1250	1500	1750	2000	2250	2500	2750	3000
3000	0	-	-	-	-	-	-	-	-
4000	20%	0	-	-	-	-	-	-	-
5000	20%	20%	-	-	-	-	-	-	-
6000	40%	20%	0	-	-	-	-	-	-
7000	40%	40%	0	0	-	-	-	-	-
8000	60%	40%	20%	20%	0	-	-	-	-
9000	60%	60%	20%	20%	0	0	-	-	-
10000	60%	60%	40%	20%	20%	0	0	-	-
12500	60%	60%	60%	40%	40%	40%	20%	0	-
15000	60%	60%	60%	60%	40%	20%	20%	20%	0

8-15: Ratio of PT unbonded length to total connection diameter.

Cantilever Length (mm)	Diameter (mm)								
	1000	1250	1500	1750	2000	2250	2500	2750	3000
3000	3.0	2.4	2.0	1.7	1.5	1.3	1.2	1.1	1.0
4000	4.0	3.2	2.7	2.3	2.0	1.8	1.6	1.5	1.3
5000	5.0	4.0	3.3	2.9	2.5	2.2	2.0	1.8	1.7
6000	6.0	4.8	4.0	3.4	3.0	2.7	2.4	2.2	2.0
7000	7.0	5.6	4.7	4.0	3.5	3.1	2.8	2.5	2.3
8000	8.0	6.4	5.3	4.6	4.0	3.6	3.2	2.9	2.7
9000	9.0	7.2	6.0	5.1	4.5	4.0	3.6	3.3	3.0
10000	10.0	8.0	6.7	5.7	5.0	4.4	4.0	3.6	3.3
12500	12.5	10.0	8.3	7.1	6.3	5.6	5.0	4.5	4.2
15000	15.0	12.0	10.0	8.6	7.5	6.7	6.0	5.5	5.0

The above table (Table 8-15) shows the maximum allowable geometric ratio of the cantilever length/connection diameter. Adhering to these ratios will ensure that PT will not yield until drifts larger than 4.5%. The $\frac{L_{ub}}{D}$ ratio pertains to the squatness of the pier. For ductile DCR piers a $\frac{L_{ub}}{D}$ ratio as low as 3 enables the PT, as long as the initial prestressing is low (less than $0.3f_{pty}$), to reach a CALS drift of 4.5% before yielding the PT. In addition, $\frac{L_{ub}}{D}$ ratios larger than 8 can utilise very large levels of prestress while still reaching a suitable CALS drift in excess of 4.5%.

8.7.2 Dissipation Devices

Geometric ratios for dissipaters are less important as the displacement capacity required can be altered based on the design requirements. In addition, dissipative devices which can be designed for large displacements are available (Marriott et al., 2009; Rodgers et al., 2009) Therefore, this has not been specifically investigated.

8.8 DESIGN TABLES

In the past a number of design charts have been developed to simplify the design of DCR connections (Palermo, 2004; Pampanin et al., 2010). The design tables

followed herein are developed specifically for bridges and typical typologies used in industry. In addition, they use the most recent materials and properties currently commonly used in design. In particular, Macalloy PT and four groove type dissipaters. The tables have also been developed to ensure they are very user friendly and can be implemented within the DBD framework. The intent is for users to simply look up known parameters to find the required connection capacity.

The modelling and material inputs previously discussed in this chapter are used to develop the design tables, shown in Appendix B. The following assumptions were made in order to develop the tables:

- The PT unbonded length is equal to the pier cantilever length (effective height).
- G300 dissipaters, Grade 1030MPa Macalloy bar and 40MPa concrete.
- Concrete has a linear distribution of stress due to steel armouring distributing stress.
- Anti-buckling tube sufficient to prevent global instability (buckling of dissipater tube).
- Dissipaters placed 100mm from column edge and evenly distributed.
- Cantilever length is equal to the effective height.
- Initial stress in PT is 10% of yield.
- Yield moment based on rotation defined in Table 8-3.
- Strain hardening of dissipaters is included.

The tables are intended to be used to quickly derive a suitable connection configuration using the mass and cantilever length (L_{cant}) of the structure which are typically fixed. Then, using a given drift level, a suitable arrangement of pier diameter and PT diameter can be obtained using the moment demand from force or displacement-based design methods. Consider the case of a 3m tall pier, with an axial load of 1000kN and a seismic demand of 1400kNm at the CALS drift. Preliminary design of this connection can be carried out using Table 8-16 (for N=1000kN and L_{cant} = 3m), looking down the 4% drift column (close to the CALS design drift) in the table for a connection with a capacity in excess of that required. In Appendix B a number of these tables are given for each connection diameter. Therefore, given the cantilever length, axial load and

demand, the connection diameter, PT diameter, and total dissipater area can be retrieved. An example of how these tables are used is shown in Chapter 9.

Table 8-16: Example of a Design Table.

Initial Pt Force 0.1Fyield			Axial Load (exluding PT) 1000kN				Cantilever Length (3000mm)		Grade 300 Dissipaters
PT Diameter	Fuse Length (mm)	Yield (kNm)	1%drift (kNm)	2%drift (kNm)	3%drift (kNm)	4%drift (kNm)	6%drift (kNm)	λ	Fuse Area (mm^2)
36mm	250	578	717	769	809	844	883	1.1	2682
	500	594	704	749	784	815	846	1.1	2682
	750	605	699	742	775	805	834	1.2	2682
	1000	616	693	738	770	800	828	1.2	2682
50mm	250	640	819	919	1005	1086	1165	1.1	3109
	500	657	805	894	973	1050	1124	1.2	3109
	750	670	800	885	962	1036	1109	1.2	3109
	1000	685	794	881	956	1029	1101	1.2	3109
75mm	250	797	1072	1277	1472	1663	1851	1.2	4217
	500	819	1060	1252	1435	1616	1796	1.3	4217
	750	836	1052	1237	1417	1593	1769	1.3	4217
	1000	859	1045	1230	1407	1581	1755	1.3	4217
100mm	250	1011	1407	1739	2060	2377	2691	1.2	5769
	500	1040	1396	1704	2012	2316	2620	1.3	5769
	750	1061	1386	1695	1995	2294	2592	1.3	5769
	1000	1093	1377	1684	1984	2283	2578	1.3	5769
125mm	250	1283	1817	2281	2742	3201	3659	1.2	7764
	500	1320	1802	2242	2682	3124	3567	1.3	7764
	750	1342	1793	2227	2661	3102	3532	1.3	7764
	1000	1383	1780	2227	2649	3081	3514	1.3	7764
150mm	250	1607	2299	2898	3506	4112	4716	1.2	10202
	500	1650	2270	2847	3430	4015	4600	1.2	10202
	750	1673	2261	2834	3409	3981	4559	1.2	10202
	1000	1724	2246	2828	3394	3960	4533	1.3	10202

8.9 CONCLUSIONS

This chapter proposed important parameters required for displacement and force -based design of DCR connections. The following was found from the parametric analysis:

- The yield rotation (based on the material non-linearity in the dissipaters) can be estimated using the following equation:

$$\vartheta_{yield} = 1.62\frac{\varepsilon_y L_{ub}}{D} + 0.00056$$

- The neutral axis location was described most simply at the SLS, DCLS and CALS by the following three equations where the cantilever length (Lcant) is in mm:

	Equation
Yield	$NA_{yield} = 24Lcant + 370$
DCLS	$NA_{DCLS} = 11Lcant + 170$
CALS	$NA_{CALS} = 8.5Lcant + 350$

- Limits on the geometric ratio ($3 < \frac{L_{ub}}{D} < 8$) and initial prestress (Table 8-14) were proposed, which ensure that the PT does not yield at CALS drift levels.
- Limits on the PT diameter (Table 8-11) were proposed to limit the increase in capacity beyond yield (to limit overstrength demands when using traditional design methods).
- Design tables were developed, which improve the efficiency of the design process by providing designers with suitable values of the main variables as a starting point in the design of DCR systems.

8.9.1 Further Research

Most of the research presented in this chapter, particularly pertaining to design efficiencies is for G300 mild steel dissipaters and Grade 1030 Macalloy bar. This process could be repeated for G500 dissipaters and PT strands, giving design tables for a wider range of connections. However, the dissipater and PT diameters could be

resolved into forces at each drift level. This would allow the estimation of alternative material sizes.

Chapter 9: Case Study – Implementing Design Tables and Alternative Design Philosophy

9.1 INTRODUCTION

The previous three chapters have proposed an alternative design philosophy, developed suitable strain limits and proposed relationships to determine key design parameters. This chapter has the following key objectives:

- Show the design procedure for the alternative design philosophy.
- Validate neutral axis and yield rotation relations.
- Illustrate the benefits of the alternative design philosophy.
- Show how design tables in Chapter 8 can be used within the design framework.
- Compare performance of connections designed with traditional displacement-based design and the alternative design philosophy.

These key objectives will be carried out through a design example for both the traditional and alternative design philosophy. The designs will then be compared in terms of structural demands and connection sizes. A detailed performance comparison will also be undertaken using a multi-axial spring model (procedure described in Chapter 7) and NLTH analysis.

9.2 DESIGN PARAMETERS

Given DCR connections will be most applicable to sites with high seismicity and poor soil conditions, the study investigates an arbitrary IL3 structure founded on soil Class C with a hazard factor of 0.3 as shown in Table 9-1. This case study is intended to show the displacement-based design process only. Knowledge on how section analysis is carried out for DCR connection will be beneficial to the reader.

Table 9-1: Summary of design constraints

Parameter	SLS	DCLS	CALS
Importance Level	3+	3+	3+
Hazard factor, Z	0.3	0.3	0.3
Soil Class	C	C	C
Return period, RP	1/100 years	1/1500years	~1/6500 years
Return period factor, R	0.375	1.5	2.25
Near fault factor	1	1	1
Structural performance factor, sp	1	1	1

The prototype bridge is a two-lane structure with super-T beams spanning each of the 20m spans. The spans are supported on single column hammerhead piers with a 6m high dynamic mass Figure 9-1. The resulting axial load on the pier is 2000kN. It is assumed that the spans are simply supported, and that the transverse direction is critical. In the transverse direction, a single pier model carrying the tributary mass is assumed to represent the response of the pier accurately. Grade 300 steel and 30MPa concrete is assumed for the examples.

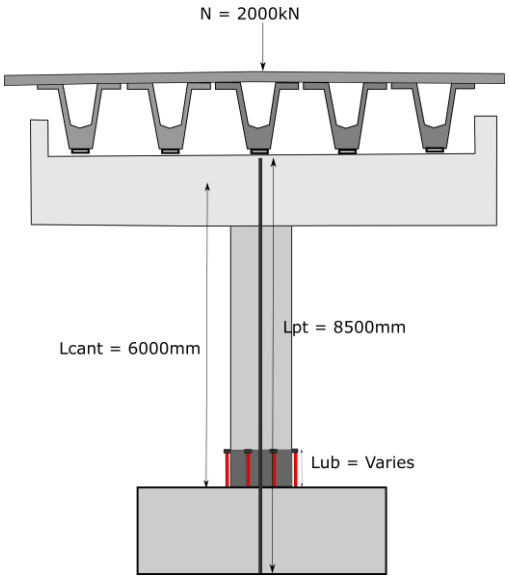

Figure 9-1: General layout of the pier.

9.3 CURRENT DESIGN PHILOSOPHY

9.3.1 Damage Control Limit State

The current design philosophy dictates that the connection be designed for the DCLS. This will be carried out in accordance with the NZTA Bridge Manual (2018). For comparative purposes soil interaction has been excluded. The design drift is assumed to be 2%. Given the yield displacement is largely determined by the fuse length of the dissipater it is assumed that the yield drift is:

$$\theta_{yield} = \frac{\theta_{design}}{\mu} = \frac{2\%}{4} = 0.5\% \qquad 9\text{-}1$$

This is assumed on the basis that there is no evidence to suggest the ductility limits stipulated in the BM for a ductile frame in which plastic hinges form can be ignored for DCR connections. Given the height of the dynamic mass is 6m the approximate design displacement and yield displacement are as follows (increased when elastic contribution included):

$$\Delta_{yield} = 0.5\% \times 6000mm = 30mm \qquad 9\text{-}2$$

$$\Delta_{design} = 2\% \times 6000mm = 120mm \qquad 9\text{-}3$$

Given the PT and mild steel contribution is not yet known the equivalent viscous damping can be found using the PRESSS design handbook (Pampanin et al., 2010). The desired recentering ratio is typically around between 1.15 and 2, 1.5 is assumed and will be checked in subsequent steps.

$$\xi_{eq} = 0.05 + \frac{0.577}{1+\lambda}\left(\frac{\mu-1}{\mu\pi}\right) \qquad 9\text{-}4$$

$$\xi_{eq} = 0.05 + \frac{0.577}{2.5}\left(\frac{4-1}{4\pi}\right) = 10.5\% \qquad 9\text{-}5$$

The factor for reducing the design displacement spectrum can be found in the NZTA Bridge Manual (Eq 5.17, BM) or DBD guidelines:

$$M_\xi = \left(\frac{0.07}{0.02 + \xi_{eq}}\right)^{\alpha} \qquad 9\text{-}6$$

$$M_\xi = \left(\frac{0.07}{0.02 + 0.105}\right)^{0.5} = 0.748 \qquad 9\text{-}7$$

Thus the earthquake demand displacement can be calculated using Eq 5-4 in the BM.:

$$\Delta_d(T) = M_\xi NZRu\Delta_h(T) \qquad 9\text{-}8$$

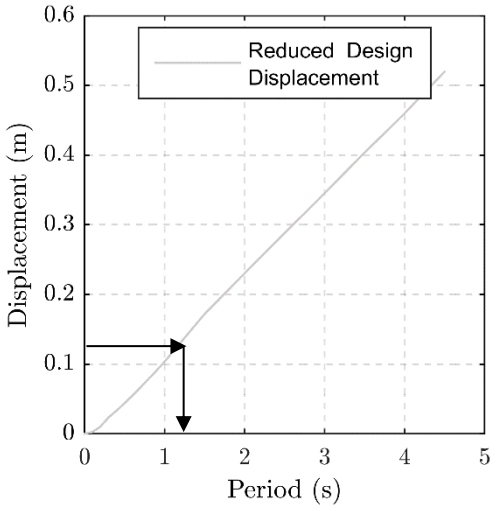

Figure 9-2: Reduced displacement spectrum from Table 5.4 in the BM

The effective period derived from Figure 9-2 is 1.12 secs. The resulting effective stiffness is then calculated:

$$k_e = \frac{4\pi^2 m_e}{T_e^2} \qquad 9\text{-}9$$

$$k_e = \frac{4\pi^2 204}{1.16^2} = 6006kN/m \qquad 9\text{-}10$$

The base shear demand and moment at the design displacement are:

$$F_f = k_e \Delta_d \qquad 9\text{-}11$$

$$F_f = 721kN, M = 4324kNm \qquad 9\text{-}12$$

Table 9-2: Design table for connection with 1800mm diameter, N = 2000kN, Lcant = 6000mm, Grade 300 steel, 30MPa Concrete, Grade 1030 Macalloy bar.

Initial Pt Force 0.1Fyield		**Axial Load (exluding PT) 2000**			**Cantilever Length (6000mm)**			**Grade 300 Dissipaters**		
	PT Diameter	Fuse Length (mm)	Yield (kNm)	1%drift (kNm)	2%drift (kNm)	3%drift (kNm)	4%drift (kNm)	6%drift (kNm)	**λ**	Fuse Area (mm^2)
Diameter (1800mm)	36mm	250	2320	2855	3058	3231	3290	3274	1.4	4020
		500	2337	2799	2960	3097	3135	3110	1.5	4020
		750	2386	2780	2925	3045	3068	3031	1.6	4020
		1000	2410	2770	2907	3017	3031	2988	1.6	4020
	50mm	250	2459	3153	3514	3853	4012	4036	1.5	4451
		500	2477	3091	3410	3707	3841	3856	1.6	4451
		750	2534	3070	3372	3649	3768	3769	1.7	4451
		1000	2560	3058	3352	3620	3728	3721	1.7	4451
	75mm	250	2818	3910	4675	5400	5851	5978	1.7	5570
		500	2839	3831	4542	5227	5641	5755	1.8	5570
		750	2910	3803	4493	5161	5551	5650	1.9	5570
		1000	2947	3788	4468	5126	5504	5591	1.9	5570
	100mm	250	3310	4923	6232	7486	8366	8629	1.8	7137
		500	3335	4831	6056	7258	8104	8347	2.0	7137
		750	3428	4792	5991	7169	7993	8217	2.0	7137
		1000	3476	4774	5958	7122	7934	8146	2.1	7137
	125mm	250	3926	6169	8111	10003	11540	11985	1.9	9152
		500	3965	6062	7907	9728	11208	11620	2.0	9152
		750	4078	6015	7825	9613	11060	11451	2.1	9152
		1000	4142	5986	7779	9549	10979	11358	2.1	9152
	150mm	250	4668	7630	10288	12889	15279	15955	1.9	11614
		500	4719	7495	10037	12551	14868	15511	2.1	11614
		750	4856	7449	9945	12420	14694	15306	2.1	11614
		1000	4935	7407	9896	12350	14601	15190	2.2	11614

From the parametric analysis, the approximate design can be determined relatively quickly. The axial load is 2000kN and the cantilever length is 6m. From design tables in Appendix B a suitable connection can be selected. For a 2000kN axial load and 6m cantilever length there are a range of suitable connections (

Table 9-2). Either 1200mm connection diameter and large PT bar diameter can be used, or a larger connection with less PT can be used. From Table 8-11 the PT bar diameter should be kept to around 100mm for a 1500mm diameter connection, and 70mm for a 1800mm diameter connection. Therefore, a starting point for the design is a 1800mm diameter column with a dissipater area of 5570mm^2 and a 75mm diameter Macalloy bar. These tables assume a low initial prestress (10% of yield of PT) so there is the potential to increase the capacity slightly by increasing the initial prestress.

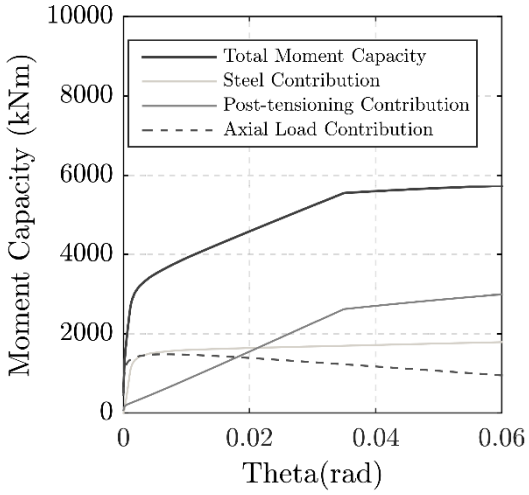

Figure 9-3: Left – Moment capacity and the various contributions, Right – Shows the yield rotation.

A pushover of the connection with D_{pt} = 75mm, Unbonded length of PT = 8.5m, dissipater area = 5890mm^2 (12x25mm diameter dissipaters gives an area of 5890 mm^2) and D = 1800mm gives a moment capacity of 4696kNm at the design level drift. Section analysis gives a re-centering ratio of 1.66. This section analysis was carried out using the ptMBA and section analysis procedure defined in Chapter 8. Though this is not required for design, it verifies the design procedure and yield rotations are correct (Yield rotation relationships are defined in Chapter 8). Following the selection of a suitable connection it is important to ensure the assumptions made at the beginning of design hold true (particularly the yield displacement and design displacement). Since the design drift is known, the minimum unbonded length of the dissipater can be estimated assuming the location of the neutral axis at the design drift. This should be verified during detailed design (using section analysis at the design drift) but a preliminary value can be assumed based on the relations proposed in Chapter 8.

$$NA_{DCLS} = 11Lcant + 170 \quad (9\text{-}13)$$

$$NA_{DCLS} = 11 \times 6 + 170 = 236mm \quad (9\text{-}14)$$

$$\Delta_{gap} = \vartheta_{des}(D - NA + 50) \quad (9\text{-}15)$$

$$\Delta_{gap} = 0.02(1800 - 236 + 50) = 32.3mm \quad (9\text{-}16)$$

$$L_{ub} = \frac{\Delta_{gap}}{\varepsilon_{DCLS}} = \frac{32.3}{0.05} \approx 540mm \quad (9\text{-}17)$$

The unbonded length required to satisfy the DCLS is 540mm. From the pushover curve the neutral axis was 232mm so in this case the estimation of the NA location was very close to the value calculated through section analysis.

Given current codes stipulate a displacement ductility of 4 the following unbonded length must be sufficient to ensure the yield displacement is at least 4 (alternatively increase the capacity of the connection and reduce the design drift). The contribution to the yield displacement from rotation can be estimated from (assuming a larger unboned length of 1000mm is required to meet design requirements):

$$\vartheta_{yield} = 0.0024\frac{L_{ub}}{D} + 0.00056 \quad (9\text{-}18)$$

$$\vartheta_{yield} = 0.0024\frac{1000}{1800} + 0.00056 = 0.0019 \quad (9\text{-}19)$$

Therefore, the yield displacement resulting from rotation of the joint is:

$$\Delta_{rot} = 0.0019 \times 6000mm = 11.4mm \quad (9\text{-}20)$$

The contribution from the elastic contribution of the pier:

$$EI_{eff} = 0.3EI_g = 4.595e + 15\ Nmm^2 \quad (9\text{-}21)$$

$$\Delta_{el} = \frac{F_y \times L^3}{3EI_{eff}} \quad (9\text{-}22)$$

$$\Delta_{el} = \frac{491000 \times 6000^3}{3 \times 4.595e+15} = 7.7mm \quad (9\text{-}23)$$

$$\Delta_{yield} = \Delta_{el} + \Delta_{rot} = 8mm + 11.4mm = 19.4mm \quad (9\text{-}24)$$

In this case the F_y can be estimated from the design table presented in Appendix B. As shown in Eq 9-24 the assumed yield displacement is below what was assumed to meet the ductility limit (4). In this situation, it would be suitable to simply increase

the fuse length of the dissipater. However, this may not be practical, and iterating through design to reduce the design displacement may be required to limit the ductility used. This is further evidence to support the fact that current bridge design guidelines (NZTA, 2018) do not accommodate the design of DCR, particularly for large diameter connections. For this example it is assumed that the connection ductility of 6 is acceptable although the current NZ BM limits the ductility to 4.

9.3.2 Collapse Avoidance Limit State

Typically, with the positive post yielding stiffness, the CALS will be easily satisfied. In this case a CALS displacement of 220mm (approx.3.5% drift or 0.035 rad) is used. Typically, 3% would be assumed (1.5x2% the design drift) but DCR connections typically have less damping and hence the increase between the DCLS and CALS is slightly larger than for monolithic connections. The damping is based on Eq 9-4 and is 11.7% for a re-centering ratio of 1.5 and ductility of 11 (recentering ratio is relatively constant for most connections beyond the design drift). Though this ductility is extremely high for monolithic connections, it is not for DCR connections due to the lower yield level (differently defined) and lack of damage/degradation.

In the same way as the DCLS displacement, the effective stiffness can be calculated for the increased return period factor R = 2.25:

$$M_\xi = \left(\frac{0.07}{0.02 + 0.12}\right)^{0.5} = 0.707 \quad 9\text{-}25$$

Which results in:

$$k_e = \frac{4\pi^2 204}{1.41^2} = 4057 kN/m \quad 9\text{-}26$$

The base shear demand and moment at the design displacement are:

$$F_f = k_e \Delta_d \quad 9\text{-}27$$

$$F_f = 888kN, M = 5330kNm \quad 9\text{-}28$$

Capacity at CALS displacement of 220mm (from pushover):

$$F_{cap} = 943kN, M_{cap} = 5659kNm \quad 9\text{-}29$$

F_{cap} and M_{cap} were determined from the pushover previously shown in Figure 9-3, although these could be found using the design tables or a simple section analysis at the desired drifts. The connection has enough capacity to survive a CALS event.

The final step is to check that the strain limits do not exceed 7.5% (PRESSS) at the CALS drift of 3.5%. Calculating the gap opening at the extreme fibre dissipater (assuming the dissipater is 50mm beyond the edge of the concrete section):

$$\Delta_{gap} = \vartheta_{Cals}(D - NA + 50) \quad 9\text{-}30$$

$$NA = 8.5Lcant + 130 = 206.5mm \quad 9\text{-}31$$

$$\Delta_{gap} = 0.035(1800 - 206.5 + 50) = 58 \quad 9\text{-}32$$

$$\varepsilon_{strain} = \frac{\Delta_{gap}}{L_{ub}} = \frac{58}{1000} \approx 5.8\% \quad 9\text{-}33$$

So, the design just meets the requirements. In Chapter 7, dissipater strain limits of 6% and 9% were recommended for DCLS and CALS respectively. In this example the DCLS strain in dissipater is about 3%. Therefore, dissipater design results in strains well within the previously recommended strain limits. This was specifically achieved to reduce ductility in accordance with bridge manual requirements and illustrate the shortfalls of ductility requirements for DCR connections. In this case the ductility at the design displacement is around 6 which conforms to the previous version of the Bridge Manual (2013). From the pushover the recentering ratio λ was 1.6 and the neutral axis location was 180mm at the CALS drift (compared to 206.5mm from simplified relationships (Eq. 9-3)). Therefore, the procedures for estimating these levels are sufficient for preliminary design.

9.3.3 Alternative Design Philosophy

This design method is somewhat different to the design example shown previously. The main difference being that some design requirements such as ductility are are not required as inputs to the design. In addition, the DCLS is not used directly in the design, and provides a means for the designer to understand when dissipaters should be replaced but nothing more.

9.3.4 Design Procedure

The design procedure is very similar to checking the DCR connection satisfies the CALS (as in the previous section) with one distinct difference: the CALS drift level is defined by the yielding of PT, failure of the dissipaters or P-Delta effects. Typically, a design will have a predefined pier height and hence PT length. The unbonded length of dissipaters can generally be altered in length in order to accommodate the CALS displacement. Therefore, to determine the target drift, a connection diameter needs to be assumed. The following procedure can then be adopted for design:

1. Assume a typical connection Diameter (D).
2. Estimate the drift the PT yields at for low levels of prestress.
3. Determine desired unbonded length of dissipaters based on the CALS drift.
4. Estimate the yield rotation and yield force.
5. Calculate damping and associated reduction factor.
6. Determine effective period, stiffness and hence moment demands.
7. Refer to design tables to obtain a suitable connection.
8. Optimise connection capacity to be close to demands.
9. Carry out detailed section analysis using ptMBA and the iterative analysis procedure.
10. Check the strain in dissipater and PT at the CALS.
11. Check damping is similar to the initial calculation.
12. Check P-Delta.
13. Check strain limits in the dissipaters at the DCLS.

These steps are explained further in the following design example.

9.4 ALTERNATIVE DESIGN PHILOSOPHY – DESIGN EXAMPLE

In this design example the parameters used in the conventional DBD method are adopted (6m height of dynamic mass, 2000kN axial load and 8.5m unbonded length of PT).

1.Assume a logical pier Diameter (D)

For this example, we will assume a pier diameter of 1500mm.

2.Estimate the drift the PT yields at for low levels of prestress

Using Eq 9-31 to estimate NA location at the CALS drift, the rotation that PT yields at can be determined:

$$\varepsilon_{pty} = 0.037 \qquad 9\text{-}34$$

$$T_{pti} = 0.1 \times 720 = 72\text{Mpa} \qquad 9\text{-}35$$

$$\varepsilon_{pti} = \frac{72}{190000} = 0.00038 \qquad 9\text{-}36$$

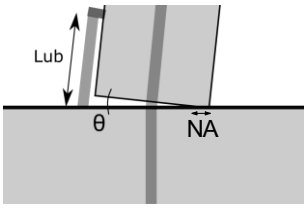

$$\vartheta_{CALS} = \frac{\varepsilon_p \times L_{ubp}}{\frac{D}{2} - NA} \qquad 9\text{-}37$$

$$\vartheta_{CALS} = \frac{(0.0035 - 0.00038) \times 8500mm}{\frac{1500mm}{2} - 206mm} = 0.048 \qquad 9\text{-}38$$

This is a suitable target drift, however to give the PT some level of protection against yield, 4.5% will be set as the target drift. From (Chapter 8 – table 8.3) we can see that a 1500mm diameter pier can achieve 4.5% drift with low levels of initial prestress. A CALS drift of 4.5% correlates to a displacement of around 270mm (excluding the elastic displacement of the pier (conservative)).

3.Determine desired unbonded length of dissipater based on CALS drift

The CALS strain limit for grooved type dissipaters was defined in Chapter 8 as 9%. As the centreline of the dissipaters is assumed to be located 50 mm outside the section. The unbonded length of the dissipater is determined by:

$$\Delta = 0.045(D - NA_{CALS} + 50) = 60.5mm \qquad 9\text{-}39$$

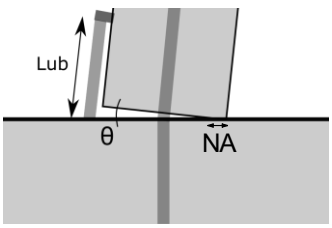

$$L_{ub} = \frac{\Delta L}{\varepsilon_{CALS}} = \frac{60.5}{0.09} = 672mm \qquad 9\text{-}40$$

Therefore, the unbonded length of dissipaters, can be 672mm or longer. A 1000mm unbonded length is assumed to be consistent with the previous example.This will allow the damage between the two connections to be fairly evaluated and account

for the fact that alternative dissipative devices can displace further than axial dissipaters (Marriott, 2009).

4.Estimate the yield rotation and yield force

The yield rotation can then be estimated using the unbonded length of the dissipater (1000mm)

$$\vartheta_{yield} = 0.0024\frac{L_{ub}}{D} + 0.00056 \quad (9\text{-}41)$$

$$\vartheta_{yield} = 0.0024\frac{1000}{1500} + 0.00056 = 0.0022\text{rad} \quad (9\text{-}42)$$

Since a diameter has been assumed, the yield displacement can be estimated by obtaining the yield force (from design tables in Appendix C). The yield moment for a 1500mm connection with 6m cantilever length, 2000kN axial load, area of dissipaters of 5329mm^2 and 75mm diameter PT is 2334kNm, which results in a base shear of 389kN

$$\Delta_{el} = \frac{F_y \times L^3}{3EI_{eff}} \quad (9\text{-}43)$$

$$\Delta_{el} = \frac{389000\times6000^3}{3\times2.216e+15} = 12.6mm \quad (9\text{-}44)$$

$$\Delta_{yield} = \Delta_{el} + \Delta_{rot} = 12.6mm + 13.2mm = 25.8mm \quad (9\text{-}45)$$

5.Calculate damping and associated reduction factor

Similar to the previous design example, the contribution of PT and mild steel is unknown. Therefore, the damping and reduction factor are calculated in accordance with the PRESSS design handbook:

$$\xi_{eq} = 0.05 + \frac{0.577}{1+\lambda}\left(\frac{\mu-1}{\mu\pi}\right) \quad (9\text{-}46)$$

$$\xi_{eq} = 0.05 + \frac{0.577}{2.8}\left(\frac{10.4-1}{10.4\pi}\right) = 11\% \quad (9\text{-}47)$$

$$M_{\xi} = \left(\frac{0.07}{0.02+0.11}\right)^{0.5} = 0.736 \quad (9\text{-}48)$$

Where **λ** was obtained from the design tables and the displacement ductility is 270mm/25.8mm.

6.Determine effective period, stiffness and hence moment demands

Using the BM reduced displacement spectrum for a R=2.25, Z = 0.3 soil class C and the above damping reduction the following effective stiffness is obtained:

$$k_e = \frac{4\pi^2 204}{1.66^2} = 2916 kN/m \quad \text{9-49}$$

The base shear and moment demand at the design (CALS) displacement of 270mm calculated above from the yield strain in the PT:

$$F_f = k_e \Delta_d \quad \text{9-50}$$

$$F_f = 787 kN, M = 4723 kNm \quad \text{9-51}$$

7.Refer to design tables to obtain a suitable connection

Table 9-3: Design table for connection with 1500mm diameter, N = 2000kN, Lcant = 6000mm, Grade 300 steel, 30MPa Concrete, Grade 1030 Macalloy bar.

Initial Pt Force 0.1Fyield		**Axial Load (exluding PT) 2000**			**Cantilever Length (6000mm)**			**Grade 300 Dissipaters**		
	PT Diameter	Fuse Length (mm)	Yield (kNm)	1%drift (kNm)	2%drift (kNm)	3%drift (kNm)	4%drift (kNm)	6%drift (kNm)	λ	Fuse Area (mm^2)
Diameter (1500mm)	36mm	250	1847	2271	2389	2471	2545	2525	1.3	3964
		500	1880	2230	2317	2374	2427	2394	1.4	3964
		750	1910	2214	2292	2339	2379	2337	1.5	3964
		1000	1937	2208	2278	2321	2354	2305	1.5	3964
	50mm	250	1949	2476	2706	2892	3074	3107	1.4	4344
		500	1984	2433	2626	2790	2947	2965	1.5	4344
		750	2018	2416	2598	2751	2896	2902	1.6	4344
		1000	2049	2408	2583	2731	2871	2868	1.6	4344
	75mm	250	2211	2995	3499	3960	4395	4585	1.6	5329
		500	2253	2948	3401	3827	4244	4416	1.7	5329
		750	2295	2926	3364	3777	4182	4344	1.7	5329
		1000	2334	2913	3345	3751	4151	4306	1.8	5329
	100mm	250	2571	3694	4540	5351	6142	6630	1.7	6708
		500	2625	3636	4429	5197	5957	6414	1.8	6708
		750	2676	3612	4385	5133	5874	6317	1.8	6708
		1000	2727	3594	4358	5097	5830	6265	1.9	6708
	125mm	250	3023	4552	5804	7019	8211	9143	1.7	8481
		500	3096	4481	5668	6831	7985	8882	1.8	8481
		750	3155	4459	5620	6760	7895	8770	1.9	8481
		1000	3217	4433	5592	6724	7846	8708	1.9	8481
	150mm	250	3564	5550	7259	8927	10570	12111	1.7	10648
		500	3661	5464	7094	8700	10295	11791	1.9	10648
		750	3723	5437	7035	8613	10185	11654	1.9	10648
		1000	3795	5415	7006	8568	10127	11579	1.9	10648

From the design tables (Table 9.3) the connection highlighted in grey is close to the demands.

8.Optimise connection to be close to demands

The connection initially chosen does not have sufficient capacity. However, lamda is 1.8 which allows the amount of steel to be increased, which will increase the damping. So, use a connection with D = 1500mm, Dpt = 75mm, Adisp = 6000mm^2.

9. Carry out detailed section analysis using ptMBA

See chapter 8 for modelling methodology. This step is optional and the next size up in the design tables will satisfy design (though less efficiently). The results from the analysis are shown below.

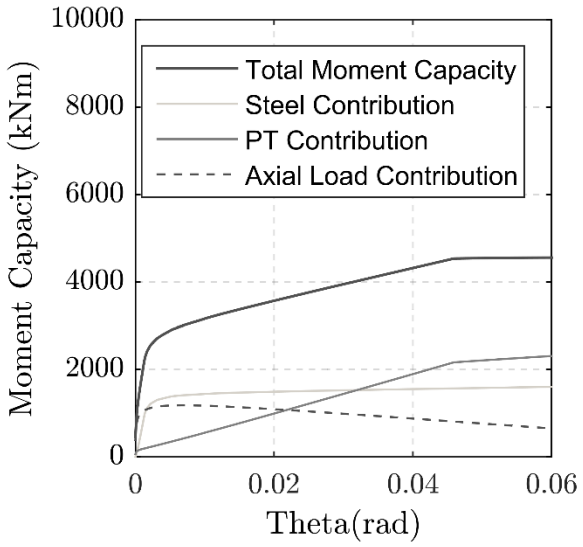

Figure 9-4: Left – Moment-rotation response for the connection design at the CALS

$$F_{cap} = 755kN, M_{cap} = 4532kNm \quad 9\text{-}52$$

Steps 10 – 13: Check the assumptions made at the start of design are correct.

All force and λ values used herein are obtained from the section analysis.

Yield displacement resulting from rotation of the joint is:

$$\Delta_{rot} = 0.0022 \times 6000mm = 13.2mm \quad 9\text{-}53$$

The contribution from elastic contribution of the pier:

$$EI_{eff} = 0.3EI_g = 2.22e + 15\ Nmm^2 \quad 9\text{-}54$$

$$\Delta_{el} = \frac{F_y \times L^3}{3EI_{eff}} \quad 9\text{-}55$$

$$\Delta_{el} = \frac{426000 \times 6000^3}{3 \times 2.22e+15} = 13.8mm \quad 9\text{-}56$$

$$\Delta_{yield} = \Delta_{el} + \Delta_{rot} = 13.8mm + 13.2mm = 27mm \quad 9\text{-}57$$

Check CALS displacement:

$$\Delta_{el} = \frac{756000 \times 6000^3}{3 \times 2.22e+15} = 24.5mm \quad 9\text{-}58$$

$$\Delta_{CALS} = \Delta_{el} + \Delta_{rot} = 24.5mm + 270mm = 294mm \quad 9\text{-}59$$

Therefore, the force demands are even lower than assumed due to the additional displacement capacity. For correctness double check displacement-based design:

$$\xi_{eq} = 0.05 + \frac{0.577}{2.4}\left(\frac{12-1}{12\pi}\right) = 12\% \quad 9\text{-}60$$

$$M_{\xi} = \left(\frac{0.07}{0.02 + 0.12.2}\right)^{0.5} = 0.708 \quad 9\text{-}61$$

Which results in:

$$k_e = \frac{4\pi^2 204}{1.88^2} = 2282kN/m \quad 9\text{-}62$$

The base shear demand and moment at the CALS displacement are:

$$F_f = k_e \Delta_d \quad 9\text{-}63$$

$$F_f = 669kN, M = 4015kNm \quad 9\text{-}64$$

Design is still suitable. From Figure 9-3 the moment capacity at 4.5% drift is about 4,532 kNm.

Check dissipater strain at CALS is less than 9%:

$$\Delta_{gap} = \vartheta_{cals}(D - NA + 50) = 60.5mm \quad 9\text{-}65$$

$$\varepsilon_{strain} = \frac{\Delta_{gap}}{L_{ub}} = \frac{60.5}{1000} \approx 6.0\% \quad 9\text{-}66$$

Check the PT strain at CALS is less than yield:

$$\Delta_{gap} = \vartheta_{cals}(D/2 - NA) = 24.5mm \quad 9\text{-}67$$

$$\varepsilon_{strain} = \frac{\Delta_{gap}}{L_{ub}} = \frac{24.5}{8500} \approx 0.29\% < 0.37\% \quad 9\text{-}68$$

This CALS strain significantly less than the recommended limit of 9%, indicating that the dissipater length could be reduced for efficiency. Given the smaller diameter of the pier (and same length of dissipaters) than that used in the previous

analysis, by inspection the dissipater strain developed in a DCLS event is smaller for the alternative design philosophy than for the conventional analysis. Therefore, although this pier would displace more in a CALS earthquake it is likely the dissipaters would be less damaged! Given the 4500kNm capacity is significantly larger than the 4015kNm demand, the steel area, Adisp was reduced to 5890mm^2 (for comparative purposes – following section). If practicable possible, fewer dissipaters could have been used.

9.5 COMPARISON BETWEEN DESIGN METHODS

The previous section illustrated how to design a DCR connection using traditional displacement-based design where ductility is considered. In addition, design of a DCR connection using the alternative design philosophy where the ductility limits were excluded was shown. The basis of excluding specified ductility limits at the DCLS was discussed in depth in Chapter 7. Basically, because DCR connections (and any other low damage connections) can be easily repaired for any level of damage below a collapse avoidance limit state event, the damage is always controlled (occurs only in replaceable devices). Therefore, the DCLS can simply be set based on the cost of repair or neglected all together (Chapter 6).

Using the alternative design philosophy has significant benefits on the connection sizes and materials required. As shown in Table 9-4, the connection interface area is reduced by 30%. Perhaps the more significant reduction is the reduction in base shear demands which have reduced by around 20%. This will have direct implications for capacity designed elements such as the piles giving greater flexibility to the construction methods available. It is noted that this reduction was from a connection with a ductility of 6 rather than the current upper limit of 4. Therefore, this reduction in base shear could be even larger in an example complying with the current Bridge Manual ductility limit of 4.

Table 9-4: Comparison of connections and demands found using displacement-based design.

	Traditional Design	Alternative Design	% Difference
Pier Diameter	1800mm	1500mm	30%
Dissipater Area	5890mm^2 (12xdia.25mm)	5890mm^2 (12xdia.24mm)	-
PT diameter	75mm Macalloy	75mm Macalloy	-
Initial Stress	318kN	318kN	-
Recentering ratio	1.7	1.5	-
Base Shear Demands Foundation	888kN	669kN	20%

Figure 9-5 shows a visual representation of the reduced base shear demands for the two connections. The ADRS curve for CALS, DCLS and SLS, which correspond to a 1/6500, 1/1500 and 1/50 annual exceedance probability events are overlaid on the pushover curves (CSM). Both connections perform satisfactorily at the CALS, which is not surprising as these levels were designed for using displacement-based design. Using the alternative design philosophy results in larger displacements. Therefore, the application of this design strategy may be limited by the interaction with the superstructure, which should be checked regardless of the design strategy used.

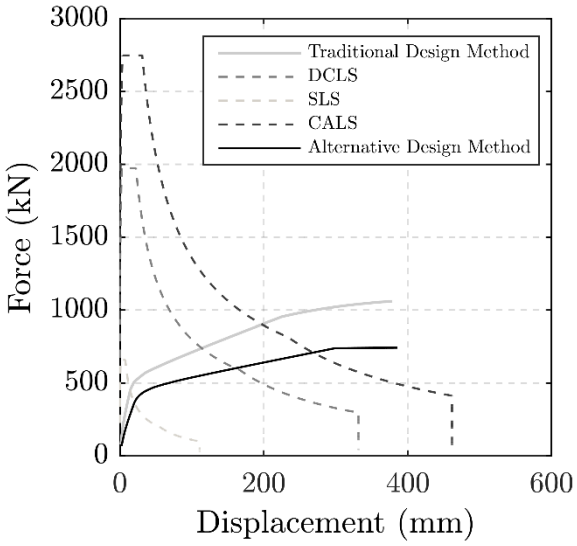

Figure 9-5: Pushover comparison of the connections.

One drawback of the proposed design philosophy is that for a given DCLS demand, with 1/1000 year annual exceedance probability, the displacement is higher (in the example this was around 35mm). On the surface this would increase the strain in the PT (which has been designed for) and potentially increase the strain in the steel. However, given the control the designer has over the unbonded length this can be easily offset. Doing this would lead to inefficiency if using axial dissipaters, as increasing the fuse length increases the construction difficulty. However, since the pier diameter reduces, the lever arm to the extreme fibre dissipater and PT also decreases. This means that the strain in the dissipaters and PT could even be reduced, rather than increased, if the reduction in diameter is sufficient. For this example, this is further quantified and discussed using NLTH in the following section.

The initial stiffness and apparent yield point of the connection designed using the alternative design philosophy are also reduced. This could result in premature yielding of the external dissipative devices in SLS level shaking. This would not affect the performance of the connections but could potentially result in unacceptable superstructure displacements in low level events. In the cases examined within this Thesis the has never governed design, so it is probably unlikely to do so. However, it cannot be ignored. One reason the ductility level is set at 4 for traditional plastic hinges is to ensure that SLS does not govern design. Therefore, since ductility is being ignored for this philosophy the SLS needs to be checked. For the above example both design

procedures give connections with yield displacements less than 20mm, which is acceptable.

The connections previously designed were modelled in OpenSEES to provide a more comprehensive comparison. The modelling and ground motion scaling was carried out using the same strategy applied in Chapter 8. The scaled ground motions for the CALS are shown in Appendix B.

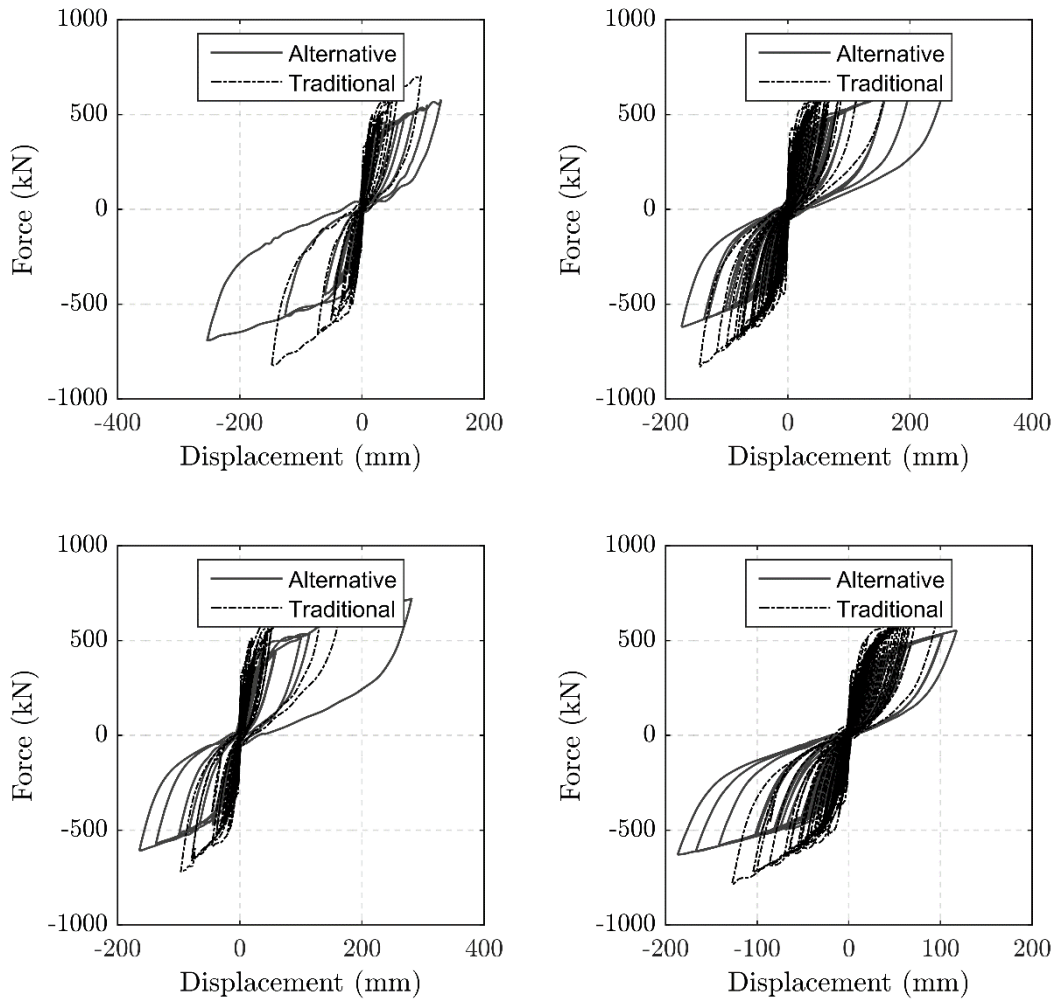

Figure 9-6: Shows the response of a selection of the connections to scaled ground motions.

Similar to the CSM, the connections designed using the alternative design philosophy undergo reduced based shear but increased displacement (Figure 9-6). The peak increase in displacement was 109mm (Table 9-5). Which is larger than the designed 50mm increase in displacement. This is due to the traditional connection reaching a 155mm displacement which is well below the 200mm design displacement. In addition, the peak displacement of the connection designed using the alternative design philosophy is 277mm, which is similar to the CALS design displacement of 294mm.

Table 9-5: Peak displacement (mm) recorded from NLTH analysis (Refer to Appendix B).

	GM1	GM2	GM3	GM4	GM5	GM6	GM7	Max
Traditional	148	173	175	155	127	214	172	214
Alternative	254	236	282	263	187	277	261	282
Increase	106	63	106	109	60	63	89	109
% Increase	42%	27%	38%	41%	32%	23%	34%	42%

The minimum force reduction (Table 9-6) as a result of using the alternative design philosophy is 18%, similar to that estimated using displacement-based design. This has a direct implication on both the connection and foundation size. Smaller foundations are expected to lead to significant foundation efficiencies and save significant cost.

Table 9-6: Peak force (kN) recorded from NLTH analysis (Refer to Appendix B).

	GM1	GM2	GM3	GM4	GM5	GM6	GM7	Max
Traditional	823	904	898	841	787	1016	896	1016
Alternative	694	686	724	714	631	719	708	724
Increase	-129	-218	-174	-127	-156	-296	-189	-127
% Reduction	19%	32%	24%	18%	25%	41%	27%	41%

So far, the alternative design philosophy has proven to be an efficient means of reducing the design base shear provided that additional displacement demands and increased risk of damage to dissipaters can be accepted. However, it is important to ensure the elements within the connection are not significantly compromised as a result of this efficiency.

Table 9-7 shows the peak levels of strain in the dissipaters for the CALS ground motions. For the traditional design method, the peak strain was 6.4%, which increased to 7.1% when using the alternative design philosophy (the unbonded length was the same for both connections). The fatigue damage, estimated using the same procedure shown in Chapter 7, to the dissipaters increased from 16% to 21% as a result of allowing the additional displacements. These strains and the level of damage are negligible and well below the proposed limits outlined in Chapter 7. The force in the PT was at 87% of the yield force which is acceptable for the CALS. Therefore, due to

the reduced lever arm of the section, the increased design displacements do not significantly increase the demand on the critical components.

Table 9-7: Component damage after CALS earthquake

	Alternative	**Traditional**	**%**
Dissipater Strain	7.1%	6.4%	9.8%
Dissipater Damage	21%	16%	23.8%
% Yield PT	87%	75%	13.7%

9.6 CONCLUSIONS

This chapter presented in depth design examples for DCR connections. It showed that the yield rotation and neutral axis relationships presented in Chapter 8 are suitable, especially at a preliminary design stage. It also illustrated how the design tables can be used with the design framework to speed up design and reduce iterations.

The design example showed that using the alternative design philosophy resulted in a 20% reduction in base shear and 30% reduction in cross section area. The 20% reduction in base shear directly reduces the overstrength demands in foundations and pier caps (for bents). The downside of this was a 30% increase in the CALS displacement. This was further verified by NLTH analysis which showed similar reduction in base shear and increases in displacement.

The performance of the connection, in terms of damage to the dissipative devices was also investigated. Since the connection designed using the alternative design philosophy is smaller, it will have a reduced lever arm (compared to the traditionally designed connection), which reduces peak strain in the dissipaters and PT. This resulted in the increased design displacements having an insignificant effect on the strains (and hence low-cycle fatigue demands) in the elements at the CALS. The traditional design philosophy and alternative design philosophy resulted in fatigue damage of 16% and 21% respectively. These values are low as the ductility limits imposed on the traditional design philosophy forced the use of long dissipaters (low strain).

Chapter 10: Optimisation of DCR connections through experimental testing

10.1 INTRODUCTION

DCR connections have been well developed over the past two decades. However, there are still some aspects that could be improved to further optimise the connections. The Wigram Magdala Bridge, recently designed and constructed in Christchurch, recently implemented DCR in the first known bridge application. A key complexity with the project was the detailing associated with not only the grooved dissipater itself, but also the provisions for access and replacement of the dissipater. Therefore, the development of dissipaters is important to ensure the future use of this system.

In this chapter, alternative dissipative devices are proposed for application within DCR connections. The key objectives of this chapter are:

- To develop alternative dissipative devices to alleviate issues and cost associated with the current axial dissipaters
- Investigate the cyclic performance of these devices, benchmarked against the currently preferred grooved axial dissipater.
- Determine the conservatism currently implemented in the design of axial dissipaters.

Alternative dissipaters, including two axial type dissipaters and one lead extrusion damper, will be designed and investigated through an experimental regime. The axial dissipaters will be designed to improve the cost and ease of fabrication. Performance and manufacturing cost of all three dissipater types will be compared against the benchmark grooved type dissipater. The application and detailing of the lead extrusion damper will be shown through a mini case study on the Wigram Magdala Bridge.

Lead extrusion dampers were developed and tested to try and work around some of the current issues associated with using axial mild steel dissipaters. Lead extrusion dampers could offer improved performance over axial dissipaters as they are not susceptible to low cycle fatigue and buckling.

10.2 EXPERIMENTAL TEST SETUP

The experimental testing on a scaled bridge pier was carried out in conjunction with another PhD student Royce Liu. Liu (2019) designed the pier for testing of foundation rocking and hierarchical activation as discussed in the Literature Review. Design inputs to the pier, design of additional dissipative devices and review were carried out by myself. Furthermore, as part of this testing design of alternative dissipative devices was undertaken by myself. Given the nature of DCR connections, which limit damage to external dissipative devices, multiple tests can be carried out on a range of devices using the same pier model. For this reason, dissipater component testing was carried out on the large-scale bridge pier that was used by Liu. The pier model provides more realistic demands on components since a simple axial push-pull test cannot simulate the same bending demands and secondary load and displacement effects that are put on these devices when loaded by a pier.

The prototype pier used for the experimental testing was based on a 20m span simply supported structure using a model scale of 2/3. The scaled model pier has similar geometry, and seismic mass to the Lower Mason River Bridge examined in Chapter 3. A SDOF model and hence experimental test can accurately capture the demands expected at the central pier of a multi-span bridge with simply supported spans. The axial load was determined for a superstructure consisting of four 1500mm deep precast I – beams and a 180mm reinforced concrete deck. The layout is illustrated in Figure 10-1. The foundation was detailed as a pile cap with the ability to rock. However, for the experimental testing reported in this chapter the cap was locked up and unable to rock. This is the equivalent of assuming a fully fixed foundation with no soil-structure interaction. The implication of this assumption is that the connection has to provide the full drift/rotation capacity.

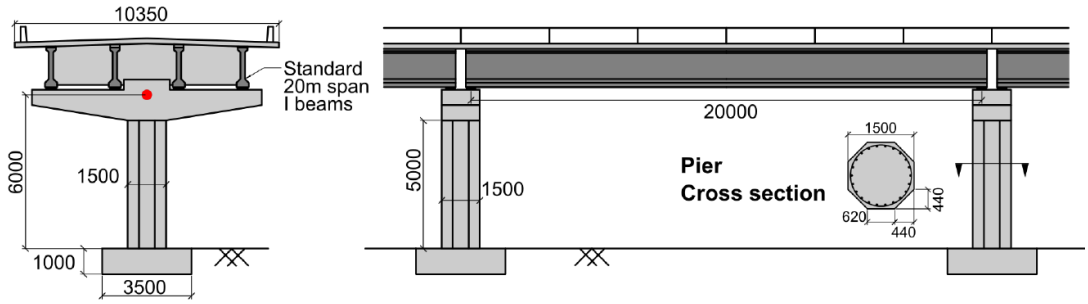

Figure 10-1: Shows the general layout of the prototype bridge pier (Liu, 2018).

The design of the prototype bridge was based on an importance level 2 structure founded on soil class C. However, after the design was completed the NZTA Bridge Manual (NZTA, 2018) was revised and the importance levels altered. As such this structure would now be classified as an importance level 3 structure on soil class C. The design spectra were derived using the parameters listed in Table 10-1.

Table 10-1: Inputs used to derive NZS 1170.5 spectra demands

	DCLS	**CALS**
Hazard factor, Z	0.3	0.3
Soil Class	C	C
Return period, RP	1000 years	2500 years
Return period factor, R	1.3	1.8
Near fault factor	1	1
Structural performance factor, S_p	1	1

The force and moment demands were derived for the single pier using displacement-based design assuming a design drift of 2%. The moment demands were derived by Liu and thus the dissipater demands, and detailing were predefined. Table 10-2 shows the demands on the scaled model pier.

Table 10-2: Design demands for the pier.

	DCLS Demand
Axial Load, N	1028 kN
Lateral Load, V	317 kN
Effective height, H_e	4000mm
Pier Diameter, D	1000mm
Design Moment, M_d	1268kNm

Design Displacement, D_d	68mm

The low damage cantilever pier was designed to operate in three different configurations, segmented column, conventional DCR and DCR with pile cap rocking (Liu, 2018). The test model was essentially a 2/3rd scale specimen of the prototype bridge but is approximately the same size as the piers used on many single-lane structures constructed throughout the 1960-1980's (including the Lower Mason River Bridge).

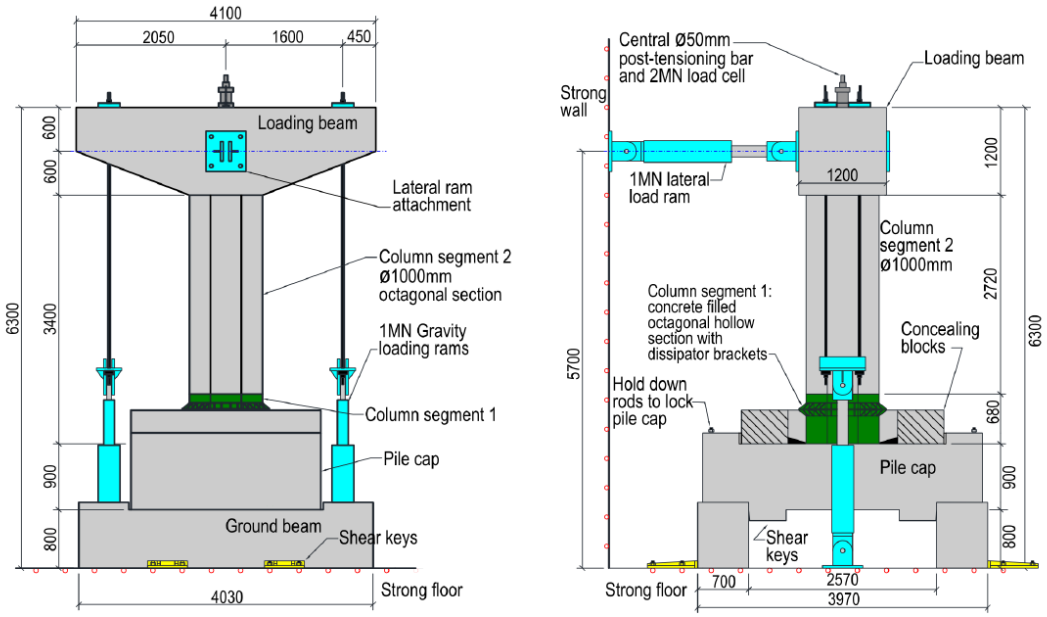

Figure 10-2: Schematic of the specimen testing arrangement (Liu, 2018)

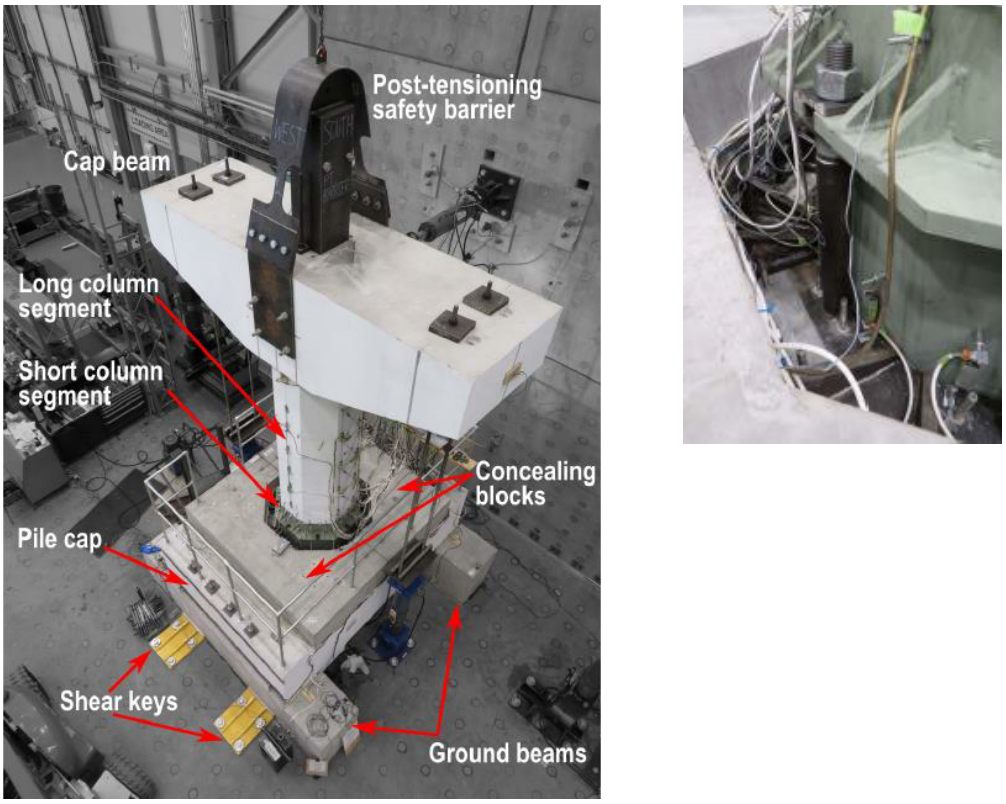

Figure 10-3: Left – Overview of the specimen (Liu, 2018), Right top – Close up of connection interface, Right bottom – Close up of interface with dissipater installed.

The model pier has an octagonal cross section which is 1000m wide and is post-tensioned by a 50mm diameter Macalloy bar which is anchored at the bottom of the pile cap and top of the cap beam. There are eight dissipaters which can be fastened to the stiffened bracket, shown in Figure 10-3, and screwed into the top of the pile cap. The column interface with the pile cap is armoured by a 10mm thick steel band around the column. The method for setting different connection configurations is described by (Liu, 2018).

10.2.1 Loading Protocol used for Testing

The testing was carried out with the loading protocol determined from ACI T1.1-01 (ACI Innovation Task Group 1, 2001). The drifts are shown in Table 10-3 and illustrated in Figure 10-4. The largest drift, while in excess of the designed CALS event, was limited by yielding of the PT and ultimately the maximum displacement the hydraulic loading ram could reach.

Table 10-3:Drift and corresponding displacements used in experiment.

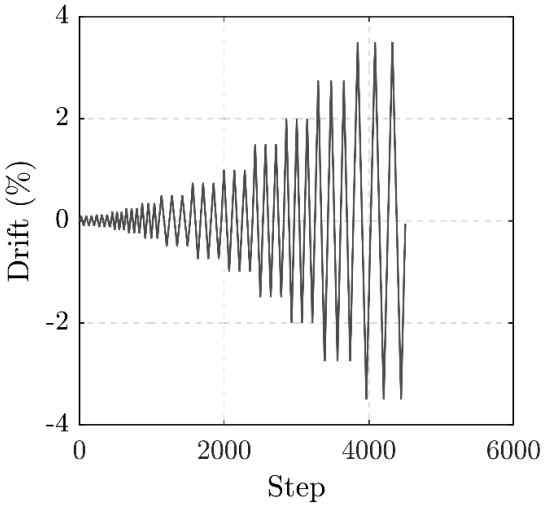

Drift (%)	Displacement (mm)
0.1	4
0.125	5
0.175	7.11
0.25	10
0.35	14
0.5	20
0.75	30
1.0	40
1.5	60
2.0	80
2.75	110
3.5	140

Figure 10-4: Plot of the loading protocol used in testing.

10.3 CURRENT SHORTFALLS OF EXISTING DISSIPATERS

Dissipaters with four cut grooves have been shown to have the best performance of "dry" type dissipaters (Liu, 2018; White, 2014). In particular, the fatigue behaviour is superior to unsymmetrical dissipater cross-sections. However, two key issues with machining grooved dissipaters have emerged (Routledge et al., 2016):

1) Fabrication difficulties: removing material unevenly causes a distortion of the bar.
2) Maximum available diameter of Grade 500 reinforcement (40mm) means increased number of dissipaters to provide moment capacity.

The testing discussed herein is specifically carried out to address these two issues. To reduce the difficulty in fabrication, alternative axial dissipater detailing could be considered. Wet type dissipaters such as the buckling restrained fuse type dissipaters, or dry type dissipaters (also known as "plug and play") such as the supported bar type (Pampanin, 2005; Liu, 2018; Palermo & Mashal, 2012; White, 2014) are alternative options. However, these all have machining requirements and hence significant cost to manufacture. In addition, development of these dissipaters

has resulted in the recommendation that the fused area of the dissipater is 60% or less of the threaded area to ensure the threaded portion of the dissipater is protected against yielding. These lead to potentially conservative designs which are difficult to manufacture. Therefore, the intent in this chapter is to develop a dissipater which is simple to fabricate and in addition to examine whether increasing the ratio of the grooved to threaded area affects the performance.

10.4 DOUBLE TUBE DISSIPATER

The double tube dissipater utilises two confining tubes, rather than the traditional single confining tube, to reduce manufacturing difficulty and hence cost. The bar is turned down in a lathe over the desired fuse length. This eliminates the need for machining in grooves which can pose issues as discussed in the previous section. The fused area, A_f, can be determined based on the required area to ensure that the threaded area of the dissipaters is protected against yielding. However, to further reduce manufacturing cost some consideration could be given to the internal diameter of the inner tube. The innertube diameter, d_i, should be designed such that the expansion of the fused diameter is not restricted. For a simple circular diameter fuse the expansion of the fused area can be calculated using Poisson's ratio as shown in equation 10-1.

$$\Delta d_f = \nu d_f \varepsilon_{cmax} \qquad 10\text{-}1$$

$$d_i = d_f(\nu\varepsilon_{cmax} + 1) \qquad 10\text{-}2$$

Where, d_f is the fuse diameter of the inner tube and ε_{cmax} is the maximum compression strain (typically 20% of the maximum tensile strain). The typical expansion of the fused diameter is small (less than 0.5mm for diameters up to 30mm). The poisson ratio ν is 0.25 to 0.3 for steel. The wall thickness of the innertube can be designed to match the reduction in diameter of the machined down fuse length. The innertube acts as a simple packer between the fused area of the dissipater and the main confining sleeve. The main confining tube then slips over both the inner tube and the dissipater threaded ends. The only machining required for such a dissipater, depending on material availability, is machining down the fused length to match the required fuse diameter. This results in an efficient dissipater, with buckling restraint over the full length. Drilling out the main confining tube to make sure the correct spacing between the confining tube and the dissipater is achieved is an additional cost.

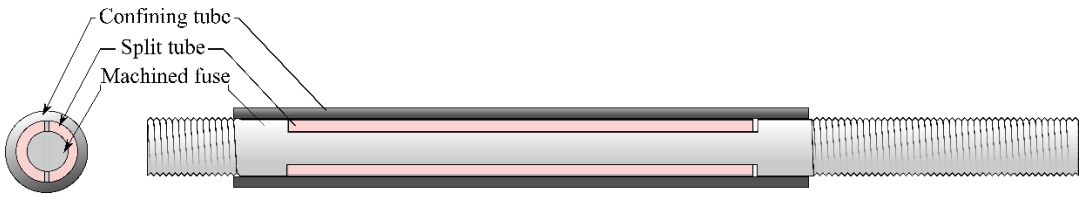

Figure 10-5: Double tube type dissipater

10.5 OPTIMISED DOUBLE TUBE DISSIPATER

One of the larger costs associated with implementing DCR connections is the cost of manufacturing dissipaters, particularly when a long unbonded length is required. Currently, the simplest and best performing dissipaters are the grooved dissipater which can be either constructed with 3 or 4 grooves. These dissipaters have good low cycle fatigue characteristics but are typically quite difficult to machine. The key difficulty is forming the grooves without bending or causing bends in the dissipater as this will prevent it from fitting in the anti-buckling sleeve.

The effective area of the grooved length of dissipaters, also known as the unbonded length, has to be designed so that the full development strength in the unbonded length does not exceed the capacity of the threaded region. Typically, for Grade 300 steel the increase in stress due to strain hardening is around 1.5. To avoid damage to the threaded area the grooved area should therefore be less than 66% of the threaded area.

$$A_{grooved} \times f_u \leq A_{threaded} \times f_y \qquad 10\text{-}3$$

$$\frac{f_u}{f_y} = 1.5 \qquad 10\text{-}4$$

$$\frac{A_{threaded}}{A_{grooved}} = 1.5 \qquad 10\text{-}5$$

$$\frac{A_{grooved}}{A_{threaded}} = 0.66 \qquad 10\text{-}6$$

For Grade 500 the increase in stress due to strain hardening is 1.3 therefore the reduction required is 0.77 (Equation 10-6). Having the grooved portion of the dissipater at 66% of the threaded portion has some practical implications since the maximum available sizes of reinforcement or mild steel bar are often limited. For

example, in New Zealand the maximum diameter of Grade 500 seismic reinforcement readily available is 40mm. This limits the maximum permissible force in a dissipater and hence increases the number of dissipaters required. Larger diameters in plain round mild steel are available but the seismic performance of these would need to be validated before application.

Several studies on the ratio of the threaded area over the fused area have been conducted. In 2016, a range of dissipaters with threaded area to fused area ratios ($\frac{A_t}{A_f}$) between 1.12 and 1.39 (Sarti et al., 2016) were tested with global instability an issue for dissipaters which developed stresses larger than yield in the threaded region. This would enforce an ($\frac{A_t}{A_f}$) ratio of 1.5. A further study by (Liu, 2018) also noted global instability issues for ($\frac{A_t}{A_f}$) ratios less than 1.5 and confining tube thickness less than $0.3d_t$. Where d_t is the outer tube diameter.

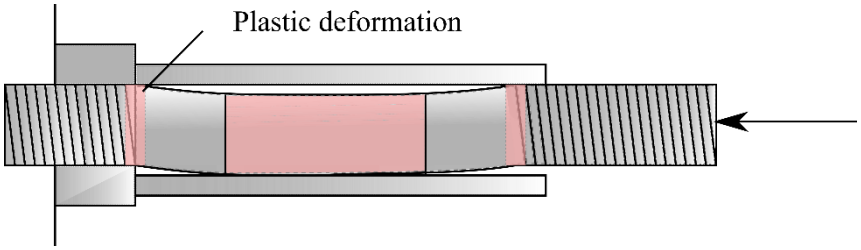

Figure 10-6: Global instability of dissipater.

Two key geometric properties of the dissipaters were found to contribute to the global instability. The first is the development of a mechanism. For the mechanism to form plastic deformation would need to occur at both ends of the dissipater ($\frac{A_t}{A_f} < 1.5$ for Grade 300 steel). Additionally, the moment induced in the confining tube by the deformed dissipater must exceed the plastic moment capacity of the tube. Global instability can only be caused when both conditions exist. Experimental results have shown that global instability is avoided provided the confining tube wall thickness is greater than $0.3d_t$. Therefore, in an effort to allow the fused area to be a larger portion of threaded area, a dissipater with $\frac{A_t}{A_f} < 1.5$ but with wall thickness equal to $0.3d_t$ was examined.

10.6 LEAD EXTRUSION DAMPER

The lead extrusion damper is a passive energy dissipation device that can be used to dissipate energy in an earthquake. As discussed in Chapter 5 the devices have been applied to both PRESSS-Hybrid connections and steel beam column joints. In addition, it has been applied between bridge superstructures and substructures (Chapman &Kirkcaldie, 1990). Although the performance of such devices was verified in testing for these applications, the devices were generally small with relatively short strokes. Though, (Chapman &Kirkcaldie, 1990) reported the use of much larger devices which were subjected to extensive testing. However, the application of lead extrusion dampers to rocking type connections which are designed to reduce damage to the dissipative devices is limited. This is probably due to the additional cost associated with constructing the lead extrusion damper compared to the more common axial mild steel dissipater. Asset owners are happy to accept some damage to replaceable elements on the basis that if there is a seismic event, these can be easily and cheaply replaced. In a building structure, most connections are readily accessible and hence the cost of replacement is dominated by the cost of dissipative devices.

The application of a connection that does not need to be repaired after a seismic event is most applicable to sites where access might be difficult or impossible. As discussed in Chapter 7, energy dissipating connections that are inaccessible are penalised by a lower permitted ductility to ensure that after a DCLS event the cost of repair is small. This may force the designer to design connections that essentially remain elastic, which will be very expensive using traditional design methods.

The current “Ferrari” of DCR connections combines steel armouring, PT and mild steel (typically grooved) dissipaters which all combine to give a low damage connection. However, after a seismic event exceeding the DCLS the mild steel dissipaters may still need replacing. In remote locations where access is expensive/dangerous or on high importance level structures replacement of dissipaters may not be acceptable. Therefore, the need to develop the “Tesla” of DCR emerges. Something that performs as well as a Ferrari without the cost associated with refuelling (repairing the connection).

An alternative to this and more than likely a cost-effective alternative will be to use lead extrusion dampers (Figure 10-7) that avoid damage altogether rather than axial dissipaters. As such, it is the authors opinion that the lead extrusion damper may

have a niche in bridge structures which are remote, and where access is either costly or dangerous. An additional application that may warrant the use of DCR with lead extrusion dampers is on structures with high importance levels that are required to be at full capacity after large seismic events. Therefore, the application of lead extrusion dampers to a DCR connection was investigated through experimental testing on the model pier.

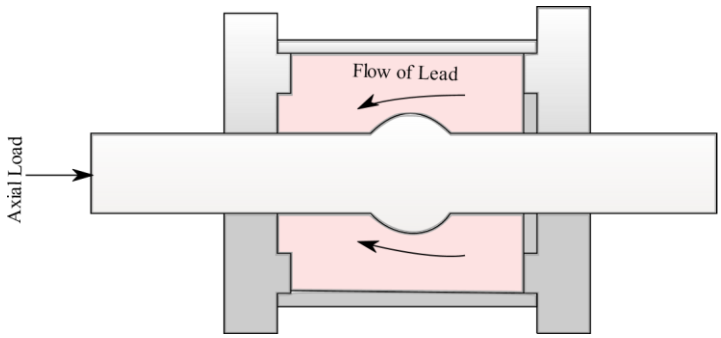

Figure 10-7: General layout of lead extrusion damper.

An alternative device already examined by Marriot (2009) is the viscous damper. These devices were found to perform in the same way as the lead extrusion damper, with reduced damage (if any) to the devices. However, velocity dependence and the cost of the devices currently limits their application to DCR connections.

10.7 DISSIPATER PERFORMANCE

As discussed, three types of dissipater have been developed for experimental testing on the 2/3 scale bridge pier. The two axial mild steel dissipaters were designed with the intention of minimising the cost of the dissipater and maximising their force capacity. The lead extrusion damper designed and constructed by the University of Canterbury's mechanical department, has been developed with the intent of developing a no damage DCR connection.

The performance of the three dissipater types was benchmarked against the most common and extensively tested four groove type axial dissipater (Figure 10-8). The four grooved dissipaters were machined down from Grade 300, 39mm diameter plain round bar. The confining tubes were manufactured from 50NB x XXS seamless ASTM A106 Grade B line pipe. The wall thickness of the confining tubes was 11.97mm.

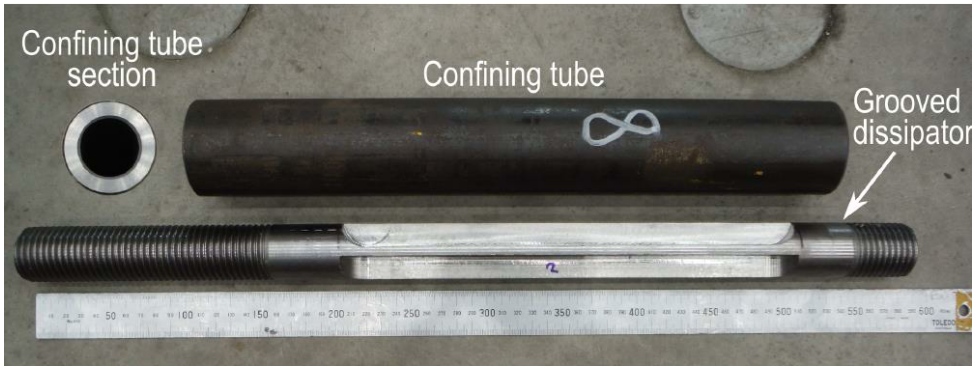

Figure 10-8: Typical four groove type dissipater, tested by Liu, 2018.

10.7.1 Double Tube Dissipater Details

The double tube dissipater was manufactured from a Grade 300 plain round bar. The fused area was machined down in the lathe to 20mm which gives an $(\frac{A_t}{A_f})$ ratio of 1.66. This was designed to match the cross-sectional area of the grooved dissipater used for the benchmark. The split tube had an inner diameter of 20.5mm with a wall thickness of 7.75mm which was designed to fill the gap between the fuse and inner diameter of the outer confining tube. The split tube and confining tube required no machining apart for the cut along the centre of the split tube to allow installation onto the fused section of the dissipater. The total effective wall thickness of the confining tubes in this case was 19.5mm (Figure 10-9).

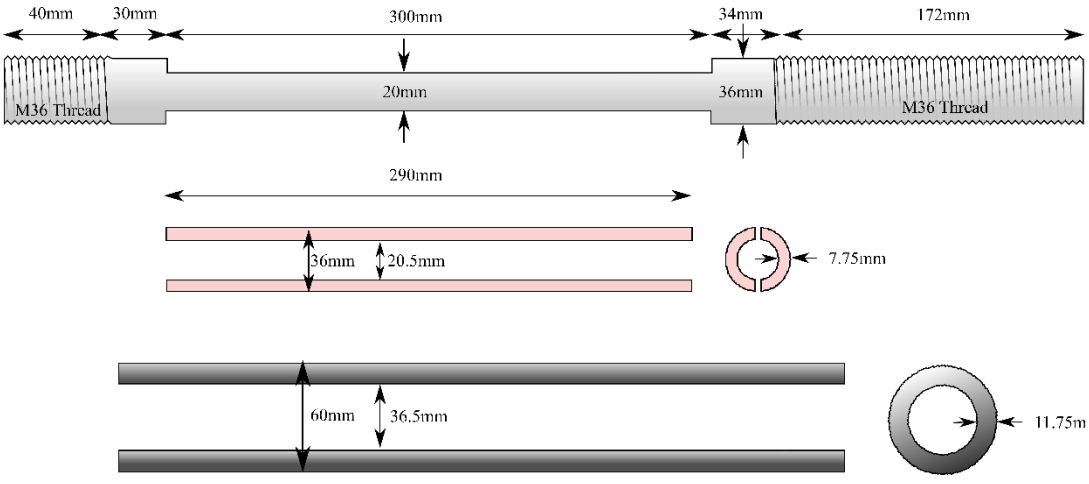

Figure 10-9: Dimensions of the double tube dissipater.

The thread dimensions, dissipater and fuse length were defined by the experiment test setup discussed previously. The shorter threaded end was screwed into

the pile cap and the longer threaded end was connected to stiffened casing on the pier using steel washers and nuts.

Figure 10-10: Detail of how the dissipater was connected to the pier.

The force displacement response of the dissipater is compared in Figure 10-11 with the benchmark. The somewhat unusual hysteresis behaviour is due to a construction imperfection. More precisely an imperfect interface between the bottom of the pier and top of the pile cap. The result is a lower than expected initial stiffness, Figure 8-7 shows the expected initial stiffness from numerical modelling. The testing was terminated after the first dissipater fractured. In the test carried out on the four-groove dissipater, fracture occurred in the first of the intended 4.35% drift cycles and before reaching the maximum displacement. The double tube dissipater fractured on the second 3.5% drift cycle. Essentially, the grooved dissipater fractured on the fourth 3.5% strain cycle while the double tubed dissipater fractured on the second 3.5% drift cycle. In addition, the grooved dissipater appears to provide a slightly higher compression capacity than the double tube dissipater.

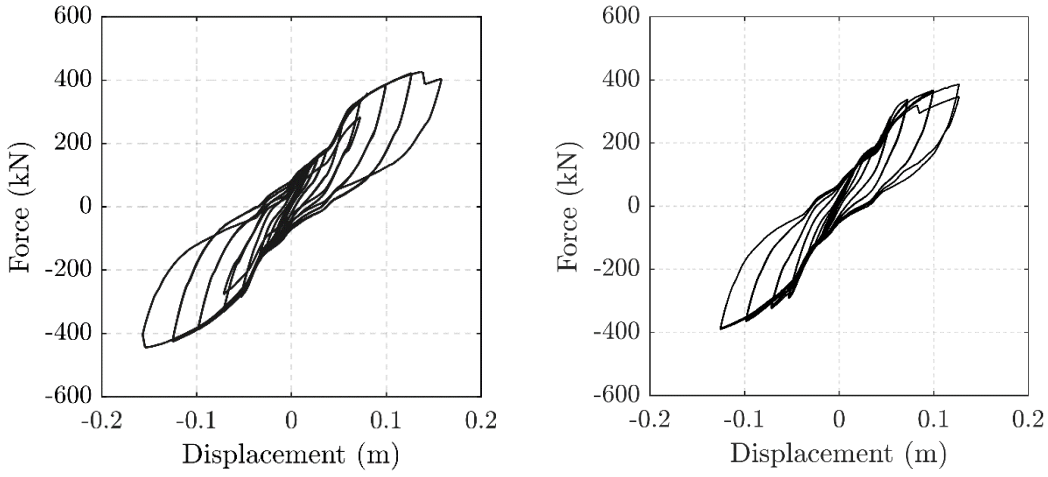

Figure 10-11: Left - Benchmark test with 4 groove dissipater, Right – Response of the double tube dissipater.

Fracture of the dissipater occurred at the extreme fibre dissipater. The fracture was near the end of the buckling tube where a 10mm gap between the split tube and end of the fuse length exists to allow compression of the fuse (Figure 10-12).

Figure 10-12: Left – Cross-section of the damaged dissipater, Right – Mode of buckling.

Figure 10-13: Mode of buckling in the grooved type dissipater.

As shown in Figure 10-12 and Figure 10-13 both the grooved type and double tube type dissipaters exhibit buckling. However, a key difference, which likely influenced the cyclic capacity, is the mode of buckling. The four-groove dissipater exhibited a much shorter buckling length which is expected to lead to a more stable hysteretic behaviour.

10.7.2 Optimised Double Tube Dissipaters

The optimised double tube dissipater (Figure 10-14) is a variation of the double tube dissipater with a reduced threaded area ratio $\frac{A_t}{A_f}$ of 1.25. The dissipater was manufactured from a Grade 300 plain round bar. The fused area was machined down in the lathe to 20mm, the same as the standard double tube dissipater. This was designed to match the cross-sectional area of the grooved dissipater used for the benchmark. The split tube had an inner diameter of 20.5mm with a wall thickness of 3.25mm which was designed to fill the gap between the fuse and inner diameter of the outer confining tube. The split tube and confining tube required no machining apart

for the cut along the centre of the slit tube to allow installation onto the fused section of the dissipater. The total effective wall thickness of the confining tubes in this case was 13.75mm. This is approximately $0.5d_t$, larger than the minimum $0.3d_t$ recommended by (Liu, 2018). However, the two tubes combined have a lower section modulus than a single tube of the same total thickness.

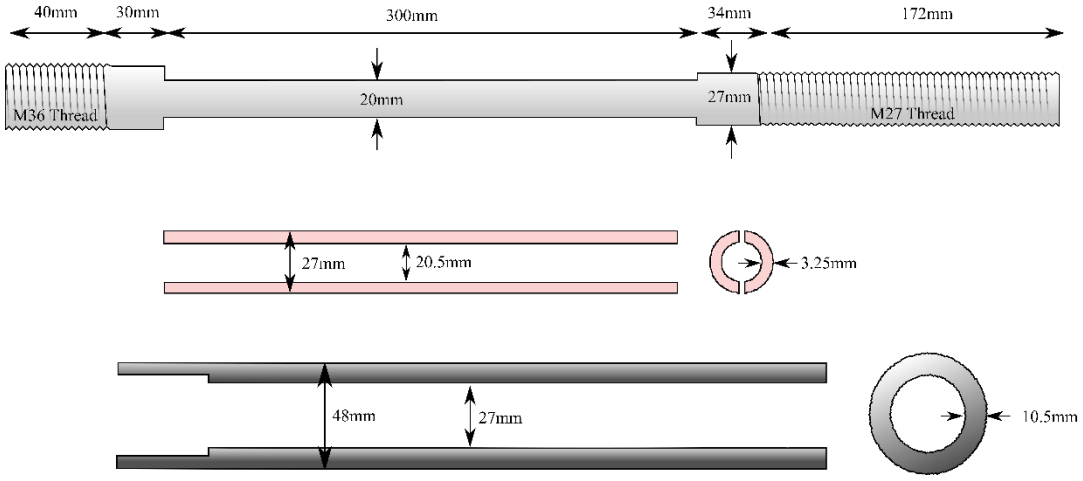

Figure 10-14: Dimensions of the optimised double tube dissipater.

The experimental testing plot for the optimised double tube dissipater is shown in Figure 10-14. The dissipater fractured on the first 3.5% drift cycle. Therefore, reducing the threaded area resulted in poorer performance than the double tube dissipater. Overall the hysteretic behaviour is stable with similar force-displacement characteristics (Figure 10-15) and worse fatigue characteristics (due to failing sooner than the benchmark).

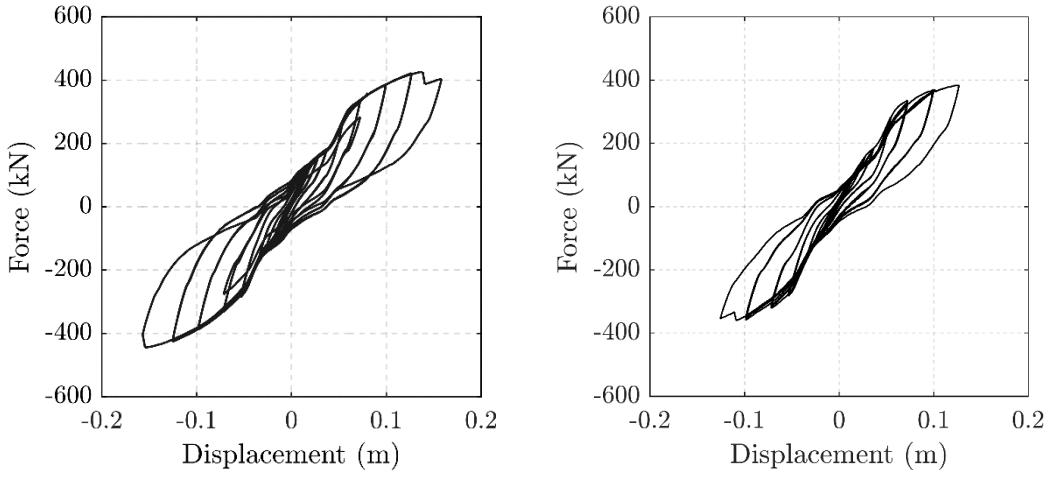

Figure 10-15: Left - Benchmark test with four grooved dissipater, Right – Test with optimised double tube

The fractured dissipater was at the extreme fibre. This is not surprising given higher strains would be expected at this location.

Figure 10-16: Fracture of the optimised double tube dissipater.

The main concern is the fracture of the double tube dissipater at ductility's less than the benchmark. Not surprisingly the fracture occurred near the end of the inner split tube, where there is a 10mm gap between the split tube and the end of the fuse, essentially creating a zone where the fuse is unrestrained (Figure 10-16).

10.7.3 Analysis

Overall both types of double tube dissipaters exhibited similar force displacement characteristics. However, the fracture of the critical dissipater occurred at lower drifts than the grooved dissipater in both tests (Table 10-4).

Table 10-4: Number of cycles, drifts and levels of strain at failure in the different dissipater types.

	Grooved	Double Tube	Optimised Double Tube
Ultimate Drift	1cycle @ 4.35%	2cycles @ 3.5%	1cycle @ 3.5%
Ultimate Strain	1cycle @ 10%	2cycles @ 8.5%	1cycle @ 8.5%

The strain was determined by transducers which measured the displacements and gap openings at the interface giving the change in length of the dissipater. Damage shown in Figure 10-16 indicates significant contact of the fused area with inner tube near the point where fracture occurred. This indicates that the fuse has essentially wedged inside the tube. Geometrically this is a more significant issue than would be expected for a grooved dissipater. The reason for this is that, as shown in Figure 10-17,

the expansion (due to Poisson's ratio) of the double tube dissipater is entirely radial. Conversely, with the groove type dissipater some of the expansion is into the grooves. The only part that can interact with the confining tube is the non-grooved section, which does not have the same ability to lockup against the confining tubes.

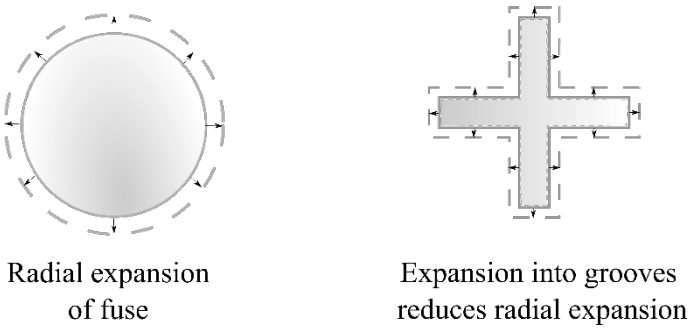

Figure 10-17: Left – Expansion characteristics of double tube dissipater, Right – Expansion characteristics of grooved type dissipater.

The consequence of the fuse becoming wedged within the confining tube is a possible failure mechanism whereby the tensile strain occurs over a much shorter length than desired. This will generate much higher strains over a short length leading to a tensile failure.

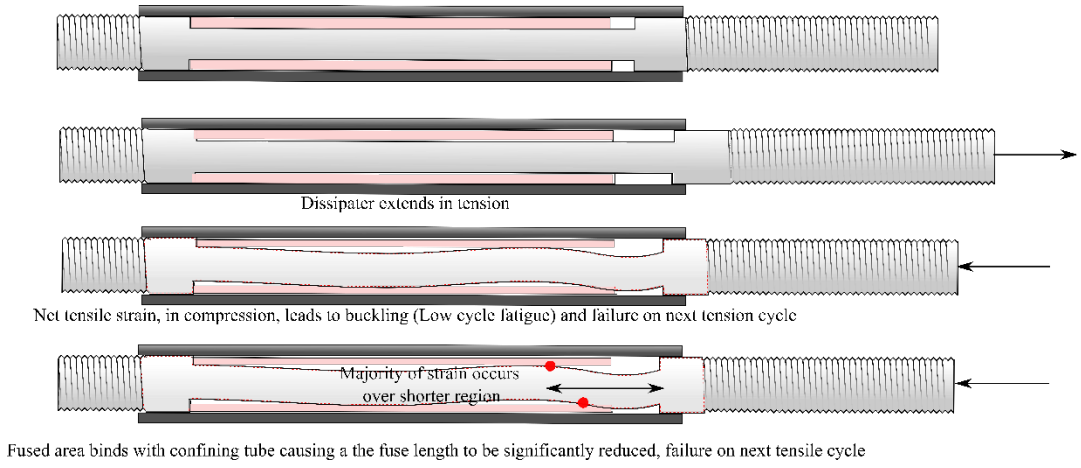

Figure 10-18: Failure mechanisms of double tube dissipater.

The second possible and more likely failure mechanism is due to low cycle fatigue. This is due to the unrestrained section of fuse, which increases as the dissipater elongates in tension. Buckling then occurs while the dissipater has a net tensile strain but is under a compressive load. This results in local strains from the buckling curvature leading to low cycle fatigue. Other possible reasons for failing earlier are:

- Less resistance against buckling due to a lower second moment of inertia.
- Higher mode of buckling (shorter lengths) than can form in the grooved dissipater.

The failure of the double tube dissipaters at strains less than the grooved dissipaters is not surprising, although fatigue damage was expected to form at the sudden change in cross sectional area, where larger concentrated stresses develop. However, the effect this section reduction has on performance at high strains is small. The CALS drift for this connection is 3.5% corresponding to a strain in the dissipaters of around 8.5%. Essentially the dissipaters fractured at the CALS level drift. So the dissipaters performed adequately. As discussed in Chapter 5 and 7, fracture of a single dissipater or several dissipaters would be acceptable in a CALS event given the redundancy of the DCR connection. Therefore, as far as performance objectives go the double tube dissipater meets expectations.

Due to cost and time constraints only one set of each type of dissipater could be tested on the model pier. Further investigation into the low cycle fatigue characteristics would need to be undertaken to ensure that the performance observed during the experimental testing was representative of a number of these dissipaters. In addition, a range of experimental tests needs to be undertaken with varying ratios of fuse thickness to threaded area and wall thickness to fully understand when yielding of threads occurs and when global instability may occur. Testing on the optimised double tube dissipater has shown there might be the potential to develop more stress in the threaded regions. However, until a more stringent testing regime is undertaken it appears best to use a minimum wall thickness of $0.3d_t$ and ensure that the tensile capacity of threaded area exceeds the ultimate strength of the fused area.

10.7.4 Axial Dissipater Cost

The double tube dissipaters were manufactured by a local fabricator from Grade 300 plain round bar and seamless Grade B line pipe. The cost per dissipater was $235 for the manufacture of 16 dissipaters. However, this cost would reduce when a larger number of dissipaters is fabricated. Quotes were also obtained for a four groove dissipater (Liu, 2018), manufactured from Grade 300 plain round bar and seamless

Grade B line pipe (the same as the double tube dissipaters). The estimated cost (from quotes) to manufacture these products ranged between $350 and $520.

10.8 LEAD EXTRUSION DAMPER PERFORMANCE

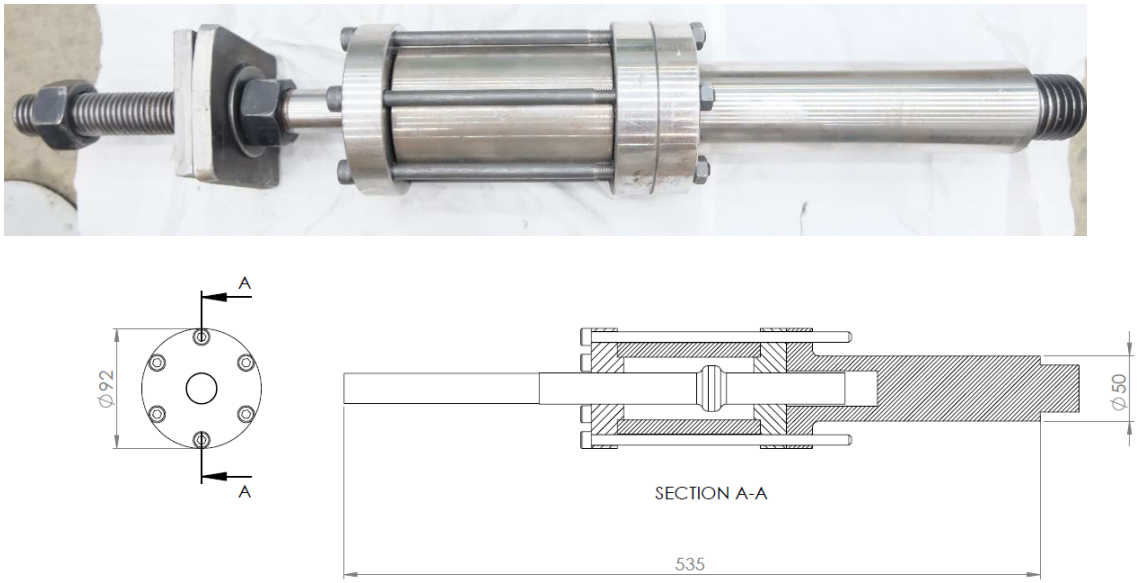

Figure 10-19: Lead extrusion damper experimentally tested.

As shown in Figure 10-20 the lead extrusion damper (Figure 10-19) had very good performance with stable hysteretic behaviour. In addition, the hysteretic damping of the device is slightly better than the grooved type dissipater

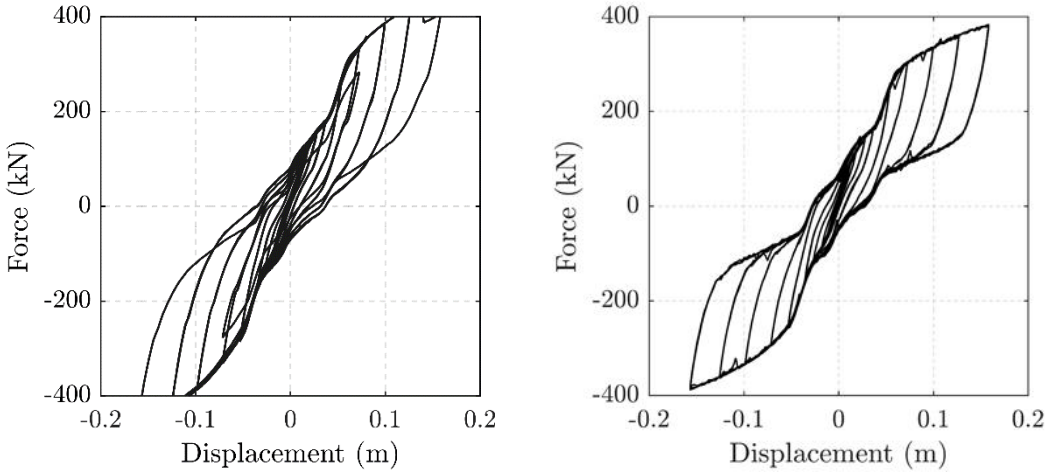

Figure 10-20: Left – Benchmark performance of grooved type dissipater, Right – Performance of lead extrusion dampers.

The damage to the lead extrusion damper after 3 cycles at 4.35% drift was limited to some slithers of lead squeezing out between the casing and shaft. No other damage was observed. Further testing was carried out following the loading protocol shown in Figure 10-4 using a pseudo dynamic protocol displacement of the pier model.

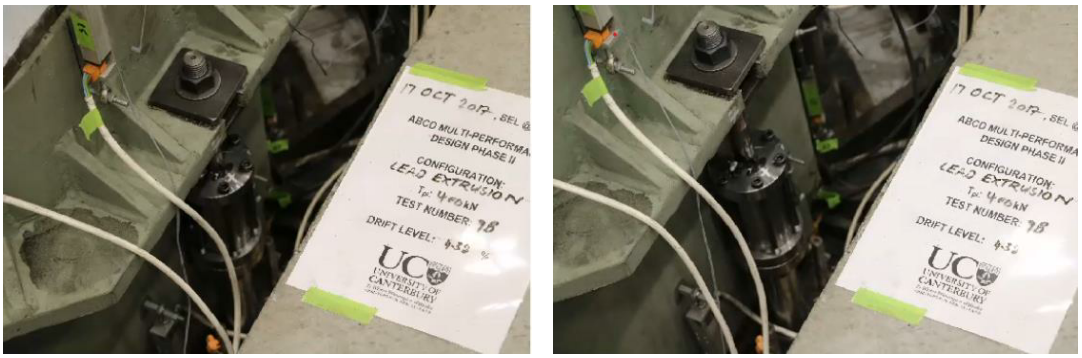

Figure 10-21: Left – Lead extrusion damper after 3 4.35% drift cycles, Right – Lead extrusion damper at peak displacement (4.35% drift).

10.8.1 Future Applications

The lead extrusion damper has the potential to greatly reduce damage to bridges in large seismic events. When the lead extrusion damper is combined with DCR, damage can be completely avoided. Typically, damage is confined to dissipative devices which as previously discussed are usually axial buckling restrained fused type which need replacement after cycles at large strain levels. However, the alternative lead extrusion dampers, if designed properly, can sustain large axial displacements with no damage.

10.8.2 Lead Extrusion Damper Cost

The lead extrusion dampers used in this pier model test cost approximately $900 per device. However, given they were designed to fit into a location which was designed to accommodate axial dissipaters the length of the device was much larger than would typically be required and resulted in additional material and machining costs. The devices used in the experimental setup had an approximate axial capacity of 100kN to match the axial dissipaters. However, increasing the axial capacity has a very small impact on the cost since machining costs would be similar. Testing on similar devices in a beam-column joint (Rodgers, Mander et al., 2016) used devices which had an axial capacity of close to 300kN. The cost of these devices was approximately $800 per device. The additional axial capacity is a large advantage over

axial mild steel dissipaters which have some limitation in size due to material availability. Using this experimental regime as an example, one lead extrusion damper with an axial capacity of 300kN and a cost of $800 is similar to using 3 axial dissipaters which have a combined capacity of 300kN and a combined cost of between $700 and $1050 (dependant of axial dissipater type). The dissipaters used in the Wigram Magdala Bridge, which had an axial capacity of around 190kN, cost around $800 to $1000 per device. Therefore, the cost for developing a system which remains undamaged in an earthquake could be cost competitive or even cheaper than the currently preferred axial mild stell dissipater.

10.8.3 Application in Bridge Design Framework

Other than the obvious application in IL4 structures which will require minimal downtime and post-earthquake functionality these devices could have an application in situations where designing accessible plastic hinges is difficult or expensive. In the BM and other seismic codes there is a design advantage from the increase in permitted ductility for accessible plastic hinges. This is clearly shown Figure 10-22 reproduced from the BM which depicts the fact that a plastic hinge which is accessible (above ground level) can be designed for a higher ductility and hence reduced base shear than structures with plastic hinges that are difficult to inspect and repair (below ground).

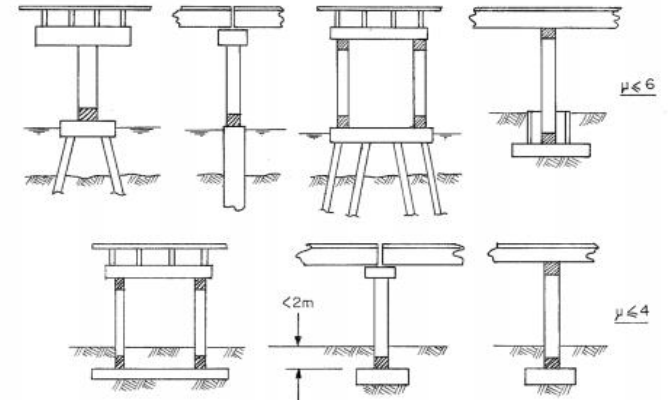

Figure 10-22: Shows the allowable ductility is dependent upon the accessibility and hence inspect ability and repairability of the hinge (BM).

Essentially additional damage is accepted on the basis that it can be inspected and repaired. Therefore, connections that are very difficult to inspect and repair would need to be designed to very low levels of ductility to reduce damage. In such cases utilising the lead extrusion damper, which could be designed for lower base shears, could become cost-effective.

The Wigram-Magdala Link Bridge located in Christchurch, New Zealand links several suburbs to the City Centre. The superstructure (Figure 10-23) comprises simply supported 1525 mm deep prestressed concrete Super Tee beams with a 200 mm thick insitu deck. The abutments comprise spill-through piled bank seats. The two piers each comprise a headstock beam supported by two 1500 mm diameter columns.

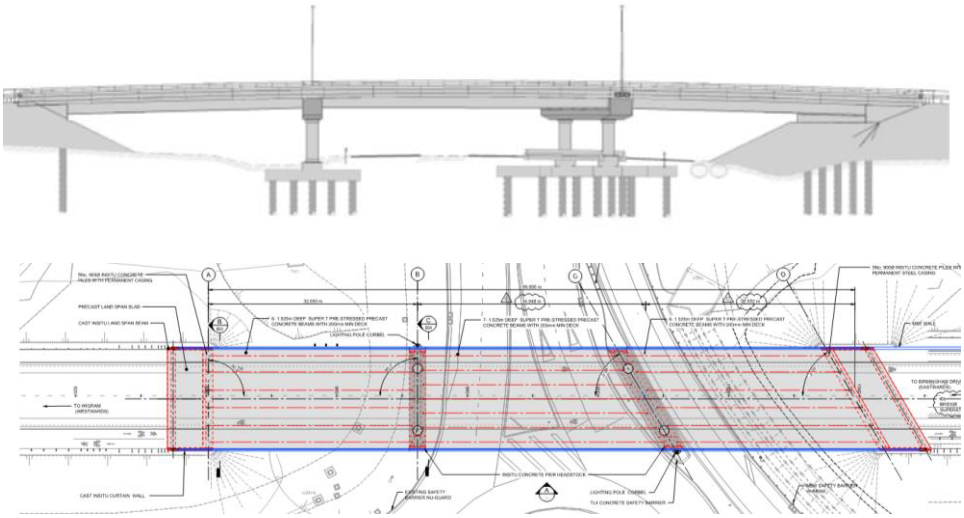

Figure 10-23: Elevation and Plan view of the Wigram Magdala Bridge (Routledge et al., 2016)

The substructure design incorporated low-damage joints, enabling easy replacement of the ductile elements that would be damaged during a major earthquake. This was achieved by adopting a hybrid joint detail (Figure 10-24) which in this case comprised of:

- Circular steel-cased, concrete-filled columns on piled footings
- Replaceable dissipater bolts connecting the stiffened column endplates to anchorages cast-into the footing and headstock
- Vertical unbonded PT across the joints

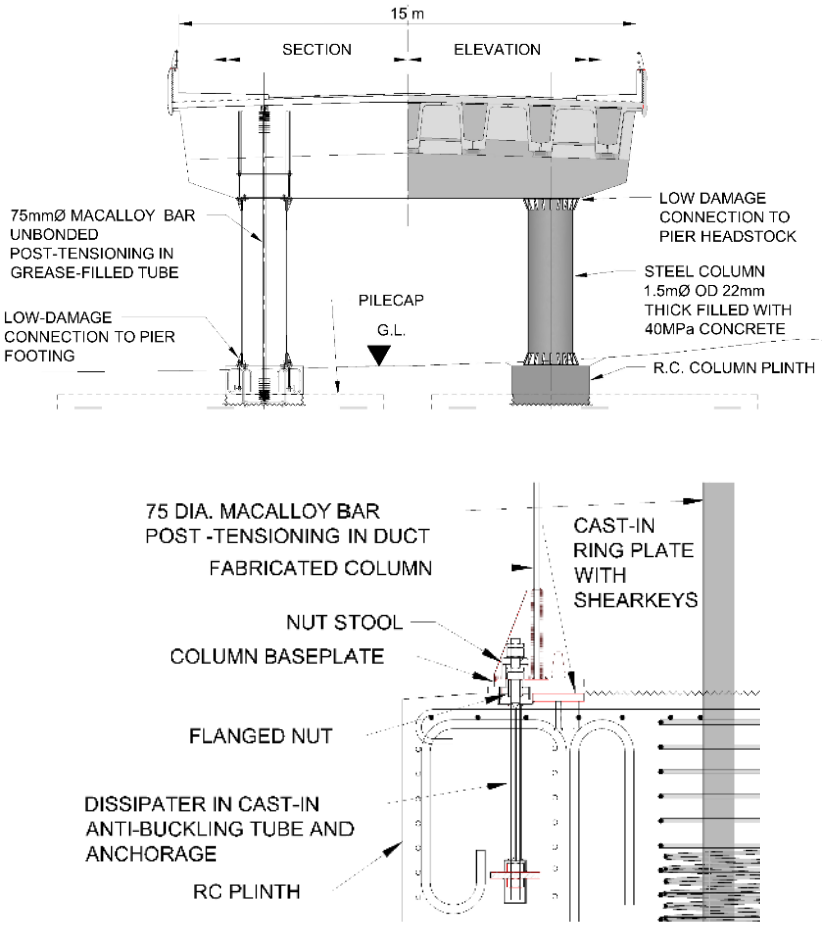

Figure 10-24: Detailing used on the Wigram Magdala Bridge (Routledge et al., 2016)

Whilst the low-damage details used were based on a prototype tested at the University of Canterbury (Mustafa & Palermo, 2019), they were modified to enable the detail to be hidden within the reinforced concrete footing and headstock for aesthetic reasons which leads to additional considerations that need to be addressed including:

- Ease of replacing the dissipaters and PT
- Durability of the dissipaters, PT, shear keys and hidden steel interfaces
- Buckling restraint to the dissipaters
- The availability and size limitations of a suitable seismic steel grade for fabricating the dissipaters
- Avoidance of thread damage (as this would hinder dissipater removal in a buried detail)

Additional complexities were also discovered during construction, which include (Routledge, 2016):

1. Machining the dissipaters to form the grooves was complicated by the fact that if too much material was removed from one side at a time then the bar would tend to distort or 'banana'. Furthermore, the deformations on the 40 mm diameter Grade 500E reinforcing bar used to make the dissipaters made the bar difficult to machine and machining would have been much easier if round bar had been available.

2. The machining difficulties and the limitations on the availability and size of a suitable grade of steel for the dissipaters resulted in them being a relatively significant cost item in the low-damage detail. Further development is required to explore ways of minimising the cost of producing the dissipaters. The availability of alternative grades of steel (other than 500E) with suitable material properties and supplied in larger diameters of plain round bar would increase the options for the size and profile of dissipaters, reduce the costs of machining and enable the use of a lesser number of larger dissipaters.

3. Further research is required to maximise the net cross-sectional area of the grooved portion of the dissipater whilst still reliably avoiding yielding in the threaded portions as this would further increase the efficiency of the dissipaters.

4. It had been recognised during the design that to ensure the threads align between the multiple threaded components fixed by welding a threaded bar would need to be temporarily installed to set the thread alignment. However, it had not been appreciated that the thread alignment would be disrupted by the heating and cooling effects of the welding itself which tended to jam the bolt within the tube and nuts. A better detail would avoid welding by fixing with screws or clamps.

5. Some of the fabricated components such as the flanged nut and nut stool had been detailed with the intention that they would be welded. However, the Contractor's preference was to machine these components out of solid steel billet. This was considered a more efficient way to fabricate

them and also provided more reliable quality assurance by avoiding welding.

Figure 10-25: Low damage connection implemented on the Wigram Magdala Bridge.

The additional requirement of having to bury the dissipaters (Figure 10-25), which is likely to be a common request from clients, leads to significant difficulties associated with the dissipater design (Figure 10-26). Additionally, full scale construction has led to further difficulties associated with constructing the dissipaters. Implementation of the Lead Extrusion Damper would eliminate all the issues associated with constructing dissipaters. In addition, given the dampers do not require replacement, burying the dissipaters requires no consideration of access and replacement details further simplifying things for construction and design. As shown in Figure 10-26 the lead extrusion damper could simply be embedded in the concrete with an unbonded shaft that is welded to the baseplate of the pier or column. However,

it is important that provisions for inspection and replacement of these devices is allowed for.

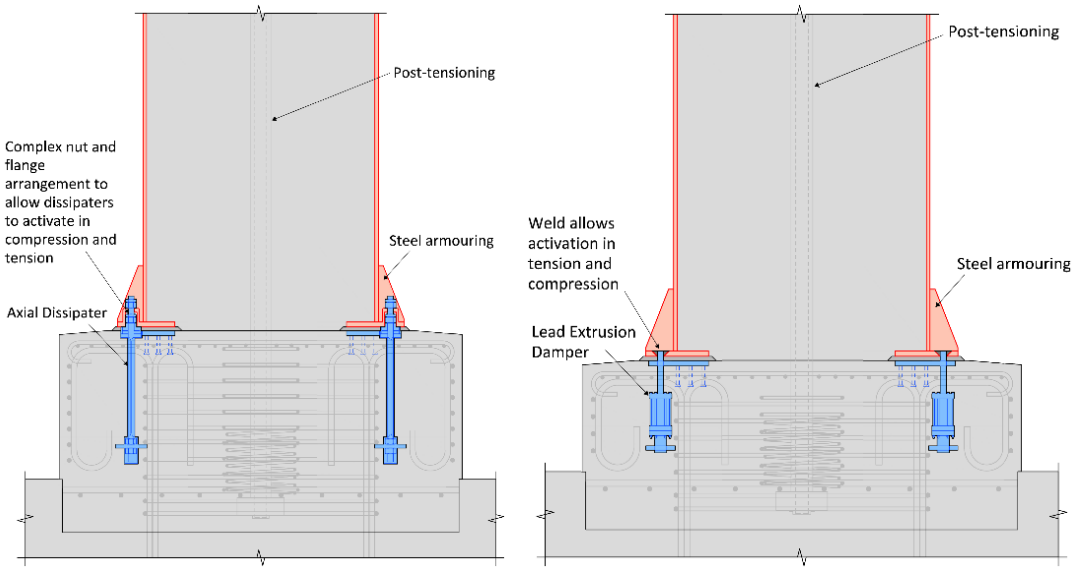

Figure 10-26: Left – as designed Wigram Magdala Bridge pier-foundation connection, Right – Wigram Magdala pier-foundation connections adapted

10.9 CONCLUSIONS

This chapter introduced three new types of dissipaters, two of which can provide a cheaper alternative to grooved mild steel axial dissipaters. The first two dissipater types, the double tube and optimised double tube dissipater, were significantly cheaper than the currently preferred four groove axial dissipater (~30% cheaper per device). However, the double tube dissipaters fractured on the second 8.5% strain cycle, before the grooved axial dissipater which underwent three 8.5% strain cycles and fracture on the following 10% strain cycle. This failure is through to be caused by low-cycle fatigue. The reason for the reduced cyclic capacity is related to the small unrestrained length of the fuse, which is detailed in this way to allow compression of the dissipater. Unfortunately, this also contributes to the buckling tendency of the fuse. A further reason for earlier onset of buckling is due to the lower rigidity (lower section modulus) than the four grooved dissipaters making it more susceptible to buckling.

The third type of dissipater examined was the lead extrusion damper. It is conceivable that these dissipaters can be cost competitive to axial dissipaters as the axial load capacity of a single device can be up to 3-4 times that of an axial dissipater. In addition, the lead extrusion damper eliminates many, if not all, of the issues associated with using axial dissipaters. The main advantages being that it can survive multiple earthquakes without damage and that because of this, the damper can be hidden within the connection without provisions for access and repair. The lead extrusion damper would fit easily within the alternative design framework proposed in Chapter 6. The key difference being that because there is no damage to the device, the DCLS can be omitted all together. The devices can be designed to have a displacement limit above yielding of the PT and below the P-Delta limit.

The key outcomes of this chapter are:

- The cheaper double tube dissipaters can be used which are cheaper but have reduced cyclic capacity (the grooved dissipater survived an additional 8.5% strain cycle)
- Lead extrusion dampers offer a now damage solution which could even work out cheaper than the currently preferred axial dissipaters (for bridges)

- Lead extrusion dampers can easily be embedded in the pier cap without any provision for access and repair.
- Lead extrusion dampers would all of the dissipater design issues encountered during design and construction of the Wigram Magdala Bridge.

Chapter 11: Conclusions

11.1 SUMMARY

This thesis has investigated, in depth, two systems that can be implemented in bridge piers to resist seismic demands, plastic hinges and DCR. Given the recent Kaikōura Earthquake, and relatively small amount of research using back analysis that can correlate damage to design and expected damage, plastic hinges were inspected, analysed and observed damage was compared to expected damage. This investigation allowed the shortfalls of plastic hinges and current design standards to be examined. Buckling of longitudinal reinforcement and residual drifts were found to be the most concerning.

This research was taken a step further for a single bridge, the River Road Bridge, which had moderate plastic hinge damage following the Kaikōura Earthquake. Due to the structural form, repair of this structure was expected to be difficult and costly. In addition, there was data on the input ground motion available. This allowed a strategy for estimating the residual capacity of a plastic hinge to be proposed. It was found that the hinge has sufficient capacity to survive future CALS events with minimal repairs.

The second section of this thesis focused on the development of displacement-based design methods for DCR connections. In particular, an alternative design philosophy was proposed were the CALS is the key design level and the DCLS level can be altered based on the acceptable risk of replacing dissipaters – a higher risk of dissipater replacement means the dissipaters can be designed to a lower DCLS strain limit.

Due to the proposal of the alternative design philosophy, there were several gaps in the design framework, such as CALS performance limits. Therefore, dissipater, PT and P-Delta limits were proposed for the CALS. A parametric analysis was carried out to allow the estimation of key preliminary design inputs such as the yield rotation and neutral axis location. This research was also used to propose geometric ratios that ensure DCR connections can achieve the desired performance limits. Design tables

were also developed to allow the quick and easy preliminary design of DCR connections.

Experimental testing of alternative dissipation devices was carried out on the double tube and optimised double tube axial dissipaters. These dissipaters were found to have a lower cost than the currently preferred four groove axial dissipater but poorer low-cycle fatigue performance. An alternative device, the lead extrusion damper was tested and was found to have good performance after a number of tests. No damage was observed during testing and therefore it could offer a no-damage (no replacement/repair at DCLS design level) alternative to axial mild steel dissipaters.

11.2 SECTION 1 - PLASITC HINGES

11.2.1 Performance of Bridge Structures Damaged in the Kaikōura Earthquake

A number of bridge structures that were damaged as a result of the 14 November 2016 Kaikōura earthquake were examined. Specifically, those that had severe plastic hinge damage. Each structure was analysed, using NLTH, CSM, and ground motion inputs from the nearest strong motion recording station. The NLTH analysis was carried out on all investigated structures with the exception of the Wandle River Bridge, where geometric complexities led to a response that could not be replicated by simple analysis. In general, it was found that structures (likely designed using FBD) typically had damage that was worse than that which would be expected given the level of shaking at the sites. However, displacement-based design accurately predicted displacements and damage levels. It was the detailing of the plastic hinge zone that led to the poorer than expected performance. Residual drifts and buckling of longitudinal reinforcement were noted as the main area of concern.

An investigation indicated that current standards such as the New Zealand concrete standards and other international displacement based guidelines (NZS 3101, 1995; NZTA, 2018; Priestley et al., 2007) provide anti-buckling requirements that are insufficient to ensure buckling does not occur. This is based on the observed damage and the fact that the plastic hinges investigated met the latest provisions for anti-buckling. The recently released Bridge Manual (NZTA, 2018) limits the ultimate tensile strain based on the volumetric ratio of transverse reinforcement to core concrete. This formula is much more conservative than the others examined and would appear, at least in the cases examined in this chapter to provide a more conservative

approach to protect against anti-buckling (provided the maximum tensile strain is used). A more evidence based approach, the method proposed by Dhakal et al., 2018, resulted in overly larger transverse stirrup requirements (>25mm). Therefore, at this stage designing to the following is recommended:

$$\rho_s = \frac{0.5\varepsilon_{sul} - 0.015}{6} + 0.005$$

Unfortunately, the basis for this relationship is unknown, other than it being recommended by Priestley for use in the NZTA Bridge Manual.

Further experimental research to verify the applicability of the approach proposed by Dhakal et al., (2018) to larger scale bridge piers where a number of longitudinal bars (typically three) require restraint should be carried out to determine the applicability of the theory to larger connections and ensure the theory results in practically achievable solutions.

11.2.2 Assessing the Residual Capacity of Moderately Damaged Plastic Hinges

The Mason River Bridge sustained plastic hinge damage as a result of the Kaikōura Earthquake. Simplified analysis indicated that the outermost bar underwent a maximum strain of 3.2%. Hardness testing confirmed that the strain experienced by the steel was around 4% and was used to verify the level of strain hardening, strain ageing and the residual strain capacity of the yielded bars. Monotonic tensile testing of the bars indicated the residual strain capacity was larger than 14%. This is larger than the strain capacity assumed in design (12%). Therefore, the monotonic strain capacity was assumed to be sufficient to survive future CALS events even when strain ageing is accounted for. The cyclic capacity was estimated using a fatigue model proposed by Kunnath, Kanvinde and Xiao et al (2009) and was found to be sufficient to sustain a future CALS event.

The analysis assumes that bars are adequately restrained against buckling so the spiral spacings where checked with additional stirrups installed to ensure a maximum spacing of 90mm. Replacement of buckled reinforcement and concrete have restored the capacity of the hinge so that it can service a future CALS event. The testing and analysis costs were around 5-10% of the original estimated repair costs and provided considerable cost savings compared with the alternative of extensive column repairs and strengthening.

Though this chapter provided a logic-based strategy for estimating the residual capacity of a hinge, it could be further developed and verified through experimental testing i.e pseudo-dynamic testing, which would provide a realistic strain history. After being damaged the residual capacity could be assessed, failure predicted, and further testing carried out to determine how failure correlates to that predicted using the method presented in this chapter.

11.3 SECTION 2 – DISSIPATIVE CONTROLLED ROCKING

This chapter introduced an alternative design philosophy which can increase the cost-competitiveness of DCR connections (or any easily repairable connections with reliable CALS performance). The change in philosophy, of designing to the CALS and neglecting the DCLS, is a simple one that can promote the efficient design of DCR connections. Although the alternative design philosophy results in higher displacements, it was shown that the connection is still likely to have better performance than the monolithic connection. A simple case study comparing the two philosophies resulted in a reduction in base shear of 23%, which results in a reduced moment demand in the foundations.

11.3.1 Appropriate CALS Limits for DCR connections

As discussed in the previous section, due to the development of an alternative design philosophy, performance limits at this level needed to be defined. For PT this was defined as yield (70% of the ultimate stress). P-Delta effects were investigated through NLTH and found to be significant. It was recommended that reductions in capacity and increases in demands be accounted for during design. Upper limits on the P-Delta displacements, proportional to the diameter, were proposed based on geometric considerations. Dissipater strain levels were investigated through ground motions scaling, NLTH and a fatigue model. Dissipater strain levels were recommended at 9% for the CALS and 6% for the DCLS. It was noted that these strain limits can be altered when using the alternative design philosophy. The altered strain limits would be based on the acceptable risk/frequency of repair. For example, for a client willing to accept a high risk of repair being required, a low DCLS strain and higher (than 9%) CALS strain could be implemented.

To further this research, similar fatigue relationships for G500 dissipaters can be developed. These relations can then be used to derive DCLS and CALS strain limits

for these higher-grade dissipaters. Moreover, further development on the type of GM and the expected number of cycles experienced in an earthquake can be completed. Further increases in the strain limits, for G300 dissipaters, could be used if strain ageing affects could be accounted for.

11.3.2 Parametric Analysis of DCR Connections

Relationships were proposed for the yield rotation of DCR connections that use either G300 or G500 mild steel dissipaters. In addition, relationships defining the neutral axis location were defined. Additionally, limits on the geometric ratio ($3 < \frac{L_{ub}}{D} < 8$) and initial prestress were proposed, which ensure that the PT does not yield at CALS drift limits. Limits on the upper PT diameter were proposed to limit the increase in capacity beyond yield (to limit overstrength demands when using traditional design methods). Design tables were developed, which improve the efficiency of the design process by providing designers with suitable values of the main variables as a starting point in the design of DCR systems.

Most of the research presented in this chapter, particularly pertaining to design efficiencies is for G300 mild steel dissipaters and Grade 1030 Macalloy bar. This process could be repeated for G500 dissipaters and PT strands, giving design tables for a wider range of connections. However, it is noted that the dissipater and PT diameters could be resolved into forces at each drift level. This would allow the estimation of alternative material sizes.

11.3.3 Case Study – Implementing Design Tables and the Alternative Design Philosophy

The alternative design philosophy process was developed and illustrated. A design example, NLTH and CSM showed that DCR connections can significantly reduce base shear demands. This is done by allowing a higher ductility or DCLS displacement than is currently possible. Since the weaker connection will typically be smaller, it will have a reduced lever arm (compared to the traditionally designed connection), which reduces peak strain in dissipaters and PT. This resulted in the increased design displacements having an insignificant effect on the strains (and hence low-cycle fatigue demands) in the elements at the CALS.

The lower base shear demands result in significant cost savings, which will offset some of the additional cost associated with using DCR. Firstly, the connection and components can be smaller. Secondly, and probably more importantly, the reduced base shear result in lower foundations demands and smaller foundations.

11.3.4 Optimisation of DCR connections through experimental testing

This chapter introduced three new types of dissipater, two of which can provide a cheaper alternative to axial dissipaters. The first dissipaters, the double tube and optimised double tube dissipater were significantly cheaper than the currently preferred four groove axial dissipater (~30% cheaper per device). However, the dissipaters fractured sooner than the four groove dissipaters. This was likely a low-cycle fatigue type failure. The reason for this is the small unrestrained length of the fuse which is designed to allow compression of the dissipater. Unfortunately, this also contributes to the buckling tendency of the fuse. Further reason for earlier onset of buckling is due to the lower rigidity (lower section modulus) than the four grooved dissipaters making it more susceptible to buckling.

The third type of dissipater examined was the lead extrusion damper. It is conceivable that these dissipaters can be cost competitive to axial dissipaters as axial load capacity of a single device can be up 3-4 time that of an axial dissipater.

Bibliography

AASHTO. (2011). *AASHTO Guide Specifications for LRFD Seismic Bridge Design, Second Edition, LRFDSEIS-2*.

AASHTO. (2017). *AASHTO LRFD Bridge Design Specifications, Eighth Edition*.

ACI Innovation Task Group 1. (2001). *Acceptance criteria for moment frames based on structural testing.*

AISC. (2011). Seismic Provisions for Structural Steel Buildings, ANSI/AISC 341-10. *Structural Analysis and Design of Tall Buildings*, 355–410. https://doi.org/10.1201/b11248-8

Allington, C. (2011). *Materials Testing in Buildings of Interest. Gallery Apartments, Westpac centre, IRD building*.

B Mander, B. J., N Priestley, M. J., & Park, R. (1988). *OBSERVED STRESS-STRAIN BEHAVIOR OF CONFINED CONCRETE*.

Berry, M. P., & Eberhard, M. O. (2005). Practical performance model for bar buckling. *Journal of Structural Engineering*, *131*(7), 1060–1070. https://doi.org/10.1061/(ASCE)0733-9445(2005)131:7(1060)

Bresler, B., & Gilbert, P. H. (1961). Tie Requirements for Reinforced Concrete Columns. *ACI Journal Proceedings*, *58*(11), 555–570. https://doi.org/10.14359/7997

Calvi, G. M., Priestley, M. J. N., & Kowalsky, M. J. (2008). Displacement Based Seismic Design of Structures - MJN Priestley high resolution.pdf. *5th New Zealand Society for Earthquake Engineering Conference*.

Carr, A. J. (2004). *RUAUMOKO Program for Inelastic Dynamic Analysis - Users Manual*.

Chegini, Z. (2018). *LOW-DAMAGE SEISMIC DESIGN OF BRIDGE SUPERSTRUCTURES*.

Christopoulos, C., Filiatrault, A., Uang, C.-M., & Folz, B. (2002). Posttensioned Energy Dissipating Connections for Moment-Resisting Steel Frames. *Journal of Structural Engineering*, *128*(9), 1111–1120. https://doi.org/10.1061/(ASCE)0733-9445(2002)128:9(1111)

Coffin, L. (1954). A study of the effects of cyclic thermal stresses on a ductile metal. *Transactions of the American Society of Mechanical Engineers*, *76-931–950*.

Collins, M. P., & Mitchell, D. (1997). Stress-strain response of reinforcement. In *Prestressed concrete structures* (p. 89). Reponse Publications.

Constantinou, M. C., Reinhorn, A. M., Mokha, A., & Watson, R. (1991). Displacement Control Device for Base-Isolated Bridges. *Earthquake Spectra*, *7*(2), 179–200. https://doi.org/10.1193/1.1585625

Cuevas, A., & Pampanin, S. (2014). Accounting for residual capacity of reinforced concrete plastic hinges : current practice and proposed framework. *Proceedings of the New Zealand Society of Earthquake Engineering Conference, Auckland, New Zealand.*, 1–12.

Cuevas, A., & Pampanin, S. (2017). *Post-Seismic Capacity of Damaged and Repaired Reinforced Concrete Plastic Hinges Extracted from a Real Building 2017 NZSEE Conference*.

Dhakal, Rajesh P. (2005). Strategy for anti-buckling design of transverse reinforcement. *2005 NZSEE Conference*, *38*.

Dhakal, Rajesh Prasad, & Maekawa, K. (2002). Path-dependent cyclic stress-strain relationship of reinforcing bar including buckling. *Engineering Structures*, *24*(11), 1383–1396. https://doi.org/10.1016/S0141-0296(02)00080-9

Dhakal, Rajesh Prasad, & Su, J. (2018). Design of transverse reinforcement to avoid premature buckling of main bars. *Earthquake Engineering and Structural Dynamics*, *47*(1), 147–168. https://doi.org/10.1002/eqe.2944

Dutta, A., & Mander, J. B. (1998). Capacity design and fatigue analysis of confined concrete columns. *Technical Report MCEER*. http://bases.bireme.br/cgi-bin/wxislind.exe/iah/online/?IsisScript=iah/iah.xis&src=google&base=DESASTRES&lang=p&nextAction=lnk&exprSearch=11283&indexSearch=ID

El Sebai, A. (2009). *Comparisons of international seismic code provisions for bridges. February*, 106. http://0-search.proquest.com.wam.city.ac.uk/docview/305104103?pq-origsite=summon

Erasmus, L. A., & Pussegoda, L. N. (1977). STRAIN AGE EMBRITTLEMENT OF REINFORCING STEELS. *New Zealand Engineering*, *32*(8), 178–183.

Freeman, S. (2004). REVIEW OF THE DEVELOPMENT OF THE CAPACITY SPECTRUM METHOD. In *ISET Journal of Earthquake Technology, Paper No. 438* (Vol. 41, Issue 1).

Freeman, S., Nicoletti, J., & Tyrell, J. (1975). Evaluations of Existing Buildings for Seismic Risk - A Case Study of Puget Sound Naval Shipyard. *Proceedings of the U.S National Conference on Earthquake Engineering*, 113–122.

GRANOR. (2018). *COMPOUND CHARACTERISTICS SERIES "BS" BEARING STRIP & PADS*.

Guerrini, G. (n.d.). *SEISMIC PERFORMANCE OF PRECAST CONCRETE DUAL-SHELL STEEL COLUMNS FOR ACCELERATED BRIDGE CONSTRUCTION*.

Guerrini, G., Asce, S. M., Restrepo, J. I., Massari, M., & Vervelidis, A. (2015). Seismic Behavior of Posttensioned Self-Centering Precast Concrete Dual-Shell Steel Columns. *Journal of Structural Engineering*, *141*(4), 1–11. https://doi.org/10.1061/(ASCE)ST.1943-541X.0001054.

Guerrini, G., Restrepo, J. I., Massari, M., & Vervelidis, A. (2012). Self-centering precast concrete dual-shell steel columns. *Proceedings of the 15th World Conference on Earthquake Engineering (15WCEE)*, *1*.

Kam, W. Y., Pampanin, S., Palermo, A., & Carr, A. J. (2010). Self-centering

structural systems with combination of hysteretic and viscous energy dissipations. *Earthquake Engineering & Structural Dynamics*, n/a-n/a. https://doi.org/10.1002/eqe.983

Kawashima, K., & Buckle, I. (2013). Structural performance of bridges in the Tohoku-oki earthquake. In *Earthquake Spectra* (Vol. 29, Issue SUPPL.1). https://doi.org/10.1193/1.4000129

Kelly, J. M., Skinner, R., & Heine, A. J. (1972). *M E C H A N I S M S OF ENERGY ABSORPTION IN SPECIAL DEVICES FOR USE IN EARTHQUAKE RESISTANT STRUCTURES*.

Kelly, T. E., Skinner, R., & Robinson, W. H. (2010). *Seismic Isolation for Designers and Structural Engineers*.

King D, J., & Priestley, M. J. N. (1986). *Computer Programs for Concrete Column Design*.

Kompatscher, M. (2004). Equotip - Rebound hardness testing after D. LEEB. *IMEKO TC5 Conference on Hardness Measurements Theory and Application in Laboratories and Industries, HARDMEKO 2004*, *1975*, 66–72.

Kunnath, S., El-Bahy, A., & Stone, A. (1997). Cumulative seismic damage of reinforced concrete bridge piers. *National Institute of Standards and Technology*.

Kunnath, S. K., Kanvinde, A., Xiao, Y., & Zhang, G. (2009). *EFFECTS OF BUCKLING AND LOW CYCLE FATIGUE ON SEISMIC PERFORMANCE OF REINFORCING BARS AND MECHANICAL COUPLERS FOR CRITICAL STRUCTURAL MEMBERS A Technical Report Submitted to the California Department of Transportation under Contract 59A0539 Sashi K . Kunna*. *June*.

Lawrance, G., & Jacks, D. (1990). *Repair Techniques C Labs Lawrence & Jacks*.

Lehman, D., Gookin, S., Nacamuli, A., & Moehle, J. (2001). Repair of Bridge Columns. *ASCE*, *98*, 233–242.

Liu, R. (2018). *Multi-Performance Seismic Design of Low Damage Bridge*.

Liu, R., & Palermo, A. (2016a). Large scale testing of a low damage substructure connection in a precast concrete bridge. *The New Zealand Concrete Industry Conference 2016*.

Liu, R., & Palermo, A. (2020). Characterization of Filler-Free Buckling Restrained Fuse-Type Energy Dissipation Device for Seismic Applications. *Journal of Structural Engineering*, *146*(5), 04020059. https://doi.org/10.1061/(ASCE)ST.1943-541X.0002591

Liu, R., & Palermo, A. (2016b). Controlled rocking, dissipative controlled rocking and multi-hierarchical activation: Numerical analysis and experimental testing. *ECCOMAS Congress 2016 - Proceedings of the 7th European Congress on Computational Methods in Applied Sciences and Engineering*, *3*, 4969–4982. https://doi.org/10.7712/100016.2160.8334

Loporcaro, G. (2017). *A least invasive method to estimate the residual strain capacity of steel reinforcing bars in earthquake damage buildings*.

Loporcaro, G., Pampanin, S., & Kral, M. V. (2018). Estimating Plastic Strain and Residual Strain Capacity of Earthquake-Damaged Steel Reinforcing Bars. *Journal of Structural Engineering*. https://doi.org/10.1061/(ASCE)ST.1943-541X.0001982.

Macalloy Bar Systems. (2009). *Post Tensioning System Macalloy 1030 Macalloy S1030 EXPERIENCE INNOVATION INNOVATION* (Issue November).

Mander, J. B., & Cheng, C. T. (1997). *Seismic resistance of bridge piers based on damage avoidance design*. 148. https://mceer.buffalo.edu/publications/catalog/reports/Seismic-Resistance-of-Bridge-Piers-Based-on-Damage-Avoidance-Design-NCEER-97-0014.html

Mander, J., Panthaki, F., & Kasalanati, A. (1994). Low-cycle fatigue behaviour of reinforcing steel. *Journal of Materials in Civil Engineering, 6(4):453-4*.

Mander, J., & Rodgers, G. (2013). *Cyclic fatigue demands on structures subjected to the 2010-2011Canterbury Earthquake Sequence 2013 NZSEE Conference*.

Mander, T., Rodgers, G., Chase, G., Mander, J., MacRae, G., & Dhakal, R. (2009). Damage Avoidance Design Steel Beam-Column Moment Connection Using High-Force-to-Volume Dissipators. *Journal of Structural Engineering*, *135*(11), 1390–1397. https://doi.org/10.1061/(ASCE)ST.1943-541X.0000065

Manson, S., & Halford, G. (1981). Practical implementation of the double linear damage rule and damge curve approach for treating cumulative fatigue damage. *International Journal of Fracture, 17(2):169-*.

Marriott, D. (2009). *The Development of High-Performance Post-Tensioned Rocking Systems for the Seismic Design of Structures*. University of Canterbury. Civil and Natural Resources Engineering. http://ir.canterbury.ac.nz:80/handle/10092/2678

Marriott, D., Boys, A., Pampanin, S., & Palermo, A. (2006a). *Experimental Validation of High-Performance Hybrid Bridge Piers.*

Marriott, D., Boys, A., Pampanin, S., & Palermo, A. (2006b). Experimental Validation of High-Performance Hybrid Bridge Piers. *New Zealand Society for Earthquake Engineering*.

Marriott, D., Pampanin, S., Bull, D., & Palermo, A. (2008). Dynamic testing of precast, post-tensioned rocking wall systems with alternative dissipating solutions. *Bulletin of the New Zealand Society for Earthquake Engineering*, *41*(2 SE-Articles). https://doi.org/10.5459/bnzsee.41.2.90-103

Marriott, D., Pampanin, S., & Palermo, A. (2009). Quasi-static and pseudo-dynamic testing of unbonded post-tensioned rocking bridge piers with external replaceable dissipaters. *Earthquake Engineering & Structural Dynamics*, *38*(3), 331–354. https://doi.org/10.1002/eqe.857

Mashal, M., & Palermo, A. (2014). *EXPERIMENTAL TESTING OF EMULATIVE FULLY PRECAST CONCRETE BRIDGE BENT IN SEISMIC REGIONS*.

Mehrsoroush, A., & M. Saiidi. (2016). Novel, Cyclic Response of Precast Bridge Piers with Column-Base Pipe Pins and Pocket Cap Beam Connections. *ASCE*.

Miner, M. (1945). Cumulative Damage in Fatigue. *Journal of Applied Mechanics, 12(1):A-15*.

Montejo, L. A., & Kowalsky, M. J. (2007). *Cumbia: Set of Codes for the Analysis of Reinforced Concrete Members.*

Morgen, B. G., & Kurama, Y. C. (2004). A friction damper for post-tensioned precast concrete moment frames. *PCI Journal*, *49*(4), 112–133. https://doi.org/10.15554/pcij.07012004.112.133

Moustafa, A., & Elgawady, M. A. (2016). Damage-resistant segmental double-skin bridge column with replaceable energy dissipaters. *Insights and Innovations in Structural Engineering, Mechanics and Computation - Proceedings of the 6th International Conference on Structural Engineering, Mechanics and Computation, SEMC 2016*, 370–375. https://doi.org/10.1201/9781315641645-62

Moyer, M. J., & Kowalsky, M. (2003). Influence of tension strain on buckling of reinforcement in concrete columns. *ACI Structural Journal*, *100*, 75-85.

Mustafa, M., & Palermo, A. (2019). Low-Damage Seismic Design for Accelerated Bridge Construction. *Journal of Bridge Engineering*, *24*(7), 4019066. https://doi.org/10.1061/(ASCE)BE.1943-5592.0001406

Nashid, H., Ferguson, W. G., Clifton, G. C., Hodgson, M., Battley, M., Seal, C., & Choi, J. H. (2014). Non-destructive method to investigate the hardness-plastic strain relationship in cyclically deformed structural steel elements. *Bulletin of the New Zealand Society for Earthquake Engineering*, *47*(3), 181–189.

NZS 3101. (1995). *Concrete Structure Standard*. Standard New Zealand.

NZS 3101. (2006). *Concrete Structures Standard.* Standard New Zealand.

NZTA. (2012). *Performance of highway structures during the darfield and christchurch earthquakes of 4 september 2010 and 22 february 2011*. *February*.

NZTA. (2016). *Earthquake Resistant Design of Structures, Bridge Manual 3rd Edition Amendment 2*.

NZTA. (2018). *NZTA Bridge manual*.

Ou, Y.-C. (2007). *Precast segmental post-tensioned concrete bridge columns for seismic regions*.

Ou, Y.-C., Chiewanichakorn, M., Aref, A. J., & Lee, G. C. (2007). Seismic Performance of Segmental Precast Unbonded Posttensioned Concrete Bridge Columns. *Journal of Structural Engineering*, *133*(11), 1636–1647. https://doi.org/10.1061/(ASCE)0733-9445(2007)133:11(1636)

Palermo, A. (2004). *The Use of Controlled Rocking in the Seismic Design of Bridges*.

Palermo, A., Liu, R., Rais, A., McHaffie, B., Andisheh, K., Pampanin, S., Gentile, R., Nuzzo, I., Granerio, M., Loporcaro, G., McGann, C., & Wotherspoon, L. (2017a). Performance of Road Bridges During the 14 November 2016 Kaikoura Earthquake. *Bulletin of the New Zealand Society for Earthquake Engineering*, *50*(2), 253-.

Palermo, A., Liu, R., Rais, A., McHaffie, B., Andisheh, K., Pampanin, S., Gentile, R., Nuzzo, I., Granerio, M., Loporcaro, G., McGann, C., & Wotherspoon, L. (2017b). Performance of road bridges during the 14 November 2016 Kaikōura earthquake. *Bulletin of the New Zealand Society for Earthquake Engineering*, *50*(2).

Palermo, A., & Mashal, M. (2012). Accelerated bridge construction (abc) and seismic damage resistant technology: A new zealand challenge. *Bulletin of the New Zealand Society for Earthquake Engineering*, *45*(3), 123–134. http://www.nzsee.org.nz/db/Bulletin/Archive/45(3)0123.pdf

Palermo, A., Pampanin, S., & Calvi, G. (2005). *FOR SEISMIC RESISTANT BRIDGE SYSTEMS*. *9*(6), 899–921.

PALERMO, A., PAMPANIN, S., & CALVI, G. (2005). CONCEPT AND DEVELOPMENT OF HYBRID SOLUTIONS FOR SEISMIC RESISTANT BRIDGE SYSTEMS. *Journal of Earthquake Engineering*, *9*(6), 899–921. https://doi.org/10.1080/13632460509350571

Palermo, A., Pampanin, S., & Marriott, D. (2007). Design, Modeling, and Experimental Response of Seismic Resistant Bridge Piers with Posttensioned Dissipating Connections. *Journal of Structural Engineering*, *133*(11), 1648–1661. https://doi.org/10.1061/(ASCE)0733-9445(2007)133:11(1648)

Pampanin, S., Marriott, D., Palermo, A., & Society, N. Z. C. (2010). *PRESSS Design Handbook*.

Pampanin, S., PRIESTLEY, M., & Sritharan, S. (2001). Analytical modeling of the seismic behavior of precast concrete frames designed with ductile connections. *Journal of Earthquake Engineering - J EARTHQU ENG*, *5*, 329–367. https://doi.org/10.1080/13632460109350397

Pantazopoulou, S. J. (1998). Detailing for Reinforcement Stability in RC Members. *Journal of Structural Engineering*, *124*(6), 623–632. https://doi.org/10.1061/(ASCE)0733-9445(1998)124:6(623)

Priestley, M. J. N. (1995). Myths and Fallacies in Earthquake Engineering--Conflicts Between Design and Reality. *Special Publication*, *157*, 231–254. https://doi.org/10.14359/983

Priestley, M. J. N. (1996). The PRESSS program - Current status and proposed plans for Phase III. In *PCI Journal* (Vol. 41, Issue 2). https://doi.org/10.15554/pcij.03011996.22.40

Priestley, M. J. N., Calvi, G. M., & Kowalsky, M. J. (2007). Displacement-based seismic design of structures. *Building*, *23*(33), 1453–1460. https://doi.org/10.1016/S0141-0296(01)00048-7

Priestley, M. J. N., Seible, F., & Calvi, G. (1996). *Seismic Design and Retrofit of Bridges*. https://doi.org/10.1002/9780470172858

Ramirez, C. M., Liel, A. B., Mitrani-Reiser, J., Haselton, C. B., Spear, A. D., Steiner, J., Deierlein, G. G., & Miranda, E. (2012). Expected earthquake damage and repair costs in reinforced concrete frame buildings. *Earthquake Engineering & Structural Dynamics*, *41*(11), 1455–1475. https://doi.org/10.1002/eqe.2216

Roberts, J. E. (2001). Performance of concrete bridges in recent earthquakes. *Structural Concrete*, *2*(2), 73–91. https://doi.org/10.1680/stco.2001.2.2.73

Robinson, W. H., & Greenbank, L. R. (1976). An extrusion energy absorber suitable for the protection of structures during an earthquake. *Earthquake Engineering & Structural Dynamics*, *4*(3), 251–259. https://doi.org/10.1002/eqe.4290040306

Rodgers, G. (2009). *Next Generation Structural Technologies : Implementing High Force-To-Volume Energy Absorbers*.

Rodgers, G., Chase, J., Mander, J., Leach, N., & Denmead, C. (2009). *High force-to-volume extrusion dampers and shock absorbers for civil infrastructure*.

Rodgers, G., Mander, J., Chase, J., & Dhakal, R. (2016). Beyond Ductility: Parametric Testing of a Jointed Rocking Beam-Column Connection Designed for Damage Avoidance. *Journal of Structural Engineering (United States)*, *142*(8), 1–10. https://doi.org/10.1061/(ASCE)ST.1943-541X.0001318

Routledge, P., Cowan, M., & Palermo, A. (2016). *Low-damage detailing for bridges – A case study of Wigram-Magdala Bridge*. *Mashal 2014*, 1–8.

Rutledge, S. T., Kowalsky, M. J., Seracino, R., & Nau, J. M. (2014). Repair of Reinforced Concrete Bridge Columns Containing Buckled and Fractured Reinforcement by Plastic Hinge Relocation. *Journal of Bridge Engineering*, *19*(8), A4013001. https://doi.org/10.1061/(ASCE)BE.1943-5592.0000492

Sarti, F. (2015). *Seismic Design of Low-Damage Post-Tensioned Timber Wall Systems*.

Sarti, F., Palermo, A., & Pampanin, S. (2016). Fuse-Type External Replaceable Dissipaters: Experimental Program and Numerical Modeling. *Journal of Structural Engineering*, *142*(12), 4016134. https://doi.org/10.1061/(ASCE)ST.1943-541X.0001606

Scribner, C. F. (1986). REINFORCEMENT BUCKLING IN REINFORCED CONCRETE FLEXURAL MEMBERS. *Journal of the American Concrete Institute*, *83*(6), 966–973. https://doi.org/10.14359/2648

Sideris, P., Aref, A. J., & Filiatrault, A. (2014a). Large-Scale Seismic Testing of a Hybrid Sliding-Rocking Posttensioned Segmental Bridge System. *Journal of Structural Engineering*, *140*(6), 04014025. https://doi.org/10.1061/(ASCE)ST.1943-541X.0000961

Sideris, P., Aref, A. J., & Filiatrault, A. (2014b). Quasi-static cyclic testing of a large-scale hybrid sliding-rocking segmental column with slip-dominant joints. *Journal of Bridge Engineering*, *19*(10). https://doi.org/10.1061/(ASCE)BE.1943-5592.0000605

Skinner, R., Robinson, W. H., & McVerry, G. H. (1991). Seismic isolation in New Zealand. *Nuclear Engineering and Design*, *127*(3), 281–289. https://doi.org/10.1016/0029-5493(91)90052-J

Skinner, R., Tyler, R. G., Heine, A. J., & Robinson, W. H. (1980). *HYSTERETIC DAMPERS FOR THE PROTECTION OF STRUCTURES FROM EARTHQUAKES Fig . 1 : Details of Rangitikei Bridge Plate 1 : Torsion beam hysteretic damper in test machine Plate 2 : South Rangitikei Rail Bridge under*

construction.

Solberg, K., Mashiko, N., Mander, J. B., & Dhakal, R. P. (2009). Performance of a Damage-Protected Highway Bridge Pier Subjected to Bidirectional Earthquake Attack. *Journal of Structural Engineering*, *135*(5), 469–478. https://doi.org/10.1061/(ASCE)0733-9445(2009)135:5(469)

Spieth, H. A., Carr, A. J., Murahidy, A. G., Arnolds, D., Davies, M., & Mander, J. B. (2004). *Modelling of post-tensioned precast reinforced concrete frame structures with rocking beam-column connections*.

Sritharan, S., Priestley, M. J. N., & Seible, F. (1999). Enhancing Seismic Performance of Bridge Cap Beam-to-Column Joints using Prestressing. *PCI Journal*.

Stone, W. C., Stanton, J. F., & Cheok, G. S. (1995). Performance of Hybrid Moment-Resisting Precast Beam-Column Concrete Connections Subjected to Cyclic Loading. *ACI Structural Journal*, *92*(2). https://doi.org/10.14359/1145

Stringer, M. E., Bastin, S., McGann, C., Cappellaro, C., El Kortbawi, M., McMahon, R., Wotherspoon, L. M., Green, R. A., Aricheta, J., Davis, R., McGlynn, L., Hargraves, S., Van Ballegooy, S., Cubrinovski, M., Bradley, B. A., Bellagamba, X., Foster, K., Lai, C., Ashfield, D., … Ntritsos, N. (2017). Geotechnical aspects of the 2016 Kaikōura earthquake on the South Island of New Zealand. *Bulletin of the New Zealand Society for Earthquake Engineering*, *50*(2), 117–141. https://doi.org/10.5459/bnzsee.50.2.117-141

Thonstad, T., Asce, S. M., Islam, ;, Mantawy, M., Stanton, J. F., Eberhard, M. O., Sanders, D. H., & Asce, F. (2016). *Shaking Table Performance of a New Bridge System with Pretensioned Rocking Columns*. https://doi.org/10.1061/(ASCE)BE.1943-5592.0000867

U.S. Department of Transportation Federal Highway Administration. (2014). *LRFD Seismic Analysis and Design of Bridges - Reference Manual*. *FHWA-NHI-15-004*, 608.

Wang, J.-C., Ou, Y.-C., Chang, K.-C., & Lee, G. C. (2008). Large-scale seismic tests of tall concrete bridge columns with precast segmental construction. *Earthquake Engineering & Structural Dynamics*, *37*(12), 1449–1465. https://doi.org/10.1002/eqe.824

Wang, J., Wang, Z., Tang, Y., Liu, T., & Zhang, J. (2018). Cyclic loading test of self-centering precast segmental unbonded posttensioned UHPFRC bridge columns. *Bulletin of Earthquake Engineering*, *16*(11), 5227–5255. https://doi.org/10.1007/s10518-018-0331-y

White, S. (2014). *Controlled damage rocking systems for accelerated bridge construction* (Issue March).

Wood, J. (2017). *Performance of State Highway Bridges in the 2016 Kaikoura Earthquake: Aftershock Records from Awatere River Bridge*. *March*.

Wood, J., & McHaffie, B. (2017). *Five Bridges Located Near the Epicentre at Waiau Report Prepared for NZ Transport Agency*. *June*.

Wood, J., & McHaffie, B. (2020). Performance of Modern Highway Bridges in the

2016 Kaikoura Earthquake. *Structural Engineering International*, 1–13. https://doi.org/10.1080/10168664.2019.1702913

Appendices

Appendix A – Seismic response of connection used to determine strain limits.

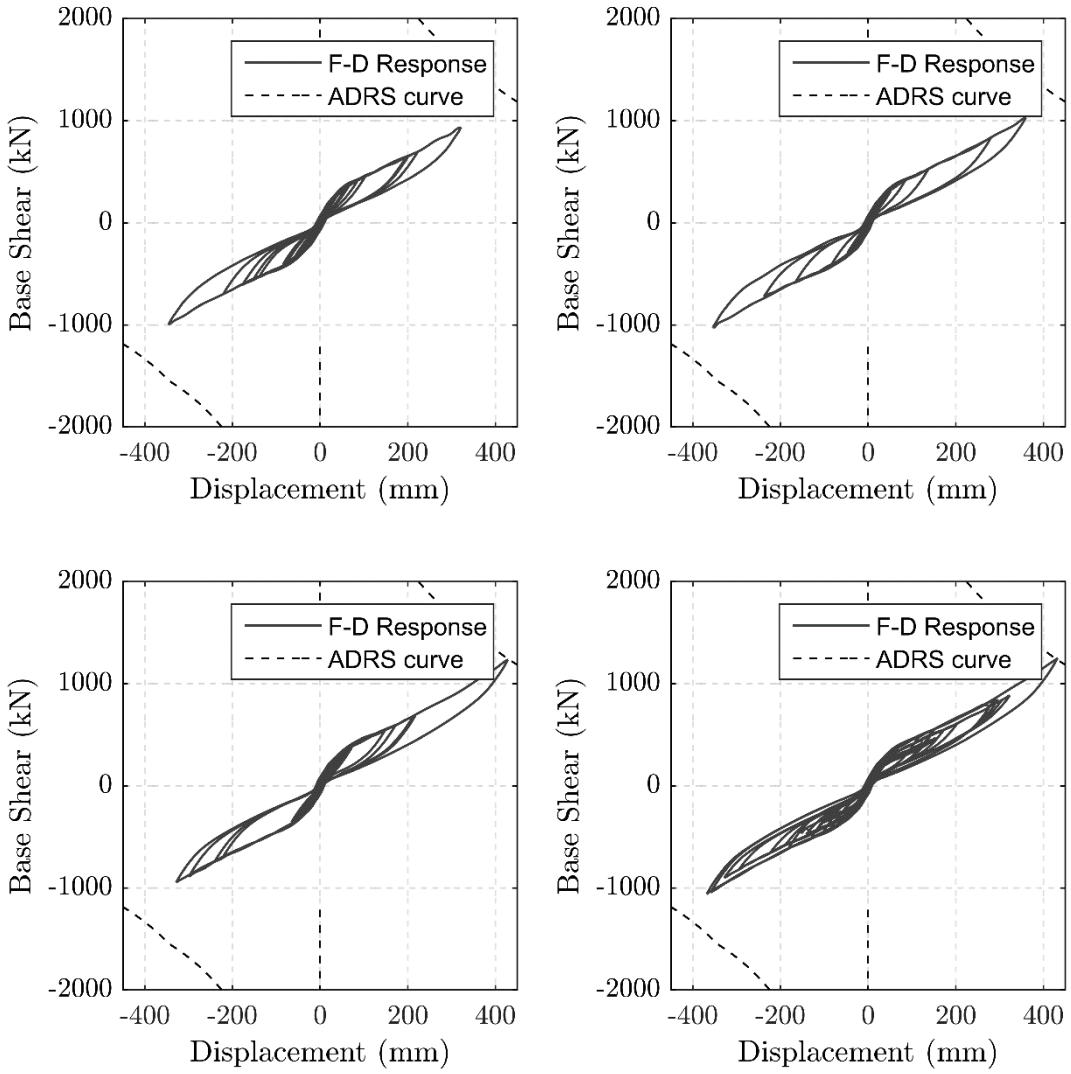

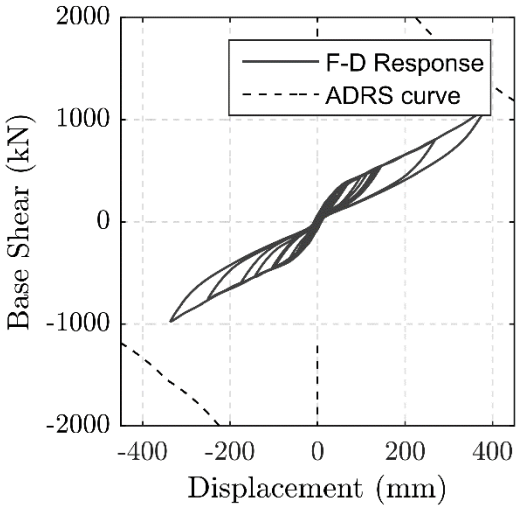
F-D Response
ADRS curve
Base Shear (kN)
Displacement (mm)
2000
1000
0
-1000
-2000
-400
-200
0
200
400

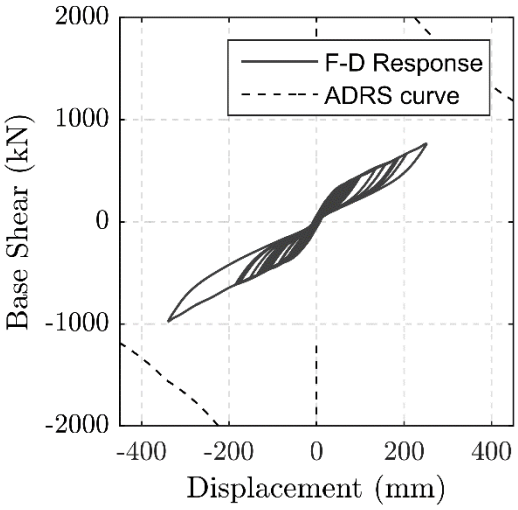
F-D Response
ADRS curve
Base Shear (kN)
Displacement (mm)
2000
1000
0
-1000
-2000
-400
-200
0
200
400

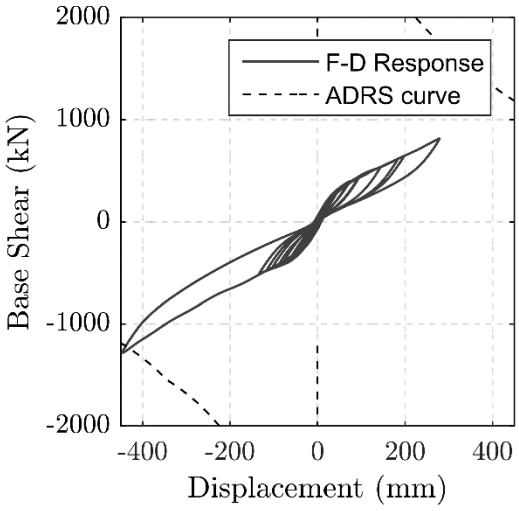
F-D Response
ADRS curve
Base Shear (kN)
Displacement (mm)
2000
1000
0
-1000
-2000
-400
-200
0
200
400

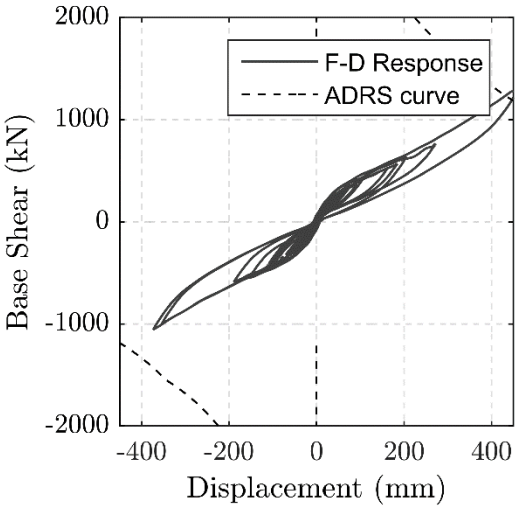
F-D Response
ADRS curve
Base Shear (kN)
Displacement (mm)
2000
1000
0
-1000
-2000
-400
-200
0
200
400

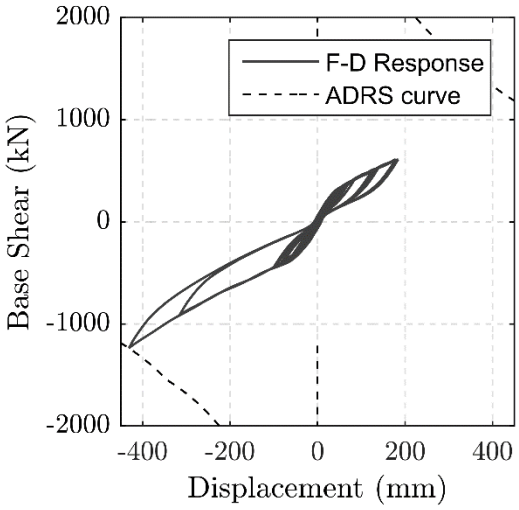
F-D Response
ADRS curve
Base Shear (kN)
Displacement (mm)
2000
1000
0
-1000
-2000
-400
-200
0
200
400

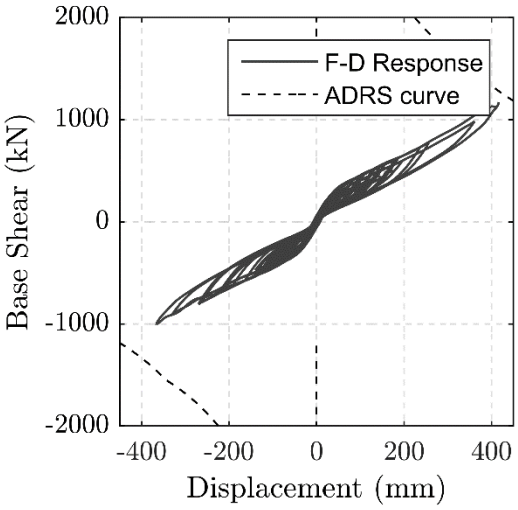
F-D Response
ADRS curve
Base Shear (kN)
Displacement (mm)
2000
1000
0
-1000
-2000
-400
-200
0
200
400

Appendix B - Ground Motions used for the CALS analysis in Chapter 9

Record Sequence Number	GM NUm	Earthquake Name	YEAR	Magnitude	EpiD (km)	HypD (km)	Soil Class	PGA (g)	PGV (cm/sec)	Scale Factor
159	GM1	Imperial Valley-06	1979	6.5	3	10	D	0.29	33.9	2.38
183	GM2	Imperial Valley-06	1979	6.5	28	30	D	0.54	56.8	1.9
292	GM3	Irpinia, Italy-01	1980	6.9	30	32	C	0.29	46.9	2.61
571	GM4	Taiwan SMART1(45)	1986	7.3	73	75	D	0.17	24.9	2.77
1077	GM5	Northridge-01	1994	6.7	22	28	D	0.59	31.2	2.28
1528	GM6	Chi-Chi, Taiwan	1999	7.62	45	46	D	0.2	61.5	2.66
1535	GM7	Chi-Chi, Taiwan	1999	7.62	126	127	D	0.0	8.0	2.57

Appendix C - Design Tables for Circular DCR Connections

Initial Pt Force 0.1F_{yield}		Axial Load (excluding PT) 1000kN			Cantilever Length (3000mm)			Grade 300 Dissipaters		
	PT Dia.	Fuse Length (mm)	Yield (kNm)	1%drift (kNm)	2%drift (kNm)	3%drift (kNm)	4%drift (kNm)	6%drift (kNm)	λ	Fuse Area (mm^2)
Diameter (800mm)	36mm	250	578	717	769	809	844	883	1.1	2682
		500	594	704	749	784	815	846	1.1	2682
		750	605	699	742	775	805	834	1.2	2682
		1000	616	693	738	770	800	828	1.2	2682
	50mm	250	640	819	919	1005	1086	1165	1.1	3109
		500	657	805	894	973	1050	1124	1.2	3109
		750	670	800	885	962	1036	1109	1.2	3109
		1000	685	794	881	956	1029	1101	1.2	3109
	75mm	250	797	1072	1277	1472	1663	1851	1.2	4217
		500	819	1060	1252	1435	1616	1796	1.3	4217
		750	836	1052	1237	1417	1593	1769	1.3	4217
		1000	859	1045	1230	1407	1581	1755	1.3	4217
	100mm	250	1011	1407	1739	2060	2377	2691	1.2	5769
		500	1040	1396	1704	2012	2316	2620	1.3	5769
		750	1061	1386	1695	1995	2294	2592	1.3	5769
		1000	1093	1377	1684	1984	2283	2578	1.3	5769
	125mm	250	1283	1817	2281	2742	3201	3659	1.2	7764
		500	1320	1802	2242	2682	3124	3567	1.3	7764
		750	1342	1793	2227	2661	3102	3532	1.3	7764
		1000	1383	1780	2227	2649	3081	3514	1.3	7764
	150mm	250	1607	2299	2898	3506	4112	4716	1.2	10202
		500	1650	2270	2847	3430	4015	4600	1.2	10202
		750	1673	2261	2834	3409	3981	4559	1.2	10202
		1000	1724	2246	2828	3394	3960	4533	1.3	10202

Initial Pt Force 0.1F_{yield}		Axial Load (excluding PT) 1000kN			Cantilever Length (3000mm)			Grade 300 Dissipaters		
	PT Dia.	Fuse Length (mm)	Yield (kNm)	1%drift (kNm)	2%drift (kNm)	3%drift (kNm)	4%drift (kNm)	6%drift (kNm)	λ	Fuse Area (mm^2)
Diameter (1000mm)	36mm	250	764	948	1037	1120	1198	1212	1.2	2756
		500	776	933	1013	1084	1151	1158	1.3	2756
		750	790	927	1004	1072	1133	1136	1.3	2756
		1000	803	919	1000	1067	1125	1125	1.3	2756
	50mm	250	853	1108	1272	1425	1580	1620	1.3	3252
		500	866	1089	1242	1386	1528	1557	1.4	3252
		750	884	1082	1231	1372	1510	1532	1.4	3252
		1000	900	1074	1226	1365	1501	1520	1.4	3252
	75mm	250	1080	1506	1855	2190	2517	2655	1.4	4539
		500	1097	1479	1807	2126	2441	2571	1.5	4539
		750	1122	1468	1790	2103	2413	2538	1.5	4539
		1000	1149	1461	1781	2091	2399	2520	1.5	4539
	100mm	250	1388	2028	2598	3157	3710	4065	1.4	6341
		500	1411	1999	2545	3081	3615	3949	1.5	6341
		750	1446	1982	2519	3048	3575	3898	1.5	6341
		1000	1484	1973	2504	3028	3550	3870	1.6	6341
	125mm	250	1775	2657	3484	4295	5098	5775	1.4	8658
		500	1805	2625	3413	4195	4974	5622	1.5	8658
		750	1850	2610	3390	4159	4926	5562	1.5	8658
		1000	1898	2593	3370	4141	4902	5530	1.5	8658
	150mm	250	2238	3386	4490	5575	6652	7720	1.4	11490
		500	2278	3351	4401	5447	6492	7534	1.4	11490
		750	2329	3340	4371	5401	6432	7462	1.5	11490
		1000	2389	3317	4352	5378	6401	7423	1.5	11490

Initial Pt Force 0.1F_{yield}		Axial Load (excluding PT) 1000kN			Cantilever Length (3000mm)			Grade 300 Dissipaters		
	PT Dia.	Fuse Length (mm)	Yield (kNm)	1%drift (kNm)	2%drift (kNm)	3%drift (kNm)	4%drift (kNm)	6%drift (kNm)	λ	Fuse Area (mm^2)
Diameter (1200mm)	36mm	250	954	1194	1336	1474	1527	1552	1.3	2830
		500	968	1176	1301	1423	1463	1480	1.4	2830
		750	983	1168	1290	1404	1438	1450	1.4	2830
		1000	997	1160	1284	1395	1425	1434	1.4	2830
	50mm	250	1075	1422	1673	1922	2035	2090	1.4	3395
		500	1090	1398	1634	1862	1960	2004	1.5	3395
		750	1110	1391	1620	1842	1930	1968	1.5	3395
		1000	1129	1381	1613	1832	1915	1949	1.6	3395
	75mm	250	1385	1995	2518	3027	3318	3446	1.5	4861
		500	1401	1957	2456	2947	3216	3327	1.6	4861
		750	1432	1944	2435	2917	3178	3277	1.7	4861
		1000	1463	1934	2423	2902	3159	3253	1.7	4861
	100mm	250	1805	2751	3628	4490	5089	5296	1.6	6914
		500	1824	2701	3539	4367	4934	5130	1.7	6914
		750	1868	2679	3504	4319	4875	5063	1.7	6914
		1000	1915	2668	3486	4294	4844	5027	1.8	6914
	125mm	250	2328	3665	4944	6203	7254	7613	1.6	9553
		500	2356	3611	4837	6054	7060	7391	1.7	9553
		750	2413	3577	4794	5999	6986	7294	1.7	9553
		1000	2477	3560	4765	5960	6941	7239	1.7	9553
	150mm	250	2952	4721	6446	8149	9799	10317	1.5	12778
		500	2990	4654	6309	7955	9548	10027	1.6	12778
		750	3058	4625	6261	7883	9452	9908	1.7	12778
		1000	3139	4600	6234	7846	9400	9846	1.7	12778

Initial Pt Force 0.1f_{yield}		Axial Load (excluding PT) 2000kN			Cantilever Length (3000mm)			Grade 300 Dissipaters		
	PT Dia.	Fuse Length (mm)	Yield (kNm)	1%drift (kNm)	2%drift (kNm)	3%drift (kNm)	4%drift (kNm)	6%drift (kNm)	λ	Fuse Area (mm^2)
Diameter (800mm)	36mm	250	1015	1256	1322	1363	1394	1412	1.0	4904
		500	1051	1244	1292	1316	1330	1339	1.0	4904
		750	1068	1234	1276	1295	1306	1312	1.0	4904
		1000	1089	1228	1267	1285	1293	1298	1.1	4904
	50mm	250	1073	1349	1457	1540	1615	1685	1.0	5331
		500	1111	1337	1425	1493	1553	1607	1.1	5331
		750	1129	1327	1410	1471	1525	1575	1.1	5331
		1000	1153	1321	1400	1459	1510	1558	1.1	5331
	75mm	250	1221	1587	1791	1975	2152	2323	1.1	6439
		500	1264	1573	1754	1920	2082	2240	1.1	6439
		750	1283	1564	1739	1901	2056	2209	1.1	6439
		1000	1315	1554	1730	1887	2039	2189	1.2	6439
	100mm	250	1424	1907	2224	2534	2837	3133	1.1	7991
		500	1474	1887	2183	2469	2754	3034	1.1	7991
		750	1494	1883	2171	2450	2724	2997	1.2	7991
		1000	1535	1869	2163	2435	2708	2979	1.2	7991
	125mm	250	1682	2305	2749	3195	3634	4072	1.1	9986
		500	1740	2277	2697	3117	3535	3953	1.1	9986
		750	1762	2268	2683	3095	3499	3910	1.2	9986
		1000	1809	2253	2677	3075	3479	3884	1.2	9986
	150mm	250	1989	2770	3352	3943	4528	5109	1.1	12424
		500	2059	2730	3298	3850	4408	4966	1.1	12424
		750	2083	2718	3274	3813	4373	4915	1.1	12424
		1000	2137	2705	3270	3806	4341	4884	1.1	12424

Initial Pt Force 0.1Fyield		Axial Load (excluding PT) 2000kN			Cantilever Length (3000mm)			Grade 300 Dissipaters		
	PT Dia.	Fuse Length (mm)	Yield (kNm)	1%drift (kNm)	2%drift (kNm)	3%drift (kNm)	4%drift (kNm)	6%drift (kNm)	λ	Fuse Area (mm^2)
Diameter (1000mm)	36mm	250	1342	1663	1775	1848	1910	1922	1.1	4978
		500	1370	1636	1721	1781	1833	1826	1.2	4978
		750	1397	1624	1703	1757	1804	1791	1.2	4978
		1000	1419	1617	1693	1745	1789	1773	1.2	4978
	50mm	250	1425	1810	1995	2148	2284	2319	1.1	5474
		500	1455	1783	1939	2071	2195	2220	1.2	5474
		750	1484	1769	1918	2043	2162	2182	1.2	5474
		1000	1510	1762	1906	2029	2144	2162	1.3	5474
	75mm	250	1639	2181	2539	2872	3195	3365	1.2	6761
		500	1673	2155	2481	2788	3085	3228	1.3	6761
		750	1709	2136	2452	2748	3038	3175	1.3	6761
		1000	1742	2126	2437	2728	3014	3146	1.3	6761
	100mm	250	1934	2677	3253	3804	4345	4732	1.3	8563
		500	1975	2645	3182	3702	4217	4578	1.3	8563
		750	2018	2629	3157	3666	4170	4517	1.4	8563
		1000	2062	2614	3136	3642	4142	4481	1.4	8563
	125mm	250	2309	3287	4112	4912	5703	6419	1.3	10880
		500	2359	3248	4026	4789	5547	6229	1.4	10880
		750	2402	3236	3997	4744	5488	6154	1.4	10880
		1000	2456	3219	3983	4721	5458	6115	1.4	10880
	150mm	250	2753	4001	5082	6162	7230	8282	1.3	13712
		500	2814	3956	4986	6009	7039	8062	1.3	13712
		750	2861	3937	4954	5956	6969	7975	1.4	13712
		1000	2924	3922	4932	5925	6932	7929	1.4	13712

Initial Pt Force 0.1Fyield		Axial Load (excluding PT) 2000kN			Cantilever Length (3000mm)			Grade 300 Dissipaters		
	PT Dia.	Fuse Length (mm)	Yield (kNm)	1%drift (kNm)	2%drift (kNm)	3%drift (kNm)	4%drift (kNm)	6%drift (kNm)	λ	Fuse Area (mm^2)
Diameter (1200mm)	36mm	250	1684	2084	2240	2371	2439	2463	1.2	5052
		500	1706	2044	2177	2285	2328	2336	1.2	5052
		750	1735	2031	2155	2255	2285	2284	1.3	5052
		1000	1760	2021	2143	2240	2264	2256	1.3	5052
	50mm	250	1796	2300	2568	2805	2935	2988	1.2	5617
		500	1821	2257	2495	2712	2813	2848	1.3	5617
		750	1854	2240	2470	2678	2768	2791	1.4	5617
		1000	1884	2231	2457	2660	2746	2760	1.4	5617
	75mm	250	2086	2841	3388	3899	4209	4320	1.3	7083
		500	2116	2792	3292	3771	4059	4151	1.4	7083
		750	2159	2770	3257	3724	4002	4085	1.5	7083
		1000	2200	2758	3239	3700	3972	4049	1.5	7083
	100mm	250	2485	3566	4452	5312	5956	6181	1.4	9136
		500	2523	3513	4348	5165	5764	5950	1.5	9136
		750	2577	3480	4300	5100	5682	5856	1.5	9136
		1000	2631	3463	4273	5064	5639	5807	1.6	9136
	125mm	250	2989	4449	5737	6994	8094	8453	1.4	11775
		500	3039	4387	5607	6809	7858	8180	1.5	11775
		750	3103	4357	5562	6742	7766	8068	1.6	11775
		1000	3174	4334	5527	6705	7718	8004	1.6	11775
	150mm	250	3597	5479	7211	8908	10585	11133	1.4	15000
		500	3659	5404	7051	8682	10306	10793	1.5	15000
		750	3730	5384	6994	8600	10197	10657	1.5	15000
		1000	3814	5349	6967	8556	10142	10583	1.6	15000

Initial Pt Force 0.1f_{yield}		Axial Load (excluding PT) 3000kN			Cantilever Length (3000mm)			Grade 300 Dissipaters		
	PT Dia.	Fuse Length (mm)	Yield (kNm)	1%drift (kNm)	2%drift (kNm)	3%drift (kNm)	4%drift (kNm)	6%drift (kNm)	λ	Fuse Area (mm^2)
Diameter (800mm)	36mm	250	1342	1690	1758	1793	1811	1820	1.0	6414
		500	1406	1674	1721	1737	1739	1734	1.1	6414
		750	1430	1669	1710	1718	1710	1694	1.1	6414
		1000	1463	1659	1699	1702	1691	1673	1.1	6414
	50mm	250	1393	1774	1881	1955	2015	2066	1.1	6798
		500	1460	1757	1842	1897	1940	1976	1.1	6798
		750	1484	1751	1827	1876	1912	1941	1.1	6798
		1000	1519	1742	1818	1862	1893	1917	1.1	6798
	75mm	250	1522	1989	2183	2353	2513	2663	1.1	7795
		500	1594	1969	2137	2288	2430	2565	1.2	7795
		750	1621	1963	2124	2268	2399	2527	1.2	7795
		1000	1660	1951	2121	2254	2384	2508	1.2	7795
	100mm	250	1703	2280	2578	2876	3151	3428	1.1	9192
		500	1783	2254	2531	2802	3056	3315	1.2	9192
		750	1811	2246	2518	2771	3022	3274	1.2	9192
		1000	1856	2233	2516	2763	3011	3251	1.2	9192
	125mm	250	1933	2643	3064	3493	3904	4315	1.1	10987
		500	2021	2607	3015	3408	3794	4185	1.2	10987
		750	2052	2594	3000	3371	3756	4137	1.2	10987
		1000	2105	2586	2987	3363	3744	4122	1.2	10987
	150mm	250	2211	3070	3630	4176	4756	5304	1.1	13182
		500	2308	3021	3564	4084	4629	5153	1.2	13182
		750	2342	3003	3543	4058	4570	5099	1.2	13182
		1000	2399	2992	3539	4045	4552	5066	1.2	13182

Initial Pt Force 0.1Fyield		Axial Load (excluding PT) 3000kN			Cantilever Length (3000mm)			Grade 300 Dissipaters		
	PT Dia.	Fuse Length (mm)	Yield (kNm)	1%drift (kNm)	2%drift (kNm)	3%drift (kNm)	4%drift (kNm)	6%drift (kNm)	λ	Fuse Area (mm^2)
Diameter (1000mm)	36mm	250	1793	2239	2365	2448	2502	2492	1.2	6480
		500	1845	2213	2308	2357	2391	2371	1.2	6480
		750	1883	2196	2280	2322	2350	2324	1.3	6480
		1000	1916	2187	2266	2304	2328	2300	1.3	6480
	50mm	250	1866	2372	2566	2719	2855	2889	1.2	6927
		500	1922	2345	2506	2629	2734	2754	1.3	6927
		750	1961	2328	2479	2590	2688	2702	1.3	6927
		1000	1998	2318	2463	2570	2664	2674	1.3	6927
	75mm	250	2055	2708	3068	3390	3698	3877	1.3	8085
		500	2117	2677	3000	3292	3573	3728	1.3	8085
		750	2159	2663	2976	3255	3523	3662	1.4	8085
		1000	2203	2649	2955	3229	3491	3626	1.4	8085
	100mm	250	2317	3162	3731	4267	4789	5192	1.3	9707
		500	2386	3127	3652	4154	4646	5018	1.4	9707
		750	2433	3116	3625	4112	4592	4950	1.4	9707
		1000	2485	3097	3609	4091	4564	4914	1.4	9707
	125mm	250	2650	3721	4526	5314	6084	6820	1.3	11792
		500	2726	3681	4434	5182	5916	6614	1.4	11792
		750	2779	3670	4403	5133	5853	6534	1.4	11792
		1000	2840	3651	4390	5108	5821	6492	1.5	11792
	150mm	250	3050	4384	5447	6498	7538	8569	1.3	14341
		500	3135	4333	5333	6339	7337	8340	1.4	14341
		750	3195	4314	5304	6284	7265	8249	1.4	14341
		1000	3266	4303	5297	6252	7222	8201	1.5	14341

Initial Pt Force 0.1F_{yield}		Axial Load (excluding PT) 3000kN			Cantilever Length (3000mm)			Grade 300 Dissipaters		
	PT Dia.	Fuse Length (mm)	Yield (kNm)	1%drift (kNm)	2%drift (kNm)	3%drift (kNm)	4%drift (kNm)	6%drift (kNm)	λ	Fuse Area (mm^2)
Diameter (1200mm)	36mm	250	2252	2812	2995	3117	3174	3189	1.2	6547
		500	2301	2767	2906	3004	3034	3027	1.3	6547
		750	2345	2746	2875	2963	2983	2960	1.4	6547
		1000	2383	2735	2859	2941	2956	2925	1.4	6547
	50mm	250	2352	3007	3300	3534	3652	3692	1.3	7056
		500	2404	2961	3204	3408	3506	3519	1.4	7056
		750	2452	2937	3169	3363	3450	3449	1.4	7056
		1000	2494	2925	3152	3339	3421	3415	1.4	7056
	75mm	250	2612	3502	4054	4566	4900	4988	1.4	8375
		500	2669	3454	3954	4418	4713	4788	1.5	8375
		750	2725	3423	3909	4358	4642	4707	1.5	8375
		1000	2776	3409	3886	4328	4605	4664	1.5	8375
	100mm	250	2968	4167	5053	5901	6565	6780	1.5	10222
		500	3037	4110	4938	5737	6355	6534	1.5	10222
		750	3100	4082	4894	5674	6269	6425	1.6	10222
		1000	3164	4062	4862	5632	6220	6368	1.6	10222
	125mm	250	3423	4983	6264	7503	8627	8971	1.5	12597
		500	3505	4920	6126	7308	8376	8681	1.6	12597
		750	3575	4896	6077	7237	8278	8563	1.6	12597
		1000	3650	4866	6050	7199	8228	8500	1.6	12597
	150mm	250	3967	5942	7656	9331	10984	11562	1.5	15500
		500	4069	5867	7492	9099	10697	11214	1.6	15500
		750	4138	5841	7435	9014	10587	11072	1.6	15500
		1000	4226	5817	7406	8969	10528	10997	1.6	15500

Initial Pt Force 0.1f_{yield}		Axial Load (excluding PT) 4000kN			Cantilever Length (3000mm)			Grade 300 Dissipaters		
	PT Dia.	Fuse Length (mm)	Yield (kNm)	1%drift (kNm)	2%drift (kNm)	3%drift (kNm)	4%drift (kNm)	6%drift (kNm)	λ	Fuse Area (mm^2)
Diameter (800mm)	36mm	250	1699	2172	2248	2278	2288	2284	1.0	8414
		500	1790	2148	2198	2209	2196	2173	1.1	8414
		750	1825	2141	2185	2182	2162	2131	1.1	8414
		1000	1865	2132	2177	2169	2144	2107	1.1	8414
	50mm	250	1746	2254	2360	2430	2481	2518	1.0	8798
		500	1842	2227	2311	2360	2386	2405	1.1	8798
		750	1875	2219	2296	2330	2351	2361	1.1	8798
		1000	1919	2210	2292	2318	2333	2339	1.1	8798
	75mm	250	1874	2459	2644	2814	2957	3093	1.0	9795
		500	1972	2428	2598	2734	2852	2970	1.1	9795
		750	2008	2419	2582	2706	2817	2923	1.1	9795
		1000	2056	2408	2573	2688	2798	2899	1.1	9795
	100mm	250	2051	2739	3031	3312	3573	3836	1.1	11192
		500	2154	2702	2976	3220	3466	3694	1.1	11192
		750	2193	2692	2962	3193	3417	3643	1.1	11192
		1000	2247	2680	2954	3176	3398	3614	1.1	11192
	125mm	250	2278	3092	3510	3902	4304	4694	1.1	12987
		500	2387	3044	3441	3803	4175	4547	1.1	12987
		750	2431	3026	3419	3774	4129	4497	1.1	12987
		1000	2488	3015	3414	3769	4114	4458	1.1	12987
	150mm	250	2553	3496	4068	4578	5133	5661	1.1	15182
		500	2670	3446	3987	4479	4980	5487	1.1	15182
		750	2720	3425	3958	4448	4929	5423	1.1	15182
		1000	2778	3408	3940	4432	4922	5395	1.1	15182

Initial Pt Force 0.1Fyield		Axial Load (excluding PT) 4000kN			Cantilever Length (3000mm)			Grade 300 Dissipaters		
	PT Dia.	Fuse Length (mm)	Yield (kNm)	1%drift (kNm)	2%drift (kNm)	3%drift (kNm)	4%drift (kNm)	6%drift (kNm)	λ	Fuse Area (mm^2)
Diameter (1000mm)	36mm	250	2277	2873	3023	3109	3169	3173	1.1	8480
		500	2355	2843	2950	3002	3029	3001	1.2	8480
		750	2403	2828	2924	2958	2970	2934	1.2	8480
		1000	2447	2813	2903	2932	2940	2900	1.2	8480
	50mm	250	2349	3001	3215	3369	3499	3553	1.1	8927
		500	2430	2966	3139	3258	3359	3380	1.2	8927
		750	2477	2955	3113	3217	3298	3307	1.2	8927
		1000	2523	2939	3092	3188	3265	3269	1.3	8927
	75mm	250	2533	3323	3696	4016	4314	4509	1.2	10085
		500	2617	3287	3613	3895	4161	4326	1.3	10085
		750	2669	3276	3584	3852	4104	4253	1.3	10085
		1000	2721	3258	3567	3828	4071	4209	1.3	10085
	100mm	250	2786	3765	4336	4868	5379	5805	1.2	11707
		500	2877	3721	4244	4732	5207	5598	1.3	11707
		750	2934	3709	4210	4683	5143	5516	1.3	11707
		1000	2995	3692	4193	4658	5110	5473	1.4	11707
	125mm	250	3105	4312	5109	5885	6647	7389	1.3	13792
		500	3209	4262	5005	5739	6452	7161	1.3	13792
		750	3273	4244	4976	5684	6379	7072	1.4	13792
		1000	3339	4233	4962	5647	6340	7025	1.4	13792
	150mm	250	3495	4964	6008	7058	8087	9101	1.3	16341
		500	3608	4893	5893	6870	7849	8822	1.3	16341
		750	3678	4872	5850	6806	7765	8720	1.4	16341
		1000	3753	4863	5841	6785	7717	8661	1.4	16341

Initial Pt Force 0.1f_{yield}		Axial Load (excluding PT) 4000kN			Cantilever Length (3000mm)			Grade 300 Dissipaters		
	PT Dia.	Fuse Length (mm)	Yield (kNm)	1%drift (kNm)	2%drift (kNm)	3%drift (kNm)	4%drift (kNm)	6%drift (kNm)	λ	Fuse Area (mm^2)
Diameter (1200mm)	36mm	250	2871	3611	3829	3973	4024	4020	1.2	8547
		500	2948	3561	3721	3815	3843	3811	1.3	8547
		750	3005	3533	3677	3758	3773	3731	1.3	8547
		1000	3055	3517	3654	3728	3737	3689	1.3	8547
	50mm	250	2967	3799	4119	4376	4507	4517	1.2	9056
		500	3048	3748	4011	4210	4310	4305	1.3	9056
		750	3107	3719	3963	4147	4234	4218	1.4	9056
		1000	3162	3702	3938	4115	4195	4173	1.4	9056
	75mm	250	3218	4277	4850	5364	5729	5829	1.3	10375
		500	3306	4216	4730	5193	5507	5569	1.4	10375
		750	3369	4189	4682	5121	5414	5464	1.4	10375
		1000	3432	4169	4652	5081	5366	5408	1.5	10375
	100mm	250	3564	4920	5823	6669	7367	7580	1.4	12222
		500	3666	4852	5686	6474	7119	7294	1.5	12222
		750	3731	4832	5638	6404	7023	7171	1.5	12222
		1000	3802	4804	5606	6361	6966	7100	1.5	12222
	125mm	250	4005	5713	7007	8243	9409	9752	1.4	14597
		500	4120	5645	6849	8018	9119	9416	1.5	14597
		750	4189	5619	6793	7937	9008	9281	1.5	14597
		1000	4273	5596	6766	7893	8950	9208	1.6	14597
	150mm	250	4536	6658	8367	10044	11687	12322	1.4	17500
		500	4665	6569	8192	9784	11364	11930	1.5	17500
		750	4742	6542	8129	9687	11239	11771	1.6	17500
		1000	4839	6521	8090	9639	11174	11687	1.6	17500

Initial Pt Force 0.1F_{yield}		Axial Load (excluding PT) 5000kN			Cantilever Length (3000mm)			Grade 300 Dissipaters		
	PT Dia.	Fuse Length (mm)	Yield (kNm)	1%drift (kNm)	2%drift (kNm)	3%drift (kNm)	4%drift (kNm)	6%drift (kNm)	λ	Fuse Area (mm^2)
Diameter (800mm)	36mm	250	2044	2645	2722	2752	2755	2739	1.0	10414
		500	2158	2611	2668	2666	2643	2604	1.0	10414
		750	2206	2599	2650	2638	2602	2553	1.0	10414
		1000	2256	2591	2645	2620	2581	2527	1.1	10414
	50mm	250	2091	2723	2829	2900	2938	2964	1.0	10798
		500	2208	2685	2775	2809	2823	2826	1.0	10798
		750	2256	2675	2759	2778	2782	2773	1.1	10798
		1000	2308	2666	2749	2765	2761	2746	1.1	10798
	75mm	250	2215	2922	3104	3264	3394	3520	1.0	11795
		500	2336	2879	3051	3166	3273	3370	1.1	11795
		750	2387	2867	3033	3133	3228	3315	1.1	11795
		1000	2442	2856	3020	3123	3209	3286	1.1	11795
	100mm	250	2391	3190	3483	3743	3998	4229	1.0	13192
		500	2517	3143	3420	3636	3858	4073	1.1	13192
		750	2571	3126	3398	3604	3810	4013	1.1	13192
		1000	2626	3115	3386	3596	3792	3979	1.1	13192
	125mm	250	2613	3523	3954	4320	4702	5073	1.0	14987
		500	2747	3476	3873	4217	4553	4903	1.1	14987
		750	2803	3453	3842	4183	4501	4838	1.1	14987
		1000	2863	3436	3828	4162	4477	4800	1.1	14987
	150mm	250	2887	3914	4501	4994	5496	6021	1.0	17182
		500	3026	3871	4399	4874	5339	5823	1.1	17182
		750	3088	3837	4361	4831	5290	5751	1.1	17182
		1000	3148	3819	4349	4813	5265	5719	1.1	17182

Initial Pt Force 0.1F_{yield}		Axial Load (excluding PT) 5000kN			Cantilever Length (3000mm)			Grade 300 Dissipaters		
	PT Dia.	Fuse Length (mm)	Yield (kNm)	1%drift (kNm)	2%drift (kNm)	3%drift (kNm)	4%drift (kNm)	6%drift (kNm)	λ	Fuse Area (mm^2)
Diameter (1000mm)	36mm	250	2737	3496	3668	3758	3815	3822	1.1	10480
		500	2846	3455	3580	3629	3651	3628	1.2	10480
		750	2905	3444	3550	3583	3587	3541	1.2	10480
		1000	2961	3428	3531	3553	3546	3495	1.2	10480
	50mm	250	2804	3619	3851	4009	4134	4191	1.1	10927
		500	2918	3576	3761	3876	3965	3991	1.2	10927
		750	2979	3565	3730	3828	3901	3909	1.2	10927
		1000	3034	3549	3714	3801	3862	3859	1.2	10927
	75mm	250	2983	3932	4314	4635	4926	5133	1.2	12085
		500	3100	3886	4215	4492	4745	4916	1.2	12085
		750	3166	3870	4182	4441	4676	4831	1.3	12085
		1000	3227	3859	4169	4414	4641	4785	1.3	12085
	100mm	250	3231	4362	4932	5464	5965	6412	1.2	13707
		500	3354	4307	4829	5306	5765	6172	1.3	13707
		750	3424	4289	4795	5250	5691	6078	1.3	13707
		1000	3492	4280	4776	5221	5651	6028	1.3	13707
	125mm	250	3546	4899	5692	6466	7213	7934	1.2	15792
		500	3673	4831	5569	6281	6985	7674	1.3	15792
		750	3754	4811	5535	6218	6901	7572	1.3	15792
		1000	3829	4802	5519	6188	6859	7519	1.3	15792
	150mm	250	3932	5533	6558	7595	8611	9621	1.2	18341
		500	4064	5454	6445	7408	8354	9308	1.3	18341
		750	4154	5431	6398	7337	8260	9193	1.3	18341
		1000	4233	5414	6377	7295	8216	9139	1.3	18341

Initial Pt Force 0.1F_{yield}		Axial Load (excluding PT) 5000kN			Cantilever Length (3000mm)			Grade 300 Dissipaters		
	PT Dia.	Fuse Length (mm)	Yield (kNm)	1%drift (kNm)	2%drift (kNm)	3%drift (kNm)	4%drift (kNm)	6%drift (kNm)	λ	Fuse Area (mm^2)
Diameter (1200mm)	36mm	250	3461	4392	4646	4807	4882	4857	1.2	10547
		500	3575	4336	4522	4622	4647	4604	1.3	10547
		750	3637	4309	4471	4547	4557	4501	1.3	10547
		1000	3699	4286	4441	4509	4510	4446	1.3	10547
	50mm	250	3555	4573	4928	5192	5357	5365	1.2	11056
		500	3672	4514	4799	5008	5110	5093	1.3	11056
		750	3737	4488	4749	4927	5014	4983	1.3	11056
		1000	3802	4463	4717	4886	4963	4925	1.3	11056
	75mm	250	3798	5037	5637	6156	6543	6652	1.3	12375
		500	3923	4971	5496	5955	6288	6349	1.4	12375
		750	3989	4947	5447	5880	6183	6219	1.4	12375
		1000	4062	4918	5413	5831	6123	6150	1.4	12375
	100mm	250	4137	5661	6586	7433	8162	8374	1.3	14222
		500	4269	5587	6429	7210	7876	8043	1.4	14222
		750	4342	5567	6374	7127	7765	7908	1.4	14222
		1000	4426	5539	6346	7084	7708	7830	1.5	14222
	125mm	250	4571	6444	7745	8980	10182	10526	1.4	16597
		500	4709	6364	7568	8727	9858	10148	1.4	16597
		750	4790	6337	7505	8633	9732	9994	1.5	16597
		1000	4885	6316	7474	8585	9667	9913	1.5	16597
	150mm	250	5096	7369	9089	10755	12388	13077	1.4	19500
		500	5246	7275	8881	10465	12030	12642	1.5	19500
		750	5331	7238	8817	10360	11892	12467	1.5	19500
		1000	5435	7229	8785	10305	11820	12372	1.5	19500

Initial Pt Force 0.1f_{yield}		Axial Load (excluding PT) 1000kN			Cantilever Length (4000mm)			Grade 300 Dissipaters		
	PT Dia.	Fuse Length (mm)	Yield (kNm)	1%drift (kNm)	2%drift (kNm)	3%drift (kNm)	4%drift (kNm)	6%drift (kNm)	λ	Fuse Area (mm^2)
Diameter (800mm)	36mm	250	500	616	649	669	684	696	1.2	2106
		500	517	607	633	648	659	669	1.3	2106
		750	527	604	627	640	651	659	1.3	2106
		1000	538	600	623	636	646	654	1.3	2106
	50mm	250	546	696	765	825	878	927	1.3	2411
		500	566	687	748	799	847	893	1.4	2411
		750	578	682	740	789	836	881	1.4	2411
		1000	591	679	736	784	830	874	1.4	2411
	75mm	250	665	893	1046	1189	1330	1467	1.4	3202
		500	691	886	1027	1162	1295	1426	1.5	3202
		750	706	880	1018	1151	1280	1409	1.5	3202
		1000	725	875	1012	1143	1271	1398	1.5	3202
	100mm	250	829	1155	1408	1652	1893	2132	1.4	4310
		500	861	1147	1381	1617	1848	2079	1.5	4310
		750	880	1141	1374	1605	1832	2059	1.5	4310
		1000	907	1134	1371	1598	1824	2049	1.5	4310
	125mm	250	1035	1476	1832	2187	2540	2892	1.4	5734
		500	1073	1460	1803	2141	2485	2822	1.5	5734
		750	1095	1455	1796	2127	2462	2799	1.5	5734
		1000	1129	1448	1793	2118	2458	2784	1.5	5734
	150mm	250	1276	1847	2307	2780	3254	3725	1.4	7475
		500	1326	1822	2280	2726	3191	3636	1.4	7475
		750	1347	1815	2266	2708	3156	3607	1.5	7475
		1000	1390	1807	2265	2702	3141	3588	1.5	7475

Initial Pt Force 0.1F_{yield}		Axial Load (excluding PT) 1000kN			Cantilever Length (4000mm)			Grade 300 Dissipaters		
	PT Dia.	Fuse Length (mm)	Yield (kNm)	1%drift (kNm)	2%drift (kNm)	3%drift (kNm)	4%drift (kNm)	6%drift (kNm)	λ	Fuse Area (mm^2)
Diameter (1000mm)	36mm	250	665	823	884	934	987	1022	1.4	2155
		500	679	810	864	908	951	980	1.5	2155
		750	693	806	857	899	938	963	1.5	2155
		1000	705	800	853	894	933	954	1.5	2155
	50mm	250	733	949	1071	1182	1289	1386	1.5	2506
		500	748	932	1046	1150	1251	1338	1.6	2506
		750	765	927	1037	1139	1238	1321	1.6	2506
		1000	780	922	1033	1133	1230	1312	1.7	2506
	75mm	250	904	1257	1527	1788	2044	2294	1.6	3417
		500	925	1238	1494	1740	1984	2226	1.7	3417
		750	949	1229	1480	1722	1961	2200	1.8	3417
		1000	971	1226	1473	1712	1950	2186	1.8	3417
	100mm	250	1137	1660	2110	2548	2982	3411	1.7	4691
		500	1166	1643	2071	2493	2912	3330	1.8	4691
		750	1198	1631	2056	2473	2886	3298	1.8	4691
		1000	1229	1624	2044	2457	2869	3279	1.8	4691
	125mm	250	1430	2149	2802	3443	4078	4706	1.7	6330
		500	1469	2130	2752	3371	3987	4602	1.8	6330
		750	1508	2118	2734	3345	3954	4560	1.8	6330
		1000	1550	2109	2725	3331	3936	4539	1.8	6330
	150mm	250	1780	2715	3586	4441	5292	6145	1.6	8333
		500	1827	2689	3515	4351	5183	6011	1.7	8333
		750	1870	2682	3502	4314	5141	5958	1.7	8333
		1000	1922	2667	3488	4301	5117	5931	1.8	8333

Initial Pt Force $0.1f_{yield}$		Axial Load (excluding PT) 1000kN			Cantilever Length (4000mm)			Grade 300 Dissipaters		
	PT Dia.	Fuse Length (mm)	Yield (kNm)	1%drift (kNm)	2%drift (kNm)	3%drift (kNm)	4%drift (kNm)	6%drift (kNm)	λ	Fuse Area (mm^2)
Diameter (1200mm)	36mm	250	836	1039	1140	1238	1317	1325	1.5	2205
		500	849	1024	1114	1198	1268	1269	1.6	2205
		750	864	1018	1105	1184	1249	1246	1.7	2205
		1000	877	1013	1101	1178	1238	1233	1.7	2205
	50mm	250	928	1218	1410	1596	1769	1802	1.6	2602
		500	942	1199	1379	1551	1712	1737	1.8	2602
		750	962	1192	1368	1536	1690	1710	1.8	2602
		1000	979	1186	1362	1528	1679	1696	1.8	2602
	75mm	250	1160	1664	2080	2482	2877	3003	1.8	3631
		500	1180	1636	2032	2419	2804	2916	1.9	3631
		750	1208	1625	2015	2396	2776	2882	2.0	3631
		1000	1235	1619	2006	2385	2762	2864	2.0	3631
	100mm	250	1475	2251	2948	3633	4311	4653	1.9	5073
		500	1503	2216	2888	3551	4209	4526	2.0	5073
		750	1542	2199	2861	3513	4163	4474	2.0	5073
		1000	1583	2192	2847	3494	4139	4446	2.1	5073
	125mm	250	1868	2957	3979	4985	5981	6665	1.9	6926
		500	1906	2919	3902	4878	5849	6506	2.0	6926
		750	1959	2899	3876	4837	5797	6441	2.0	6926
		1000	2012	2886	3854	4815	5770	6407	2.1	6926
	150mm	250	2338	3771	5152	6512	7859	9026	1.8	9192
		500	2389	3729	5054	6373	7689	8821	1.9	9192
		750	2451	3713	5020	6323	7624	8737	2.0	9192
		1000	2518	3690	5003	6297	7589	8694	2.0	9192

Initial Pt Force $0.1f_{yield}$		Axial Load (excluding PT) 2000kN			Cantilever Length (4000mm)			Grade 300 Dissipaters		
	PT Dia.	Fuse Length (mm)	Yield (kNm)	1%drift (kNm)	2%drift (kNm)	3%drift (kNm)	4%drift (kNm)	6%drift (kNm)	λ	Fuse Area (mm^2)
Diameter (800mm)	36mm	250	871	1082	1111	1117	1114	1105	1.1	3884
		500	911	1072	1088	1083	1070	1049	1.2	3884
		750	928	1067	1079	1069	1049	1026	1.2	3884
		1000	949	1061	1072	1060	1039	1014	1.2	3884
	50mm	250	913	1153	1216	1256	1288	1314	1.1	4189
		500	956	1144	1190	1220	1241	1259	1.2	4189
		750	974	1138	1183	1207	1223	1235	1.2	4189
		1000	997	1133	1175	1197	1210	1220	1.2	4189
	75mm	250	1024	1338	1475	1596	1709	1818	1.2	4980
		500	1073	1326	1446	1554	1656	1755	1.3	4980
		750	1091	1322	1438	1540	1637	1731	1.3	4980
		1000	1119	1314	1432	1532	1627	1719	1.3	4980
	100mm	250	1176	1584	1813	2030	2249	2455	1.2	6087
		500	1231	1570	1779	1982	2181	2381	1.3	6087
		750	1254	1564	1771	1966	2159	2353	1.3	6087
		1000	1288	1555	1766	1956	2152	2338	1.3	6087
	125mm	250	1369	1891	2218	2549	2868	3187	1.2	7512
		500	1433	1866	2185	2485	2795	3100	1.3	7512
		750	1459	1859	2171	2466	2774	3069	1.3	7512
		1000	1497	1851	2169	2465	2754	3050	1.3	7512
	150mm	250	1602	2252	2688	3115	3568	3995	1.2	9252
		500	1677	2216	2643	3053	3470	3892	1.3	9252
		750	1704	2204	2632	3035	3440	3855	1.3	9252
		1000	1750	2196	2620	3027	3428	3832	1.3	9252

Initial Pt Force 0.1f_{yield}		Axial Load (excluding PT) 2000kN			Cantilever Length (4000mm)			Grade 300 Dissipaters		
	PT Dia.	Fuse Length (mm)	Yield (kNm)	1%drift (kNm)	2%drift (kNm)	3%drift (kNm)	4%drift (kNm)	6%drift (kNm)	λ	Fuse Area (mm^2)
Diameter (1000mm)	36mm	250	1165	1444	1514	1556	1578	1591	1.3	3933
		500	1200	1428	1477	1499	1513	1520	1.3	3933
		750	1226	1417	1461	1479	1489	1492	1.4	3933
		1000	1248	1411	1452	1468	1476	1477	1.4	3933
	50mm	250	1228	1559	1686	1788	1876	1952	1.3	4284
		500	1265	1541	1648	1729	1802	1870	1.4	4284
		750	1293	1529	1629	1705	1774	1839	1.4	4284
		1000	1318	1523	1620	1693	1760	1822	1.5	4284
	75mm	250	1388	1844	2110	2352	2585	2811	1.4	5194
		500	1431	1824	2067	2289	2506	2719	1.5	5194
		750	1463	1815	2050	2265	2472	2678	1.5	5194
		1000	1494	1805	2037	2248	2452	2655	1.6	5194
	100mm	250	1609	2227	2666	3084	3492	3894	1.5	6469
		500	1659	2204	2614	3008	3398	3784	1.6	6469
		750	1696	2196	2596	2981	3362	3740	1.6	6469
		1000	1735	2184	2585	2967	3343	3717	1.6	6469
	125mm	250	1886	2698	3334	3951	4560	5161	1.5	8108
		500	1947	2672	3271	3859	4445	5027	1.6	8108
		750	1989	2661	3244	3827	4402	4975	1.6	8108
		1000	2034	2651	3237	3810	4380	4947	1.6	8108
	150mm	250	2220	3248	4084	4923	5748	6562	1.5	10111
		500	2289	3212	4016	4813	5610	6400	1.6	10111
		750	2337	3199	3989	4781	5560	6339	1.6	10111
		1000	2393	3192	3986	4753	5530	6310	1.6	10111

Initial Pt Force 0.1F_{yield}		Axial Load (excluding PT) 2000kN			Cantilever Length (4000mm)			Grade 300 Dissipaters		
	PT Dia.	Fuse Length (mm)	Yield (kNm)	1%drift (kNm)	2%drift (kNm)	3%drift (kNm)	4%drift (kNm)	6%drift (kNm)	λ	Fuse Area (mm^2)
Diameter (1200mm)	36mm	250	1582	1960	2082	2166	2245	2246	1.1	4729
		500	1611	1926	2019	2086	2144	2129	1.2	4729
		750	1640	1912	1997	2057	2107	2080	1.3	4729
		1000	1664	1904	1986	2042	2088	2055	1.3	4729
	50mm	250	1676	2139	2356	2531	2691	2726	1.2	5200
		500	1709	2103	2284	2439	2586	2599	1.3	5200
		750	1741	2087	2259	2406	2546	2548	1.3	5200
		1000	1769	2077	2246	2389	2524	2522	1.3	5200
	75mm	250	1921	2588	3023	3430	3824	3965	1.3	6423
		500	1960	2551	2946	3317	3680	3808	1.4	6423
		750	1998	2529	2912	3272	3625	3745	1.4	6423
		1000	2035	2516	2894	3248	3596	3711	1.5	6423
	100mm	250	2260	3190	3902	4586	5256	5644	1.4	8135
		500	2306	3144	3811	4457	5096	5454	1.5	8135
		750	2352	3123	3778	4409	5034	5373	1.5	8135
		1000	2401	3108	3752	4376	4994	5326	1.5	8135
	125mm	250	2688	3926	4963	5969	6959	7705	1.4	10336
		500	2745	3874	4851	5811	6763	7469	1.5	10336
		750	2796	3855	4812	5752	6687	7374	1.5	10336
		1000	2855	3835	4792	5722	6648	7323	1.6	10336
	150mm	250	3196	4786	6175	7542	8886	10129	1.4	13027
		500	3273	4724	6045	7348	8646	9841	1.5	13027
		750	3323	4704	5998	7276	8554	9725	1.5	13027
		1000	3391	4686	5968	7241	8506	9662	1.6	13027

Initial Pt Force $0.1f_{yield}$		Axial Load (excluding PT) 2000kN			Cantilever Length (4000mm)			Grade 300 Dissipaters		
	PT Dia.	Fuse Length (mm)	Yield (kNm)	1%drift (kNm)	2%drift (kNm)	3%drift (kNm)	4%drift (kNm)	6%drift (kNm)	λ	Fuse Area (mm^2)
Diameter (1500mm)	36mm	250	2096	2583	2787	2975	3030	3051	1.2	4817
		500	2115	2534	2704	2854	2884	2890	1.3	4817
		750	2145	2517	2674	2808	2824	2819	1.4	4817
		1000	2172	2507	2659	2786	2792	2780	1.4	4817
	50mm	250	2237	2867	3219	3550	3668	3725	1.3	5370
		500	2257	2810	3125	3417	3506	3547	1.4	5370
		750	2292	2790	3091	3370	3440	3469	1.5	5370
		1000	2325	2781	3074	3345	3405	3426	1.5	5370
	75mm	250	2598	3582	4305	4988	5290	5442	1.5	6806
		500	2623	3510	4180	4827	5089	5220	1.6	6806
		750	2667	3483	4136	4767	5012	5123	1.6	6806
		1000	2712	3470	4112	4735	4971	5070	1.6	6806
	100mm	250	3091	4537	5745	6917	7529	7780	1.5	8815
		500	3127	4455	5588	6698	7269	7506	1.7	8815
		750	3183	4416	5525	6613	7165	7386	1.7	8815
		1000	3245	4397	5493	6569	7110	7322	1.7	8815
	125mm	250	3716	5711	7478	9207	10320	10767	1.6	11399
		500	3763	5614	7292	8950	10000	10401	1.7	11399
		750	3833	5567	7222	8853	9864	10236	1.8	11399
		1000	3912	5539	7175	8789	9788	10148	1.8	11399
	150mm	250	4468	7079	9477	11832	13607	14258	1.6	14556
		500	4529	6960	9248	11516	13208	13810	1.7	14556
		750	4610	6919	9167	11396	13047	13616	1.8	14556
		1000	4707	6876	9125	11334	12962	13511	1.8	14556

Initial Pt Force 0.1F_{yield}		Axial Load (excluding PT) 3000kN			Cantilever Length (4000mm)			Grade 300 Dissipaters		
	PT Dia.	Fuse Length (mm)	Yield (kNm)	1%drift (kNm)	2%drift (kNm)	3%drift (kNm)	4%drift (kNm)	6%drift (kNm)	λ	Fuse Area (mm^2)
Diameter (800mm)	36mm	250	1134	1442	1462	1449	1420	1382	1.2	4954
		500	1203	1429	1433	1407	1366	1317	1.3	4954
		750	1229	1424	1426	1392	1345	1292	1.3	4954
		1000	1260	1419	1421	1385	1334	1276	1.3	4954
	50mm	250	1172	1506	1555	1573	1578	1574	1.2	5221
		500	1243	1491	1524	1529	1522	1507	1.3	5221
		750	1270	1487	1517	1515	1501	1481	1.3	5221
		1000	1302	1481	1513	1506	1490	1468	1.3	5221
	75mm	250	1268	1670	1784	1883	1964	2042	1.3	5913
		500	1344	1651	1753	1832	1902	1968	1.3	5913
		750	1374	1646	1745	1815	1880	1939	1.4	5913
		1000	1409	1639	1740	1810	1869	1925	1.4	5913
	100mm	250	1402	1890	2088	2279	2465	2633	1.3	6882
		500	1482	1867	2060	2226	2389	2551	1.4	6882
		750	1515	1860	2047	2205	2365	2521	1.4	6882
		1000	1555	1853	2044	2203	2357	2503	1.4	6882
	125mm	250	1573	2163	2465	2756	3041	3327	1.3	8128
		500	1661	2132	2425	2692	2963	3239	1.4	8128
		750	1699	2123	2415	2679	2940	3194	1.4	8128
		1000	1741	2117	2405	2671	2919	3179	1.4	8128
	150mm	250	1781	2477	2907	3286	3696	4098	1.3	9651
		500	1877	2445	2852	3222	3594	3977	1.4	9651
		750	1919	2431	2834	3209	3570	3938	1.4	9651
		1000	1966	2420	2825	3191	3557	3929	1.4	9651

Initial Pt Force 0.1f_{yield}		Axial Load (excluding PT) 3000kN			Cantilever Length (4000mm)			Grade 300 Dissipaters		
	PT Dia.	Fuse Length (mm)	Yield (kNm)	1%drift (kNm)	2%drift (kNm)	3%drift (kNm)	4%drift (kNm)	6%drift (kNm)	λ	Fuse Area (mm^2)
Diameter (1000mm)	36mm	250	1538	1934	2003	2029	2037	2030	1.4	4997
		500	1600	1913	1960	1966	1953	1931	1.5	4997
		750	1637	1905	1943	1938	1919	1892	1.5	4997
		1000	1670	1896	1931	1923	1901	1872	1.5	4997
	50mm	250	1592	2034	2158	2240	2306	2363	1.4	5304
		500	1657	2014	2113	2174	2223	2261	1.5	5304
		750	1695	2005	2097	2149	2186	2218	1.5	5304
		1000	1729	1995	2084	2132	2166	2195	1.6	5304
	75mm	250	1730	2289	2545	2763	2967	3162	1.5	6101
		500	1801	2268	2494	2690	2875	3055	1.6	6101
		750	1844	2259	2477	2664	2840	3012	1.6	6101
		1000	1883	2250	2466	2649	2821	2987	1.6	6101
	100mm	250	1922	2635	3053	3445	3822	4190	1.6	7216
		500	1999	2609	2998	3362	3717	4067	1.7	7216
		750	2048	2602	2979	3332	3677	4019	1.7	7216
		1000	2095	2591	2967	3316	3657	3994	1.7	7216
	125mm	250	2162	3063	3666	4260	4832	5397	1.6	8650
		500	2251	3032	3603	4163	4710	5256	1.7	8650
		750	2307	3021	3580	4121	4664	5201	1.7	8650
		1000	2361	3015	3570	4106	4640	5171	1.7	8650
	150mm	250	2456	3566	4365	5170	5959	6735	1.6	10403
		500	2550	3525	4300	5058	5817	6570	1.7	10403
		750	2616	3512	4278	5025	5766	6507	1.7	10403
		1000	2679	3506	4267	4996	5736	6488	1.7	10403

Initial Pt Force 0.1F_{yield}		Axial Load (excluding PT) 3000kN			Cantilever Length (4000mm)			Grade 300 Dissipaters		
	PT Dia.	Fuse Length (mm)	Yield (kNm)	1%drift (kNm)	2%drift (kNm)	3%drift (kNm)	4%drift (kNm)	6%drift (kNm)	λ	Fuse Area (mm^2)
Diameter (1200mm)	36mm	250	2218	2770	2920	3016	3071	3051	1.1	6840
		500	2274	2732	2836	2889	2925	2888	1.2	6840
		750	2315	2709	2800	2842	2869	2823	1.2	6840
		1000	2351	2696	2782	2819	2840	2789	1.2	6840
	50mm	250	2309	2937	3176	3362	3516	3532	1.1	7312
		500	2368	2898	3090	3231	3355	3358	1.2	7312
		750	2411	2876	3051	3179	3294	3287	1.2	7312
		1000	2449	2862	3031	3153	3262	3249	1.3	7312
	75mm	250	2544	3368	3816	4217	4596	4771	1.2	8534
		500	2611	3320	3718	4077	4424	4559	1.3	8534
		750	2657	3299	3682	4021	4347	4470	1.3	8534
		1000	2702	3283	3656	3988	4306	4423	1.3	8534
	100mm	250	2867	3947	4667	5341	5994	6410	1.3	10246
		500	2946	3893	4553	5179	5794	6173	1.4	10246
		750	2993	3878	4514	5120	5717	6076	1.4	10246
		1000	3050	3855	4490	5090	5676	6023	1.4	10246
	125mm	250	3279	4664	5699	6693	7666	8447	1.3	12447
		500	3369	4603	5566	6503	7430	8166	1.4	12447
		750	3419	4582	5519	6434	7339	8052	1.4	12447
		1000	3486	4564	5496	6398	7292	7991	1.4	12447
	150mm	250	3776	5506	6890	8236	9562	10849	1.3	15138
		500	3876	5432	6729	8012	9284	10514	1.4	15138
		750	3933	5410	6679	7931	9178	10381	1.4	15138
		1000	4008	5396	6654	7889	9123	10309	1.5	15138

Initial Pt Force $0.1F_{yield}$		Axial Load (excluding PT) 3000kN			Cantilever Length (4000mm)			Grade 300 Dissipaters		
	PT Dia.	Fuse Length (mm)	Yield (kNm)	1%drift (kNm)	2%drift (kNm)	3%drift (kNm)	4%drift (kNm)	6%drift (kNm)	Lambda	Fuse Area (mm^2)
Diameter (1500mm)	36mm	250	2944	3656	3893	4071	4139	4155	1.2	6929
		500	2988	3585	3767	3904	3932	3926	1.3	6929
		750	3033	3558	3722	3842	3847	3825	1.3	6929
		1000	3075	3545	3699	3810	3803	3770	1.3	6929
	50mm	250	3079	3928	4314	4633	4766	4818	1.2	7482
		500	3125	3852	4176	4455	4544	4573	1.3	7482
		750	3174	3822	4127	4388	4454	4465	1.4	7482
		1000	3220	3808	4101	4353	4409	4406	1.4	7482
	75mm	250	3424	4614	5371	6060	6371	6511	1.3	8917
		500	3478	4531	5206	5839	6116	6223	1.5	8917
		750	3536	4495	5144	5756	6013	6098	1.5	8917
		1000	3593	4473	5112	5712	5958	6034	1.5	8917
	100mm	250	3905	5540	6765	7936	8608	8854	1.4	10926
		500	3967	5447	6583	7684	8282	8503	1.5	10926
		750	4035	5404	6507	7574	8149	8351	1.6	10926
		1000	4106	5374	6464	7517	8079	8269	1.6	10926
	125mm	250	4510	6686	8465	10189	11357	11800	1.5	13510
		500	4590	6571	8247	9888	10979	11379	1.6	13510
		750	4666	6529	8169	9774	10828	11186	1.6	13510
		1000	4756	6491	8120	9710	10740	11078	1.7	13510
	150mm	250	5237	8025	10434	12782	14620	15266	1.5	16667
		500	5341	7892	10172	12421	14165	14756	1.6	16667
		750	5427	7845	10080	12284	13982	14536	1.7	16667
		1000	5522	7805	10032	12214	13885	14416	1.7	16667

Initial Pt Force 0.1F_{yield}		Axial Load (excluding PT) 4000kN			Cantilever Length (4000mm)			Grade 300 Dissipaters		
	PT Dia.	Fuse Length (mm)	Yield (kNm)	1%drift (kNm)	2%drift (kNm)	3%drift (kNm)	4%drift (kNm)	6%drift (kNm)	λ	Fuse Area (mm^2)
Diameter (800mm)	36mm	250	1699	2172	2248	2278	2288	2284	1.0	8414
		500	1790	2148	2198	2209	2196	2173	1.1	8414
		750	1825	2141	2185	2182	2162	2131	1.1	8414
		1000	1865	2132	2177	2169	2144	2107	1.1	8414
	50mm	250	1746	2254	2360	2430	2481	2518	1.0	8798
		500	1842	2227	2311	2360	2386	2405	1.1	8798
		750	1875	2219	2296	2330	2351	2361	1.1	8798
		1000	1919	2210	2292	2318	2333	2339	1.1	8798
	75mm	250	1874	2459	2644	2814	2957	3093	1.0	9795
		500	1972	2428	2598	2734	2852	2970	1.1	9795
		750	2008	2419	2582	2706	2817	2923	1.1	9795
		1000	2056	2408	2573	2688	2798	2899	1.1	9795
	100mm	250	2051	2739	3031	3312	3573	3836	1.1	11192
		500	2154	2702	2976	3220	3466	3694	1.1	11192
		750	2193	2692	2962	3193	3417	3643	1.1	11192
		1000	2247	2680	2954	3176	3398	3614	1.1	11192
	125mm	250	2278	3092	3510	3902	4304	4694	1.1	12987
		500	2387	3044	3441	3803	4175	4547	1.1	12987
		750	2431	3026	3419	3774	4129	4497	1.1	12987
		1000	2488	3015	3414	3769	4114	4458	1.1	12987
	150mm	250	2553	3496	4068	4578	5133	5661	1.1	15182
		500	2670	3446	3987	4479	4980	5487	1.1	15182
		750	2720	3425	3958	4448	4929	5423	1.1	15182
		1000	2778	3408	3940	4432	4922	5395	1.1	15182

Initial Pt Force 0.1f_{yield}		Axial Load (excluding PT) 4000kN			Cantilever Length (4000mm)			Grade 300 Dissipaters		
	PT Dia.	Fuse Length (mm)	Yield (kNm)	1%drift (kNm)	2%drift (kNm)	3%drift (kNm)	4%drift (kNm)	6%drift (kNm)	λ	Fuse Area (mm^2)
Diameter (1000mm)	36mm	250	2277	2873	3023	3109	3169	3173	1.1	8480
		500	2355	2843	2950	3002	3029	3001	1.2	8480
		750	2403	2828	2924	2958	2970	2934	1.2	8480
		1000	2447	2813	2903	2932	2940	2900	1.2	8480
	50mm	250	2349	3001	3215	3369	3499	3553	1.1	8927
		500	2430	2966	3139	3258	3359	3380	1.2	8927
		750	2477	2955	3113	3217	3298	3307	1.2	8927
		1000	2523	2939	3092	3188	3265	3269	1.3	8927
	75mm	250	2533	3323	3696	4016	4314	4509	1.2	10085
		500	2617	3287	3613	3895	4161	4326	1.3	10085
		750	2669	3276	3584	3852	4104	4253	1.3	10085
		1000	2721	3258	3567	3828	4071	4209	1.3	10085
	100mm	250	2786	3765	4336	4868	5379	5805	1.2	11707
		500	2877	3721	4244	4732	5207	5598	1.3	11707
		750	2934	3709	4210	4683	5143	5516	1.3	11707
		1000	2995	3692	4193	4658	5110	5473	1.4	11707
	125mm	250	3105	4312	5109	5885	6647	7389	1.3	13792
		500	3209	4262	5005	5739	6452	7161	1.3	13792
		750	3273	4244	4976	5684	6379	7072	1.4	13792
		1000	3339	4233	4962	5647	6340	7025	1.4	13792
	150mm	250	3495	4964	6008	7058	8087	9101	1.3	16341
		500	3608	4893	5893	6870	7849	8822	1.3	16341
		750	3678	4872	5850	6806	7765	8720	1.4	16341
		1000	3753	4863	5841	6785	7717	8661	1.4	16341

Initial Pt Force 0.1F_{yield}		Axial Load (excluding PT) 4000kN			Cantilever Length (4000mm)			Grade 300 Dissipaters		
	PT Dia.	Fuse Length (mm)	Yield (kNm)	1%drift (kNm)	2%drift (kNm)	3%drift (kNm)	4%drift (kNm)	6%drift (kNm)	λ	Fuse Area (mm^2)
Diameter (1200mm)	36mm	250	2871	3611	3829	3973	4024	4020	1.2	8547
		500	2948	3561	3721	3815	3843	3811	1.3	8547
		750	3005	3533	3677	3758	3773	3731	1.3	8547
		1000	3055	3517	3654	3728	3737	3689	1.3	8547
	50mm	250	2967	3799	4119	4376	4507	4517	1.2	9056
		500	3048	3748	4011	4210	4310	4305	1.3	9056
		750	3107	3719	3963	4147	4234	4218	1.4	9056
		1000	3162	3702	3938	4115	4195	4173	1.4	9056
	75mm	250	3218	4277	4850	5364	5729	5829	1.3	10375
		500	3306	4216	4730	5193	5507	5569	1.4	10375
		750	3369	4189	4682	5121	5414	5464	1.4	10375
		1000	3432	4169	4652	5081	5366	5408	1.5	10375
	100mm	250	3564	4920	5823	6669	7367	7580	1.4	12222
		500	3666	4852	5686	6474	7119	7294	1.5	12222
		750	3731	4832	5638	6404	7023	7171	1.5	12222
		1000	3802	4804	5606	6361	6966	7100	1.5	12222
	125mm	250	4005	5713	7007	8243	9409	9752	1.4	14597
		500	4120	5645	6849	8018	9119	9416	1.5	14597
		750	4189	5619	6793	7937	9008	9281	1.5	14597
		1000	4273	5596	6766	7893	8950	9208	1.6	14597
	150mm	250	4536	6658	8367	10044	11687	12322	1.4	17500
		500	4665	6569	8192	9784	11364	11930	1.5	17500
		750	4742	6542	8129	9687	11239	11771	1.6	17500
		1000	4839	6521	8090	9639	11174	11687	1.6	17500

Initial Pt Force 0.1f_{yield}		Axial Load (excluding PT) 4000kN			Cantilever Length (4000mm)			Grade 300 Dissipaters		
	PT Dia.	Fuse Length (mm)	Yield (kNm)	1%drift (kNm)	2%drift (kNm)	3%drift (kNm)	4%drift (kNm)	6%drift (kNm)	λ	Fuse Area (mm^2)
Diameter (1500mm)	36mm	250	3668	4594	4873	5042	5099	5103	1.2	8564
		500	3743	4517	4710	4835	4846	4823	1.3	8564
		750	3805	4481	4652	4756	4746	4700	1.3	8564
		1000	3862	4460	4622	4715	4694	4632	1.4	8564
	50mm	250	3793	4849	5271	5591	5709	5749	1.3	9088
		500	3874	4768	5102	5368	5447	5454	1.4	9088
		750	3936	4731	5040	5284	5343	5324	1.4	9088
		1000	3998	4708	5007	5240	5287	5255	1.4	9088
	75mm	250	4114	5497	6272	6970	7301	7402	1.4	10447
		500	4204	5408	6094	6710	6993	7073	1.5	10447
		750	4276	5368	6018	6610	6870	6931	1.5	10447
		1000	4348	5341	5979	6557	6804	6854	1.5	10447
	100mm	250	4558	6377	7613	8773	9472	9727	1.4	12351
		500	4666	6274	7409	8491	9120	9320	1.5	12351
		750	4745	6235	7334	8378	8966	9145	1.6	12351
		1000	4827	6200	7284	8311	8885	9050	1.6	12351
	125mm	250	5126	7466	9253	10963	12162	12591	1.5	14799
		500	5253	7351	9015	10634	11751	12131	1.6	14799
		750	5336	7307	8930	10510	11586	11931	1.6	14799
		1000	5428	7271	8886	10445	11498	11813	1.7	14799
	150mm	250	5805	8747	11155	13486	15359	15991	1.5	17790
		500	5962	8607	10878	13101	14876	15448	1.6	17790
		750	6042	8561	10780	12957	14682	15213	1.7	17790
		1000	6149	8526	10730	12881	14579	15087	1.7	17790

Initial Pt Force 0.1F_{yield}		Axial Load (excluding PT) 5000kN			Cantilever Length (4000mm)			Grade 300 Dissipaters		
	PT Dia.	Fuse Length (mm)	Yield (kNm)	1%drift (kNm)	2%drift (kNm)	3%drift (kNm)	4%drift (kNm)	6%drift (kNm)	λ	Fuse Area (mm^2)
Diameter (800mm)	36mm	250	2044	2645	2722	2752	2755	2739	1.0	10414
		500	2158	2611	2668	2666	2643	2604	1.0	10414
		750	2206	2599	2650	2638	2602	2553	1.0	10414
		1000	2256	2591	2645	2620	2581	2527	1.1	10414
	50mm	250	2091	2723	2829	2900	2938	2964	1.0	10798
		500	2208	2685	2775	2809	2823	2826	1.0	10798
		750	2256	2675	2759	2778	2782	2773	1.1	10798
		1000	2308	2666	2749	2765	2761	2746	1.1	10798
	75mm	250	2215	2922	3104	3264	3394	3520	1.0	11795
		500	2336	2879	3051	3166	3273	3370	1.1	11795
		750	2387	2867	3033	3133	3228	3315	1.1	11795
		1000	2442	2856	3020	3123	3209	3286	1.1	11795
	100mm	250	2391	3190	3483	3743	3998	4229	1.0	13192
		500	2517	3143	3420	3636	3858	4073	1.1	13192
		750	2571	3126	3398	3604	3810	4013	1.1	13192
		1000	2626	3115	3386	3596	3792	3979	1.1	13192
	125mm	250	2613	3523	3954	4320	4702	5073	1.0	14987
		500	2747	3476	3873	4217	4553	4903	1.1	14987
		750	2803	3453	3842	4183	4501	4838	1.1	14987
		1000	2863	3436	3828	4162	4477	4800	1.1	14987
	150mm	250	2887	3914	4501	4994	5496	6021	1.0	17182
		500	3026	3871	4399	4874	5339	5823	1.1	17182
		750	3088	3837	4361	4831	5290	5751	1.1	17182
		1000	3148	3819	4349	4813	5265	5719	1.1	17182

Initial Pt Force 0.1f_{yield}		Axial Load (excluding PT) 5000kN			Cantilever Length (4000mm)			Grade 300 Dissipaters		
	PT Dia.	Fuse Length (mm)	Yield (kNm)	1%drift (kNm)	2%drift (kNm)	3%drift (kNm)	4%drift (kNm)	6%drift (kNm)	λ	Fuse Area (mm^2)
Diameter (1000mm)	36mm	250	2737	3496	3668	3758	3815	3822	1.1	10480
		500	2846	3455	3580	3629	3651	3628	1.2	10480
		750	2905	3444	3550	3583	3587	3541	1.2	10480
		1000	2961	3428	3531	3553	3546	3495	1.2	10480
	50mm	250	2804	3619	3851	4009	4134	4191	1.1	10927
		500	2918	3576	3761	3876	3965	3991	1.2	10927
		750	2979	3565	3730	3828	3901	3909	1.2	10927
		1000	3034	3549	3714	3801	3862	3859	1.2	10927
	75mm	250	2983	3932	4314	4635	4926	5133	1.2	12085
		500	3100	3886	4215	4492	4745	4916	1.2	12085
		750	3166	3870	4182	4441	4676	4831	1.3	12085
		1000	3227	3859	4169	4414	4641	4785	1.3	12085
	100mm	250	3231	4362	4932	5464	5965	6412	1.2	13707
		500	3354	4307	4829	5306	5765	6172	1.3	13707
		750	3424	4289	4795	5250	5691	6078	1.3	13707
		1000	3492	4280	4776	5221	5651	6028	1.3	13707
	125mm	250	3546	4899	5692	6466	7213	7934	1.2	15792
		500	3673	4831	5569	6281	6985	7674	1.3	15792
		750	3754	4811	5535	6218	6901	7572	1.3	15792
		1000	3829	4802	5519	6188	6859	7519	1.3	15792
	150mm	250	3932	5533	6558	7595	8611	9621	1.2	18341
		500	4064	5454	6445	7408	8354	9308	1.3	18341
		750	4154	5431	6398	7337	8260	9193	1.3	18341
		1000	4233	5414	6377	7295	8216	9139	1.3	18341

Initial Pt Force 0.1F_{yield}		Axial Load (excluding PT) 5000kN			Cantilever Length (4000mm)			Grade 300 Dissipaters		
	PT Dia.	Fuse Length (mm)	Yield (kNm)	1%drift (kNm)	2%drift (kNm)	3%drift (kNm)	4%drift (kNm)	6%drift (kNm)	λ	Fuse Area (mm^2)
Diameter (1200mm)	36mm	250	3461	4392	4646	4807	4882	4857	1.2	10547
		500	3575	4336	4522	4622	4647	4604	1.3	10547
		750	3637	4309	4471	4547	4557	4501	1.3	10547
		1000	3699	4286	4441	4509	4510	4446	1.3	10547
	50mm	250	3555	4573	4928	5192	5357	5365	1.2	11056
		500	3672	4514	4799	5008	5110	5093	1.3	11056
		750	3737	4488	4749	4927	5014	4983	1.3	11056
		1000	3802	4463	4717	4886	4963	4925	1.3	11056
	75mm	250	3798	5037	5637	6156	6543	6652	1.3	12375
		500	3923	4971	5496	5955	6288	6349	1.4	12375
		750	3989	4947	5447	5880	6183	6219	1.4	12375
		1000	4062	4918	5413	5831	6123	6150	1.4	12375
	100mm	250	4137	5661	6586	7433	8162	8374	1.3	14222
		500	4269	5587	6429	7210	7876	8043	1.4	14222
		750	4342	5567	6374	7127	7765	7908	1.4	14222
		1000	4426	5539	6346	7084	7708	7830	1.5	14222
	125mm	250	4571	6444	7745	8980	10182	10526	1.4	16597
		500	4709	6364	7568	8727	9858	10148	1.4	16597
		750	4790	6337	7505	8633	9732	9994	1.5	16597
		1000	4885	6316	7474	8585	9667	9913	1.5	16597
	150mm	250	5096	7369	9089	10755	12388	13077	1.4	19500
		500	5246	7275	8881	10465	12030	12642	1.5	19500
		750	5331	7238	8817	10360	11892	12467	1.5	19500
		1000	5435	7229	8785	10305	11820	12372	1.5	19500

Initial Pt Force 0.1F_{yield}		Axial Load (excluding PT) 5000kN			Cantilever Length (4000mm)			Grade 300 Dissipaters		
	PT Dia.	Fuse Length (mm)	Yield (kNm)	1%drift (kNm)	2%drift (kNm)	3%drift (kNm)	4%drift (kNm)	6%drift (kNm)	λ	Fuse Area (mm^2)
Diameter (1500mm)	36mm	250	4425	5598	5918	6114	6155	6148	1.2	10564
		500	4543	5507	5730	5849	5852	5805	1.3	10564
		750	4618	5467	5655	5749	5730	5655	1.3	10564
		1000	4686	5438	5617	5697	5664	5577	1.3	10564
	50mm	250	4545	5845	6304	6655	6773	6786	1.2	11088
		500	4671	5751	6114	6372	6450	6428	1.3	11088
		750	4746	5710	6033	6266	6320	6278	1.4	11088
		1000	4816	5680	5992	6211	6251	6196	1.4	11088
	75mm	250	4859	6476	7280	7983	8361	8448	1.3	12447
		500	4995	6370	7072	7692	7986	8049	1.4	12447
		750	5074	6330	6991	7567	7835	7876	1.4	12447
		1000	5154	6295	6943	7502	7755	7783	1.5	12447
	100mm	250	5294	7333	8593	9754	10489	10745	1.4	14351
		500	5447	7218	8358	9428	10085	10285	1.5	14351
		750	5529	7174	8275	9305	9917	10077	1.5	14351
		1000	5616	7137	8224	9231	9820	9965	1.5	14351
	125mm	250	5847	8400	10203	11911	13157	13581	1.4	16799
		500	6025	8267	9936	11541	12694	13061	1.5	16799
		750	6103	8220	9842	11400	12507	12836	1.6	16799
		1000	6207	8185	9793	11328	12408	12713	1.6	16799
	150mm	250	6518	9652	12077	14402	16332	16958	1.5	19790
		500	6711	9508	11771	13979	15796	16357	1.6	19790
		750	6797	9451	11663	13818	15582	16099	1.6	19790
		1000	6912	9427	11607	13735	15467	15957	1.6	19790

Initial Pt Force 0.1f_{yield}		Axial Load (excluding PT) 1500kN			Cantilever Length (5000mm)			Grade 300 Dissipaters		
	PT Dia.	Fuse Length (mm)	Yield (kNm)	1%drift (kNm)	2%drift (kNm)	3%drift (kNm)	4%drift (kNm)	6%drift (kNm)	λ	Fuse Area (mm^2)
Diameter (1000mm)	36mm	250	938	1151	1201	1227	1238	1244	1.1	3385
		500	962	1137	1168	1179	1183	1183	1.1	3385
		750	981	1126	1154	1161	1162	1160	1.2	3385
		1000	996	1122	1147	1152	1151	1147	1.2	3385
	50mm	250	1002	1262	1361	1440	1509	1567	1.1	3743
		500	1028	1246	1328	1389	1444	1495	1.2	3743
		750	1048	1235	1311	1368	1419	1468	1.2	3743
		1000	1066	1230	1303	1358	1407	1453	1.3	3743
	75mm	250	1165	1537	1756	1956	2148	2335	1.2	4671
		500	1196	1519	1717	1899	2077	2252	1.3	4671
		750	1220	1511	1702	1878	2049	2217	1.3	4671
		1000	1243	1502	1691	1863	2030	2195	1.4	4671
	100mm	250	1387	1905	2273	2623	2965	3301	1.3	5971
		500	1426	1886	2225	2554	2878	3199	1.4	5971
		750	1453	1877	2208	2529	2845	3159	1.4	5971
		1000	1484	1868	2200	2516	2828	3138	1.4	5971
	125mm	250	1669	2358	2888	3414	3924	4430	1.3	7642
		500	1713	2333	2829	3324	3817	4304	1.4	7642
		750	1745	2323	2814	3294	3777	4256	1.4	7642
		1000	1783	2315	2806	3277	3756	4230	1.4	7642
	150mm	250	2002	2891	3594	4297	4993	5682	1.3	9685
		500	2058	2852	3527	4191	4860	5526	1.4	9685
		750	2093	2840	3502	4155	4812	5468	1.4	9685
		1000	2137	2834	3491	4138	4796	5448	1.4	9685

Initial Pt Force $0.1f_{yield}$		Axial Load (excluding PT) 1500kN			Cantilever Length (5000mm)			Grade 300 Dissipaters		
	PT Dia.	Fuse Length (mm)	Yield (kNm)	1%drift (kNm)	2%drift (kNm)	3%drift (kNm)	4%drift (kNm)	6%drift (kNm)	λ	Fuse Area (mm^2)
Diameter (1200mm)	36mm	250	1181	1456	1539	1596	1652	1677	1.2	3433
		500	1203	1430	1494	1539	1578	1592	1.3	3433
		750	1224	1421	1478	1518	1551	1557	1.3	3433
		1000	1242	1415	1470	1507	1537	1538	1.3	3433
	50mm	250	1267	1614	1779	1913	2037	2131	1.3	3835
		500	1291	1588	1726	1847	1961	2037	1.4	3835
		750	1314	1576	1708	1822	1931	2000	1.4	3835
		1000	1336	1569	1698	1810	1916	1981	1.4	3835
	75mm	250	1485	2012	2363	2695	3016	3298	1.4	4878
		500	1515	1984	2305	2609	2907	3177	1.5	4878
		750	1546	1966	2279	2575	2865	3128	1.5	4878
		1000	1575	1957	2265	2557	2843	3102	1.5	4878
	100mm	250	1785	2542	3129	3695	4250	4795	1.5	6339
		500	1824	2506	3058	3594	4125	4653	1.5	6339
		750	1862	2490	3033	3557	4077	4596	1.6	6339
		1000	1901	2478	3013	3532	4048	4560	1.6	6339
	125mm	250	2163	3188	4049	4886	5712	6525	1.5	8217
		500	2215	3147	3960	4761	5556	6349	1.6	8217
		750	2256	3132	3929	4715	5497	6277	1.6	8217
		1000	2303	3117	3913	4691	5466	6238	1.6	8217
	150mm	250	2613	3940	5095	6237	7360	8470	1.5	10513
		500	2680	3892	4992	6082	7168	8251	1.6	10513
		750	2721	3875	4955	6025	7095	8162	1.6	10513
		1000	2780	3862	4931	5997	7057	8116	1.6	10513

Initial Pt Force 0.1F_{yield}		Axial Load (excluding PT) 1500kN			Cantilever Length (5000mm)			Grade 300 Dissipaters		
	PT Dia.	Fuse Length (mm)	Yield (kNm)	1%drift (kNm)	2%drift (kNm)	3%drift (kNm)	4%drift (kNm)	6%drift (kNm)	λ	Fuse Area (mm^2)
Diameter (1500mm)	36mm	250	1567	1927	2080	2222	2302	2306	1.3	3504
		500	1582	1892	2020	2133	2195	2189	1.4	3504
		750	1605	1880	1998	2100	2151	2137	1.4	3504
		1000	1625	1872	1987	2083	2128	2109	1.5	3504
	50mm	250	1693	2176	2455	2721	2901	2939	1.4	3973
		500	1709	2135	2386	2622	2781	2807	1.5	3973
		750	1736	2120	2361	2586	2732	2749	1.5	3973
		1000	1761	2113	2349	2568	2706	2717	1.6	3973
	75mm	250	2012	2802	3397	3962	4419	4544	1.5	5189
		500	2034	2747	3302	3840	4269	4375	1.7	5189
		750	2070	2727	3268	3794	4210	4301	1.7	5189
		1000	2105	2717	3251	3770	4179	4262	1.7	5189
	100mm	250	2449	3635	4641	5620	6518	6736	1.6	6891
		500	2480	3573	4521	5452	6310	6517	1.8	6891
		750	2526	3543	4471	5384	6227	6422	1.8	6891
		1000	2577	3527	4446	5350	6183	6371	1.8	6891
	125mm	250	2998	4655	6136	7584	9011	9490	1.7	9080
		500	3040	4578	5989	7382	8767	9207	1.8	9080
		750	3099	4545	5936	7305	8670	9081	1.8	9080
		1000	3166	4521	5898	7258	8613	9008	1.9	9080
	150mm	250	3656	5842	7855	9832	11782	12719	1.7	11755
		500	3714	5745	7671	9579	11475	12361	1.8	11755
		750	3782	5713	7606	9481	11353	12207	1.8	11755
		1000	3864	5684	7572	9432	11287	12124	1.9	11755

Initial Pt Force 0.1f_{yield}		Axial Load (excluding PT) 1500kN			Cantilever Length (5000mm)			Grade 300 Dissipaters		
	PT Dia.	Fuse Length (mm)	Yield (kNm)	1%drift (kNm)	2%drift (kNm)	3%drift (kNm)	4%drift (kNm)	6%drift (kNm)	λ	Fuse Area (mm^2)
Diameter (1800mm)	36mm	250	1951	2424	2680	2892	2938	2958	1.4	3576
		500	1964	2377	2590	2770	2797	2811	1.5	3576
		750	2001	2361	2557	2722	2737	2740	1.5	3576
		1000	2016	2350	2541	2697	2704	2700	1.5	3576
	50mm	250	2122	2779	3224	3627	3723	3787	1.5	4111
		500	2135	2725	3122	3489	3564	3619	1.6	4111
		750	2180	2706	3086	3434	3495	3538	1.7	4111
		1000	2200	2695	3068	3406	3458	3493	1.7	4111
	75mm	250	2560	3679	4582	5471	5724	5899	1.7	5499
		500	2572	3604	4456	5294	5514	5678	1.8	5499
		750	2635	3578	4409	5226	5424	5572	1.9	5499
		1000	2667	3565	4385	5192	5375	5513	1.9	5499
	100mm	250	3162	4892	6416	7895	8449	8782	1.8	7443
		500	3171	4787	6236	7666	8171	8487	1.9	7443
		750	3258	4750	6170	7576	8057	8347	2.0	7443
		1000	3305	4730	6136	7528	7995	8269	2.0	7443
	125mm	250	3919	6374	8647	10871	11897	12393	1.8	9942
		500	3926	6251	8417	10563	11525	12012	2.0	9942
		750	4038	6196	8324	10434	11367	11833	2.0	9942
		1000	4100	6167	8274	10366	11283	11734	2.1	9942
	150mm	250	4813	8105	11214	14264	15982	16756	1.8	12997
		500	4828	7954	10929	13883	15517	16253	2.0	12997
		750	4968	7893	10826	13732	15319	16008	2.0	12997
		1000	5048	7851	10758	13650	15204	15873	2.1	12997

Initial Pt Force 0.1F_{yield}		Axial Load (excluding PT) 3000kN			Cantilever Length (5000mm)			Grade 300 Dissipaters		
	PT Dia.	Fuse Length (mm)	Yield (kNm)	1%drift (kNm)	2%drift (kNm)	3%drift (kNm)	4%drift (kNm)	6%drift (kNm)	λ	Fuse Area (mm^2)
Diameter (1000mm)	36mm	250	578	717	769	809	844	883	1.1	2682
		500	594	704	749	784	815	846	1.1	2682
		750	605	699	742	775	805	834	1.2	2682
		1000	616	693	738	770	800	828	1.2	2682
	50mm	250	640	819	919	1005	1086	1165	1.1	3109
		500	657	805	894	973	1050	1124	1.2	3109
		750	670	800	885	962	1036	1109	1.2	3109
		1000	685	794	881	956	1029	1101	1.2	3109
	75mm	250	797	1072	1277	1472	1663	1851	1.2	4217
		500	819	1060	1252	1435	1616	1796	1.3	4217
		750	836	1052	1237	1417	1593	1769	1.3	4217
		1000	859	1045	1230	1407	1581	1755	1.3	4217
	100mm	250	1011	1407	1739	2060	2377	2691	1.2	5769
		500	1040	1396	1704	2012	2316	2620	1.3	5769
		750	1061	1386	1695	1995	2294	2592	1.3	5769
		1000	1093	1377	1684	1984	2283	2578	1.3	5769
	125mm	250	1283	1817	2281	2742	3201	3659	1.2	7764
		500	1320	1802	2242	2682	3124	3567	1.3	7764
		750	1342	1793	2227	2661	3102	3532	1.3	7764
		1000	1383	1780	2227	2649	3081	3514	1.3	7764
	150mm	250	1607	2299	2898	3506	4112	4716	1.2	10202
		500	1650	2270	2847	3430	4015	4600	1.2	10202
		750	1673	2261	2834	3409	3981	4559	1.2	10202
		1000	1724	2246	2828	3394	3960	4533	1.3	10202

Initial Pt Force $0.1F_{yield}$		Axial Load (excluding PT) 3000kN			Cantilever Length (5000mm)			Grade 300 Dissipaters		
	PT Dia.	Fuse Length (mm)	Yield (kNm)	1%drift (kNm)	2%drift (kNm)	3%drift (kNm)	4%drift (kNm)	6%drift (kNm)	λ	Fuse Area (mm^2)
Diameter (1200mm)	36mm	250	764	948	1037	1120	1198	1212	1.2	2756
		500	776	933	1013	1084	1151	1158	1.3	2756
		750	790	927	1004	1072	1133	1136	1.3	2756
		1000	803	919	1000	1067	1125	1125	1.3	2756
	50mm	250	853	1108	1272	1425	1580	1620	1.3	3252
		500	866	1089	1242	1386	1528	1557	1.4	3252
		750	884	1082	1231	1372	1510	1532	1.4	3252
		1000	900	1074	1226	1365	1501	1520	1.4	3252
	75mm	250	1080	1506	1855	2190	2517	2655	1.4	4539
		500	1097	1479	1807	2126	2441	2571	1.5	4539
		750	1122	1468	1790	2103	2413	2538	1.5	4539
		1000	1149	1461	1781	2091	2399	2520	1.5	4539
	100mm	250	1388	2028	2598	3157	3710	4065	1.4	6341
		500	1411	1999	2545	3081	3615	3949	1.5	6341
		750	1446	1982	2519	3048	3575	3898	1.5	6341
		1000	1484	1973	2504	3028	3550	3870	1.6	6341
	125mm	250	1775	2657	3484	4295	5098	5775	1.4	8658
		500	1805	2625	3413	4195	4974	5622	1.5	8658
		750	1850	2610	3390	4159	4926	5562	1.5	8658
		1000	1898	2593	3370	4141	4902	5530	1.5	8658
	150mm	250	2238	3386	4490	5575	6652	7720	1.4	11490
		500	2278	3351	4401	5447	6492	7534	1.4	11490
		750	2329	3340	4371	5401	6432	7462	1.5	11490
		1000	2389	3317	4352	5378	6401	7423	1.5	11490

Initial Pt Force 0.1F_{yield}		Axial Load (excluding PT) 3000kN			Cantilever Length (5000mm)			Grade 300 Dissipaters		
	PT Dia.	Fuse Length (mm)	Yield (kNm)	1%drift (kNm)	2%drift (kNm)	3%drift (kNm)	4%drift (kNm)	6%drift (kNm)	λ	Fuse Area (mm^2)
Diameter (1500mm)	36mm	250	954	1194	1336	1474	1527	1552	1.3	2830
		500	968	1176	1301	1423	1463	1480	1.4	2830
		750	983	1168	1290	1404	1438	1450	1.4	2830
		1000	997	1160	1284	1395	1425	1434	1.4	2830
	50mm	250	1075	1422	1673	1922	2035	2090	1.4	3395
		500	1090	1398	1634	1862	1960	2004	1.5	3395
		750	1110	1391	1620	1842	1930	1968	1.5	3395
		1000	1129	1381	1613	1832	1915	1949	1.6	3395
	75mm	250	1385	1995	2518	3027	3318	3446	1.5	4861
		500	1401	1957	2456	2947	3216	3327	1.6	4861
		750	1432	1944	2435	2917	3178	3277	1.7	4861
		1000	1463	1934	2423	2902	3159	3253	1.7	4861
	100mm	250	1805	2751	3628	4490	5089	5296	1.6	6914
		500	1824	2701	3539	4367	4934	5130	1.7	6914
		750	1868	2679	3504	4319	4875	5063	1.7	6914
		1000	1915	2668	3486	4294	4844	5027	1.8	6914
	125mm	250	2328	3665	4944	6203	7254	7613	1.6	9553
		500	2356	3611	4837	6054	7060	7391	1.7	9553
		750	2413	3577	4794	5999	6986	7294	1.7	9553
		1000	2477	3560	4765	5960	6941	7239	1.7	9553
	150mm	250	2952	4721	6446	8149	9799	10317	1.5	12778
		500	2990	4654	6309	7955	9548	10027	1.6	12778
		750	3058	4625	6261	7883	9452	9908	1.7	12778
		1000	3139	4600	6234	7846	9400	9846	1.7	12778

Initial Pt Force 0.1Fyield		Axial Load (excluding PT) 3000kN			Cantilever Length (5000mm)			Grade 300 Dissipaters		
	PT Dia.	Fuse Length (mm)	Yield (kNm)	1%drift (kNm)	2%drift (kNm)	3%drift (kNm)	4%drift (kNm)	6%drift (kNm)	λ	Fuse Area (mm^2)
Diameter (1800mm)	36mm	250	954	1194	1336	1474	1527	1552	1.3	2830
		500	968	1176	1301	1423	1463	1480	1.4	2830
		750	983	1168	1290	1404	1438	1450	1.4	2830
		1000	997	1160	1284	1395	1425	1434	1.4	2830
	50mm	250	1075	1422	1673	1922	2035	2090	1.4	3395
		500	1090	1398	1634	1862	1960	2004	1.5	3395
		750	1110	1391	1620	1842	1930	1968	1.5	3395
		1000	1129	1381	1613	1832	1915	1949	1.6	3395
	75mm	250	1385	1995	2518	3027	3318	3446	1.5	4861
		500	1401	1957	2456	2947	3216	3327	1.6	4861
		750	1432	1944	2435	2917	3178	3277	1.7	4861
		1000	1463	1934	2423	2902	3159	3253	1.7	4861
	100mm	250	1805	2751	3628	4490	5089	5296	1.6	6914
		500	1824	2701	3539	4367	4934	5130	1.7	6914
		750	1868	2679	3504	4319	4875	5063	1.7	6914
		1000	1915	2668	3486	4294	4844	5027	1.8	6914
	125mm	250	2328	3665	4944	6203	7254	7613	1.6	9553
		500	2356	3611	4837	6054	7060	7391	1.7	9553
		750	2413	3577	4794	5999	6986	7294	1.7	9553
		1000	2477	3560	4765	5960	6941	7239	1.7	9553
	150mm	250	2952	4721	6446	8149	9799	10317	1.5	12778
		500	2990	4654	6309	7955	9548	10027	1.6	12778
		750	3058	4625	6261	7883	9452	9908	1.7	12778
		1000	3139	4600	6234	7846	9400	9846	1.7	12778

Initial Pt Force 0.1f_{yield}		Axial Load (excluding PT) 4500kN			Cantilever Length (5000mm)			Grade 300 Dissipaters		
	PT Dia.	Fuse Length (mm)	Yield (kNm)	1%drift (kNm)	2%drift (kNm)	3%drift (kNm)	4%drift (kNm)	6%drift (kNm)	λ	Fuse Area (mm^2)
Diameter (1000mm)	36mm	250	2047	2640	2669	2631	2561	2473	1.2	7299
		500	2155	2611	2612	2545	2450	2343	1.3	7299
		750	2219	2602	2591	2513	2409	2291	1.3	7299
		1000	2261	2598	2582	2497	2387	2264	1.3	7299
	50mm	250	2094	2725	2793	2799	2775	2733	1.2	7578
		500	2201	2693	2733	2710	2661	2600	1.3	7578
		750	2268	2683	2713	2677	2618	2547	1.3	7578
		1000	2313	2679	2704	2661	2596	2519	1.4	7578
	75mm	250	2215	2936	3100	3218	3304	3376	1.3	8300
		500	2325	2900	3038	3119	3183	3234	1.4	8300
		750	2395	2890	3015	3085	3137	3178	1.4	8300
		1000	2444	2882	3007	3071	3114	3149	1.4	8300
	100mm	250	2381	3226	3513	3764	4000	4213	1.3	9311
		500	2498	3182	3448	3666	3862	4058	1.4	9311
		750	2573	3170	3427	3629	3812	3998	1.4	9311
		1000	2624	3162	3413	3605	3789	3965	1.5	9311
	125mm	250	2593	3583	4023	4427	4827	5201	1.4	10611
		500	2717	3537	3947	4311	4673	5026	1.4	10611
		750	2798	3519	3927	4278	4619	4960	1.5	10611
		1000	2854	3506	3910	4254	4599	4928	1.5	10611
	150mm	250	2847	3999	4623	5177	5752	6310	1.4	12199
		500	2985	3953	4535	5058	5586	6132	1.4	12199
		750	3073	3932	4502	5017	5527	6042	1.5	12199
		1000	3130	3912	4486	4996	5498	6007	1.5	12199

Initial Pt Force 0.1F_{yield}		Axial Load (excluding PT) 4500kN			Cantilever Length (5000mm)			Grade 300 Dissipaters		
	PT Dia.	Fuse Length (mm)	Yield (kNm)	1%drift (kNm)	2%drift (kNm)	3%drift (kNm)	4%drift (kNm)	6%drift (kNm)	λ	Fuse Area (mm^2)
Diameter (1200mm)	36mm	250	2923	3726	3859	3898	3898	3873	1.1	9433
		500	3033	3675	3752	3744	3705	3651	1.1	9433
		750	3092	3659	3715	3687	3630	3551	1.1	9433
		1000	3144	3648	3696	3655	3583	3497	1.2	9433
	50mm	250	2998	3863	4061	4171	4244	4292	1.1	9835
		500	3110	3811	3952	4013	4046	4064	1.1	9835
		750	3171	3792	3913	3954	3969	3969	1.2	9835
		1000	3225	3784	3894	3924	3925	3911	1.2	9835
	75mm	250	3189	4209	4573	4858	5107	5333	1.1	10878
		500	3305	4151	4454	4686	4894	5088	1.2	10878
		750	3372	4134	4413	4623	4811	4988	1.2	10878
		1000	3431	4124	4392	4591	4768	4935	1.2	10878
	100mm	250	3457	4680	5256	5769	6245	6699	1.2	12339
		500	3578	4617	5128	5580	6010	6428	1.2	12339
		750	3654	4595	5079	5511	5919	6319	1.3	12339
		1000	3716	4589	5059	5476	5872	6261	1.3	12339
	125mm	250	3799	5278	6094	6869	7614	8334	1.2	14217
		500	3928	5197	5947	6667	7352	8031	1.3	14217
		750	4011	5173	5903	6582	7250	7909	1.3	14217
		1000	4080	5162	5879	6549	7198	7844	1.3	14217
	150mm	250	4210	5983	7068	8135	9183	10188	1.2	16513
		500	4346	5885	6906	7895	8874	9845	1.3	16513
		750	4445	5858	6854	7820	8758	9709	1.3	16513
		1000	4517	5846	6835	7764	8701	9636	1.3	16513

Initial Pt Force 0.1Fyield		Axial Load (excluding PT) 4500kN			Cantilever Length (5000mm)			Grade 300 Dissipaters		
	PT Dia.	Fuse Length (mm)	Yield (kNm)	1%drift (kNm)	2%drift (kNm)	3%drift (kNm)	4%drift (kNm)	6%drift (kNm)	λ	Fuse Area (mm^2)
Diameter (1500mm)	36mm	250	3917	4956	5197	5335	5382	5315	1.1	9504
		500	4036	4874	5034	5094	5103	5010	1.2	9504
		750	4095	4841	4968	5002	4991	4881	1.3	9504
		1000	4154	4815	4932	4954	4932	4811	1.3	9504
	50mm	250	4028	5173	5533	5791	5967	5922	1.2	9973
		500	4151	5088	5364	5547	5670	5607	1.3	9973
		750	4211	5055	5297	5449	5551	5470	1.3	9973
		1000	4273	5027	5259	5398	5488	5396	1.3	9973
	75mm	250	4311	5729	6382	6939	7443	7510	1.3	11189
		500	4444	5636	6196	6680	7124	7141	1.3	11189
		750	4507	5600	6130	6577	6984	6982	1.4	11189
		1000	4574	5572	6087	6516	6910	6896	1.4	11189
	100mm	250	4704	6483	7523	8469	9369	9637	1.3	12891
		500	4851	6380	7315	8179	9019	9235	1.4	12891
		750	4917	6338	7240	8069	8877	9060	1.5	12891
		1000	4993	6315	7202	8011	8802	8955	1.5	12891
	125mm	250	5205	7425	8922	10332	11694	12293	1.4	15080
		500	5364	7301	8686	10001	11294	11832	1.5	15080
		750	5435	7263	8602	9877	11135	11633	1.5	15080
		1000	5525	7244	8558	9813	11050	11525	1.5	15080
	150mm	250	5812	8527	10550	12482	14363	15450	1.4	17755
		500	5977	8398	10279	12104	13906	14916	1.5	17755
		750	6061	8351	10183	11961	13724	14688	1.5	17755
		1000	6160	8332	10133	11887	13627	14564	1.6	17755

Initial Pt Force 0.1Fyield		Axial Load (excluding PT) 4500kN			Cantilever Length (5000mm)			Grade 300 Dissipaters		
	PT Dia.	Fuse Length (mm)	Yield (kNm)	1%drift (kNm)	2%drift (kNm)	3%drift (kNm)	4%drift (kNm)	6%drift (kNm)	λ	Fuse Area (mm^2)
Diameter (1800mm)	36mm	250	4942	6219	6578	6803	6864	6847	1.2	9576
		500	5014	6097	6342	6500	6501	6462	1.3	9576
		750	5132	6046	6257	6382	6345	6279	1.3	9576
		1000	5185	6021	6212	6320	6262	6178	1.4	9576
	50mm	250	5091	6540	7088	7492	7617	7644	1.2	10111
		500	5169	6415	6836	7173	7235	7240	1.4	10111
		750	5290	6361	6745	7048	7073	7048	1.4	10111
		1000	5349	6334	6698	6982	6988	6941	1.4	10111
	75mm	250	5482	7358	8364	9244	9547	9686	1.3	11499
		500	5567	7219	8090	8872	9126	9231	1.5	11499
		750	5701	7162	7983	8728	8947	9016	1.5	11499
		1000	5769	7127	7928	8652	8851	8899	1.5	11499
	100mm	250	6020	8473	10079	11573	12251	12503	1.4	13443
		500	6120	8317	9775	11160	11742	11981	1.6	13443
		750	6273	8257	9656	10984	11528	11737	1.6	13443
		1000	6345	8211	9588	10891	11413	11602	1.6	13443
	125mm	250	6704	9864	12190	14402	15605	16104	1.5	15942
		500	6827	9679	11840	13927	15031	15477	1.6	15942
		750	6996	9621	11711	13741	14785	15178	1.7	15942
		1000	7073	9563	11638	13638	14643	15013	1.7	15942
	150mm	250	7534	11503	14652	17684	19600	20347	1.5	18997
		500	7680	11287	14246	17133	18928	19622	1.7	18997
		750	7869	11215	14098	16920	18646	19285	1.7	18997
		1000	7943	11167	14022	16807	18493	19100	1.8	18997

Initial Pt Force 0.1F_{yield}		Axial Load (excluding PT) 4500kN			Cantilever Length (5000mm)			Grade 300 Dissipaters		
	PT Dia.	Fuse Length (mm)	Yield (kNm)	1%drift (kNm)	2%drift (kNm)	3%drift (kNm)	4%drift (kNm)	6%drift (kNm)	λ	Fuse Area (mm^2)
Diameter (2000mm)	36mm	250	5967	7408	7886	8205	8304	8316	1.1	10693
		500	6024	7234	7581	7796	7838	7841	1.2	10693
		750	6087	7171	7469	7632	7631	7599	1.2	10693
		1000	6155	7139	7410	7547	7517	7463	1.3	10693
	50mm	250	6166	7828	8541	9051	9213	9278	1.1	11336
		500	6226	7647	8218	8620	8721	8775	1.3	11336
		750	6293	7578	8098	8451	8503	8520	1.3	11336
		1000	6368	7545	8036	8362	8384	8377	1.3	11336
	75mm	250	6682	8900	10212	11230	11544	11744	1.2	13007
		500	6752	8703	9835	10748	10986	11172	1.4	13007
		750	6827	8620	9696	10554	10740	10883	1.4	13007
		1000	6912	8579	9624	10452	10608	10721	1.4	13007
	100mm	250	7392	10361	12457	14266	14755	15137	1.3	15346
		500	7484	10138	12029	13683	14113	14468	1.5	15346
		750	7564	10047	11860	13452	13831	14134	1.5	15346
		1000	7669	9995	11772	13330	13678	13949	1.5	15346
	125mm	250	8297	12183	15215	18054	18876	19440	1.4	18353
		500	8414	11922	14728	17389	18086	18650	1.5	18353
		750	8504	11829	14542	17113	17742	18258	1.6	18353
		1000	8623	11764	14431	16962	17556	18039	1.6	18353
	150mm	250	9383	14338	18447	22395	23739	24654	1.4	22028
		500	9535	14037	17877	21638	22834	23706	1.6	22028
		750	9637	13930	17666	21336	22439	23224	1.6	22028
		1000	9776	13856	17557	21176	22209	22954	1.7	22028

Initial Pt Force 0.1f_{yield}		Axial Load (excluding PT) 6000kN			Cantilever Length (5000mm)			Grade 300 Dissipaters		
	PT Dia.	Fuse Length (mm)	Yield (kNm)	1%drift (kNm)	2%drift (kNm)	3%drift (kNm)	4%drift (kNm)	6%drift (kNm)	λ	Fuse Area (mm^2)
Diameter (1000mm)	36mm	250	2749	3597	3633	3582	3489	3368	1.0	11009
		500	2893	3551	3549	3455	3327	3176	1.1	11009
		750	2982	3534	3523	3411	3266	3101	1.1	11009
		1000	3040	3520	3511	3387	3234	3061	1.1	11009
	50mm	250	2798	3678	3750	3746	3697	3619	1.1	11327
		500	2943	3631	3667	3617	3530	3423	1.1	11327
		750	3034	3613	3641	3568	3468	3347	1.1	11327
		1000	3093	3598	3625	3547	3436	3307	1.1	11327
	75mm	250	2926	3890	4062	4152	4206	4244	1.1	12152
		500	3074	3841	3969	4016	4038	4039	1.1	12152
		750	3168	3821	3943	3964	3969	3959	1.2	12152
		1000	3230	3802	3928	3942	3939	3917	1.2	12152
	100mm	250	3101	4179	4477	4687	4891	5059	1.1	13308
		500	3256	4129	4378	4543	4701	4844	1.2	13308
		750	3356	4107	4345	4496	4631	4758	1.2	13308
		1000	3422	4083	4330	4477	4597	4714	1.2	13308
	125mm	250	3332	4540	5001	5344	5700	6050	1.1	14793
		500	3489	4492	4889	5195	5511	5806	1.2	14793
		750	3594	4461	4850	5152	5429	5713	1.2	14793
		1000	3668	4436	4827	5120	5392	5674	1.2	14793
	150mm	250	3606	4967	5618	6124	6632	7150	1.1	16609
		500	3769	4913	5476	5959	6414	6892	1.2	16609
		750	3882	4878	5432	5903	6352	6791	1.2	16609
		1000	3962	4852	5410	5874	6304	6751	1.2	16609

Initial Pt Force 0.1F_{yield}		Axial Load (excluding PT) 6000kN			Cantilever Length (5000mm)			Grade 300 Dissipaters		
	PT Dia.	Fuse Length (mm)	Yield (kNm)	1%drift (kNm)	2%drift (kNm)	3%drift (kNm)	4%drift (kNm)	6%drift (kNm)	λ	Fuse Area (mm^2)
Diameter (1200mm)	36mm	250	3509	4568	4699	4713	4673	4600	1.2	11051
		500	3665	4508	4580	4537	4452	4345	1.2	11051
		750	3762	4492	4538	4472	4366	4240	1.3	11051
		1000	3831	4483	4515	4439	4321	4184	1.3	11051
	50mm	250	3575	4689	4883	4966	4996	4994	1.2	11409
		500	3733	4628	4759	4786	4769	4733	1.2	11409
		750	3833	4612	4718	4719	4682	4626	1.3	11409
		1000	3901	4602	4696	4686	4636	4570	1.3	11409
	75mm	250	3746	5004	5355	5602	5803	5976	1.2	12336
		500	3907	4939	5218	5411	5564	5700	1.3	12336
		750	4016	4918	5176	5341	5473	5588	1.3	12336
		1000	4087	4908	5155	5305	5424	5528	1.3	12336
	100mm	250	3980	5433	5985	6453	6874	7270	1.2	13635
		500	4150	5358	5837	6244	6617	6973	1.3	13635
		750	4263	5335	5795	6169	6518	6852	1.4	13635
		1000	4341	5325	5772	6130	6466	6789	1.4	13635
	125mm	250	4285	5979	6752	7486	8165	8823	1.3	15304
		500	4463	5890	6601	7260	7886	8500	1.4	15304
		750	4583	5859	6555	7171	7777	8369	1.4	15304
		1000	4668	5848	6532	7136	7722	8300	1.4	15304
	150mm	250	4648	6614	7663	8672	9635	10581	1.3	17345
		500	4847	6520	7498	8416	9341	10242	1.4	17345
		750	4970	6485	7446	8324	9211	10084	1.4	17345
		1000	5063	6466	7413	8283	9161	10022	1.4	17345

Initial Pt Force 0.1f_{yield}		Axial Load (excluding PT) 6000kN			Cantilever Length (5000mm)			Grade 300 Dissipaters		
	PT Dia.	Fuse Length (mm)	Yield (kNm)	1%drift (kNm)	2%drift (kNm)	3%drift (kNm)	4%drift (kNm)	6%drift (kNm)	λ	Fuse Area (mm^2)
Diameter (1500mm)	36mm	250	4743	6096	6356	6473	6520	6404	1.3	11115
		500	4916	6003	6170	6211	6189	6044	1.4	11115
		750	5005	5969	6103	6104	6053	5889	1.4	11115
		1000	5085	5944	6062	6046	5981	5805	1.4	11115
	50mm	250	4840	6293	6666	6901	7069	7001	1.3	11531
		500	5015	6199	6475	6632	6736	6622	1.4	11531
		750	5104	6161	6407	6527	6593	6459	1.4	11531
		1000	5190	6141	6367	6465	6517	6371	1.4	11531
	75mm	250	5092	6798	7455	7980	8448	8502	1.4	12612
		500	5269	6694	7249	7692	8099	8106	1.5	12612
		750	5369	6659	7176	7583	7957	7922	1.5	12612
		1000	5458	6636	7139	7524	7874	7822	1.5	12612
	100mm	250	5443	7488	8517	9425	10276	10545	1.4	14125
		500	5626	7376	8293	9110	9894	10108	1.5	14125
		750	5736	7336	8213	8991	9740	9918	1.6	14125
		1000	5831	7318	8172	8929	9660	9816	1.6	14125
	125mm	250	5888	8350	9827	11189	12495	13106	1.5	16071
		500	6079	8226	9577	10841	12073	12617	1.6	16071
		750	6202	8184	9489	10709	11904	12407	1.6	16071
		1000	6307	8160	9443	10640	11814	12293	1.6	16071
	150mm	250	6434	9367	11353	13229	15050	16153	1.5	18449
		500	6629	9228	11078	12840	14577	15602	1.6	18449
		750	6764	9184	10975	12693	14390	15366	1.7	18449
		1000	6880	9159	10925	12617	14289	15238	1.7	18449

Initial Pt Force $0.1f_{yield}$		Axial Load (excluding PT) 6000kN			Cantilever Length (5000mm)			Grade 300 Dissipaters		
	PT Dia.	Fuse Length (mm)	Yield (kNm)	1%drift (kNm)	2%drift (kNm)	3%drift (kNm)	4%drift (kNm)	6%drift (kNm)	λ	Fuse Area (mm^2)
Diameter (1800mm)	36mm	250	6004	7670	8066	8283	8300	8246	1.3	11179
		500	6150	7535	7796	7923	7880	7800	1.4	11179
		750	6309	7482	7692	7782	7707	7589	1.5	11179
		1000	6375	7446	7639	7709	7614	7471	1.5	11179
	50mm	250	6137	7965	8537	8942	9022	9012	1.4	11654
		500	6290	7823	8261	8564	8594	8548	1.5	11654
		750	6451	7770	8152	8416	8413	8330	1.5	11654
		1000	6518	7732	8096	8339	8315	8209	1.6	11654
	75mm	250	6481	8716	9730	10598	10909	10976	1.4	12888
		500	6647	8564	9436	10187	10428	10471	1.6	12888
		750	6820	8511	9320	10020	10225	10239	1.6	12888
		1000	6889	8464	9255	9933	10115	10110	1.7	12888
	100mm	250	6964	9743	11344	12801	13498	13729	1.5	14616
		500	7140	9574	11017	12358	12960	13149	1.7	14616
		750	7326	9515	10899	12181	12723	12880	1.7	14616
		1000	7404	9470	10827	12077	12596	12731	1.7	14616
	125mm	250	7575	11029	13335	15501	16727	17179	1.6	16838
		500	7763	10838	12969	15005	16122	16530	1.7	16838
		750	7969	10770	12836	14810	15868	16218	1.8	16838
		1000	8057	10726	12767	14707	15727	16041	1.8	16838
	150mm	250	8312	12552	15665	18641	20581	21276	1.6	19553
		500	8517	12334	15250	18077	19891	20533	1.8	19553
		750	8748	12252	15099	17858	19603	20188	1.8	19553
		1000	8841	12210	15022	17744	19447	19999	1.9	19553

Initial Pt Force 0.1f_{yield}		Axial Load (excluding PT) 6000kN			Cantilever Length (5000mm)			Grade 300 Dissipaters		
	PT Dia.	Fuse Length (mm)	Yield (kNm)	1%drift (kNm)	2%drift (kNm)	3%drift (kNm)	4%drift (kNm)	6%drift (kNm)	λ	Fuse Area (mm^2)
Diameter (2000mm)	36mm	250	7447	9378	9943	10262	10364	10358	1.1	13325
		500	7585	9178	9556	9766	9789	9769	1.2	13325
		750	7672	9096	9413	9568	9534	9472	1.3	13325
		1000	7765	9055	9340	9463	9395	9304	1.3	13325
	50mm	250	7634	9775	10575	11094	11249	11295	1.2	13936
		500	7777	9568	10168	10575	10650	10680	1.3	13936
		750	7866	9485	10018	10368	10385	10371	1.3	13936
		1000	7965	9439	9940	10258	10242	10196	1.4	13936
	75mm	250	8113	10791	12166	13241	13520	13701	1.3	15523
		500	8268	10565	11727	12657	12863	13021	1.4	15523
		750	8364	10476	11557	12424	12577	12680	1.4	15523
		1000	8474	10424	11469	12300	12422	12488	1.4	15523
	100mm	250	8776	12180	14315	16191	16693	17017	1.3	17745
		500	8955	11927	13838	15533	15939	16247	1.5	17745
		750	9059	11837	13649	15261	15609	15871	1.5	17745
		1000	9184	11773	13545	15117	15431	15661	1.5	17745
	125mm	250	9620	13921	16978	19853	20700	21274	1.4	20602
		500	9828	13633	16435	19131	19841	20371	1.5	20602
		750	9943	13533	16236	18842	19449	19928	1.6	20602
		1000	10082	13459	16121	18676	19237	19679	1.6	20602
	150mm	250	10644	15979	20103	24035	25462	26352	1.4	24093
		500	10888	15654	19485	23211	24476	25325	1.6	24093
		750	11012	15538	19256	22882	24046	24811	1.6	24093
		1000	11151	15463	19138	22707	23811	24513	1.7	24093

Initial Pt Force 0.1f_{yield}		Axial Load (excluding PT) 7500kN			Cantilever Length (5000mm)			Grade 300 Dissipaters		
	PT Dia.	Fuse Length (mm)	Yield (kNm)	1%drift (kNm)	2%drift (kNm)	3%drift (kNm)	4%drift (kNm)	6%drift (kNm)	λ	Fuse Area (mm^2)
Diameter (1000mm)	36mm	250	3303	4365	4420	4338	4214	4050	1.0	13676
		500	3471	4319	4316	4182	4012	3815	1.1	13676
		750	3585	4291	4281	4128	3942	3724	1.1	13676
		1000	3672	4268	4265	4102	3904	3676	1.1	13676
	50mm	250	3348	4443	4534	4488	4403	4287	1.0	13994
		500	3517	4397	4429	4335	4204	4050	1.1	13994
		750	3637	4367	4393	4277	4133	3958	1.1	13994
		1000	3721	4344	4374	4256	4090	3909	1.1	13994
	75mm	250	3474	4640	4832	4870	4892	4887	1.0	14819
		500	3642	4592	4716	4710	4689	4641	1.1	14819
		750	3765	4562	4679	4656	4607	4539	1.1	14819
		1000	3853	4538	4659	4630	4567	4490	1.1	14819
	100mm	250	3648	4917	5236	5389	5548	5666	1.1	15974
		500	3819	4866	5109	5224	5322	5409	1.1	15974
		750	3944	4830	5069	5173	5239	5306	1.1	15974
		1000	4041	4806	5042	5144	5198	5255	1.1	15974
	125mm	250	3873	5260	5734	6038	6325	6610	1.1	17460
		500	4044	5204	5600	5865	6102	6339	1.1	17460
		750	4176	5173	5546	5794	6012	6230	1.1	17460
		1000	4274	5148	5519	5763	5974	6176	1.2	17460
	150mm	250	4146	5674	6314	6808	7228	7686	1.1	19275
		500	4317	5609	6177	6605	6990	7387	1.1	19275
		750	4458	5576	6112	6522	6909	7288	1.1	19275
		1000	4564	5549	6082	6483	6871	7229	1.2	19275

Initial Pt Force $0.1F_{yield}$		Axial Load (excluding PT) 7500kN			Cantilever Length (5000mm)			Grade 300 Dissipaters		
	PT Dia.	Fuse Length (mm)	Yield (kNm)	1%drift (kNm)	2%drift (kNm)	3%drift (kNm)	4%drift (kNm)	6%drift (kNm)	λ	Fuse Area (mm^2)
Diameter (1200mm)	36mm	250	4205	5571	5715	5722	5656	5548	1.1	13718
		500	4414	5497	5572	5508	5386	5234	1.2	13718
		750	4547	5470	5518	5429	5282	5108	1.2	13718
		1000	4630	5460	5495	5389	5228	5040	1.2	13718
	50mm	250	4269	5687	5895	5963	5965	5926	1.1	14075
		500	4481	5612	5746	5745	5691	5608	1.2	14075
		750	4613	5584	5693	5665	5585	5479	1.2	14075
		1000	4701	5574	5665	5624	5530	5410	1.3	14075
	75mm	250	4436	5993	6338	6569	6742	6874	1.2	15003
		500	4651	5907	6182	6346	6455	6541	1.2	15003
		750	4791	5879	6128	6256	6345	6407	1.3	15003
		1000	4880	5867	6102	6215	6287	6335	1.3	15003
	100mm	250	4667	6402	6940	7391	7776	8128	1.2	16301
		500	4886	6314	6781	7142	7472	7776	1.3	16301
		750	5032	6282	6723	7052	7356	7634	1.3	16301
		1000	5128	6265	6697	7008	7295	7558	1.3	16301
	125mm	250	4963	6920	7695	8389	9026	9642	1.2	17971
		500	5193	6822	7521	8120	8709	9264	1.3	17971
		750	5343	6787	7460	8023	8574	9111	1.3	17971
		1000	5446	6767	7430	7979	8510	9030	1.4	17971
	150mm	250	5321	7534	8584	9541	10461	11361	1.3	20011
		500	5561	7433	8389	9248	10111	10955	1.3	20011
		750	5720	7386	8321	9153	9972	10786	1.4	20011
		1000	5830	7362	8295	9105	9904	10701	1.4	20011

Initial Pt Force 0.1Fyield		Axial Load (excluding PT) 7500kN			Cantilever Length (5000mm)			Grade 300 Dissipaters		
	PT Dia.	Fuse Length (mm)	Yield (kNm)	1%drift (kNm)	2%drift (kNm)	3%drift (kNm)	4%drift (kNm)	6%drift (kNm)	λ	Fuse Area (mm^2)
Diameter (1500mm)	36mm	250	5716	7442	7749	7870	7908	7795	1.2	13782
		500	5923	7325	7524	7551	7518	7348	1.3	13782
		750	6053	7289	7443	7430	7356	7149	1.4	13782
		1000	6154	7267	7402	7363	7264	7041	1.4	13782
	50mm	250	5811	7631	8051	8283	8438	8368	1.3	14198
		500	6017	7512	7818	7957	8040	7921	1.4	14198
		750	6154	7472	7735	7833	7880	7712	1.4	14198
		1000	6258	7454	7693	7769	7786	7600	1.4	14198
	75mm	250	6053	8116	8809	9329	9773	9835	1.3	15279
		500	6267	7995	8565	8985	9354	9360	1.4	15279
		750	6407	7953	8478	8854	9186	9154	1.4	15279
		1000	6517	7930	8433	8787	9095	9036	1.5	15279
	100mm	250	6392	8782	9838	10735	11558	11851	1.4	16792
		500	6612	8649	9576	10365	11108	11336	1.5	16792
		750	6764	8606	9482	10225	10928	11113	1.5	16792
		1000	6882	8582	9435	10152	10831	10993	1.5	16792
	125mm	250	6821	9620	11111	12457	13733	14384	1.4	18738
		500	7054	9473	10824	12054	13243	13817	1.5	18738
		750	7220	9428	10722	11902	13046	13575	1.5	18738
		1000	7342	9403	10671	11823	12943	13443	1.6	18738
	150mm	250	7345	10616	12592	14455	16242	17399	1.4	21116
		500	7594	10460	12287	14013	15705	16772	1.5	21116
		750	7773	10405	12172	13847	15490	16504	1.6	21116
		1000	7900	10378	12112	13760	15376	16359	1.6	21116

Initial Pt Force 0.1F_{yield}		Axial Load (excluding PT) 7500kN			Cantilever Length (5000mm)			Grade 300 Dissipaters		
	PT Dia.	Fuse Length (mm)	Yield (kNm)	1%drift (kNm)	2%drift (kNm)	3%drift (kNm)	4%drift (kNm)	6%drift (kNm)	λ	Fuse Area (mm^2)
Diameter (1800mm)	36mm	250	7245	9378	9842	10099	10101	10007	1.3	13845
		500	7447	9215	9522	9646	9587	9459	1.4	13845
		750	7651	9159	9399	9468	9369	9203	1.5	13845
		1000	7731	9111	9330	9375	9252	9065	1.5	13845
	50mm	250	7375	9664	10298	10732	10830	10763	1.3	14321
		500	7579	9496	9970	10274	10294	10200	1.4	14321
		750	7789	9437	9847	10088	10068	9941	1.5	14321
		1000	7867	9389	9774	9991	9946	9797	1.5	14321
	75mm	250	7709	10392	11459	12334	12699	12735	1.4	15555
		500	7924	10212	11109	11855	12113	12123	1.5	15555
		750	8142	10146	10981	11660	11863	11838	1.6	15555
		1000	8226	10102	10906	11551	11728	11680	1.6	15555
	100mm	250	8179	11391	13032	14491	15234	15468	1.5	17283
		500	8397	11195	12652	13971	14610	14783	1.6	17283
		750	8634	11120	12513	13768	14341	14460	1.6	17283
		1000	8725	11077	12442	13657	14188	14281	1.7	17283
	125mm	250	8773	12641	14982	17143	18431	18866	1.5	19504
		500	9002	12420	14562	16571	17737	18118	1.7	19504
		750	9259	12346	14408	16348	17444	17770	1.7	19504
		1000	9359	12304	14331	16231	17286	17571	1.7	19504
	150mm	250	9501	14126	17267	20234	22252	22931	1.6	22220
		500	9730	13873	16800	19598	21474	22090	1.7	22220
		750	10023	13798	16630	19352	21147	21702	1.8	22220
		1000	10126	13755	16544	19220	20972	21487	1.8	22220

Initial Pt Force $0.1f_{yield}$		Axial Load (excluding PT) 7500kN			Cantilever Length (5000mm)			Grade 300 Dissipaters		
	PT Dia.	Fuse Length (mm)	Yield (kNm)	1%drift (kNm)	2%drift (kNm)	3%drift (kNm)	4%drift (kNm)	6%drift (kNm)	λ	Fuse Area (mm^2)
Diameter (2000mm)	36mm	250	9001	11478	12150	12523	12608	12595	1.1	16491
		500	9219	11238	11681	11903	11903	11870	1.2	16491
		750	9331	11149	11501	11656	11595	11505	1.3	16491
		1000	9451	11093	11408	11526	11429	11300	1.3	16491
	50mm	250	9179	11863	12759	13350	13481	13521	1.1	17103
		500	9404	11616	12281	12705	12756	12770	1.3	17103
		750	9523	11528	12092	12447	12440	12394	1.3	17103
		1000	9640	11466	11995	12312	12269	12183	1.3	17103
	75mm	250	9646	12853	14308	15473	15754	15901	1.2	18690
		500	9888	12584	13800	14769	14964	15086	1.3	18690
		750	10010	12494	13601	14484	14617	14681	1.4	18690
		1000	10131	12423	13491	14334	14429	14458	1.4	18690
	100mm	250	10292	14206	16414	18369	18920	19213	1.3	20912
		500	10555	13916	15857	17612	18022	18308	1.4	20912
		750	10691	13814	15651	17300	17628	17861	1.4	20912
		1000	10815	13737	15529	17128	17415	17611	1.5	20912
	125mm	250	11123	15906	19028	21921	22861	23454	1.3	23768
		500	11407	15583	18408	21093	21880	22413	1.5	23768
		750	11554	15466	18180	20762	21445	21896	1.5	23768
		1000	11685	15391	18063	20588	21198	21607	1.5	23768
	150mm	250	12127	17930	22104	26048	27587	28474	1.4	27260
		500	12437	17561	21410	25120	26478	27314	1.5	27260
		750	12587	17428	21154	24751	25993	26746	1.6	27260
		1000	12732	17352	21022	24554	25730	26418	1.6	27260

Initial Pt Force 0.1f_{yield}		Axial Load (excluding PT) 9000kN			Cantilever Length (5000mm)			Grade 300 Dissipaters		
	PT Dia.	Fuse Length (mm)	Yield (kNm)	1%drift (kNm)	2%drift (kNm)	3%drift (kNm)	4%drift (kNm)	6%drift (kNm)	λ	Fuse Area (mm^2)
Diameter (1000mm)	36mm	250	3835	5108	5198	5072	4913	4717	1.0	16342
		500	4021	5056	5066	4899	4682	4437	1.0	16342
		750	4161	5025	5023	4838	4600	4331	1.1	16342
		1000	4270	4996	5001	4803	4556	4277	1.1	16342
	50mm	250	3882	5181	5309	5217	5099	4940	1.0	16660
		500	4069	5128	5174	5039	4868	4661	1.1	16660
		750	4211	5096	5133	4981	4776	4554	1.1	16660
		1000	4321	5072	5108	4946	4731	4500	1.1	16660
	75mm	250	4008	5372	5589	5593	5569	5509	1.0	17486
		500	4190	5314	5454	5411	5328	5222	1.1	17486
		750	4336	5282	5401	5346	5232	5112	1.1	17486
		1000	4448	5257	5376	5312	5193	5059	1.1	17486
	100mm	250	4174	5635	5968	6105	6193	6265	1.0	18641
		500	4362	5574	5833	5908	5932	5967	1.1	18641
		750	4514	5543	5776	5832	5845	5859	1.1	18641
		1000	4630	5518	5752	5802	5801	5788	1.1	18641
	125mm	250	4391	5968	6437	6744	6943	7175	1.0	20126
		500	4587	5896	6299	6524	6698	6863	1.1	20126
		750	4742	5874	6237	6444	6596	6752	1.1	20126
		1000	4856	5842	6211	6398	6559	6682	1.1	20126
	150mm	250	4658	6367	6993	7475	7863	8218	1.0	21942
		500	4854	6288	6846	7245	7569	7906	1.1	21942
		750	5018	6261	6784	7146	7469	7771	1.1	21942
		1000	5138	6236	6755	7108	7425	7714	1.1	21942

Initial Pt Force 0.1F_{yield}		Axial Load (excluding PT) 9000kN			Cantilever Length (5000mm)			Grade 300 Dissipaters		
	PT Dia.	Fuse Length (mm)	Yield (kNm)	1%drift (kNm)	2%drift (kNm)	3%drift (kNm)	4%drift (kNm)	6%drift (kNm)	λ	Fuse Area (mm^2)
Diameter (1200mm)	36mm	250	4879	6548	6708	6707	6621	6478	1.1	16385
		500	5129	6460	6545	6456	6303	6109	1.2	16385
		750	5298	6429	6486	6366	6182	5960	1.2	16385
		1000	5412	6412	6455	6319	6118	5880	1.2	16385
	50mm	250	4943	6661	6880	6940	6918	6843	1.1	16742
		500	5196	6571	6708	6686	6596	6469	1.2	16742
		750	5362	6539	6652	6591	6472	6317	1.2	16742
		1000	5478	6522	6618	6544	6408	6237	1.2	16742
	75mm	250	5103	6947	7310	7522	7666	7759	1.1	17670
		500	5362	6857	7130	7263	7333	7372	1.2	17670
		750	5532	6824	7071	7164	7205	7216	1.3	17670
		1000	5653	6802	7040	7112	7139	7133	1.3	17670
	100mm	250	5329	7346	7898	8309	8662	8977	1.2	18968
		500	5592	7250	7709	8038	8323	8570	1.2	18968
		750	5768	7207	7649	7929	8180	8408	1.3	18968
		1000	5896	7184	7613	7880	8111	8321	1.3	18968
	125mm	250	5621	7841	8631	9282	9883	10449	1.2	20638
		500	5893	7744	8434	8977	9520	10018	1.3	20638
		750	6070	7698	8358	8875	9366	9840	1.3	20638
		1000	6203	7665	8325	8822	9294	9749	1.3	20638
	150mm	250	5979	8437	9512	10391	11281	12137	1.2	22678
		500	6247	8332	9280	10086	10884	11689	1.3	22678
		750	6433	8288	9205	9986	10747	11486	1.3	22678
		1000	6575	8245	9159	9934	10651	11390	1.3	22678

Initial Pt Force 0.1f_{yield}		Axial Load (excluding PT) 9000kN			Cantilever Length (5000mm)			Grade 300 Dissipaters		
	PT Dia.	Fuse Length (mm)	Yield (kNm)	1%drift (kNm)	2%drift (kNm)	3%drift (kNm)	4%drift (kNm)	6%drift (kNm)	λ	Fuse Area (mm^2)
Diameter (1500mm)	36mm	250	6633	8756	9122	9246	9270	9141	1.2	16448
		500	6899	8625	8856	8871	8811	8625	1.3	16448
		750	7074	8583	8761	8729	8626	8400	1.4	16448
		1000	7194	8559	8714	8655	8528	8267	1.4	16448
	50mm	250	6723	8936	9411	9647	9786	9705	1.2	16865
		500	6993	8804	9140	9266	9318	9179	1.3	16865
		750	7171	8761	9046	9121	9131	8951	1.4	16865
		1000	7293	8738	8995	9046	9031	8820	1.4	16865
	75mm	250	6958	9408	10148	10663	11086	11154	1.3	17946
		500	7236	9272	9863	10264	10598	10600	1.4	17946
		750	7422	9222	9765	10113	10402	10361	1.4	17946
		1000	7546	9204	9715	10034	10298	10231	1.4	17946
	100mm	250	7287	10054	11142	12032	12830	13145	1.3	19459
		500	7572	9906	10844	11608	12312	12552	1.4	19459
		750	7768	9861	10737	11447	12106	12297	1.5	19459
		1000	7900	9835	10683	11365	11996	12159	1.5	19459
	125mm	250	7708	10878	12380	13715	14962	15649	1.4	21404
		500	8007	10713	12059	13259	14407	15007	1.5	21404
		750	8211	10658	11946	13087	14183	14732	1.5	21404
		1000	8352	10632	11891	12999	14066	14583	1.5	21404
	150mm	250	8215	11855	13830	15673	17428	18637	1.4	23782
		500	8530	11670	13481	15180	16826	17934	1.5	23782
		750	8751	11612	13355	14994	16587	17635	1.5	23782
		1000	8903	11584	13305	14897	16458	17473	1.6	23782

Initial Pt Force $0.1f_{yield}$		Axial Load (excluding PT) 9000kN			Cantilever Length (5000mm)			Grade 300 Dissipaters		
	PT Dia.	Fuse Length (mm)	Yield (kNm)	1%drift (kNm)	2%drift (kNm)	3%drift (kNm)	4%drift (kNm)	6%drift (kNm)	λ	Fuse Area (mm^2)
Diameter (1800mm)	36mm	250	8446	11059	11594	11871	11911	11762	1.3	16512
		500	8687	10869	11223	11356	11284	11117	1.4	16512
		750	8948	10796	11083	11142	11020	10815	1.4	16512
		1000	9044	10753	11005	11028	10879	10648	1.5	16512
	50mm	250	8570	11335	12038	12488	12626	12527	1.3	16987
		500	8813	11140	11655	11963	11985	11858	1.4	16987
		750	9084	11067	11516	11749	11712	11546	1.5	16987
		1000	9182	11024	11438	11631	11565	11374	1.5	16987
	75mm	250	8900	12043	13169	14054	14447	14503	1.4	18222
		500	9147	11838	12765	13500	13785	13769	1.5	18222
		750	9428	11755	12621	13283	13492	13429	1.5	18222
		1000	9531	11717	12542	13161	13332	13242	1.6	18222
	100mm	250	9359	13014	14707	16169	16956	17172	1.4	19949
		500	9605	12790	14274	15574	16241	16403	1.5	19949
		750	9912	12705	14115	15343	15938	16034	1.6	19949
		1000	10016	12663	14034	15221	15773	15824	1.6	19949
	125mm	250	9947	14238	16617	18777	20123	20541	1.5	22171
		500	10197	13991	16145	18130	19339	19695	1.6	22171
		750	10525	13905	15972	17880	19009	19303	1.7	22171
		1000	10637	13861	15884	17748	18832	19086	1.7	22171
	150mm	250	10660	15678	18862	21824	23915	24578	1.5	24886
		500	10913	15417	18344	21113	23047	23639	1.7	24886
		750	11273	15317	18154	20839	22685	23207	1.7	24886
		1000	11386	15274	18059	20695	22488	22968	1.7	24886

Initial Pt Force 0.1f_{yield}		Axial Load (excluding PT) 9000kN			Cantilever Length (5000mm)			Grade 300 Dissipaters		
	PT Dia.	Fuse Length (mm)	Yield (kNm)	1%drift (kNm)	2%drift (kNm)	3%drift (kNm)	4%drift (kNm)	6%drift (kNm)	λ	Fuse Area (mm^2)
Diameter (2000mm)	36mm	250	10505	13545	14322	14778	14842	14811	1.1	19658
		500	10800	13268	13783	14027	14012	13950	1.2	19658
		750	10947	13170	13572	13730	13648	13520	1.2	19658
		1000	11072	13096	13458	13572	13450	13280	1.3	19658
	50mm	250	10680	13923	14916	15587	15722	15726	1.1	20270
		500	10981	13635	14363	14823	14863	14841	1.2	20270
		750	11131	13535	14152	14514	14486	14400	1.3	20270
		1000	11258	13461	14033	14350	14282	14158	1.3	20270
	75mm	250	11138	14888	16432	17665	17996	18091	1.2	21857
		500	11449	14581	15845	16868	17056	17149	1.3	21857
		750	11602	14475	15632	16533	16647	16682	1.3	21857
		1000	11738	14399	15501	16356	16425	16421	1.4	21857
	100mm	250	11773	16210	18497	20501	21100	21423	1.2	24078
		500	12106	15881	17862	19649	20097	20363	1.4	24078
		750	12262	15758	17628	19308	19639	19843	1.4	24078
		1000	12403	15688	17506	19116	19391	19553	1.4	24078
	125mm	250	12589	17875	21066	23977	25009	25597	1.3	26935
		500	12943	17514	20371	23045	23904	24445	1.4	26935
		750	13103	17373	20113	22674	23421	23859	1.5	26935
		1000	13255	17303	19981	22477	23151	23528	1.5	26935
	150mm	250	13575	19862	24095	28053	29700	30585	1.3	30426
		500	13955	19458	23328	27024	28469	29295	1.5	30426
		750	14124	19307	23044	26613	27932	28663	1.5	30426
		1000	14282	19223	22898	26396	27641	28310	1.5	30426

Initial Pt Force 0.1f_{yield}		Axial Load (excluding PT) 1500kN			Cantilever Length (6000mm)			Grade 300 Dissipaters		
	PT Dia.	Fuse Length (mm)	Yield (kNm)	1%drift (kNm)	2%drift (kNm)	3%drift (kNm)	4%drift (kNm)	6%drift (kNm)	λ	Fuse Area (mm^2)
Diameter (1000mm)	36mm	250	938	1151	1201	1227	1238	1244	1.1	3385
		500	962	1137	1168	1179	1183	1183	1.1	3385
		750	981	1126	1154	1161	1162	1160	1.2	3385
		1000	996	1122	1147	1152	1151	1147	1.2	3385
	50mm	250	1002	1262	1361	1440	1509	1567	1.1	3743
		500	1028	1246	1328	1389	1444	1495	1.2	3743
		750	1048	1235	1311	1368	1419	1468	1.2	3743
		1000	1066	1230	1303	1358	1407	1453	1.3	3743
	75mm	250	1165	1537	1756	1956	2148	2335	1.2	4671
		500	1196	1519	1717	1899	2077	2252	1.3	4671
		750	1220	1511	1702	1878	2049	2217	1.3	4671
		1000	1243	1502	1691	1863	2030	2195	1.4	4671
	100mm	250	1387	1905	2273	2623	2965	3301	1.3	5971
		500	1426	1886	2225	2554	2878	3199	1.4	5971
		750	1453	1877	2208	2529	2845	3159	1.4	5971
		1000	1484	1868	2200	2516	2828	3138	1.4	5971
	125mm	250	1669	2358	2888	3414	3924	4430	1.3	7642
		500	1713	2333	2829	3324	3817	4304	1.4	7642
		750	1745	2323	2814	3294	3777	4256	1.4	7642
		1000	1783	2315	2806	3277	3756	4230	1.4	7642
	150mm	250	2002	2891	3594	4297	4993	5682	1.3	9685
		500	2058	2852	3527	4191	4860	5526	1.4	9685
		750	2093	2840	3502	4155	4812	5468	1.4	9685
		1000	2137	2834	3491	4138	4796	5448	1.4	9685

Initial Pt Force 0.1f_{yield}		Axial Load (excluding PT) 1500kN			Cantilever Length (6000mm)			Grade 300 Dissipaters		
	PT Dia.	Fuse Length (mm)	Yield (kNm)	1%drift (kNm)	2%drift (kNm)	3%drift (kNm)	4%drift (kNm)	6%drift (kNm)	λ	Fuse Area (mm^2)
Diameter (1200mm)	36mm	250	1181	1456	1539	1596	1652	1677	1.2	3433
		500	1203	1430	1494	1539	1578	1592	1.3	3433
		750	1224	1421	1478	1518	1551	1557	1.3	3433
		1000	1242	1415	1470	1507	1537	1538	1.3	3433
	50mm	250	1267	1614	1779	1913	2037	2131	1.3	3835
		500	1291	1588	1726	1847	1961	2037	1.4	3835
		750	1314	1576	1708	1822	1931	2000	1.4	3835
		1000	1336	1569	1698	1810	1916	1981	1.4	3835
	75mm	250	1485	2012	2363	2695	3016	3298	1.4	4878
		500	1515	1984	2305	2609	2907	3177	1.5	4878
		750	1546	1966	2279	2575	2865	3128	1.5	4878
		1000	1575	1957	2265	2557	2843	3102	1.5	4878
	100mm	250	1785	2542	3129	3695	4250	4795	1.5	6339
		500	1824	2506	3058	3594	4125	4653	1.5	6339
		750	1862	2490	3033	3557	4077	4596	1.6	6339
		1000	1901	2478	3013	3532	4048	4560	1.6	6339
	125mm	250	2163	3188	4049	4886	5712	6525	1.5	8217
		500	2215	3147	3960	4761	5556	6349	1.6	8217
		750	2256	3132	3929	4715	5497	6277	1.6	8217
		1000	2303	3117	3913	4691	5466	6238	1.6	8217
	150mm	250	2613	3940	5095	6237	7360	8470	1.5	10513
		500	2680	3892	4992	6082	7168	8251	1.6	10513
		750	2721	3875	4955	6025	7095	8162	1.6	10513
		1000	2780	3862	4931	5997	7057	8116	1.6	10513

Initial Pt Force 0.1F_{yield}		Axial Load (excluding PT) 1500kN			Cantilever Length (6000mm)			Grade 300 Dissipaters		
	PT Dia.	Fuse Length (mm)	Yield (kNm)	1%drift (kNm)	2%drift (kNm)	3%drift (kNm)	4%drift (kNm)	6%drift (kNm)	λ	Fuse Area (mm^2)
Diameter (1500mm)	36mm	250	1567	1927	2080	2222	2302	2306	1.3	3504
		500	1582	1892	2020	2133	2195	2189	1.4	3504
		750	1605	1880	1998	2100	2151	2137	1.4	3504
		1000	1625	1872	1987	2083	2128	2109	1.5	3504
	50mm	250	1693	2176	2455	2721	2901	2939	1.4	3973
		500	1709	2135	2386	2622	2781	2807	1.5	3973
		750	1736	2120	2361	2586	2732	2749	1.5	3973
		1000	1761	2113	2349	2568	2706	2717	1.6	3973
	75mm	250	2012	2802	3397	3962	4419	4544	1.5	5189
		500	2034	2747	3302	3840	4269	4375	1.7	5189
		750	2070	2727	3268	3794	4210	4301	1.7	5189
		1000	2105	2717	3251	3770	4179	4262	1.7	5189
	100mm	250	2449	3635	4641	5620	6518	6736	1.6	6891
		500	2480	3573	4521	5452	6310	6517	1.8	6891
		750	2526	3543	4471	5384	6227	6422	1.8	6891
		1000	2577	3527	4446	5350	6183	6371	1.8	6891
	125mm	250	2998	4655	6136	7584	9011	9490	1.7	9080
		500	3040	4578	5989	7382	8767	9207	1.8	9080
		750	3099	4545	5936	7305	8670	9081	1.8	9080
		1000	3166	4521	5898	7258	8613	9008	1.9	9080
	150mm	250	3656	5842	7855	9832	11782	12719	1.7	11755
		500	3714	5745	7671	9579	11475	12361	1.8	11755
		750	3782	5713	7606	9481	11353	12207	1.8	11755
		1000	3864	5684	7572	9432	11287	12124	1.9	11755

Initial Pt Force 0.1f_{yield}		Axial Load (excluding PT) 1500kN			Cantilever Length (6000mm)			Grade 300 Dissipaters		
	PT Dia.	Fuse Length (mm)	Yield (kNm)	1%drift (kNm)	2%drift (kNm)	3%drift (kNm)	4%drift (kNm)	6%drift (kNm)	λ	Fuse Area (mm^2)
Diameter (1800mm)	36mm	250	1951	2424	2680	2892	2938	2958	1.4	3576
		500	1964	2377	2590	2770	2797	2811	1.5	3576
		750	2001	2361	2557	2722	2737	2740	1.5	3576
		1000	2016	2350	2541	2697	2704	2700	1.5	3576
	50mm	250	2122	2779	3224	3627	3723	3787	1.5	4111
		500	2135	2725	3122	3489	3564	3619	1.6	4111
		750	2180	2706	3086	3434	3495	3538	1.7	4111
		1000	2200	2695	3068	3406	3458	3493	1.7	4111
	75mm	250	2560	3679	4582	5471	5724	5899	1.7	5499
		500	2572	3604	4456	5294	5514	5678	1.8	5499
		750	2635	3578	4409	5226	5424	5572	1.9	5499
		1000	2667	3565	4385	5192	5375	5513	1.9	5499
	100mm	250	3162	4892	6416	7895	8449	8782	1.8	7443
		500	3171	4787	6236	7666	8171	8487	1.9	7443
		750	3258	4750	6170	7576	8057	8347	2.0	7443
		1000	3305	4730	6136	7528	7995	8269	2.0	7443
	125mm	250	3919	6374	8647	10871	11897	12393	1.8	9942
		500	3926	6251	8417	10563	11525	12012	2.0	9942
		750	4038	6196	8324	10434	11367	11833	2.0	9942
		1000	4100	6167	8274	10366	11283	11734	2.1	9942
	150mm	250	4813	8105	11214	14264	15982	16756	1.8	12997
		500	4828	7954	10929	13883	15517	16253	2.0	12997
		750	4968	7893	10826	13732	15319	16008	2.0	12997
		1000	5048	7851	10758	13650	15204	15873	2.1	12997

Initial Pt Force 0.1F_{yield}		Axial Load (excluding PT) 2000			Cantilever Length (6000mm)			Grade 300 Dissipaters		
	PT Dia.	Fuse Length (mm)	Yield (kNm)	1%drift (kNm)	2%drift (kNm)	3%drift (kNm)	4%drift (kNm)	6%drift (kNm)	λ	Fuse Area (mm^2)
Diameter (1000mm)	36mm	250	1092	1340	1361	1348	1324	1293	1.1	3871
		500	1131	1325	1327	1300	1261	1214	1.2	3871
		750	1152	1319	1315	1280	1234	1183	1.2	3871
		1000	1172	1312	1306	1268	1220	1167	1.2	3871
	50mm	250	1144	1430	1492	1523	1542	1554	1.1	4165
		500	1184	1415	1457	1471	1477	1477	1.2	4165
		750	1207	1409	1445	1453	1450	1443	1.2	4165
		1000	1229	1401	1435	1439	1434	1424	1.2	4165
	75mm	250	1277	1660	1820	1952	2074	2189	1.2	4926
		500	1322	1641	1780	1893	2000	2103	1.3	4926
		750	1349	1635	1766	1872	1972	2069	1.3	4926
		1000	1375	1627	1758	1862	1958	2051	1.3	4926
	100mm	250	1459	1971	2248	2510	2760	3003	1.3	5992
		500	1514	1947	2201	2442	2674	2902	1.4	5992
		750	1543	1939	2188	2417	2641	2862	1.4	5992
		1000	1575	1932	2178	2404	2625	2842	1.4	5992
	125mm	250	1689	2352	2764	3169	3572	3957	1.3	7363
		500	1750	2320	2709	3094	3464	3837	1.4	7363
		750	1789	2311	2697	3059	3426	3790	1.4	7363
		1000	1825	2307	2686	3046	3404	3766	1.4	7363
	150mm	250	1968	2804	3358	3922	4471	5011	1.3	9038
		500	2037	2760	3298	3821	4348	4874	1.4	9038
		750	2083	2745	3282	3786	4303	4820	1.4	9038
		1000	2126	2743	3272	3775	4277	4787	1.4	9038

Initial Pt Force 0.1f_{yield}		Axial Load (excluding PT) 2000			Cantilever Length (6000mm)			Grade 300 Dissipaters		
	PT Dia.	Fuse Length (mm)	Yield (kNm)	1%drift (kNm)	2%drift (kNm)	3%drift (kNm)	4%drift (kNm)	6%drift (kNm)	λ	Fuse Area (mm^2)
Diameter (1200mm)	36mm	250	1384	1704	1763	1785	1783	1776	1.2	3908
		500	1423	1682	1714	1713	1701	1684	1.3	3908
		750	1451	1669	1694	1686	1669	1647	1.3	3908
		1000	1474	1662	1684	1673	1653	1628	1.3	3908
	50mm	250	1454	1834	1958	2048	2119	2175	1.3	4236
		500	1496	1811	1909	1972	2026	2075	1.4	4236
		750	1526	1799	1886	1942	1990	2034	1.4	4236
		1000	1550	1789	1874	1927	1972	2012	1.4	4236
	75mm	250	1632	2165	2445	2693	2929	3155	1.4	5087
		500	1684	2137	2387	2611	2827	3039	1.5	5087
		750	1715	2125	2366	2578	2783	2984	1.5	5087
		1000	1747	2113	2350	2558	2758	2955	1.5	5087
	100mm	250	1880	2607	3087	3536	3972	4399	1.5	6278
		500	1939	2575	3018	3438	3851	4260	1.6	6278
		750	1975	2564	2993	3402	3804	4203	1.6	6278
		1000	2014	2550	2981	3383	3779	4173	1.6	6278
	125mm	250	2192	3152	3858	4543	5211	5868	1.5	7810
		500	2260	3112	3777	4425	5065	5701	1.6	7810
		750	2302	3100	3749	4382	5009	5633	1.6	7810
		1000	2350	3088	3734	4360	4980	5597	1.7	7810
	150mm	250	2565	3788	4741	5680	6609	7521	1.5	9682
		500	2645	3739	4648	5542	6434	7320	1.6	9682
		750	2694	3726	4616	5490	6367	7239	1.6	9682
		1000	2749	3717	4602	5461	6332	7195	1.7	9682

Initial Pt Force 0.1Fyield		Axial Load (excluding PT) 2000			Cantilever Length (6000mm)			Grade 300 Dissipaters		
	PT Dia.	Fuse Length (mm)	Yield (kNm)	1%drift (kNm)	2%drift (kNm)	3%drift (kNm)	4%drift (kNm)	6%drift (kNm)	λ	Fuse Area (mm^2)
Diameter (1500mm)	36mm	250	1847	2271	2389	2471	2545	2525	1.3	3964
		500	1880	2230	2317	2374	2427	2394	1.4	3964
		750	1910	2214	2292	2339	2379	2337	1.5	3964
		1000	1937	2208	2278	2321	2354	2305	1.5	3964
	50mm	250	1949	2476	2706	2892	3074	3107	1.4	4344
		500	1984	2433	2626	2790	2947	2965	1.5	4344
		750	2018	2416	2598	2751	2896	2902	1.6	4344
		1000	2049	2408	2583	2731	2871	2868	1.6	4344
	75mm	250	2211	2995	3499	3960	4395	4585	1.6	5329
		500	2253	2948	3401	3827	4244	4416	1.7	5329
		750	2295	2926	3364	3777	4182	4344	1.7	5329
		1000	2334	2913	3345	3751	4151	4306	1.8	5329
	100mm	250	2571	3694	4540	5351	6142	6630	1.7	6708
		500	2625	3636	4429	5197	5957	6414	1.8	6708
		750	2676	3612	4385	5133	5874	6317	1.8	6708
		1000	2727	3594	4358	5097	5830	6265	1.9	6708
	125mm	250	3023	4552	5804	7019	8211	9143	1.7	8481
		500	3096	4481	5668	6831	7985	8882	1.8	8481
		750	3155	4459	5620	6760	7895	8770	1.9	8481
		1000	3217	4433	5592	6724	7846	8708	1.9	8481
	150mm	250	3564	5550	7259	8927	10570	12111	1.7	10648
		500	3661	5464	7094	8700	10295	11791	1.9	10648
		750	3723	5437	7035	8613	10185	11654	1.9	10648
		1000	3795	5415	7006	8568	10127	11579	1.9	10648

Initial Pt Force 0.1f_{yield}		Axial Load (excluding PT) 2000			Cantilever Length (6000mm)			Grade 300 Dissipaters		
	PT Dia.	Fuse Length (mm)	Yield (kNm)	1%drift (kNm)	2%drift (kNm)	3%drift (kNm)	4%drift (kNm)	6%drift (kNm)	λ	Fuse Area (mm^2)
Diameter (1800mm)	36mm	250	2320	2855	3058	3231	3290	3274	1.4	4020
		500	2337	2799	2960	3097	3135	3110	1.5	4020
		750	2386	2780	2925	3045	3068	3031	1.6	4020
		1000	2410	2770	2907	3017	3031	2988	1.6	4020
	50mm	250	2459	3153	3514	3853	4012	4036	1.5	4451
		500	2477	3091	3410	3707	3841	3856	1.6	4451
		750	2534	3070	3372	3649	3768	3769	1.7	4451
		1000	2560	3058	3352	3620	3728	3721	1.7	4451
	75mm	250	2818	3910	4675	5400	5851	5978	1.7	5570
		500	2839	3831	4542	5227	5641	5755	1.8	5570
		750	2910	3803	4493	5161	5551	5650	1.9	5570
		1000	2947	3788	4468	5126	5504	5591	1.9	5570
	100mm	250	3310	4923	6232	7486	8366	8629	1.8	7137
		500	3335	4831	6056	7258	8104	8347	2.0	7137
		750	3428	4792	5991	7169	7993	8217	2.0	7137
		1000	3476	4774	5958	7122	7934	8146	2.1	7137
	125mm	250	3926	6169	8111	10003	11540	11985	1.9	9152
		500	3965	6062	7907	9728	11208	11620	2.0	9152
		750	4078	6015	7825	9613	11060	11451	2.1	9152
		1000	4142	5986	7779	9549	10979	11358	2.1	9152
	150mm	250	4668	7630	10288	12889	15279	15955	1.9	11614
		500	4719	7495	10037	12551	14868	15511	2.1	11614
		750	4856	7449	9945	12420	14694	15306	2.1	11614
		1000	4935	7407	9896	12350	14601	15190	2.2	11614

Initial Pt Force 0.1Fyield		Axial Load (excluding PT) 2000			Cantilever Length (6000mm)			Grade 300 Dissipaters		
	PT Dia.	Fuse Length (mm)	Yield (kNm)	1%drift (kNm)	2%drift (kNm)	3%drift (kNm)	4%drift (kNm)	6%drift (kNm)	λ	Fuse Area (mm^2)
Diameter (2000mm)	36mm	250	2656	3256	3532	3763	3790	3782	1.4	4057
		500	2686	3191	3412	3603	3610	3599	1.6	4057
		750	2713	3168	3367	3538	3529	3506	1.6	4057
		1000	2741	3156	3345	3504	3485	3453	1.7	4057
	50mm	250	2824	3623	4103	4545	4634	4672	1.6	4522
		500	2857	3551	3970	4371	4434	4469	1.7	4522
		750	2890	3525	3923	4300	4345	4366	1.8	4522
		1000	2921	3512	3899	4263	4296	4307	1.8	4522
	75mm	250	3258	4555	5536	6489	6786	6944	1.7	5731
		500	3297	4462	5378	6274	6537	6690	1.9	5731
		750	3340	4430	5319	6188	6427	6561	2.0	5731
		1000	3387	4414	5289	6145	6366	6489	2.0	5731
	100mm	250	3858	5818	7477	9076	9728	10053	1.9	7423
		500	3903	5696	7266	8810	9411	9728	2.1	7423
		750	3960	5652	7189	8704	9272	9565	2.1	7423
		1000	4024	5630	7148	8648	9198	9473	2.2	7423
	125mm	250	4616	7368	9853	12276	13439	13954	2.0	9599
		500	4668	7226	9588	11922	13033	13540	2.1	9599
		750	4739	7165	9482	11777	12856	13338	2.2	9599
		1000	4824	7134	9428	11700	12759	13225	2.3	9599
	150mm	250	5528	9187	12597	15935	17870	18668	2.0	12258
		500	5582	9012	12277	15511	17365	18130	2.2	12258
		750	5670	8945	12159	15342	17140	17864	2.2	12258
		1000	5776	8902	12084	15243	17012	17715	2.3	12258

Initial Pt Force 0.1f_{yield}		Axial Load (excluding PT) 3000kN			Cantilever Length (6000mm)			Grade 300 Dissipaters		
	PT Dia.	Fuse Length (mm)	Yield (kNm)	1%drift (kNm)	2%drift (kNm)	3%drift (kNm)	4%drift (kNm)	6%drift (kNm)	λ	Fuse Area (mm^2)
Diameter (1000mm)	36mm	250	1092	1340	1361	1348	1324	1293	1.1	3871
		500	1131	1325	1327	1300	1261	1214	1.2	3871
		750	1152	1319	1315	1280	1234	1183	1.2	3871
		1000	1172	1312	1306	1268	1220	1167	1.2	3871
	50mm	250	1144	1430	1492	1523	1542	1554	1.1	4165
		500	1184	1415	1457	1471	1477	1477	1.2	4165
		750	1207	1409	1445	1453	1450	1443	1.2	4165
		1000	1229	1401	1435	1439	1434	1424	1.2	4165
	75mm	250	1277	1660	1820	1952	2074	2189	1.2	4926
		500	1322	1641	1780	1893	2000	2103	1.3	4926
		750	1349	1635	1766	1872	1972	2069	1.3	4926
		1000	1375	1627	1758	1862	1958	2051	1.3	4926
	100mm	250	1459	1971	2248	2510	2760	3003	1.3	5992
		500	1514	1947	2201	2442	2674	2902	1.4	5992
		750	1543	1939	2188	2417	2641	2862	1.4	5992
		1000	1575	1932	2178	2404	2625	2842	1.4	5992
	125mm	250	1689	2352	2764	3169	3572	3957	1.3	7363
		500	1750	2320	2709	3094	3464	3837	1.4	7363
		750	1789	2311	2697	3059	3426	3790	1.4	7363
		1000	1825	2307	2686	3046	3404	3766	1.4	7363
	150mm	250	1968	2804	3358	3922	4471	5011	1.3	9038
		500	2037	2760	3298	3821	4348	4874	1.4	9038
		750	2083	2745	3282	3786	4303	4820	1.4	9038
		1000	2126	2743	3272	3775	4277	4787	1.4	9038

Initial Pt Force 0.1Fyield		Axial Load (excluding PT) 3000kN			Cantilever Length (6000mm)			Grade 300 Dissipaters		
	PT Dia.	Fuse Length (mm)	Yield (kNm)	1%drift (kNm)	2%drift (kNm)	3%drift (kNm)	4%drift (kNm)	6%drift (kNm)	λ	Fuse Area (mm^2)
Diameter (1200mm)	36mm	250	1384	1704	1763	1785	1783	1776	1.2	3908
		500	1423	1682	1714	1713	1701	1684	1.3	3908
		750	1451	1669	1694	1686	1669	1647	1.3	3908
		1000	1474	1662	1684	1673	1653	1628	1.3	3908
	50mm	250	1454	1834	1958	2048	2119	2175	1.3	4236
		500	1496	1811	1909	1972	2026	2075	1.4	4236
		750	1526	1799	1886	1942	1990	2034	1.4	4236
		1000	1550	1789	1874	1927	1972	2012	1.4	4236
	75mm	250	1632	2165	2445	2693	2929	3155	1.4	5087
		500	1684	2137	2387	2611	2827	3039	1.5	5087
		750	1715	2125	2366	2578	2783	2984	1.5	5087
		1000	1747	2113	2350	2558	2758	2955	1.5	5087
	100mm	250	1880	2607	3087	3536	3972	4399	1.5	6278
		500	1939	2575	3018	3438	3851	4260	1.6	6278
		750	1975	2564	2993	3402	3804	4203	1.6	6278
		1000	2014	2550	2981	3383	3779	4173	1.6	6278
	125mm	250	2192	3152	3858	4543	5211	5868	1.5	7810
		500	2260	3112	3777	4425	5065	5701	1.6	7810
		750	2302	3100	3749	4382	5009	5633	1.6	7810
		1000	2350	3088	3734	4360	4980	5597	1.7	7810
	150mm	250	2565	3788	4741	5680	6609	7521	1.5	9682
		500	2645	3739	4648	5542	6434	7320	1.6	9682
		750	2694	3726	4616	5490	6367	7239	1.6	9682
		1000	2749	3717	4602	5461	6332	7195	1.7	9682

Initial Pt Force 0.1f_{yield}		Axial Load (excluding PT) 3000kN			Cantilever Length (6000mm)			Grade 300 Dissipaters		
	PT Dia.	Fuse Length (mm)	Yield (kNm)	1%drift (kNm)	2%drift (kNm)	3%drift (kNm)	4%drift (kNm)	6%drift (kNm)	λ	Fuse Area (mm^2)
Diameter (1500mm)	36mm	250	1847	2271	2389	2471	2545	2525	1.3	3964
		500	1880	2230	2317	2374	2427	2394	1.4	3964
		750	1910	2214	2292	2339	2379	2337	1.5	3964
		1000	1937	2208	2278	2321	2354	2305	1.5	3964
	50mm	250	1949	2476	2706	2892	3074	3107	1.4	4344
		500	1984	2433	2626	2790	2947	2965	1.5	4344
		750	2018	2416	2598	2751	2896	2902	1.6	4344
		1000	2049	2408	2583	2731	2871	2868	1.6	4344
	75mm	250	2211	2995	3499	3960	4395	4585	1.6	5329
		500	2253	2948	3401	3827	4244	4416	1.7	5329
		750	2295	2926	3364	3777	4182	4344	1.7	5329
		1000	2334	2913	3345	3751	4151	4306	1.8	5329
	100mm	250	2571	3694	4540	5351	6142	6630	1.7	6708
		500	2625	3636	4429	5197	5957	6414	1.8	6708
		750	2676	3612	4385	5133	5874	6317	1.8	6708
		1000	2727	3594	4358	5097	5830	6265	1.9	6708
	125mm	250	3023	4552	5804	7019	8211	9143	1.7	8481
		500	3096	4481	5668	6831	7985	8882	1.8	8481
		750	3155	4459	5620	6760	7895	8770	1.9	8481
		1000	3217	4433	5592	6724	7846	8708	1.9	8481
	150mm	250	3564	5550	7259	8927	10570	12111	1.7	10648
		500	3661	5464	7094	8700	10295	11791	1.9	10648
		750	3723	5437	7035	8613	10185	11654	1.9	10648
		1000	3795	5415	7006	8568	10127	11579	1.9	10648

Initial Pt Force 0.1Fyield		Axial Load (excluding PT) 3000kN			Cantilever Length (6000mm)			Grade 300 Dissipaters		
	PT Dia.	Fuse Length (mm)	Yield (kNm)	1%drift (kNm)	2%drift (kNm)	3%drift (kNm)	4%drift (kNm)	6%drift (kNm)	λ	Fuse Area (mm^2)
Diameter (1800mm)	36mm	250	2320	2855	3058	3231	3290	3274	1.4	4020
		500	2337	2799	2960	3097	3135	3110	1.5	4020
		750	2386	2780	2925	3045	3068	3031	1.6	4020
		1000	2410	2770	2907	3017	3031	2988	1.6	4020
	50mm	250	2459	3153	3514	3853	4012	4036	1.5	4451
		500	2477	3091	3410	3707	3841	3856	1.6	4451
		750	2534	3070	3372	3649	3768	3769	1.7	4451
		1000	2560	3058	3352	3620	3728	3721	1.7	4451
	75mm	250	2818	3910	4675	5400	5851	5978	1.7	5570
		500	2839	3831	4542	5227	5641	5755	1.8	5570
		750	2910	3803	4493	5161	5551	5650	1.9	5570
		1000	2947	3788	4468	5126	5504	5591	1.9	5570
	100mm	250	3310	4923	6232	7486	8366	8629	1.8	7137
		500	3335	4831	6056	7258	8104	8347	2.0	7137
		750	3428	4792	5991	7169	7993	8217	2.0	7137
		1000	3476	4774	5958	7122	7934	8146	2.1	7137
	125mm	250	3926	6169	8111	10003	11540	11985	1.9	9152
		500	3965	6062	7907	9728	11208	11620	2.0	9152
		750	4078	6015	7825	9613	11060	11451	2.1	9152
		1000	4142	5986	7779	9549	10979	11358	2.1	9152
	150mm	250	4668	7630	10288	12889	15279	15955	1.9	11614
		500	4719	7495	10037	12551	14868	15511	2.1	11614
		750	4856	7449	9945	12420	14694	15306	2.1	11614
		1000	4935	7407	9896	12350	14601	15190	2.2	11614

Initial Pt Force 0.1f_{yield}		Axial Load (excluding PT) 3000kN			Cantilever Length (6000mm)			Grade 300 Dissipaters		
	PT Dia.	Fuse Length (mm)	Yield (kNm)	1%drift (kNm)	2%drift (kNm)	3%drift (kNm)	4%drift (kNm)	6%drift (kNm)	λ	Fuse Area (mm^2)
Diameter (2000mm)	36mm	250	2656	3256	3532	3763	3790	3782	1.4	4057
		500	2686	3191	3412	3603	3610	3599	1.6	4057
		750	2713	3168	3367	3538	3529	3506	1.6	4057
		1000	2741	3156	3345	3504	3485	3453	1.7	4057
	50mm	250	2824	3623	4103	4545	4634	4672	1.6	4522
		500	2857	3551	3970	4371	4434	4469	1.7	4522
		750	2890	3525	3923	4300	4345	4366	1.8	4522
		1000	2921	3512	3899	4263	4296	4307	1.8	4522
	75mm	250	3258	4555	5536	6489	6786	6944	1.7	5731
		500	3297	4462	5378	6274	6537	6690	1.9	5731
		750	3340	4430	5319	6188	6427	6561	2.0	5731
		1000	3387	4414	5289	6145	6366	6489	2.0	5731
	100mm	250	3858	5818	7477	9076	9728	10053	1.9	7423
		500	3903	5696	7266	8810	9411	9728	2.1	7423
		750	3960	5652	7189	8704	9272	9565	2.1	7423
		1000	4024	5630	7148	8648	9198	9473	2.2	7423
	125mm	250	4616	7368	9853	12276	13439	13954	2.0	9599
		500	4668	7226	9588	11922	13033	13540	2.1	9599
		750	4739	7165	9482	11777	12856	13338	2.2	9599
		1000	4824	7134	9428	11700	12759	13225	2.3	9599
	150mm	250	5528	9187	12597	15935	17870	18668	2.0	12258
		500	5582	9012	12277	15511	17365	18130	2.2	12258
		750	5670	8945	12159	15342	17140	17864	2.2	12258
		1000	5776	8902	12084	15243	17012	17715	2.3	12258

Initial Pt Force 0.1F_{yield}		Axial Load (excluding PT) 4500kN			Cantilever Length (6000mm)			Grade 300 Dissipaters		
	PT Dia.	Fuse Length (mm)	Yield (kNm)	1%drift (kNm)	2%drift (kNm)	3%drift (kNm)	4%drift (kNm)	6%drift (kNm)	λ	Fuse Area (mm^2)
Diameter (1000mm)	36mm	250	1092	1340	1361	1348	1324	1293	1.1	3871
		500	1131	1325	1327	1300	1261	1214	1.2	3871
		750	1152	1319	1315	1280	1234	1183	1.2	3871
		1000	1172	1312	1306	1268	1220	1167	1.2	3871
	50mm	250	1144	1430	1492	1523	1542	1554	1.1	4165
		500	1184	1415	1457	1471	1477	1477	1.2	4165
		750	1207	1409	1445	1453	1450	1443	1.2	4165
		1000	1229	1401	1435	1439	1434	1424	1.2	4165
	75mm	250	1277	1660	1820	1952	2074	2189	1.2	4926
		500	1322	1641	1780	1893	2000	2103	1.3	4926
		750	1349	1635	1766	1872	1972	2069	1.3	4926
		1000	1375	1627	1758	1862	1958	2051	1.3	4926
	100mm	250	1459	1971	2248	2510	2760	3003	1.3	5992
		500	1514	1947	2201	2442	2674	2902	1.4	5992
		750	1543	1939	2188	2417	2641	2862	1.4	5992
		1000	1575	1932	2178	2404	2625	2842	1.4	5992
	125mm	250	1689	2352	2764	3169	3572	3957	1.3	7363
		500	1750	2320	2709	3094	3464	3837	1.4	7363
		750	1789	2311	2697	3059	3426	3790	1.4	7363
		1000	1825	2307	2686	3046	3404	3766	1.4	7363
	150mm	250	1968	2804	3358	3922	4471	5011	1.3	9038
		500	2037	2760	3298	3821	4348	4874	1.4	9038
		750	2083	2745	3282	3786	4303	4820	1.4	9038
		1000	2126	2743	3272	3775	4277	4787	1.4	9038

Initial Pt Force 0.1f_{yield}		Axial Load (excluding PT) 4500kN			Cantilever Length (6000mm)			Grade 300 Dissipaters		
	PT Dia.	Fuse Length (mm)	Yield (kNm)	1%drift (kNm)	2%drift (kNm)	3%drift (kNm)	4%drift (kNm)	6%drift (kNm)	λ	Fuse Area (mm^2)
Diameter (1200mm)	36mm	250	1384	1704	1763	1785	1783	1776	1.2	3908
		500	1423	1682	1714	1713	1701	1684	1.3	3908
		750	1451	1669	1694	1686	1669	1647	1.3	3908
		1000	1474	1662	1684	1673	1653	1628	1.3	3908
	50mm	250	1454	1834	1958	2048	2119	2175	1.3	4236
		500	1496	1811	1909	1972	2026	2075	1.4	4236
		750	1526	1799	1886	1942	1990	2034	1.4	4236
		1000	1550	1789	1874	1927	1972	2012	1.4	4236
	75mm	250	1632	2165	2445	2693	2929	3155	1.4	5087
		500	1684	2137	2387	2611	2827	3039	1.5	5087
		750	1715	2125	2366	2578	2783	2984	1.5	5087
		1000	1747	2113	2350	2558	2758	2955	1.5	5087
	100mm	250	1880	2607	3087	3536	3972	4399	1.5	6278
		500	1939	2575	3018	3438	3851	4260	1.6	6278
		750	1975	2564	2993	3402	3804	4203	1.6	6278
		1000	2014	2550	2981	3383	3779	4173	1.6	6278
	125mm	250	2192	3152	3858	4543	5211	5868	1.5	7810
		500	2260	3112	3777	4425	5065	5701	1.6	7810
		750	2302	3100	3749	4382	5009	5633	1.6	7810
		1000	2350	3088	3734	4360	4980	5597	1.7	7810
	150mm	250	2565	3788	4741	5680	6609	7521	1.5	9682
		500	2645	3739	4648	5542	6434	7320	1.6	9682
		750	2694	3726	4616	5490	6367	7239	1.6	9682
		1000	2749	3717	4602	5461	6332	7195	1.7	9682

Initial Pt Force 0.1F_{yield}		Axial Load (excluding PT) 4500kN			Cantilever Length (6000mm)			Grade 300 Dissipaters		
	PT Dia.	Fuse Length (mm)	Yield (kNm)	1%drift (kNm)	2%drift (kNm)	3%drift (kNm)	4%drift (kNm)	6%drift (kNm)	λ	Fuse Area (mm^2)
Diameter (1500mm)	36mm	250	1847	2271	2389	2471	2545	2525	1.3	3964
		500	1880	2230	2317	2374	2427	2394	1.4	3964
		750	1910	2214	2292	2339	2379	2337	1.5	3964
		1000	1937	2208	2278	2321	2354	2305	1.5	3964
	50mm	250	1949	2476	2706	2892	3074	3107	1.4	4344
		500	1984	2433	2626	2790	2947	2965	1.5	4344
		750	2018	2416	2598	2751	2896	2902	1.6	4344
		1000	2049	2408	2583	2731	2871	2868	1.6	4344
	75mm	250	2211	2995	3499	3960	4395	4585	1.6	5329
		500	2253	2948	3401	3827	4244	4416	1.7	5329
		750	2295	2926	3364	3777	4182	4344	1.7	5329
		1000	2334	2913	3345	3751	4151	4306	1.8	5329
	100mm	250	2571	3694	4540	5351	6142	6630	1.7	6708
		500	2625	3636	4429	5197	5957	6414	1.8	6708
		750	2676	3612	4385	5133	5874	6317	1.8	6708
		1000	2727	3594	4358	5097	5830	6265	1.9	6708
	125mm	250	3023	4552	5804	7019	8211	9143	1.7	8481
		500	3096	4481	5668	6831	7985	8882	1.8	8481
		750	3155	4459	5620	6760	7895	8770	1.9	8481
		1000	3217	4433	5592	6724	7846	8708	1.9	8481
	150mm	250	3564	5550	7259	8927	10570	12111	1.7	10648
		500	3661	5464	7094	8700	10295	11791	1.9	10648
		750	3723	5437	7035	8613	10185	11654	1.9	10648
		1000	3795	5415	7006	8568	10127	11579	1.9	10648

Initial Pt Force 0.1f_{yield}		Axial Load (excluding PT) 4500kN			Cantilever Length (6000mm)			Grade 300 Dissipaters		
	PT Dia.	Fuse Length (mm)	Yield (kNm)	1%drift (kNm)	2%drift (kNm)	3%drift (kNm)	4%drift (kNm)	6%drift (kNm)	λ	Fuse Area (mm^2)
Diameter (1800mm)	36mm	250	2320	2855	3058	3231	3290	3274	1.4	4020
		500	2337	2799	2960	3097	3135	3110	1.5	4020
		750	2386	2780	2925	3045	3068	3031	1.6	4020
		1000	2410	2770	2907	3017	3031	2988	1.6	4020
	50mm	250	2459	3153	3514	3853	4012	4036	1.5	4451
		500	2477	3091	3410	3707	3841	3856	1.6	4451
		750	2534	3070	3372	3649	3768	3769	1.7	4451
		1000	2560	3058	3352	3620	3728	3721	1.7	4451
	75mm	250	2818	3910	4675	5400	5851	5978	1.7	5570
		500	2839	3831	4542	5227	5641	5755	1.8	5570
		750	2910	3803	4493	5161	5551	5650	1.9	5570
		1000	2947	3788	4468	5126	5504	5591	1.9	5570
	100mm	250	3310	4923	6232	7486	8366	8629	1.8	7137
		500	3335	4831	6056	7258	8104	8347	2.0	7137
		750	3428	4792	5991	7169	7993	8217	2.0	7137
		1000	3476	4774	5958	7122	7934	8146	2.1	7137
	125mm	250	3926	6169	8111	10003	11540	11985	1.9	9152
		500	3965	6062	7907	9728	11208	11620	2.0	9152
		750	4078	6015	7825	9613	11060	11451	2.1	9152
		1000	4142	5986	7779	9549	10979	11358	2.1	9152
	150mm	250	4668	7630	10288	12889	15279	15955	1.9	11614
		500	4719	7495	10037	12551	14868	15511	2.1	11614
		750	4856	7449	9945	12420	14694	15306	2.1	11614
		1000	4935	7407	9896	12350	14601	15190	2.2	11614

Initial Pt Force 0.1F_{yield}		Axial Load (excluding PT) 4500kN			Cantilever Length (6000mm)			Grade 300 Dissipaters		
	PT Dia.	Fuse Length (mm)	Yield (kNm)	1%drift (kNm)	2%drift (kNm)	3%drift (kNm)	4%drift (kNm)	6%drift (kNm)	λ	Fuse Area (mm^2)
Diameter (2000mm)	36mm	250	2656	3256	3532	3763	3790	3782	1.4	4057
		500	2686	3191	3412	3603	3610	3599	1.6	4057
		750	2713	3168	3367	3538	3529	3506	1.6	4057
		1000	2741	3156	3345	3504	3485	3453	1.7	4057
	50mm	250	2824	3623	4103	4545	4634	4672	1.6	4522
		500	2857	3551	3970	4371	4434	4469	1.7	4522
		750	2890	3525	3923	4300	4345	4366	1.8	4522
		1000	2921	3512	3899	4263	4296	4307	1.8	4522
	75mm	250	3258	4555	5536	6489	6786	6944	1.7	5731
		500	3297	4462	5378	6274	6537	6690	1.9	5731
		750	3340	4430	5319	6188	6427	6561	2.0	5731
		1000	3387	4414	5289	6145	6366	6489	2.0	5731
	100mm	250	3858	5818	7477	9076	9728	10053	1.9	7423
		500	3903	5696	7266	8810	9411	9728	2.1	7423
		750	3960	5652	7189	8704	9272	9565	2.1	7423
		1000	4024	5630	7148	8648	9198	9473	2.2	7423
	125mm	250	4616	7368	9853	12276	13439	13954	2.0	9599
		500	4668	7226	9588	11922	13033	13540	2.1	9599
		750	4739	7165	9482	11777	12856	13338	2.2	9599
		1000	4824	7134	9428	11700	12759	13225	2.3	9599
	150mm	250	5528	9187	12597	15935	17870	18668	2.0	12258
		500	5582	9012	12277	15511	17365	18130	2.2	12258
		750	5670	8945	12159	15342	17140	17864	2.2	12258
		1000	5776	8902	12084	15243	17012	17715	2.3	12258

Initial Pt Force 0.1f_{yield}		Axial Load (excluding PT) 6000kN			Cantilever Length (6000mm)			Grade 300 Dissipaters		
	PT Dia.	Fuse Length (mm)	Yield (kNm)	1%drift (kNm)	2%drift (kNm)	3%drift (kNm)	4%drift (kNm)	6%drift (kNm)	λ	Fuse Area (mm^2)
Diameter (1000mm)	36mm	250	2657.97	3460	3446	3325	3169	2981	1.0	10982
		500	2791.73	3420	3362	3201	3006	2792	1.0	10982
		750	2882	3399	3333	3154	2949	2718	1.0	10982
		1000	2945	3381	3319	3137	2919	2680	1.0	10982
	50mm	250	2702	3532	3551	3465	3346	3197	1.0	11276
		500	2837	3495	3467	3339	3180	3005	1.0	11276
		750	2929	3472	3439	3295	3123	2930	1.0	11276
		1000	2996	3453	3425	3271	3092	2891	1.0	11276
	75mm	250	2820	3721	3825	3818	3791	3739	1.0	12037
		500	2958	3682	3735	3683	3617	3533	1.0	12037
		750	3050	3655	3703	3639	3559	3456	1.1	12037
		1000	3121	3635	3689	3618	3521	3419	1.1	12037
	100mm	250	2985	3978	4203	4283	4375	4442	1.0	13103
		500	3122	3936	4098	4152	4202	4231	1.1	13103
		750	3220	3908	4061	4111	4130	4147	1.1	13103
		1000	3295	3892	4041	4083	4096	4105	1.1	13103
	125mm	250	3197	4305	4659	4882	5092	5290	1.0	14474
		500	3335	4255	4545	4730	4892	5066	1.1	14474
		750	3440	4229	4503	4676	4833	4975	1.1	14474
		1000	3518	4208	4487	4650	4792	4931	1.1	14474
	150mm	250	3453	4687	5194	5582	5914	6252	1.0	16149
		500	3592	4639	5076	5401	5702	6018	1.1	16149
		750	3706	4611	5028	5337	5629	5912	1.1	16149
		1000	3791	4583	5000	5315	5604	5871	1.1	16149

Initial Pt Force 0.1Fyield		Axial Load (excluding PT) 6000kN			Cantilever Length (6000mm)			Grade 300 Dissipaters		
	PT Dia.	Fuse Length (mm)	Yield (kNm)	1%drift (kNm)	2%drift (kNm)	3%drift (kNm)	4%drift (kNm)	6%drift (kNm)	λ	Fuse Area (mm^2)
Diameter (1200mm)	36mm	250	3390	4428	4491	4441	4334	4193	1.1	11020
		500	3554	4368	4375	4269	4116	3941	1.1	11020
		750	3654	4350	4335	4205	4033	3838	1.2	11020
		1000	3721	4338	4312	4173	3989	3784	1.2	11020
	50mm	250	3451	4536	4653	4660	4613	4533	1.1	11347
		500	3614	4475	4535	4485	4391	4277	1.2	11347
		750	3719	4456	4493	4420	4306	4172	1.2	11347
		1000	3785	4448	4472	4387	4261	4116	1.2	11347
	75mm	250	3606	4822	5065	5214	5314	5383	1.1	12198
		500	3776	4752	4939	5028	5081	5113	1.2	12198
		750	3886	4728	4895	4960	4991	5005	1.2	12198
		1000	3955	4719	4873	4925	4944	4946	1.3	12198
	100mm	250	3824	5203	5614	5949	6244	6506	1.2	13389
		500	3999	5130	5485	5756	5995	6218	1.2	13389
		750	4115	5104	5437	5678	5899	6101	1.3	13389
		1000	4190	5090	5415	5646	5849	6039	1.3	13389
	125mm	250	4098	5682	6305	6850	7373	7857	1.2	14921
		500	4284	5606	6161	6642	7093	7544	1.3	14921
		750	4408	5572	6107	6557	6993	7418	1.3	14921
		1000	4491	5561	6082	6525	6946	7351	1.3	14921
	150mm	250	4434	6250	7121	7887	8651	9403	1.2	16793
		500	4631	6171	6949	7661	8367	9045	1.3	16793
		750	4764	6132	6892	7581	8243	8922	1.3	16793
		1000	4853	6112	6870	7542	8186	8833	1.3	16793

Initial Pt Force 0.1f_{yield}		Axial Load (excluding PT) 6000kN			Cantilever Length (6000mm)			Grade 300 Dissipaters		
	PT Dia.	Fuse Length (mm)	Yield (kNm)	1%drift (kNm)	2%drift (kNm)	3%drift (kNm)	4%drift (kNm)	6%drift (kNm)	λ	Fuse Area (mm^2)
Diameter (1500mm)	36mm	250	4609	5935	6131	6177	6156	6050	1.2	11075
		500	4771	5843	5951	5919	5843	5687	1.3	11075
		750	4871	5814	5886	5822	5710	5528	1.3	11075
		1000	4951	5796	5851	5766	5636	5442	1.3	11075
	50mm	250	4698	6111	6403	6549	6632	6601	1.2	11455
		500	4861	6018	6217	6286	6311	6239	1.3	11455
		750	4964	5984	6150	6186	6181	6071	1.4	11455
		1000	5046	5969	6115	6133	6103	5981	1.4	11455
	75mm	250	4924	6555	7093	7491	7827	8011	1.3	12440
		500	5094	6460	6895	7210	7486	7624	1.4	12440
		750	5205	6425	6823	7104	7348	7456	1.4	12440
		1000	5289	6406	6788	7049	7275	7363	1.4	12440
	100mm	250	5242	7170	8026	8752	9420	9942	1.3	13819
		500	5418	7060	7811	8448	9051	9519	1.4	13819
		750	5540	7025	7733	8333	8902	9337	1.5	13819
		1000	5631	7010	7694	8274	8823	9238	1.5	13819
	125mm	250	5644	7937	9177	10296	11357	12362	1.4	15592
		500	5833	7821	8939	9961	10951	11893	1.5	15592
		750	5964	7778	8854	9835	10788	11692	1.5	15592
		1000	6064	7763	8811	9770	10702	11583	1.6	15592
	150mm	250	6129	8852	10512	12082	13589	15049	1.4	17759
		500	6334	8721	10256	11712	13137	14544	1.5	17759
		750	6480	8675	10166	11573	12957	14330	1.6	17759
		1000	6590	8652	10109	11500	12861	14213	1.6	17759

Initial Pt Force 0.1Fyield		Axial Load (excluding PT) 6000kN			Cantilever Length (6000mm)			Grade 300 Dissipaters		
	PT Dia.	Fuse Length (mm)	Yield (kNm)	1%drift (kNm)	2%drift (kNm)	3%drift (kNm)	4%drift (kNm)	6%drift (kNm)	λ	Fuse Area (mm^2)
Diameter (1800mm)	36mm	250	5840	7496	7820	7980	7976	7850	1.3	11131
		500	6001	7364	7563	7614	7563	7409	1.4	11131
		750	6160	7319	7462	7471	7389	7201	1.4	11131
		1000	6220	7279	7407	7396	7295	7090	1.5	11131
	50mm	250	5960	7758	8233	8548	8674	8575	1.3	11562
		500	6124	7622	7967	8175	8243	8118	1.4	11562
		750	6287	7573	7865	8025	8060	7909	1.5	11562
		1000	6352	7533	7808	7947	7962	7793	1.5	11562
	75mm	250	6275	8423	9279	9981	10464	10461	1.4	12681
		500	6445	8276	8993	9591	9988	9962	1.5	12681
		750	6621	8224	8889	9430	9784	9729	1.5	12681
		1000	6687	8184	8827	9342	9675	9601	1.6	12681
	100mm	250	6709	9334	10695	11907	12889	13063	1.5	14248
		500	6887	9172	10381	11480	12376	12507	1.6	14248
		750	7079	9111	10267	11313	12158	12239	1.6	14248
		1000	7152	9075	10209	11222	12032	12090	1.7	14248
	125mm	250	7266	10476	12446	14272	15939	16300	1.5	16263
		500	7450	10292	12096	13796	15363	15679	1.7	16263
		750	7661	10223	11969	13610	15120	15391	1.7	16263
		1000	7743	10195	11904	13513	14990	15232	1.7	16263
	150mm	250	7939	11822	14495	17022	19466	20166	1.6	18725
		500	8124	11617	14102	16488	18838	19460	1.7	18725
		750	8368	11546	13960	16279	18574	19135	1.8	18725
		1000	8453	11510	13886	16170	18430	18956	1.8	18725

Initial Pt Force 0.1f_{yield}		Axial Load (excluding PT) 6000kN			Cantilever Length (6000mm)			Grade 300 Dissipaters		
	PT Dia.	Fuse Length (mm)	Yield (kNm)	1%drift (kNm)	2%drift (kNm)	3%drift (kNm)	4%drift (kNm)	6%drift (kNm)	λ	Fuse Area (mm^2)
Diameter (2000mm)	36mm	250	6768	8553	8975	9187	9201	9102	1.3	11168
		500	6938	8390	8650	8772	8722	8610	1.4	11168
		750	7036	8326	8529	8606	8510	8362	1.5	11168
		1000	7131	8288	8467	8518	8397	8222	1.5	11168
	50mm	250	6915	8881	9496	9912	10006	9954	1.3	11634
		500	7091	8710	9164	9478	9508	9443	1.5	11634
		750	7192	8647	9037	9305	9292	9185	1.5	11634
		1000	7291	8607	8971	9213	9175	9041	1.5	11634
	75mm	250	7295	9717	10822	11758	12082	12141	1.4	12842
		500	7486	9533	10471	11270	11542	11581	1.6	12842
		750	7595	9469	10329	11076	11304	11301	1.6	12842
		1000	7703	9420	10255	10974	11175	11147	1.6	12842
	100mm	250	7824	10863	12618	14207	14979	15169	1.5	14534
		500	8037	10659	12229	13689	14353	14543	1.7	14534
		750	8156	10588	12085	13469	14081	14232	1.7	14534
		1000	8269	10533	11998	13350	13933	14059	1.7	14534
	125mm	250	8498	12296	14840	17219	18581	19034	1.6	16710
		500	8734	12063	14404	16637	17893	18308	1.7	16710
		750	8866	11986	14243	16406	17591	17944	1.8	16710
		1000	8987	11931	14160	16281	17417	17740	1.8	16710
	150mm	250	9315	13994	17447	20733	22890	23609	1.7	19369
		500	9576	13729	16953	20073	22104	22787	1.8	19369
		750	9721	13635	16772	19812	21762	22385	1.9	19369
		1000	9851	13583	16679	19674	21576	22159	1.9	19369

Initial Pt Force 0.1f_{yield}		Axial Load (excluding PT) 7500kN			Cantilever Length (6000mm)			Grade 300 Dissipaters		
	PT Dia.	Fuse Length (mm)	Yield (kNm)	1%drift (kNm)	2%drift (kNm)	3%drift (kNm)	4%drift (kNm)	6%drift (kNm)	λ	Fuse Area (mm^2)
Diameter (1000mm)	36mm	250	2992	3950	3933	3739	3518	3268	1.1	11943
		500	3146	3912	3834	3609	3350	3066	1.1	11943
		750	3262	3887	3804	3565	3286	2984	1.1	11943
		1000	3350	3869	3788	3546	3254	2943	1.2	11943
	50mm	250	3032	4015	4031	3865	3686	3464	1.1	12200
		500	3189	3976	3932	3736	3510	3260	1.1	12200
		750	3305	3950	3899	3694	3450	3185	1.1	12200
		1000	3391	3932	3879	3668	3412	3138	1.2	12200
	75mm	250	3135	4181	4273	4195	4089	3963	1.1	12866
		500	3292	4140	4172	4056	3917	3753	1.1	12866
		750	3413	4116	4137	4008	3846	3670	1.2	12866
		1000	3502	4093	4116	3987	3812	3628	1.2	12866
	100mm	250	3281	4410	4608	4635	4639	4630	1.1	13799
		500	3441	4361	4500	4490	4447	4402	1.2	13799
		750	3567	4339	4463	4438	4380	4324	1.2	13799
		1000	3659	4321	4439	4413	4348	4271	1.2	13799
	125mm	250	3465	4698	5011	5195	5289	5427	1.1	14998
		500	3628	4645	4913	5023	5111	5184	1.2	14998
		750	3758	4625	4866	4972	5036	5092	1.2	14998
		1000	3854	4600	4839	4942	4999	5046	1.2	14998
	150mm	250	3691	5035	5494	5824	6081	6320	1.1	16463
		500	3860	4977	5381	5648	5869	6075	1.2	16463
		750	3995	4958	5339	5577	5789	5983	1.2	16463
		1000	4096	4940	5309	5544	5758	5943	1.2	16463

Initial Pt Force 0.1f_{yield}		Axial Load (excluding PT) 7500kN			Cantilever Length (6000mm)			Grade 300 Dissipaters		
	PT Dia.	Fuse Length (mm)	Yield (kNm)	1%drift (kNm)	2%drift (kNm)	3%drift (kNm)	4%drift (kNm)	6%drift (kNm)	λ	Fuse Area (mm^2)
Diameter (1200mm)	36mm	250	3829	5100	5141	5046	4878	4670	1.2	11975
		500	4039	5036	5017	4861	4646	4399	1.3	11975
		750	4175	5013	4977	4793	4556	4290	1.3	11975
		1000	4267	5004	4954	4759	4509	4232	1.3	11975
	50mm	250	3883	5198	5288	5249	5138	4989	1.2	12262
		500	4091	5135	5161	5058	4902	4715	1.3	12262
		750	4233	5112	5119	4991	4811	4604	1.3	12262
		1000	4327	5099	5098	4954	4764	4545	1.4	12262
	75mm	250	4021	5448	5665	5759	5792	5790	1.3	13007
		500	4236	5382	5533	5560	5547	5505	1.3	13007
		750	4378	5357	5487	5494	5453	5389	1.4	13007
		1000	4476	5341	5467	5452	5404	5328	1.4	13007
	100mm	250	4212	5792	6175	6439	6661	6850	1.3	14049
		500	4436	5721	6039	6241	6409	6550	1.4	14049
		750	4580	5693	5985	6165	6303	6428	1.4	14049
		1000	4684	5671	5965	6121	6252	6364	1.4	14049
	125mm	250	4458	6221	6817	7276	7719	8123	1.3	15389
		500	4685	6150	6659	7065	7439	7805	1.4	15389
		750	4836	6114	6611	6981	7344	7673	1.4	15389
		1000	4946	6090	6583	6943	7290	7607	1.5	15389
	150mm	250	4759	6737	7572	8244	8931	9585	1.3	17027
		500	4989	6653	7398	8026	8630	9235	1.4	17027
		750	5150	6619	7332	7934	8530	9112	1.5	17027
		1000	5267	6592	7302	7903	8456	9022	1.5	17027

Initial Pt Force 0.1f_{yield}		Axial Load (excluding PT) 7500kN			Cantilever Length (6000mm)			Grade 300 Dissipaters		
	PT Dia.	Fuse Length (mm)	Yield (kNm)	1%drift (kNm)	2%drift (kNm)	3%drift (kNm)	4%drift (kNm)	6%drift (kNm)	λ	Fuse Area (mm^2)
Diameter (1500mm)	36mm	250	5234	6865	7061	7064	6987	6824	1.4	12024
		500	5457	6774	6868	6790	6651	6447	1.5	12024
		750	5606	6742	6801	6686	6515	6280	1.5	12024
		1000	5708	6725	6764	6631	6442	6183	1.5	12024
	50mm	250	5312	7027	7313	7414	7437	7354	1.4	12356
		500	5539	6930	7118	7133	7094	6968	1.5	12356
		750	5690	6899	7045	7027	6956	6801	1.5	12356
		1000	5791	6881	7011	6972	6883	6705	1.5	12356
	75mm	250	5509	7433	7952	8298	8568	8711	1.4	13218
		500	5745	7333	7745	8003	8209	8304	1.5	13218
		750	5903	7296	7670	7891	8065	8127	1.6	13218
		1000	6010	7278	7635	7834	7989	8032	1.6	13218
	100mm	250	5788	7989	8819	9485	10082	10572	1.5	14425
		500	6034	7880	8600	9171	9699	10134	1.6	14425
		750	6198	7847	8517	9053	9545	9945	1.6	14425
		1000	6313	7828	8476	8991	9463	9843	1.7	14425
	125mm	250	6144	8698	9892	10942	11927	12864	1.5	15976
		500	6400	8575	9645	10602	11513	12402	1.6	15976
		750	6576	8534	9562	10473	11348	12203	1.7	15976
		1000	6701	8514	9522	10407	11259	12097	1.7	15976
	150mm	250	6571	9541	11135	12631	14054	15431	1.6	17872
		500	6842	9401	10882	12261	13604	14925	1.7	17872
		750	7034	9357	10783	12121	13423	14710	1.7	17872
		1000	7169	9328	10736	12049	13327	14593	1.7	17872

Initial Pt Force 0.1f_{yield}		Axial Load (excluding PT) 7500kN			Cantilever Length (6000mm)			Grade 300 Dissipaters		
	PT Dia.	Fuse Length (mm)	Yield (kNm)	1%drift (kNm)	2%drift (kNm)	3%drift (kNm)	4%drift (kNm)	6%drift (kNm)	λ	Fuse Area (mm^2)
Diameter (1800mm)	36mm	250	7395	9621	10056	10262	10319	10150	1.1	15522
		500	7589	9445	9705	9780	9729	9539	1.2	15522
		750	7805	9374	9577	9583	9480	9254	1.2	15522
		1000	7874	9337	9506	9475	9346	9097	1.3	15522
	50mm	250	7523	9884	10468	10828	11014	10902	1.1	16007
		500	7718	9703	10110	10334	10418	10266	1.2	16007
		750	7940	9631	9978	10137	10159	9971	1.3	16007
		1000	8010	9595	9908	10025	10020	9808	1.3	16007
	75mm	250	7857	10561	11519	12261	12798	12822	1.2	17266
		500	8051	10367	11138	11738	12173	12138	1.3	17266
		750	8287	10296	10999	11533	11905	11814	1.3	17266
		1000	8361	10257	10928	11422	11752	11635	1.4	17266
	100mm	250	8323	11489	12948	14195	15253	15428	1.2	19029
		500	8519	11276	12536	13631	14574	14697	1.3	19029
		750	8770	11197	12386	13411	14288	14357	1.4	19029
		1000	8849	11164	12309	13294	14134	14159	1.4	19029
	125mm	250	8916	12660	14719	16581	18331	18714	1.3	21295
		500	9109	12422	14269	15963	17598	17905	1.4	21295
		750	9390	12341	14104	15722	17284	17531	1.4	21295
		1000	9475	12301	14021	15596	17115	17325	1.5	21295
	150mm	250	9638	14036	16802	19364	21814	22642	1.3	24065
		500	9832	13779	16305	18681	21009	21740	1.4	24065
		750	10138	13696	16124	18418	20673	21327	1.5	24065
		1000	10222	13655	16031	18279	20492	21098	1.5	24065

Initial Pt Force 0.1F_{yield}		Axial Load (excluding PT) 7500kN			Cantilever Length (6000mm)			Grade 300 Dissipaters		
	PT Dia.	Fuse Length (mm)	Yield (kNm)	1%drift (kNm)	2%drift (kNm)	3%drift (kNm)	4%drift (kNm)	6%drift (kNm)	λ	Fuse Area (mm^2)
Diameter (2000mm)	36mm	250	8564	10984	11537	11841	11849	11742	1.1	15564
		500	8808	10762	11110	11248	11193	11060	1.2	15564
		750	8935	10688	10942	11012	10905	10719	1.3	15564
		1000	9039	10629	10852	10888	10748	10529	1.3	15564
	50mm	250	8721	11317	12061	12563	12678	12603	1.2	16088
		500	8970	11089	11622	11957	11996	11901	1.3	16088
		750	9100	11010	11454	11712	11697	11552	1.3	16088
		1000	9202	10951	11359	11583	11535	11359	1.3	16088
	75mm	250	9124	12169	13396	14387	14817	14831	1.2	17447
		500	9388	11925	12927	13758	14065	14078	1.3	17447
		750	9521	11843	12755	13492	13738	13706	1.4	17447
		1000	9631	11780	12654	13349	13561	13497	1.4	17447
	100mm	250	9688	13340	15212	16853	17724	17962	1.3	19351
		500	9966	13073	14702	16169	16922	17104	1.4	19351
		750	10104	12978	14514	15897	16559	16685	1.5	19351
		1000	10223	12922	14418	15743	16359	16451	1.5	19351
	125mm	250	10407	14809	17467	19899	21387	21854	1.4	21799
		500	10710	14513	16906	19145	20497	20923	1.5	21799
		750	10852	14404	16700	18846	20108	20463	1.5	21799
		1000	10982	14348	16593	18688	19896	20193	1.6	21799
	150mm	250	11281	16554	20124	23461	25775	26513	1.4	24790
		500	11610	16222	19500	22623	24776	25466	1.5	24790
		750	11755	16103	19269	22293	24342	24956	1.6	24790
		1000	11897	16047	19150	22115	24107	24669	1.6	24790

Initial Pt Force 0.1f_{yield}		Axial Load (excluding PT) 9000kN			Cantilever Length (6000mm)			Grade 300 Dissipaters		
	PT Dia.	Fuse Length (mm)	Yield (kNm)	1%drift (kNm)	2%drift (kNm)	3%drift (kNm)	4%drift (kNm)	6%drift (kNm)	λ	Fuse Area (mm^2)
Diameter (1000mm)	36mm	250	3232	4327	4290	4046	3746	3419	1.2	12237
		500	3412	4284	4202	3912	3580	3219	1.3	12237
		750	3555	4267	4164	3869	3516	3136	1.3	12237
		1000	3652	4248	4144	3844	3480	3098	1.3	12237
	50mm	250	3266	4382	4376	4165	3895	3603	1.2	12457
		500	3449	4337	4287	4032	3728	3399	1.3	12457
		750	3589	4321	4249	3984	3663	3318	1.3	12457
		1000	3691	4306	4228	3961	3632	3276	1.3	12457
	75mm	250	3361	4531	4594	4468	4272	4067	1.2	13028
		500	3543	4482	4502	4325	4094	3862	1.3	13028
		750	3687	4466	4461	4272	4037	3775	1.3	13028
		1000	3788	4447	4444	4252	4000	3737	1.3	13028
	100mm	250	3484	4730	4894	4880	4781	4684	1.2	13827
		500	3673	4680	4794	4722	4594	4463	1.3	13827
		750	3821	4660	4758	4667	4538	4387	1.3	13827
		1000	3926	4646	4734	4639	4499	4334	1.3	13827
	125mm	250	3650	4982	5258	5383	5407	5425	1.3	14855
		500	3838	4931	5160	5214	5213	5195	1.3	14855
		750	3988	4911	5122	5160	5141	5110	1.3	14855
		1000	4098	4898	5095	5121	5106	5071	1.4	14855
	150mm	250	3845	5280	5696	5956	6154	6289	1.3	16112
		500	4043	5222	5584	5787	5929	6054	1.3	16112
		750	4195	5211	5548	5718	5845	5958	1.3	16112
		1000	4312	5199	5519	5691	5816	5912	1.4	16112

Initial Pt Force 0.1Fyield		Axial Load (excluding PT) 9000kN			Cantilever Length (6000mm)			Grade 300 Dissipaters		
	PT Dia.	Fuse Length (mm)	Yield (kNm)	1%drift (kNm)	2%drift (kNm)	3%drift (kNm)	4%drift (kNm)	6%drift (kNm)	λ	Fuse Area (mm^2)
Diameter (1200mm)	36mm	250	4165	5639	5659	5505	5269	4988	1.4	12265
		500	4405	5577	5534	5319	5035	4714	1.5	12265
		750	4570	5553	5491	5251	4944	4604	1.5	12265
		1000	4696	5536	5470	5214	4897	4544	1.5	12265
	50mm	250	4209	5726	5789	5687	5512	5288	1.4	12511
		500	4450	5663	5663	5499	5274	5011	1.5	12511
		750	4622	5638	5621	5433	5183	4899	1.5	12511
		1000	4749	5620	5602	5396	5136	4840	1.6	12511
	75mm	250	4332	5944	6137	6158	6127	6043	1.4	13149
		500	4577	5884	6003	5968	5875	5757	1.5	13149
		750	4748	5858	5960	5899	5788	5643	1.6	13149
		1000	4879	5836	5935	5858	5732	5581	1.6	13149
	100mm	250	4499	6250	6611	6794	6938	7046	1.5	14042
		500	4749	6186	6464	6591	6689	6748	1.6	14042
		750	4927	6158	6420	6518	6585	6628	1.6	14042
		1000	5058	6131	6391	6483	6540	6565	1.6	14042
	125mm	250	4717	6634	7201	7581	7943	8252	1.5	15191
		500	4968	6566	7045	7368	7670	7950	1.6	15191
		750	5154	6542	6991	7296	7558	7814	1.6	15191
		1000	5292	6508	6964	7250	7513	7757	1.6	15191
	150mm	250	4984	7097	7894	8488	9085	9640	1.5	16595
		500	5237	7016	7721	8262	8786	9302	1.6	16595
		750	5428	6991	7659	8183	8674	9166	1.6	16595
		1000	5578	6955	7630	8149	8624	9098	1.7	16595

Initial Pt Force 0.1Fyield		Axial Load (excluding PT) 9000kN			Cantilever Length (6000mm)			Grade 300 Dissipaters		
	PT Dia.	Fuse Length (mm)	Yield (kNm)	1%drift (kNm)	2%drift (kNm)	3%drift (kNm)	4%drift (kNm)	6%drift (kNm)	λ	Fuse Area (mm^2)
Diameter (1500mm)	36mm	250	5716	7637	7818	7767	7623	7394	1.6	12306
		500	6008	7543	7624	7489	7283	7011	1.7	12306
		750	6200	7515	7552	7384	7146	6846	1.7	12306
		1000	6328	7499	7517	7329	7073	6756	1.7	12306
	50mm	250	5782	7782	8051	8094	8048	7904	1.6	12591
		500	6077	7688	7851	7812	7703	7514	1.7	12591
		750	6273	7654	7783	7705	7564	7345	1.7	12591
		1000	6403	7638	7745	7650	7490	7254	1.8	12591
	75mm	250	5960	8152	8643	8924	9123	9212	1.6	13330
		500	6258	8049	8435	8631	8764	8803	1.7	13330
		750	6461	8020	8364	8520	8619	8627	1.8	13330
		1000	6597	8003	8326	8463	8542	8532	1.8	13330
	100mm	250	6202	8664	9444	10044	10561	11007	1.7	14364
		500	6510	8556	9229	9733	10183	10572	1.8	14364
		750	6722	8520	9150	9616	10032	10386	1.8	14364
		1000	6867	8503	9109	9556	9951	10285	1.9	14364
	125mm	250	6513	9309	10444	11417	12320	13170	1.7	15694
		500	6829	9188	10204	11086	11914	12715	1.8	15694
		750	7051	9143	10124	10962	11752	12522	1.9	15694
		1000	7208	9125	10081	10896	11667	12417	1.9	15694
	150mm	250	6892	10074	11601	13018	14349	15634	1.8	17319
		500	7224	9934	11356	12649	13913	15146	1.9	17319
		750	7456	9895	11273	12529	13739	14937	1.9	17319
		1000	7623	9867	11218	12445	13648	14825	2.0	17319

Initial Pt Force 0.1Fyield		Axial Load (excluding PT) 9000kN			Cantilever Length (6000mm)			Grade 300 Dissipaters		
	PT Dia.	Fuse Length (mm)	Yield (kNm)	1%drift (kNm)	2%drift (kNm)	3%drift (kNm)	4%drift (kNm)	6%drift (kNm)	λ	Fuse Area (mm^2)
Diameter (1800mm)	36mm	250	8628	11342	11849	12071	12126	11973	1.1	18522
		500	8841	11131	11438	11504	11452	11225	1.2	18522
		750	9130	11051	11288	11281	11155	10879	1.2	18522
		1000	9212	11011	11211	11160	10992	10689	1.3	18522
	50mm	250	8751	11600	12253	12622	12812	12701	1.1	19007
		500	8969	11382	11830	12043	12123	11947	1.2	19007
		750	9260	11302	11680	11816	11828	11589	1.3	19007
		1000	9348	11262	11602	11697	11659	11393	1.3	19007
	75mm	250	9077	12253	13275	14020	14573	14571	1.2	20266
		500	9297	12023	12831	13412	13847	13789	1.3	20266
		750	9603	11942	12671	13175	13540	13419	1.3	20266
		1000	9689	11901	12592	13050	13374	13205	1.3	20266
	100mm	250	9527	13156	14665	15912	17000	17150	1.2	22029
		500	9752	12905	14195	15264	16221	16308	1.3	22029
		750	10077	12823	14023	15013	15893	15918	1.4	22029
		1000	10168	12782	13935	14880	15716	15702	1.4	22029
	125mm	250	10097	14290	16398	18252	19976	20405	1.3	24295
		500	10336	14021	15890	17553	19148	19487	1.4	24295
		750	10679	13938	15704	17281	18802	19064	1.4	24295
		1000	10777	13896	15610	17139	18615	18830	1.4	24295
	150mm	250	10793	15638	18439	20990	23407	24302	1.3	27065
		500	11042	15360	17886	20228	22507	23292	1.4	27065
		750	11414	15264	17684	19933	22132	22829	1.4	27065
		1000	11513	15222	17581	19779	21929	22573	1.5	27065

Initial Pt Force 0.1f_{yield}		Axial Load (excluding PT) 9000kN			Cantilever Length (6000mm)			Grade 300 Dissipaters		
	PT Dia.	Fuse Length (mm)	Yield (kNm)	1%drift (kNm)	2%drift (kNm)	3%drift (kNm)	4%drift (kNm)	6%drift (kNm)	λ	Fuse Area (mm^2)
Diameter (2000mm)	36mm	250	9988	12962	13604	13934	13974	13796	1.1	18564
		500	10307	12700	13102	13254	13179	12993	1.2	18564
		750	10460	12609	12916	12968	12831	12596	1.3	18564
		1000	10583	12551	12810	12817	12643	12374	1.3	18564
	50mm	250	10145	13284	14112	14636	14799	14660	1.2	19088
		500	10464	13018	13599	13943	13976	13835	1.3	19088
		750	10618	12922	13409	13654	13617	13426	1.3	19088
		1000	10744	12866	13307	13498	13423	13197	1.3	19088
	75mm	250	10540	14115	15419	16422	16887	16905	1.2	20447
		500	10871	13834	14877	15692	16031	16006	1.3	20447
		750	11026	13728	14673	15399	15642	15564	1.4	20447
		1000	11158	13671	14570	15233	15431	15317	1.4	20447
	100mm	250	11094	15257	17192	18842	19760	19978	1.3	22351
		500	11430	14954	16610	18059	18839	19017	1.4	22351
		750	11603	14839	16396	17747	18436	18526	1.4	22351
		1000	11738	14778	16285	17582	18209	18252	1.4	22351
	125mm	250	11799	16698	19405	21839	23391	23835	1.3	24799
		500	12147	16361	18773	20987	22383	22781	1.4	24799
		750	12331	16240	18540	20649	21944	22264	1.5	24799
		1000	12483	16173	18419	20469	21705	21973	1.5	24799
	150mm	250	12657	18402	22016	25351	27744	28462	1.4	27790
		500	13018	18031	21322	24417	26630	27292	1.5	27790
		750	13224	17896	21067	24048	26147	26723	1.5	27790
		1000	13373	17840	20934	23851	25886	26405	1.6	27790

Initial Pt Force $0.1f_{yield}$		Axial Load (excluding PT) 1500kN			Cantilever Length (7000mm)			Grade 300 Dissipaters		
	PT Dia.	Fuse Length (mm)	Yield (kNm)	1%drift (kNm)	2%drift (kNm)	3%drift (kNm)	4%drift (kNm)	6%drift (kNm)	λ	Fuse Area (mm^2)
Diameter (1000mm)	36mm	250	844	1020	1027	1010	984	947	1.1	2962
		500	871	1009	1002	972	932	889	1.1	2962
		750	887	1002	991	955	913	866	1.1	2962
		1000	900	998	984	947	902	855	1.2	2962
	50mm	250	893	1108	1152	1173	1185	1193	1.1	3236
		500	923	1094	1124	1132	1135	1131	1.2	3236
		750	940	1088	1114	1116	1112	1104	1.2	3236
		1000	956	1083	1106	1106	1100	1091	1.2	3236
	75mm	250	1023	1326	1459	1572	1676	1775	1.2	3948
		500	1057	1310	1427	1525	1617	1706	1.3	3948
		750	1077	1305	1415	1508	1595	1679	1.3	3948
		1000	1098	1298	1409	1499	1583	1665	1.3	3948
	100mm	250	1198	1620	1862	2088	2306	2519	1.3	4944
		500	1240	1600	1823	2031	2235	2436	1.4	4944
		750	1265	1593	1808	2011	2208	2403	1.4	4944
		1000	1290	1587	1805	2001	2194	2386	1.4	4944
	125mm	250	1419	1981	2340	2697	3042	3387	1.3	6225
		500	1469	1954	2295	2628	2958	3287	1.4	6225
		750	1501	1946	2285	2604	2930	3247	1.4	6225
		1000	1531	1942	2275	2596	2908	3227	1.4	6225
	150mm	250	1683	2406	2893	3388	3867	4350	1.3	7791
		500	1743	2369	2841	3300	3766	4226	1.4	7791
		750	1782	2356	2828	3278	3733	4179	1.4	7791
		1000	1817	2354	2819	3261	3705	4164	1.4	7791

Initial Pt Force $0.1f_{yield}$		Axial Load (excluding PT) 1500kN			Cantilever Length (7000mm)			Grade 300 Dissipaters		
	PT Dia.	Fuse Length (mm)	Yield (kNm)	1%drift (kNm)	2%drift (kNm)	3%drift (kNm)	4%drift (kNm)	6%drift (kNm)	λ	Fuse Area (mm^2)
Diameter (1200mm)	36mm	250	1068	1302	1341	1348	1343	1338	1.2	2995
		500	1096	1284	1301	1295	1281	1265	1.3	2995
		750	1115	1274	1286	1275	1258	1237	1.3	2995
		1000	1133	1268	1279	1265	1245	1222	1.3	2995
	50mm	250	1136	1425	1523	1596	1650	1697	1.3	3300
		500	1166	1407	1482	1534	1579	1620	1.4	3300
		750	1188	1396	1465	1512	1552	1589	1.4	3300
		1000	1207	1390	1456	1500	1538	1573	1.4	3300
	75mm	250	1309	1737	1976	2190	2395	2592	1.4	4091
		500	1346	1715	1929	2123	2312	2496	1.5	4091
		750	1372	1705	1911	2096	2276	2453	1.5	4091
		1000	1398	1695	1899	2080	2256	2430	1.5	4091
	100mm	250	1546	2154	2570	2964	3346	3720	1.5	5199
		500	1593	2128	2513	2882	3245	3605	1.6	5199
		750	1622	2117	2493	2852	3206	3559	1.6	5199
		1000	1655	2107	2482	2837	3186	3533	1.6	5199
	125mm	250	1842	2664	3282	3885	4473	5051	1.5	6623
		500	1900	2631	3215	3785	4349	4910	1.6	6623
		750	1934	2620	3190	3748	4301	4853	1.6	6623
		1000	1974	2609	3179	3730	4277	4821	1.7	6623
	150mm	250	2199	3261	4097	4931	5741	6545	1.5	8363
		500	2266	3218	4017	4802	5591	6371	1.6	8363
		750	2306	3203	3989	4758	5533	6301	1.6	8363
		1000	2356	3196	3977	4742	5503	6264	1.7	8363

Initial Pt Force 0.1F_{yield}		Axial Load (excluding PT) 1500kN			Cantilever Length (7000mm)			Grade 300 Dissipaters		
	PT Dia.	Fuse Length (mm)	Yield (kNm)	1%drift (kNm)	2%drift (kNm)	3%drift (kNm)	4%drift (kNm)	6%drift (kNm)	λ	Fuse Area (mm^2)
Diameter (1500mm)	36mm	250	1426	1740	1828	1895	1953	1967	1.3	3044
		500	1447	1708	1774	1819	1863	1866	1.4	3044
		750	1470	1696	1755	1792	1825	1822	1.5	3044
		1000	1489	1691	1745	1778	1806	1798	1.5	3044
	50mm	250	1523	1933	2121	2279	2436	2531	1.4	3395
		500	1548	1898	2059	2199	2336	2420	1.5	3395
		750	1573	1885	2037	2169	2295	2371	1.6	3395
		1000	1597	1879	2026	2154	2276	2345	1.6	3395
	75mm	250	1774	2418	2853	3252	3633	3961	1.6	4306
		500	1805	2378	2772	3145	3512	3826	1.7	4306
		750	1838	2361	2743	3105	3463	3767	1.8	4306
		1000	1870	2351	2727	3085	3437	3736	1.8	4306
	100mm	250	2118	3069	3809	4520	5216	5896	1.7	5580
		500	2159	3021	3716	4393	5063	5726	1.8	5580
		750	2200	3001	3679	4339	4993	5645	1.9	5580
		1000	2244	2985	3657	4309	4956	5601	1.9	5580
	125mm	250	2548	3864	4966	6036	7087	8121	1.7	7219
		500	2606	3807	4851	5877	6895	7908	1.9	7219
		750	2655	3785	4809	5816	6818	7817	1.9	7219
		1000	2709	3766	4786	5785	6777	7767	1.9	7219
	150mm	250	3060	4790	6296	7767	9215	10644	1.7	9222
		500	3141	4716	6154	7571	8978	10381	1.9	9222
		750	3193	4693	6103	7495	8884	10268	1.9	9222
		1000	3256	4679	6077	7457	8833	10207	1.9	9222

Initial Pt Force 0.1f_{yield}		Axial Load (excluding PT) 1500kN			Cantilever Length (7000mm)			Grade 300 Dissipaters		
	PT Dia.	Fuse Length (mm)	Yield (kNm)	1%drift (kNm)	2%drift (kNm)	3%drift (kNm)	4%drift (kNm)	6%drift (kNm)	λ	Fuse Area (mm^2)
Diameter (1800mm)	36mm	250	1788	2193	2358	2499	2588	2568	1.4	3094
		500	1800	2151	2281	2396	2468	2442	1.5	3094
		750	1838	2136	2255	2355	2416	2381	1.6	3094
		1000	1854	2129	2241	2334	2388	2348	1.6	3094
	50mm	250	1921	2470	2777	3066	3287	3305	1.5	3490
		500	1935	2422	2694	2951	3152	3163	1.7	3490
		750	1978	2405	2664	2906	3095	3096	1.7	3490
		1000	1997	2397	2649	2883	3064	3058	1.7	3490
	75mm	250	2263	3172	3836	4473	5062	5177	1.7	4520
		500	2278	3107	3729	4331	4892	4996	1.9	4520
		750	2336	3085	3690	4278	4819	4911	1.9	4520
		1000	2365	3074	3670	4250	4781	4863	2.0	4520
	100mm	250	2729	4110	5258	6360	7434	7725	1.8	5962
		500	2749	4032	5110	6170	7220	7491	2.0	5962
		750	2825	3999	5056	6096	7130	7384	2.1	5962
		1000	2865	3984	5028	6058	7082	7325	2.1	5962
	125mm	250	3315	5261	6969	8637	10273	10948	1.9	7815
		500	3343	5169	6796	8403	10001	10639	2.1	7815
		750	3440	5127	6726	8307	9879	10493	2.1	7815
		1000	3494	5104	6686	8251	9810	10412	2.2	7815
	150mm	250	4013	6605	8949	11245	13503	14741	1.9	10081
		500	4054	6490	8732	10952	13162	14359	2.1	10081
		750	4173	6450	8653	10839	13019	14181	2.1	10081
		1000	4241	6412	8611	10778	12940	14083	2.2	10081

Initial Pt Force 0.1f_{yield}		Axial Load (excluding PT) 3000kN			Cantilever Length (7000mm)			Grade 300 Dissipaters		
	PT Dia.	Fuse Length (mm)	Yield (kNm)	1%drift (kNm)	2%drift (kNm)	3%drift (kNm)	4%drift (kNm)	6%drift (kNm)	λ	Fuse Area (mm^2)
Diameter (1000mm)	36mm	250	1469	1834	1809	1736	1641	1535	1.0	5628
		500	1536	1811	1764	1669	1556	1434	1.0	5628
		750	1573	1804	1748	1645	1524	1394	1.0	5628
		1000	1598	1801	1740	1632	1507	1373	1.0	5628
	50mm	250	1515	1912	1917	1881	1824	1754	1.0	5903
		500	1583	1887	1871	1812	1735	1650	1.0	5903
		750	1623	1880	1855	1787	1702	1609	1.1	5903
		1000	1649	1877	1849	1774	1684	1587	1.1	5903
	75mm	250	1633	2111	2196	2243	2274	2293	1.0	6614
		500	1706	2083	2146	2170	2178	2180	1.1	6614
		750	1749	2075	2128	2143	2142	2136	1.1	6614
		1000	1778	2069	2121	2126	2123	2112	1.1	6614
	100mm	250	1799	2384	2563	2720	2859	2992	1.1	7611
		500	1877	2349	2509	2639	2753	2866	1.1	7611
		750	1924	2339	2492	2608	2712	2818	1.2	7611
		1000	1957	2332	2486	2591	2693	2792	1.2	7611
	125mm	250	2006	2717	3026	3296	3564	3816	1.1	8892
		500	2094	2682	2960	3196	3436	3674	1.2	8892
		750	2148	2665	2938	3170	3399	3618	1.2	8892
		1000	2183	2655	2926	3150	3369	3587	1.2	8892
	150mm	250	2259	3110	3565	3948	4354	4739	1.1	10458
		500	2356	3072	3481	3844	4207	4578	1.2	10458
		750	2417	3052	3453	3809	4166	4515	1.2	10458
		1000	2457	3034	3439	3792	4135	4492	1.2	10458

Initial Pt Force 0.1f_{yield}		Axial Load (excluding PT) 3000kN			Cantilever Length (7000mm)			Grade 300 Dissipaters		
	PT Dia.	Fuse Length (mm)	Yield (kNm)	1%drift (kNm)	2%drift (kNm)	3%drift (kNm)	4%drift (kNm)	6%drift (kNm)	λ	Fuse Area (mm^2)
Diameter (1200mm)	36mm	250	1879	2342	2369	2334	2275	2201	1.1	5661
		500	1950	2313	2305	2241	2159	2063	1.2	5661
		750	1987	2303	2282	2207	2110	2003	1.2	5661
		1000	2020	2295	2269	2185	2083	1971	1.2	5661
	50mm	250	1941	2454	2535	2555	2553	2536	1.1	5966
		500	2014	2422	2467	2458	2432	2397	1.2	5966
		750	2053	2412	2444	2423	2385	2336	1.2	5966
		1000	2088	2405	2432	2403	2356	2302	1.2	5966
	75mm	250	2098	2739	2950	3107	3242	3363		6758
		500	2176	2705	2877	3001	3110	3211	1.3	6758
		750	2220	2692	2851	2961	3058	3149	1.3	6758
		1000	2260	2686	2837	2941	3031	3116	1.3	6758
	100mm	250	2316	3128	3503	3836	4146	4442	1.3	7865
		500	2401	3085	3422	3716	3996	4270	1.3	7865
		750	2453	3073	3393	3671	3939	4200	1.4	7865
		1000	2498	3067	3379	3649	3908	4163	1.4	7865
	125mm	250	2592	3609	4177	4711	5225	5724	1.3	9289
		500	2686	3560	4086	4574	5055	5527	1.4	9289
		750	2748	3544	4049	4523	4989	5449	1.4	9289
		1000	2799	3537	4034	4503	4955	5406	1.4	9289
	150mm	250	2928	4184	4957	5711	6448	7168	1.3	11030
		500	3031	4119	4847	5553	6251	6945	1.4	11030
		750	3105	4101	4818	5495	6175	6855	1.4	11030
		1000	3160	4088	4795	5467	6144	6806	1.5	11030

Initial Pt Force 0.1F_{yield}		Axial Load (excluding PT) 3000kN			Cantilever Length (7000mm)			Grade 300 Dissipaters		
	PT Dia.	Fuse Length (mm)	Yield (kNm)	1%drift (kNm)	2%drift (kNm)	3%drift (kNm)	4%drift (kNm)	6%drift (kNm)	λ	Fuse Area (mm^2)
Diameter (1500mm)	36mm	250	2526	3142	3242	3270	3256	3218	1.2	5711
		500	2602	3092	3141	3126	3092	3033	1.3	5711
		750	2645	3071	3101	3072	3026	2955	1.4	5711
		1000	2682	3055	3080	3044	2991	2913	1.4	5711
	50mm	250	2615	3318	3512	3639	3724	3765	1.3	6062
		500	2695	3267	3408	3487	3547	3576	1.4	6062
		750	2739	3245	3365	3429	3476	3493	1.4	6062
		1000	2780	3228	3343	3398	3438	3448	1.4	6062
	75mm	250	2846	3768	4191	4551	4882	5193	1.4	6972
		500	2935	3710	4075	4390	4686	4966	1.5	6972
		750	2983	3688	4034	4324	4599	4867	1.5	6972
		1000	3029	3669	4006	4287	4554	4813	1.5	6972
	100mm	250	3165	4377	5100	5760	6391	6999	1.5	8247
		500	3269	4313	4967	5575	6168	6751	1.6	8247
		750	3317	4286	4919	5505	6078	6644	1.6	8247
		1000	3374	4268	4895	5468	6029	6585	1.6	8247
	125mm	250	3569	5135	6210	7224	8209	9168	1.5	9886
		500	3685	5055	6055	7009	7949	8880	1.6	9886
		750	3742	5026	6000	6927	7844	8755	1.7	9886
		1000	3808	5014	5972	6885	7789	8688	1.7	9886
	150mm	250	4056	6023	7494	8906	10288	11641	1.6	11889
		500	4182	5928	7314	8656	9984	11302	1.7	11889
		750	4251	5897	7249	8562	9863	11157	1.7	11889
		1000	4327	5885	7217	8512	9797	11080	1.7	11889

Initial Pt Force 0.1f_{yield}		Axial Load (excluding PT) 3000kN			Cantilever Length (7000mm)			Grade 300 Dissipaters		
	PT Dia.	Fuse Length (mm)	Yield (kNm)	1%drift (kNm)	2%drift (kNm)	3%drift (kNm)	4%drift (kNm)	6%drift (kNm)	λ	Fuse Area (mm^2)
Diameter (1800mm)	36mm	250	3195	3963	4141	4243	4309	4236	1.3	5760
		500	3240	3887	4000	4058	4090	4004	1.4	5760
		750	3317	3857	3949	3987	3997	3894	1.5	5760
		1000	3352	3842	3923	3950	3946	3833	1.5	5760
	50mm	250	3317	4221	4545	4783	4989	4954	1.4	6157
		500	3366	4142	4393	4590	4757	4708	1.5	6157
		750	3447	4110	4338	4515	4657	4591	1.5	6157
		1000	3487	4093	4310	4475	4606	4526	1.6	6157
	75mm	250	3631	4876	5561	6160	6711	6787	1.5	7187
		500	3689	4790	5387	5929	6453	6503	1.6	7187
		750	3782	4751	5321	5839	6343	6369	1.7	7187
		1000	3828	4732	5286	5792	6285	6298	1.7	7187
	100mm	250	4063	5767	6913	7987	9019	9317	1.6	8629
		500	4135	5665	6719	7724	8702	8977	1.7	8629
		750	4244	5626	6642	7610	8564	8819	1.8	8629
		1000	4301	5597	6598	7550	8490	8731	1.8	8629
	125mm	250	4611	6871	8572	10196	11775	12490	1.7	10482
		500	4703	6750	8343	9886	11412	12088	1.8	10482
		750	4828	6709	8259	9764	11259	11900	1.9	10482
		1000	4887	6674	8212	9699	11174	11789	1.9	10482
	150mm	250	5272	8164	10500	12750	14949	16242	1.7	12747
		500	5390	8025	10229	12383	14518	15761	1.9	12747
		750	5531	7977	10130	12240	14338	15539	1.9	12747
		1000	5590	7943	10079	12166	14240	15417	2.0	12747

Initial Pt Force 0.1f_{yield}		Axial Load (excluding PT) 3000kN			Cantilever Length (7000mm)			Grade 300 Dissipaters		
	PT Dia.	Fuse Length (mm)	Yield (kNm)	1%drift (kNm)	2%drift (kNm)	3%drift (kNm)	4%drift (kNm)	6%drift (kNm)	λ	Fuse Area (mm^2)
Diameter (2000mm)	36mm	250	3863	4746	5008	5206	5272	5220	1.2	6518
		500	3904	4637	4824	4956	4987	4930	1.3	6518
		750	3948	4600	4755	4856	4861	4782	1.3	6518
		1000	3993	4580	4720	4804	4792	4699	1.4	6518
	50mm	250	4026	5081	5527	5900	6086	6080	1.3	6998
		500	4070	4968	5328	5635	5783	5769	1.4	6998
		750	4115	4926	5255	5530	5648	5612	1.4	6998
		1000	4164	4905	5217	5476	5574	5523	1.4	6998
	75mm	250	4444	5936	6844	7648	8169	8279	1.4	8246
		500	4493	5809	6606	7349	7816	7916	1.5	8246
		750	4547	5758	6519	7229	7660	7734	1.6	8246
		1000	4607	5732	6474	7166	7578	7632	1.6	8246
	100mm	250	5015	7098	8613	10033	11037	11292	1.5	9993
		500	5082	6951	8334	9656	10616	10858	1.6	9993
		750	5143	6892	8224	9506	10431	10645	1.7	9993
		1000	5216	6858	8167	9428	10331	10526	1.7	9993
	125mm	250	5736	8542	10776	12912	14660	15128	1.6	12240
		500	5827	8367	10452	12481	14154	14589	1.7	12240
		750	5897	8305	10330	12304	13922	14326	1.8	12240
		1000	5988	8262	10256	12202	13795	14178	1.8	12240
	150mm	250	6605	10240	13299	16249	18948	19676	1.6	14985
		500	6725	10034	12915	15737	18339	19040	1.7	14985
		750	6807	9966	12772	15533	18073	18728	1.8	14985
		1000	6912	9915	12699	15425	17928	18549	1.8	14985

Initial Pt Force 0.1f_{yield}		Axial Load (excluding PT) 4500kN			Cantilever Length (7000mm)			Grade 300 Dissipaters		
	PT Dia.	Fuse Length (mm)	Yield (kNm)	1%drift (kNm)	2%drift (kNm)	3%drift (kNm)	4%drift (kNm)	6%drift (kNm)	λ	Fuse Area (mm^2)
Diameter (1000mm)	36mm	250	1469	1834	1809	1736	1641	1535	1.0	5628
		500	1536	1811	1764	1669	1556	1434	1.0	5628
		750	1573	1804	1748	1645	1524	1394	1.0	5628
		1000	1598	1801	1740	1632	1507	1373	1.0	5628
	50mm	250	1515	1912	1917	1881	1824	1754	1.0	5903
		500	1583	1887	1871	1812	1735	1650	1.0	5903
		750	1623	1880	1855	1787	1702	1609	1.1	5903
		1000	1649	1877	1849	1774	1684	1587	1.1	5903
	75mm	250	1633	2111	2196	2243	2274	2293	1.0	6614
		500	1706	2083	2146	2170	2178	2180	1.1	6614
		750	1749	2075	2128	2143	2142	2136	1.1	6614
		1000	1778	2069	2121	2126	2123	2112	1.1	6614
	100mm	250	1799	2384	2563	2720	2859	2992	1.1	7611
		500	1877	2349	2509	2639	2753	2866	1.1	7611
		750	1924	2339	2492	2608	2712	2818	1.2	7611
		1000	1957	2332	2486	2591	2693	2792	1.2	7611
	125mm	250	2006	2717	3026	3296	3564	3816	1.1	8892
		500	2094	2682	2960	3196	3436	3674	1.2	8892
		750	2148	2665	2938	3170	3399	3618	1.2	8892
		1000	2183	2655	2926	3150	3369	3587	1.2	8892
	150mm	250	2259	3110	3565	3948	4354	4739	1.1	10458
		500	2356	3072	3481	3844	4207	4578	1.2	10458
		750	2417	3052	3453	3809	4166	4515	1.2	10458
		1000	2457	3034	3439	3792	4135	4492	1.2	10458

Initial Pt Force 0.1F_{yield}		Axial Load (excluding PT) 4500kN			Cantilever Length (7000mm)			Grade 300 Dissipaters		
	PT Dia.	Fuse Length (mm)	Yield (kNm)	1%drift (kNm)	2%drift (kNm)	3%drift (kNm)	4%drift (kNm)	6%drift (kNm)	λ	Fuse Area (mm^2)
Diameter (1200mm)	36mm	250	1879	2342	2369	2334	2275	2201	1.1	5661
		500	1950	2313	2305	2241	2159	2063	1.2	5661
		750	1987	2303	2282	2207	2110	2003	1.2	5661
		1000	2020	2295	2269	2185	2083	1971	1.2	5661
	50mm	250	1941	2454	2535	2555	2553	2536	1.1	5966
		500	2014	2422	2467	2458	2432	2397	1.2	5966
		750	2053	2412	2444	2423	2385	2336	1.2	5966
		1000	2088	2405	2432	2403	2356	2302	1.2	5966
	75mm	250	2098	2739	2950	3107	3242	3363	1.2	6758
		500	2176	2705	2877	3001	3110	3211	1.3	6758
		750	2220	2692	2851	2961	3058	3149	1.3	6758
		1000	2260	2686	2837	2941	3031	3116	1.3	6758
	100mm	250	2316	3128	3503	3836	4146	4442	1.3	7865
		500	2401	3085	3422	3716	3996	4270	1.3	7865
		750	2453	3073	3393	3671	3939	4200	1.4	7865
		1000	2498	3067	3379	3649	3908	4163	1.4	7865
	125mm	250	2592	3609	4177	4711	5225	5724	1.3	9289
		500	2686	3560	4086	4574	5055	5527	1.4	9289
		750	2748	3544	4049	4523	4989	5449	1.4	9289
		1000	2799	3537	4034	4503	4955	5406	1.4	9289
	150mm	250	2928	4184	4957	5711	6448	7168	1.3	11030
		500	3031	4119	4847	5553	6251	6945	1.4	11030
		750	3105	4101	4818	5495	6175	6855	1.4	11030
		1000	3160	4088	4795	5467	6144	6806	1.5	11030

Initial Pt Force 0.1f_{yield}		Axial Load (excluding PT) 4500kN			Cantilever Length (7000mm)			Grade 300 Dissipaters		
	PT Dia.	Fuse Length (mm)	Yield (kNm)	1%drift (kNm)	2%drift (kNm)	3%drift (kNm)	4%drift (kNm)	6%drift (kNm)	λ	Fuse Area (mm^2)
Diameter (1500mm)	36mm	250	2526	3142	3242	3270	3256	3218	1.2	5711
		500	2602	3092	3141	3126	3092	3033	1.3	5711
		750	2645	3071	3101	3072	3026	2955	1.4	5711
		1000	2682	3055	3080	3044	2991	2913	1.4	5711
	50mm	250	2615	3318	3512	3639	3724	3765	1.3	6062
		500	2695	3267	3408	3487	3547	3576	1.4	6062
		750	2739	3245	3365	3429	3476	3493	1.4	6062
		1000	2780	3228	3343	3398	3438	3448	1.4	6062
	75mm	250	2846	3768	4191	4551	4882	5193	1.4	6972
		500	2935	3710	4075	4390	4686	4966	1.5	6972
		750	2983	3688	4034	4324	4599	4867	1.5	6972
		1000	3029	3669	4006	4287	4554	4813	1.5	6972
	100mm	250	3165	4377	5100	5760	6391	6999	1.5	8247
		500	3269	4313	4967	5575	6168	6751	1.6	8247
		750	3317	4286	4919	5505	6078	6644	1.6	8247
		1000	3374	4268	4895	5468	6029	6585	1.6	8247
	125mm	250	3569	5135	6210	7224	8209	9168	1.5	9886
		500	3685	5055	6055	7009	7949	8880	1.6	9886
		750	3742	5026	6000	6927	7844	8755	1.7	9886
		1000	3808	5014	5972	6885	7789	8688	1.7	9886
	150mm	250	4056	6023	7494	8906	10288	11641	1.6	11889
		500	4182	5928	7314	8656	9984	11302	1.7	11889
		750	4251	5897	7249	8562	9863	11157	1.7	11889
		1000	4327	5885	7217	8512	9797	11080	1.7	11889

Initial Pt Force 0.1F_{yield}		Axial Load (excluding PT) 4500kN			Cantilever Length (7000mm)			Grade 300 Dissipaters		
	PT Dia.	Fuse Length (mm)	Yield (kNm)	1%drift (kNm)	2%drift (kNm)	3%drift (kNm)	4%drift (kNm)	6%drift (kNm)	λ	Fuse Area (mm^2)
Diameter (1800mm)	36mm	250	3195	3963	4141	4243	4309	4236	1.3	5760
		500	3240	3887	4000	4058	4090	4004	1.4	5760
		750	3317	3857	3949	3987	3997	3894	1.5	5760
		1000	3352	3842	3923	3950	3946	3833	1.5	5760
	50mm	250	3317	4221	4545	4783	4989	4954	1.4	6157
		500	3366	4142	4393	4590	4757	4708	1.5	6157
		750	3447	4110	4338	4515	4657	4591	1.5	6157
		1000	3487	4093	4310	4475	4606	4526	1.6	6157
	75mm	250	3631	4876	5561	6160	6711	6787	1.5	7187
		500	3689	4790	5387	5929	6453	6503	1.6	7187
		750	3782	4751	5321	5839	6343	6369	1.7	7187
		1000	3828	4732	5286	5792	6285	6298	1.7	7187
	100mm	250	4063	5767	6913	7987	9019	9317	1.6	8629
		500	4135	5665	6719	7724	8702	8977	1.7	8629
		750	4244	5626	6642	7610	8564	8819	1.8	8629
		1000	4301	5597	6598	7550	8490	8731	1.8	8629
	125mm	250	4611	6871	8572	10196	11775	12490	1.7	10482
		500	4703	6750	8343	9886	11412	12088	1.8	10482
		750	4828	6709	8259	9764	11259	11900	1.9	10482
		1000	4887	6674	8212	9699	11174	11789	1.9	10482
	150mm	250	5272	8164	10500	12750	14949	16242	1.7	12747
		500	5390	8025	10229	12383	14518	15761	1.9	12747
		750	5531	7977	10130	12240	14338	15539	1.9	12747
		1000	5590	7943	10079	12166	14240	15417	2.0	12747

Initial Pt Force 0.1F_{yield}		Axial Load (excluding PT) 4500kN			Cantilever Length (7000mm)			Grade 300 Dissipaters		
	PT Dia.	Fuse Length (mm)	Yield (kNm)	1%drift (kNm)	2%drift (kNm)	3%drift (kNm)	4%drift (kNm)	6%drift (kNm)	λ	Fuse Area (mm^2)
Diameter (2000mm)	36mm	250	5441	6801	7131	7299	7356	7262	1.1	9518
		500	5550	6659	6853	6947	6946	6841	1.3	9518
		750	5616	6601	6751	6806	6765	6629	1.3	9518
		1000	5686	6571	6698	6731	6666	6510	1.3	9518
	50mm	250	5594	7120	7633	7978	8154	8106	1.2	9998
		500	5709	6974	7341	7608	7726	7666	1.3	9998
		750	5777	6915	7233	7460	7538	7445	1.3	9998
		1000	5848	6882	7178	7382	7437	7320	1.4	9998
	75mm	250	5987	7941	8896	9707	10209	10270	1.3	11246
		500	6115	7779	8584	9283	9737	9780	1.4	11246
		750	6190	7718	8460	9115	9529	9534	1.4	11246
		1000	6273	7679	8395	9026	9416	9399	1.5	11246
	100mm	250	6535	9060	10603	12009	13073	13264	1.4	12993
		500	6683	8877	10255	11546	12516	12702	1.5	12993
		750	6764	8813	10123	11346	12272	12424	1.5	12993
		1000	6858	8766	10045	11241	12140	12269	1.6	12993
	125mm	250	7228	10459	12713	14826	16630	17066	1.4	15240
		500	7405	10248	12315	14295	16004	16413	1.6	15240
		750	7496	10175	12168	14085	15730	16079	1.6	15240
		1000	7593	10124	12091	13969	15575	15892	1.7	15240
	150mm	250	8067	12113	15183	18108	20875	21566	1.5	17985
		500	8271	11869	14727	17496	20149	20804	1.6	17985
		750	8376	11783	14557	17253	19833	20433	1.7	17985
		1000	8475	11732	14471	17126	19661	20226	1.7	17985

Initial Pt Force $0.1f_{yield}$		Axial Load (excluding PT) 6000kN			Cantilever Length (7000mm)			Grade 300 Dissipaters		
	PT Dia.	Fuse Length (mm)	Yield (kNm)	1%drift (kNm)	2%drift (kNm)	3%drift (kNm)	4%drift (kNm)	6%drift (kNm)	λ	Fuse Area (mm^2)
Diameter (1000mm)	36mm	250	2422	3139	3059	2853	2624	2361	1.0	9592
		500	2545	3108	2987	2747	2484	2200	1.0	9592
		750	2634	3087	2960	2715	2436	2135	1.1	9592
		1000	2700	3072	2947	2694	2406	2102	1.1	9592
	50mm	250	2463	3199	3154	2974	2773	2550	1.0	9832
		500	2584	3168	3074	2865	2637	2380	1.1	9832
		750	2673	3149	3049	2829	2582	2317	1.1	9832
		1000	2741	3134	3035	2812	2558	2286	1.1	9832
	75mm	250	2561	3362	3389	3275	3154	3013	1.0	10454
		500	2687	3326	3306	3166	3008	2836	1.1	10454
		750	2780	3304	3274	3128	2959	2774	1.1	10454
		1000	2848	3289	3263	3113	2926	2733	1.1	10454
	100mm	250	2700	3579	3704	3688	3658	3617	1.1	11326
		500	2826	3543	3614	3575	3503	3442	1.1	11326
		750	2925	3523	3582	3528	3449	3366	1.1	11326
		1000	2997	3507	3567	3508	3423	3334	1.1	11326
	125mm	250	2877	3856	4092	4203	4274	4348	1.1	12447
		500	3007	3811	4001	4068	4108	4152	1.1	12447
		750	3113	3797	3962	4026	4059	4087	1.2	12447
		1000	3186	3776	3945	3997	4024	4038	1.2	12447
	150mm	250	3088	4184	4538	4806	4993	5185	1.1	13817
		500	3228	4132	4447	4653	4815	4967	1.2	13817
		750	3340	4115	4407	4589	4748	4897	1.2	13817
		1000	3418	4099	4385	4561	4722	4857	1.2	13817

Initial Pt Force 0.1f_{yield}		Axial Load (excluding PT) 6000kN			Cantilever Length (7000mm)			Grade 300 Dissipaters		
	PT Dia.	Fuse Length (mm)	Yield (kNm)	1%drift (kNm)	2%drift (kNm)	3%drift (kNm)	4%drift (kNm)	6%drift (kNm)	λ	Fuse Area (mm^2)
Diameter (1200mm)	36mm	250	3102	4065	4043	3909	3720	3499	1.2	9620
		500	3267	4013	3941	3761	3532	3281	1.2	9620
		750	3373	3994	3909	3706	3460	3192	1.3	9620
		1000	3442	3987	3889	3678	3422	3145	1.3	9620
	50mm	250	3153	4157	4183	4095	3960	3793	1.2	9887
		500	3321	4104	4080	3946	3769	3571	1.3	9887
		750	3428	4085	4042	3890	3696	3481	1.3	9887
		1000	3499	4077	4027	3862	3657	3433	1.3	9887
	75mm	250	3284	4397	4531	4569	4564	4527	1.2	10579
		500	3455	4340	4426	4414	4364	4294	1.3	10579
		750	3569	4319	4390	4353	4287	4200	1.3	10579
		1000	3641	4308	4371	4326	4246	4151	1.3	10579
	100mm	250	3468	4721	5009	5206	5369	5497	1.3	11549
		500	3647	4663	4896	5039	5148	5249	1.3	11549
		750	3765	4640	4857	4973	5069	5150	1.4	11549
		1000	3845	4625	4834	4941	5031	5097	1.4	11549
	125mm	250	3702	5133	5604	5977	6329	6660	1.3	12795
		500	3889	5068	5479	5793	6103	6390	1.4	12795
		750	4010	5043	5431	5728	6013	6287	1.4	12795
		1000	4098	5020	5415	5706	5969	6238	1.4	12795
	150mm	250	3989	5615	6306	6876	7437	7998	1.3	14318
		500	4181	5549	6159	6677	7199	7696	1.4	14318
		750	4307	5521	6108	6617	7094	7577	1.4	14318
		1000	4402	5494	6086	6574	7054	7518	1.4	14318

Initial Pt Force 0.1F_{yield}		Axial Load (excluding PT) 6000kN			Cantilever Length (7000mm)			Grade 300 Dissipaters		
	PT Dia.	Fuse Length (mm)	Yield (kNm)	1%drift (kNm)	2%drift (kNm)	3%drift (kNm)	4%drift (kNm)	6%drift (kNm)	λ	Fuse Area (mm^2)
Diameter (1500mm)	36mm	250	4246	5491	5591	5542	5429	5273	1.3	9664
		500	4417	5410	5434	5320	5157	4970	1.4	9664
		750	4528	5384	5380	5235	5048	4831	1.4	9664
		1000	4610	5373	5350	5192	4985	4754	1.5	9664
	50mm	250	4319	5640	5825	5863	5840	5775	1.3	9971
		500	4493	5559	5664	5636	5563	5466	1.4	9971
		750	4610	5533	5607	5550	5451	5331	1.5	9971
		1000	4691	5518	5578	5505	5391	5250	1.5	9971
	75mm	250	4507	6020	6420	6675	6874	7034	1.4	10767
		500	4692	5936	6247	6435	6581	6707	1.5	10767
		750	4814	5909	6187	6343	6463	6565	1.5	10767
		1000	4900	5894	6156	6296	6401	6488	1.6	10767
	100mm	250	4773	6545	7219	7764	8253	8704	1.5	11883
		500	4965	6453	7035	7504	7938	8351	1.6	11883
		750	5097	6425	6969	7407	7811	8200	1.6	11883
		1000	5190	6409	6936	7356	7743	8117	1.6	11883
	125mm	250	5109	7207	8207	9095	9930	10726	1.5	13317
		500	5315	7102	8004	8812	9584	10340	1.6	13317
		750	5459	7068	7935	8705	9446	10175	1.7	13317
		1000	5557	7057	7895	8649	9373	10085	1.7	13317
	150mm	250	5516	7989	9365	10637	11859	13043	1.5	15069
		500	5737	7877	9141	10324	11479	12616	1.7	15069
		750	5895	7833	9065	10207	11328	12435	1.7	15069
		1000	6003	7816	9019	10145	11248	12337	1.7	15069

Initial Pt Force 0.1f_{yield}		Axial Load (excluding PT) 6000kN			Cantilever Length (7000mm)			Grade 300 Dissipaters		
	PT Dia.	Fuse Length (mm)	Yield (kNm)	1%drift (kNm)	2%drift (kNm)	3%drift (kNm)	4%drift (kNm)	6%drift (kNm)	λ	Fuse Area (mm^2)
Diameter (1800mm)	36mm	250	5417	6970	7183	7234	7190	6977	1.4	9707
		500	5581	6857	6961	6924	6826	6597	1.5	9707
		750	5751	6815	6879	6798	6673	6420	1.6	9707
		1000	5813	6787	6830	6732	6591	6323	1.6	9707
	50mm	250	5517	7193	7538	7724	7830	7660	1.4	10054
		500	5686	7077	7309	7411	7449	7268	1.6	10054
		750	5857	7032	7226	7280	7289	7085	1.6	10054
		1000	5925	7004	7176	7210	7204	6983	1.6	10054
	75mm	250	5781	7762	8439	8964	9416	9436	1.5	10955
		500	5954	7637	8194	8629	9022	8996	1.6	10955
		750	6138	7590	8105	8499	8846	8792	1.7	10955
		1000	6208	7563	8058	8422	8750	8680	1.7	10955
	100mm	250	6147	8540	9659	10630	11531	11834	1.6	12217
		500	6323	8403	9392	10266	11101	11363	1.7	12217
		750	6525	8350	9295	10124	10920	11144	1.8	12217
		1000	6604	8324	9245	10049	10823	11014	1.8	12217
	125mm	250	6615	9513	11166	12675	14113	14844	1.7	13838
		500	6796	9357	10871	12273	13639	14318	1.8	13838
		750	7020	9304	10764	12116	13440	14076	1.9	13838
		1000	7103	9277	10709	12033	13332	13941	1.9	13838
	150mm	250	7179	10670	12930	15053	17102	18434	1.7	15821
		500	7366	10498	12601	14604	16574	17842	1.9	15821
		750	7617	10435	12482	14430	16351	17569	1.9	15821
		1000	7707	10408	12421	14339	16233	17420	2.0	15821

Initial Pt Force 0.1f_{yield}		Axial Load (excluding PT) 6000kN			Cantilever Length (7000mm)			Grade 300 Dissipaters		
	PT Dia.	Fuse Length (mm)	Yield (kNm)	1%drift (kNm)	2%drift (kNm)	3%drift (kNm)	4%drift (kNm)	6%drift (kNm)	λ	Fuse Area (mm^2)
Diameter (2000mm)	36mm	250	6933	8807	9206	9397	9406	9272	1.1	12518
		500	7121	8627	8861	8924	8879	8723	1.2	12518
		750	7220	8567	8722	8735	8647	8448	1.3	12518
		1000	7302	8520	8650	8636	8521	8293	1.3	12518
	50mm	250	7080	9116	9690	10064	10202	10103	1.2	12998
		500	7273	8931	9331	9569	9654	9535	1.3	12998
		750	7376	8867	9190	9373	9414	9251	1.3	12998
		1000	7459	8819	9115	9269	9283	9094	1.3	12998
	75mm	250	7460	9908	10911	11726	12263	12243	1.2	14246
		500	7665	9707	10527	11210	11650	11630	1.3	14246
		750	7774	9638	10385	10991	11384	11327	1.4	14246
		1000	7862	9587	10300	10875	11239	11156	1.4	14246
	100mm	250	7988	10992	12573	13968	15064	15251	1.3	15993
		500	8213	10771	12151	13403	14401	14541	1.4	15993
		750	8325	10692	11995	13177	14103	14195	1.5	15993
		1000	8423	10644	11912	13048	13937	14001	1.5	15993
	125mm	250	8666	12351	14633	16730	18583	18981	1.4	18240
		500	8910	12103	14163	16100	17838	18203	1.5	18240
		750	9026	12010	13990	15849	17514	17822	1.5	18240
		1000	9135	11963	13900	15717	17338	17599	1.6	18240
	150mm	250	9485	13963	17054	19957	22739	23442	1.4	20985
		500	9753	13685	16527	19248	21923	22558	1.5	20985
		750	9877	13583	16332	18967	21571	22127	1.6	20985
		1000	9992	13526	16232	18819	21379	21887	1.6	20985

Initial Pt Force 0.1f_{yield}		Axial Load (excluding PT) 6000kN			Cantilever Length (7000mm)			Grade 300 Dissipaters		
	PT Dia.	Fuse Length (mm)	Yield (kNm)	1%drift (kNm)	2%drift (kNm)	3%drift (kNm)	4%drift (kNm)	6%drift (kNm)	λ	Fuse Area (mm^2)
Diameter (2200mm)	36mm	250	7751	9920	10424	10679	10716	10589	1.1	12555
		500	7982	9700	9999	10146	10114	9994	1.3	12555
		750	8112	9616	9841	9928	9836	9674	1.3	12555
		1000	8232	9570	9759	9811	9683	9490	1.3	12555
	50mm	250	7925	10299	11020	11493	11626	11552	1.2	13070
		500	8160	10071	10581	10938	11001	10933	1.3	13070
		750	8294	9986	10416	10711	10714	10601	1.3	13070
		1000	8419	9937	10330	10590	10558	10412	1.4	13070
	75mm	250	8369	11268	12531	13570	13963	14024	1.3	14407
		500	8626	11021	12067	12953	13288	13347	1.4	14407
		750	8766	10933	11881	12701	12979	12985	1.4	14407
		1000	8903	10877	11785	12567	12809	12779	1.5	14407
	100mm	250	8989	12598	14584	16362	17236	17434	1.3	16280
		500	9269	12326	14073	15689	16461	16679	1.5	16280
		750	9427	12229	13878	15399	16109	16281	1.5	16280
		1000	9579	12170	13766	15245	15916	16054	1.6	16280
	125mm	250	9775	14266	17134	19791	21341	21818	1.4	18687
		500	10091	13956	16561	19039	20475	20929	1.5	18687
		750	10265	13852	16347	18732	20073	20466	1.6	18687
		1000	10428	13787	16233	18560	19848	20204	1.6	18687
	150mm	250	10734	16244	20136	23804	26239	27012	1.5	21629
		500	11082	15897	19488	22953	25251	26017	1.6	21629
		750	11274	15777	19246	22608	24804	25498	1.7	21629
		1000	11448	15702	19119	22423	24559	25192	1.7	21629

Initial Pt Force 0.1F_{yield}		Axial Load (excluding PT) 7500kN			Cantilever Length (7000mm)			Grade 300 Dissipaters		
	PT Dia.	Fuse Length (mm)	Yield (kNm)	1%drift (kNm)	2%drift (kNm)	3%drift (kNm)	4%drift (kNm)	6%drift (kNm)	λ	Fuse Area (mm^2)
Diameter (1000mm)	36mm	250	2703	3552	3450	3169	2850	2503	1.1	10221
		500	2852	3518	3372	3061	2706	2333	1.2	10221
		750	2964	3503	3341	3021	2657	2266	1.2	10221
		1000	3044	3486	3327	3002	2629	2232	1.2	10221
	50mm	250	2737	3606	3530	3276	2991	2673	1.1	10427
		500	2884	3570	3453	3169	2846	2505	1.2	10427
		750	3001	3556	3421	3126	2789	2434	1.2	10427
		1000	3078	3539	3408	3107	2766	2402	1.2	10427
	75mm	250	2823	3745	3736	3559	3335	3100	1.2	10961
		500	2975	3709	3656	3444	3185	2921	1.2	10961
		750	3092	3691	3622	3402	3131	2858	1.2	10961
		1000	3172	3678	3607	3377	3105	2816	1.2	10961
	100mm	250	2945	3940	4014	3945	3796	3663	1.2	11708
		500	3100	3895	3932	3811	3647	3476	1.2	11708
		750	3217	3882	3901	3764	3591	3412	1.3	11708
		1000	3305	3869	3880	3741	3562	3367	1.3	11708
	125mm	250	3098	4180	4357	4404	4378	4342	1.2	12669
		500	3258	4132	4277	4272	4213	4146	1.3	12669
		750	3381	4116	4241	4214	4151	4074	1.3	12669
		1000	3470	4104	4218	4193	4121	4047	1.3	12669
	150mm	250	3288	4466	4762	4941	5058	5133	1.2	13843
		500	3453	4416	4673	4795	4870	4924	1.3	13843
		750	3579	4400	4639	4741	4799	4857	1.3	13843
		1000	3676	4390	4621	4713	4762	4817	1.3	13843

Initial Pt Force 0.1f_{yield}		Axial Load (excluding PT) 7500kN			Cantilever Length (7000mm)			Grade 300 Dissipaters		
	PT Dia.	Fuse Length (mm)	Yield (kNm)	1%drift (kNm)	2%drift (kNm)	3%drift (kNm)	4%drift (kNm)	6%drift (kNm)	λ	Fuse Area (mm^2)
Diameter (1200mm)	36mm	250	3484	4647	4591	4391	4126	3819	1.3	10246
		500	3682	4599	4490	4236	3929	3590	1.4	10246
		750	3820	4575	4452	4178	3853	3497	1.4	10246
		1000	3921	4562	4434	4152	3814	3448	1.5	10246
	50mm	250	3529	4732	4719	4563	4348	4093	1.3	10475
		500	3729	4679	4610	4408	4149	3861	1.4	10475
		750	3868	4659	4574	4347	4072	3768	1.5	10475
		1000	3966	4645	4556	4321	4032	3718	1.5	10475
	75mm	250	3645	4943	5037	5002	4905	4781	1.4	11068
		500	3848	4887	4929	4838	4700	4541	1.5	11068
		750	3988	4865	4892	4778	4626	4444	1.5	11068
		1000	4094	4848	4871	4743	4578	4393	1.5	11068
	100mm	250	3804	5231	5475	5587	5651	5694	1.4	11899
		500	4012	5177	5356	5415	5441	5440	1.5	11899
		750	4158	5148	5316	5353	5352	5339	1.5	11899
		1000	4269	5131	5297	5323	5315	5285	1.6	11899
	125mm	250	4013	5591	6023	6303	6558	6786	1.5	12967
		500	4219	5533	5890	6117	6326	6523	1.5	12967
		750	4378	5507	5848	6061	6248	6413	1.6	12967
		1000	4491	5484	5821	6022	6193	6358	1.6	12967
	150mm	250	4265	6024	6668	7144	7599	8055	1.5	14273
		500	4478	5961	6519	6951	7350	7756	1.6	14273
		750	4638	5933	6465	6883	7254	7639	1.6	14273
		1000	4764	5902	6441	6848	7211	7581	1.6	14273

Initial Pt Force $0.1F_{yield}$		Axial Load (excluding PT) 7500kN			Cantilever Length (7000mm)			Grade 300 Dissipaters		
	PT Dia.	Fuse Length (mm)	Yield (kNm)	1%drift (kNm)	2%drift (kNm)	3%drift (kNm)	4%drift (kNm)	6%drift (kNm)	λ	Fuse Area (mm^2)
Diameter (1500mm)	36mm	250	4789	6324	6400	6289	6101	5861	1.5	10283
		500	5029	6245	6237	6057	5815	5542	1.6	10283
		750	5186	6217	6181	5969	5701	5404	1.7	10283
		1000	5290	6203	6152	5924	5640	5327	1.7	10283
	50mm	250	4854	6457	6615	6589	6487	6337	1.5	10546
		500	5093	6377	6451	6352	6198	6012	1.6	10546
		750	5253	6349	6392	6263	6081	5872	1.7	10546
		1000	5359	6335	6362	6217	6019	5796	1.7	10546
	75mm	250	5018	6801	7163	7348	7463	7533	1.6	11229
		500	5264	6718	6990	7100	7160	7193	1.7	11229
		750	5435	6689	6927	7007	7039	7048	1.7	11229
		1000	5543	6675	6893	6958	6975	6969	1.8	11229
	100mm	250	5248	7278	7903	8368	8768	9125	1.6	12185
		500	5505	7186	7713	8105	8447	8765	1.8	12185
		750	5681	7155	7650	8006	8318	8610	1.8	12185
		1000	5801	7140	7616	7954	8250	8527	1.8	12185
	125mm	250	5544	7879	8817	9619	10359	11056	1.7	13414
		500	5810	7774	8612	9336	10013	10668	1.8	13414
		750	5996	7742	8548	9230	9876	10504	1.9	13414
		1000	6127	7727	8512	9175	9803	10414	1.9	13414
	150mm	250	5903	8594	9884	11075	12194	13274	1.7	14917
		500	6184	8474	9667	10757	11817	12853	1.9	14917
		750	6381	8440	9596	10640	11668	12676	1.9	14917
		1000	6521	8416	9560	10582	11590	12580	1.9	14917

Initial Pt Force 0.1f_{yield}		Axial Load (excluding PT) 7500kN			Cantilever Length (7000mm)			Grade 300 Dissipaters		
	PT Dia.	Fuse Length (mm)	Yield (kNm)	1%drift (kNm)	2%drift (kNm)	3%drift (kNm)	4%drift (kNm)	6%drift (kNm)	λ	Fuse Area (mm^2)
Diameter (1800mm)	36mm	250	6172	8065	8256	8247	8145	7858	1.6	10320
		500	6381	7945	8024	7927	7760	7450	1.8	10320
		750	6612	7899	7939	7801	7593	7260	1.8	10320
		1000	6702	7876	7895	7728	7504	7155	1.8	10320
	50mm	250	6260	8266	8586	8709	8742	8525	1.6	10618
		500	6470	8145	8349	8382	8356	8101	1.8	10618
		750	6707	8099	8262	8254	8183	7904	1.8	10618
		1000	6799	8076	8220	8181	8090	7796	1.9	10618
	75mm	250	6490	8783	9425	9879	10247	10216	1.7	11390
		500	6704	8656	9175	9535	9842	9774	1.9	11390
		750	6954	8604	9084	9400	9670	9558	1.9	11390
		1000	7051	8581	9039	9330	9571	9439	2.0	11390
	100mm	250	6814	9494	10564	11457	12267	12526	1.8	12471
		500	7030	9351	10295	11087	11831	12048	1.9	12471
		750	7298	9304	10197	10944	11648	11826	2.0	12471
		1000	7396	9275	10147	10868	11550	11704	2.0	12471
	125mm	250	7216	10383	11974	13397	14739	15433	1.9	13862
		500	7448	10227	11682	12996	14264	14909	2.0	13862
		750	7733	10173	11576	12840	14067	14667	2.1	13862
		1000	7840	10149	11522	12758	13960	14533	2.1	13862
	150mm	250	7702	11439	13629	15656	17602	18902	1.9	15561
		500	7950	11268	13308	15215	17082	18322	2.1	15561
		750	8261	11213	13192	15046	16865	18056	2.2	15561
		1000	8377	11189	13131	14956	16751	17909	2.2	15561

Initial Pt Force 0.1f_{yield}		Axial Load (excluding PT) 7500kN			Cantilever Length (7000mm)			Grade 300 Dissipaters		
	PT Dia.	Fuse Length (mm)	Yield (kNm)	1%drift (kNm)	2%drift (kNm)	3%drift (kNm)	4%drift (kNm)	6%drift (kNm)	λ	Fuse Area (mm^2)
Diameter (2000mm)	36mm	250	8367	10777	11246	11459	11470	11255	1.1	15518
		500	8626	10560	10825	10887	10806	10581	1.2	15518
		750	8749	10483	10670	10648	10516	10250	1.2	15518
		1000	8850	10431	10580	10523	10359	10064	1.3	15518
	50mm	250	8511	11076	11715	12097	12263	12083	1.1	15998
		500	8775	10853	11281	11516	11575	11392	1.2	15998
		750	8900	10774	11125	11271	11274	11050	1.3	15998
		1000	9003	10723	11033	11141	11112	10858	1.3	15998
	75mm	250	8881	11843	12902	13717	14275	14241	1.2	17246
		500	9158	11605	12445	13101	13555	13482	1.3	17246
		750	9285	11518	12276	12855	13227	13109	1.3	17246
		1000	9395	11466	12189	12714	13049	12901	1.4	17246
	100mm	250	9401	12897	14523	15911	17036	17186	1.2	18993
		500	9686	12639	14028	15245	16255	16372	1.4	18993
		750	9824	12539	13846	14981	15914	15957	1.4	18993
		1000	9942	12490	13752	14840	15724	15724	1.4	18993
	125mm	250	10060	14221	16539	18623	20519	20880	1.3	21240
		500	10356	13933	15997	17894	19658	19980	1.4	21240
		750	10510	13830	15798	17605	19284	19539	1.5	21240
		1000	10633	13772	15695	17451	19081	19292	1.5	21240
	150mm	250	10863	15792	18913	21798	24540	25307	1.3	23985
		500	11170	15471	18316	20993	23611	24300	1.5	23985
		750	11344	15366	18096	20675	23208	23811	1.5	23985
		1000	11477	15307	17982	20505	22991	23538	1.5	23985

Initial Pt Force 0.1f_{yield}		Axial Load (excluding PT) 7500kN			Cantilever Length (7000mm)			Grade 300 Dissipaters		
	PT Dia.	Fuse Length (mm)	Yield (kNm)	1%drift (kNm)	2%drift (kNm)	3%drift (kNm)	4%drift (kNm)	6%drift (kNm)	λ	Fuse Area (mm^2)
Diameter (2200mm)	36mm	250	9362	12146	12741	13031	13031	12868	1.1	15555
		500	9686	11882	12236	12363	12292	12134	1.2	15555
		750	9865	11789	12038	12090	11958	11741	1.3	15555
		1000	10010	11733	11932	11945	11774	11517	1.3	15555
	50mm	250	9528	12515	13316	13834	13930	13819	1.2	16070
		500	9863	12242	12801	13140	13175	13062	1.3	16070
		750	10043	12148	12597	12857	12830	12658	1.3	16070
		1000	10189	12088	12489	12708	12640	12427	1.3	16070
	75mm	250	9962	13457	14790	15854	16278	16265	1.2	17407
		500	10310	13167	14241	15121	15451	15449	1.3	17407
		750	10502	13065	14032	14812	15076	15021	1.4	17407
		1000	10658	13003	13913	14647	14870	14777	1.4	17407
	100mm	250	10564	14754	16800	18580	19513	19681	1.3	19280
		500	10937	14437	16202	17793	18604	18776	1.4	19280
		750	11137	14325	15979	17470	18183	18300	1.5	19280
		1000	11306	14258	15857	17282	17952	18031	1.5	19280
	125mm	250	11339	16380	19300	21953	23566	24012	1.4	21687
		500	11739	16030	18643	21087	22567	23005	1.5	21687
		750	11947	15907	18396	20735	22114	22463	1.5	21687
		1000	12127	15834	18269	20545	21859	22155	1.6	21687
	150mm	250	12277	18321	22252	25912	28427	29167	1.4	24629
		500	12702	17931	21520	24948	27308	28035	1.5	24629
		750	12932	17783	21248	24557	26803	27447	1.6	24629
		1000	13130	17705	21106	24350	26524	27114	1.6	24629

Initial Pt Force 0.1F_{yield}		Axial Load (excluding PT) 8500kN			Cantilever Length (7000mm)			Grade 300 Dissipaters		
	PT Dia.	Fuse Length (mm)	Yield (kNm)	1%drift (kNm)	2%drift (kNm)	3%drift (kNm)	4%drift (kNm)	6%drift (kNm)	λ	Fuse Area (mm^2)
Diameter (1000mm)	36mm	250	2990	3947	3834	3522	3148	2752	1.1	11555
		500	3153	3903	3749	3400	2988	2563	1.2	11555
		750	3274	3886	3717	3353	2934	2488	1.2	11555
		1000	3365	3875	3702	3332	2906	2449	1.2	11555
	50mm	250	3022	3998	3912	3629	3280	2921	1.1	11760
		500	3183	3952	3829	3500	3123	2723	1.2	11760
		750	3309	3936	3793	3458	3067	2653	1.2	11760
		1000	3398	3929	3778	3432	3033	2615	1.2	11760
	75mm	250	3109	4133	4106	3905	3614	3329	1.1	12294
		500	3275	4084	4023	3766	3454	3129	1.2	12294
		750	3400	4068	3989	3717	3400	3055	1.2	12294
		1000	3492	4062	3972	3695	3366	3019	1.2	12294
	100mm	250	3230	4316	4375	4271	4077	3874	1.1	13041
		500	3398	4267	4285	4126	3904	3668	1.2	13041
		750	3523	4252	4258	4075	3843	3591	1.2	13041
		1000	3619	4242	4235	4045	3811	3560	1.2	13041
	125mm	250	3380	4543	4707	4714	4650	4531	1.2	14002
		500	3552	4497	4620	4570	4458	4326	1.2	14002
		750	3683	4482	4585	4511	4390	4247	1.2	14002
		1000	3784	4479	4567	4479	4353	4217	1.2	14002
	150mm	250	3569	4824	5101	5234	5305	5328	1.2	15177
		500	3746	4773	5001	5076	5112	5092	1.2	15177
		750	3879	4760	4972	5028	5022	5003	1.2	15177
		1000	3988	4752	4954	4992	4981	4960	1.3	15177

Initial Pt Force 0.1f_{yield}		Axial Load (excluding PT) 8500kN			Cantilever Length (7000mm)			Grade 300 Dissipaters		
	PT Dia.	Fuse Length (mm)	Yield (kNm)	1%drift (kNm)	2%drift (kNm)	3%drift (kNm)	4%drift (kNm)	6%drift (kNm)	λ	Fuse Area (mm^2)
Diameter (1200mm)	36mm	250	3853	5178	5119	4887	4577	4227	1.3	11579
		500	4066	5125	5005	4714	4360	3971	1.4	11579
		750	4224	5103	4962	4653	4276	3867	1.4	11579
		1000	4341	5080	4941	4619	4232	3813	1.4	11579
	50mm	250	3898	5258	5242	5055	4794	4494	1.3	11808
		500	4113	5204	5123	4877	4575	4234	1.4	11808
		750	4269	5181	5084	4815	4486	4130	1.4	11808
		1000	4387	5157	5062	4783	4442	4074	1.5	11808
	75mm	250	4014	5463	5558	5473	5336	5163	1.4	12401
		500	4228	5407	5429	5291	5108	4896	1.4	12401
		750	4388	5383	5384	5226	5019	4789	1.5	12401
		1000	4510	5356	5368	5193	4974	4731	1.5	12401
	100mm	250	4172	5744	5988	6041	6064	6049	1.4	13232
		500	4391	5680	5846	5858	5832	5771	1.5	13232
		750	4557	5655	5800	5792	5734	5657	1.5	13232
		1000	4683	5632	5776	5752	5692	5599	1.5	13232
	125mm	250	4372	6095	6522	6741	6958	7127	1.4	14300
		500	4594	6032	6369	6546	6697	6830	1.5	14300
		750	4769	6006	6320	6475	6599	6716	1.5	14300
		1000	4900	5977	6295	6439	6549	6662	1.5	14300
	150mm	250	4621	6517	7140	7574	7968	8369	1.4	15606
		500	4850	6443	6982	7367	7696	8044	1.5	15606
		750	5030	6415	6924	7288	7610	7916	1.5	15606
		1000	5162	6385	6893	7239	7549	7852	1.6	15606

Initial Pt Force 0.1F_{yield}		Axial Load (excluding PT) 8500kN			Cantilever Length (7000mm)			Grade 300 Dissipaters		
	PT Dia.	Fuse Length (mm)	Yield (kNm)	1%drift (kNm)	2%drift (kNm)	3%drift (kNm)	4%drift (kNm)	6%drift (kNm)	λ	Fuse Area (mm^2)
Diameter (1500mm)	36mm	250	5290	7063	7147	7016	6792	6509	1.5	11617
		500	5566	6975	6970	6757	6473	6151	1.6	11617
		750	5751	6946	6903	6658	6345	5997	1.6	11617
		1000	5879	6931	6869	6608	6277	5913	1.7	11617
	50mm	250	5355	7194	7355	7308	7171	6976	1.5	11880
		500	5633	7105	7172	7044	6847	6612	1.6	11880
		750	5821	7075	7108	6945	6717	6456	1.7	11880
		1000	5947	7061	7071	6893	6648	6371	1.7	11880
	75mm	250	5517	7532	7889	8049	8126	8149	1.6	12562
		500	5799	7439	7699	7775	7789	7772	1.7	12562
		750	5996	7409	7626	7672	7655	7610	1.7	12562
		1000	6129	7394	7590	7617	7583	7522	1.7	12562
	100mm	250	5742	8003	8607	9048	9406	9715	1.6	13518
		500	6034	7894	8410	8759	9052	9317	1.7	13518
		750	6239	7862	8333	8650	8911	9146	1.8	13518
		1000	6381	7847	8298	8593	8836	9055	1.8	13518
	125mm	250	6033	8588	9509	10276	10971	11619	1.7	14748
		500	6338	8470	9285	9967	10593	11195	1.8	14748
		750	6547	8437	9215	9851	10443	11014	1.8	14748
		1000	6700	8414	9177	9791	10363	10916	1.9	14748
	150mm	250	6385	9282	10556	11694	12779	13809	1.7	16250
		500	6702	9157	10318	11373	12372	13352	1.8	16250
		750	6921	9113	10239	11238	12211	13159	1.9	16250
		1000	7087	9096	10207	11183	12126	13054	1.9	16250

Initial Pt Force 0.1f_{yield}		Axial Load (excluding PT) 8500kN			Cantilever Length (7000mm)			Grade 300 Dissipaters		
	PT Dia.	Fuse Length (mm)	Yield (kNm)	1%drift (kNm)	2%drift (kNm)	3%drift (kNm)	4%drift (kNm)	6%drift (kNm)	λ	Fuse Area (mm^2)
Diameter (1800mm)	36mm	250	6836	9021	9233	9209	9076	8779	1.6	11654
		500	7077	8887	8977	8852	8654	8309	1.7	11654
		750	7352	8836	8881	8712	8468	8091	1.8	11654
		1000	7454	8812	8835	8636	8365	7971	1.8	11654
	50mm	250	6923	9220	9556	9662	9663	9429	1.6	11951
		500	7168	9082	9292	9298	9232	8955	1.8	11951
		750	7447	9029	9197	9156	9049	8731	1.8	11951
		1000	7548	9006	9147	9081	8942	8607	1.9	11951
	75mm	250	7143	9723	10378	10811	11144	11095	1.7	12723
		500	7396	9580	10105	10430	10694	10604	1.8	12723
		750	7688	9527	10001	10281	10503	10375	1.9	12723
		1000	7794	9504	9952	10203	10401	10240	1.9	12723
	100mm	250	7453	10413	11500	12364	13136	13389	1.8	13805
		500	7718	10265	11205	11958	12657	12861	1.9	13805
		750	8022	10211	11094	11799	12455	12617	2.0	13805
		1000	8134	10187	11043	11717	12345	12483	2.0	13805
	125mm	250	7849	11285	12882	14276	15578	16277	1.8	15195
		500	8123	11125	12565	13839	15060	15704	2.0	15195
		750	8453	11070	12449	13669	14844	15440	2.0	15195
		1000	8574	11038	12390	13581	14728	15295	2.1	15195
	150mm	250	8330	12324	14511	16507	18411	19727	1.9	16894
		500	8620	12150	14166	16032	17849	19097	2.0	16894
		750	8970	12093	14040	15848	17616	18810	2.1	16894
		1000	9101	12060	13977	15751	17489	18651	2.1	16894

Initial Pt Force 0.1F_{yield}		Axial Load (excluding PT) 8500kN			Cantilever Length (7000mm)			Grade 300 Dissipaters		
	PT Dia.	Fuse Length (mm)	Yield (kNm)	1%drift (kNm)	2%drift (kNm)	3%drift (kNm)	4%drift (kNm)	6%drift (kNm)	λ	Fuse Area (mm^2)
Diameter (2000mm)	36mm	250	8640	11207	11623	11759	11711	11413	1.3	14598
		500	8942	11006	11230	11228	11082	10783	1.4	14598
		750	9100	10930	11082	11006	10809	10471	1.5	14598
		1000	9226	10886	11003	10887	10660	10296	1.5	14598
	50mm	250	8762	11479	12059	12362	12464	12214	1.3	14999
		500	9068	11273	11654	11820	11821	11563	1.5	14999
		750	9234	11194	11509	11599	11538	11241	1.5	14999
		1000	9358	11150	11428	11475	11384	11060	1.5	14999
	75mm	250	9082	12176	13166	13896	14380	14284	1.4	16039
		500	9396	11958	12743	13325	13715	13572	1.5	16039
		750	9567	11872	12587	13097	13416	13224	1.6	16039
		1000	9702	11828	12506	12972	13249	13030	1.6	16039
	100mm	250	9533	13137	14678	15972	17023	17090	1.5	17494
		500	9853	12898	14225	15361	16306	16341	1.6	17494
		750	10036	12811	14059	15118	15993	15967	1.7	17494
		1000	10176	12763	13972	14990	15822	15751	1.7	17494
	125mm	250	10101	14335	16561	18540	20359	20631	1.5	19366
		500	10433	14077	16069	17878	19575	19809	1.7	19366
		750	10634	13981	15888	17614	19234	19408	1.7	19366
		1000	10783	13932	15794	17475	19050	19184	1.8	19366
	150mm	250	10787	15774	18777	21545	24178	24873	1.6	21654
		500	11139	15485	18240	20821	23342	23964	1.7	21654
		750	11357	15386	18042	20533	22980	23523	1.8	21654
		1000	11515	15336	17941	20382	22782	23277	1.8	21654

Initial Pt Force 0.1f_{yield}		Axial Load (excluding PT) 8500kN			Cantilever Length (7000mm)			Grade 300 Dissipaters		
	PT Dia.	Fuse Length (mm)	Yield (kNm)	1%drift (kNm)	2%drift (kNm)	3%drift (kNm)	4%drift (kNm)	6%drift (kNm)	λ	Fuse Area (mm^2)
Diameter (2200mm)	36mm	250	9683	12645	13176	13403	13316	13077	1.3	14629
		500	10065	12399	12709	12771	12627	12387	1.5	14629
		750	10277	12315	12523	12513	12313	12019	1.5	14629
		1000	10445	12261	12425	12376	12140	11809	1.6	14629
	50mm	250	9828	12983	13717	14161	14184	13987	1.4	15058
		500	10217	12727	13236	13510	13475	13278	1.5	15058
		750	10431	12641	13051	13244	13151	12901	1.6	15058
		1000	10604	12588	12949	13104	12973	12687	1.6	15058
	75mm	250	10201	13842	15096	16069	16431	16328	1.4	16173
		500	10608	13573	14587	15398	15659	15574	1.6	16173
		750	10829	13479	14401	15109	15310	15178	1.6	16173
		1000	11012	13424	14289	14956	15118	14952	1.7	16173
	100mm	250	10720	15024	16977	18656	19513	19609	1.5	17733
		500	11151	14733	16429	17933	18685	18772	1.7	17733
		750	11382	14635	16225	17639	18297	18335	1.7	17733
		1000	11579	14570	16119	17472	18084	18086	1.8	17733
	125mm	250	11389	16514	19321	21859	23390	23743	1.6	19739
		500	11834	16195	18723	21071	22481	22830	1.7	19739
		750	12092	16082	18500	20751	22070	22340	1.8	19739
		1000	12300	16012	18383	20580	21842	22059	1.8	19739
	150mm	250	12197	18283	22085	25617	28040	28681	1.7	22191
		500	12663	17931	21427	24750	27032	27661	1.8	22191
		750	12949	17800	21181	24398	26577	27131	1.9	22191
		1000	13170	17728	21055	24210	26328	26831	1.9	22191

Initial Pt Force 0.1F_{yield}		Axial Load (excluding PT) 8500kN			Cantilever Length (7000mm)			Grade 300 Dissipaters		
	PT Dia.	Fuse Length (mm)	Yield (kNm)	1%drift (kNm)	2%drift (kNm)	3%drift (kNm)	4%drift (kNm)	6%drift (kNm)	λ	Fuse Area (mm^2)
Diameter (2500mm)	36mm	250	11599	14830	15544	15869	15822	13116	1.4	14675
		500	11813	14508	14943	15119	15019	14836	1.5	14675
		750	12088	14388	14713	14801	14624	14387	1.6	14675
		1000	12189	14321	14597	14630	14402	14124	1.6	14675
	50mm	250	11783	15273	16271	16842	16867	14147	1.4	15148
		500	12003	14941	15649	16074	16040	15918	1.6	15148
		750	12284	14821	15412	15747	15634	15457	1.6	15148
		1000	12386	14751	15288	15571	15407	15187	1.7	15148
	75mm	250	12261	16410	18110	19369	19559	16799	1.5	16374
		500	12494	16058	17455	18536	18671	18706	1.6	16374
		750	12791	15931	17197	18183	18236	18211	1.7	16374
		1000	12895	15855	17063	17993	17995	17922	1.8	16374
	100mm	250	12926	17977	20621	22871	23286	22448	1.6	18091
		500	13170	17593	19917	21948	22317	22561	1.7	18091
		750	13493	17456	19638	21556	21845	22020	1.8	18091
		1000	13596	17376	19488	21346	21581	21705	1.9	18091
	125mm	250	13776	19945	23752	27234	28063	27323	1.7	20298
		500	14036	19521	22979	26250	26960	27455	1.8	20298
		750	14397	19374	22683	25825	26427	26860	1.9	20298
		1000	14497	19293	22518	25585	26131	26513	2.0	20298
	150mm	250	14802	22291	27453	32283	33762	33264	1.7	22996
		500	15089	21819	26594	31188	32544	33384	1.9	22996
		750	15489	21656	26266	30726	31952	32704	2.0	22996
		1000	15575	21572	26096	30478	31612	32310	2.0	22996

Initial Pt Force 0.1F_{yield}		Axial Load (excluding PT) 10000kN			Cantilever Length (7000mm)			Grade 300 Dissipaters		
	PT Dia.	Fuse Length (mm)	Yield (kNm)	1%drift (kNm)	2%drift (kNm)	3%drift (kNm)	4%drift (kNm)	6%drift (kNm)	λ	Fuse Area (mm^2)
Diameter (1000mm)	36mm	250	3412	4511	4395	4048	3587	3113	1.1	13555
		500	3594	4463	4301	3898	3410	2894	1.1	13555
		750	3728	4449	4267	3839	3343	2813	1.1	13555
		1000	3833	4442	4245	3815	3306	2769	1.2	13555
	50mm	250	3448	4555	4467	4143	3716	3274	1.1	13760
		500	3627	4513	4372	3995	3532	3047	1.1	13760
		750	3762	4495	4338	3938	3465	2966	1.1	13760
		1000	3868	4493	4320	3913	3430	2918	1.2	13760
	75mm	250	3532	4682	4652	4397	4047	3666	1.1	14294
		500	3710	4636	4555	4251	3860	3433	1.1	14294
		750	3849	4623	4525	4188	3785	3355	1.2	14294
		1000	3958	4616	4501	4160	3753	3313	1.2	14294
	100mm	250	3647	4858	4907	4742	4497	4183	1.1	15041
		500	3832	4813	4807	4591	4291	3956	1.2	15041
		750	3970	4795	4776	4528	4213	3878	1.2	15041
		1000	4084	4794	4758	4494	4181	3827	1.2	15041
	125mm	250	3804	5080	5228	5170	5040	4849	1.1	16002
		500	3992	5030	5122	5008	4834	4603	1.2	16002
		750	4130	5019	5083	4951	4741	4508	1.2	16002
		1000	4249	5013	5065	4910	4699	4460	1.2	16002
	150mm	250	3989	5349	5601	5663	5656	5625	1.1	17177
		500	4175	5300	5490	5493	5440	5351	1.2	17177
		750	4320	5284	5449	5433	5365	5244	1.2	17177
		1000	4447	5278	5437	5406	5314	5187	1.2	17177

Initial Pt Force 0.1f_{yield}		Axial Load (excluding PT) 10000kN			Cantilever Length (7000mm)			Grade 300 Dissipaters		
	PT Dia.	Fuse Length (mm)	Yield (kNm)	1%drift (kNm)	2%drift (kNm)	3%drift (kNm)	4%drift (kNm)	6%drift (kNm)	λ	Fuse Area (mm^2)
Diameter (1200mm)	36mm	250	4389	5957	5905	5608	5243	4826	1.3	13579
		500	4628	5896	5761	5411	4990	4529	1.4	13579
		750	4812	5871	5714	5342	4898	4410	1.4	13579
		1000	4946	5843	5690	5306	4848	4347	1.4	13579
	50mm	250	4431	6032	6022	5768	5451	5081	1.3	13808
		500	4672	5970	5877	5568	5195	4782	1.4	13808
		750	4859	5943	5829	5499	5103	4662	1.4	13808
		1000	4994	5915	5804	5460	5046	4598	1.4	13808
	75mm	250	4540	6224	6325	6174	5971	5722	1.3	14401
		500	4787	6161	6173	5969	5709	5415	1.4	14401
		750	4977	6135	6123	5893	5615	5293	1.4	14401
		1000	5116	6107	6098	5861	5564	5228	1.4	14401
	100mm	250	4697	6494	6730	6721	6671	6581	1.3	15232
		500	4941	6427	6576	6516	6400	6263	1.4	15232
		750	5137	6397	6524	6440	6295	6144	1.5	15232
		1000	5281	6368	6490	6400	6251	6078	1.5	15232
	125mm	250	4891	6835	7239	7420	7528	7625	1.4	16300
		500	5145	6759	7082	7183	7252	7295	1.5	16300
		750	5343	6728	7018	7105	7144	7158	1.5	16300
		1000	5493	6700	6990	7060	7092	7090	1.5	16300
	150mm	250	5135	7234	7833	8236	8515	8824	1.4	17606
		500	5396	7160	7672	7982	8230	8486	1.5	17606
		750	5596	7121	7607	7882	8126	8333	1.5	17606
		1000	5754	7101	7567	7835	8059	8259	1.5	17606

Initial Pt Force 0.1f_{yield}		Axial Load (excluding PT) 10000kN			Cantilever Length (7000mm)			Grade 300 Dissipaters		
	PT Dia.	Fuse Length (mm)	Yield (kNm)	1%drift (kNm)	2%drift (kNm)	3%drift (kNm)	4%drift (kNm)	6%drift (kNm)	λ	Fuse Area (mm^2)
Diameter (1500mm)	36mm	250	6022	8163	8253	8090	7815	7469	1.5	13617
		500	6351	8056	8047	7790	7446	7054	1.6	13617
		750	6576	8025	7966	7677	7298	6875	1.6	13617
		1000	6738	8005	7931	7619	7220	6778	1.6	13617
	50mm	250	6087	8291	8454	8372	8181	7921	1.5	13880
		500	6414	8183	8245	8068	7807	7501	1.6	13880
		750	6645	8145	8168	7954	7658	7320	1.6	13880
		1000	6805	8130	8126	7894	7579	7223	1.7	13880
	75mm	250	6246	8617	8963	9088	9108	9063	1.5	14562
		500	6581	8501	8746	8775	8722	8629	1.6	14562
		750	6813	8469	8670	8656	8568	8444	1.7	14562
		1000	6983	8447	8629	8596	8487	8343	1.7	14562
	100mm	250	6466	9066	9659	10057	10355	10592	1.6	15518
		500	6811	8947	9436	9729	9952	10138	1.7	15518
		750	7049	8907	9347	9605	9791	9944	1.7	15518
		1000	7224	8884	9307	9541	9706	9840	1.8	15518
	125mm	250	6752	9634	10527	11253	11883	12456	1.6	16748
		500	7106	9510	10293	10907	11457	11976	1.7	16748
		750	7348	9460	10203	10768	11287	11773	1.8	16748
		1000	7531	9442	10163	10701	11198	11662	1.8	16748
	150mm	250	7098	10301	11550	12646	13646	14607	1.6	18250
		500	7469	10173	11301	12278	13193	14095	1.8	18250
		750	7715	10126	11210	12128	13027	13878	1.8	18250
		1000	7901	10100	11158	12056	12915	13761	1.8	18250

Initial Pt Force 0.1F_{yield}		Axial Load (excluding PT) 10000kN			Cantilever Length (7000mm)			Grade 300 Dissipaters		
	PT Dia.	Fuse Length (mm)	Yield (kNm)	1%drift (kNm)	2%drift (kNm)	3%drift (kNm)	4%drift (kNm)	6%drift (kNm)	λ	Fuse Area (mm^2)
Diameter (1800mm)	36mm	250	7783	10434	10685	10637	10461	10115	1.6	13654
		500	8095	10279	10384	10224	9970	9585	1.7	13654
		750	8429	10225	10276	10062	9762	9330	1.8	13654
		1000	8555	10201	10222	9978	9648	9186	1.8	13654
	50mm	250	7867	10621	10998	11078	11032	10756	1.6	13951
		500	8182	10465	10692	10658	10534	10216	1.7	13951
		750	8521	10411	10582	10494	10324	9963	1.8	13951
		1000	8648	10387	10528	10408	10210	9816	1.8	13951
	75mm	250	8087	11107	11793	12198	12480	12403	1.7	14723
		500	8405	10949	11481	11761	11963	11838	1.8	14723
		750	8756	10894	11366	11591	11745	11576	1.9	14723
		1000	8888	10870	11308	11502	11627	11432	1.9	14723
	100mm	250	8388	11783	12881	13714	14432	14672	1.7	15805
		500	8716	11613	12549	13254	13886	14073	1.9	15805
		750	9084	11558	12427	13075	13657	13795	1.9	15805
		1000	9224	11527	12365	12981	13533	13642	1.9	15805
	125mm	250	8772	12633	14235	15588	16830	17533	1.8	17195
		500	9112	12449	13885	15097	16248	16889	1.9	17195
		750	9500	12392	13755	14908	16006	16592	2.0	17195
		1000	9647	12360	13689	14807	15875	16428	2.0	17195
	150mm	250	9242	13652	15824	17778	19622	20954	1.8	18894
		500	9597	13451	15443	17252	18995	20254	2.0	18894
		750	10002	13383	15300	17047	18735	19935	2.0	18894
		1000	10162	13360	15235	16939	18595	19759	2.1	18894

Initial Pt Force 0.1f_{yield}		Axial Load (excluding PT) 10000kN			Cantilever Length (7000mm)			Grade 300 Dissipaters		
	PT Dia.	Fuse Length (mm)	Yield (kNm)	1%drift (kNm)	2%drift (kNm)	3%drift (kNm)	4%drift (kNm)	6%drift (kNm)	λ	Fuse Area (mm^2)
Diameter (2000mm)	36mm	250	9894	12984	13461	13598	13538	13217	1.3	17098
		500	10242	12755	13006	12983	12822	12464	1.4	17098
		750	10458	12660	12838	12737	12497	12095	1.5	17098
		1000	10607	12612	12752	12600	12320	11887	1.5	17098
	50mm	250	10017	13249	13882	14187	14275	14015	1.3	17499
		500	10368	13012	13424	13561	13547	13238	1.4	17499
		750	10587	12917	13254	13311	13220	12859	1.5	17499
		1000	10739	12869	13166	13176	13038	12646	1.5	17499
	75mm	250	10324	13928	14965	15687	16171	16030	1.4	18539
		500	10688	13671	14483	15034	15407	15234	1.5	18539
		750	10916	13582	14305	14773	15073	14827	1.5	18539
		1000	11070	13533	14213	14635	14887	14600	1.6	18539
	100mm	250	10764	14863	16448	17723	18787	18809	1.4	19994
		500	11132	14588	15937	17030	17972	17957	1.6	19994
		750	11373	14490	15748	16755	17618	17538	1.6	19994
		1000	11536	14440	15646	16609	17424	17302	1.6	19994
	125mm	250	11322	16029	18294	20245	22049	22321	1.5	21866
		500	11700	15738	17745	19503	21188	21397	1.6	21866
		750	11953	15639	17536	19209	20816	20946	1.7	21866
		1000	12134	15589	17438	19053	20614	20695	1.7	21866
	150mm	250	12001	17431	20472	23207	25793	26531	1.5	24154
		500	12386	17120	19870	22403	24859	25520	1.7	24154
		750	12662	17008	19651	22086	24459	25032	1.7	24154
		1000	12850	16958	19538	21916	24240	24759	1.8	24154

Initial Pt Force 0.1f_{yield}		Axial Load (excluding PT) 10000kN			Cantilever Length (7000mm)			Grade 300 Dissipaters		
	PT Dia.	Fuse Length (mm)	Yield (kNm)	1%drift (kNm)	2%drift (kNm)	3%drift (kNm)	4%drift (kNm)	6%drift (kNm)	λ	Fuse Area (mm^2)
Diameter (2200mm)	36mm	250	11098	14664	15270	15511	15421	15106	1.3	17129
		500	11556	14381	14728	14787	14608	14302	1.5	17129
		750	11819	14282	14522	14482	14238	13877	1.5	17129
		1000	12020	14221	14409	14319	14035	13637	1.5	17129
	50mm	250	11238	14991	15795	16245	16287	16007	1.4	17558
		500	11700	14701	15245	15513	15449	15187	1.5	17558
		750	11973	14600	15039	15200	15069	14755	1.5	17558
		1000	12173	14536	14923	15034	14860	14509	1.6	17558
	75mm	250	11608	15829	17149	18117	18503	18356	1.4	18673
		500	12075	15523	16565	17349	17620	17481	1.6	18673
		750	12362	15418	16352	17035	17212	17020	1.6	18673
		1000	12571	15348	16236	16856	16989	16759	1.6	18673
	100mm	250	12117	16985	18988	20660	21543	21619	1.5	20233
		500	12604	16659	18371	19842	20606	20662	1.6	20233
		750	12903	16540	18140	19509	20180	20158	1.7	20233
		1000	13125	16469	18025	19331	19935	19872	1.7	20233
	125mm	250	12772	18441	21297	23817	25389	25702	1.5	22239
		500	13270	18087	20624	22933	24371	24675	1.7	22239
		750	13593	17950	20374	22575	23912	24139	1.8	22239
		1000	13831	17883	20246	22385	23658	23825	1.8	22239
	150mm	250	13567	20177	24011	27525	30006	30607	1.6	24691
		500	14084	19784	23285	26564	28889	29476	1.7	24691
		750	14433	19643	23014	26175	28387	28889	1.8	24691
		1000	14684	19564	22875	25967	28112	28557	1.8	24691

Initial Pt Force 0.1f_{yield}		Axial Load (excluding PT) 10000kN			Cantilever Length (7000mm)			Grade 300 Dissipaters		
	PT Dia.	Fuse Length (mm)	Yield (kNm)	1%drift (kNm)	2%drift (kNm)	3%drift (kNm)	4%drift (kNm)	6%drift (kNm)	λ	Fuse Area (mm^2)
Diameter (2500mm)	36mm	250	13630	17646	18519	18914	18869	15538	1.3	18320
		500	13914	17252	17783	17982	17872	17676	1.4	18320
		750	14265	17114	17495	17586	17383	17120	1.5	18320
		1000	14352	17031	17345	17373	17111	16794	1.5	18320
	50mm	250	13819	18093	19237	19901	19918	16568	1.3	18824
		500	14109	17687	18489	18942	18896	18762	1.4	18824
		750	14466	17546	18192	18536	18396	18192	1.5	18824
		1000	14553	17464	18037	18317	18120	17860	1.5	18824
	75mm	250	14313	19234	21074	22452	22622	21435	1.4	20132
		500	14610	18807	20286	21420	21543	21562	1.5	20132
		750	14986	18658	19977	20985	21016	20957	1.6	20132
		1000	15065	18573	19813	20751	20722	20604	1.6	20132
	100mm	250	14996	20808	23586	25951	26411	25301	1.4	21963
		500	15304	20347	22746	24857	25223	25436	1.6	21963
		750	15708	20187	22418	24379	24649	24787	1.7	21963
		1000	15787	20102	22238	24122	24327	24411	1.7	21963
	125mm	250	15867	22792	26726	30258	31209	30238	1.5	24318
		500	16199	22290	25807	29084	29907	30385	1.7	24318
		750	16637	22115	25456	28588	29266	29669	1.7	24318
		1000	16700	22022	25274	28311	28908	29253	1.8	24318
	150mm	250	16923	25163	30446	35326	36949	36217	1.6	27196
		500	17283	24610	29438	34035	35515	36373	1.7	27196
		750	17748	24419	29053	33493	34823	35565	1.8	27196
		1000	17811	24307	28854	33200	34432	35096	1.8	27196

Initial Pt Force 0.1F_{yield}		Axial Load (excluding PT) 4500kN			Cantilever Length (8000mm)			Grade 300 Dissipaters		
	PT Dia.	Fuse Length (mm)	Yield (kNm)	1%drift (kNm)	2%drift (kNm)	3%drift (kNm)	4%drift (kNm)	6%drift (kNm)	λ	Fuse Area (mm^2)
Diameter (1000mm)	36mm	250	1868	2369	2259	2074	1857	1622	0.9	7244
		500	1965	2343	2207	1992	1754	1497	1.0	7244
		750	2030	2329	2188	1963	1714	1448	1.0	7244
		1000	2073	2317	2179	1949	1694	1423	1.0	7244
	50mm	250	1906	2431	2349	2190	2003	1799	1.0	7470
		500	2004	2404	2294	2105	1898	1672	1.0	7470
		750	2068	2389	2275	2075	1857	1623	1.0	7470
		1000	2113	2379	2266	2061	1837	1596	1.0	7470
	75mm	250	2004	2589	2577	2478	2368	2238	1.0	8058
		500	2102	2563	2515	2390	2255	2105	1.1	8058
		750	2172	2545	2494	2362	2212	2053	1.1	8058
		1000	2218	2532	2485	2348	2191	2026	1.1	8058
	100mm	250	2138	2805	2889	2871	2850	2817	1.0	8881
		500	2240	2776	2816	2778	2729	2673	1.1	8881
		750	2313	2757	2792	2746	2683	2616	1.1	8881
		1000	2365	2743	2780	2730	2660	2588	1.1	8881
	125mm	250	2311	3074	3265	3354	3428	3512	1.1	9940
		500	2418	3043	3191	3251	3296	3355	1.1	9940
		750	2495	3026	3162	3214	3257	3289	1.1	9940
		1000	2553	3008	3147	3197	3229	3255	1.2	9940
	150mm	250	2520	3394	3704	3926	4099	4279	1.1	11233
		500	2631	3359	3626	3801	3965	4108	1.1	11233
		750	2717	3342	3592	3757	3905	4047	1.2	11233
		1000	2778	3323	3569	3734	3879	4020	1.2	11233

Initial Pt Force 0.1Fyield		Axial Load (excluding PT) 4500kN			Cantilever Length (8000mm)			Grade 300 Dissipaters		
	PT Dia.	Fuse Length (mm)	Yield (kNm)	1%drift (kNm)	2%drift (kNm)	3%drift (kNm)	4%drift (kNm)	6%drift (kNm)	λ	Fuse Area (mm^2)
Diameter (1200mm)	36mm	250	2398	3070	3016	2877	2698	2495	1.1	7270
		500	2518	3030	2939	2763	2554	2329	1.2	7270
		750	2592	3015	2910	2721	2499	2261	1.2	7270
		1000	2639	3010	2899	2699	2470	2225	1.2	7270
	50mm	250	2447	3159	3151	3057	2926	2772	1.1	7520
		500	2570	3118	3071	2941	2779	2602	1.2	7520
		750	2645	3105	3043	2898	2722	2533	1.2	7520
		1000	2694	3100	3029	2875	2693	2496	1.3	7520
	75mm	250	2575	3393	3489	3510	3498	3463	1.2	8171
		500	2704	3349	3404	3387	3341	3282	1.3	8171
		750	2783	3333	3377	3341	3281	3209	1.3	8171
		1000	2835	3327	3359	3317	3250	3170	1.3	8171
	100mm	250	2752	3713	3941	4115	4252	4371	1.2	9082
		500	2888	3663	3853	3977	4083	4175	1.3	9082
		750	2976	3645	3823	3927	4019	4097	1.4	9082
		1000	3031	3635	3809	3903	3985	4055	1.4	9082
	125mm	250	2981	4108	4506	4843	5166	5458	1.3	10253
		500	3125	4056	4406	4695	4975	5244	1.4	10253
		750	3218	4036	4373	4648	4903	5158	1.4	10253
		1000	3282	4023	4356	4616	4867	5112	1.4	10253
	150mm	250	3257	4577	5175	5691	6204	6687	1.3	11684
		500	3411	4523	5056	5521	5992	6448	1.4	11684
		750	3512	4495	5017	5467	5912	6351	1.4	11684
		1000	3583	4478	4996	5446	5880	6303	1.5	11684

Initial Pt Force 0.1F_{yield}		Axial Load (excluding PT) 4500kN			Cantilever Length (8000mm)			Grade 300 Dissipaters		
	PT Dia.	Fuse Length (mm)	Yield (kNm)	1%drift (kNm)	2%drift (kNm)	3%drift (kNm)	4%drift (kNm)	6%drift (kNm)	λ	Fuse Area (mm^2)
Diameter (1500mm)	36mm	250	3278	4158	4197	4127	4011	3864	1.3	7309
		500	3403	4097	4076	3957	3804	3624	1.4	7309
		750	3476	4075	4035	3892	3715	3519	1.4	7309
		1000	3534	4066	4011	3855	3666	3463	1.4	7309
	50mm	250	3351	4302	4419	4430	4397	4332	1.3	7596
		500	3478	4238	4295	4255	4184	4094	1.4	7596
		750	3554	4219	4252	4189	4097	3983	1.5	7596
		1000	3614	4206	4228	4153	4045	3923	1.5	7596
	75mm	250	3538	4667	4983	5194	5363	5502	1.4	8340
		500	3669	4601	4849	5006	5134	5248	1.5	8340
		750	3754	4578	4802	4935	5042	5138	1.5	8340
		1000	3819	4569	4777	4898	4994	5077	1.6	8340
	100mm	250	3797	5172	5741	6214	6646	7049	1.5	9382
		500	3935	5099	5595	6008	6396	6769	1.6	9382
		750	4030	5075	5543	5930	6295	6649	1.6	9382
		1000	4102	5062	5516	5890	6241	6584	1.6	9382
	125mm	250	4124	5803	6672	7457	8201	8914	1.5	10722
		500	4275	5721	6511	7228	7922	8603	1.6	10722
		750	4383	5691	6452	7142	7811	8470	1.7	10722
		1000	4459	5682	6423	7097	7752	8398	1.7	10722
	150mm	250	4518	6549	7758	8892	9984	11046	1.6	12360
		500	4684	6454	7579	8635	9671	10696	1.7	12360
		750	4806	6422	7506	8539	9548	10548	1.7	12360
		1000	4891	6407	7477	8489	9481	10468	1.8	12360

Initial Pt Force $0.1f_{yield}$		Axial Load (excluding PT) 4500kN			Cantilever Length (8000mm)			Grade 300 Dissipaters		
	PT Dia.	Fuse Length (mm)	Yield (kNm)	1%drift (kNm)	2%drift (kNm)	3%drift (kNm)	4%drift (kNm)	6%drift (kNm)	λ	Fuse Area (mm^2)
Diameter (1800mm)	36mm	250	4171	5282	5413	5424	5357	5210	1.4	7348
		500	4294	5194	5243	5183	5087	4919	1.5	7348
		750	4413	5164	5175	5089	4973	4782	1.5	7348
		1000	4458	5138	5139	5040	4911	4708	1.6	7348
	50mm	250	4270	5495	5748	5885	5948	5872	1.4	7671
		500	4395	5405	5571	5637	5664	5570	1.5	7671
		750	4518	5373	5503	5538	5544	5431	1.6	7671
		1000	4565	5347	5465	5486	5479	5354	1.6	7671
	75mm	250	4524	6038	6595	7041	7432	7591	1.5	8509
		500	4656	5938	6403	6779	7118	7254	1.7	8509
		750	4789	5904	6333	6672	6981	7097	1.7	8509
		1000	4844	5877	6291	6612	6908	7010	1.7	8509
	100mm	250	4879	6778	7738	8588	9385	9937	1.6	9683
		500	5018	6668	7525	8298	9045	9563	1.8	9683
		750	5166	6627	7448	8185	8901	9387	1.8	9683
		1000	5225	6604	7408	8125	8819	9285	1.8	9683
	125mm	250	5327	7702	9147	10483	11763	12861	1.7	11192
		500	5475	7575	8907	10156	11379	12435	1.8	11192
		750	5645	7529	8820	10029	11219	12239	1.9	11192
		1000	5710	7512	8775	9962	11131	12131	1.9	11192
	150mm	250	5872	8794	10791	12680	14511	16291	1.8	13037
		500	6024	8646	10519	12309	14073	15822	1.9	13037
		750	6221	8599	10419	12165	13891	15607	2.0	13037
		1000	6294	8576	10369	12090	13794	15488	2.0	13037

Initial Pt Force 0.1F_{yield}		Axial Load (excluding PT) 4500kN			Cantilever Length (8000mm)			Grade 300 Dissipaters		
	PT Dia.	Fuse Length (mm)	Yield (kNm)	1%drift (kNm)	2%drift (kNm)	3%drift (kNm)	4%drift (kNm)	6%drift (kNm)	λ	Fuse Area (mm^2)
Diameter (2000mm)	36mm	250	5333	6681	6959	7070	7109	6970	1.1	9480
		500	5459	6543	6686	6716	6703	6553	1.2	9480
		750	5525	6490	6583	6575	6525	6343	1.3	9480
		1000	5596	6459	6530	6500	6430	6225	1.3	9480
	50mm	250	5476	6974	7410	7687	7876	7780	1.1	9927
		500	5607	6831	7130	7315	7456	7345	1.3	9927
		750	5675	6777	7021	7166	7273	7127	1.3	9927
		1000	5746	6743	6965	7088	7173	7004	1.3	9927
	75mm	250	5843	7724	8556	9247	9835	9856	1.2	11085
		500	5988	7566	8254	8833	9368	9376	1.3	11085
		750	6062	7513	8135	8665	9164	9140	1.4	11085
		1000	6136	7471	8071	8576	9054	9008	1.4	11085
	100mm	250	6349	8749	10106	11323	12457	12758	1.3	12707
		500	6512	8572	9768	10872	11940	12198	1.4	12707
		750	6600	8510	9644	10688	11700	11923	1.5	12707
		1000	6676	8465	9572	10583	11569	11770	1.5	12707
	125mm	250	6995	10029	12024	13874	15636	16374	1.4	14792
		500	7181	9827	11641	13362	15049	15744	1.5	14792
		750	7276	9755	11500	13158	14793	15435	1.6	14792
		1000	7359	9714	11427	13051	14653	15255	1.6	14792
	150mm	250	7779	11547	14272	16848	19327	20683	1.4	17341
		500	7988	11315	13834	16262	18655	19954	1.6	17341
		750	8085	11230	13673	16029	18361	19599	1.6	17341
		1000	8183	11185	13590	15907	18202	19399	1.6	17341

Initial Pt Force 0.1f_{yield}		Axial Load (excluding PT) 6000kN			Cantilever Length (8000mm)			Grade 300 Dissipaters		
	PT Dia.	Fuse Length (mm)	Yield (kNm)	1%drift (kNm)	2%drift (kNm)	3%drift (kNm)	4%drift (kNm)	6%drift (kNm)	λ	Fuse Area (mm^2)
Diameter (1000mm)	36mm	250	2199	2828	2685	2400	2094	1756	1.1	8209
		500	2313	2802	2619	2311	1977	1619	1.1	8209
		750	2401	2787	2595	2280	1932	1564	1.1	8209
		1000	2463	2772	2585	2266	1912	1536	1.1	8209
	50mm	250	2229	2882	2764	2501	2222	1917	1.1	8403
		500	2349	2854	2696	2414	2108	1778	1.1	8403
		750	2438	2840	2673	2382	2064	1723	1.1	8403
		1000	2498	2825	2662	2368	2037	1695	1.2	8403
	75mm	250	2312	3018	2962	2769	2556	2320	1.1	8907
		500	2434	2990	2894	2674	2433	2173	1.2	8907
		750	2527	2973	2867	2645	2385	2122	1.2	8907
		1000	2592	2961	2855	2629	2366	2087	1.2	8907
	100mm	250	2430	3205	3231	3130	2994	2848	1.1	9613
		500	2555	3172	3166	3031	2862	2703	1.2	9613
		750	2651	3160	3136	2990	2823	2639	1.2	9613
		1000	2720	3144	3121	2976	2795	2605	1.2	9613
	125mm	250	2579	3441	3566	3579	3526	3486	1.2	10520
		500	2709	3405	3491	3458	3393	3323	1.2	10520
		750	2812	3389	3463	3417	3350	3259	1.2	10520
		1000	2882	3378	3444	3396	3325	3232	1.2	10520
	150mm	250	2762	3719	3950	4079	4166	4210	1.2	11629
		500	2898	3680	3872	3961	4009	4041	1.2	11629
		750	3005	3665	3849	3911	3959	3979	1.3	11629
		1000	3081	3655	3827	3892	3922	3946	1.3	11629

Initial Pt Force 0.1F_{yield}		Axial Load (excluding PT) 6000kN			Cantilever Length (8000mm)			Grade 300 Dissipaters		
	PT Dia.	Fuse Length (mm)	Yield (kNm)	1%drift (kNm)	2%drift (kNm)	3%drift (kNm)	4%drift (kNm)	6%drift (kNm)	λ	Fuse Area (mm^2)
Diameter (1200mm)	36mm	250	2835	3712	3608	3393	3123	2823	1.3	8231
		500	2996	3667	3523	3267	2964	2638	1.3	8231
		750	3102	3651	3493	3219	2903	2563	1.4	8231
		1000	3176	3645	3478	3196	2871	2523	1.4	8231
	50mm	250	2878	3791	3728	3557	3333	3080	1.3	8446
		500	3041	3748	3643	3426	3171	2891	1.4	8446
		750	3149	3728	3613	3379	3109	2815	1.4	8446
		1000	3223	3721	3596	3358	3076	2775	1.4	8446
	75mm	250	2989	3993	4033	3969	3859	3722	1.3	9004
		500	3155	3951	3943	3835	3689	3525	1.4	9004
		750	3268	3930	3910	3786	3625	3446	1.4	9004
		1000	3346	3919	3897	3759	3591	3404	1.5	9004
	100mm	250	3144	4273	4449	4519	4555	4570	1.4	9784
		500	3316	4228	4352	4377	4375	4362	1.5	9784
		750	3431	4208	4316	4327	4313	4278	1.5	9784
		1000	3514	4189	4300	4303	4270	4233	1.5	9784
	125mm	250	3343	4625	4962	5194	5398	5584	1.4	10788
		500	3518	4576	4854	5036	5215	5371	1.5	10788
		750	3641	4554	4818	4985	5135	5273	1.5	10788
		1000	3733	4533	4799	4964	5103	5234	1.6	10788
	150mm	250	3586	5041	5575	5969	6366	6756	1.5	12015
		500	3765	4983	5446	5817	6157	6505	1.5	12015
		750	3898	4962	5408	5759	6077	6407	1.6	12015
		1000	3995	4935	5383	5729	6048	6366	1.6	12015

Initial Pt Force 0.1f_{yield}		Axial Load (excluding PT) 6000kN			Cantilever Length (8000mm)			Grade 300 Dissipaters		
	PT Dia.	Fuse Length (mm)	Yield (kNm)	1%drift (kNm)	2%drift (kNm)	3%drift (kNm)	4%drift (kNm)	6%drift (kNm)	λ	Fuse Area (mm^2)
Diameter (1500mm)	36mm	250	3902	5061	5068	4927	4724	4481	1.5	8265
		500	4086	4994	4936	4738	4494	4224	1.6	8265
		750	4204	4974	4889	4667	4401	4112	1.6	8265
		1000	4283	4962	4865	4630	4351	4045	1.6	8265
	50mm	250	3963	5190	5271	5207	5084	4922	1.5	8511
		500	4150	5122	5137	5015	4849	4659	1.6	8511
		750	4271	5102	5089	4942	4754	4546	1.6	8511
		1000	4352	5090	5065	4904	4704	4483	1.7	8511
	75mm	250	4121	5521	5786	5916	5990	6028	1.6	9149
		500	4316	5450	5643	5713	5742	5751	1.7	9149
		750	4444	5426	5592	5636	5643	5631	1.7	9149
		1000	4533	5413	5566	5596	5590	5566	1.7	9149
	100mm	250	4345	5974	6482	6866	7198	7495	1.6	10042
		500	4550	5896	6328	6649	6933	7198	1.7	10042
		750	4687	5870	6276	6566	6826	7070	1.8	10042
		1000	4780	5861	6244	6524	6769	7001	1.8	10042
	125mm	250	4628	6545	7339	8029	8666	9271	1.7	11191
		500	4846	6456	7171	7792	8378	8947	1.8	11191
		750	4995	6428	7109	7703	8263	8809	1.9	11191
		1000	5097	6415	7082	7657	8202	8734	1.9	11191
	150mm	250	4974	7219	8345	9369	10356	11304	1.7	12595
		500	5200	7123	8155	9120	10039	10950	1.9	12595
		750	5364	7087	8090	9021	9914	10799	1.9	12595
		1000	5478	7073	8064	8972	9847	10718	1.9	12595

Initial Pt Force 0.1F_{yield}		Axial Load (excluding PT) 6000kN			Cantilever Length (8000mm)			Grade 300 Dissipaters		
	PT Dia.	Fuse Length (mm)	Yield (kNm)	1%drift (kNm)	2%drift (kNm)	3%drift (kNm)	4%drift (kNm)	6%drift (kNm)	λ	Fuse Area (mm^2)
Diameter (1800mm)	36mm	250	5015	6462	6567	6513	6383	6128	1.6	8298
		500	5183	6368	6381	6254	6068	5804	1.7	8298
		750	5359	6330	6311	6147	5935	5653	1.8	8298
		1000	5430	6310	6272	6090	5864	5569	1.8	8298
	50mm	250	5102	6654	6876	6942	6936	6778	1.6	8575
		500	5272	6557	6683	6677	6617	6439	1.8	8575
		750	5452	6520	6613	6570	6479	6281	1.8	8575
		1000	5523	6500	6574	6510	6404	6194	1.8	8575
	75mm	250	5324	7147	7660	8026	8325	8434	1.7	9294
		500	5498	7043	7455	7745	7993	8069	1.8	9294
		750	5691	6999	7380	7635	7850	7894	1.9	9294
		1000	5766	6979	7342	7574	7767	7797	1.9	9294
	100mm	250	5632	7817	8723	9485	10182	10681	1.8	10300
		500	5813	7703	8500	9180	9822	10287	1.9	10300
		750	6021	7662	8419	9061	9670	10104	2.0	10300
		1000	6103	7637	8377	8998	9589	10002	2.0	10300
	125mm	250	6025	8660	10036	11276	12451	13504	1.9	11593
		500	6212	8526	9790	10939	12055	13066	2.0	11593
		750	6442	8486	9701	10809	11889	12864	2.1	11593
		1000	6531	8466	9655	10741	11799	12752	2.1	11593
	150mm	250	6499	9651	11571	13356	15074	16741	1.9	13174
		500	6693	9511	11300	12984	14635	16268	2.1	13174
		750	6952	9462	11201	12839	14452	16052	2.2	13174
		1000	7045	9442	11150	12763	14353	15932	2.2	13174

Initial Pt Force 0.1f_{yield}		Axial Load (excluding PT) 6000kN			Cantilever Length (8000mm)			Grade 300 Dissipaters		
	PT Dia.	Fuse Length (mm)	Yield (kNm)	1%drift (kNm)	2%drift (kNm)	3%drift (kNm)	4%drift (kNm)	6%drift (kNm)	λ	Fuse Area (mm^2)
Diameter (2000mm)	36mm	250	6794	8653	8983	9111	9097	8890	1.1	12480
		500	6992	8477	8642	8640	8569	8345	1.2	12480
		750	7089	8416	8513	8450	8338	8075	1.2	12480
		1000	7171	8371	8440	8350	8212	7925	1.2	12480
	50mm	250	6930	8935	9418	9702	9856	9687	1.1	12927
		500	7134	8754	9070	9224	9306	9127	1.2	12927
		750	7232	8691	8937	9026	9066	8852	1.3	12927
		1000	7316	8645	8861	8921	8936	8697	1.3	12927
	75mm	250	7285	9659	10527	11201	11767	11770	1.2	14085
		500	7502	9463	10151	10695	11178	11154	1.3	14085
		750	7603	9392	10012	10490	10912	10850	1.3	14085
		1000	7689	9350	9936	10373	10768	10681	1.4	14085
	100mm	250	7776	10648	12032	13225	14309	14627	1.2	15707
		500	8011	10433	11622	12674	13674	13954	1.4	15707
		750	8115	10355	11470	12454	13398	13610	1.4	15707
		1000	8209	10310	11393	12337	13238	13417	1.4	15707
	125mm	250	8406	11895	13903	15723	17431	18198	1.3	17792
		500	8654	11653	13449	15112	16727	17444	1.4	17792
		750	8771	11563	13281	14869	16421	17075	1.5	17792
		1000	8874	11517	13194	14741	16255	16869	1.5	17792
	150mm	250	9172	13365	16102	18642	21065	22468	1.4	20341
		500	9427	13099	15595	17960	20279	21614	1.5	20341
		750	9562	12998	15407	17690	19938	21202	1.5	20341
		1000	9670	12956	15312	17547	19752	20970	1.5	20341

Initial Pt Force 0.1Fyield		Axial Load (excluding PT) 6000kN			Cantilever Length (8000mm)			Grade 300 Dissipaters		
	PT Dia.	Fuse Length (mm)	Yield (kNm)	1%drift (kNm)	2%drift (kNm)	3%drift (kNm)	4%drift (kNm)	6%drift (kNm)	λ	Fuse Area (mm^2)
Diameter (2200mm)	36mm	250	7601	9758	10191	10377	10388	10202	1.1	12514
		500	7853	9543	9778	9842	9790	9611	1.2	12514
		750	7985	9466	9618	9624	9517	9293	1.3	12514
		1000	8102	9418	9536	9507	9369	9112	1.3	12514
	50mm	250	7758	10103	10728	11115	11260	11124	1.1	12991
		500	8017	9882	10306	10558	10643	10512	1.3	12991
		750	8153	9804	10139	10331	10364	10184	1.3	12991
		1000	8278	9754	10053	10210	10211	9997	1.3	12991
	75mm	250	8173	10988	12096	12989	13523	13493	1.2	14230
		500	8448	10749	11645	12381	12850	12826	1.3	14230
		750	8596	10665	11468	12129	12544	12472	1.4	14230
		1000	8723	10613	11372	11996	12375	12274	1.4	14230
	100mm	250	8747	12203	13957	15498	16657	16788	1.3	15965
		500	9041	11939	13461	14845	15903	16040	1.4	15965
		750	9204	11846	13275	14571	15555	15647	1.5	15965
		1000	9341	11791	13170	14418	15364	15424	1.5	15965
	125mm	250	9480	13725	16270	18598	20573	20965	1.4	18195
		500	9803	13430	15717	17869	19735	20123	1.5	18195
		750	9979	13330	15510	17574	19356	19668	1.5	18195
		1000	10127	13266	15402	17415	19144	19410	1.6	18195
	150mm	250	10369	15535	18995	22228	25261	25931	1.4	20921
		500	10724	15203	18373	21411	24312	24972	1.5	20921
		750	10908	15082	18141	21077	23884	24473	1.6	20921
		1000	11077	15013	18020	20901	23650	24190	1.6	20921

Initial Pt Force 0.1f_{yield}		Axial Load (excluding PT) 7500kN			Cantilever Length (8000mm)			Grade 300 Dissipaters		
	PT Dia.	Fuse Length (mm)	Yield (kNm)	1%drift (kNm)	2%drift (kNm)	3%drift (kNm)	4%drift (kNm)	6%drift (kNm)	λ	Fuse Area (mm^2)
Diameter (1000mm)	36mm	250	2627	3408	3233	2890	2481	2063	1.0	10209
		500	2764	3368	3161	2776	2344	1890	1.1	10209
		750	2869	3354	3134	2739	2290	1829	1.1	10209
		1000	2942	3344	3117	2716	2265	1795	1.1	10209
	50mm	250	2659	3457	3307	2989	2604	2213	1.0	10403
		500	2798	3416	3234	2875	2466	2039	1.1	10403
		750	2901	3402	3207	2835	2416	1975	1.1	10403
		1000	2978	3393	3189	2812	2386	1943	1.1	10403
	75mm	250	2740	3582	3494	3243	2916	2588	1.0	10907
		500	2883	3544	3416	3124	2776	2415	1.1	10907
		750	2989	3530	3388	3081	2720	2346	1.1	10907
		1000	3067	3521	3374	3059	2699	2311	1.1	10907
	100mm	250	2855	3761	3745	3585	3342	3097	1.1	11613
		500	3001	3719	3665	3460	3189	2909	1.1	11613
		750	3108	3706	3639	3408	3135	2841	1.1	11613
		1000	3193	3698	3621	3388	3110	2813	1.1	11613
	125mm	250	3003	3978	4057	3998	3875	3701	1.1	12520
		500	3153	3938	3980	3873	3709	3518	1.1	12520
		750	3266	3926	3948	3820	3639	3453	1.2	12520
		1000	3349	3919	3933	3788	3606	3410	1.2	12520
	150mm	250	3182	4243	4428	4471	4474	4439	1.1	13629
		500	3338	4200	4342	4344	4297	4221	1.1	13629
		750	3453	4189	4305	4296	4232	4141	1.2	13629
		1000	3543	4182	4293	4264	4185	4109	1.2	13629

Initial Pt Force 0.1F_{yield}		Axial Load (excluding PT) 7500kN			Cantilever Length (8000mm)			Grade 300 Dissipaters		
	PT Dia.	Fuse Length (mm)	Yield (kNm)	1%drift (kNm)	2%drift (kNm)	3%drift (kNm)	4%drift (kNm)	6%drift (kNm)	λ	Fuse Area (mm^2)
Diameter (1200mm)	36mm	250	3389	4498	4371	4090	3746	3363	1.2	10231
		500	3574	4447	4269	3940	3554	3137	1.3	10231
		750	3710	4431	4235	3881	3480	3046	1.3	10231
		1000	3809	4411	4214	3856	3441	2997	1.4	10231
	50mm	250	3432	4572	4489	4246	3948	3607	1.3	10446
		500	3617	4525	4383	4093	3752	3378	1.3	10446
		750	3755	4504	4345	4036	3673	3286	1.4	10446
		1000	3856	4483	4326	4008	3634	3237	1.4	10446
	75mm	250	3544	4764	4781	4635	4450	4220	1.3	11004
		500	3729	4715	4667	4477	4241	3983	1.4	11004
		750	3868	4692	4627	4415	4168	3888	1.4	11004
		1000	3972	4672	4612	4387	4122	3837	1.4	11004
	100mm	250	3693	5028	5178	5163	5111	5033	1.3	11784
		500	3883	4976	5059	4992	4900	4782	1.4	11784
		750	4028	4952	5017	4934	4817	4685	1.4	11784
		1000	4136	4932	4996	4909	4776	4638	1.4	11784
	125mm	250	3885	5363	5672	5808	5925	6025	1.4	12788
		500	4081	5307	5543	5640	5697	5753	1.4	12788
		750	4234	5282	5499	5577	5621	5646	1.5	12788
		1000	4343	5256	5477	5545	5570	5592	1.5	12788
	150mm	250	4121	5760	6252	6577	6855	7152	1.4	14015
		500	4320	5699	6118	6381	6617	6860	1.5	14015
		750	4484	5672	6062	6311	6534	6746	1.5	14015
		1000	4598	5646	6039	6284	6486	6689	1.5	14015

Initial Pt Force 0.1f_{yield}		Axial Load (excluding PT) 7500kN			Cantilever Length (8000mm)			Grade 300 Dissipaters		
	PT Dia.	Fuse Length (mm)	Yield (kNm)	1%drift (kNm)	2%drift (kNm)	3%drift (kNm)	4%drift (kNm)	6%drift (kNm)	λ	Fuse Area (mm^2)
Diameter (1500mm)	36mm	250	4657	6161	6166	5975	5704	5382	1.4	10265
		500	4898	6083	6005	5746	5423	5066	1.5	10265
		750	5059	6057	5949	5659	5310	4930	1.6	10265
		1000	5169	6045	5918	5614	5250	4856	1.6	10265
	50mm	250	4718	6287	6357	6244	6051	5807	1.5	10511
		500	4962	6208	6196	6011	5764	5487	1.6	10511
		750	5124	6178	6135	5923	5650	5348	1.6	10511
		1000	5234	6165	6108	5877	5589	5273	1.6	10511
	75mm	250	4875	6606	6848	6924	6925	6877	1.5	11149
		500	5122	6519	6680	6681	6627	6543	1.6	11149
		750	5290	6493	6621	6590	6507	6399	1.7	11149
		1000	5409	6475	6589	6542	6444	6322	1.7	11149
	100mm	250	5090	7043	7516	7842	8095	8303	1.6	12042
		500	5348	6947	7335	7585	7780	7949	1.7	12042
		750	5523	6918	7271	7488	7654	7799	1.7	12042
		1000	5647	6905	7238	7437	7587	7717	1.7	12042
	125mm	250	5367	7591	8342	8966	9523	10037	1.6	13191
		500	5634	7491	8148	8692	9186	9658	1.7	13191
		750	5817	7455	8087	8589	9051	9496	1.8	13191
		1000	5956	7435	8045	8535	8981	9409	1.8	13191
	150mm	250	5702	8240	9318	10269	11174	12029	1.6	14595
		500	5985	8133	9104	9981	10808	11619	1.8	14595
		750	6179	8094	9034	9860	10665	11446	1.8	14595
		1000	6326	8072	9001	9810	10588	11352	1.8	14595

Initial Pt Force 0.1F_{yield}		Axial Load (excluding PT) 7500kN			Cantilever Length (8000mm)			Grade 300 Dissipaters		
	PT Dia.	Fuse Length (mm)	Yield (kNm)	1%drift (kNm)	2%drift (kNm)	3%drift (kNm)	4%drift (kNm)	6%drift (kNm)	λ	Fuse Area (mm^2)
Diameter (1800mm)	36mm	250	6023	7891	8010	7915	7726	7432	1.6	10298
		500	6235	7773	7780	7599	7353	7018	1.7	10298
		750	6475	7727	7697	7476	7189	6826	1.7	10298
		1000	6563	7707	7654	7410	7098	6719	1.8	10298
	50mm	250	6103	8077	8308	8330	8261	8062	1.6	10575
		500	6318	7955	8073	8008	7880	7646	1.7	10575
		750	6563	7909	7988	7882	7719	7447	1.8	10575
		1000	6653	7889	7946	7816	7624	7337	1.8	10575
	75mm	250	6313	8548	9062	9381	9611	9677	1.7	11294
		500	6536	8419	8820	9043	9212	9243	1.8	11294
		750	6792	8373	8728	8911	9043	9040	1.8	11294
		1000	6888	8352	8685	8843	8952	8923	1.9	11294
	100mm	250	6609	9189	10091	10801	11425	11898	1.7	12300
		500	6840	9058	9829	10440	10999	11429	1.9	12300
		750	7112	9011	9734	10300	10819	11213	1.9	12300
		1000	7214	8984	9685	10226	10723	11093	2.0	12300
	125mm	250	6981	10006	11367	12549	13647	14685	1.8	13593
		500	7229	9857	11083	12159	13186	14178	1.9	13593
		750	7521	9809	10980	12008	12994	13944	2.0	13593
		1000	7627	9781	10928	11928	12889	13815	2.0	13593
	150mm	250	7437	10971	12864	14586	16226	17801	1.8	15174
		500	7697	10809	12555	14160	15722	17258	2.0	15174
		750	8014	10759	12442	13995	15513	17011	2.1	15174
		1000	8129	10730	12385	13910	15399	16873	2.1	15174

Initial Pt Force 0.1Fyield		Axial Load (excluding PT) 7500kN			Cantilever Length (8000mm)			Grade 300 Dissipaters		
	PT Dia.	Fuse Length (mm)	Yield (kNm)	1%drift (kNm)	2%drift (kNm)	3%drift (kNm)	4%drift (kNm)	6%drift (kNm)	λ	Fuse Area (mm^2)
Diameter (2000mm)	36mm	250	8198	10584	10974	11099	11083	10806	1.1	15480
		500	8454	10371	10560	10538	10420	10131	1.2	15480
		750	8591	10291	10409	10309	10128	9799	1.2	15480
		1000	8690	10245	10327	10181	9970	9613	1.2	15480
	50mm	250	8332	10856	11398	11673	11811	11611	1.1	15927
		500	8590	10638	10974	11100	11143	10912	1.2	15927
		750	8727	10556	10818	10871	10841	10569	1.2	15927
		1000	8828	10510	10735	10739	10677	10376	1.3	15927
	75mm	250	8679	11559	12475	13133	13657	13668	1.1	17085
		500	8944	11326	12024	12527	12959	12924	1.2	17085
		750	9089	11235	11858	12286	12653	12550	1.3	17085
		1000	9195	11189	11773	12158	12474	12341	1.3	17085
	100mm	250	9157	12519	13942	15111	16147	16470	1.2	18707
		500	9431	12260	13457	14460	15397	15672	1.3	18707
		750	9589	12169	13279	14201	15070	15281	1.3	18707
		1000	9698	12125	13188	14065	14891	15056	1.4	18707
	125mm	250	9768	13726	15764	17558	19216	20006	1.2	20792
		500	10057	13444	15240	16851	18398	19129	1.4	20792
		750	10224	13343	15047	16570	18043	18701	1.4	20792
		1000	10343	13299	14948	16421	17850	18462	1.4	20792
	150mm	250	10511	15163	17918	20428	22797	24239	1.3	23341
		500	10812	14858	17342	19650	21895	23265	1.4	23341
		750	10996	14745	17130	19342	21507	22794	1.5	23341
		1000	11127	14702	17021	19180	21296	22530	1.5	23341

Initial Pt Force 0.1F_{yield}		Axial Load (excluding PT) 7500kN			Cantilever Length (8000mm)			Grade 300 Dissipaters		
	PT Dia.	Fuse Length (mm)	Yield (kNm)	1%drift (kNm)	2%drift (kNm)	3%drift (kNm)	4%drift (kNm)	6%drift (kNm)	λ	Fuse Area (mm^2)
Diameter (2200mm)	36mm	250	9176	11948	12455	12675	12638	12390	1.1	15514
		500	9516	11686	11960	12004	11905	11660	1.2	15514
		750	9689	11597	11770	11731	11571	11271	1.2	15514
		1000	9832	11543	11665	11585	11388	11050	1.3	15514
	50mm	250	9329	12283	12977	13387	13513	13301	1.1	15991
		500	9676	12015	12470	12707	12755	12550	1.2	15991
		750	9855	11924	12279	12423	12410	12152	1.3	15991
		1000	9998	11866	12170	12272	12220	11928	1.3	15991
	75mm	250	9731	13142	14310	15199	15770	15657	1.2	17230
		500	10094	12856	13775	14488	14945	14853	1.3	17230
		750	10279	12759	13573	14188	14570	14429	1.3	17230
		1000	10431	12699	13459	14023	14365	14188	1.4	17230
	100mm	250	10293	14322	16132	17657	18841	18954	1.2	18965
		500	10666	14015	15550	16889	17962	18054	1.4	18965
		750	10867	13908	15328	16576	17558	17581	1.4	18965
		1000	11030	13840	15219	16404	17330	17314	1.4	18965
	125mm	250	11012	15807	18399	20704	22720	23063	1.3	21195
		500	11400	15469	17756	19862	21750	22086	1.4	21195
		750	11623	15344	17518	19521	21313	21575	1.5	21195
		1000	11795	15275	17394	19338	21072	21276	1.5	21195
	150mm	250	11882	17576	21068	24280	27316	27994	1.4	23921
		500	12287	17201	20365	23350	26266	26899	1.5	23921
		750	12537	17066	20102	22973	25796	26332	1.5	23921
		1000	12724	16985	19965	22772	25536	26011	1.6	23921

Initial Pt Force $0.1f_{yield}$		Axial Load (excluding PT) 8500kN			Cantilever Length (8000mm)			Grade 300 Dissipaters		
	PT Dia.	Fuse Length (mm)	Yield (kNm)	1%drift (kNm)	2%drift (kNm)	3%drift (kNm)	4%drift (kNm)	6%drift (kNm)	λ	Fuse Area (mm^2)
Diameter (1000mm)	36mm	250	2909	3775	3590	3208	2733	2249	1.0	11542
		500	3058	3731	3510	3078	2579	2062	1.0	11542
		750	3168	3719	3481	3035	2527	1994	1.1	11542
		1000	3252	3712	3462	3010	2495	1951	1.1	11542
	50mm	250	2940	3819	3660	3305	2854	2395	1.0	11737
		500	3091	3781	3579	3173	2702	2206	1.0	11737
		750	3202	3769	3550	3127	2645	2132	1.1	11737
		1000	3287	3762	3530	3101	2612	2099	1.1	11737
	75mm	250	3022	3944	3834	3542	3163	2759	1.0	12240
		500	3174	3902	3756	3417	2999	2567	1.1	12240
		750	3287	3891	3725	3363	2944	2493	1.1	12240
		1000	3376	3884	3710	3336	2908	2461	1.1	12240
	100mm	250	3136	4112	4081	3865	3583	3245	1.0	12946
		500	3289	4071	3995	3738	3405	3049	1.1	12946
		750	3407	4060	3963	3681	3342	2978	1.1	12946
		1000	3500	4054	3947	3655	3307	2938	1.1	12946
	125mm	250	3282	4327	4381	4269	4100	3862	1.0	13853
		500	3439	4282	4290	4128	3907	3650	1.1	13853
		750	3558	4272	4263	4083	3840	3567	1.1	13853
		1000	3656	4266	4247	4044	3803	3526	1.1	13853
	150mm	250	3461	4581	4738	4729	4677	4581	1.0	14962
		500	3622	4537	4641	4581	4489	4343	1.1	14962
		750	3743	4529	4613	4529	4412	4249	1.1	14962
		1000	3844	4524	4595	4505	4362	4200	1.1	14962

Initial Pt Force 0.1F_{yield}		Axial Load (excluding PT) 8500kN			Cantilever Length (8000mm)			Grade 300 Dissipaters		
	PT Dia.	Fuse Length (mm)	Yield (kNm)	1%drift (kNm)	2%drift (kNm)	3%drift (kNm)	4%drift (kNm)	6%drift (kNm)	λ	Fuse Area (mm^2)
Diameter (1200mm)	36mm	250	3747	5007	4875	4548	4154	3712	1.2	11565
		500	3946	4951	4756	4377	3938	3460	1.3	11565
		750	4102	4931	4715	4314	3852	3358	1.3	11565
		1000	4212	4907	4695	4283	3809	3304	1.3	11565
	50mm	250	3789	5080	4986	4691	4343	3949	1.2	11779
		500	3990	5023	4866	4521	4128	3693	1.3	11779
		750	4144	5002	4825	4462	4040	3591	1.3	11779
		1000	4255	4977	4804	4431	3997	3536	1.3	11779
	75mm	250	3896	5263	5273	5074	4827	4548	1.3	12337
		500	4097	5208	5143	4896	4603	4285	1.3	12337
		750	4256	5183	5100	4830	4522	4173	1.4	12337
		1000	4370	5159	5079	4800	4471	4117	1.4	12337
	100mm	250	4040	5519	5653	5589	5483	5334	1.3	13118
		500	4250	5462	5527	5407	5240	5061	1.4	13118
		750	4414	5437	5475	5341	5158	4959	1.4	13118
		1000	4533	5412	5453	5307	5112	4901	1.4	13118
	125mm	250	4231	5845	6137	6225	6268	6298	1.3	14121
		500	4445	5784	6001	6034	6030	6019	1.4	14121
		750	4612	5753	5946	5957	5931	5895	1.4	14121
		1000	4737	5728	5914	5928	5892	5842	1.4	14121
	150mm	250	4463	6232	6695	6985	7183	7396	1.3	15348
		500	4685	6161	6550	6763	6928	7094	1.4	15348
		750	4856	6127	6497	6682	6845	6969	1.4	15348
		1000	4989	6109	6462	6647	6794	6921	1.5	15348

Initial Pt Force $0.1f_{yield}$		Axial Load (excluding PT) 8500kN			Cantilever Length (8000mm)			Grade 300 Dissipaters		
	PT Dia.	Fuse Length (mm)	Yield (kNm)	1%drift (kNm)	2%drift (kNm)	3%drift (kNm)	4%drift (kNm)	6%drift (kNm)	λ	Fuse Area (mm^2)
Diameter (1500mm)	36mm	250	5145	6883	6880	6662	6347	5973	1.4	11598
		500	5421	6795	6703	6406	6032	5618	1.5	11598
		750	5612	6768	6641	6309	5906	5465	1.6	11598
		1000	5742	6751	6606	6259	5839	5383	1.6	11598
	50mm	250	5205	7007	7072	6923	6685	6389	1.4	11844
		500	5484	6914	6887	6663	6365	6029	1.5	11844
		750	5673	6886	6823	6566	6237	5874	1.6	11844
		1000	5805	6868	6787	6515	6170	5791	1.6	11844
	75mm	250	5356	7313	7545	7587	7539	7437	1.5	12482
		500	5643	7219	7359	7318	7208	7064	1.6	12482
		750	5837	7186	7295	7216	7076	6904	1.6	12482
		1000	5975	7172	7259	7164	7006	6819	1.7	12482
	100mm	250	5571	7742	8200	8483	8686	8837	1.5	13375
		500	5863	7639	8002	8200	8338	8446	1.6	13375
		750	6065	7604	7932	8094	8200	8279	1.7	13375
		1000	6209	7584	7897	8039	8126	8189	1.7	13375
	125mm	250	5842	8274	9009	9581	10090	10542	1.6	14524
		500	6144	8167	8802	9287	9721	10127	1.7	14524
		750	6356	8129	8724	9166	9574	9951	1.7	14524
		1000	6506	8108	8684	9109	9496	9855	1.8	14524
	150mm	250	6176	8915	9960	10868	11706	12507	1.6	15928
		500	6490	8796	9743	10541	11312	12061	1.7	15928
		750	6702	8755	9664	10431	11167	11872	1.8	15928
		1000	6865	8732	9623	10368	11086	11772	1.8	15928

Initial Pt Force 0.1Fyield		Axial Load (excluding PT) 8500kN			Cantilever Length (8000mm)			Grade 300 Dissipaters		
	PT Dia.	Fuse Length (mm)	Yield (kNm)	1%drift (kNm)	2%drift (kNm)	3%drift (kNm)	4%drift (kNm)	6%drift (kNm)	λ	Fuse Area (mm^2)
Diameter (1800mm)	36mm	250	6656	8821	8955	8837	8609	8273	1.5	11631
		500	6912	8692	8703	8484	8190	7821	1.7	11631
		750	7193	8645	8610	8346	8013	7601	1.7	11631
		1000	7297	8624	8560	8274	7914	7480	1.7	11631
	50mm	250	6733	9004	9245	9244	9133	8896	1.6	11908
		500	6996	8868	8986	8884	8708	8436	1.7	11908
		750	7282	8821	8892	8745	8528	8218	1.8	11908
		1000	7383	8800	8845	8671	8431	8093	1.8	11908
	75mm	250	6941	9459	9989	10275	10461	10498	1.6	12627
		500	7209	9321	9718	9900	10017	10014	1.8	12627
		750	7506	9273	9619	9755	9830	9789	1.8	12627
		1000	7617	9253	9569	9677	9730	9665	1.8	12627
	100mm	250	7230	10091	10998	11670	12248	12701	1.7	13633
		500	7508	9944	10707	11273	11777	12183	1.8	13633
		750	7821	9895	10606	11119	11579	11945	1.9	13633
		1000	7934	9874	10552	11038	11473	11813	1.9	13633
	125mm	250	7598	10886	12247	13391	14441	15420	1.8	14927
		500	7888	10734	11938	12965	13936	14877	1.9	14927
		750	8216	10677	11830	12801	13725	14627	2.0	14927
		1000	8339	10656	11773	12714	13612	14489	2.0	14927
	150mm	250	8045	11845	13717	15402	16991	18508	1.8	16508
		500	8345	11669	13390	14941	16444	17916	1.9	16508
		750	8695	11609	13266	14762	16217	17647	2.0	16508
		1000	8836	11589	13203	14670	16094	17500	2.0	16508

Initial Pt Force 0.1f_{yield}		Axial Load (excluding PT) 8500kN			Cantilever Length (8000mm)			Grade 300 Dissipaters		
	PT Dia.	Fuse Length (mm)	Yield (kNm)	1%drift (kNm)	2%drift (kNm)	3%drift (kNm)	4%drift (kNm)	6%drift (kNm)	λ	Fuse Area (mm^2)
Diameter (2000mm)	36mm	250	8452	11003	11324	11366	11263	10922	1.3	14567
		500	8749	10799	10940	10841	10651	10282	1.4	14567
		750	8924	10723	10797	10631	10375	9968	1.4	14567
		1000	9049	10681	10723	10512	10225	9792	1.5	14567
	50mm	250	8566	11247	11716	11908	11957	11695	1.3	14939
		500	8865	11042	11322	11373	11339	11033	1.4	14939
		750	9048	10965	11176	11159	11057	10709	1.5	14939
		1000	9171	10923	11101	11042	10903	10528	1.5	14939
	75mm	250	8862	11880	12721	13287	13716	13651	1.4	15904
		500	9169	11662	12307	12725	13068	12968	1.5	15904
		750	9361	11585	12154	12501	12785	12619	1.5	15904
		1000	9490	11542	12072	12383	12624	12424	1.6	15904
	100mm	250	9276	12753	14084	15155	16091	16339	1.4	17256
		500	9592	12517	13642	14557	15401	15604	1.5	17256
		750	9791	12432	13480	14320	15100	15244	1.6	17256
		1000	9934	12389	13400	14194	14936	15042	1.6	17256
	125mm	250	9807	13845	15786	17468	19017	19731	1.5	18994
		500	10135	13591	15309	16825	18272	18930	1.6	18994
		750	10350	13505	15134	16569	17949	18542	1.7	18994
		1000	10498	13461	15043	16434	17772	18323	1.7	18994
	150mm	250	10446	15156	17793	20181	22433	23794	1.5	21117
		500	10785	14874	17274	19478	21620	22912	1.7	21117
		750	11023	14786	17083	19200	21268	22487	1.7	21117
		1000	11178	14742	16985	19054	21078	22250	1.7	21117

Initial Pt Force 0.1F_{yield}		Axial Load (excluding PT) 8500kN			Cantilever Length (8000mm)			Grade 300 Dissipaters		
	PT Dia.	Fuse Length (mm)	Yield (kNm)	1%drift (kNm)	2%drift (kNm)	3%drift (kNm)	4%drift (kNm)	6%drift (kNm)	λ	Fuse Area (mm^2)
Diameter (2200mm)	36mm	250	9479	12431	12869	13001	12891	12547	1.3	14595
		500	9870	12188	12405	12380	12199	11861	1.4	14595
		750	10089	12104	12232	12121	11885	11497	1.5	14595
		1000	10254	12052	12134	11983	11711	11293	1.5	14595
	50mm	250	9613	12735	13359	13676	13731	13420	1.3	14993
		500	10009	12486	12886	13048	13016	12717	1.5	14993
		750	10232	12402	12709	12780	12691	12349	1.5	14993
		1000	10401	12347	12608	12638	12514	12139	1.5	14993
	75mm	250	9964	13517	14601	15392	15878	15690	1.4	16025
		500	10365	13254	14106	14732	15120	14938	1.5	16025
		750	10601	13166	13916	14461	14770	14544	1.6	16025
		1000	10779	13105	13823	14307	14579	14319	1.6	16025
	100mm	250	10450	14593	16305	17722	18819	18838	1.5	17471
		500	10860	14311	15766	17015	18011	18017	1.6	17471
		750	11113	14210	15571	16727	17644	17581	1.7	17471
		1000	11303	14152	15463	16574	17434	17333	1.7	17471
	125mm	250	11071	15948	18419	20609	22534	22778	1.5	19329
		500	11497	15644	17840	19843	21652	21887	1.7	19329
		750	11773	15527	17622	19532	21253	21422	1.7	19329
		1000	11972	15464	17511	19366	21034	21154	1.8	19329
	150mm	250	11821	17562	20921	24000	26911	27505	1.6	21600
		500	12265	17219	20287	23161	25964	26516	1.7	21600
		750	12566	17096	20049	22821	25539	26005	1.8	21600
		1000	12784	17037	19927	22640	25307	25715	1.8	21600

Initial Pt Force $0.1f_{yield}$		Axial Load (excluding PT) 8500kN			Cantilever Length (8000mm)			Grade 300 Dissipaters		
	PT Dia.	Fuse Length (mm)	Yield (kNm)	1%drift (kNm)	2%drift (kNm)	3%drift (kNm)	4%drift (kNm)	6%drift (kNm)	λ	Fuse Area (mm^2)
Diameter (2500mm)	36mm	250	11369	14603	15227	15467	15366	12593	1.3	14637
		500	11608	14286	14632	14725	14569	14302	1.5	14637
		750	11896	14175	14402	14411	14177	13857	1.5	14637
		1000	11981	14108	14282	14241	13958	13597	1.6	14637
	50mm	250	11540	15007	15877	16371	16368	13586	1.4	15073
		500	11783	14681	15270	15607	15549	15341	1.5	15073
		750	12078	14568	15032	15283	15147	14884	1.6	15073
		1000	12162	14499	14909	15109	14925	14617	1.6	15073
	75mm	250	11980	16042	17538	18684	18947	17912	1.4	16206
		500	12236	15695	16899	17858	18076	18015	1.6	16206
		750	12549	15575	16647	17510	17652	17528	1.7	16206
		1000	12632	15505	16512	17323	17415	17244	1.7	16206
	100mm	250	12595	17464	19802	21809	22549	21602	1.5	17793
		500	12862	17092	19117	20931	21588	21711	1.7	17793
		750	13205	16958	18855	20545	21123	21186	1.8	17793
		1000	13285	16891	18706	20337	20862	20881	1.8	17793
	125mm	250	13381	19257	22634	25679	27108	26307	1.6	19832
		500	13670	18847	21884	24721	26051	26426	1.8	19832
		750	14044	18705	21597	24317	25528	25841	1.8	19832
		1000	14112	18633	21449	24089	25235	25501	1.9	19832
	150mm	250	14335	21396	25983	30233	32559	31984	1.7	22325
		500	14646	20943	25155	29176	31384	32114	1.8	22325
		750	15052	20786	24839	28731	30818	31455	1.9	22325
		1000	15115	20698	24676	28492	30502	31070	2.0	22325

Initial Pt Force 0.1f_{yield}		Axial Load (excluding PT) 10000kN			Cantilever Length (8000mm)			Grade 300 Dissipaters		
	PT Dia.	Fuse Length (mm)	Yield (kNm)	1%drift (kNm)	2%drift (kNm)	3%drift (kNm)	4%drift (kNm)	6%drift (kNm)	λ	Fuse Area (mm^2)
Diameter (1000mm)	36mm	250	3069	3998	3765	3301	2739	2136	1.1	11285
		500	3235	3964	3689	3186	2588	1951	1.2	11285
		750	3360	3952	3666	3139	2531	1882	1.2	11285
		1000	3458	3948	3653	3112	2498	1849	1.2	11285
	50mm	250	3099	4040	3830	3384	2853	2265	1.1	11447
		500	3263	4006	3754	3271	2692	2088	1.2	11447
		750	3389	3995	3726	3223	2635	2015	1.2	11447
		1000	3488	3990	3712	3195	2610	1982	1.2	11447
	75mm	250	3169	4147	3984	3604	3140	2602	1.2	11867
		500	3337	4113	3906	3482	2970	2421	1.2	11867
		750	3461	4102	3877	3437	2909	2352	1.2	11867
		1000	3564	4098	3869	3407	2877	2322	1.3	11867
	100mm	250	3270	4294	4198	3892	3512	3073	1.2	12455
		500	3439	4256	4117	3766	3351	2876	1.2	12455
		750	3568	4246	4093	3723	3279	2810	1.3	12455
		1000	3674	4242	4079	3701	3246	2773	1.3	12455
	125mm	250	3398	4480	4466	4248	3975	3651	1.2	13211
		500	3568	4443	4382	4126	3809	3434	1.2	13211
		750	3698	4433	4357	4076	3741	3362	1.3	13211
		1000	3809	4430	4342	4051	3697	3313	1.3	13211
	150mm	250	3553	4706	4786	4667	4504	4301	1.2	14135
		500	3727	4670	4697	4540	4319	4092	1.3	14135
		750	3862	4660	4663	4488	4254	3990	1.3	14135
		1000	3975	4651	4647	4461	4217	3944	1.3	14135

Initial Pt Force 0.1f_{yield}		Axial Load (excluding PT) 10000kN			Cantilever Length (8000mm)			Grade 300 Dissipaters		
	PT Dia.	Fuse Length (mm)	Yield (kNm)	1%drift (kNm)	2%drift (kNm)	3%drift (kNm)	4%drift (kNm)	6%drift (kNm)	λ	Fuse Area (mm^2)
Diameter (1200mm)	36mm	250	3965	5376	5202	4775	4278	3734	1.4	11304
		500	4199	5323	5087	4616	4074	3493	1.5	11304
		750	4373	5298	5044	4554	3991	3390	1.6	11304
		1000	4507	5278	5024	4523	3950	3339	1.6	11304
	50mm	250	4001	5439	5297	4911	4456	3954	1.5	11483
		500	4236	5390	5186	4748	4251	3709	1.5	11483
		750	4413	5364	5142	4692	4166	3608	1.6	11483
		1000	4547	5344	5122	4658	4128	3556	1.6	11483
	75mm	250	4091	5600	5555	5260	4914	4511	1.5	11948
		500	4332	5547	5439	5097	4697	4260	1.6	11948
		750	4512	5520	5393	5033	4610	4157	1.6	11948
		1000	4646	5506	5373	5003	4567	4104	1.6	11948
	100mm	250	4222	5825	5897	5738	5511	5256	1.5	12598
		500	4461	5772	5784	5568	5287	5004	1.6	12598
		750	4646	5745	5734	5504	5204	4892	1.6	12598
		1000	4790	5726	5713	5465	5163	4843	1.6	12598
	125mm	250	4384	6112	6334	6335	6259	6171	1.5	13435
		500	4632	6049	6208	6151	6021	5890	1.6	13435
		750	4819	6024	6162	6080	5934	5779	1.6	13435
		1000	4969	6005	6132	6044	5900	5723	1.7	13435
	150mm	250	4587	6452	6837	7025	7121	7198	1.5	14457
		500	4843	6384	6704	6834	6875	6910	1.6	14457
		750	5032	6354	6664	6748	6795	6800	1.7	14457
		1000	5190	6343	6630	6716	6749	6748	1.7	14457

Initial Pt Force 0.1F_{yield}		Axial Load (excluding PT) 10000kN			Cantilever Length (8000mm)			Grade 300 Dissipaters		
	PT Dia.	Fuse Length (mm)	Yield (kNm)	1%drift (kNm)	2%drift (kNm)	3%drift (kNm)	4%drift (kNm)	6%drift (kNm)	λ	Fuse Area (mm^2)
Diameter (1500mm)	36mm	250	6044	8186	8203	7960	7599	7163	1.3	14731
		500	6371	8073	7979	7641	7205	6718	1.4	14731
		750	6587	8036	7898	7521	7048	6527	1.4	14731
		1000	6747	8016	7857	7459	6964	6424	1.4	14731
	50mm	250	6108	8302	8386	8216	7930	7570	1.3	14997
		500	6431	8192	8157	7893	7531	7121	1.4	14997
		750	6649	8154	8076	7772	7372	6928	1.4	14997
		1000	6811	8133	8035	7709	7287	6823	1.5	14997
	75mm	250	6265	8608	8858	8871	8767	8599	1.3	15689
		500	6593	8498	8623	8536	8357	8135	1.4	15689
		750	6816	8453	8543	8412	8193	7938	1.5	15689
		1000	6982	8437	8502	8344	8106	7830	1.5	15689
	100mm	250	6486	9037	9494	9748	9897	9979	1.4	16657
		500	6816	8919	9261	9403	9469	9496	1.5	16657
		750	7046	8871	9172	9270	9299	9290	1.5	16657
		1000	7218	8849	9131	9203	9208	9179	1.5	16657
	125mm	250	6769	9572	10307	10835	11278	11665	1.4	17901
		500	7106	9446	10049	10467	10833	11157	1.5	17901
		750	7341	9400	9960	10338	10654	10940	1.6	17901
		1000	7520	9376	9910	10259	10560	10825	1.6	17901
	150mm	250	7116	10210	11262	12117	12900	13606	1.4	19422
		500	7457	10076	10991	11727	12409	13075	1.5	19422
		750	7703	10024	10889	11571	12221	12847	1.6	19422
		1000	7889	9998	10837	11510	12122	12724	1.6	19422

Initial Pt Force 0.1f_{yield}		Axial Load (excluding PT) 10000kN			Cantilever Length (8000mm)			Grade 300 Dissipaters		
	PT Dia.	Fuse Length (mm)	Yield (kNm)	1%drift (kNm)	2%drift (kNm)	3%drift (kNm)	4%drift (kNm)	6%drift (kNm)	λ	Fuse Area (mm^2)
Diameter (1800mm)	36mm	250	7797	10487	10686	10561	10298	9917	1.4	14767
		500	8116	10328	10369	10120	9773	9349	1.5	14767
		750	8460	10276	10254	9949	9552	9085	1.6	14767
		1000	8591	10247	10195	9858	9432	8937	1.6	14767
	50mm	250	7879	10668	10973	10962	10815	10540	1.4	15067
		500	8201	10502	10652	10514	10282	9962	1.5	15067
		750	8544	10449	10532	10340	10058	9694	1.6	15067
		1000	8678	10421	10475	10248	9937	9545	1.6	15067
	75mm	250	8094	11124	11706	11981	12126	12140	1.5	15846
		500	8419	10955	11369	11516	11574	11537	1.6	15846
		750	8777	10902	11251	11336	11342	11258	1.6	15846
		1000	8912	10873	11188	11241	11218	11104	1.7	15846
	100mm	250	8390	11758	12707	13362	13896	14340	1.5	16936
		500	8725	11585	12355	12874	13316	13705	1.6	16936
		750	9092	11523	12227	12686	13074	13412	1.7	16936
		1000	9241	11493	12163	12586	12942	13251	1.7	16936
	125mm	250	8772	12566	13952	15073	16076	16990	1.6	18337
		500	9115	12369	13576	14555	15460	16324	1.7	18337
		750	9500	12306	13442	14355	15203	16018	1.7	18337
		1000	9660	12275	13364	14249	15066	15851	1.8	18337
	150mm	250	9233	13528	15416	17076	18615	20066	1.6	20050
		500	9593	13321	15020	16522	17955	19352	1.7	20050
		750	9997	13246	14875	16307	17681	19026	1.8	20050
		1000	10166	13214	14792	16195	17535	18849	1.8	20050

Initial Pt Force 0.1F_{yield}		Axial Load (excluding PT) 10000kN			Cantilever Length (8000mm)			Grade 300 Dissipaters		
	PT Dia.	Fuse Length (mm)	Yield (kNm)	1%drift (kNm)	2%drift (kNm)	3%drift (kNm)	4%drift (kNm)	6%drift (kNm)	λ	Fuse Area (mm^2)
Diameter (2000mm)	36mm	250	9669	12735	13113	13142	12998	12627	1.3	17067
		500	10013	12502	12667	12535	12293	11881	1.4	17067
		750	10249	12417	12505	12292	11985	11507	1.4	17067
		1000	10400	12373	12418	12164	11807	11299	1.4	17067
	50mm	250	9783	12975	13497	13671	13676	13376	1.3	17439
		500	10129	12736	13043	13053	12960	12626	1.4	17439
		750	10364	12650	12874	12808	12647	12243	1.4	17439
		1000	10523	12607	12788	12678	12472	12029	1.5	17439
	75mm	250	10074	13594	14470	15017	15399	15305	1.3	18404
		500	10424	13341	14001	14375	14654	14518	1.4	18404
		750	10669	13247	13823	14119	14329	14132	1.5	18404
		1000	10829	13204	13733	13984	14153	13910	1.5	18404
	100mm	250	10483	14431	15804	16848	17731	17967	1.4	19756
		500	10832	14174	15308	16169	16944	17129	1.5	19756
		750	11095	14078	15120	15899	16602	16720	1.5	19756
		1000	11262	14034	15026	15758	16416	16491	1.6	19756
	125mm	250	10997	15502	17469	19118	20608	21330	1.4	21494
		500	11357	15221	16935	18393	19769	20426	1.6	21494
		750	11630	15123	16743	18107	19405	19989	1.6	21494
		1000	11817	15079	16642	17955	19208	19744	1.6	21494
	150mm	250	11618	16780	19442	21784	23975	25359	1.5	23617
		500	11991	16479	18860	21004	23070	24377	1.6	23617
		750	12283	16379	18649	20697	22680	23905	1.7	23617
		1000	12488	16324	18546	20534	22469	23640	1.7	23617

Initial Pt Force 0.1f_{yield}		Axial Load (excluding PT) 10000kN			Cantilever Length (8000mm)			Grade 300 Dissipaters		
	PT Dia.	Fuse Length (mm)	Yield (kNm)	1%drift (kNm)	2%drift (kNm)	3%drift (kNm)	4%drift (kNm)	6%drift (kNm)	λ	Fuse Area (mm^2)
Diameter (2200mm)	36mm	250	11140	14781	15329	15495	15415	15003	1.2	18235
		500	11580	14483	14760	14738	14544	14150	1.3	18235
		750	11868	14374	14548	14426	14147	13699	1.4	18235
		1000	12066	14307	14437	14251	13930	13444	1.4	18235
	50mm	250	11275	15084	15816	16164	16244	15894	1.2	18659
		500	11724	14781	15234	15393	15364	15015	1.4	18659
		750	12011	14666	15017	15078	14957	14554	1.4	18659
		1000	12213	14603	14906	14901	14733	14292	1.4	18659
	75mm	250	11634	15867	17054	17868	18380	18188	1.3	19760
		500	12088	15549	16446	17062	17463	17249	1.4	19760
		750	12392	15425	16223	16735	17043	16757	1.5	19760
		1000	12597	15362	16105	16560	16804	16478	1.5	19760
	100mm	250	12128	16949	18750	20187	21329	21316	1.3	21302
		500	12599	16604	18102	19333	20351	20329	1.5	21302
		750	12915	16481	17862	18986	19908	19810	1.5	21302
		1000	13133	16409	17738	18801	19664	19505	1.5	21302
	125mm	250	12764	18307	20862	23070	25060	25274	1.4	23284
		500	13250	17934	20172	22153	24002	24202	1.5	23284
		750	13587	17801	19915	21781	23526	23647	1.6	23284
		1000	13820	17727	19786	21583	23265	23332	1.6	23284
	150mm	250	13525	19928	23368	26462	29352	30027	1.4	25707
		500	14036	19523	22628	25469	28227	28854	1.6	25707
		750	14401	19377	22342	25067	27726	28249	1.6	25707
		1000	14646	19302	22197	24854	27449	27907	1.7	25707

Initial Pt Force 0.1f_{yield}		Axial Load (excluding PT) 10000kN			Cantilever Length (8000mm)			Grade 300 Dissipaters		
	PT Dia.	Fuse Length (mm)	Yield (kNm)	1%drift (kNm)	2%drift (kNm)	3%drift (kNm)	4%drift (kNm)	6%drift (kNm)	λ	Fuse Area (mm^2)
Diameter (2500mm)	36mm	250	13359	17379	18143	18454	18330	16931	1.2	18279
		500	13664	16991	17420	17521	17341	17047	1.4	18279
		750	14039	16856	17140	17127	16861	16496	1.4	18279
		1000	14099	16783	16989	16914	16593	16174	1.5	18279
	50mm	250	13534	17781	18790	19360	19336	17970	1.3	18745
		500	13844	17385	18053	18400	18329	18088	1.4	18745
		750	14223	17247	17767	17996	17838	17524	1.5	18745
		1000	14285	17176	17611	17778	17563	17195	1.5	18745
	75mm	250	13990	18818	20443	21646	21955	20647	1.3	19953
		500	14307	18400	19675	20650	20878	20770	1.5	19953
		750	14699	18255	19376	20217	20355	20175	1.5	19953
		1000	14762	18182	19215	19984	20063	19832	1.6	19953
	100mm	250	14620	20248	22710	24757	25587	24361	1.4	21645
		500	14945	19801	21885	23699	24414	24499	1.5	21645
		750	15363	19645	21570	23251	23845	23863	1.6	21645
		1000	15422	19562	21406	22994	23527	23491	1.6	21645
	125mm	250	15425	22054	25554	28629	30152	29133	1.5	23821
		500	15759	21568	24655	27486	28890	29256	1.6	23821
		750	16211	21400	24321	27004	28281	28550	1.7	23821
		1000	16272	21304	24144	26745	27928	28140	1.7	23821
	150mm	250	16406	24207	28909	33197	35642	36278	1.5	26480
		500	16751	23675	27945	31948	34252	34966	1.7	26480
		750	17234	23491	27566	31423	33585	34202	1.7	26480
		1000	17298	23380	27373	31141	33214	33749	1.8	26480

Initial Pt Force $0.1f_{yield}$		Axial Load (excluding PT) 1500kN			Cantilever Length (10000mm)			Grade 300 Dissipaters		
	PT Dia.	Fuse Length (mm)	Yield (kNm)	1%drift (kNm)	2%drift (kNm)	3%drift (kNm)	4%drift (kNm)	6%drift (kNm)	λ	Fuse Area (mm^2)
Diameter (1000mm)	36mm	250	844	1020	1027	1010	984	947	1.1	2962
		500	871	1009	1002	972	932	889	1.1	2962
		750	887	1002	991	955	913	866	1.1	2962
		1000	900	998	984	947	902	855	1.2	2962
	50mm	250	893	1108	1152	1173	1185	1193	1.1	3236
		500	923	1094	1124	1132	1135	1131	1.2	3236
		750	940	1088	1114	1116	1112	1104	1.2	3236
		1000	956	1083	1106	1106	1100	1091	1.2	3236
	75mm	250	1023	1326	1459	1572	1676	1775	1.2	3948
		500	1057	1310	1427	1525	1617	1706	1.3	3948
		750	1077	1305	1415	1508	1595	1679	1.3	3948
		1000	1098	1298	1409	1499	1583	1665	1.3	3948
	100mm	250	1198	1620	1862	2088	2306	2519	1.3	4944
		500	1240	1600	1823	2031	2235	2436	1.4	4944
		750	1265	1593	1808	2011	2208	2403	1.4	4944
		1000	1290	1587	1805	2001	2194	2386	1.4	4944
	125mm	250	1419	1981	2340	2697	3042	3387	1.3	6225
		500	1469	1954	2295	2628	2958	3287	1.4	6225
		750	1501	1946	2285	2604	2930	3247	1.4	6225
		1000	1531	1942	2275	2596	2908	3227	1.4	6225
	150mm	250	1683	2406	2893	3388	3867	4350	1.3	7791
		500	1743	2369	2841	3300	3766	4226	1.4	7791
		750	1782	2356	2828	3278	3733	4179	1.4	7791
		1000	1817	2354	2819	3261	3705	4164	1.4	7791

Initial Pt Force 0.1f_{yield}		Axial Load (excluding PT) 1500kN			Cantilever Length (10000mm)			Grade 300 Dissipaters		
	PT Dia.	Fuse Length (mm)	Yield (kNm)	1%drift (kNm)	2%drift (kNm)	3%drift (kNm)	4%drift (kNm)	6%drift (kNm)	λ	Fuse Area (mm^2)
Diameter (1200mm)	36mm	250	1068	1302	1341	1348	1343	1338	1.2	2995
		500	1096	1284	1301	1295	1281	1265	1.3	2995
		750	1115	1274	1286	1275	1258	1237	1.3	2995
		1000	1133	1268	1279	1265	1245	1222	1.3	2995
	50mm	250	1136	1425	1523	1596	1650	1697	1.3	3300
		500	1166	1407	1482	1534	1579	1620	1.4	3300
		750	1188	1396	1465	1512	1552	1589	1.4	3300
		1000	1207	1390	1456	1500	1538	1573	1.4	3300
	75mm	250	1309	1737	1976	2190	2395	2592	1.4	4091
		500	1346	1715	1929	2123	2312	2496	1.5	4091
		750	1372	1705	1911	2096	2276	2453	1.5	4091
		1000	1398	1695	1899	2080	2256	2430	1.5	4091
	100mm	250	1546	2154	2570	2964	3346	3720	1.5	5199
		500	1593	2128	2513	2882	3245	3605	1.6	5199
		750	1622	2117	2493	2852	3206	3559	1.6	5199
		1000	1655	2107	2482	2837	3186	3533	1.6	5199
	125mm	250	1842	2664	3282	3885	4473	5051	1.5	6623
		500	1900	2631	3215	3785	4349	4910	1.6	6623
		750	1934	2620	3190	3748	4301	4853	1.6	6623
		1000	1974	2609	3179	3730	4277	4821	1.7	6623
	150mm	250	2199	3261	4097	4931	5741	6545	1.5	8363
		500	2266	3218	4017	4802	5591	6371	1.6	8363
		750	2306	3203	3989	4758	5533	6301	1.6	8363
		1000	2356	3196	3977	4742	5503	6264	1.7	8363

Initial Pt Force 0.1Fyield		Axial Load (excluding PT) 1500kN			Cantilever Length (10000mm)			Grade 300 Dissipaters		
	PT Dia.	Fuse Length (mm)	Yield (kNm)	1%drift (kNm)	2%drift (kNm)	3%drift (kNm)	4%drift (kNm)	6%drift (kNm)	λ	Fuse Area (mm^2)
Diameter (1500mm)	36mm	250	1426	1740	1828	1895	1953	1967	1.3	3044
		500	1447	1708	1774	1819	1863	1866	1.4	3044
		750	1470	1696	1755	1792	1825	1822	1.5	3044
		1000	1489	1691	1745	1778	1806	1798	1.5	3044
	50mm	250	1523	1933	2121	2279	2436	2531	1.4	3395
		500	1548	1898	2059	2199	2336	2420	1.5	3395
		750	1573	1885	2037	2169	2295	2371	1.6	3395
		1000	1597	1879	2026	2154	2276	2345	1.6	3395
	75mm	250	1774	2418	2853	3252	3633	3961	1.6	4306
		500	1805	2378	2772	3145	3512	3826	1.7	4306
		750	1838	2361	2743	3105	3463	3767	1.8	4306
		1000	1870	2351	2727	3085	3437	3736	1.8	4306
	100mm	250	2118	3069	3809	4520	5216	5896	1.7	5580
		500	2159	3021	3716	4393	5063	5726	1.8	5580
		750	2200	3001	3679	4339	4993	5645	1.9	5580
		1000	2244	2985	3657	4309	4956	5601	1.9	5580
	125mm	250	2548	3864	4966	6036	7087	8121	1.7	7219
		500	2606	3807	4851	5877	6895	7908	1.9	7219
		750	2655	3785	4809	5816	6818	7817	1.9	7219
		1000	2709	3766	4786	5785	6777	7767	1.9	7219
	150mm	250	3060	4790	6296	7767	9215	10644	1.7	9222
		500	3141	4716	6154	7571	8978	10381	1.9	9222
		750	3193	4693	6103	7495	8884	10268	1.9	9222
		1000	3256	4679	6077	7457	8833	10207	1.9	9222

Initial Pt Force $0.1f_{yield}$		Axial Load (excluding PT) 1500kN			Cantilever Length (10000mm)			Grade 300 Dissipaters		
	PT Dia.	Fuse Length (mm)	Yield (kNm)	1%drift (kNm)	2%drift (kNm)	3%drift (kNm)	4%drift (kNm)	6%drift (kNm)	λ	Fuse Area (mm^2)
Diameter (1800mm)	36mm	250	1788	2193	2358	2499	2588	2568	1.4	3094
		500	1800	2151	2281	2396	2468	2442	1.5	3094
		750	1838	2136	2255	2355	2416	2381	1.6	3094
		1000	1854	2129	2241	2334	2388	2348	1.6	3094
	50mm	250	1921	2470	2777	3066	3287	3305	1.5	3490
		500	1935	2422	2694	2951	3152	3163	1.7	3490
		750	1978	2405	2664	2906	3095	3096	1.7	3490
		1000	1997	2397	2649	2883	3064	3058	1.7	3490
	75mm	250	2263	3172	3836	4473	5062	5177	1.7	4520
		500	2278	3107	3729	4331	4892	4996	1.9	4520
		750	2336	3085	3690	4278	4819	4911	1.9	4520
		1000	2365	3074	3670	4250	4781	4863	2.0	4520
	100mm	250	2729	4110	5258	6360	7434	7725	1.8	5962
		500	2749	4032	5110	6170	7220	7491	2.0	5962
		750	2825	3999	5056	6096	7130	7384	2.1	5962
		1000	2865	3984	5028	6058	7082	7325	2.1	5962
	125mm	250	3315	5261	6969	8637	10273	10948	1.9	7815
		500	3343	5169	6796	8403	10001	10639	2.1	7815
		750	3440	5127	6726	8307	9879	10493	2.1	7815
		1000	3494	5104	6686	8251	9810	10412	2.2	7815
	150mm	250	4013	6605	8949	11245	13503	14741	1.9	10081
		500	4054	6490	8732	10952	13162	14359	2.1	10081
		750	4173	6450	8653	10839	13019	14181	2.1	10081
		1000	4241	6412	8611	10778	12940	14083	2.2	10081

Initial Pt Force $0.1f_{yield}$		Axial Load (excluding PT) 3000kN			Cantilever Length (10000mm)			Grade 300 Dissipaters		
	PT Dia.	Fuse Length (mm)	Yield (kNm)	1%drift (kNm)	2%drift (kNm)	3%drift (kNm)	4%drift (kNm)	6%drift (kNm)	λ	Fuse Area (mm^2)
Diameter (1000mm)	36mm	250	1469	1834	1809	1736	1641	1535	1.0	5628
		500	1536	1811	1764	1669	1556	1434	1.0	5628
		750	1573	1804	1748	1645	1524	1394	1.0	5628
		1000	1598	1801	1740	1632	1507	1373	1.0	5628
	50mm	250	1515	1912	1917	1881	1824	1754	1.0	5903
		500	1583	1887	1871	1812	1735	1650	1.0	5903
		750	1623	1880	1855	1787	1702	1609	1.1	5903
		1000	1649	1877	1849	1774	1684	1587	1.1	5903
	75mm	250	1633	2111	2196	2243	2274	2293	1.0	6614
		500	1706	2083	2146	2170	2178	2180	1.1	6614
		750	1749	2075	2128	2143	2142	2136	1.1	6614
		1000	1778	2069	2121	2126	2123	2112	1.1	6614
	100mm	250	1799	2384	2563	2720	2859	2992	1.1	7611
		500	1877	2349	2509	2639	2753	2866	1.1	7611
		750	1924	2339	2492	2608	2712	2818	1.2	7611
		1000	1957	2332	2486	2591	2693	2792	1.2	7611
	125mm	250	2006	2717	3026	3296	3564	3816	1.1	8892
		500	2094	2682	2960	3196	3436	3674	1.2	8892
		750	2148	2665	2938	3170	3399	3618	1.2	8892
		1000	2183	2655	2926	3150	3369	3587	1.2	8892
	150mm	250	2259	3110	3565	3948	4354	4739	1.1	10458
		500	2356	3072	3481	3844	4207	4578	1.2	10458
		750	2417	3052	3453	3809	4166	4515	1.2	10458
		1000	2457	3034	3439	3792	4135	4492	1.2	10458

Initial Pt Force 0.1F_{yield}		Axial Load (excluding PT) 3000kN			Cantilever Length (10000mm)			Grade 300 Dissipaters		
	PT Dia.	Fuse Length (mm)	Yield (kNm)	1%drift (kNm)	2%drift (kNm)	3%drift (kNm)	4%drift (kNm)	6%drift (kNm)	λ	Fuse Area (mm^2)
Diameter (1200mm)	36mm	250	1879	2342	2369	2334	2275	2201	1.1	5661
		500	1950	2313	2305	2241	2159	2063	1.2	5661
		750	1987	2303	2282	2207	2110	2003	1.2	5661
		1000	2020	2295	2269	2185	2083	1971	1.2	5661
	50mm	250	1941	2454	2535	2555	2553	2536	1.1	5966
		500	2014	2422	2467	2458	2432	2397	1.2	5966
		750	2053	2412	2444	2423	2385	2336	1.2	5966
		1000	2088	2405	2432	2403	2356	2302	1.2	5966
	75mm	250	2098	2739	2950	3107	3242	3363	1.2	6758
		500	2176	2705	2877	3001	3110	3211	1.3	6758
		750	2220	2692	2851	2961	3058	3149	1.3	6758
		1000	2260	2686	2837	2941	3031	3116	1.3	6758
	100mm	250	2316	3128	3503	3836	4146	4442	1.3	7865
		500	2401	3085	3422	3716	3996	4270	1.3	7865
		750	2453	3073	3393	3671	3939	4200	1.4	7865
		1000	2498	3067	3379	3649	3908	4163	1.4	7865
	125mm	250	2592	3609	4177	4711	5225	5724	1.3	9289
		500	2686	3560	4086	4574	5055	5527	1.4	9289
		750	2748	3544	4049	4523	4989	5449	1.4	9289
		1000	2799	3537	4034	4503	4955	5406	1.4	9289
	150mm	250	2928	4184	4957	5711	6448	7168	1.3	11030
		500	3031	4119	4847	5553	6251	6945	1.4	11030
		750	3105	4101	4818	5495	6175	6855	1.4	11030
		1000	3160	4088	4795	5467	6144	6806	1.5	11030

Initial Pt Force 0.1f_{yield}		Axial Load (excluding PT) 3000kN			Cantilever Length (10000mm)			Grade 300 Dissipaters		
	PT Dia.	Fuse Length (mm)	Yield (kNm)	1%drift (kNm)	2%drift (kNm)	3%drift (kNm)	4%drift (kNm)	6%drift (kNm)	λ	Fuse Area (mm^2)
Diameter (1500mm)	36mm	250	2526	3142	3242	3270	3256	3218	1.2	5711
		500	2602	3092	3141	3126	3092	3033	1.3	5711
		750	2645	3071	3101	3072	3026	2955	1.4	5711
		1000	2682	3055	3080	3044	2991	2913	1.4	5711
	50mm	250	2615	3318	3512	3639	3724	3765	1.3	6062
		500	2695	3267	3408	3487	3547	3576	1.4	6062
		750	2739	3245	3365	3429	3476	3493	1.4	6062
		1000	2780	3228	3343	3398	3438	3448	1.4	6062
	75mm	250	2846	3768	4191	4551	4882	5193	1.4	6972
		500	2935	3710	4075	4390	4686	4966	1.5	6972
		750	2983	3688	4034	4324	4599	4867	1.5	6972
		1000	3029	3669	4006	4287	4554	4813	1.5	6972
	100mm	250	3165	4377	5100	5760	6391	6999	1.5	8247
		500	3269	4313	4967	5575	6168	6751	1.6	8247
		750	3317	4286	4919	5505	6078	6644	1.6	8247
		1000	3374	4268	4895	5468	6029	6585	1.6	8247
	125mm	250	3569	5135	6210	7224	8209	9168	1.5	9886
		500	3685	5055	6055	7009	7949	8880	1.6	9886
		750	3742	5026	6000	6927	7844	8755	1.7	9886
		1000	3808	5014	5972	6885	7789	8688	1.7	9886
	150mm	250	4056	6023	7494	8906	10288	11641	1.6	11889
		500	4182	5928	7314	8656	9984	11302	1.7	11889
		750	4251	5897	7249	8562	9863	11157	1.7	11889
		1000	4327	5885	7217	8512	9797	11080	1.7	11889

Initial Pt Force $0.1f_{yield}$		Axial Load (excluding PT) 3000kN			Cantilever Length (10000mm)			Grade 300 Dissipaters		
	PT Dia.	Fuse Length (mm)	Yield (kNm)	1%drift (kNm)	2%drift (kNm)	3%drift (kNm)	4%drift (kNm)	6%drift (kNm)	λ	Fuse Area (mm^2)
Diameter (1800mm)	36mm	250	3195	3963	4141	4243	4309	4236	1.3	5760
		500	3240	3887	4000	4058	4090	4004	1.4	5760
		750	3317	3857	3949	3987	3997	3894	1.5	5760
		1000	3352	3842	3923	3950	3946	3833	1.5	5760
	50mm	250	3317	4221	4545	4783	4989	4954	1.4	6157
		500	3366	4142	4393	4590	4757	4708	1.5	6157
		750	3447	4110	4338	4515	4657	4591	1.5	6157
		1000	3487	4093	4310	4475	4606	4526	1.6	6157
	75mm	250	3631	4876	5561	6160	6711	6787	1.5	7187
		500	3689	4790	5387	5929	6453	6503	1.6	7187
		750	3782	4751	5321	5839	6343	6369	1.7	7187
		1000	3828	4732	5286	5792	6285	6298	1.7	7187
	100mm	250	4063	5767	6913	7987	9019	9317	1.6	8629
		500	4135	5665	6719	7724	8702	8977	1.7	8629
		750	4244	5626	6642	7610	8564	8819	1.8	8629
		1000	4301	5597	6598	7550	8490	8731	1.8	8629
	125mm	250	4611	6871	8572	10196	11775	12490	1.7	10482
		500	4703	6750	8343	9886	11412	12088	1.8	10482
		750	4828	6709	8259	9764	11259	11900	1.9	10482
		1000	4887	6674	8212	9699	11174	11789	1.9	10482
	150mm	250	5272	8164	10500	12750	14949	16242	1.7	12747
		500	5390	8025	10229	12383	14518	15761	1.9	12747
		750	5531	7977	10130	12240	14338	15539	1.9	12747
		1000	5590	7943	10079	12166	14240	15417	2.0	12747

Initial Pt Force 0.1f_{yield}		Axial Load (excluding PT) 3000kN			Cantilever Length (10000mm)			Grade 300 Dissipaters		
	PT Dia.	Fuse Length (mm)	Yield (kNm)	1%drift (kNm)	2%drift (kNm)	3%drift (kNm)	4%drift (kNm)	6%drift (kNm)	λ	Fuse Area (mm^2)
Diameter (2000mm)	36mm	250	3503	4292	4413	4437	4431	4340	1.2	5711
		500	3574	4207	4248	4225	4186	4088	1.3	5711
		750	3618	4171	4187	4140	4077	3960	1.4	5711
		1000	3662	4154	4155	4096	4018	3889	1.4	5711
	50mm	250	3627	4546	4804	4957	5081	5097	1.3	6062
		500	3702	4456	4627	4734	4823	4830	1.4	6062
		750	3748	4419	4562	4645	4709	4696	1.4	6062
		1000	3795	4400	4529	4598	4649	4621	1.5	6062
	75mm	250	3942	5192	5786	6283	6718	7030	1.4	6972
		500	4030	5091	5591	6022	6431	6727	1.5	6972
		750	4083	5052	5514	5918	6304	6576	1.6	6972
		1000	4137	5028	5474	5863	6236	6494	1.6	6972
	100mm	250	4379	6070	7105	8048	8938	9706	1.5	8247
		500	4484	5955	6884	7755	8594	9344	1.6	8247
		750	4545	5914	6800	7629	8440	9166	1.7	8247
		1000	4611	5882	6751	7561	8356	9066	1.7	8247
	125mm	250	4931	7164	8729	10198	11609	12967	1.6	9886
		500	5061	7028	8472	9856	11216	12561	1.7	9886
		750	5132	6981	8377	9719	11044	12361	1.8	9886
		1000	5200	6949	8328	9646	10951	12247	1.8	9886
	150mm	250	5596	8455	10626	12694	14699	16644	1.6	11889
		500	5750	8293	10326	12293	14238	16163	1.8	11889
		750	5833	8235	10215	12133	14037	15932	1.8	11889
		1000	5910	8206	10157	12049	13928	15801	1.9	11889

Initial Pt Force $0.1f_{yield}$		Axial Load (excluding PT) 4500kN			Cantilever Length (10000mm)			Grade 300 Dissipaters		
	PT Dia.	Fuse Length (mm)	Yield (kNm)	1%drift (kNm)	2%drift (kNm)	3%drift (kNm)	4%drift (kNm)	6%drift (kNm)	λ	Fuse Area (mm^2)
Diameter (1000mm)	36mm	250	1469	1834	1809	1736	1641	1535	1.0	5628
		500	1536	1811	1764	1669	1556	1434	1.0	5628
		750	1573	1804	1748	1645	1524	1394	1.0	5628
		1000	1598	1801	1740	1632	1507	1373	1.0	5628
	50mm	250	1515	1912	1917	1881	1824	1754	1.0	5903
		500	1583	1887	1871	1812	1735	1650	1.0	5903
		750	1623	1880	1855	1787	1702	1609	1.1	5903
		1000	1649	1877	1849	1774	1684	1587	1.1	5903
	75mm	250	1633	2111	2196	2243	2274	2293	1.0	6614
		500	1706	2083	2146	2170	2178	2180	1.1	6614
		750	1749	2075	2128	2143	2142	2136	1.1	6614
		1000	1778	2069	2121	2126	2123	2112	1.1	6614
	100mm	250	1799	2384	2563	2720	2859	2992	1.1	7611
		500	1877	2349	2509	2639	2753	2866	1.1	7611
		750	1924	2339	2492	2608	2712	2818	1.2	7611
		1000	1957	2332	2486	2591	2693	2792	1.2	7611
	125mm	250	2006	2717	3026	3296	3564	3816	1.1	8892
		500	2094	2682	2960	3196	3436	3674	1.2	8892
		750	2148	2665	2938	3170	3399	3618	1.2	8892
		1000	2183	2655	2926	3150	3369	3587	1.2	8892
	150mm	250	2259	3110	3565	3948	4354	4739	1.1	10458
		500	2356	3072	3481	3844	4207	4578	1.2	10458
		750	2417	3052	3453	3809	4166	4515	1.2	10458
		1000	2457	3034	3439	3792	4135	4492	1.2	10458

Initial Pt Force 0.1F_{yield}		Axial Load (excluding PT) 4500kN			Cantilever Length (10000mm)			Grade 300 Dissipaters		
	PT Dia.	Fuse Length (mm)	Yield (kNm)	1%drift (kNm)	2%drift (kNm)	3%drift (kNm)	4%drift (kNm)	6%drift (kNm)	λ	Fuse Area (mm^2)
Diameter (1200mm)	36mm	250	1879	2342	2369	2334	2275	2201	1.1	5661
		500	1950	2313	2305	2241	2159	2063	1.2	5661
		750	1987	2303	2282	2207	2110	2003	1.2	5661
		1000	2020	2295	2269	2185	2083	1971	1.2	5661
	50mm	250	1941	2454	2535	2555	2553	2536	1.1	5966
		500	2014	2422	2467	2458	2432	2397	1.2	5966
		750	2053	2412	2444	2423	2385	2336	1.2	5966
		1000	2088	2405	2432	2403	2356	2302	1.2	5966
	75mm	250	2098	2739	2950	3107	3242	3363	1.2	6758
		500	2176	2705	2877	3001	3110	3211	1.3	6758
		750	2220	2692	2851	2961	3058	3149	1.3	6758
		1000	2260	2686	2837	2941	3031	3116	1.3	6758
	100mm	250	2316	3128	3503	3836	4146	4442	1.3	7865
		500	2401	3085	3422	3716	3996	4270	1.3	7865
		750	2453	3073	3393	3671	3939	4200	1.4	7865
		1000	2498	3067	3379	3649	3908	4163	1.4	7865
	125mm	250	2592	3609	4177	4711	5225	5724	1.3	9289
		500	2686	3560	4086	4574	5055	5527	1.4	9289
		750	2748	3544	4049	4523	4989	5449	1.4	9289
		1000	2799	3537	4034	4503	4955	5406	1.4	9289
	150mm	250	2928	4184	4957	5711	6448	7168	1.3	11030
		500	3031	4119	4847	5553	6251	6945	1.4	11030
		750	3105	4101	4818	5495	6175	6855	1.4	11030
		1000	3160	4088	4795	5467	6144	6806	1.5	11030

Initial Pt Force $0.1f_{yield}$		Axial Load (excluding PT) 4500kN			Cantilever Length (10000mm)			Grade 300 Dissipaters		
	PT Dia.	Fuse Length (mm)	Yield (kNm)	1%drift (kNm)	2%drift (kNm)	3%drift (kNm)	4%drift (kNm)	6%drift (kNm)	λ	Fuse Area (mm^2)
Diameter (1500mm)	36mm	250	2526	3142	3242	3270	3256	3218	1.2	5711
		500	2602	3092	3141	3126	3092	3033	1.3	5711
		750	2645	3071	3101	3072	3026	2955	1.4	5711
		1000	2682	3055	3080	3044	2991	2913	1.4	5711
	50mm	250	2615	3318	3512	3639	3724	3765	1.3	6062
		500	2695	3267	3408	3487	3547	3576	1.4	6062
		750	2739	3245	3365	3429	3476	3493	1.4	6062
		1000	2780	3228	3343	3398	3438	3448	1.4	6062
	75mm	250	2846	3768	4191	4551	4882	5193	1.4	6972
		500	2935	3710	4075	4390	4686	4966	1.5	6972
		750	2983	3688	4034	4324	4599	4867	1.5	6972
		1000	3029	3669	4006	4287	4554	4813	1.5	6972
	100mm	250	3165	4377	5100	5760	6391	6999	1.5	8247
		500	3269	4313	4967	5575	6168	6751	1.6	8247
		750	3317	4286	4919	5505	6078	6644	1.6	8247
		1000	3374	4268	4895	5468	6029	6585	1.6	8247
	125mm	250	3569	5135	6210	7224	8209	9168	1.5	9886
		500	3685	5055	6055	7009	7949	8880	1.6	9886
		750	3742	5026	6000	6927	7844	8755	1.7	9886
		1000	3808	5014	5972	6885	7789	8688	1.7	9886
	150mm	250	4056	6023	7494	8906	10288	11641	1.6	11889
		500	4182	5928	7314	8656	9984	11302	1.7	11889
		750	4251	5897	7249	8562	9863	11157	1.7	11889
		1000	4327	5885	7217	8512	9797	11080	1.7	11889

Initial Pt Force 0.1f_{yield}		Axial Load (excluding PT) 4500kN			Cantilever Length (10000mm)			Grade 300 Dissipaters		
	PT Dia.	Fuse Length (mm)	Yield (kNm)	1%drift (kNm)	2%drift (kNm)	3%drift (kNm)	4%drift (kNm)	6%drift (kNm)	λ	Fuse Area (mm^2)
Diameter (1800mm)	36mm	250	3195	3963	4141	4243	4309	4236	1.3	5760
		500	3240	3887	4000	4058	4090	4004	1.4	5760
		750	3317	3857	3949	3987	3997	3894	1.5	5760
		1000	3352	3842	3923	3950	3946	3833	1.5	5760
	50mm	250	3317	4221	4545	4783	4989	4954	1.4	6157
		500	3366	4142	4393	4590	4757	4708	1.5	6157
		750	3447	4110	4338	4515	4657	4591	1.5	6157
		1000	3487	4093	4310	4475	4606	4526	1.6	6157
	75mm	250	3631	4876	5561	6160	6711	6787	1.5	7187
		500	3689	4790	5387	5929	6453	6503	1.6	7187
		750	3782	4751	5321	5839	6343	6369	1.7	7187
		1000	3828	4732	5286	5792	6285	6298	1.7	7187
	100mm	250	4063	5767	6913	7987	9019	9317	1.6	8629
		500	4135	5665	6719	7724	8702	8977	1.7	8629
		750	4244	5626	6642	7610	8564	8819	1.8	8629
		1000	4301	5597	6598	7550	8490	8731	1.8	8629
	125mm	250	4611	6871	8572	10196	11775	12490	1.7	10482
		500	4703	6750	8343	9886	11412	12088	1.8	10482
		750	4828	6709	8259	9764	11259	11900	1.9	10482
		1000	4887	6674	8212	9699	11174	11789	1.9	10482
	150mm	250	5272	8164	10500	12750	14949	16242	1.7	12747
		500	5390	8025	10229	12383	14518	15761	1.9	12747
		750	5531	7977	10130	12240	14338	15539	1.9	12747
		1000	5590	7943	10079	12166	14240	15417	2.0	12747

Initial Pt Force $0.1f_{yield}$		Axial Load (excluding PT) 4500kN			Cantilever Length (10000mm)			Grade 300 Dissipaters		
	PT Dia.	Fuse Length (mm)	Yield (kNm)	1%drift (kNm)	2%drift (kNm)	3%drift (kNm)	4%drift (kNm)	6%drift (kNm)	λ	Fuse Area (mm^2)
Diameter (2000mm)	36mm	250	4915	6156	6289	6274	6163	5991	1.2	8378
		500	5059	6035	6059	5956	5812	5624	1.3	8378
		750	5136	5994	5967	5830	5658	5441	1.3	8378
		1000	5195	5963	5918	5763	5574	5338	1.3	8378
	50mm	250	5031	6395	6658	6778	6800	6732	1.2	8728
		500	5179	6272	6420	6449	6433	6351	1.3	8728
		750	5258	6229	6327	6316	6272	6164	1.4	8728
		1000	5320	6198	6276	6247	6185	6059	1.4	8728
	75mm	250	5330	7012	7597	8043	8416	8653	1.3	9639
		500	5493	6877	7338	7696	8006	8232	1.4	9639
		750	5573	6831	7243	7551	7826	8025	1.5	9639
		1000	5640	6796	7187	7472	7728	7909	1.5	9639
	100mm	250	5749	7853	8869	9746	10548	11287	1.4	10914
		500	5925	7704	8583	9363	10108	10824	1.5	10914
		750	6012	7649	8477	9209	9915	10588	1.6	10914
		1000	6087	7617	8422	9126	9801	10454	1.6	10914
	125mm	250	6277	8907	10444	11841	13160	14412	1.5	12552
		500	6475	8736	10123	11411	12664	13896	1.6	12552
		750	6569	8674	10004	11239	12449	13644	1.6	12552
		1000	6653	8641	9943	11148	12332	13503	1.7	12552
	150mm	250	6920	10152	12290	14284	16194	18030	1.5	14555
		500	7130	9960	11927	13796	15631	17442	1.6	14555
		750	7240	9888	11794	13604	15389	17159	1.7	14555
		1000	7333	9859	11725	13501	15257	17001	1.7	14555

Initial Pt Force $0.1f_{yield}$		Axial Load (excluding PT) 6000kN			Cantilever Length (10000mm)			Grade 300 Dissipaters		
	PT Dia.	Fuse Length (mm)	Yield (kNm)	1%drift (kNm)	2%drift (kNm)	3%drift (kNm)	4%drift (kNm)	6%drift (kNm)	λ	Fuse Area (mm^2)
Diameter (1000mm)	36mm	250	2422	3139	3059	2853	2624	2361	1.0	9592
		500	2545	3108	2987	2747	2484	2200	1.0	9592
		750	2634	3087	2960	2715	2436	2135	1.1	9592
		1000	2700	3072	2947	2694	2406	2102	1.1	9592
	50mm	250	2463	3199	3154	2974	2773	2550	1.0	9832
		500	2584	3168	3074	2865	2637	2380	1.1	9832
		750	2673	3149	3049	2829	2582	2317	1.1	9832
		1000	2741	3134	3035	2812	2558	2286	1.1	9832
	75mm	250	2561	3362	3389	3275	3154	3013	1.0	10454
		500	2687	3326	3306	3166	3008	2836	1.1	10454
		750	2780	3304	3274	3128	2959	2774	1.1	10454
		1000	2848	3289	3263	3113	2926	2733	1.1	10454
	100mm	250	2700	3579	3704	3688	3658	3617	1.1	11326
		500	2826	3543	3614	3575	3503	3442	1.1	11326
		750	2925	3523	3582	3528	3449	3366	1.1	11326
		1000	2997	3507	3567	3508	3423	3334	1.1	11326
	125mm	250	2877	3856	4092	4203	4274	4348	1.1	12447
		500	3007	3811	4001	4068	4108	4152	1.1	12447
		750	3113	3797	3962	4026	4059	4087	1.2	12447
		1000	3186	3776	3945	3997	4024	4038	1.2	12447
	150mm	250	3088	4184	4538	4806	4993	5185	1.1	13817
		500	3228	4132	4447	4653	4815	4967	1.2	13817
		750	3340	4115	4407	4589	4748	4897	1.2	13817
		1000	3418	4099	4385	4561	4722	4857	1.2	13817

Initial Pt Force 0.1F_{yield}		Axial Load (excluding PT) 6000kN			Cantilever Length (10000mm)			Grade 300 Dissipaters		
	PT Dia.	Fuse Length (mm)	Yield (kNm)	1%drift (kNm)	2%drift (kNm)	3%drift (kNm)	4%drift (kNm)	6%drift (kNm)	λ	Fuse Area (mm^2)
Diameter (1200mm)	36mm	250	3102	4065	4043	3909	3720	3499	1.2	9620
		500	3267	4013	3941	3761	3532	3281	1.2	9620
		750	3373	3994	3909	3706	3460	3192	1.3	9620
		1000	3442	3987	3889	3678	3422	3145	1.3	9620
	50mm	250	3153	4157	4183	4095	3960	3793	1.2	9887
		500	3321	4104	4080	3946	3769	3571	1.3	9887
		750	3428	4085	4042	3890	3696	3481	1.3	9887
		1000	3499	4077	4027	3862	3657	3433	1.3	9887
	75mm	250	3284	4397	4531	4569	4564	4527	1.2	10579
		500	3455	4340	4426	4414	4364	4294	1.3	10579
		750	3569	4319	4390	4353	4287	4200	1.3	10579
		1000	3641	4308	4371	4326	4246	4151	1.3	10579
	100mm	250	3468	4721	5009	5206	5369	5497	1.3	11549
		500	3647	4663	4896	5039	5148	5249	1.3	11549
		750	3765	4640	4857	4973	5069	5150	1.4	11549
		1000	3845	4625	4834	4941	5031	5097	1.4	11549
	125mm	250	3702	5133	5604	5977	6329	6660	1.3	12795
		500	3889	5068	5479	5793	6103	6390	1.4	12795
		750	4010	5043	5431	5728	6013	6287	1.4	12795
		1000	4098	5020	5415	5706	5969	6238	1.4	12795
	150mm	250	3989	5615	6306	6876	7437	7998	1.3	14318
		500	4181	5549	6159	6677	7199	7696	1.4	14318
		750	4307	5521	6108	6617	7094	7577	1.4	14318
		1000	4402	5494	6086	6574	7054	7518	1.4	14318

Initial Pt Force 0.1f_{yield}		Axial Load (excluding PT) 6000kN			Cantilever Length (10000mm)			Grade 300 Dissipaters		
	PT Dia.	Fuse Length (mm)	Yield (kNm)	1%drift (kNm)	2%drift (kNm)	3%drift (kNm)	4%drift (kNm)	6%drift (kNm)	λ	Fuse Area (mm^2)
Diameter (1500mm)	36mm	250	4246	5491	5591	5542	5429	5273	1.3	9664
		500	4417	5410	5434	5320	5157	4970	1.4	9664
		750	4528	5384	5380	5235	5048	4831	1.4	9664
		1000	4610	5373	5350	5192	4985	4754	1.5	9664
	50mm	250	4319	5640	5825	5863	5840	5775	1.3	9971
		500	4493	5559	5664	5636	5563	5466	1.4	9971
		750	4610	5533	5607	5550	5451	5331	1.5	9971
		1000	4691	5518	5578	5505	5391	5250	1.5	9971
	75mm	250	4507	6020	6420	6675	6874	7034	1.4	10767
		500	4692	5936	6247	6435	6581	6707	1.5	10767
		750	4814	5909	6187	6343	6463	6565	1.5	10767
		1000	4900	5894	6156	6296	6401	6488	1.6	10767
	100mm	250	4773	6545	7219	7764	8253	8704	1.5	11883
		500	4965	6453	7035	7504	7938	8351	1.6	11883
		750	5097	6425	6969	7407	7811	8200	1.6	11883
		1000	5190	6409	6936	7356	7743	8117	1.6	11883
	125mm	250	5109	7207	8207	9095	9930	10726	1.5	13317
		500	5315	7102	8004	8812	9584	10340	1.6	13317
		750	5459	7068	7935	8705	9446	10175	1.7	13317
		1000	5557	7057	7895	8649	9373	10085	1.7	13317
	150mm	250	5516	7989	9365	10637	11859	13043	1.5	15069
		500	5737	7877	9141	10324	11479	12616	1.7	15069
		750	5895	7833	9065	10207	11328	12435	1.7	15069
		1000	6003	7816	9019	10145	11248	12337	1.7	15069

Initial Pt Force $0.1f_{yield}$		Axial Load (excluding PT) 6000kN			Cantilever Length (10000mm)			Grade 300 Dissipaters		
	PT Dia.	Fuse Length (mm)	Yield (kNm)	1%drift (kNm)	2%drift (kNm)	3%drift (kNm)	4%drift (kNm)	6%drift (kNm)	λ	Fuse Area (mm^2)
Diameter (1800mm)	36mm	250	5417	6970	7183	7234	7190	6977	1.4	9707
		500	5581	6857	6961	6924	6826	6597	1.5	9707
		750	5751	6815	6879	6798	6673	6420	1.6	9707
		1000	5813	6787	6830	6732	6591	6323	1.6	9707
	50mm	250	5517	7193	7538	7724	7830	7660	1.4	10054
		500	5686	7077	7309	7411	7449	7268	1.6	10054
		750	5857	7032	7226	7280	7289	7085	1.6	10054
		1000	5925	7004	7176	7210	7204	6983	1.6	10054
	75mm	250	5781	7762	8439	8964	9416	9436	1.5	10955
		500	5954	7637	8194	8629	9022	8996	1.6	10955
		750	6138	7590	8105	8499	8846	8792	1.7	10955
		1000	6208	7563	8058	8422	8750	8680	1.7	10955
	100mm	250	6147	8540	9659	10630	11531	11834	1.6	12217
		500	6323	8403	9392	10266	11101	11363	1.7	12217
		750	6525	8350	9295	10124	10920	11144	1.8	12217
		1000	6604	8324	9245	10049	10823	11014	1.8	12217
	125mm	250	6615	9513	11166	12675	14113	14844	1.7	13838
		500	6796	9357	10871	12273	13639	14318	1.8	13838
		750	7020	9304	10764	12116	13440	14076	1.9	13838
		1000	7103	9277	10709	12033	13332	13941	1.9	13838
	150mm	250	7179	10670	12930	15053	17102	18434	1.7	15821
		500	7366	10498	12601	14604	16574	17842	1.9	15821
		750	7617	10435	12482	14430	16351	17569	1.9	15821
		1000	7707	10408	12421	14339	16233	17420	2.0	15821

Initial Pt Force 0.1Fyield		Axial Load (excluding PT) 6000kN			Cantilever Length (10000mm)			Grade 300 Dissipaters		
	PT Dia.	Fuse Length (mm)	Yield (kNm)	1%drift (kNm)	2%drift (kNm)	3%drift (kNm)	4%drift (kNm)	6%drift (kNm)	λ	Fuse Area (mm^2)
Diameter (2000mm)	36mm	250	6251	7967	8117	8064	7906	7619	1.1	11044
		500	6458	7815	7820	7663	7430	7140	1.2	11044
		750	6564	7757	7713	7497	7223	6903	1.3	11044
		1000	6647	7725	7652	7407	7110	6771	1.3	11044
	50mm	250	6365	8198	8474	8546	8517	8364	1.2	11395
		500	6572	8040	8170	8135	8036	7865	1.3	11395
		750	6684	7981	8056	7970	7821	7620	1.3	11395
		1000	6765	7949	7998	7875	7704	7482	1.3	11395
	75mm	250	6654	8789	9377	9770	10063	10263	1.2	12306
		500	6868	8622	9054	9334	9560	9731	1.3	12306
		750	6989	8556	8935	9160	9339	9461	1.4	12306
		1000	7075	8523	8873	9067	9209	9310	1.4	12306
	100mm	250	7053	9602	10608	11426	12143	12778	1.3	13580
		500	7279	9416	10259	10954	11599	12213	1.4	13580
		750	7412	9345	10129	10767	11362	11935	1.5	13580
		1000	7505	9315	10066	10667	11232	11779	1.5	13580
	125mm	250	7565	10613	12138	13471	14702	15846	1.4	15219
		500	7802	10409	11755	12954	14104	15224	1.5	15219
		750	7949	10337	11614	12748	13845	14920	1.5	15219
		1000	8051	10300	11541	12640	13703	14751	1.6	15219
	150mm	250	8185	11821	13938	15862	17680	19410	1.4	17222
		500	8437	11594	13515	15289	17017	18715	1.5	17222
		750	8596	11520	13359	15064	16732	18382	1.6	17222
		1000	8710	11482	13278	14945	16578	18194	1.6	17222

Initial Pt Force 0.1Fyield		Axial Load (excluding PT) 6000kN			Cantilever Length (10000mm)			Grade 300 Dissipaters		
	PT Dia.	Fuse Length (mm)	Yield (kNm)	1%drift (kNm)	2%drift (kNm)	3%drift (kNm)	4%drift (kNm)	6%drift (kNm)	λ	Fuse Area (mm^2)
Diameter (2200mm)	36mm	250	7006	9012	9251	9269	9132	8844	1.2	11069
		500	7274	8826	8899	8789	8613	8323	1.3	11069
		750	7416	8763	8760	8594	8376	8044	1.3	11069
		1000	7529	8723	8687	8490	8245	7886	1.4	11069
	50mm	250	7137	9295	9689	9867	9895	9684	1.2	11443
		500	7411	9103	9325	9377	9356	9147	1.3	11443
		750	7555	9038	9187	9175	9112	8862	1.4	11443
		1000	7671	8995	9109	9067	8977	8702	1.4	11443
	75mm	250	7473	10017	10806	11383	11838	11858	1.3	12413
		500	7762	9813	10421	10870	11247	11278	1.4	12413
		750	7912	9742	10272	10652	10979	10973	1.5	12413
		1000	8036	9700	10192	10534	10832	10799	1.5	12413
	100mm	250	7939	11011	12331	13435	14420	14877	1.4	13771
		500	8242	10786	11908	12877	13795	14232	1.5	13771
		750	8410	10707	11747	12649	13508	13888	1.5	13771
		1000	8546	10658	11665	12525	13341	13693	1.6	13771
	125mm	250	8538	12255	14220	15973	17601	18647	1.4	15517
		500	8857	12009	13754	15359	16909	17932	1.6	15517
		750	9044	11916	13580	15108	16597	17561	1.6	15517
		1000	9189	11866	13490	14974	16425	17350	1.7	15517
	150mm	250	9266	13742	16451	18949	21314	23157	1.5	17651
		500	9596	13458	15932	18264	20542	22351	1.6	17651
		750	9808	13354	15738	17986	20197	21937	1.7	17651
		1000	9967	13304	15639	17838	20005	21701	1.7	17651

Initial Pt Force $0.1f_{yield}$		Axial Load (excluding PT) 7500kN			Cantilever Length (10000mm)			Grade 300 Dissipaters		
	PT Dia.	Fuse Length (mm)	Yield (kNm)	1%drift (kNm)	2%drift (kNm)	3%drift (kNm)	4%drift (kNm)	6%drift (kNm)	λ	Fuse Area (mm^2)
Diameter (1000mm)	36mm	250	2703	3552	3450	3169	2850	2503	1.1	10221
		500	2852	3518	3372	3061	2706	2333	1.2	10221
		750	2964	3503	3341	3021	2657	2266	1.2	10221
		1000	3044	3486	3327	3002	2629	2232	1.2	10221
	50mm	250	2737	3606	3530	3276	2991	2673	1.1	10427
		500	2884	3570	3453	3169	2846	2505	1.2	10427
		750	3001	3556	3421	3126	2789	2434	1.2	10427
		1000	3078	3539	3408	3107	2766	2402	1.2	10427
	75mm	250	2823	3745	3736	3559	3335	3100	1.2	10961
		500	2975	3709	3656	3444	3185	2921	1.2	10961
		750	3092	3691	3622	3402	3131	2858	1.2	10961
		1000	3172	3678	3607	3377	3105	2816	1.2	10961
	100mm	250	2945	3940	4014	3945	3796	3663	1.2	11708
		500	3100	3895	3932	3811	3647	3476	1.2	11708
		750	3217	3882	3901	3764	3591	3412	1.3	11708
		1000	3305	3869	3880	3741	3562	3367	1.3	11708
	125mm	250	3098	4180	4357	4404	4378	4342	1.2	12669
		500	3258	4132	4277	4272	4213	4146	1.3	12669
		750	3381	4116	4241	4214	4151	4074	1.3	12669
		1000	3470	4104	4218	4193	4121	4047	1.3	12669
	150mm	250	3288	4466	4762	4941	5058	5133	1.2	13843
		500	3453	4416	4673	4795	4870	4924	1.3	13843
		750	3579	4400	4639	4741	4799	4857	1.3	13843
		1000	3676	4390	4621	4713	4762	4817	1.3	13843

Initial Pt Force 0.1f_{yield}		Axial Load (excluding PT) 7500kN			Cantilever Length (10000mm)			Grade 300 Dissipaters		
	PT Dia.	Fuse Length (mm)	Yield (kNm)	1%drift (kNm)	2%drift (kNm)	3%drift (kNm)	4%drift (kNm)	6%drift (kNm)	λ	Fuse Area (mm^2)
Diameter (1200mm)	36mm	250	3484	4647	4591	4391	4126	3819	1.3	10246
		500	3682	4599	4490	4236	3929	3590	1.4	10246
		750	3820	4575	4452	4178	3853	3497	1.4	10246
		1000	3921	4562	4434	4152	3814	3448	1.5	10246
	50mm	250	3529	4732	4719	4563	4348	4093	1.3	10475
		500	3729	4679	4610	4408	4149	3861	1.4	10475
		750	3868	4659	4574	4347	4072	3768	1.5	10475
		1000	3966	4645	4556	4321	4032	3718	1.5	10475
	75mm	250	3645	4943	5037	5002	4905	4781	1.4	11068
		500	3848	4887	4929	4838	4700	4541	1.5	11068
		750	3988	4865	4892	4778	4626	4444	1.5	11068
		1000	4094	4848	4871	4743	4578	4393	1.5	11068
	100mm	250	3804	5231	5475	5587	5651	5694	1.4	11899
		500	4012	5177	5356	5415	5441	5440	1.5	11899
		750	4158	5148	5316	5353	5352	5339	1.5	11899
		1000	4269	5131	5297	5323	5315	5285	1.6	11899
	125mm	250	4013	5591	6023	6303	6558	6786	1.5	12967
		500	4219	5533	5890	6117	6326	6523	1.5	12967
		750	4378	5507	5848	6061	6248	6413	1.6	12967
		1000	4491	5484	5821	6022	6193	6358	1.6	12967
	150mm	250	4265	6024	6668	7144	7599	8055	1.5	14273
		500	4478	5961	6519	6951	7350	7756	1.6	14273
		750	4638	5933	6465	6883	7254	7639	1.6	14273
		1000	4764	5902	6441	6848	7211	7581	1.6	14273

Initial Pt Force 0.1f_{yield}		Axial Load (excluding PT) 7500kN			Cantilever Length (10000mm)			Grade 300 Dissipaters		
	PT Dia.	Fuse Length (mm)	Yield (kNm)	1%drift (kNm)	2%drift (kNm)	3%drift (kNm)	4%drift (kNm)	6%drift (kNm)	λ	Fuse Area (mm^2)
Diameter (1500mm)	36mm	250	4789	6324	6400	6289	6101	5861	1.5	10283
		500	5029	6245	6237	6057	5815	5542	1.6	10283
		750	5186	6217	6181	5969	5701	5404	1.7	10283
		1000	5290	6203	6152	5924	5640	5327	1.7	10283
	50mm	250	4854	6457	6615	6589	6487	6337	1.5	10546
		500	5093	6377	6451	6352	6198	6012	1.6	10546
		750	5253	6349	6392	6263	6081	5872	1.7	10546
		1000	5359	6335	6362	6217	6019	5796	1.7	10546
	75mm	250	5018	6801	7163	7348	7463	7533	1.6	11229
		500	5264	6718	6990	7100	7160	7193	1.7	11229
		750	5435	6689	6927	7007	7039	7048	1.7	11229
		1000	5543	6675	6893	6958	6975	6969	1.8	11229
	100mm	250	5248	7278	7903	8368	8768	9125	1.6	12185
		500	5505	7186	7713	8105	8447	8765	1.8	12185
		750	5681	7155	7650	8006	8318	8610	1.8	12185
		1000	5801	7140	7616	7954	8250	8527	1.8	12185
	125mm	250	5544	7879	8817	9619	10359	11056	1.7	13414
		500	5810	7774	8612	9336	10013	10668	1.8	13414
		750	5996	7742	8548	9230	9876	10504	1.9	13414
		1000	6127	7727	8512	9175	9803	10414	1.9	13414
	150mm	250	5903	8594	9884	11075	12194	13274	1.7	14917
		500	6184	8474	9667	10757	11817	12853	1.9	14917
		750	6381	8440	9596	10640	11668	12676	1.9	14917
		1000	6521	8416	9560	10582	11590	12580	1.9	14917

Initial Pt Force 0.1F_{yield}		Axial Load (excluding PT) 7500kN			Cantilever Length (10000mm)			Grade 300 Dissipaters		
	PT Dia.	Fuse Length (mm)	Yield (kNm)	1%drift (kNm)	2%drift (kNm)	3%drift (kNm)	4%drift (kNm)	6%drift (kNm)	λ	Fuse Area (mm^2)
Diameter (1800mm)	36mm	250	6172	8065	8256	8247	8145	7858	1.6	10320
		500	6381	7945	8024	7927	7760	7450	1.8	10320
		750	6612	7899	7939	7801	7593	7260	1.8	10320
		1000	6702	7876	7895	7728	7504	7155	1.8	10320
	50mm	250	6260	8266	8586	8709	8742	8525	1.6	10618
		500	6470	8145	8349	8382	8356	8101	1.8	10618
		750	6707	8099	8262	8254	8183	7904	1.8	10618
		1000	6799	8076	8220	8181	8090	7796	1.9	10618
	75mm	250	6490	8783	9425	9879	10247	10216	1.7	11390
		500	6704	8656	9175	9535	9842	9774	1.9	11390
		750	6954	8604	9084	9400	9670	9558	1.9	11390
		1000	7051	8581	9039	9330	9571	9439	2.0	11390
	100mm	250	6814	9494	10564	11457	12267	12526	1.8	12471
		500	7030	9351	10295	11087	11831	12048	1.9	12471
		750	7298	9304	10197	10944	11648	11826	2.0	12471
		1000	7396	9275	10147	10868	11550	11704	2.0	12471
	125mm	250	7216	10383	11974	13397	14739	15433	1.9	13862
		500	7448	10227	11682	12996	14264	14909	2.0	13862
		750	7733	10173	11576	12840	14067	14667	2.1	13862
		1000	7840	10149	11522	12758	13960	14533	2.1	13862
	150mm	250	7702	11439	13629	15656	17602	18902	1.9	15561
		500	7950	11268	13308	15215	17082	18322	2.1	15561
		750	8261	11213	13192	15046	16865	18056	2.2	15561
		1000	8377	11189	13131	14956	16751	17909	2.2	15561

Initial Pt Force 0.1f_{yield}		Axial Load (excluding PT) 7500kN			Cantilever Length (10000mm)			Grade 300 Dissipaters		
	PT Dia.	Fuse Length (mm)	Yield (kNm)	1%drift (kNm)	2%drift (kNm)	3%drift (kNm)	4%drift (kNm)	6%drift (kNm)	λ	Fuse Area (mm^2)
Diameter (2000mm)	36mm	250	7525	9738	9912	9818	9592	9256	1.1	13711
		500	7780	9550	9552	9329	9025	8652	1.2	13711
		750	7938	9478	9419	9133	8772	8353	1.3	13711
		1000	8046	9442	9351	9030	8630	8186	1.3	13711
	50mm	250	7633	9958	10253	10286	10185	9978	1.1	14062
		500	7890	9763	9888	9787	9607	9370	1.2	14062
		750	8052	9696	9753	9587	9354	9062	1.3	14062
		1000	8162	9660	9681	9482	9209	8889	1.3	14062
	75mm	250	7914	10531	11131	11474	11690	11805	1.2	14972
		500	8176	10319	10744	10951	11084	11174	1.3	14972
		750	8347	10252	10603	10742	10819	10863	1.3	14972
		1000	8459	10215	10528	10632	10676	10684	1.4	14972
	100mm	250	8303	11310	12324	13088	13723	14259	1.3	16247
		500	8568	11086	11913	12529	13077	13584	1.4	16247
		750	8759	11013	11761	12308	12796	13254	1.4	16247
		1000	8879	10975	11683	12190	12644	13070	1.4	16247
	125mm	250	8805	12288	13813	15086	16230	17273	1.3	17886
		500	9074	12059	13370	14484	15533	16543	1.4	17886
		750	9275	11976	13206	14245	15231	16188	1.5	17886
		1000	9408	11939	13122	14118	15066	15990	1.5	17886
	150mm	250	9399	13469	15576	17430	19158	20781	1.4	19889
		500	9683	13214	15093	16773	18398	19982	1.5	19889
		750	9907	13130	14909	16515	18069	19598	1.5	19889
		1000	10056	13083	14818	16377	17891	19383	1.5	19889

Initial Pt Force 0.1Fyield		Axial Load (excluding PT) 7500kN			Cantilever Length (10000mm)			Grade 300 Dissipaters		
	PT Dia.	Fuse Length (mm)	Yield (kNm)	1%drift (kNm)	2%drift (kNm)	3%drift (kNm)	4%drift (kNm)	6%drift (kNm)	λ	Fuse Area (mm^2)
Diameter (2200mm)	36mm	250	8448	11028	11306	11294	11121	10715	1.2	13736
		500	8779	10805	10876	10721	10464	10075	1.3	13736
		750	8979	10723	10714	10480	10166	9737	1.3	13736
		1000	9121	10674	10627	10349	10003	9545	1.3	13736
	50mm	250	8576	11300	11729	11874	11863	11559	1.2	14109
		500	8906	11072	11289	11289	11193	10898	1.3	14109
		750	9115	10988	11126	11047	10886	10550	1.3	14109
		1000	9260	10938	11041	10912	10718	10352	1.4	14109
	75mm	250	8901	12002	12817	13351	13735	13735	1.2	15080
		500	9244	11757	12353	12735	13042	13017	1.4	15080
		750	9460	11665	12177	12484	12719	12642	1.4	15080
		1000	9612	11615	12087	12347	12538	12429	1.4	15080
	100mm	250	9356	12965	14300	15357	16266	16692	1.3	16438
		500	9711	12702	13799	14697	15523	15931	1.4	16438
		750	9946	12600	13616	14430	15186	15535	1.5	16438
		1000	10106	12549	13521	14287	15002	15300	1.5	16438
	125mm	250	9937	14173	16145	17846	19392	20425	1.4	18184
		500	10306	13887	15610	17130	18585	19592	1.5	18184
		750	10557	13781	15404	16839	18222	19159	1.6	18184
		1000	10735	13722	15300	16685	18023	18915	1.6	18184
	150mm	250	10642	15620	18329	20770	23051	24899	1.4	20318
		500	11031	15303	17738	19986	22165	23973	1.6	20318
		750	11305	15186	17519	19670	21768	23500	1.6	20318
		1000	11495	15126	17404	19500	21551	23231	1.6	20318

Initial Pt Force $0.1f_{yield}$		Axial Load (excluding PT) 8500kN			Cantilever Length (10000mm)			Grade 300 Dissipaters		
	PT Dia.	Fuse Length (mm)	Yield (kNm)	1%drift (kNm)	2%drift (kNm)	3%drift (kNm)	4%drift (kNm)	6%drift (kNm)	λ	Fuse Area (mm^2)
Diameter (1000mm)	36mm	250	2990	3947	3834	3522	3148	2752	1.1	11555
		500	3153	3903	3749	3400	2988	2563	1.2	11555
		750	3274	3886	3717	3353	2934	2488	1.2	11555
		1000	3365	3875	3702	3332	2906	2449	1.2	11555
	50mm	250	3022	3998	3912	3629	3280	2921	1.1	11760
		500	3183	3952	3829	3500	3123	2723	1.2	11760
		750	3309	3936	3793	3458	3067	2653	1.2	11760
		1000	3398	3929	3778	3432	3033	2615	1.2	11760
	75mm	250	3109	4133	4106	3905	3614	3329	1.1	12294
		500	3275	4084	4023	3766	3454	3129	1.2	12294
		750	3400	4068	3989	3717	3400	3055	1.2	12294
		1000	3492	4062	3972	3695	3366	3019	1.2	12294
	100mm	250	3230	4316	4375	4271	4077	3874	1.1	13041
		500	3398	4267	4285	4126	3904	3668	1.2	13041
		750	3523	4252	4258	4075	3843	3591	1.2	13041
		1000	3619	4242	4235	4045	3811	3560	1.2	13041
	125mm	250	3380	4543	4707	4714	4650	4531	1.2	14002
		500	3552	4497	4620	4570	4458	4326	1.2	14002
		750	3683	4482	4585	4511	4390	4247	1.2	14002
		1000	3784	4479	4567	4479	4353	4217	1.2	14002
	150mm	250	3569	4824	5101	5234	5305	5328	1.2	15177
		500	3746	4773	5001	5076	5112	5092	1.2	15177
		750	3879	4760	4972	5028	5022	5003	1.2	15177
		1000	3988	4752	4954	4992	4981	4960	1.3	15177

Initial Pt Force 0.1f_{yield}		Axial Load (excluding PT) 8500kN			Cantilever Length (10000mm)			Grade 300 Dissipaters		
	PT Dia.	Fuse Length (mm)	Yield (kNm)	1%drift (kNm)	2%drift (kNm)	3%drift (kNm)	4%drift (kNm)	6%drift (kNm)	λ	Fuse Area (mm^2)
Diameter (1200mm)	36mm	250	3853	5178	5119	4887	4577	4227	1.3	11579
		500	4066	5125	5005	4714	4360	3971	1.4	11579
		750	4224	5103	4962	4653	4276	3867	1.4	11579
		1000	4341	5080	4941	4619	4232	3813	1.4	11579
	50mm	250	3898	5258	5242	5055	4794	4494	1.3	11808
		500	4113	5204	5123	4877	4575	4234	1.4	11808
		750	4269	5181	5084	4815	4486	4130	1.4	11808
		1000	4387	5157	5062	4783	4442	4074	1.5	11808
	75mm	250	4014	5463	5558	5473	5336	5163	1.4	12401
		500	4228	5407	5429	5291	5108	4896	1.4	12401
		750	4388	5383	5384	5226	5019	4789	1.5	12401
		1000	4510	5356	5368	5193	4974	4731	1.5	12401
	100mm	250	4172	5744	5988	6041	6064	6049	1.4	13232
		500	4391	5680	5846	5858	5832	5771	1.5	13232
		750	4557	5655	5800	5792	5734	5657	1.5	13232
		1000	4683	5632	5776	5752	5692	5599	1.5	13232
	125mm	250	4372	6095	6522	6741	6958	7127	1.4	14300
		500	4594	6032	6369	6546	6697	6830	1.5	14300
		750	4769	6006	6320	6475	6599	6716	1.5	14300
		1000	4900	5977	6295	6439	6549	6662	1.5	14300
	150mm	250	4621	6517	7140	7574	7968	8369	1.4	15606
		500	4850	6443	6982	7367	7696	8044	1.5	15606
		750	5030	6415	6924	7288	7610	7916	1.5	15606
		1000	5162	6385	6893	7239	7549	7852	1.6	15606

Initial Pt Force 0.1Fyield		Axial Load (excluding PT) 8500kN			Cantilever Length (10000mm)			Grade 300 Dissipaters		
	PT Dia.	Fuse Length (mm)	Yield (kNm)	1%drift (kNm)	2%drift (kNm)	3%drift (kNm)	4%drift (kNm)	6%drift (kNm)	λ	Fuse Area (mm^2)
Diameter (1500mm)	36mm	250	5290	7063	7147	7016	6792	6509	1.5	11617
		500	5566	6975	6970	6757	6473	6151	1.6	11617
		750	5751	6946	6903	6658	6345	5997	1.6	11617
		1000	5879	6931	6869	6608	6277	5913	1.7	11617
	50mm	250	5355	7194	7355	7308	7171	6976	1.5	11880
		500	5633	7105	7172	7044	6847	6612	1.6	11880
		750	5821	7075	7108	6945	6717	6456	1.7	11880
		1000	5947	7061	7071	6893	6648	6371	1.7	11880
	75mm	250	5517	7532	7889	8049	8126	8149	1.6	12562
		500	5799	7439	7699	7775	7789	7772	1.7	12562
		750	5996	7409	7626	7672	7655	7610	1.7	12562
		1000	6129	7394	7590	7617	7583	7522	1.7	12562
	100mm	250	5742	8003	8607	9048	9406	9715	1.6	13518
		500	6034	7894	8410	8759	9052	9317	1.7	13518
		750	6239	7862	8333	8650	8911	9146	1.8	13518
		1000	6381	7847	8298	8593	8836	9055	1.8	13518
	125mm	250	6033	8588	9509	10276	10971	11619	1.7	14748
		500	6338	8470	9285	9967	10593	11195	1.8	14748
		750	6547	8437	9215	9851	10443	11014	1.8	14748
		1000	6700	8414	9177	9791	10363	10916	1.9	14748
	150mm	250	6385	9282	10556	11694	12779	13809	1.7	16250
		500	6702	9157	10318	11373	12372	13352	1.8	16250
		750	6921	9113	10239	11238	12211	13159	1.9	16250
		1000	7087	9096	10207	11183	12126	13054	1.9	16250

Initial Pt Force 0.1F_{yield}		Axial Load (excluding PT) 8500kN			Cantilever Length (10000mm)			Grade 300 Dissipaters		
	PT Dia.	Fuse Length (mm)	Yield (kNm)	1%drift (kNm)	2%drift (kNm)	3%drift (kNm)	4%drift (kNm)	6%drift (kNm)	λ	Fuse Area (mm^2)
Diameter (1800mm)	36mm	250	6836	9021	9233	9209	9076	8779	1.6	11654
		500	7077	8887	8977	8852	8654	8309	1.7	11654
		750	7352	8836	8881	8712	8468	8091	1.8	11654
		1000	7454	8812	8835	8636	8365	7971	1.8	11654
	50mm	250	6923	9220	9556	9662	9663	9429	1.6	11951
		500	7168	9082	9292	9298	9232	8955	1.8	11951
		750	7447	9029	9197	9156	9049	8731	1.8	11951
		1000	7548	9006	9147	9081	8942	8607	1.9	11951
	75mm	250	7143	9723	10378	10811	11144	11095	1.7	12723
		500	7396	9580	10105	10430	10694	10604	1.8	12723
		750	7688	9527	10001	10281	10503	10375	1.9	12723
		1000	7794	9504	9952	10203	10401	10240	1.9	12723
	100mm	250	7453	10413	11500	12364	13136	13389	1.8	13805
		500	7718	10265	11205	11958	12657	12861	1.9	13805
		750	8022	10211	11094	11799	12455	12617	2.0	13805
		1000	8134	10187	11043	11717	12345	12483	2.0	13805
	125mm	250	7849	11285	12882	14276	15578	16277	1.8	15195
		500	8123	11125	12565	13839	15060	15704	2.0	15195
		750	8453	11070	12449	13669	14844	15440	2.0	15195
		1000	8574	11038	12390	13581	14728	15295	2.1	15195
	150mm	250	8330	12324	14511	16507	18411	19727	1.9	16894
		500	8620	12150	14166	16032	17849	19097	2.0	16894
		750	8970	12093	14040	15848	17616	18810	2.1	16894
		1000	9101	12060	13977	15751	17489	18651	2.1	16894

Initial Pt Force 0.1f_{yield}		Axial Load (excluding PT) 8500kN			Cantilever Length (10000mm)			Grade 300 Dissipaters		
	PT Dia.	Fuse Length (mm)	Yield (kNm)	1%drift (kNm)	2%drift (kNm)	3%drift (kNm)	4%drift (kNm)	6%drift (kNm)	λ	Fuse Area (mm^2)
Diameter (2000mm)	36mm	250	8349	10895	11091	10973	10703	10313	1.1	15489
		500	8625	10681	10690	10425	10066	9648	1.2	15489
		750	8824	10607	10542	10207	9788	9313	1.3	15489
		1000	8954	10570	10464	10092	9635	9122	1.3	15489
	50mm	250	8452	11109	11427	11432	11285	11022	1.1	15839
		500	8731	10893	11019	10874	10638	10347	1.2	15839
		750	8939	10819	10868	10653	10356	10015	1.3	15839
		1000	9067	10782	10790	10535	10202	9818	1.3	15839
	75mm	250	8725	11661	12283	12599	12766	12818	1.2	16750
		500	9014	11437	11859	12018	12091	12112	1.3	16750
		750	9225	11362	11699	11787	11797	11767	1.3	16750
		1000	9361	11325	11621	11664	11637	11574	1.3	16750
	100mm	250	9099	12423	13456	14186	14769	15239	1.2	18025
		500	9401	12194	13004	13570	14055	14492	1.3	18025
		750	9624	12112	12841	13327	13745	14128	1.4	18025
		1000	9771	12074	12752	13197	13577	13925	1.4	18025
	125mm	250	9581	13390	14920	16154	17244	18219	1.3	19664
		500	9898	13147	14441	15496	16479	17417	1.4	19664
		750	10132	13055	14258	15236	16149	17029	1.4	19664
		1000	10298	13017	14166	15098	15970	16813	1.5	19664
	150mm	250	10167	14549	16656	18466	20139	21693	1.3	21667
		500	10497	14280	16134	17757	19312	20823	1.4	21667
		750	10755	14194	15937	17476	18956	20405	1.5	21667
		1000	10933	14147	15843	17329	18764	20174	1.5	21667

Initial Pt Force 0.1Fyield		Axial Load (excluding PT) 8500kN			Cantilever Length (10000mm)			Grade 300 Dissipaters		
	PT Dia.	Fuse Length (mm)	Yield (kNm)	1%drift (kNm)	2%drift (kNm)	3%drift (kNm)	4%drift (kNm)	6%drift (kNm)	λ	Fuse Area (mm^2)
Diameter (2200mm)	36mm	250	9373	12351	12656	12628	12420	11976	1.2	15513
		500	9746	12103	12177	11987	11691	11244	1.3	15513
		750	9994	12006	11997	11725	11352	10860	1.3	15513
		1000	10157	11952	11902	11579	11166	10642	1.3	15513
	50mm	250	9501	12619	13073	13198	13146	12817	1.2	15887
		500	9874	12365	12585	12546	12409	12062	1.3	15887
		750	10125	12264	12400	12279	12063	11668	1.3	15887
		1000	10292	12212	12305	12134	11872	11444	1.4	15887
	75mm	250	9820	13305	14142	14652	14990	14955	1.2	16857
		500	10206	13037	13628	13968	14219	14172	1.3	16857
		750	10464	12932	13436	13690	13868	13749	1.4	16857
		1000	10639	12877	13337	13542	13670	13509	1.4	16857
	100mm	250	10262	14250	15601	16630	17489	17892	1.3	18215
		500	10665	13957	15050	15903	16669	17052	1.4	18215
		750	10940	13851	14846	15607	16298	16615	1.5	18215
		1000	11126	13792	14741	15451	16094	16366	1.5	18215
	125mm	250	10821	15440	17422	19087	20580	21604	1.3	19962
		500	11248	15116	16830	18304	19697	20690	1.5	19962
		750	11546	15009	16610	17988	19299	20217	1.5	19962
		1000	11746	14950	16498	17819	19082	19950	1.5	19962
	150mm	250	11503	16861	19572	21977	24204	26052	1.4	22096
		500	11951	16516	18941	21128	23244	25049	1.5	22096
		750	12273	16397	18697	20786	22814	24535	1.6	22096
		1000	12495	16337	18580	20604	22577	24244	1.6	22096

Initial Pt Force 0.1f_{yield}		Axial Load (excluding PT) 8500kN			Cantilever Length (10000mm)			Grade 300 Dissipaters		
	PT Dia.	Fuse Length (mm)	Yield (kNm)	1%drift (kNm)	2%drift (kNm)	3%drift (kNm)	4%drift (kNm)	6%drift (kNm)	λ	Fuse Area (mm^2)
Diameter (2500mm)	36mm	250	11256	14562	15048	15153	14968	13615	1.2	15551
		500	11516	14235	14439	14356	14132	13712	1.3	15551
		750	11832	14121	14204	14019	13724	13245	1.4	15551
		1000	11880	14063	14074	13839	13496	12972	1.4	15551
	50mm	250	11412	14914	15603	15915	15924	14593	1.2	15959
		500	11675	14579	14979	15104	15064	14692	1.3	15959
		750	11998	14463	14743	14759	14646	14214	1.4	15959
		1000	12050	14404	14610	14573	14412	13935	1.4	15959
	75mm	250	11817	15818	17020	17856	18394	17109	1.3	17018
		500	12085	15464	16366	17016	17468	17216	1.4	17018
		750	12425	15341	16119	16649	17022	16715	1.5	17018
		1000	12479	15276	15981	16449	16772	16423	1.5	17018
	100mm	250	12387	17066	18963	20502	21781	20625	1.3	18502
		500	12656	16686	18262	19602	20797	20730	1.5	18502
		750	13026	16554	17996	19222	20312	20184	1.5	18502
		1000	13077	16477	17857	19009	20039	19866	1.6	18502
	125mm	250	13109	18637	21395	23793	25961	25071	1.4	20409
		500	13393	18224	20635	22818	24907	25189	1.6	20409
		750	13785	18081	20346	22407	24401	24590	1.6	20409
		1000	13841	17993	20195	22186	24118	24237	1.7	20409
	150mm	250	13982	20510	24277	27676	30834	31640	1.5	22740
		500	14280	20063	23447	26608	29676	30515	1.6	22740
		750	14707	19894	23130	26161	29127	29864	1.7	22740
		1000	14761	19804	22966	25918	28818	29487	1.7	22740

Initial Pt Force 0.1f_{yield}		Axial Load (excluding PT) 10000kN			Cantilever Length (10000mm)			Grade 300 Dissipaters		
	PT Dia.	Fuse Length (mm)	Yield (kNm)	1%drift (kNm)	2%drift (kNm)	3%drift (kNm)	4%drift (kNm)	6%drift (kNm)	λ	Fuse Area (mm^2)
Diameter (1000mm)	36mm	250	3412	4511	4395	4048	3587	3113	1.1	13555
		500	3594	4463	4301	3898	3410	2894	1.1	13555
		750	3728	4449	4267	3839	3343	2813	1.1	13555
		1000	3833	4442	4245	3815	3306	2769	1.2	13555
	50mm	250	3448	4555	4467	4143	3716	3274	1.1	13760
		500	3627	4513	4372	3995	3532	3047	1.1	13760
		750	3762	4495	4338	3938	3465	2966	1.1	13760
		1000	3868	4493	4320	3913	3430	2918	1.2	13760
	75mm	250	3532	4682	4652	4397	4047	3666	1.1	14294
		500	3710	4636	4555	4251	3860	3433	1.1	14294
		750	3849	4623	4525	4188	3785	3355	1.2	14294
		1000	3958	4616	4501	4160	3753	3313	1.2	14294
	100mm	250	3647	4858	4907	4742	4497	4183	1.1	15041
		500	3832	4813	4807	4591	4291	3956	1.2	15041
		750	3970	4795	4776	4528	4213	3878	1.2	15041
		1000	4084	4794	4758	4494	4181	3827	1.2	15041
	125mm	250	3804	5080	5228	5170	5040	4849	1.1	16002
		500	3992	5030	5122	5008	4834	4603	1.2	16002
		750	4130	5019	5083	4951	4741	4508	1.2	16002
		1000	4249	5013	5065	4910	4699	4460	1.2	16002
	150mm	250	3989	5349	5601	5663	5656	5625	1.1	17177
		500	4175	5300	5490	5493	5440	5351	1.2	17177
		750	4320	5284	5449	5433	5365	5244	1.2	17177
		1000	4447	5278	5437	5406	5314	5187	1.2	17177

Initial Pt Force 0.1F_{yield}		Axial Load (excluding PT) 10000kN			Cantilever Length (10000mm)			Grade 300 Dissipaters		
	PT Dia.	Fuse Length (mm)	Yield (kNm)	1%drift (kNm)	2%drift (kNm)	3%drift (kNm)	4%drift (kNm)	6%drift (kNm)	λ	Fuse Area (mm^2)
Diameter (1200mm)	36mm	250	4389	5957	5905	5608	5243	4826	1.3	13579
		500	4628	5896	5761	5411	4990	4529	1.4	13579
		750	4812	5871	5714	5342	4898	4410	1.4	13579
		1000	4946	5843	5690	5306	4848	4347	1.4	13579
	50mm	250	4431	6032	6022	5768	5451	5081	1.3	13808
		500	4672	5970	5877	5568	5195	4782	1.4	13808
		750	4859	5943	5829	5499	5103	4662	1.4	13808
		1000	4994	5915	5804	5460	5046	4598	1.4	13808
	75mm	250	4540	6224	6325	6174	5971	5722	1.3	14401
		500	4787	6161	6173	5969	5709	5415	1.4	14401
		750	4977	6135	6123	5893	5615	5293	1.4	14401
		1000	5116	6107	6098	5861	5564	5228	1.4	14401
	100mm	250	4697	6494	6730	6721	6671	6581	1.3	15232
		500	4941	6427	6576	6516	6400	6263	1.4	15232
		750	5137	6397	6524	6440	6295	6144	1.5	15232
		1000	5281	6368	6490	6400	6251	6078	1.5	15232
	125mm	250	4891	6835	7239	7420	7528	7625	1.4	16300
		500	5145	6759	7082	7183	7252	7295	1.5	16300
		750	5343	6728	7018	7105	7144	7158	1.5	16300
		1000	5493	6700	6990	7060	7092	7090	1.5	16300
	150mm	250	5135	7234	7833	8236	8515	8824	1.4	17606
		500	5396	7160	7672	7982	8230	8486	1.5	17606
		750	5596	7121	7607	7882	8126	8333	1.5	17606
		1000	5754	7101	7567	7835	8059	8259	1.5	17606

Initial Pt Force $0.1f_{yield}$		Axial Load (excluding PT) 10000kN			Cantilever Length (10000mm)			Grade 300 Dissipaters		
	PT Dia.	Fuse Length (mm)	Yield (kNm)	1%drift (kNm)	2%drift (kNm)	3%drift (kNm)	4%drift (kNm)	6%drift (kNm)	λ	Fuse Area (mm^2)
Diameter (1500mm)	36mm	250	6022	8163	8253	8090	7815	7469	1.5	13617
		500	6351	8056	8047	7790	7446	7054	1.6	13617
		750	6576	8025	7966	7677	7298	6875	1.6	13617
		1000	6738	8005	7931	7619	7220	6778	1.6	13617
	50mm	250	6087	8291	8454	8372	8181	7921	1.5	13880
		500	6414	8183	8245	8068	7807	7501	1.6	13880
		750	6645	8145	8168	7954	7658	7320	1.6	13880
		1000	6805	8130	8126	7894	7579	7223	1.7	13880
	75mm	250	6246	8617	8963	9088	9108	9063	1.5	14562
		500	6581	8501	8746	8775	8722	8629	1.6	14562
		750	6813	8469	8670	8656	8568	8444	1.7	14562
		1000	6983	8447	8629	8596	8487	8343	1.7	14562
	100mm	250	6466	9066	9659	10057	10355	10592	1.6	15518
		500	6811	8947	9436	9729	9952	10138	1.7	15518
		750	7049	8907	9347	9605	9791	9944	1.7	15518
		1000	7224	8884	9307	9541	9706	9840	1.8	15518
	125mm	250	6752	9634	10527	11253	11883	12456	1.6	16748
		500	7106	9510	10293	10907	11457	11976	1.7	16748
		750	7348	9460	10203	10768	11287	11773	1.8	16748
		1000	7531	9442	10163	10701	11198	11662	1.8	16748
	150mm	250	7098	10301	11550	12646	13646	14607	1.6	18250
		500	7469	10173	11301	12278	13193	14095	1.8	18250
		750	7715	10126	11210	12128	13027	13878	1.8	18250
		1000	7901	10100	11158	12056	12915	13761	1.8	18250

Initial Pt Force 0.1f_{yield}		Axial Load (excluding PT) 10000kN			Cantilever Length (10000mm)			Grade 300 Dissipaters		
	PT Dia.	Fuse Length (mm)	Yield (kNm)	1%drift (kNm)	2%drift (kNm)	3%drift (kNm)	4%drift (kNm)	6%drift (kNm)	λ	Fuse Area (mm^2)
Diameter (1800mm)	36mm	250	7783	10434	10685	10637	10461	10115	1.6	13654
		500	8095	10279	10384	10224	9970	9585	1.7	13654
		750	8429	10225	10276	10062	9762	9330	1.8	13654
		1000	8555	10201	10222	9978	9648	9186	1.8	13654
	50mm	250	7867	10621	10998	11078	11032	10756	1.6	13951
		500	8182	10465	10692	10658	10534	10216	1.7	13951
		750	8521	10411	10582	10494	10324	9963	1.8	13951
		1000	8648	10387	10528	10408	10210	9816	1.8	13951
	75mm	250	8087	11107	11793	12198	12480	12403	1.7	14723
		500	8405	10949	11481	11761	11963	11838	1.8	14723
		750	8756	10894	11366	11591	11745	11576	1.9	14723
		1000	8888	10870	11308	11502	11627	11432	1.9	14723
	100mm	250	8388	11783	12881	13714	14432	14672	1.7	15805
		500	8716	11613	12549	13254	13886	14073	1.9	15805
		750	9084	11558	12427	13075	13657	13795	1.9	15805
		1000	9224	11527	12365	12981	13533	13642	1.9	15805
	125mm	250	8772	12633	14235	15588	16830	17533	1.8	17195
		500	9112	12449	13885	15097	16248	16889	1.9	17195
		750	9500	12392	13755	14908	16006	16592	2.0	17195
		1000	9647	12360	13689	14807	15875	16428	2.0	17195
	150mm	250	9242	13652	15824	17778	19622	20954	1.8	18894
		500	9597	13451	15443	17252	18995	20254	2.0	18894
		750	10002	13383	15300	17047	18735	19935	2.0	18894
		1000	10162	13360	15235	16939	18595	19759	2.1	18894

Initial Pt Force $0.1f_{yield}$		Axial Load (excluding PT) 10000kN			Cantilever Length (10000mm)			Grade 300 Dissipaters		
	PT Dia.	Fuse Length (mm)	Yield (kNm)	1%drift (kNm)	2%drift (kNm)	3%drift (kNm)	4%drift (kNm)	6%drift (kNm)	λ	Fuse Area (mm^2)
Diameter (2000mm)	36mm	250	8349	10895	11091	10973	10703	10313	1.1	15489
		500	8625	10681	10690	10425	10066	9648	1.2	15489
		750	8824	10607	10542	10207	9788	9313	1.3	15489
		1000	8954	10570	10464	10092	9635	9122	1.3	15489
	50mm	250	8452	11109	11427	11432	11285	11022	1.1	15839
		500	8731	10893	11019	10874	10638	10347	1.2	15839
		750	8939	10819	10868	10653	10356	10015	1.3	15839
		1000	9067	10782	10790	10535	10202	9818	1.3	15839
	75mm	250	8725	11661	12283	12599	12766	12818	1.2	16750
		500	9014	11437	11859	12018	12091	12112	1.3	16750
		750	9225	11362	11699	11787	11797	11767	1.3	16750
		1000	9361	11325	11621	11664	11637	11574	1.3	16750
	100mm	250	9099	12423	13456	14186	14769	15239	1.2	18025
		500	9401	12194	13004	13570	14055	14492	1.3	18025
		750	9624	12112	12841	13327	13745	14128	1.4	18025
		1000	9771	12074	12752	13197	13577	13925	1.4	18025
	125mm	250	9581	13390	14920	16154	17244	18219	1.3	19664
		500	9898	13147	14441	15496	16479	17417	1.4	19664
		750	10132	13055	14258	15236	16149	17029	1.4	19664
		1000	10298	13017	14166	15098	15970	16813	1.5	19664
	150mm	250	10167	14549	16656	18466	20139	21693	1.3	21667
		500	10497	14280	16134	17757	19312	20823	1.4	21667
		750	10755	14194	15937	17476	18956	20405	1.5	21667
		1000	10933	14147	15843	17329	18764	20174	1.5	21667

Initial Pt Force 0.1Fyield		Axial Load (excluding PT) 10000kN			Cantilever Length (10000mm)			Grade 300 Dissipaters		
	PT Dia.	Fuse Length (mm)	Yield (kNm)	1%drift (kNm)	2%drift (kNm)	3%drift (kNm)	4%drift (kNm)	6%drift (kNm)	λ	Fuse Area (mm^2)
Diameter (2200mm)	36mm	250	10695	14312	14661	14609	14342	13846	1.1	18180
		500	11156	14014	14109	13867	13501	12989	1.2	18180
		750	11470	13906	13902	13565	13119	12534	1.3	18180
		1000	11677	13848	13792	13403	12900	12276	1.3	18180
	50mm	250	10816	14572	15070	15166	15052	14663	1.2	18554
		500	11277	14266	14506	14412	14198	13801	1.3	18554
		750	11596	14158	14296	14105	13810	13336	1.3	18554
		1000	11811	14099	14187	13942	13593	13071	1.3	18554
	75mm	250	11125	15240	16106	16587	16859	16770	1.2	19524
		500	11599	14919	15523	15802	15971	15867	1.3	19524
		750	11929	14803	15304	15485	15570	15396	1.4	19524
		1000	12150	14751	15188	15315	15349	15122	1.4	19524
	100mm	250	11553	16150	17534	18525	19313	19680	1.2	20882
		500	12040	15820	16912	17698	18376	18720	1.4	20882
		750	12386	15703	16685	17364	17955	18222	1.4	20882
		1000	12628	15643	16562	17186	17724	17939	1.4	20882
	125mm	250	12105	17300	19317	20936	22355	23359	1.3	22628
		500	12614	16955	18654	20056	21356	22326	1.4	22628
		750	12974	16837	18413	19701	20910	21794	1.5	22628
		1000	13235	16767	18282	19511	20664	21494	1.5	22628
	150mm	250	12772	18688	21432	23779	25927	27775	1.3	24763
		500	13302	18313	20724	22834	24853	26651	1.5	24763
		750	13687	18193	20456	22453	24374	26079	1.5	24763
		1000	13971	18121	20324	22252	24112	25756	1.5	24763

Initial Pt Force 0.1Fyield		Axial Load (excluding PT) 10000kN			Cantilever Length (10000mm)			Grade 300 Dissipaters		
	PT Dia.	Fuse Length (mm)	Yield (kNm)	1%drift (kNm)	2%drift (kNm)	3%drift (kNm)	4%drift (kNm)	6%drift (kNm)	λ	Fuse Area (mm^2)
Diameter (2500mm)	36mm	250	12893	16892	17444	17542	17332	15715	1.2	18217
		500	13198	16515	16741	16634	16344	15827	1.3	18217
		750	13602	16385	16472	16239	15866	15287	1.4	18217
		1000	13670	16307	16332	16025	15599	14973	1.4	18217
	50mm	250	13046	17235	17989	18288	18284	16683	1.2	18625
		500	13352	16852	17270	17364	17270	16800	1.3	18625
		750	13763	16719	17000	16966	16780	16251	1.4	18625
		1000	13833	16637	16858	16746	16507	15930	1.4	18625
	75mm	250	13445	18118	19380	20193	20713	19201	1.3	19685
		500	13757	17716	18628	19228	19659	19319	1.4	19685
		750	14179	17577	18343	18821	19139	18738	1.4	19685
		1000	14251	17487	18194	18592	18849	18400	1.5	19685
	100mm	250	13997	19336	21282	22794	24039	22701	1.3	21168
		500	14321	18908	20488	21770	22934	22817	1.4	21168
		750	14765	18754	20187	21340	22401	22187	1.5	21168
		1000	14835	18664	20029	21107	22093	21822	1.5	21168
	125mm	250	14708	20875	23670	26035	28130	28371	1.4	23076
		500	15033	20415	22824	24938	26944	27227	1.5	23076
		750	15507	20240	22501	24478	26375	26560	1.6	23076
		1000	15581	20144	22331	24229	26057	26170	1.6	23076
	150mm	250	15568	22712	26512	29866	32947	33773	1.4	25407
		500	15898	22225	25592	28679	31660	32516	1.6	25407
		750	16408	22025	25242	28181	31046	31794	1.6	25407
		1000	16490	21922	25060	27913	30704	31375	1.7	25407

Initial Pt Force 0.1Fyield		Axial Load (excluding PT) 1500kN			Cantilever Length (12000mm)			Grade 300 Dissipaters		
	PT Dia.	Fuse Length (mm)	Yield (kNm)	1%drift (kNm)	2%drift (kNm)	3%drift (kNm)	4%drift (kNm)	6%drift (kNm)	λ	Fuse Area (mm^2)
Diameter (1000mm)	36mm	250	844	1020	1027	1010	984	947	1.1	2962
		500	871	1009	1002	972	932	889	1.1	2962
		750	887	1002	991	955	913	866	1.1	2962
		1000	900	998	984	947	902	855	1.2	2962
	50mm	250	893	1108	1152	1173	1185	1193	1.1	3236
		500	923	1094	1124	1132	1135	1131	1.2	3236
		750	940	1088	1114	1116	1112	1104	1.2	3236
		1000	956	1083	1106	1106	1100	1091	1.2	3236
	75mm	250	1023	1326	1459	1572	1676	1775	1.2	3948
		500	1057	1310	1427	1525	1617	1706	1.3	3948
		750	1077	1305	1415	1508	1595	1679	1.3	3948
		1000	1098	1298	1409	1499	1583	1665	1.3	3948
	100mm	250	1198	1620	1862	2088	2306	2519	1.3	4944
		500	1240	1600	1823	2031	2235	2436	1.4	4944
		750	1265	1593	1808	2011	2208	2403	1.4	4944
		1000	1290	1587	1805	2001	2194	2386	1.4	4944
	125mm	250	1419	1981	2340	2697	3042	3387	1.3	6225
		500	1469	1954	2295	2628	2958	3287	1.4	6225
		750	1501	1946	2285	2604	2930	3247	1.4	6225
		1000	1531	1942	2275	2596	2908	3227	1.4	6225
	150mm	250	1683	2406	2893	3388	3867	4350	1.3	7791
		500	1743	2369	2841	3300	3766	4226	1.4	7791
		750	1782	2356	2828	3278	3733	4179	1.4	7791
		1000	1817	2354	2819	3261	3705	4164	1.4	7791

Initial Pt Force 0.1Fyield		Axial Load (excluding PT) 1500kN			Cantilever Length (12000mm)			Grade 300 Dissipaters		
	PT Dia.	Fuse Length (mm)	Yield (kNm)	1%drift (kNm)	2%drift (kNm)	3%drift (kNm)	4%drift (kNm)	6%drift (kNm)	λ	Fuse Area (mm^2)
Diameter (1200mm)	36mm	250	1068	1302	1341	1348	1343	1338	1.2	2995
		500	1096	1284	1301	1295	1281	1265	1.3	2995
		750	1115	1274	1286	1275	1258	1237	1.3	2995
		1000	1133	1268	1279	1265	1245	1222	1.3	2995
	50mm	250	1136	1425	1523	1596	1650	1697	1.3	3300
		500	1166	1407	1482	1534	1579	1620	1.4	3300
		750	1188	1396	1465	1512	1552	1589	1.4	3300
		1000	1207	1390	1456	1500	1538	1573	1.4	3300
	75mm	250	1309	1737	1976	2190	2395	2592	1.4	4091
		500	1346	1715	1929	2123	2312	2496	1.5	4091
		750	1372	1705	1911	2096	2276	2453	1.5	4091
		1000	1398	1695	1899	2080	2256	2430	1.5	4091
	100mm	250	1546	2154	2570	2964	3346	3720	1.5	5199
		500	1593	2128	2513	2882	3245	3605	1.6	5199
		750	1622	2117	2493	2852	3206	3559	1.6	5199
		1000	1655	2107	2482	2837	3186	3533	1.6	5199
	125mm	250	1842	2664	3282	3885	4473	5051	1.5	6623
		500	1900	2631	3215	3785	4349	4910	1.6	6623
		750	1934	2620	3190	3748	4301	4853	1.6	6623
		1000	1974	2609	3179	3730	4277	4821	1.7	6623
	150mm	250	2199	3261	4097	4931	5741	6545	1.5	8363
		500	2266	3218	4017	4802	5591	6371	1.6	8363
		750	2306	3203	3989	4758	5533	6301	1.6	8363
		1000	2356	3196	3977	4742	5503	6264	1.7	8363

Initial Pt Force 0.1f_{yield}		Axial Load (excluding PT) 1500kN			Cantilever Length (12000mm)			Grade 300 Dissipaters		
	PT Dia.	Fuse Length (mm)	Yield (kNm)	1%drift (kNm)	2%drift (kNm)	3%drift (kNm)	4%drift (kNm)	6%drift (kNm)	λ	Fuse Area (mm^2)
Diameter (1500mm)	36mm	250	1426	1740	1828	1895	1953	1967	1.3	3044
		500	1447	1708	1774	1819	1863	1866	1.4	3044
		750	1470	1696	1755	1792	1825	1822	1.5	3044
		1000	1489	1691	1745	1778	1806	1798	1.5	3044
	50mm	250	1523	1933	2121	2279	2436	2531	1.4	3395
		500	1548	1898	2059	2199	2336	2420	1.5	3395
		750	1573	1885	2037	2169	2295	2371	1.6	3395
		1000	1597	1879	2026	2154	2276	2345	1.6	3395
	75mm	250	1774	2418	2853	3252	3633	3961	1.6	4306
		500	1805	2378	2772	3145	3512	3826	1.7	4306
		750	1838	2361	2743	3105	3463	3767	1.8	4306
		1000	1870	2351	2727	3085	3437	3736	1.8	4306
	100mm	250	2118	3069	3809	4520	5216	5896	1.7	5580
		500	2159	3021	3716	4393	5063	5726	1.8	5580
		750	2200	3001	3679	4339	4993	5645	1.9	5580
		1000	2244	2985	3657	4309	4956	5601	1.9	5580
	125mm	250	2548	3864	4966	6036	7087	8121	1.7	7219
		500	2606	3807	4851	5877	6895	7908	1.9	7219
		750	2655	3785	4809	5816	6818	7817	1.9	7219
		1000	2709	3766	4786	5785	6777	7767	1.9	7219
	150mm	250	3060	4790	6296	7767	9215	10644	1.7	9222
		500	3141	4716	6154	7571	8978	10381	1.9	9222
		750	3193	4693	6103	7495	8884	10268	1.9	9222
		1000	3256	4679	6077	7457	8833	10207	1.9	9222

Initial Pt Force 0.1Fyield		Axial Load (excluding PT) 1500kN			Cantilever Length (12000mm)			Grade 300 Dissipaters		
	PT Dia.	Fuse Length (mm)	Yield (kNm)	1%drift (kNm)	2%drift (kNm)	3%drift (kNm)	4%drift (kNm)	6%drift (kNm)	λ	Fuse Area (mm^2)
Diameter (1800mm)	36mm	250	1788	2193	2358	2499	2588	2568	1.4	3094
		500	1800	2151	2281	2396	2468	2442	1.5	3094
		750	1838	2136	2255	2355	2416	2381	1.6	3094
		1000	1854	2129	2241	2334	2388	2348	1.6	3094
	50mm	250	1921	2470	2777	3066	3287	3305	1.5	3490
		500	1935	2422	2694	2951	3152	3163	1.7	3490
		750	1978	2405	2664	2906	3095	3096	1.7	3490
		1000	1997	2397	2649	2883	3064	3058	1.7	3490
	75mm	250	2263	3172	3836	4473	5062	5177	1.7	4520
		500	2278	3107	3729	4331	4892	4996	1.9	4520
		750	2336	3085	3690	4278	4819	4911	1.9	4520
		1000	2365	3074	3670	4250	4781	4863	2.0	4520
	100mm	250	2729	4110	5258	6360	7434	7725	1.8	5962
		500	2749	4032	5110	6170	7220	7491	2.0	5962
		750	2825	3999	5056	6096	7130	7384	2.1	5962
		1000	2865	3984	5028	6058	7082	7325	2.1	5962
	125mm	250	3315	5261	6969	8637	10273	10948	1.9	7815
		500	3343	5169	6796	8403	10001	10639	2.1	7815
		750	3440	5127	6726	8307	9879	10493	2.1	7815
		1000	3494	5104	6686	8251	9810	10412	2.2	7815
	150mm	250	4013	6605	8949	11245	13503	14741	1.9	10081
		500	4054	6490	8732	10952	13162	14359	2.1	10081
		750	4173	6450	8653	10839	13019	14181	2.1	10081
		1000	4241	6412	8611	10778	12940	14083	2.2	10081

Initial Pt Force 0.1f_{yield}		Axial Load (excluding PT) 1500kN			Cantilever Length (12000mm)			Grade 300 Dissipaters		
	PT Dia.	Fuse Length (mm)	Yield (kNm)	1%drift (kNm)	2%drift (kNm)	3%drift (kNm)	4%drift (kNm)	6%drift (kNm)	λ	Fuse Area (mm^2)
Diameter (2000mm)	36mm	250	1913	2287	2364	2410	2431	2430	1.2	3009
		500	1935	2237	2278	2294	2299	2297	1.3	3009
		750	1956	2220	2247	2247	2241	2229	1.4	3009
		1000	1977	2211	2230	2222	2209	2191	1.4	3009
	50mm	250	2037	2530	2723	2885	3023	3140	1.3	3327
		500	2061	2474	2630	2759	2880	2994	1.5	3327
		750	2084	2455	2595	2708	2817	2920	1.5	3327
		1000	2108	2445	2577	2682	2782	2879	1.5	3327
	75mm	250	2355	3143	3635	4074	4499	4900	1.5	4152
		500	2383	3078	3516	3924	4325	4723	1.6	4152
		750	2412	3052	3472	3864	4248	4633	1.7	4152
		1000	2445	3040	3450	3833	4209	4583	1.7	4152
	100mm	250	2787	3971	4855	5686	6473	7229	1.6	5308
		500	2827	3894	4708	5486	6252	7009	1.8	5308
		750	2863	3862	4649	5407	6156	6900	1.9	5308
		1000	2907	3845	4619	5365	6103	6839	1.9	5308
	125mm	250	3323	4995	6340	7624	8871	10083	1.7	6793
		500	3385	4898	6160	7387	8600	9804	1.9	6793
		750	3430	4865	6095	7292	8482	9664	1.9	6793
		1000	3485	4841	6054	7236	8410	9579	2.0	6793
	150mm	250	3964	6194	8064	9865	11621	13335	1.8	8609
		500	4053	6077	7845	9573	11286	12987	1.9	8609
		750	4109	6038	7764	9457	11140	12819	2.0	8609
		1000	4175	6011	7722	9396	11062	12723	2.0	8609

Initial Pt Force $0.1f_{yield}$		Axial Load (excluding PT) 3000kN			Cantilever Length (12000mm)			Grade 300 Dissipaters		
	PT Dia.	Fuse Length (mm)	Yield (kNm)	1%drift (kNm)	2%drift (kNm)	3%drift (kNm)	4%drift (kNm)	6%drift (kNm)	λ	Fuse Area (mm^2)
Diameter (1000mm)	36mm	250	1469	1834	1809	1736	1641	1535	1.0	5628
		500	1536	1811	1764	1669	1556	1434	1.0	5628
		750	1573	1804	1748	1645	1524	1394	1.0	5628
		1000	1598	1801	1740	1632	1507	1373	1.0	5628
	50mm	250	1515	1912	1917	1881	1824	1754	1.0	5903
		500	1583	1887	1871	1812	1735	1650	1.0	5903
		750	1623	1880	1855	1787	1702	1609	1.1	5903
		1000	1649	1877	1849	1774	1684	1587	1.1	5903
	75mm	250	1633	2111	2196	2243	2274	2293	1.0	6614
		500	1706	2083	2146	2170	2178	2180	1.1	6614
		750	1749	2075	2128	2143	2142	2136	1.1	6614
		1000	1778	2069	2121	2126	2123	2112	1.1	6614
	100mm	250	1799	2384	2563	2720	2859	2992	1.1	7611
		500	1877	2349	2509	2639	2753	2866	1.1	7611
		750	1924	2339	2492	2608	2712	2818	1.2	7611
		1000	1957	2332	2486	2591	2693	2792	1.2	7611
	125mm	250	2006	2717	3026	3296	3564	3816	1.1	8892
		500	2094	2682	2960	3196	3436	3674	1.2	8892
		750	2148	2665	2938	3170	3399	3618	1.2	8892
		1000	2183	2655	2926	3150	3369	3587	1.2	8892
	150mm	250	2259	3110	3565	3948	4354	4739	1.1	10458
		500	2356	3072	3481	3844	4207	4578	1.2	10458
		750	2417	3052	3453	3809	4166	4515	1.2	10458
		1000	2457	3034	3439	3792	4135	4492	1.2	10458

Initial Pt Force 0.1Fyield		Axial Load (excluding PT) 3000kN			Cantilever Length (12000mm)			Grade 300 Dissipaters		
	PT Dia.	Fuse Length (mm)	Yield (kNm)	1%drift (kNm)	2%drift (kNm)	3%drift (kNm)	4%drift (kNm)	6%drift (kNm)	λ	Fuse Area (mm^2)
Diameter (1200mm)	36mm	250	1879	2342	2369	2334	2275	2201	1.1	5661
		500	1950	2313	2305	2241	2159	2063	1.2	5661
		750	1987	2303	2282	2207	2110	2003	1.2	5661
		1000	2020	2295	2269	2185	2083	1971	1.2	5661
	50mm	250	1941	2454	2535	2555	2553	2536	1.1	5966
		500	2014	2422	2467	2458	2432	2397	1.2	5966
		750	2053	2412	2444	2423	2385	2336	1.2	5966
		1000	2088	2405	2432	2403	2356	2302	1.2	5966
	75mm	250	2098	2739	2950	3107	3242	3363	1.2	6758
		500	2176	2705	2877	3001	3110	3211	1.3	6758
		750	2220	2692	2851	2961	3058	3149	1.3	6758
		1000	2260	2686	2837	2941	3031	3116	1.3	6758
	100mm	250	2316	3128	3503	3836	4146	4442	1.3	7865
		500	2401	3085	3422	3716	3996	4270	1.3	7865
		750	2453	3073	3393	3671	3939	4200	1.4	7865
		1000	2498	3067	3379	3649	3908	4163	1.4	7865
	125mm	250	2592	3609	4177	4711	5225	5724	1.3	9289
		500	2686	3560	4086	4574	5055	5527	1.4	9289
		750	2748	3544	4049	4523	4989	5449	1.4	9289
		1000	2799	3537	4034	4503	4955	5406	1.4	9289
	150mm	250	2928	4184	4957	5711	6448	7168	1.3	11030
		500	3031	4119	4847	5553	6251	6945	1.4	11030
		750	3105	4101	4818	5495	6175	6855	1.4	11030
		1000	3160	4088	4795	5467	6144	6806	1.5	11030

Initial Pt Force $0.1f_{yield}$		Axial Load (excluding PT) 3000kN			Cantilever Length (12000mm)			Grade 300 Dissipaters		
	PT Dia.	Fuse Length (mm)	Yield (kNm)	1%drift (kNm)	2%drift (kNm)	3%drift (kNm)	4%drift (kNm)	6%drift (kNm)	λ	Fuse Area (mm^2)
Diameter (1500mm)	36mm	250	2526	3142	3242	3270	3256	3218	1.2	5711
		500	2602	3092	3141	3126	3092	3033	1.3	5711
		750	2645	3071	3101	3072	3026	2955	1.4	5711
		1000	2682	3055	3080	3044	2991	2913	1.4	5711
	50mm	250	2615	3318	3512	3639	3724	3765	1.3	6062
		500	2695	3267	3408	3487	3547	3576	1.4	6062
		750	2739	3245	3365	3429	3476	3493	1.4	6062
		1000	2780	3228	3343	3398	3438	3448	1.4	6062
	75mm	250	2846	3768	4191	4551	4882	5193	1.4	6972
		500	2935	3710	4075	4390	4686	4966	1.5	6972
		750	2983	3688	4034	4324	4599	4867	1.5	6972
		1000	3029	3669	4006	4287	4554	4813	1.5	6972
	100mm	250	3165	4377	5100	5760	6391	6999	1.5	8247
		500	3269	4313	4967	5575	6168	6751	1.6	8247
		750	3317	4286	4919	5505	6078	6644	1.6	8247
		1000	3374	4268	4895	5468	6029	6585	1.6	8247
	125mm	250	3569	5135	6210	7224	8209	9168	1.5	9886
		500	3685	5055	6055	7009	7949	8880	1.6	9886
		750	3742	5026	6000	6927	7844	8755	1.7	9886
		1000	3808	5014	5972	6885	7789	8688	1.7	9886
	150mm	250	4056	6023	7494	8906	10288	11641	1.6	11889
		500	4182	5928	7314	8656	9984	11302	1.7	11889
		750	4251	5897	7249	8562	9863	11157	1.7	11889
		1000	4327	5885	7217	8512	9797	11080	1.7	11889

Initial Pt Force 0.1Fyield		Axial Load (excluding PT) 3000kN			Cantilever Length (12000mm)			Grade 300 Dissipaters		
	PT Dia.	Fuse Length (mm)	Yield (kNm)	1%drift (kNm)	2%drift (kNm)	3%drift (kNm)	4%drift (kNm)	6%drift (kNm)	λ	Fuse Area (mm^2)
Diameter (1800mm)	36mm	250	3195	3963	4141	4243	4309	4236	1.3	5760
		500	3240	3887	4000	4058	4090	4004	1.4	5760
		750	3317	3857	3949	3987	3997	3894	1.5	5760
		1000	3352	3842	3923	3950	3946	3833	1.5	5760
	50mm	250	3317	4221	4545	4783	4989	4954	1.4	6157
		500	3366	4142	4393	4590	4757	4708	1.5	6157
		750	3447	4110	4338	4515	4657	4591	1.5	6157
		1000	3487	4093	4310	4475	4606	4526	1.6	6157
	75mm	250	3631	4876	5561	6160	6711	6787	1.5	7187
		500	3689	4790	5387	5929	6453	6503	1.6	7187
		750	3782	4751	5321	5839	6343	6369	1.7	7187
		1000	3828	4732	5286	5792	6285	6298	1.7	7187
	100mm	250	4063	5767	6913	7987	9019	9317	1.6	8629
		500	4135	5665	6719	7724	8702	8977	1.7	8629
		750	4244	5626	6642	7610	8564	8819	1.8	8629
		1000	4301	5597	6598	7550	8490	8731	1.8	8629
	125mm	250	4611	6871	8572	10196	11775	12490	1.7	10482
		500	4703	6750	8343	9886	11412	12088	1.8	10482
		750	4828	6709	8259	9764	11259	11900	1.9	10482
		1000	4887	6674	8212	9699	11174	11789	1.9	10482
	150mm	250	5272	8164	10500	12750	14949	16242	1.7	12747
		500	5390	8025	10229	12383	14518	15761	1.9	12747
		750	5531	7977	10130	12240	14338	15539	1.9	12747
		1000	5590	7943	10079	12166	14240	15417	2.0	12747

Initial Pt Force 0.1f_{yield}		Axial Load (excluding PT) 3000kN			Cantilever Length (12000mm)			Grade 300 Dissipaters		
	PT Dia.	Fuse Length (mm)	Yield (kNm)	1%drift (kNm)	2%drift (kNm)	3%drift (kNm)	4%drift (kNm)	6%drift (kNm)	λ	Fuse Area (mm^2)
Diameter (2000mm)	36mm	250	3405	4165	4217	4160	4066	3938	1.1	5676
		500	3489	4081	4052	3949	3824	3690	1.2	5676
		750	3533	4049	3991	3865	3718	3565	1.3	5676
		1000	3578	4031	3959	3820	3661	3494	1.3	5676
	50mm	250	3518	4390	4556	4618	4628	4614	1.2	5994
		500	3606	4302	4386	4393	4377	4354	1.3	5994
		750	3652	4270	4320	4304	4268	4224	1.3	5994
		1000	3700	4249	4286	4257	4208	4151	1.4	5994
	75mm	250	3806	4964	5414	5772	6066	6310	1.3	6819
		500	3907	4867	5229	5518	5778	6024	1.4	6819
		750	3958	4833	5157	5415	5653	5882	1.5	6819
		1000	4008	4807	5116	5360	5585	5802	1.5	6819
	100mm	250	4203	5746	6573	7304	7983	8615	1.4	7974
		500	4320	5636	6362	7022	7660	8276	1.5	7974
		750	4383	5597	6284	6910	7511	8103	1.6	7974
		1000	4435	5571	6240	6843	7429	8007	1.6	7974
	125mm	250	4708	6723	8003	9182	10305	11378	1.5	9460
		500	4843	6595	7759	8857	9931	10989	1.6	9460
		750	4912	6547	7669	8727	9768	10799	1.7	9460
		1000	4975	6520	7622	8658	9679	10694	1.7	9460
	150mm	250	5316	7875	9673	11366	12996	14569	1.5	11275
		500	5474	7728	9392	10988	12559	14115	1.7	11275
		750	5549	7669	9287	10838	12372	13895	1.7	11275
		1000	5621	7645	9233	10758	12269	13772	1.8	11275

Initial Pt Force 0.1f_{yield}		Axial Load (excluding PT) 3000kN			Cantilever Length (12000mm)			Grade 300 Dissipaters		
	PT Dia.	Fuse Length (mm)	Yield (kNm)	1%drift (kNm)	2%drift (kNm)	3%drift (kNm)	4%drift (kNm)	6%drift (kNm)	λ	Fuse Area (mm^2)
Diameter (2200mm)	36mm	250	3631	4469	4541	4521	4457	4325	1.3	4985
		500	3734	4379	4374	4305	4217	4088	1.5	4985
		750	3797	4344	4312	4217	4106	3960	1.5	4985
		1000	3853	4326	4280	4171	4045	3886	1.6	4985
	50mm	250	3750	4728	4942	5057	5132	5133	1.4	5280
		500	3859	4635	4765	4831	4881	4883	1.5	5280
		750	3926	4597	4699	4740	4765	4748	1.6	5280
		1000	3985	4578	4665	4692	4701	4671	1.6	5280
	75mm	250	4058	5389	5961	6420	6831	7199	1.6	6047
		500	4181	5284	5759	6165	6548	6915	1.7	6047
		750	4256	5244	5682	6061	6422	6764	1.8	6047
		1000	4326	5221	5643	6006	6352	6677	1.8	6047
	100mm	250	4482	6291	7327	8265	9135	9940	1.7	7121
		500	4626	6170	7102	7966	8800	9618	1.8	7121
		750	4715	6127	7013	7840	8649	9448	1.9	7121
		1000	4797	6100	6965	7773	8567	9352	2.0	7121
	125mm	250	5018	7415	9013	10508	11939	13311	1.8	8501
		500	5192	7273	8752	10167	11557	12930	2.0	8501
		750	5294	7226	8654	10027	11383	12725	2.0	8501
		1000	5392	7194	8600	9948	11280	12604	2.1	8501
	150mm	250	5664	8741	10986	13119	15182	17177	1.9	10188
		500	5868	8574	10682	12721	14734	16729	2.0	10188
		750	5993	8520	10568	12558	14533	16496	2.1	10188
		1000	6098	8484	10509	12472	14422	16364	2.1	10188

Initial Pt Force 0.1Fyield		Axial Load (excluding PT) 4500kN			Cantilever Length (12000mm)			Grade 300 Dissipaters		
	PT Dia.	Fuse Length (mm)	Yield (kNm)	1%drift (kNm)	2%drift (kNm)	3%drift (kNm)	4%drift (kNm)	6%drift (kNm)	λ	Fuse Area (mm^2)
Diameter (1200mm)	36mm	250	1879	2342	2369	2334	2275	2201	1.1	5661
		500	1950	2313	2305	2241	2159	2063	1.2	5661
		750	1987	2303	2282	2207	2110	2003	1.2	5661
		1000	2020	2295	2269	2185	2083	1971	1.2	5661
	50mm	250	1941	2454	2535	2555	2553	2536	1.1	5966
		500	2014	2422	2467	2458	2432	2397	1.2	5966
		750	2053	2412	2444	2423	2385	2336	1.2	5966
		1000	2088	2405	2432	2403	2356	2302	1.2	5966
	75mm	250	2098	2739	2950	3107	3242	3363	1.2	6758
		500	2176	2705	2877	3001	3110	3211	1.3	6758
		750	2220	2692	2851	2961	3058	3149	1.3	6758
		1000	2260	2686	2837	2941	3031	3116	1.3	6758
	100mm	250	2316	3128	3503	3836	4146	4442	1.3	7865
		500	2401	3085	3422	3716	3996	4270	1.3	7865
		750	2453	3073	3393	3671	3939	4200	1.4	7865
		1000	2498	3067	3379	3649	3908	4163	1.4	7865
	125mm	250	2592	3609	4177	4711	5225	5724	1.3	9289
		500	2686	3560	4086	4574	5055	5527	1.4	9289
		750	2748	3544	4049	4523	4989	5449	1.4	9289
		1000	2799	3537	4034	4503	4955	5406	1.4	9289
	150mm	250	2928	4184	4957	5711	6448	7168	1.3	11030
		500	3031	4119	4847	5553	6251	6945	1.4	11030
		750	3105	4101	4818	5495	6175	6855	1.4	11030
		1000	3160	4088	4795	5467	6144	6806	1.5	11030

Initial Pt Force 0.1f_{yield}		Axial Load (excluding PT) 4500kN			Cantilever Length (12000mm)			Grade 300 Dissipaters		
	PT Dia.	Fuse Length (mm)	Yield (kNm)	1%drift (kNm)	2%drift (kNm)	3%drift (kNm)	4%drift (kNm)	6%drift (kNm)	λ	Fuse Area (mm^2)
Diameter (1500mm)	36mm	250	2526	3142	3242	3270	3256	3218	1.2	5711
		500	2602	3092	3141	3126	3092	3033	1.3	5711
		750	2645	3071	3101	3072	3026	2955	1.4	5711
		1000	2682	3055	3080	3044	2991	2913	1.4	5711
	50mm	250	2615	3318	3512	3639	3724	3765	1.3	6062
		500	2695	3267	3408	3487	3547	3576	1.4	6062
		750	2739	3245	3365	3429	3476	3493	1.4	6062
		1000	2780	3228	3343	3398	3438	3448	1.4	6062
	75mm	250	2846	3768	4191	4551	4882	5193	1.4	6972
		500	2935	3710	4075	4390	4686	4966	1.5	6972
		750	2983	3688	4034	4324	4599	4867	1.5	6972
		1000	3029	3669	4006	4287	4554	4813	1.5	6972
	100mm	250	3165	4377	5100	5760	6391	6999	1.5	8247
		500	3269	4313	4967	5575	6168	6751	1.6	8247
		750	3317	4286	4919	5505	6078	6644	1.6	8247
		1000	3374	4268	4895	5468	6029	6585	1.6	8247
	125mm	250	3569	5135	6210	7224	8209	9168	1.5	9886
		500	3685	5055	6055	7009	7949	8880	1.6	9886
		750	3742	5026	6000	6927	7844	8755	1.7	9886
		1000	3808	5014	5972	6885	7789	8688	1.7	9886
	150mm	250	4056	6023	7494	8906	10288	11641	1.6	11889
		500	4182	5928	7314	8656	9984	11302	1.7	11889
		750	4251	5897	7249	8562	9863	11157	1.7	11889
		1000	4327	5885	7217	8512	9797	11080	1.7	11889

Initial Pt Force 0.1Fyield		Axial Load (excluding PT) 4500kN			Cantilever Length (12000mm)			Grade 300 Dissipaters		
	PT Dia.	Fuse Length (mm)	Yield (kNm)	1%drift (kNm)	2%drift (kNm)	3%drift (kNm)	4%drift (kNm)	6%drift (kNm)	λ	Fuse Area (mm^2)
Diameter (1800mm)	36mm	250	3195	3963	4141	4243	4309	4236	1.3	5760
		500	3240	3887	4000	4058	4090	4004	1.4	5760
		750	3317	3857	3949	3987	3997	3894	1.5	5760
		1000	3352	3842	3923	3950	3946	3833	1.5	5760
	50mm	250	3317	4221	4545	4783	4989	4954	1.4	6157
		500	3366	4142	4393	4590	4757	4708	1.5	6157
		750	3447	4110	4338	4515	4657	4591	1.5	6157
		1000	3487	4093	4310	4475	4606	4526	1.6	6157
	75mm	250	3631	4876	5561	6160	6711	6787	1.5	7187
		500	3689	4790	5387	5929	6453	6503	1.6	7187
		750	3782	4751	5321	5839	6343	6369	1.7	7187
		1000	3828	4732	5286	5792	6285	6298	1.7	7187
	100mm	250	4063	5767	6913	7987	9019	9317	1.6	8629
		500	4135	5665	6719	7724	8702	8977	1.7	8629
		750	4244	5626	6642	7610	8564	8819	1.8	8629
		1000	4301	5597	6598	7550	8490	8731	1.8	8629
	125mm	250	4611	6871	8572	10196	11775	12490	1.7	10482
		500	4703	6750	8343	9886	11412	12088	1.8	10482
		750	4828	6709	8259	9764	11259	11900	1.9	10482
		1000	4887	6674	8212	9699	11174	11789	1.9	10482
	150mm	250	5272	8164	10500	12750	14949	16242	1.7	12747
		500	5390	8025	10229	12383	14518	15761	1.9	12747
		750	5531	7977	10130	12240	14338	15539	1.9	12747
		1000	5590	7943	10079	12166	14240	15417	2.0	12747

Initial Pt Force 0.1f_{yield}		Axial Load (excluding PT) 4500kN			Cantilever Length (12000mm)			Grade 300 Dissipaters		
	PT Dia.	Fuse Length (mm)	Yield (kNm)	1%drift (kNm)	2%drift (kNm)	3%drift (kNm)	4%drift (kNm)	6%drift (kNm)	λ	Fuse Area (mm^2)
Diameter (2000mm)	36mm	250	4772	5969	6005	5888	5682	5406	1.1	8342
		500	4926	5853	5779	5581	5326	5047	1.2	8342
		750	5001	5811	5696	5452	5171	4870	1.2	8342
		1000	5057	5784	5647	5385	5087	4770	1.3	8342
	50mm	250	4880	6182	6328	6321	6237	6067	1.1	8660
		500	5036	6062	6095	6007	5864	5694	1.2	8660
		750	5112	6019	6007	5875	5702	5510	1.3	8660
		1000	5173	5993	5959	5804	5614	5407	1.3	8660
	75mm	250	5153	6729	7147	7418	7614	7748	1.2	9486
		500	5318	6600	6896	7080	7225	7334	1.3	9486
		750	5398	6550	6804	6946	7049	7129	1.4	9486
		1000	5464	6523	6756	6870	6950	7015	1.4	9486
	100mm	250	5534	7479	8260	8899	9461	9959	1.3	10641
		500	5708	7334	7988	8529	9034	9516	1.4	10641
		750	5799	7278	7884	8381	8848	9298	1.4	10641
		1000	5871	7249	7831	8303	8746	9173	1.5	10641
	125mm	250	6015	8415	9641	10724	11727	12663	1.4	12126
		500	6202	8251	9336	10311	11251	12166	1.5	12126
		750	6307	8191	9223	10147	11044	11925	1.5	12126
		1000	6386	8161	9164	10061	10931	11790	1.6	12126
	150mm	250	6599	9518	11264	12854	14362	15797	1.4	13942
		500	6797	9337	10920	12391	13825	15236	1.5	13942
		750	6921	9275	10793	12208	13594	14965	1.6	13942
		1000	7007	9244	10728	12110	13469	14815	1.6	13942

Initial Pt Force 0.1f_{yield}		Axial Load (excluding PT) 4500kN			Cantilever Length (12000mm)			Grade 300 Dissipaters		
	PT Dia.	Fuse Length (mm)	Yield (kNm)	1%drift (kNm)	2%drift (kNm)	3%drift (kNm)	4%drift (kNm)	6%drift (kNm)	λ	Fuse Area (mm^2)
Diameter (2200mm)	36mm	250	5089	6416	6477	6372	6185	5941	1.3	7318
		500	5284	6290	6237	6058	5838	5596	1.4	7318
		750	5391	6246	6143	5930	5681	5411	1.5	7318
		1000	5474	6220	6095	5862	5595	5305	1.5	7318
	50mm	250	5204	6662	6857	6896	6836	6734	1.3	7613
		500	5402	6533	6613	6568	6481	6375	1.5	7613
		750	5514	6488	6516	6435	6319	6184	1.5	7613
		1000	5600	6460	6464	6364	6230	6075	1.6	7613
	75mm	250	5494	7292	7829	8217	8510	8720	1.4	8380
		500	5706	7153	7564	7865	8115	8340	1.6	8380
		750	5825	7104	7465	7716	7936	8138	1.6	8380
		1000	5918	7074	7407	7637	7838	8024	1.7	8380
	100mm	250	5898	8158	9148	9991	10750	11438	1.5	9454
		500	6129	8001	8855	9607	10320	10998	1.7	9454
		750	6258	7948	8747	9450	10117	10765	1.8	9454
		1000	6363	7916	8688	9359	10003	10634	1.8	9454
	125mm	250	6410	9238	10784	12179	13487	14718	1.6	10834
		500	6666	9064	10457	11748	13003	14233	1.8	10834
		750	6807	9000	10334	11573	12785	13980	1.9	10834
		1000	6924	8965	10271	11479	12664	13837	1.9	10834
	150mm	250	7030	10519	12707	14736	16673	18526	1.7	12521
		500	7302	10322	12337	14249	16125	17974	1.9	12521
		750	7469	10248	12200	14051	15879	17691	1.9	12521
		1000	7600	10209	12128	13947	15744	17529	2.0	12521

Initial Pt Force 0.1Fyield		Axial Load (excluding PT) 6000kN			Cantilever Length (12000mm)			Grade 300 Dissipaters		
	PT Dia.	Fuse Length (mm)	Yield (kNm)	1%drift (kNm)	2%drift (kNm)	3%drift (kNm)	4%drift (kNm)	6%drift (kNm)	λ	Fuse Area (mm^2)
Diameter (1000mm)	36mm	250	2422	3139	3059	2853	2624	2361	1.0	9592
		500	2545	3108	2987	2747	2484	2200	1.0	9592
		750	2634	3087	2960	2715	2436	2135	1.1	9592
		1000	2700	3072	2947	2694	2406	2102	1.1	9592
	50mm	250	2463	3199	3154	2974	2773	2550	1.0	9832
		500	2584	3168	3074	2865	2637	2380	1.1	9832
		750	2673	3149	3049	2829	2582	2317	1.1	9832
		1000	2741	3134	3035	2812	2558	2286	1.1	9832
	75mm	250	2561	3362	3389	3275	3154	3013	1.0	10454
		500	2687	3326	3306	3166	3008	2836	1.1	10454
		750	2780	3304	3274	3128	2959	2774	1.1	10454
		1000	2848	3289	3263	3113	2926	2733	1.1	10454
	100mm	250	2700	3579	3704	3688	3658	3617	1.1	11326
		500	2826	3543	3614	3575	3503	3442	1.1	11326
		750	2925	3523	3582	3528	3449	3366	1.1	11326
		1000	2997	3507	3567	3508	3423	3334	1.1	11326
	125mm	250	2877	3856	4092	4203	4274	4348	1.1	12447
		500	3007	3811	4001	4068	4108	4152	1.1	12447
		750	3113	3797	3962	4026	4059	4087	1.2	12447
		1000	3186	3776	3945	3997	4024	4038	1.2	12447
	150mm	250	3088	4184	4538	4806	4993	5185	1.1	13817
		500	3228	4132	4447	4653	4815	4967	1.2	13817
		750	3340	4115	4407	4589	4748	4897	1.2	13817
		1000	3418	4099	4385	4561	4722	4857	1.2	13817

Initial Pt Force 0.1Fyield		Axial Load (excluding PT) 6000kN			Cantilever Length (12000mm)			Grade 300 Dissipaters		
	PT Dia.	Fuse Length (mm)	Yield (kNm)	1%drift (kNm)	2%drift (kNm)	3%drift (kNm)	4%drift (kNm)	6%drift (kNm)	λ	Fuse Area (mm^2)
Diameter (1200mm)	36mm	250	3102	4065	4043	3909	3720	3499	1.2	9620
		500	3267	4013	3941	3761	3532	3281	1.2	9620
		750	3373	3994	3909	3706	3460	3192	1.3	9620
		1000	3442	3987	3889	3678	3422	3145	1.3	9620
	50mm	250	3153	4157	4183	4095	3960	3793	1.2	9887
		500	3321	4104	4080	3946	3769	3571	1.3	9887
		750	3428	4085	4042	3890	3696	3481	1.3	9887
		1000	3499	4077	4027	3862	3657	3433	1.3	9887
	75mm	250	3284	4397	4531	4569	4564	4527	1.2	10579
		500	3455	4340	4426	4414	4364	4294	1.3	10579
		750	3569	4319	4390	4353	4287	4200	1.3	10579
		1000	3641	4308	4371	4326	4246	4151	1.3	10579
	100mm	250	3468	4721	5009	5206	5369	5497	1.3	11549
		500	3647	4663	4896	5039	5148	5249	1.3	11549
		750	3765	4640	4857	4973	5069	5150	1.4	11549
		1000	3845	4625	4834	4941	5031	5097	1.4	11549
	125mm	250	3702	5133	5604	5977	6329	6660	1.3	12795
		500	3889	5068	5479	5793	6103	6390	1.4	12795
		750	4010	5043	5431	5728	6013	6287	1.4	12795
		1000	4098	5020	5415	5706	5969	6238	1.4	12795
	150mm	250	3989	5615	6306	6876	7437	7998	1.3	14318
		500	4181	5549	6159	6677	7199	7696	1.4	14318
		750	4307	5521	6108	6617	7094	7577	1.4	14318
		1000	4402	5494	6086	6574	7054	7518	1.4	14318

Initial Pt Force 0.1Fyield		Axial Load (excluding PT) 6000kN			Cantilever Length (12000mm)			Grade 300 Dissipaters		
	PT Dia.	Fuse Length (mm)	Yield (kNm)	1%drift (kNm)	2%drift (kNm)	3%drift (kNm)	4%drift (kNm)	6%drift (kNm)	λ	Fuse Area (mm^2)
Diameter (1500mm)	36mm	250	4246	5491	5591	5542	5429	5273	1.3	9664
		500	4417	5410	5434	5320	5157	4970	1.4	9664
		750	4528	5384	5380	5235	5048	4831	1.4	9664
		1000	4610	5373	5350	5192	4985	4754	1.5	9664
	50mm	250	4319	5640	5825	5863	5840	5775	1.3	9971
		500	4493	5559	5664	5636	5563	5466	1.4	9971
		750	4610	5533	5607	5550	5451	5331	1.5	9971
		1000	4691	5518	5578	5505	5391	5250	1.5	9971
	75mm	250	4507	6020	6420	6675	6874	7034	1.4	10767
		500	4692	5936	6247	6435	6581	6707	1.5	10767
		750	4814	5909	6187	6343	6463	6565	1.5	10767
		1000	4900	5894	6156	6296	6401	6488	1.6	10767
	100mm	250	4773	6545	7219	7764	8253	8704	1.5	11883
		500	4965	6453	7035	7504	7938	8351	1.6	11883
		750	5097	6425	6969	7407	7811	8200	1.6	11883
		1000	5190	6409	6936	7356	7743	8117	1.6	11883
	125mm	250	5109	7207	8207	9095	9930	10726	1.5	13317
		500	5315	7102	8004	8812	9584	10340	1.6	13317
		750	5459	7068	7935	8705	9446	10175	1.7	13317
		1000	5557	7057	7895	8649	9373	10085	1.7	13317
	150mm	250	5516	7989	9365	10637	11859	13043	1.5	15069
		500	5737	7877	9141	10324	11479	12616	1.7	15069
		750	5895	7833	9065	10207	11328	12435	1.7	15069
		1000	6003	7816	9019	10145	11248	12337	1.7	15069

v

Initial Pt Force 0.1Fyield		Axial Load (excluding PT) 6000kN			Cantilever Length (12000mm)			Grade 300 Dissipaters		
	PT Dia.	Fuse Length (mm)	Yield (kNm)	1%drift (kNm)	2%drift (kNm)	3%drift (kNm)	4%drift (kNm)	6%drift (kNm)	λ	Fuse Area (mm^2)
Diameter (1800mm)	36mm	250	5417	6970	7183	7234	7190	6977	1.4	9707
		500	5581	6857	6961	6924	6826	6597	1.5	9707
		750	5751	6815	6879	6798	6673	6420	1.6	9707
		1000	5813	6787	6830	6732	6591	6323	1.6	9707
	50mm	250	5517	7193	7538	7724	7830	7660	1.4	10054
		500	5686	7077	7309	7411	7449	7268	1.6	10054
		750	5857	7032	7226	7280	7289	7085	1.6	10054
		1000	5925	7004	7176	7210	7204	6983	1.6	10054
	75mm	250	5781	7762	8439	8964	9416	9436	1.5	10955
		500	5954	7637	8194	8629	9022	8996	1.6	10955
		750	6138	7590	8105	8499	8846	8792	1.7	10955
		1000	6208	7563	8058	8422	8750	8680	1.7	10955
	100mm	250	6147	8540	9659	10630	11531	11834	1.6	12217
		500	6323	8403	9392	10266	11101	11363	1.7	12217
		750	6525	8350	9295	10124	10920	11144	1.8	12217
		1000	6604	8324	9245	10049	10823	11014	1.8	12217
	125mm	250	6615	9513	11166	12675	14113	14844	1.7	13838
		500	6796	9357	10871	12273	13639	14318	1.8	13838
		750	7020	9304	10764	12116	13440	14076	1.9	13838
		1000	7103	9277	10709	12033	13332	13941	1.9	13838
	150mm	250	7179	10670	12930	15053	17102	18434	1.7	15821
		500	7366	10498	12601	14604	16574	17842	1.9	15821
		750	7617	10435	12482	14430	16351	17569	1.9	15821
		1000	7707	10408	12421	14339	16233	17420	2.0	15821

Initial Pt Force 0.1f_{yield}		Axial Load (excluding PT) 6000kN			Cantilever Length (12000mm)			Grade 300 Dissipaters		
	PT Dia.	Fuse Length (mm)	Yield (kNm)	1%drift (kNm)	2%drift (kNm)	3%drift (kNm)	4%drift (kNm)	6%drift (kNm)	λ	Fuse Area (mm^2)
Diameter (2000mm)	36mm	250	6062	7722	7747	7561	7267	6891	1.1	11009
		500	6263	7570	7459	7166	6811	6402	1.2	11009
		750	6384	7515	7350	7009	6605	6163	1.2	11009
		1000	6464	7485	7296	6924	6491	6030	1.2	11009
	50mm	250	6162	7926	8058	7978	7793	7526	1.1	11327
		500	6369	7768	7761	7575	7327	7034	1.2	11327
		750	6493	7713	7652	7414	7121	6787	1.2	11327
		1000	6575	7682	7593	7329	7003	6649	1.3	11327
	75mm	250	6424	8448	8847	9037	9125	9132	1.1	12152
		500	6636	8278	8533	8611	8633	8619	1.3	12152
		750	6769	8222	8418	8442	8418	8367	1.3	12152
		1000	6857	8192	8358	8352	8300	8219	1.3	12152
	100mm	250	6791	9165	9920	10472	10922	11289	1.2	13308
		500	7007	8985	9586	10015	10392	10737	1.3	13308
		750	7154	8924	9458	9833	10162	10467	1.4	13308
		1000	7248	8893	9397	9738	10037	10317	1.4	13308
	125mm	250	7258	10062	11261	12248	13135	13937	1.3	14793
		500	7478	9872	10894	11750	12558	13334	1.4	14793
		750	7640	9803	10755	11554	12308	13041	1.4	14793
		1000	7746	9772	10689	11449	12173	12877	1.5	14793
	150mm	250	7818	11136	12840	14328	15717	17015	1.3	16609
		500	8051	10924	12436	13781	15081	16349	1.4	16609
		750	8229	10853	12283	13566	14809	16030	1.5	16609
		1000	8350	10822	12211	13453	14660	15851	1.5	16609

Initial Pt Force 0.1f_{yield}		Axial Load (excluding PT) 6000kN			Cantilever Length (12000mm)			Grade 300 Dissipaters		
	PT Dia.	Fuse Length (mm)	Yield (kNm)	1%drift (kNm)	2%drift (kNm)	3%drift (kNm)	4%drift (kNm)	6%drift (kNm)	λ	Fuse Area (mm^2)
Diameter (2200mm)	36mm	250	6469	8308	8362	8197	7904	7516	1.3	9651
		500	6734	8149	8055	7791	7446	7065	1.4	9651
		750	6892	8095	7943	7618	7238	6829	1.4	9651
		1000	7005	8059	7878	7527	7124	6694	1.5	9651
	50mm	250	6577	8546	8728	8698	8550	8285	1.3	9947
		500	6846	8382	8416	8283	8074	7826	1.4	9947
		750	7009	8324	8300	8108	7860	7583	1.5	9947
		1000	7124	8288	8236	8014	7742	7445	1.5	9947
	75mm	250	6856	9151	9665	9972	10167	10266	1.4	10714
		500	7133	8977	9334	9533	9673	9760	1.5	10714
		750	7307	8914	9212	9354	9439	9496	1.6	10714
		1000	7429	8875	9148	9253	9311	9346	1.6	10714
	100mm	250	7246	9982	10947	11699	12343	12893	1.5	11787
		500	7534	9794	10588	11224	11809	12359	1.6	11787
		750	7723	9723	10452	11032	11567	12080	1.7	11787
		1000	7856	9684	10386	10929	11434	11912	1.7	11787
	125mm	250	7739	11033	12534	13835	15023	16116	1.5	13168
		500	8045	10820	12143	13317	14439	15528	1.7	13168
		750	8252	10743	11996	13107	14176	15223	1.7	13168
		1000	8398	10700	11921	12994	14030	15050	1.8	13168
	150mm	250	8338	12276	14415	16341	18156	19869	1.6	14855
		500	8664	12037	13982	15767	17507	19214	1.8	14855
		750	8893	11952	13816	15536	17217	18879	1.8	14855
		1000	9054	11915	13733	15413	17059	18687	1.9	14855

Initial Pt Force 0.1f_{yield}		Axial Load (excluding PT) 6000kN			Cantilever Length (12000mm)			Grade 300 Dissipaters		
	PT Dia.	Fuse Length (mm)	Yield (kNm)	1%drift (kNm)	2%drift (kNm)	3%drift (kNm)	4%drift (kNm)	6%drift (kNm)	λ	Fuse Area (mm^2)
Diameter (2500mm)	36mm	250	7770	9811	9986	9902	9688	7652	1.3	9679
		500	7943	9602	9598	9410	9163	8781	1.5	9679
		750	8151	9530	9447	9202	8906	8487	1.5	9679
		1000	8202	9486	9366	9090	8763	8316	1.6	9679
	50mm	250	7907	10119	10472	10570	10526	8540	1.4	10000
		500	8084	9906	10076	10062	9987	9707	1.5	10000
		750	8297	9830	9919	9847	9725	9405	1.6	10000
		1000	8348	9787	9837	9732	9579	9229	1.6	10000
	75mm	250	8258	10913	11713	12276	12664	12018	1.5	10834
		500	8445	10683	11293	11725	12089	12085	1.6	10834
		750	8674	10603	11125	11491	11809	11762	1.7	10834
		1000	8726	10560	11035	11366	11653	11575	1.7	10834
	100mm	250	8751	12002	13405	14573	15594	15302	1.5	12002
		500	8951	11751	12945	13985	14950	15377	1.7	12002
		750	9200	11664	12770	13729	14637	15024	1.8	12002
		1000	9249	11621	12674	13588	14462	14818	1.8	12002
	125mm	250	9377	13371	15514	17420	19173	19478	1.6	13503
		500	9595	13093	15007	16771	18475	19557	1.8	13503
		750	9867	12998	14814	16498	18139	19157	1.9	13503
		1000	9915	12947	14718	16351	17943	18923	1.9	13503
	150mm	250	10133	15000	18007	20766	23365	25296	1.7	15338
		500	10361	14693	17442	20044	22585	24538	1.9	15338
		750	10666	14587	17227	19741	22213	24099	2.0	15338
		1000	10717	14521	17117	19578	22004	23845	2.0	15338

Initial Pt Force 0.1Fyield		Axial Load (excluding PT) 7500kN			Cantilever Length (12000mm)			Grade 300 Dissipaters		
	PT Dia.	Fuse Length (mm)	Yield (kNm)	1%drift (kNm)	2%drift (kNm)	3%drift (kNm)	4%drift (kNm)	6%drift (kNm)	λ	Fuse Area (mm^2)
Diameter (1000mm)	36mm	250	2703	3552	3450	3169	2850	2503	1.1	10221
		500	2852	3518	3372	3061	2706	2333	1.2	10221
		750	2964	3503	3341	3021	2657	2266	1.2	10221
		1000	3044	3486	3327	3002	2629	2232	1.2	10221
	50mm	250	2737	3606	3530	3276	2991	2673	1.1	10427
		500	2884	3570	3453	3169	2846	2505	1.2	10427
		750	3001	3556	3421	3126	2789	2434	1.2	10427
		1000	3078	3539	3408	3107	2766	2402	1.2	10427
	75mm	250	2823	3745	3736	3559	3335	3100	1.2	10961
		500	2975	3709	3656	3444	3185	2921	1.2	10961
		750	3092	3691	3622	3402	3131	2858	1.2	10961
		1000	3172	3678	3607	3377	3105	2816	1.2	10961
	100mm	250	2945	3940	4014	3945	3796	3663	1.2	11708
		500	3100	3895	3932	3811	3647	3476	1.2	11708
		750	3217	3882	3901	3764	3591	3412	1.3	11708
		1000	3305	3869	3880	3741	3562	3367	1.3	11708
	125mm	250	3098	4180	4357	4404	4378	4342	1.2	12669
		500	3258	4132	4277	4272	4213	4146	1.3	12669
		750	3381	4116	4241	4214	4151	4074	1.3	12669
		1000	3470	4104	4218	4193	4121	4047	1.3	12669
	150mm	250	3288	4466	4762	4941	5058	5133	1.2	13843
		500	3453	4416	4673	4795	4870	4924	1.3	13843
		750	3579	4400	4639	4741	4799	4857	1.3	13843
		1000	3676	4390	4621	4713	4762	4817	1.3	13843

Initial Pt Force 0.1Fyield		Axial Load (excluding PT) 7500kN			Cantilever Length (12000mm)			Grade 300 Dissipaters		
	PT Dia.	Fuse Length (mm)	Yield (kNm)	1%drift (kNm)	2%drift (kNm)	3%drift (kNm)	4%drift (kNm)	6%drift (kNm)	λ	Fuse Area (mm^2)
Diameter (1200mm)	36mm	250	3484	4647	4591	4391	4126	3819	1.3	10246
		500	3682	4599	4490	4236	3929	3590	1.4	10246
		750	3820	4575	4452	4178	3853	3497	1.4	10246
		1000	3921	4562	4434	4152	3814	3448	1.5	10246
	50mm	250	3529	4732	4719	4563	4348	4093	1.3	10475
		500	3729	4679	4610	4408	4149	3861	1.4	10475
		750	3868	4659	4574	4347	4072	3768	1.5	10475
		1000	3966	4645	4556	4321	4032	3718	1.5	10475
	75mm	250	3645	4943	5037	5002	4905	4781	1.4	11068
		500	3848	4887	4929	4838	4700	4541	1.5	11068
		750	3988	4865	4892	4778	4626	4444	1.5	11068
		1000	4094	4848	4871	4743	4578	4393	1.5	11068
	100mm	250	3804	5231	5475	5587	5651	5694	1.4	11899
		500	4012	5177	5356	5415	5441	5440	1.5	11899
		750	4158	5148	5316	5353	5352	5339	1.5	11899
		1000	4269	5131	5297	5323	5315	5285	1.6	11899
	125mm	250	4013	5591	6023	6303	6558	6786	1.5	12967
		500	4219	5533	5890	6117	6326	6523	1.5	12967
		750	4378	5507	5848	6061	6248	6413	1.6	12967
		1000	4491	5484	5821	6022	6193	6358	1.6	12967
	150mm	250	4265	6024	6668	7144	7599	8055	1.5	14273
		500	4478	5961	6519	6951	7350	7756	1.6	14273
		750	4638	5933	6465	6883	7254	7639	1.6	14273
		1000	4764	5902	6441	6848	7211	7581	1.6	14273

Initial Pt Force $0.1f_{yield}$		Axial Load (excluding PT) 7500kN			Cantilever Length (12000mm)			Grade 300 Dissipaters		
	PT Dia.	Fuse Length (mm)	Yield (kNm)	1%drift (kNm)	2%drift (kNm)	3%drift (kNm)	4%drift (kNm)	6%drift (kNm)	λ	Fuse Area (mm^2)
Diameter (1500mm)	36mm	250	4789	6324	6400	6289	6101	5861	1.5	10283
		500	5029	6245	6237	6057	5815	5542	1.6	10283
		750	5186	6217	6181	5969	5701	5404	1.7	10283
		1000	5290	6203	6152	5924	5640	5327	1.7	10283
	50mm	250	4854	6457	6615	6589	6487	6337	1.5	10546
		500	5093	6377	6451	6352	6198	6012	1.6	10546
		750	5253	6349	6392	6263	6081	5872	1.7	10546
		1000	5359	6335	6362	6217	6019	5796	1.7	10546
	75mm	250	5018	6801	7163	7348	7463	7533	1.6	11229
		500	5264	6718	6990	7100	7160	7193	1.7	11229
		750	5435	6689	6927	7007	7039	7048	1.7	11229
		1000	5543	6675	6893	6958	6975	6969	1.8	11229
	100mm	250	5248	7278	7903	8368	8768	9125	1.6	12185
		500	5505	7186	7713	8105	8447	8765	1.8	12185
		750	5681	7155	7650	8006	8318	8610	1.8	12185
		1000	5801	7140	7616	7954	8250	8527	1.8	12185
	125mm	250	5544	7879	8817	9619	10359	11056	1.7	13414
		500	5810	7774	8612	9336	10013	10668	1.8	13414
		750	5996	7742	8548	9230	9876	10504	1.9	13414
		1000	6127	7727	8512	9175	9803	10414	1.9	13414
	150mm	250	5903	8594	9884	11075	12194	13274	1.7	14917
		500	6184	8474	9667	10757	11817	12853	1.9	14917
		750	6381	8440	9596	10640	11668	12676	1.9	14917
		1000	6521	8416	9560	10582	11590	12580	1.9	14917

Initial Pt Force 0.1Fyield		Axial Load (excluding PT) 7500kN			Cantilever Length (12000mm)			Grade 300 Dissipaters		
	PT Dia.	Fuse Length (mm)	Yield (kNm)	1%drift (kNm)	2%drift (kNm)	3%drift (kNm)	4%drift (kNm)	6%drift (kNm)	λ	Fuse Area (mm^2)
Diameter (1800mm)	36mm	250	6172	8065	8256	8247	8145	7858	1.6	10320
		500	6381	7945	8024	7927	7760	7450	1.8	10320
		750	6612	7899	7939	7801	7593	7260	1.8	10320
		1000	6702	7876	7895	7728	7504	7155	1.8	10320
	50mm	250	6260	8266	8586	8709	8742	8525	1.6	10618
		500	6470	8145	8349	8382	8356	8101	1.8	10618
		750	6707	8099	8262	8254	8183	7904	1.8	10618
		1000	6799	8076	8220	8181	8090	7796	1.9	10618
	75mm	250	6490	8783	9425	9879	10247	10216	1.7	11390
		500	6704	8656	9175	9535	9842	9774	1.9	11390
		750	6954	8604	9084	9400	9670	9558	1.9	11390
		1000	7051	8581	9039	9330	9571	9439	2.0	11390
	100mm	250	6814	9494	10564	11457	12267	12526	1.8	12471
		500	7030	9351	10295	11087	11831	12048	1.9	12471
		750	7298	9304	10197	10944	11648	11826	2.0	12471
		1000	7396	9275	10147	10868	11550	11704	2.0	12471
	125mm	250	7216	10383	11974	13397	14739	15433	1.9	13862
		500	7448	10227	11682	12996	14264	14909	2.0	13862
		750	7733	10173	11576	12840	14067	14667	2.1	13862
		1000	7840	10149	11522	12758	13960	14533	2.1	13862
	150mm	250	7702	11439	13629	15656	17602	18902	1.9	15561
		500	7950	11268	13308	15215	17082	18322	2.1	15561
		750	8261	11213	13192	15046	16865	18056	2.2	15561
		1000	8377	11189	13131	14956	16751	17909	2.2	15561

Initial Pt Force 0.1f_{yield}		Axial Load (excluding PT) 7500kN			Cantilever Length (12000mm)			Grade 300 Dissipaters		
	PT Dia.	Fuse Length (mm)	Yield (kNm)	1%drift (kNm)	2%drift (kNm)	3%drift (kNm)	4%drift (kNm)	6%drift (kNm)	λ	Fuse Area (mm^2)
Diameter (2000mm)	36mm	250	6903	8934	8897	8596	8167	7643	1.2	11966
		500	7157	8769	8590	8174	7676	7131	1.3	11966
		750	7339	8710	8476	8005	7462	6875	1.3	11966
		1000	7458	8683	8417	7916	7345	6727	1.4	11966
	50mm	250	6995	9118	9186	8987	8665	8248	1.2	12244
		500	7248	8947	8869	8557	8165	7727	1.3	12244
		750	7434	8893	8755	8386	7948	7471	1.4	12244
		1000	7556	8865	8693	8296	7829	7321	1.4	12244
	75mm	250	7223	9591	9917	9983	9928	9780	1.3	12967
		500	7485	9417	9587	9534	9406	9235	1.4	12967
		750	7678	9357	9468	9356	9179	8968	1.4	12967
		1000	7808	9330	9404	9261	9056	8819	1.5	12967
	100mm	250	7540	10243	10917	11336	11635	11844	1.3	13977
		500	7814	10066	10568	10860	11082	11265	1.4	13977
		750	8020	10004	10442	10672	10843	10983	1.5	13977
		1000	8160	9971	10377	10572	10713	10827	1.5	13977
	125mm	250	7944	11070	12166	13013	13743	14381	1.4	15277
		500	8234	10874	11795	12503	13150	13759	1.5	15277
		750	8454	10812	11657	12302	12894	13459	1.6	15277
		1000	8608	10777	11582	12195	12755	13291	1.6	15277
	150mm	250	8442	12061	13638	14982	16205	17336	1.4	16866
		500	8745	11850	13239	14429	15563	16659	1.6	16866
		750	8977	11778	13090	14213	15287	16336	1.6	16866
		1000	9148	11743	13010	14098	15138	16156	1.6	16866

Initial Pt Force 0.1f_{yield}		Axial Load (excluding PT) 7500kN			Cantilever Length (12000mm)			Grade 300 Dissipaters		
	PT Dia.	Fuse Length (mm)	Yield (kNm)	1%drift (kNm)	2%drift (kNm)	3%drift (kNm)	4%drift (kNm)	6%drift (kNm)	λ	Fuse Area (mm^2)
Diameter (2200mm)	36mm	250	7778	10159	10210	9979	9601	9093	1.3	11985
		500	8108	9967	9839	9484	9041	8527	1.4	11985
		750	8327	9892	9702	9282	8778	8230	1.4	11985
		1000	8476	9852	9629	9171	8634	8062	1.4	11985
	50mm	250	7877	10387	10567	10465	10219	9859	1.3	12280
		500	8216	10191	10187	9961	9651	9273	1.4	12280
		750	8440	10114	10048	9755	9386	8969	1.4	12280
		1000	8592	10071	9973	9645	9238	8797	1.5	12280
	75mm	250	8143	10974	11476	11703	11791	11765	1.3	13047
		500	8495	10765	11077	11175	11195	11167	1.5	13047
		750	8731	10681	10929	10960	10925	10847	1.5	13047
		1000	8886	10644	10855	10846	10774	10662	1.5	13047
	100mm	250	8514	11779	12718	13387	13919	14337	1.4	14121
		500	8879	11551	12296	12825	13284	13698	1.5	14121
		750	9131	11466	12136	12597	12998	13366	1.6	14121
		1000	9302	11429	12054	12475	12840	13178	1.6	14121
	125mm	250	8983	12791	14269	15477	16550	17505	1.5	15501
		500	9370	12541	13814	14872	15863	16814	1.6	15501
		750	9640	12455	13644	14627	15557	16457	1.7	15501
		1000	9828	12411	13553	14496	15388	16256	1.7	15501
	150mm	250	9554	13991	16102	17935	19628	21204	1.5	17188
		500	9967	13726	15608	17276	18883	20446	1.7	17188
		750	10260	13639	15424	17010	18550	20060	1.7	17188
		1000	10469	13594	15324	16869	18367	19841	1.8	17188

Initial Pt Force 0.1F_{yield}		Axial Load (excluding PT) 7500kN			Cantilever Length (12000mm)			Grade 300 Dissipaters		
	PT Dia.	Fuse Length (mm)	Yield (kNm)	1%drift (kNm)	2%drift (kNm)	3%drift (kNm)	4%drift (kNm)	6%drift (kNm)	λ	Fuse Area (mm^2)
Diameter (2500mm)	36mm	250	9607	12339	12577	12486	12174	10926	1.2	12871
		500	9833	12070	12073	11830	11483	11006	1.3	12871
		750	10118	11977	11882	11552	11147	10620	1.4	12871
		1000	10166	11929	11776	11402	10958	10395	1.4	12871
	50mm	250	9744	12647	13058	13143	13014	11848	1.2	13215
		500	9972	12372	12543	12478	12303	11930	1.4	13215
		750	10263	12276	12347	12191	11958	11535	1.4	13215
		1000	10316	12224	12241	12036	11765	11308	1.5	13215
	75mm	250	10101	13435	14286	14819	15160	14224	1.3	14108
		500	10334	13144	13745	14123	14395	14315	1.4	14108
		750	10641	13043	13538	13824	14027	13899	1.5	14108
		1000	10696	12984	13433	13657	13821	13657	1.5	14108
	100mm	250	10598	14523	15972	17100	18038	17547	1.4	15359
		500	10842	14210	15392	16354	17236	17627	1.5	15359
		750	11170	14102	15171	16040	16843	17171	1.6	15359
		1000	11224	14033	15053	15869	16617	16907	1.6	15359
	125mm	250	11229	15892	18076	19938	21607	22644	1.5	16968
		500	11486	15552	17447	19128	20734	21803	1.6	16968
		750	11840	15430	17203	18789	20313	21313	1.7	16968
		1000	11900	15355	17079	18605	20079	21027	1.7	16968
	150mm	250	11997	17525	20570	23282	25798	27736	1.5	18933
		500	12262	17152	19875	22395	24838	26799	1.7	18933
		750	12649	17012	19619	22025	24378	26261	1.7	18933
		1000	12714	16937	19483	21824	24123	25950	1.8	18933

Initial Pt Force 0.1Fyield		Axial Load (excluding PT) 8500kN			Cantilever Length (12000mm)			Grade 300 Dissipaters		
	PT Dia.	Fuse Length (mm)	Yield (kNm)	1%drift (kNm)	2%drift (kNm)	3%drift (kNm)	4%drift (kNm)	6%drift (kNm)	λ	Fuse Area (mm^2)
Diameter (1000mm)	36mm	250	2990	3947	3834	3522	3148	2752	1.1	11555
		500	3153	3903	3749	3400	2988	2563	1.2	11555
		750	3274	3886	3717	3353	2934	2488	1.2	11555
		1000	3365	3875	3702	3332	2906	2449	1.2	11555
	50mm	250	3022	3998	3912	3629	3280	2921	1.1	11760
		500	3183	3952	3829	3500	3123	2723	1.2	11760
		750	3309	3936	3793	3458	3067	2653	1.2	11760
		1000	3398	3929	3778	3432	3033	2615	1.2	11760
	75mm	250	3109	4133	4106	3905	3614	3329	1.1	12294
		500	3275	4084	4023	3766	3454	3129	1.2	12294
		750	3400	4068	3989	3717	3400	3055	1.2	12294
		1000	3492	4062	3972	3695	3366	3019	1.2	12294
	100mm	250	3230	4316	4375	4271	4077	3874	1.1	13041
		500	3398	4267	4285	4126	3904	3668	1.2	13041
		750	3523	4252	4258	4075	3843	3591	1.2	13041
		1000	3619	4242	4235	4045	3811	3560	1.2	13041
	125mm	250	3380	4543	4707	4714	4650	4531	1.2	14002
		500	3552	4497	4620	4570	4458	4326	1.2	14002
		750	3683	4482	4585	4511	4390	4247	1.2	14002
		1000	3784	4479	4567	4479	4353	4217	1.2	14002
	150mm	250	3569	4824	5101	5234	5305	5328	1.2	15177
		500	3746	4773	5001	5076	5112	5092	1.2	15177
		750	3879	4760	4972	5028	5022	5003	1.2	15177
		1000	3988	4752	4954	4992	4981	4960	1.3	15177

Initial Pt Force 0.1Fyield		Axial Load (excluding PT) 8500kN			Cantilever Length (12000mm)			Grade 300 Dissipaters		
	PT Dia.	Fuse Length (mm)	Yield (kNm)	1%drift (kNm)	2%drift (kNm)	3%drift (kNm)	4%drift (kNm)	6%drift (kNm)	λ	Fuse Area (mm^2)
Diameter (1200mm)	36mm	250	3853	5178	5119	4887	4577	4227	1.3	11579
		500	4066	5125	5005	4714	4360	3971	1.4	11579
		750	4224	5103	4962	4653	4276	3867	1.4	11579
		1000	4341	5080	4941	4619	4232	3813	1.4	11579
	50mm	250	3898	5258	5242	5055	4794	4494	1.3	11808
		500	4113	5204	5123	4877	4575	4234	1.4	11808
		750	4269	5181	5084	4815	4486	4130	1.4	11808
		1000	4387	5157	5062	4783	4442	4074	1.5	11808
	75mm	250	4014	5463	5558	5473	5336	5163	1.4	12401
		500	4228	5407	5429	5291	5108	4896	1.4	12401
		750	4388	5383	5384	5226	5019	4789	1.5	12401
		1000	4510	5356	5368	5193	4974	4731	1.5	12401
	100mm	250	4172	5744	5988	6041	6064	6049	1.4	13232
		500	4391	5680	5846	5858	5832	5771	1.5	13232
		750	4557	5655	5800	5792	5734	5657	1.5	13232
		1000	4683	5632	5776	5752	5692	5599	1.5	13232
	125mm	250	4372	6095	6522	6741	6958	7127	1.4	14300
		500	4594	6032	6369	6546	6697	6830	1.5	14300
		750	4769	6006	6320	6475	6599	6716	1.5	14300
		1000	4900	5977	6295	6439	6549	6662	1.5	14300
	150mm	250	4621	6517	7140	7574	7968	8369	1.4	15606
		500	4850	6443	6982	7367	7696	8044	1.5	15606
		750	5030	6415	6924	7288	7610	7916	1.5	15606
		1000	5162	6385	6893	7239	7549	7852	1.6	15606

Initial Pt Force 0.1f_{yield}		Axial Load (excluding PT) 8500kN			Cantilever Length (12000mm)			Grade 300 Dissipaters		
	PT Dia.	Fuse Length (mm)	Yield (kNm)	1%drift (kNm)	2%drift (kNm)	3%drift (kNm)	4%drift (kNm)	6%drift (kNm)	λ	Fuse Area (mm^2)
Diameter (1500mm)	36mm	250	5290	7063	7147	7016	6792	6509	1.5	11617
		500	5566	6975	6970	6757	6473	6151	1.6	11617
		750	5751	6946	6903	6658	6345	5997	1.6	11617
		1000	5879	6931	6869	6608	6277	5913	1.7	11617
	50mm	250	5355	7194	7355	7308	7171	6976	1.5	11880
		500	5633	7105	7172	7044	6847	6612	1.6	11880
		750	5821	7075	7108	6945	6717	6456	1.7	11880
		1000	5947	7061	7071	6893	6648	6371	1.7	11880
	75mm	250	5517	7532	7889	8049	8126	8149	1.6	12562
		500	5799	7439	7699	7775	7789	7772	1.7	12562
		750	5996	7409	7626	7672	7655	7610	1.7	12562
		1000	6129	7394	7590	7617	7583	7522	1.7	12562
	100mm	250	5742	8003	8607	9048	9406	9715	1.6	13518
		500	6034	7894	8410	8759	9052	9317	1.7	13518
		750	6239	7862	8333	8650	8911	##	1.8	13518
		1000	6381	7847	8298	8593	8836	9055	1.8	13518
	125mm	250	6033	8588	9509	10276	10971	11619	1.7	14748
		500	6338	8470	9285	9967	10593	11195	1.8	14748
		750	6547	8437	9215	9851	10443	11014	1.8	14748
		1000	6700	8414	9177	9791	10363	10916	1.9	14748
	150mm	250	6385	9282	10556	11694	12779	13809	1.7	16250
		500	6702	9157	10318	11373	12372	13352	1.8	16250
		750	6921	9113	10239	11238	12211	13159	1.9	16250
		1000	7087	9096	10207	11183	12126	13054	1.9	16250

Initial Pt Force $0.1f_{yield}$		Axial Load (excluding PT) 8500kN			Cantilever Length (12000mm)			Grade 300 Dissipaters		
	PT Dia.	Fuse Length (mm)	Yield (kNm)	1%drift (kNm)	2%drift (kNm)	3%drift (kNm)	4%drift (kNm)	6%drift (kNm)	λ	Fuse Area (mm^2)
Diameter (1800mm)	36mm	250	6836	9021	9233	9209	9076	8779	1.6	11654
		500	7077	8887	8977	8852	8654	8309	1.7	11654
		750	7352	8836	8881	8712	8468	8091	1.8	11654
		1000	7454	8812	8835	8636	8365	7971	1.8	11654
	50mm	250	6923	9220	9556	9662	9663	9429	1.6	11951
		500	7168	9082	9292	9298	9232	8955	1.8	11951
		750	7447	9029	9197	9156	9049	8731	1.8	11951
		1000	7548	9006	9147	9081	8942	8607	1.9	11951
	75mm	250	7143	9723	10378	10811	11144	11095	1.7	12723
		500	7396	9580	10105	10430	10694	10604	1.8	12723
		750	7688	9527	10001	10281	10503	10375	1.9	12723
		1000	7794	9504	9952	10203	10401	10240	1.9	12723
	100mm	250	7453	10413	11500	12364	13136	13389	1.8	13805
		500	7718	10265	11205	11958	12657	12861	1.9	13805
		750	8022	10211	11094	11799	12455	12617	2.0	13805
		1000	8134	10187	11043	11717	12345	12483	2.0	13805
	125mm	250	7849	11285	12882	14276	15578	16277	1.8	15195
		500	8123	11125	12565	13839	15060	15704	2.0	15195
		750	8453	11070	12449	13669	14844	15440	2.0	15195
		1000	8574	11038	12390	13581	14728	15295	2.1	15195
	150mm	250	8330	12324	14511	16507	18411	19727	1.9	16894
		500	8620	12150	14166	16032	17849	19097	2.0	16894
		750	8970	12093	14040	15848	17616	18810	2.1	16894
		1000	9101	12060	13977	15751	17489	18651	2.1	16894

Initial Pt Force 0.1f_{yield}		Axial Load (excluding PT) 8500kN			Cantilever Length (12000mm)			Grade 300 Dissipaters		
	PT Dia.	Fuse Length (mm)	Yield (kNm)	1%drift (kNm)	2%drift (kNm)	3%drift (kNm)	4%drift (kNm)	6%drift (kNm)	λ	Fuse Area (mm^2)
Diameter (2000mm)	36mm	250	7631	9979	9948	9599	9103	8497	1.2	13522
		500	7928	9804	9606	9126	8552	7921	1.3	13522
		750	8144	9744	9479	8939	8312	7638	1.3	13522
		1000	8295	9711	9413	8839	8181	7479	1.4	13522
	50mm	250	7715	10157	10229	9982	9590	9090	1.2	13800
		500	8016	9981	9879	9502	9031	8506	1.3	13800
		750	8239	9921	9750	9312	8788	8219	1.4	13800
		1000	8390	9888	9685	9211	8656	8059	1.4	13800
	75mm	250	7941	10625	10948	10958	10830	10597	1.3	14522
		500	8251	10441	10582	10460	10250	9989	1.4	14522
		750	8478	10373	10447	10262	9998	9693	1.4	14522
		1000	8636	10346	10381	10158	9861	9527	1.4	14522
	100mm	250	8254	11262	11929	12287	12511	12630	1.3	15533
		500	8572	11074	11545	11762	11899	11990	1.4	15533
		750	8810	11005	11401	11555	11635	11679	1.5	15533
		1000	8983	10971	11331	11445	11492	11506	1.5	15533
	125mm	250	8651	12079	13150	13936	14589	15135	1.4	16833
		500	8986	11871	12742	13378	13937	14452	1.5	16833
		750	9237	11800	12595	13158	13657	14122	1.5	16833
		1000	9423	11765	12515	13042	13506	13940	1.5	16833
	150mm	250	9140	13051	14594	15877	17019	18058	1.4	18422
		500	9490	12826	14160	15277	16321	17320	1.5	18422
		750	9757	12753	13998	15042	16021	16969	1.6	18422
		1000	9954	12718	13909	14917	15859	16772	1.6	18422

Initial Pt Force $0.1f_{yield}$		Axial Load (excluding PT) 8500kN			Cantilever Length (12000mm)			Grade 300 Dissipaters		
	PT Dia.	Fuse Length (mm)	Yield (kNm)	1%drift (kNm)	2%drift (kNm)	3%drift (kNm)	4%drift (kNm)	6%drift (kNm)	λ	Fuse Area (mm^2)
Diameter (2200mm)	36mm	250	8599	11372	11426	11152	10708	10134	1.2	13540
		500	8984	11153	11012	10598	10081	9495	1.4	13540
		750	9254	11069	10858	10372	9797	9158	1.4	13540
		1000	9430	11031	10778	10252	9633	8966	1.4	13540
	50mm	250	8698	11597	11776	11629	11317	10874	1.3	13836
		500	9094	11371	11355	11065	10679	10234	1.4	13836
		750	9363	11286	11196	10836	10391	9887	1.4	13836
		1000	9543	11243	11115	10715	10228	9691	1.5	13836
	75mm	250	8959	12167	12667	12845	12863	12753	1.3	14603
		500	9362	11929	12228	12259	12200	12085	1.4	14603
		750	9642	11844	12062	12021	11900	11736	1.5	14603
		1000	9836	11800	11977	11894	11735	11534	1.5	14603
	100mm	250	9320	12956	13887	14503	14962	15293	1.4	15676
		500	9740	12704	13420	13883	14259	14584	1.5	15676
		750	10035	12611	13250	13632	13944	14217	1.6	15676
		1000	10243	12567	13157	13498	13771	14009	1.6	15676
	125mm	250	9785	13945	15408	16564	17560	18426	1.4	17056
		500	10221	13673	14912	15901	16808	17666	1.6	17056
		750	10535	13585	14731	15634	16472	17275	1.6	17056
		1000	10761	13541	14632	15491	16288	17054	1.7	17056
	150mm	250	10346	15121	17218	18990	20606	22091	1.5	18744
		500	10807	14843	16683	18275	19794	21264	1.6	18744
		750	11144	14746	16480	17988	19432	20845	1.7	18744
		1000	11391	14701	16380	17835	19235	20606	1.7	18744

Initial Pt Force 0.1f_{yield}		Axial Load (excluding PT) 8500kN			Cantilever Length (12000mm)			Grade 300 Dissipaters		
	PT Dia.	Fuse Length (mm)	Yield (kNm)	1%drift (kNm)	2%drift (kNm)	3%drift (kNm)	4%drift (kNm)	6%drift (kNm)	λ	Fuse Area (mm^2)
Diameter (2500mm)	36mm	250	10659	13827	14087	13965	13610	12174	1.2	14537
		500	10918	13528	13526	13241	12822	12263	1.3	14537
		750	11260	13424	13312	12926	12442	11833	1.4	14537
		1000	11321	13361	13197	12755	12229	11583	1.4	14537
	50mm	250	10793	14130	14560	14612	14442	13090	1.2	14881
		500	11055	13824	13988	13874	13634	13184	1.4	14881
		750	11403	13718	13768	13557	13243	12746	1.4	14881
		1000	11465	13652	13654	13381	13026	12490	1.4	14881
	75mm	250	11146	14904	15770	16262	16542	15472	1.3	15775
		500	11413	14583	15170	15490	15706	15563	1.4	15775
		750	11771	14472	14939	15164	15290	15097	1.5	15775
		1000	11841	14400	14823	14982	15058	14826	1.5	15775
	100mm	250	11632	15970	17428	18515	19386	18762	1.4	17026
		500	11910	15628	16787	17692	18499	18861	1.5	17026
		750	12290	15505	16548	17347	18071	18355	1.6	17026
		1000	12359	15430	16418	17160	17827	18061	1.6	17026
	125mm	250	12254	17316	19498	21319	22918	23927	1.4	18634
		500	12539	16951	18817	20435	21960	23003	1.6	18634
		750	12952	16808	18552	20063	21502	22468	1.6	18634
		1000	13021	16732	18420	19863	21246	22157	1.7	18634
	150mm	250	13012	18933	21967	24630	27071	28993	1.5	20600
		500	13300	18523	21221	23669	26030	27975	1.6	20600
		750	13745	18376	20933	23267	25532	27392	1.7	20600
		1000	13825	18290	20792	23051	25256	27054	1.7	20600

Initial Pt Force 0.1Fyield		Axial Load (excluding PT) 8500kN			Cantilever Length (12000mm)			Grade 300 Dissipaters		
	PT Dia.	Fuse Length (mm)	Yield (kNm)	1%drift (kNm)	2%drift (kNm)	3%drift (kNm)	4%drift (kNm)	6%drift (kNm)	λ	Fuse Area (mm^2)
Diameter (2800mm)	36mm	250	12551	16000	16435	16420	16129	11102	1.2	14567
		500	12844	15619	15745	15565	15262	14709	1.4	14567
		750	13036	15484	15471	15189	14804	14198	1.4	14567
		1000	13135	15415	15323	14984	14544	13891	1.5	14567
	50mm	250	12719	16384	17042	17256	17176	12104	1.3	14939
		500	13014	15994	16337	16380	16288	15795	1.4	14939
		750	13210	15857	16057	15994	15822	15272	1.5	14939
		1000	13313	15787	15907	15785	15557	14958	1.5	14939
	75mm	250	13150	17369	18594	19396	19881	14681	1.3	15904
		500	13464	16961	17857	18467	18942	18591	1.5	15904
		750	13668	16816	17569	18057	18449	18038	1.6	15904
		1000	13773	16743	17409	17834	18169	17708	1.6	15904
	100mm	250	13758	18729	20729	22300	23591	18243	1.4	17256
		500	14087	18291	19934	21319	22567	22463	1.6	17256
		750	14297	18136	19630	20878	22038	21872	1.6	17256
		1000	14408	18057	19462	20634	21736	21518	1.7	17256
	125mm	250	14524	20447	23402	25921	28156	22774	1.5	18994
		500	14886	19972	22545	24859	27067	27400	1.6	18994
		750	15101	19803	22208	24393	26497	26748	1.7	18994
		1000	15220	19719	22038	24138	26163	26359	1.8	18994
	150mm	250	15457	22502	26576	30205	33534	30572	1.6	21117
		500	15854	21981	25633	29040	32338	33335	1.7	21117
		750	16078	21797	25277	28533	31722	32624	1.8	21117
		1000	16202	21698	25087	28257	31372	32195	1.8	21117

Initial Pt Force 0.1Fyield		Axial Load (excluding PT) 10000kN			Cantilever Length (12000mm)			Grade 300 Dissipaters		
	PT Dia.	Fuse Length (mm)	Yield (kNm)	1%drift (kNm)	2%drift (kNm)	3%drift (kNm)	4%drift (kNm)	6%drift (kNm)	λ	Fuse Area (mm^2)
Diameter (1000mm)	36mm	250	3412	4511	4395	4048	3587	3113	1.1	13555
		500	3594	4463	4301	3898	3410	2894	1.1	13555
		750	3728	4449	4267	3839	3343	2813	1.1	13555
		1000	3833	4442	4245	3815	3306	2769	1.2	13555
	50mm	250	3448	4555	4467	4143	3716	3274	1.1	13760
		500	3627	4513	4372	3995	3532	3047	1.1	13760
		750	3762	4495	4338	3938	3465	2966	1.1	13760
		1000	3868	4493	4320	3913	3430	2918	1.2	13760
	75mm	250	3532	4682	4652	4397	4047	3666	1.1	14294
		500	3710	4636	4555	4251	3860	3433	1.1	14294
		750	3849	4623	4525	4188	3785	3355	1.2	14294
		1000	3958	4616	4501	4160	3753	3313	1.2	14294
	100mm	250	3647	4858	4907	4742	4497	4183	1.1	15041
		500	3832	4813	4807	4591	4291	3956	1.2	15041
		750	3970	4795	4776	4528	4213	3878	1.2	15041
		1000	4084	4794	4758	4494	4181	3827	1.2	15041
	125mm	250	3804	5080	5228	5170	5040	4849	1.1	16002
		500	3992	5030	5122	5008	4834	4603	1.2	16002
		750	4130	5019	5083	4951	4741	4508	1.2	16002
		1000	4249	5013	5065	4910	4699	4460	1.2	16002
	150mm	250	3989	5349	5601	5663	5656	5625	1.1	17177
		500	4175	5300	5490	5493	5440	5351	1.2	17177
		750	4320	5284	5449	5433	5365	5244	1.2	17177
		1000	4447	5278	5437	5406	5314	5187	1.2	17177

Initial Pt Force 0.1F_{yield}		Axial Load (excluding PT) 10000kN			Cantilever Length (12000mm)			Grade 300 Dissipaters		
	PT Dia.	Fuse Length (mm)	Yield (kNm)	1%drift (kNm)	2%drift (kNm)	3%drift (kNm)	4%drift (kNm)	6%drift (kNm)	λ	Fuse Area (mm^2)
Diameter (1200mm)	36mm	250	4389	5957	5905	5608	5243	4826	1.3	13579
		500	4628	5896	5761	5411	4990	4529	1.4	13579
		750	4812	5871	5714	5342	4898	4410	1.4	13579
		1000	4946	5843	5690	5306	4848	4347	1.4	13579
	50mm	250	4431	6032	6022	5768	5451	5081	1.3	13808
		500	4672	5970	5877	5568	5195	4782	1.4	13808
		750	4859	5943	5829	5499	5103	4662	1.4	13808
		1000	4994	5915	5804	5460	5046	4598	1.4	13808
	75mm	250	4540	6224	6325	6174	5971	5722	1.3	14401
		500	4787	6161	6173	5969	5709	5415	1.4	14401
		750	4977	6135	6123	5893	5615	5293	1.4	14401
		1000	5116	6107	6098	5861	5564	5228	1.4	14401
	100mm	250	4697	6494	6730	6721	6671	6581	1.3	15232
		500	4941	6427	6576	6516	6400	6263	1.4	15232
		750	5137	6397	6524	6440	6295	6144	1.5	15232
		1000	5281	6368	6490	6400	6251	6078	1.5	15232
	125mm	250	4891	6835	7239	7420	7528	7625	1.4	16300
		500	5145	6759	7082	7183	7252	7295	1.5	16300
		750	5343	6728	7018	7105	7144	7158	1.5	16300
		1000	5493	6700	6990	7060	7092	7090	1.5	16300
	150mm	250	5135	7234	7833	8236	8515	8824	1.4	17606
		500	5396	7160	7672	7982	8230	8486	1.5	17606
		750	5596	7121	7607	7882	8126	8333	1.5	17606
		1000	5754	7101	7567	7835	8059	8259	1.5	17606

Initial Pt Force 0.1Fyield		Axial Load (excluding PT) 10000kN			Cantilever Length (12000mm)			Grade 300 Dissipaters		
	PT Dia.	Fuse Length (mm)	Yield (kNm)	1%drift (kNm)	2%drift (kNm)	3%drift (kNm)	4%drift (kNm)	6%drift (kNm)	λ	Fuse Area (mm^2)
Diameter (1500mm)	36mm	250	6022	8163	8253	8090	7815	7469	1.5	13617
		500	6351	8056	8047	7790	7446	7054	1.6	13617
		750	6576	8025	7966	7677	7298	6875	1.6	13617
		1000	6738	8005	7931	7619	7220	6778	1.6	13617
	50mm	250	6087	8291	8454	8372	8181	7921	1.5	13880
		500	6414	8183	8245	8068	7807	7501	1.6	13880
		750	6645	8145	8168	7954	7658	7320	1.6	13880
		1000	6805	8130	8126	7894	7579	7223	1.7	13880
	75mm	250	6246	8617	8963	9088	9108	9063	1.5	14562
		500	6581	8501	8746	8775	8722	8629	1.6	14562
		750	6813	8469	8670	8656	8568	8444	1.7	14562
		1000	6983	8447	8629	8596	8487	8343	1.7	14562
	100mm	250	6466	9066	9659	10057	10355	10592	1.6	15518
		500	6811	8947	9436	9729	9952	10138	1.7	15518
		750	7049	8907	9347	9605	9791	9944	1.7	15518
		1000	7224	8884	9307	9541	9706	9840	1.8	15518
	125mm	250	6752	9634	10527	11253	11883	12456	1.6	16748
		500	7106	9510	10293	10907	11457	11976	1.7	16748
		750	7348	9460	10203	10768	11287	11773	1.8	16748
		1000	7531	9442	10163	10701	11198	11662	1.8	16748
	150mm	250	7098	10301	11550	12646	13646	14607	1.6	18250
		500	7469	10173	11301	12278	13193	14095	1.8	18250
		750	7715	10126	11210	12128	13027	13878	1.8	18250
		1000	7901	10100	11158	12056	12915	13761	1.8	18250

Initial Pt Force 0.1F_{yield}		Axial Load (excluding PT) 10000kN			Cantilever Length (12000mm)			Grade 300 Dissipaters		
	PT Dia.	Fuse Length (mm)	Yield (kNm)	1%drift (kNm)	2%drift (kNm)	3%drift (kNm)	4%drift (kNm)	6%drift (kNm)	λ	Fuse Area (mm^2)
Diameter (1800mm)	36mm	250	7783	10434	10685	10637	10461	10115	1.6	13654
		500	8095	10279	10384	10224	9970	9585	1.7	13654
		750	8429	10225	10276	10062	9762	9330	1.8	13654
		1000	8555	10201	10222	9978	9648	9186	1.8	13654
	50mm	250	7867	10621	10998	11078	11032	10756	1.6	13951
		500	8182	10465	10692	10658	10534	10216	1.7	13951
		750	8521	10411	10582	10494	10324	9963	1.8	13951
		1000	8648	10387	10528	10408	10210	9816	1.8	13951
	75mm	250	8087	11107	11793	12198	12480	12403	1.7	14723
		500	8405	10949	11481	11761	11963	11838	1.8	14723
		750	8756	10894	11366	11591	11745	11576	1.9	14723
		1000	8888	10870	11308	11502	11627	11432	1.9	14723
	100mm	250	8388	11783	12881	13714	14432	14672	1.7	15805
		500	8716	11613	12549	13254	13886	14073	1.9	15805
		750	9084	11558	12427	13075	13657	13795	1.9	15805
		1000	9224	11527	12365	12981	13533	13642	1.9	15805
	125mm	250	8772	12633	14235	15588	16830	17533	1.8	17195
		500	9112	12449	13885	15097	16248	16889	1.9	17195
		750	9500	12392	13755	14908	16006	16592	2.0	17195
		1000	9647	12360	13689	14807	15875	16428	2.0	17195
	150mm	250	9242	13652	15824	17778	19622	20954	1.8	18894
		500	9597	13451	15443	17252	18995	20254	2.0	18894
		750	10002	13383	15300	17047	18735	19935	2.0	18894
		1000	10162	13360	15235	16939	18595	19759	2.1	18894

Initial Pt Force 0.1f_{yield}		Axial Load (excluding PT) 10000kN			Cantilever Length (12000mm)			Grade 300 Dissipaters		
	PT Dia.	Fuse Length (mm)	Yield (kNm)	1%drift (kNm)	2%drift (kNm)	3%drift (kNm)	4%drift (kNm)	6%drift (kNm)	λ	Fuse Area (mm^2)
Diameter (2000mm)	36mm	250	8688	11527	11504	11083	10486	9760	1.2	15855
		500	9054	11334	11106	10537	9847	9088	1.3	15855
		750	9324	11266	10962	10320	9570	8761	1.3	15855
		1000	9516	11232	10887	10206	9419	8577	1.3	15855
	50mm	250	8773	11705	11775	11455	10961	10339	1.2	16133
		500	9142	11503	11373	10902	10313	9659	1.3	16133
		750	9410	11435	11224	10682	10033	9328	1.3	16133
		1000	9610	11402	11148	10566	9881	9143	1.4	16133
	75mm	250	8993	12155	12470	12404	12169	11810	1.2	16855
		500	9367	11951	12053	11832	11501	11108	1.3	16855
		750	9648	11881	11902	11607	11212	10767	1.4	16855
		1000	9850	11847	11823	11487	11055	10576	1.4	16855
	100mm	250	9297	12783	13417	13698	13812	13801	1.3	17866
		500	9684	12566	12984	13101	13113	13067	1.4	17866
		750	9975	12488	12827	12866	12812	12713	1.4	17866
		1000	10187	12454	12748	12742	12650	12514	1.4	17866
	125mm	250	9687	13574	14612	15310	15845	16260	1.3	19166
		500	10092	13340	14156	14681	15109	15483	1.4	19166
		750	10390	13267	13987	14433	14793	15112	1.5	19166
		1000	10615	13225	13890	14302	14623	14904	1.5	19166
	150mm	250	10164	14529	16028	17208	18232	19135	1.4	20755
		500	10586	14275	15542	16540	17448	18307	1.5	20755
		750	10898	14191	15360	16278	17115	17913	1.5	20755
		1000	11130	14155	15255	16138	16933	17693	1.6	20755

Initial Pt Force 0.1f_{yield}		Axial Load (excluding PT) 10000kN			Cantilever Length (12000mm)			Grade 300 Dissipaters		
	PT Dia.	Fuse Length (mm)	Yield (kNm)	1%drift (kNm)	2%drift (kNm)	3%drift (kNm)	4%drift (kNm)	6%drift (kNm)	λ	Fuse Area (mm^2)
Diameter (2200mm)	36mm	250	10053	13511	13634	13336	12826	12152	1.1	17007
		500	10528	13243	13125	12649	12046	11365	1.3	17007
		750	10863	13144	12934	12371	11694	10954	1.3	17007
		1000	11094	13097	12836	12223	11500	10713	1.3	17007
	50mm	250	10158	13735	13979	13807	13426	12882	1.2	17324
		500	10637	13458	13462	13112	12636	12084	1.3	17324
		750	10972	13366	13269	12829	12279	11669	1.3	17324
		1000	11211	13312	13171	12679	12083	11431	1.3	17324
	75mm	250	10424	14296	14864	15012	14957	14742	1.2	18146
		500	10915	14017	14329	14292	14138	13915	1.3	18146
		750	11260	13917	14128	14000	13770	13485	1.4	18146
		1000	11505	13869	14023	13844	13567	13241	1.4	18146
	100mm	250	10798	15079	16076	16656	17038	17262	1.2	19296
		500	11300	14788	15514	15902	16181	16392	1.4	19296
		750	11661	14686	15304	15597	15795	15944	1.4	19296
		1000	11919	14639	15194	15434	15584	15690	1.4	19296
	125mm	250	11273	16076	17595	18707	19623	20381	1.3	20775
		500	11791	15769	16996	17907	18713	19455	1.4	20775
		750	12171	15665	16774	17585	18307	18982	1.5	20775
		1000	12445	15609	16660	17414	18084	18714	1.5	20775
	150mm	250	11847	17267	19395	21128	22663	24035	1.3	22582
		500	12393	16943	18763	20274	21687	23042	1.5	22582
		750	12795	16828	18522	19931	21257	22538	1.5	22582
		1000	13090	16771	18400	19749	21020	22254	1.5	22582

Initial Pt Force 0.1f_{yield}		Axial Load (excluding PT) 10000kN			Cantilever Length (12000mm)			Grade 300 Dissipaters		
	PT Dia.	Fuse Length (mm)	Yield (kNm)	1%drift (kNm)	2%drift (kNm)	3%drift (kNm)	4%drift (kNm)	6%drift (kNm)	λ	Fuse Area (mm^2)
Diameter (2500mm)	36mm	250	12198	16033	16326	16163	15738	14044	1.2	17037
		500	12498	15689	15680	15322	14822	14149	1.3	17037
		750	12923	15558	15431	14968	14372	13645	1.4	17037
		1000	13014	15486	15304	14771	14122	13352	1.4	17037
	50mm	250	12329	16326	16787	16795	16543	14964	1.2	17381
		500	12631	15975	16130	15942	15619	15065	1.3	17381
		750	13062	15843	15877	15582	15162	14550	1.4	17381
		1000	13155	15767	15749	15386	14905	14251	1.4	17381
	75mm	250	12673	17080	17971	18412	18599	17329	1.3	18275
		500	12977	16715	17285	17525	17638	17430	1.4	18275
		750	13423	16572	17022	17151	17174	16885	1.4	18275
		1000	13522	16496	16889	16949	16906	16570	1.5	18275
	100mm	250	13152	18126	19590	20621	21396	21652	1.3	19526
		500	13460	17734	18871	19686	20383	20682	1.5	19526
		750	13921	17582	18593	19294	19895	20117	1.5	19526
		1000	14028	17505	18450	19081	19624	19784	1.5	19526
	125mm	250	13764	19443	21629	23379	24877	25839	1.4	21134
		500	14075	19020	20859	22382	23794	24792	1.5	21134
		750	14563	18861	20567	21966	23277	24188	1.6	21134
		1000	14680	18784	20414	21740	22988	23838	1.6	21134
	150mm	250	14507	21017	24042	26639	28978	30870	1.4	23100
		500	14818	20555	23215	25569	27810	29729	1.6	23100
		750	15339	20395	22902	25122	27255	29079	1.6	23100
		1000	15469	20307	22739	24881	26947	28701	1.7	23100

Initial Pt Force 0.1Fyield		Axial Load (excluding PT) 10000kN			Cantilever Length (12000mm)			Grade 300 Dissipaters		
	PT Dia.	Fuse Length (mm)	Yield (kNm)	1%drift (kNm)	2%drift (kNm)	3%drift (kNm)	4%drift (kNm)	6%drift (kNm)	λ	Fuse Area (mm^2)
Diameter (2800mm)	36mm	250	14376	18569	19063	19034	18644	12768	1.2	17067
		500	14768	18133	18267	18031	17634	16976	1.4	17067
		750	14988	17979	17955	17589	17104	16380	1.4	17067
		1000	15116	17901	17785	17349	16802	16024	1.5	17067
	50mm	250	14541	18945	19654	19850	19688	13761	1.3	17439
		500	14939	18501	18845	18834	18656	18052	1.4	17439
		750	15160	18343	18529	18383	18115	17445	1.5	17439
		1000	15290	18264	18359	18137	17807	17082	1.5	17439
	75mm	250	14961	19908	21181	21940	22362	16315	1.3	18404
		500	15375	19443	20332	20886	21271	20823	1.5	18404
		750	15605	19278	20003	20414	20704	20191	1.5	18404
		1000	15735	19195	19831	20154	20383	19813	1.6	18404
	100mm	250	15551	21239	23274	24797	25994	19850	1.4	19756
		500	15979	20746	22374	23680	24850	24682	1.5	19756
		750	16221	20571	22029	23191	24237	24005	1.6	19756
		1000	16358	20481	21846	22918	23892	23601	1.6	19756
	125mm	250	16305	22925	25896	28367	30504	26770	1.4	21494
		500	16760	22394	24942	27171	29273	29597	1.6	21494
		750	17003	22206	24564	26648	28635	28857	1.7	21494
		1000	17148	22098	24373	26362	28274	28416	1.7	21494
	150mm	250	17220	24942	29029	32597	35824	32400	1.5	23617
		500	17701	24367	27990	31302	34490	35481	1.7	23617
		750	17954	24162	27582	30738	33803	34690	1.7	23617
		1000	18112	24037	27377	30431	33413	34218	1.8	23617